INDOLES AND BIINDOLES: SYNTHESIS OF POWERFUL TOOLS FOR PHARMACEUTICAL AND MATERIALS SCIENCES

PhD in Chemical and Environmental Sciences – XXXIII Cycle

Dipartimento di Scienza e Alta Tecnologia

Università degli Studi dell'Insubria – Como (Italy)

PhD dissertation:

Luca SCAPINELLO

Supervisor: Prof. Andrea PENONI

Academic year: 2020/2021

"We think there is colour, we think there is sweet, we think there is bitter, but in realty there are atoms and a void"

Democritus (4th century BC)

"The chemists are a strange class of mortals, impelled by an almost insane impulse to seek their pleasures amid smoke and vapour, soot and flame, poisons and poverty; yet among all these evils I seem to live so sweetly that may I die if I were to change places with the Persian king."

J. J. Becher (17th century)

Index

- Appendix -

Synthesis of novel tetrapyrazinoporphyrazines for applications in material science field

Acknowledgments

People mentioned below are gratefully acknowledged for their precious contribution to this thesis. The present work would have been impossible otherwise.

Prof. Andrea Penoni

Prof. Tiziana Benincori

Prof. Angelo Maspero

Prof. Giovanni Palmisano

Prof. Stefano Tollari

Prof. Damiano Monticelli

Dr. Luca Nardo

and all the Bachelor and Master students who have worked with us.

Prof. Dr. Sabine Ludwigs

Dr. Klaus Dirnberger

Dr. Beatrice Omiecienski

and the whole Institute für Polymerchemie (IPOC) research group.

Prof. Patrizia Romana Mussini

Dr. Serena Arnaboldi

Dr. Sara Grecchi

Dr. Sergio Rossi

Dr. Luca Vaghi   Prof. Marco Pierini

Dr. Gloria Zanotti   Prof. Giancarlo Cravotto

Dr. Giuseppe Mattioli   Prof. Alessandro Barge

Dr. Roberto Cirilli

- Chapter 1 -

Synthesis of indoles as potential bioactive compounds

1.   Foreword

In the chemical space of heterocyclic compounds, indole (Figure 1) and its derivatives play a strong relevant role. It is diffused in a huge array of different natural products[1], many of them with intriguing biological activity.[2] Other applications spread uncountable fields: material science, fragrances, agrochemicals, pigments and dyes and many more.[3] It's not surprising then that many efforts are made by organic chemists to find not only synthetic methods to achieve indole fragments but also new functionalization protocols to afford with ease complex targets.
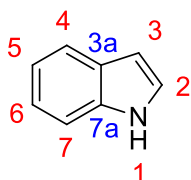
Figure 1: indole molecule and its positions numbering.

As previously stated, an incredible high number of natural bioactive molecules contains indole ring. The family of indole alkaloid contains more than 4,000 different products[4], being one of the largest in nature. Most of them are bioactive compounds very useful in medicine. All these products are *in vivo* synthetized by plants from amino acid *L*-tryptophan: its decarboxylation produces tryptamine, one of the simplest and widespread indole alkaloids. Tryptamine itself is a versatile building block for more complex products synthesis and its scaffold is clearly recognizable in many indole alkaloids (Figure 2).

Lysergic acid   Melatonin   Yohimbine
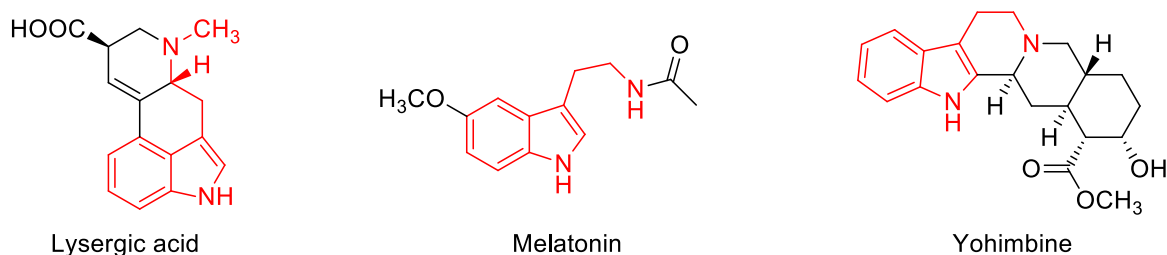
Figure 2: tryptamine-based alkaloids. Tryptamine subunit is red highlighted.

Indole is famous to be a very electron rich system. Many reviews summarize its consolidated chemistry.[5–7] A predominant aspect is extremely strong nucleophilic behaviour of 3 position. Calculations show that C3 reacts towards electrophiles 10^{13} times faster than benzene in the same conditions.[8] However, especially when C3 bears substituent, C2 nucleophilic behaviour must not be ignored when treating indoles with

electrophiles or oxidants. These chemical features and the previously cited biological predominance in natural bioactive compounds let indole be known as the *Lord of the Rings*[5] by organic chemists.

Indole appears in synthetic chemistry history in 1866, when von Baeyer on his studies on indigo dyes obtained indole by reducing oxindole with zinc metal powder.[9] First structure assignment (Figure 3) was therefore elucidated by von Baeyer himself in 1869 after cyclization of *o*-nitrocinnamic acid in presence of iron in basic solution.[10] This protocol is now known worldwide as Baeyer-Emmerling indole synthesis.

$$C_6H_4 \quad \begin{matrix} - \, C\,H \\ \parallel \\ C\,H \\ \mid \\ - \, N\,H \end{matrix}$$

Figure 3: indole structure published by von Baeyer in 1869. This is the first time ever indole molecule appears on a scientific paper.
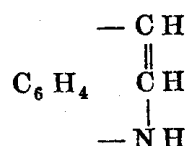
Indole core synthesis has continued to attract and challenge chemists[11] and many notable results were achieved so far. One of the most popular indole synthesis was developed by Fischer in 1883.[12] This protocol exploits a condensation reaction between a phenylhydrazine and a ketone or an aldehyde in acidic conditions (Scheme 1). Both Brønsted and Lewis acid can be employed as acid catalysts. Commonly accepted mechanism starts with carbonyl condensation forming a hydrazone, which can isomerize to respective enamine. Occurring of a [3,3]-sigmatropic rearrangement provides an imine, which goes to form an aminal. Acidic catalysis finally provides ammonia elimination to afford an indole (Scheme 1).[13,14] Hydrazone is not usually isolated.
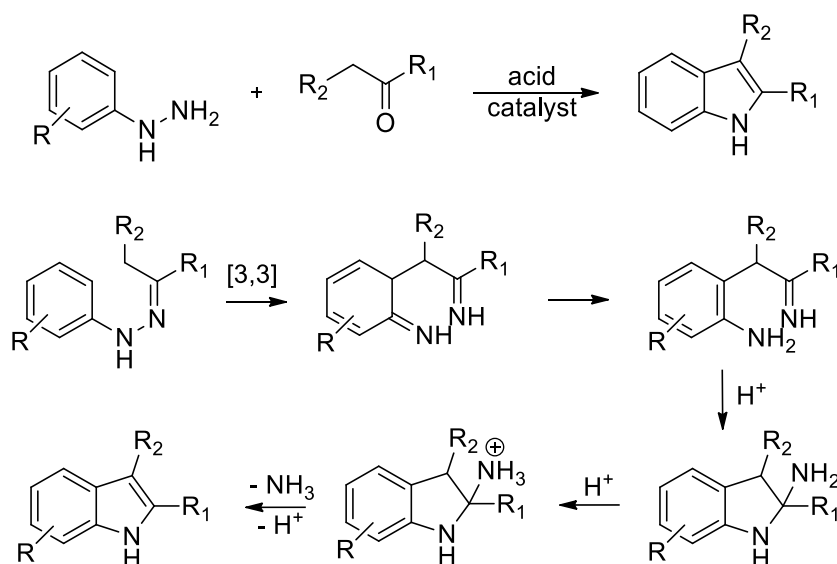
Scheme 1: Fischer indole synthesis and its mechanism.

Mechanistic investigations with 15N isotopic labeling showed that nitrogen atom in final indole product is always aryl N.[15] Hydrazone pivotal role in mechanism is confirmed by a protocol modification published by Buchwald.[16] The latter can be isolated by a palladium catalyzed cross coupling reaction starting from an aryl

halide and benzophenone hydrazone (Scheme 2). Resulting products are demonstrated to be stored for months on benchtop without any decomposition even if liquid.[17] This compound can be used as starting material to run a Fischer indolization with excellent results in presence of an enolizable ketone.
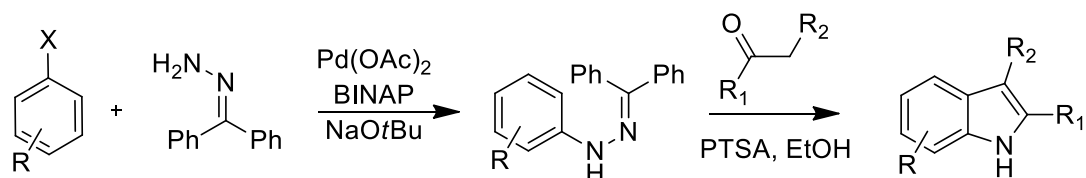
Scheme 2: Buchwald approach to Fischer reaction.

Despite being an old reaction, Fischer indole synthesis is diffused in pharmaceutical industry. Indomethacin synthetic plan, for example, exploits this protocol. Discovered in 1963[18] and approved in 1965 by US Food and Drug Administration, indomethacin expresses a strong non-selective inhibition of cyclooxygenases (COX-1 and COX-2), enzymes catalysing rate determining step in prostaglandins and thromboxanes synthesis from arachidonic acid. This action mechanism is generally common to all NSAIDs drugs. Anti-inflammatory potency in humans of indomethacin is estimated to be 0.5 times than cortisone.[19]

Merck industrial synthesis of indomethacin results is an elegant two steps sequence.[20] Key point is usage of α-angelica lactone as ketone equivalent.[21] The latter is formed in acidic conditions by enol lactone opening and directly reacts with hydrazone *via* classic Fischer indolization (Scheme 3).
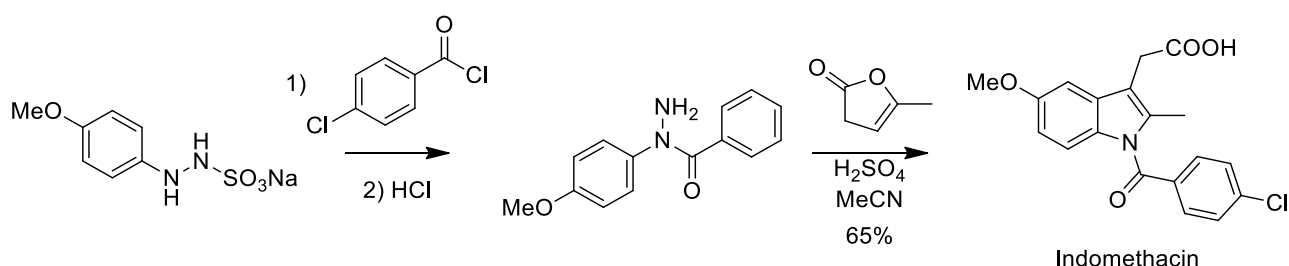
Scheme 3: modern indomethacin industrial synthesis.

Interest by pharmaceutical companies for Fischer indole synthesis is also particularly strong for triptans. These molecules are known to be effective only in migraine pain treatment. Despite their selectivity and low presence of adverse effects, nowadays triptanes are often replaced by mixtures of ergotamine and caffeine, which have broader activity spectrum.[22] Most diffused API belonging to triptane class is Glaxo's sumatriptan, patented in 1992.[23] Previously illustrated Fischer protocol is useful for sumatriptan synthesis too (Scheme 4), in which dihydropyran is seen as ketone equivalent.[21]
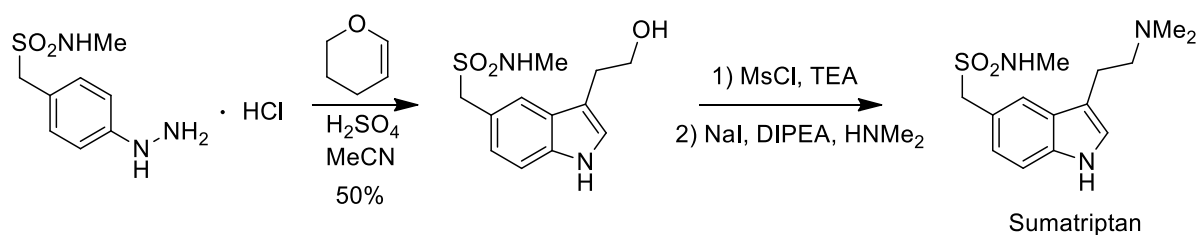
Scheme 4: sumatriptan synthesis.

Nenitzescu synthesis constitutes another classic in indoles preparation. Discovered in 1929[24], its starting materials are *p*-benzoquinone and a 3-aminocrotonic ester. Usually reaction takes place in refluxing high polar solvent.[25] Its peculiar point is the formation of 5-hydroxy-indoles (Scheme 5), making this protocol very attractive to a pharmaceutical point of view since this subunit is diffused in neurotransmitters like serotonin. Mechanism starts with a Micheal addition on *p*-benzoquinone. Subsequent step is attack on carbonyl by enamine π bond to form the indole skeleton which aromatizes after water loss.[26] A variant of this protocol was even developed for solid support synthesis[27] and optimizations for big batches have been studied.[28]
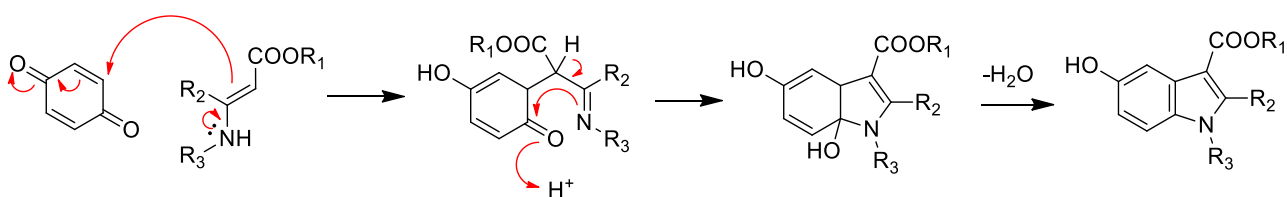
Scheme 5: Nenitzescu indole synthesis mechanism.

One of the current most interesting applications of Nenitzescu synthesis is new anticancer drug design as anthraquinone is a particularly common subunit in antitumor APIs.[29] Reacting 1,4,6,10-anthraquinone with different enamines in a modified protocol, a wide library of indoles with high toxicity for cancer cells (Scheme 6). Interestingly, their elucidated X-rays structures revealed they were not classic expected Nenitzescu products. Broad activity spectrum of 5-hydroxyindoles obtained by Nenitzescu synthesis covers also preparation of anti-HIV[30] and anti-hepatitis[31] drugs.
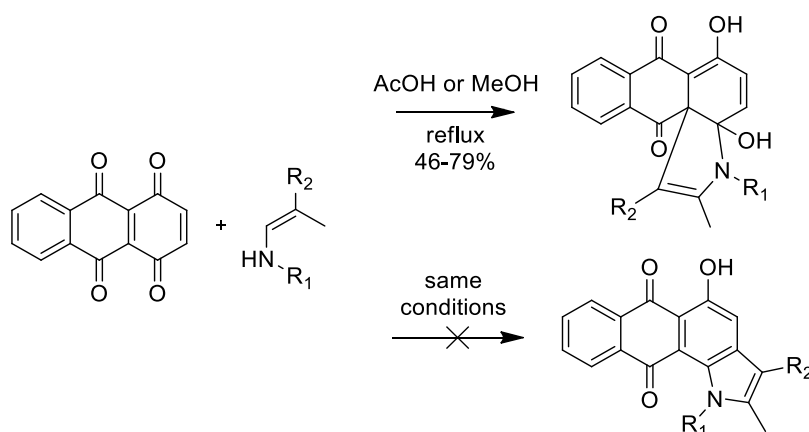
Scheme 6: Nenitzescu approach to afford new antitumor drugs.

11

With huge progresses in organometallic chemistry, metal assisted synthesis has revolutionized approach in indoles preparation. Voluminous literature has been published only concerning palladium promoted indole synthesis[32] and other metals like copper[33], rhodium[34] and gold[35–37] are nowadays common use in research labs and pharmaceutical industries for the purpose. Enormous impact for its remarkable versatility has Larock indole synthesis. Firstly proposed in 1991[38], reaction takes place with a 2-iodoaniline in presence of an alkyne (Scheme 7). Choice of alkyne is very flexible as a large survey has been successfully tested. Furthermore, high regioselectivity is observed when unsymmetrical alkynes are employed. Usually the bulkier group occupies C2 in final product.[38] *N*-acetyl and *N*-tosyl anilines have been demonstrated to give best results. Catalysis is done by Pd(OAc)$_2$ in presence of base and stoichiometric amount of LiCl. PPh$_3$ is present as catalyst ligand.[39]
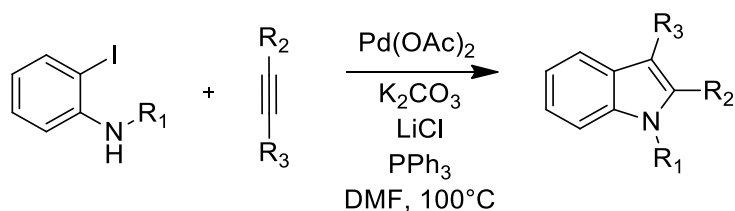

Scheme 7: Larock indole synthesis.

Great versatility of Larock synthesis is demonstrated by numerous pharmaceuticals obtained by this approach like psychedelic drug psilocin[40], antibiotic indolmycin[41], adrenergic blocking receptor aspidospermidine[42] and many more.

Naturally this foreword is not meant to summarize in few pages all key points about synthesis of pharmaceutical high interest indole-based compounds, but to underline and focus some aspects of this topic and to explain why indole is considered the *Lord of the Rings* in heterocycles chemistry. For further information on this argument, reader is sent to cited literature.[1,5,6,43]
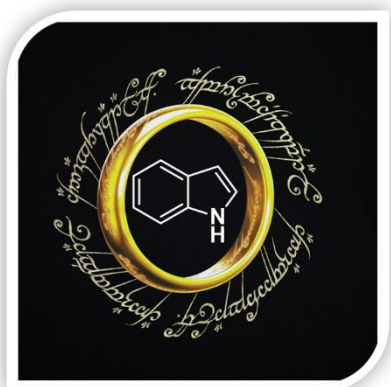
"One Ring to rule them all,

One Ring to find them,

One Ring to bring them all,

And in darkness bind them."

J. R. R. Tolkien, The Lord of the Rings, Part I – The Fellowship of the Ring

2.   Synthesis of *N*-hydroxyindoles

In *N*-hydroxyindole structure (Figure 4) a hydroxyl group is directly bonded to indole nitrogen atom. Nitrogen-oxygen bond is usually considered weak as its calculated dissociation energy is 34 kcal/mol, far less than organic chemistry core bonds carbon-carbon and carbon-hydrogen (64 and 88 kcal/mol respectively).[44]
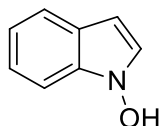
Figure 4: N-hydroxyindole structure.

For this reason stability of *N*-hydroxyindole has been topic of debate as they were considered elusive products[45]: It is known in fact tendency of some *N*-hydroxyindoles to dimerize and form kabutanes[46] (Scheme 8). Their name is justified by C2 symmetry of those products, resembling helmets used by soldiers of the former Empire of Japan. To avoid dimerization, trapping strategies like acetylation or alkylation were employed.[47,48]
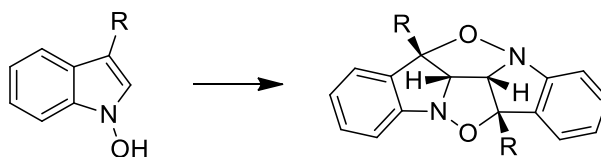
Scheme 8: N-hydroxyindoles dimerization to form kabutanes.

Although these premises, *N*-hydroxyindole moiety or its analogous nitrone form is not so rare in natural molecules: nocathiacine I[49] and coproverdine[50] (Figure 5) are two examples. Interest in *N*-hydroxyindoles is ever growing, as some of them are very useful in carcinoma treatment.[51] For example, stephacidin B displays high activity against prostate cancer.[52] Parallel to this, some synthetic strategies to afford stable *N*-hydroxyindoles were studied.
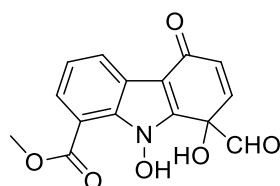
Figure 5: coproverdine, a cytotoxic marine alkaloid.

Some stable unprotected compounds were isolated by Somei in 1981, exploiting a titanium(III) chloride cyclization[53–55] (Scheme 9). Products stability was observed when R is an electron withdrawing group. Starting substrate was prepared by condensation of 2-methylnitrobenzenes with dimethylformamide dimethylacetal.

Scheme 9: Somei approach to *N*-hydroxindoles.

The same research group then focused attention on obtaining *N*-hydroxindoles by indoline oxidation. Best condition were identified in using 30% hydrogen peroxide and sodium tungstate as catalyst[56] (Scheme 10). Oxone® and *m*-chloroperbenzoic acid genera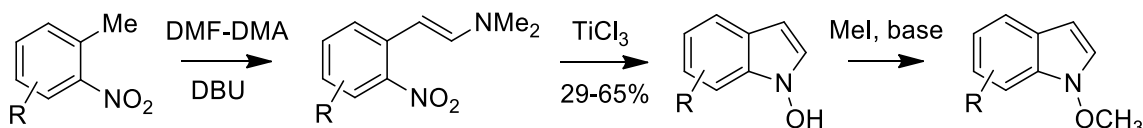lly give worse results. Halogenated indolines displayed unstable hydroxindoles. Their alkylation provided stability and opens path on possible extra transformations.[57,58]
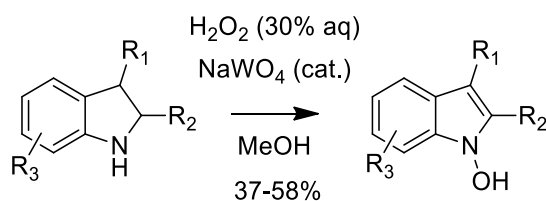
Scheme 10: indoline oxidation to *N*-hydroxyindole.

Somei applied successfully this oxidation protocol in synthesis of lespedamine (alkaloid extracted from *Lespedeza bicolor*) and novel *N*-hydroxytriptamines[59] (Scheme 11). Starting indolines are usually obtained by respective indoles hydrogenation.
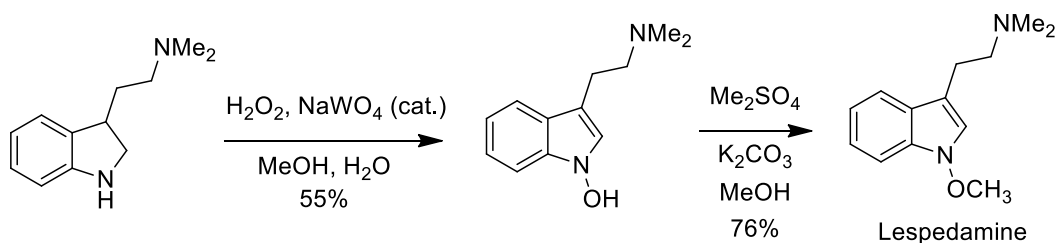
Scheme 11: lespedamine synthesis.

Pioneering works from Somei group put basis for further development of *N*-hydroxyindole synthesis, especially inspired on classical Reissert indole synthesis.[60] A protocol introduced by Wong in 2003[61] approaches problem exploiting a reductive cyclization of 2-nitrobenzyl ketones or aldehydes using lead and triethylammonium formate (Scheme 12). Protocol is respectful of hydroxy functional group avoiding its reduction. This way *N*-hydroxyindoles were obtained in good to excellent yields. Very interestingly authors report stability for all products obtained and not only for electron withdrawing group decorated ones. A later paper by Wojciechowski and co-workers reports a SnCl₂ mediated cyclization for the same substrates.[62]
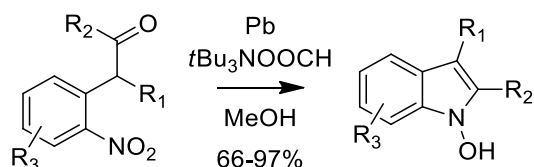
Scheme 12: Wong *N*-hydroxyindole synthesis.

Another successful strategy was pursued by Nicolaou in 2005 on the previously cited nocathiacine I total synthesis.[49] Starting material was identified in 2-nitrobenzyl ketoesters. A selective reduction mediated by $SnCl_2$ reduces chemo selectively nitro group to hydroxylamine. The latter condensates on ketone to afford a nitrone which can be converted into *N*-hydroxyindole by a nucleophile attack (Scheme 13). Both Wong's and Nicolaou's methods provide quite a general protocol to prepare a diverse library of different compounds starting off from easily available reactants in an organic chemistry laboratory.
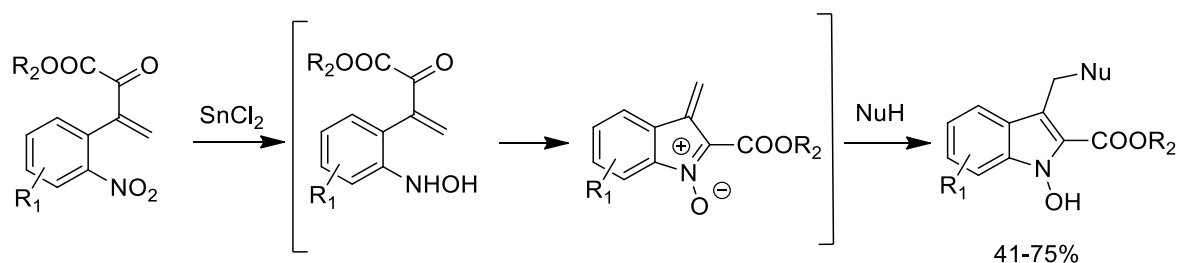
Scheme 13: Nicolaou *N*-hydroxyindole synthesis.

A straightforward preparation of *N*-alkoxyindoles was provided by Zhao[63] in 2008 (Scheme 14). Core step is oxidative mild hetero cyclization mediated by iron trichloride. Key point of this protocol is wide functional group tolerance; electron donating and electron withdrawing either. A radical mechanism initiated by a single electron transfer by $FeCl_3$ is invoked by authors to explain ring closure. In addition, nitrile group on C3 in final product is interesting starting point for further transformations.
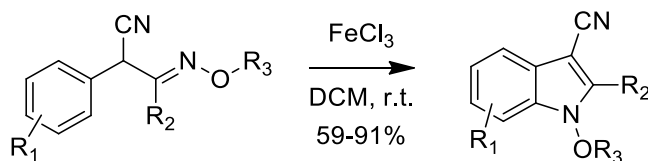
Scheme 14: Zhao *N*-alkoxyindoles synthesis.

A modification was introduced in 2009 by the same group to achieve indoles: oxidant is changed to $PhI(OAc)_2$ providing an effective metal free ring closure.[64]

3. Introduction on nitrosoarene-alkyne annulation

Nitroso group is one of the most studied functional groups due to its importance as source of oxygen and nitrogen for preparation of complex compounds. Since von Baeyer first preparation of nitrosobenzene by benzene nitrosylation,[65] chemists knowledge of nitroso compounds expanded: hetero Diels-Alder[66], nitroso-ene[67] and nitroso-aldol[68] reactions are valuable examples. A peculiar feature of nitroso compounds is their tendency to monomer/dimer equilibrium[69] (Figure 6). In addition the C-N bond energy ($\approx$ 35 kcal/mol for nitroso alkyls and $\approx$ 55 kcal/mol for nitrosoarenes) is not that high due stability of nitrosyl radical[70]: for this reason nitroso compounds are generally sensitive to heat and light. This is something which must be considered when planning new synthetic methodologies.[71]
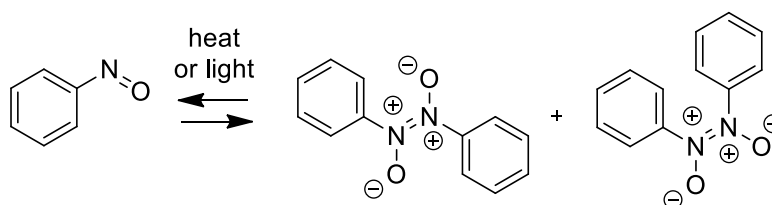
Figure 6: nitrosobenzene monomer/dimer equilibrium.

On the other hand, alkynes are reactants in huge amount of organic and metalorganic protocols and indole synthesis is not an exception. Besides aforementioned Larock cyclization, high success was Cacchi's intramolecular Larock-type approach to indole ring[32,72,73], with many improvements studied by other groups.[74] Reactivity between alkynes and nitrosoarenes is often mediated by metal catalysis like gold to afford nitrones[75] or indoles.[76] Even copper can be useful in preparation of 3-arylindoles from the same starting materials.[77] Nitrosoarenes could be also prepared *in situ* from hydroxylamine catalytic oxidation by iron phtalocyanine[78] in alkyne functional group respectful fashion. Manna and coworkers report an interesting metal free protocol to achieve *N*-oxide-imidazo[1,2-*a*]pyridines by annulation of 2-nitrosopyridines with alkynes.[79]

♦ ♦ ♦ ♦ ♦ ♦

3.1. Nitroarenes as nitrosoarenes precursors

Carbon monoxide nitroarenes reduction has been a stimulating topic and many results were achieved so far.[80–83] In particular, direct nitrogen introduction in organic molecules is very attractive goal for chemists. Transition metal complexes can be very helpful in promoting carbon nitrogen bond formation in CO reducing atmosphere.

Cenini group, for example, published an interesting ruthenium catalyzed allylic amination starting from nitroarenes (Scheme 15) and olefins.[84] Anilines were always detected as byproducts.
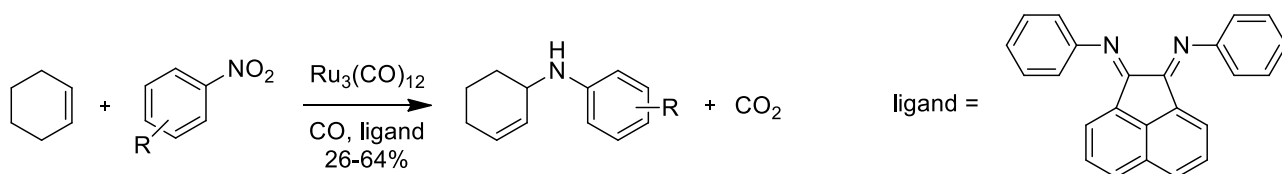
Scheme 15: Ru catalysed allylic amination of olefins.

Nicholas group developed an iron catalysed olefin allylic amination starting from usual nitroaromatics[85] (Scheme 16). Clear advantages are usage of inexpensive metal like Fe and no adding of extra ligands. *N,N*-diarylureas were detected as major byproducts.
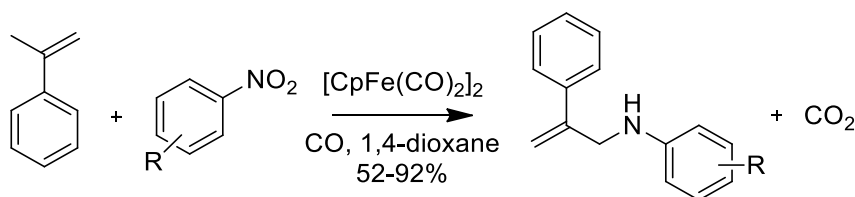
Scheme 16: Fe catalysed allylic amination of olefins.

Same research group tried to expand scope of this protocol, starting off from alkynes to achieve propargylic amination of the latter. First runs were performed with nitrobenzene and 1-phenyl-1-propyne with the same iron catalyst. Surprisingly, no trace of propargylic aminated product was detected. Indoles were obtained as major products in good yields[86] (Scheme 17). Both Fe and Ru catalysts were effective in achieving indole molecules in a regioselective fashion. 3-Substituted indoles were obtained even working with terminal alkynes, demonstrating high regioselectivity of these conditions.
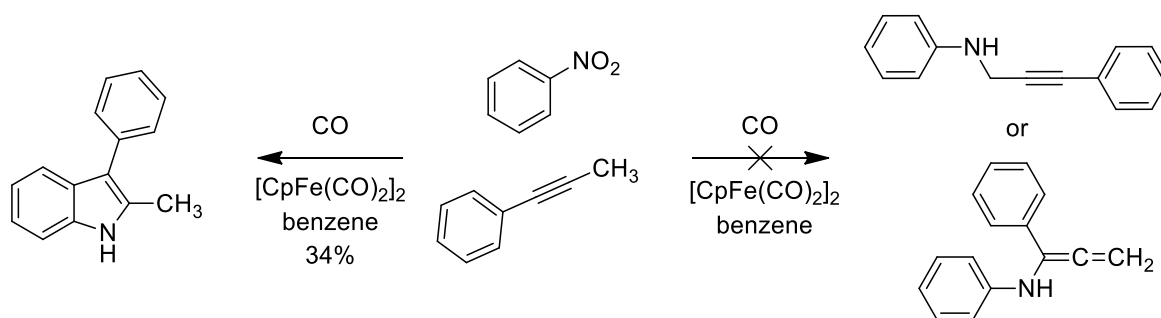
Scheme 17: unexpected obtaining of an indole product.

Stimulated by these interesting results, Nicholas group investigated more deeply mechanism behind this transformation. Given the previously cited metal promoted reduction of nitroarenes in CO atmosphere, nitrosoarenes were more likely invoked as reactive species in annulation. Experiments run in absence of carbon monoxide confirmed the hypothesis: even an uncatalyzed process was enough to promote annulation and *N*-hydroxyindoles were achieved as main product as no reducing agent was present[87] (Scheme 18).
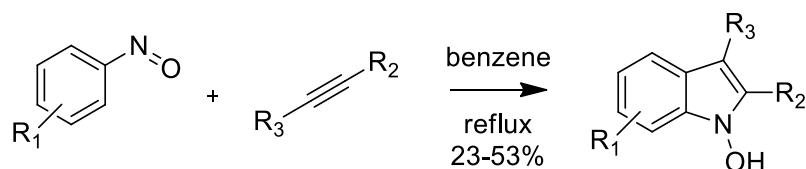
Scheme 18: uncatalyzed nitrosoarene-alkyne annulation to afford *N*-hydroxyindoles.

This result demonstrated metal catalyst is active part in nitroarene reduction to nitroso instead of annulation itself. 3 Position regioselectivity was still present when terminal alkynes were employed. High functional group tolerance was noticed. A highly favourable atom economy is clearly recognized. *N*-hydroxyindoles obtained could be easily reduced to respective indoles by catalytic hydrogenation or by carbon monoxide.

Formation of *N*-hydroxyindoles was demonstrated not only by masses analysis but also by comparation with authentic samples prepared with Somei oxidation protocol (Scheme 19).
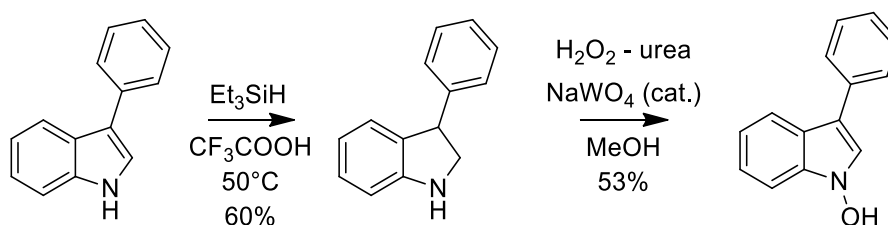
Scheme 19: preparation of 3-phenyl-*N*-hydroxyindole. Indoline was prepared following a literature procedure.[88]

♦ ♦ ♦ ♦ ♦ ♦

3.2. Nitrosoarenes direct employment

Given hypothesis nitrosoarene species are active part in the reaction, Penoni group studied direct employment of nitrosoarene compounds in annulation with alkynes. Same group reported high efficiency on nitrosoarene-alkyne cycloaddition by trapping formed N-OH indole by methylation with sodium dimethylsulfate and potassium carbonate.[89] Other electrophiles like Boc$_2$O, alkylchloroformates, allyl bromide, benzoyl and tosyl chloride were successfully employed[90] in the same one pot multi component approach (Scheme 20).

This way dimerization to kabutanes is avoided. High toxic benzene solvent was generally replaced with toluene. A slight tendency of nitrosoarenes with electron withdrawing groups to react faster and afford better yields than electron rich nitrosoaromatics was noticed: higher performances were achieved employing 4-nitronitrosobenzene. Nitroso compounds were usually used as the limiting reagents and with most of the reactions being carried out with an excess of the alkyne (10-12 excess fold). Conjugated alkynes were found to be the privileged partners: reactions carried out with unconjugated alkynes and symmetrical internal alkynes gave poor yields or no reactions at all. Terminal alkynes show better yields and faster forming of the

indole compounds. Major point was all the reactions show exclusively the formation of 3-substituted indoles without any traces of the 2-substitued isomer. Great atom economy was observed.

An interesting application of this protocol resulted in synthesis of unnatural indole based amino acids, starting off from a modified phenylalanine fragment (Scheme 21).
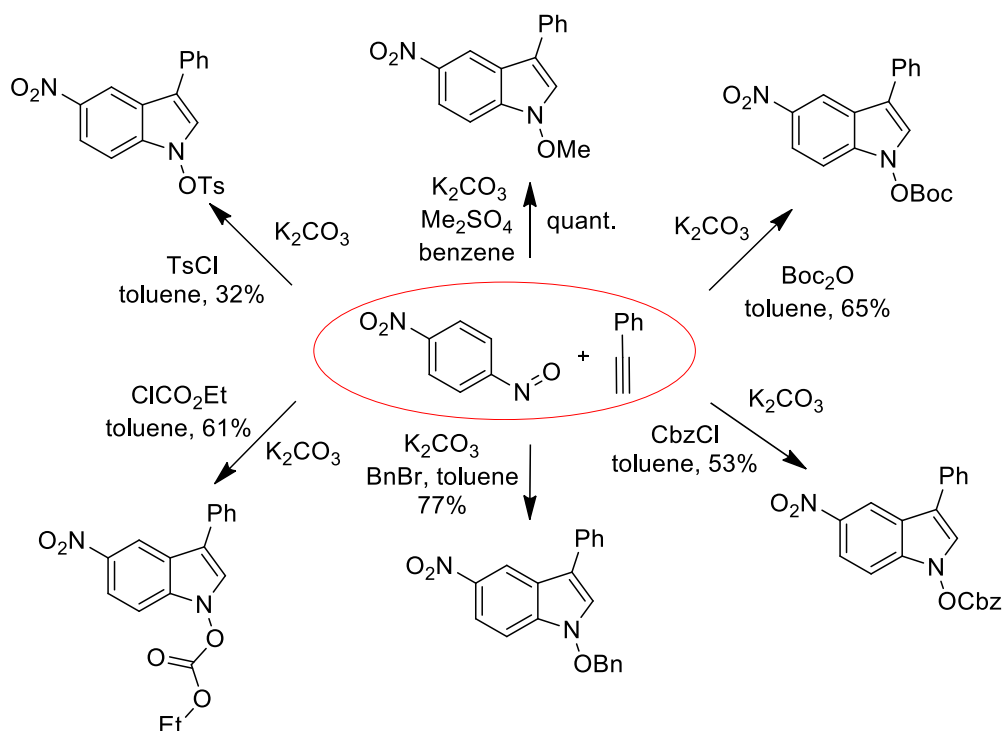
Scheme 20: one pot multi component synthesis of protected N-hydroxyindoles. All reactions were 80°C heated.
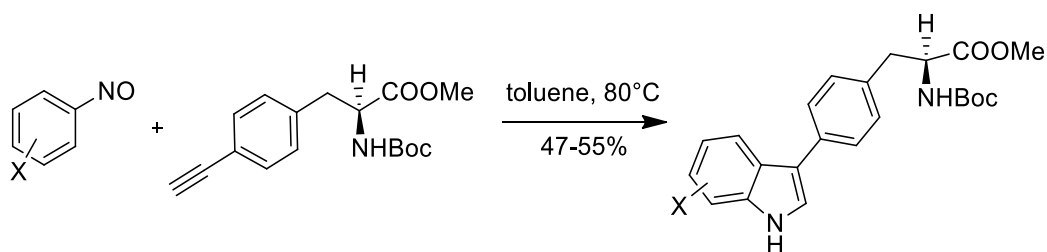
Scheme 21: preparation of unnatural phenylalanine amino acids via nitrosoarene-alkyne annulation.

Interestingly, annulation reaction these cases provided indoles instead expected N-hydroxy derivatives. Similar amino acids were known in literature already and prepared by Morera[91] exploiting classical Stille cross coupling reaction.

Penoni applied nitrosoarene-alkyne annulation reaction to achieve in an elegant way meridianins and analogues (Scheme 22) with the usual very high regioselectivity in indolization process.[92] Furthermore, indoles were afforded with no trace of expected N-OH products. Meridianines are an important family of marine alkaloids, firstly isolated from tunicate *Aplidium meridianum*:[93] extensive studies were performed investigating their potency as kinase enzymes inhibitors[94] and recently they were screened in cancer therapy.[95]

Previously reported synthetic approaches start off from preformed indole rings[96,97], except a Fischer synthesis reported by Franco in achieving isomeridianins.[98]
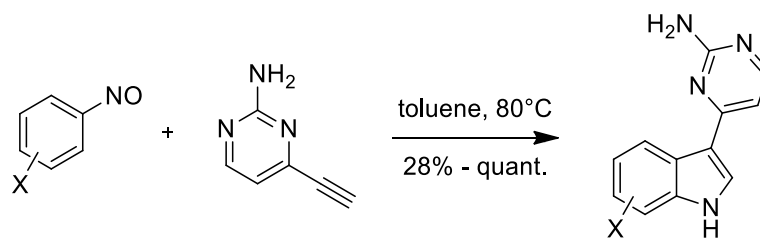
Scheme 22: synthesis of meridianins.

♦♦♦♦♦♦

3.3.   Nitrosoarene-alkyne annulation mechanism

A deep study of nitrosoarene-alkyne annulation has been performed by Penoni *et al.*[99] either combining computational and experimental techniques. Initial considerations were derived from previous papers:[86,89,92] first, yields are not so dependent from the electronic character of the nitrosoarene, being comparatively efficient with both electron rich and poor nitroso compound. Second, terminal alkynes with conjugating substituents react most efficiently and placing always alkyne substituent at the 3-position in high regioselective fashion. Third, the reaction solvent polarity has little effect on the course or efficiency of the reaction. These considerations disadvantaged an ionic mechanism.

Kinetic studies reported a first order each in alkyne and nitrosoarene, suggesting both were involved in rate determining step. Moreover, introduction in batches of radical species like TEMPO provided a complex mixture of products, suggesting mechanism could be radical and TEMPO just broke it up. Computational studies provided evidence of bond formation between terminal alkyne C and nitroso N to generate a diradical as rate determining step (Scheme 23).
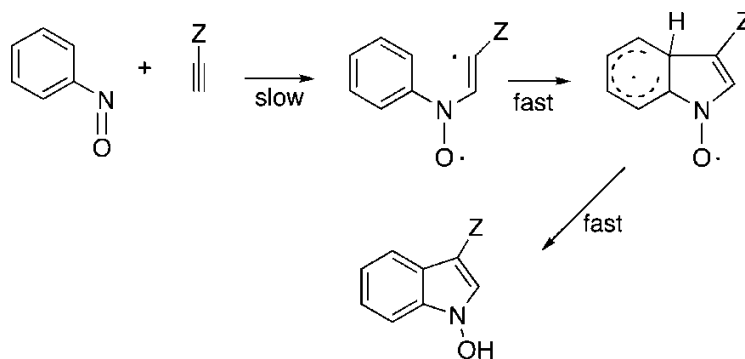
Scheme 23: proposed radical mechanism.

A detailed calculation on intermediates and transition states has been performed (Figure 7 and Figure 8), considering nitrosobenzene and acetylene as reactant models and *N*-hydroxyindole as product. Pathway to

the latter was computed to be exothermic by 59.6 kcal/mol, with an overall barrier of 19.1 kcal/mol via the vinyl radical intermediates. Energy values explains also C3 regioselectivity. However, it has still to be cleared why with some alkyne reagents products afford indoles instead of relative N-OH analogues.
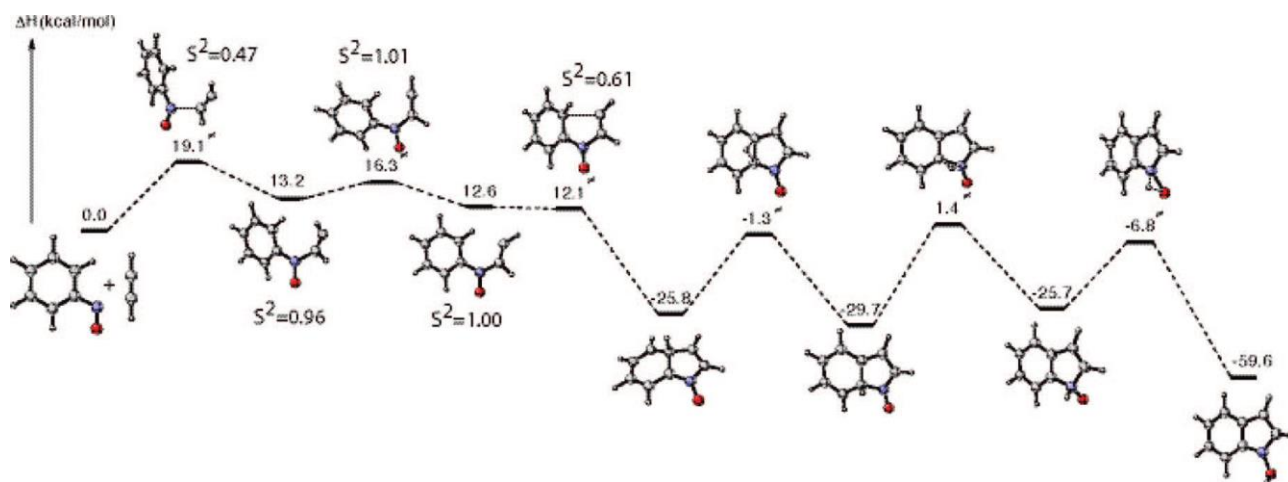
Figure 7: reaction pathway energy profile. S^2 ≠ 0 values indicates radical presence.
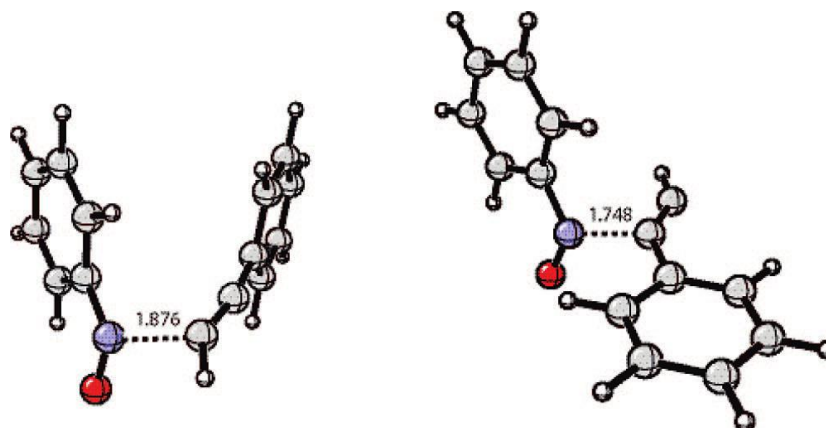
Figure 8: transition state between nitrosobenzene and phenylacetylene.

4. Aim of the research project

3-Acylindoles are known to be bioactive compounds and recent studies highlighted their interesting proper-ties[100] and various synthetic approaches.[101] Some synthetic compounds such as BPR0L075 showing 3-aroy-lindole unit were discovered to be potent antitubulin agents[102] or powerful analgesic drugs like pravadoline (Figure 9). 3-aroylindoles were differently prepared by classic synthetic approaches by acylation of pre-formed indole substrates[103] and very recently by metal[104] or acid[105] catalyzed reactions. Not many indoliza-tion protocols are known to afford directly 3-acylindoles starting from easily available reactants.

BPR0L075   Pravadoline
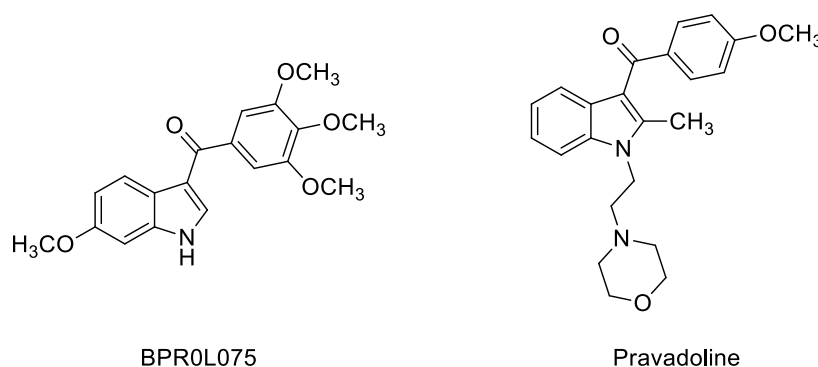
Figure 9: some 3-aroylindole based APIs.

Research project is therefore focused on applying and optimizing nitrosoarene-alkyne one pot annulation approach for the preparation of highly functionalizable compounds and/or biologically active products having the 3-aroylindole fragment (Scheme 24). Synthesis of novel compounds showing *N*-hydroxyindole moiety is also expected. The use of conjugated alkynones, instead of simply aromatic alkynes, is a natural extension of previous synthetic studies in the aim to generalize the synthetic versatility of this method.
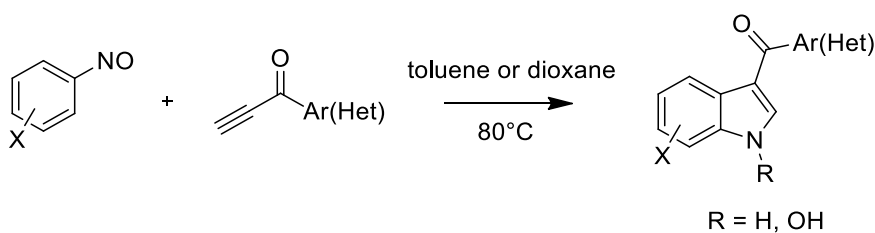
Scheme 24: synthesis of *N*-hydroxy-3-aroylindoles and 3-aroylindoles.

Deep studies on reactivity and further functionalization on obtained products are an objective too.

5.   Results and discussion

5.1.   Preliminary attempts

Previous papers highlighted a slight tendency of nitrosoaromatics with electron withdrawing groups to have faster reaction times and better product yields. Studies on optimization of reaction conditions were then carried out using 4-nitronitrosobenzene **1a** and 1-phenyl-2-propyne-1-one **2a** (Table 1). A general drawback for previous cycloaddition reactions between nitrosoarenes and alkynes was the necessary over-stoichometric employment of the latter (10–15 equivalents) to minimize formation of non indolic byproducts.

Envisioning an instability of the *N*-hydroxyindoles, first nitroso-alkyne cycloaddition reactions between 4-nitronitrosobenzene **1a** and 1-phenyl-prop-2-yn-1-one **2a** were run under alkylating conditions (K_2CO_3 and dimethyl sulfate, both 6 fold) in toluene, but this strategy was not fruitful; corresponding *N*-methoxy-3-aroylindole **3** was isolated only in traces. However, working in the absence of base and dimethyl sulphate, a solid precipitation was noticed. After spectroscopic and mass characterizations, precipitate was identified in *N*-hydroxy-5-nitro-3-benzoylindole **4**. A simple filtration without any other further purification was enough to afford clean compound. Only C3 substituted isomer was detected.

In addition, in contrast to previously cited *N*-hydroxy-3-arylindoles, *N*-hydroxy-3-aroylindoles are generally more stable and do not dimerize to kabutanes.[45,46] This was also demonstrated trying a dimerization reaction stirring compound **4** in neat TFA at r.t. for 5 days. No reaction was observed, in contrast with *N*-hydroxy-3-arylindoles which dimerize immediately without any trapping.[45,89]

Aiming for further optimizing, different molar ratios nitrosoarene/alkynone were employed but surprisingly, best yields of indole products were obtained by performing the reactions with a 1:1 nitrosoarene/alkynone molar ratio (Table 1). Only reaction faster times were noticed when alkyne excess was employed.

Toluene was chosen as standard solvent after screening between previously employed benzene (standard solvent with phenylacetylenes) and 1,4-dioxane. No significant differences in yield between benzene and toluene were detected: the latter was better choice for its lower toxicity. Since it has been proved the cycloaddition follows a radical pathway, is quite surprising that toluene, having radical sensitive benzylic hydrogens, does not interfere with the indole–forming reaction. 1,4-Dioxane instead showed a higher decomposition over time of nitrosobenzene **1a** to 4,4'-dinitro-azoxybenzene (Figure 10). Significant yield improvements were not detected. In all three solvents *N*-hydroxyindole **3** precipitated.

Optimal reaction temperature was found at 80°C. Running reaction at 50°C a slower time to form the usual precipitate of *N*-hydroxy-5-nitro-3-benzoylindole **4** was noticed. However, yield was much lower and an increasing of 4-nitronitrosobenzene **1a** degradation to 4,4'-dinitro-azoxybenzene was clearly noticed.

Given these interesting optimized results, a wide survey of reactions between different alkynones and nitrosoaromatics has been carried out. A lot of different compounds with very different electronic properties were examined in annulation reaction.
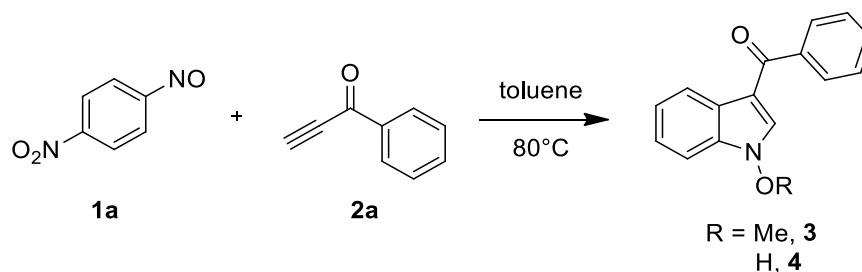
Entry[a]	Alkynone/nitrosoarene ratio	Alkylating agent, base	R	Product	Yield
1	15:1	Me_2SO_4, K_2CO_3	Me	3	traces[b]
2	5:1	Me_2SO_4, K_2CO_3	Me	3	traces[b]
3	15:1	-	H	4	35%[c]
4	12:1	-	H	4	38%[c]
5	10:1	-	H	4	40%[c]
6	5:1	-	H	4	42%[c]
7	1:1	-	H	4	53%[c]

Table 1: survey for reaction conditions optimization. [a]; 5 h, 80 °C: [b]; product chromatographated: [c]; product precipitated.
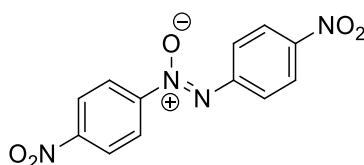
Figure 10: 4,4'-dinitro-azoxybenzene.

♦ ♦ ♦ ♦ ♦ ♦

5.2. Nitrosoarenes synthesis

Usually nitrosoarenes are not commercially available except few exceptions: Sigma Aldrich for example sells only 2-nitrosotoluene and nitrosobenzene. The latter is the only purchased as it's quite simple to afford nitrosoarenes by oxidation of correspondent commercial anilines. Oxidants employed were peroxides like Oxone® and $NaWO_4$ or *cis*-$Mo(O)_2(acac)_2/H_2O_2$ with phase transfer catalysis (Table 2). Products were purified by recrystallizations. Direct nitrosation with $NOBF_4$ was also exploited albeit with this procedure purification by chromatography is always requested.
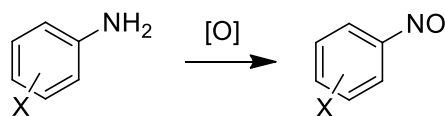
Entry	X	Product	Conditions	Yield
1	4-NO$_2$	1a	Oxone®	71%
2	4-COOH	1b	Oxone®	Quant.
3	4-COOEt	1c	NaWO$_4$/H$_2$O$_2$/TBAB	37%
4	4-CH$_3$	1d	Cis-Mo(O)$_2$(acac)$_2$/H$_2$O$_2$	41%
5	4-OCH$_3$	1e	NOBF$_4$	74%
6	2-COOMe	1f	NaWO$_4$/H$_2$O$_2$/TBAB	92%
7	4-CN	1g	NaWO$_4$/H$_2$O$_2$/TBAB	62%
8	4-Br	1h	NaWO$_4$/H$_2$O$_2$/TBAB	65%
9	4-CF$_3$	1i	Oxone®	66%
10	4-Cl	1j	Cis-Mo(O)$_2$(acac)$_2$/H$_2$O$_2$	40%
11	2-NO$_2$	1k	NaWO$_4$/H$_2$O$_2$/TBAB	70%

Table 2: anilines oxidation to nitrosobenzenes.

♦♦♦♦♦♦
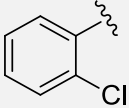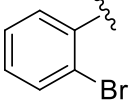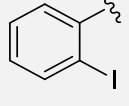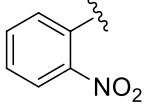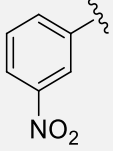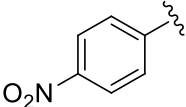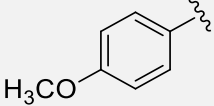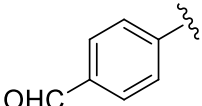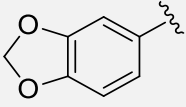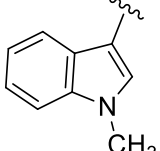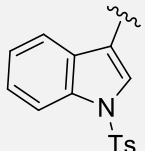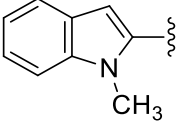
5.3. Alkynones synthesis

Synthesis of aryl-alkynones can be accomplished starting off from commercial available aromatic alde-hydes.[106] Pathway is two steps long: first, a nucleophilic addition of ethynylmagnesium halide to afford a propargylic alcohol; second, oxidation to ketone generally with transition metal based oxidants (Table 3).

Chromium based Jones oxidant is generally preferred when substrate has acidity tolerance. Possibility to oxidize directly raw alcohol from previous step is a noticeable advantage: residues of carboxylic acid formed from aldehyde oxidation can be removed in propargyl ketone work-up. When Jones conditions were incompatible with substrates (for example with indole, pyrrole and furan-based alcohols), manganese dioxide was preferred. MnO$_2$ in addition expresses selectivity for benzylic and allylic alcohols, being respectful of other oxidation sensible functional groups. On the other hand, purification of starting alcohol must be performed when MnO$_2$ is employed: furthermore, yields are generally lower. The milder oxidant Dess-Martin perio-dinane is also employed successfully but used only when strictly necessary due to its high cost. Results in alkynones synthesis by this two steps protocol is reported in Table 3.
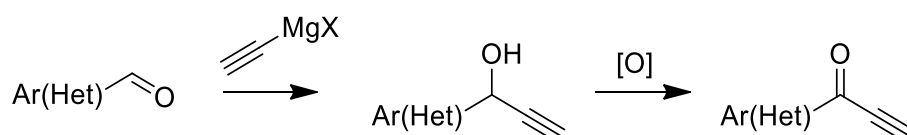
Entry	Ar(Het)	Alcohol yield	Oxidant	Alkynone yield	Alkynone product
1		Quant.	Jones	90%	**2b**
2		78%	Jones	93%	**2c**
3		78%	Jones	93%	**2d**
4		92%	Dess-Martin periodinane	Quant.	**2e**
5		61%	Jones	64%	**2f**
6		55%	Jones	64%	**2g**
7		59%	Jones	77%	**2h**
8		88%	MnO_2	63%	**2i**
9		78%	MnO_2	89%	**2j**
10[a]		-	MnO_2	52%	**2k**
11		Quant.	MnO_2	76%	**2l**
12		75%	MnO_2	78%	**2m**
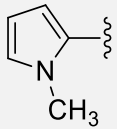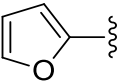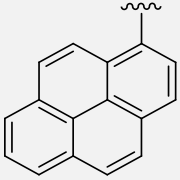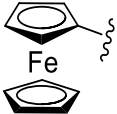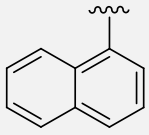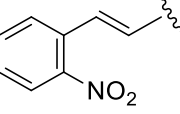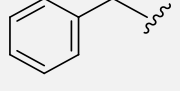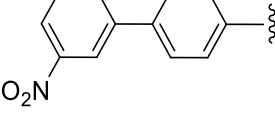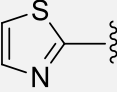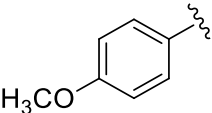
13	(1-methylpyrrol-2-yl)	76%	MnO$_2$	75%	2n
14	(furan-2-yl)	52%	MnO$_2$	65%	2o
15[b]	(pyren-1-yl)	85%	MnO$_2$	Quant.	2p
16	(ferrocenyl)	81%	MnO$_2$	Quant.	2q
17	(naphthalen-1-yl)	83%	Jones	90%	2r
18	(2-nitrocinnamyl)	Quant.	Dess-Martin periodinane	75%	2s
19	(phenethyl)	70%	Jones	90%	2t
20	(3-nitrobiphenyl)	89%	Dess-Martin periodinane	Quant.	2u
21	(thiazol-2-yl)	82%	Dess-Martin periodinane	Unstable	2v
22[c]	(4-methoxyphenyl)	Quant.	Jones	87%	2w

Table 3: two steps synthesis of alkynones. [a]; one pot reaction: [b]; TMSA/n-BuLi, then TBAF silicon group removal. [c]; prop-1-ynyl-magnesium bromide used.

Alkynone **2v** and related compounds are reported in literature to be an unstable.[107] In work-up procedure solvent evaporation was performed under reduced pressure and in inert atmosphere to avoid as much as possible decomposition of target **2v**. The latter will be immediately involved in nitrosoarene-alkynone annulation in standard conditions.

Acyl chlorides are good starting materials too. Triple bond could be introduced in just one single step by addition of TMSA and aluminum chloride catalysis. One step is then required as TMS group is removed in reaction conditions.[108] Cinnamoyl chloride has been converted to alkynone **2x** by this strategy (Scheme 25).
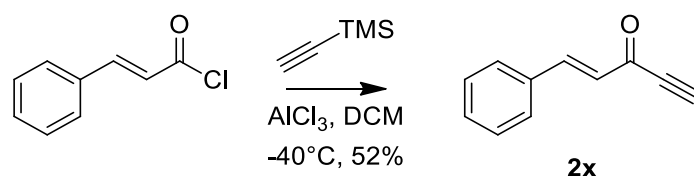
Scheme 25: synthesis of (*E*)-1-phenylpent-1-en-4-yn-3-one **2x**.

Propiolic chloride (prepared *in situ* with propiolic acid and SOCl₂) is useful reagent to synthetize alkynones by acylation of ready-available nucleophiles, like benzotriazole (Scheme 26).[109] A simple column chromatography is enough to purify crude product of interest and separate from unreacted benzotriazole. The latter is then not lost as can be easily recovered to be recycled in another batch.
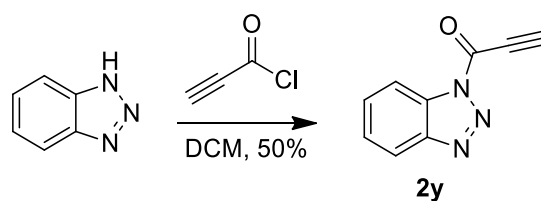
Scheme 26: synthesis of 1-(1H-benzotriazol-1-yl)prop-2-yn-1-one **2y**.

Nucleophilic addition of deprotonated TMSA to commercial isocyanates is an effective way to synthetize propargylamides.[110] Removal of TMF group is easily accomplished by TBAF addition in the same pot (Scheme 27).

This approach was chosen since no condensation reaction between anilines and propiolic acid was effective in amides formation: classic condensation with DCC/DMAP failed. Reaction was tested even with peptide synthesis coupling agents (HATU and HBTU amongst all), well known for mild conditions requested for activating properties. However, no reaction was detected.
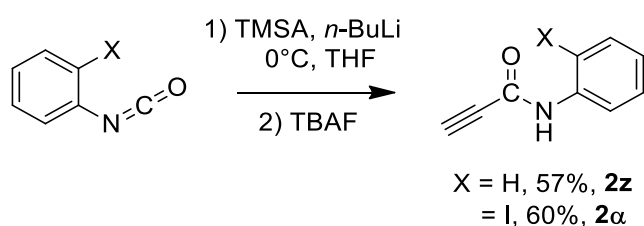
Scheme 27: synthesis of propargylamides **2z** and **2α**.

(*E*)-1-(1-tosyl-1H-indol-3-yl)pent-1-en-4-yn-3-one **2β** has been synthetized by a 5 steps sequence. First step was preparation of pyridine 3-boronic acid, which was isolated as its respective trioxaborinane condensed form. The latter was partner with 2-bromoaniline in a Suzuki coupling to afford 2-(pyridine-3-yl)aniline. Subsequent step is a BrCN mediated ring opening of pyridine to afford an indole (Scheme 28). A detailed mechanism discussion on this transformation was published by Kearney in 2006.[111]
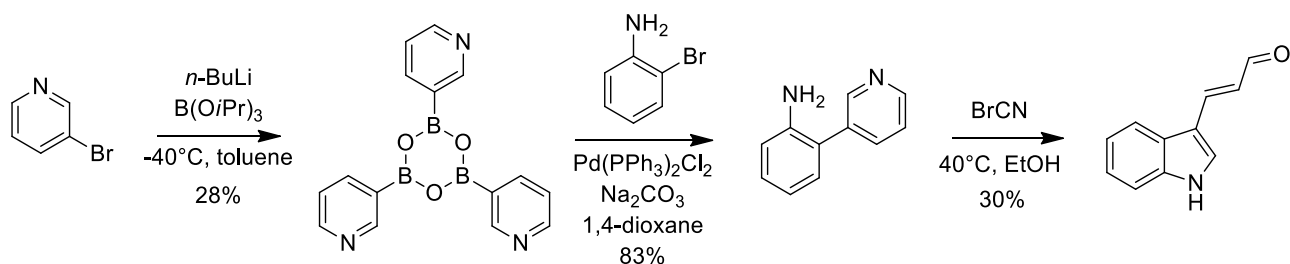
Scheme 28: synthesis of 3-indolyl-acrylaldehyde.

3-Indolyl-acrylaldehyde was then *N* protected with tosyl group by reacting with tosyl chloride. Product obtained was substrate for aforementioned Grignard addition and subsequent oxidation with Dess-Martin periodinane to afford (*E*)-1-(1-tosyl-1H-indol-3-yl)pent-1-en-4-yn-3-one **2β** (Scheme 29).
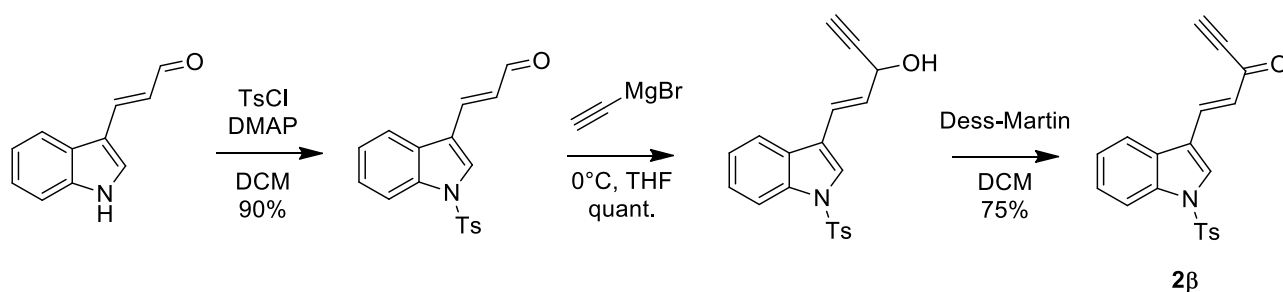
Scheme 29: synthesis of (*E*)-1-(1-tosyl-1H-indol-3-yl)pent-1-en-4-yn-3-one **2β**.

Given C3 selectivity in aroyl-NH/N-OH-indole synthesis by nitrosoarene annulation with terminal alkynes, synthesis of a brominated acetylene was an attractive idea: 2,3 disubstituted indoles can be obtained this way and studies on reactivity of resulting brominated compounds could be performed.

Model substrate was prepared by bromination of 1-phenylprop-2-yn-1-one **2a** with NBS and silver nitrate to afford 3-bromo-1-phenylprop-2-yn-1-one **2γ**. The latter is isolated by column chromatography with excellent yield (Scheme 30).
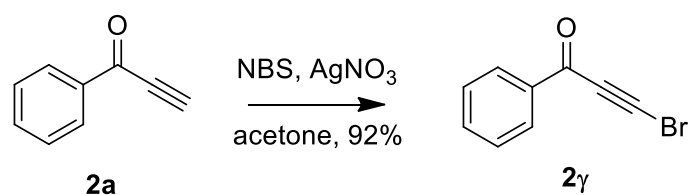
Scheme 30: bromination of compound **2a**.

♦ ♦ ♦ ♦ ♦ ♦

5.4. Synthesis of *N*-hydroxy-3-aroylindoles and 3-aroylindoles

5.4.1. Annulation between nitrosobenzenes and phenylaklynones

With optimized conditions in our hands, a wide substrate scope of was explored using previously illustrated synthetized nitrosoarenes and arylalkynones affording indole compounds in moderate to excellent yields.

Reactants were in 1:1 stoichiometric ratio. Faster times were detected using extra alkyne but no yield improvement. Only 3-substituted regioisomers were isolated: 2-substituted weren't detected neither in traces. Procedures carried out with electron-poor nitrosoaromatics registered better product yields and shorter reaction times. Electronrich nitrosoarenes show the prevalent formation of indoles instead of *N*-hydroxyindoles. Minor conversions and moderate yields were observed by using nitrosoaromatics with electron donating groups. Interestingly, when 4-nitronitrosobenzene **1a** was employed, 5-nitro-3-aroyl-*N*-hydroxyindole product always precipitated. Precipitation trend was noticed with other electron withdrawing groups like carboxylic acid.

With few nitrosoarenes, NH indoles were detected as minor products. The electronic properties of substituents on the ring of the aromatic alkynone does not seem to play a dramatic role neither in product yields nor for reaction times. Process shows an excellent atom and step economy, as indole ring is obtained *via* formation of new C-N and C-C bonds. Survey of cycloaddition between nitrosoarenes and substituted phenylalkynones is reported in Table 4.

Reactions proceeded with no use of acid/basic catalysts nor organometallic chemistry.
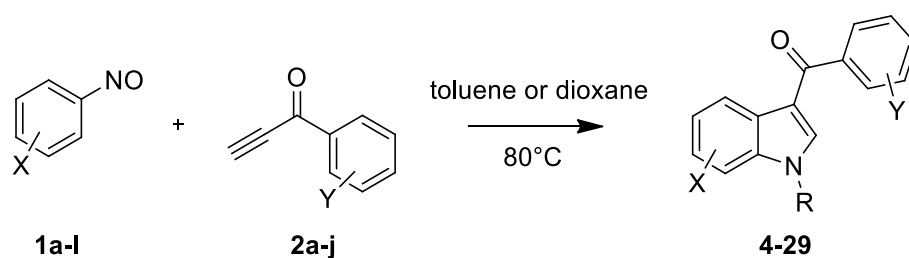
Entry	Nitro-sobenzene	X	Phenyl-alkynone	Y	R	Product	Yield
1	1a	4-NO$_2$	2a	H	OH	4	54% [a]
2	1a	4-NO$_2$	2b	2-Cl	OH	5	70% [a]
3	1a	4-NO$_2$	2c	2-Br	OH	6	52% [a]
4	1a	4-NO$_2$	2d	2-I	OH	7	37% [a]
5	1a	4-NO$_2$	2e	2-NO$_2$	OH	8	48% [a]
6	1a	4-NO$_2$	2f	3-NO$_2$	OH	9	69% [a]
7	1a	4-NO$_2$	2g	4-NO$_2$	OH	10	62% [a]

8	1a	4-NO$_2$	2h	4-OMe	OH	11	37% [a]
9	1a	4-NO$_2$	2i	4-CHO	OH	12	31% [a]
10	1a	4-NO$_2$	2j	3,4-OCH$_2$O	OH	13	61% [a]
11	1b	4-COOH	2b	2-Cl	OH	14	69% [a, b, c]
12	1b	4-COOH	2c	2-Br	OH	15	50% [b, c]
13	1b	4-COOH	2f	3-NO$_2$	OH	16	84% [a, b, c]
14	1b	4-COOH	2g	4-NO$_2$	OH	17	67% [a, b, c]
15	1l	H	2a	H	H	18	25% [d]
16	1c	4-COOEt	2a	H	H	19	27% [d]
17	1d	4-Me	2a	H	H	20	20% [d]
18	1e	4-OMe	2a	H	H	21	30% [d]
19	1g	4-CN	2a	H	H	22	41% [d]
20	1j	4-Cl	2a	H	OH	23	15% [d]
21	1j	4-Cl	2a	H	H	24	36% [d]
22	1h	4-Br	2a	H	OH	25	15% [d]
23	1h	4-Br	2a	H	H	26	35% [d]
24	1i	4-CF$_3$	2a	H	H	27	33% [d]
25	1k	2-NO$_2$	2a	H	OH	28	46% [d]
26	1f	2-COOMe	2a	H	OH	29	33% [d]

Table 4: synthesis of *N*-hydroxy-3-benzoylindoles and 3-benzoylindoles. [a]; product precipitated: [b]; reaction carried in 1,4-dioxane: [c]; product recrystallized: [d]; product chromatographated.

Confirmation of 3-regioselectivity of this annulation reaction is provided by X-rays diffraction pattern from single crystal of product **5** (*Figure 11*)**.**
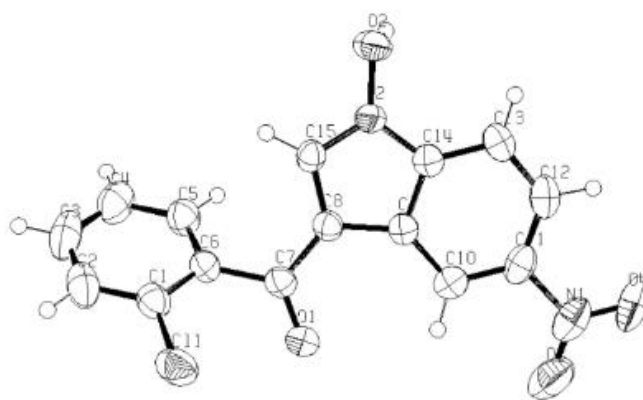
Figure 11: ORTEP plot for compound **5**. Thermal ellipsoids are drawn at the 50% level.

4-Nitrosobenzoic acid **1b** is not soluble in toluene, so reaction was carried out in 1,4-dioxane. Corresponding *N*-hydroxy-3-benzoylindoles **14**, **15**, **16** and **17** were completely insoluble in dioxane and they precipitated as yellow solids with azoxy-benzene-4,4'-dicarboxylic acid. The latter can be originated by reductive dimerization of starting nitrosoarene. Removal of this by-products was achieved by recrystallization.

All products were characterized by NMR and mass analysis. ^{1}H-NMR is a useful technique to distinguish between *N*-hydroxy and NH indoles as N–OH peak is broader and higher shifted (10-12 ppm *vs* 8-9 ppm). Mass analysis of course can distinguish too.

5.4.2.   Annulation between nitrosobenzene and more complex or heteroaryl alkynones

With the aim to generalize the application of the cycloaddition between nitrosoarenes and alkynones, ethynyl ketones containing heterocyclic frameworks or other conjugated units, organometallic moieties and polycyclic fragments were tested and an extension of the synthetic scope of the reaction was achieved (Table 5).
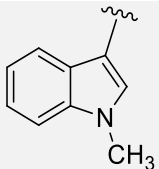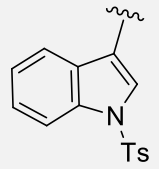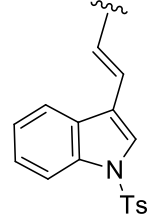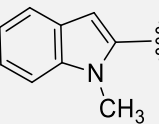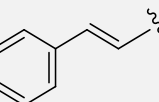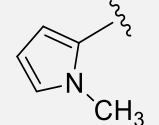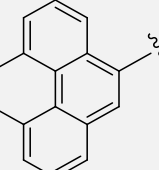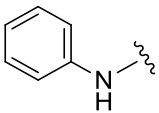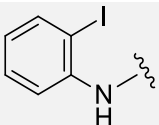
4-Nitronitrosobenzene **1a** and 4-nitrosobenzoic acid **1b** proved again to be superior reagents through stoichiometric reaction in toluene or 1,4-dioxane at 80 °C with alkynones. As previously observed, 5-nitro-*N*-hydroxy-aroylindoles were always isolated by filtration without any further purification as they precipitated during reaction run. On the other hand, 3-aroyl-1-hydroxy-1H-indole-5-carboxylic acids were another time extremely insoluble and their precipitation was polluted by azoxybenzene-4,4'-dicarboxylic acid which can be removed by recrystallization as cited before.

Many of these products were synthetized with interesting functional groups, opening possibility to examine further functionalization or transformations on them.
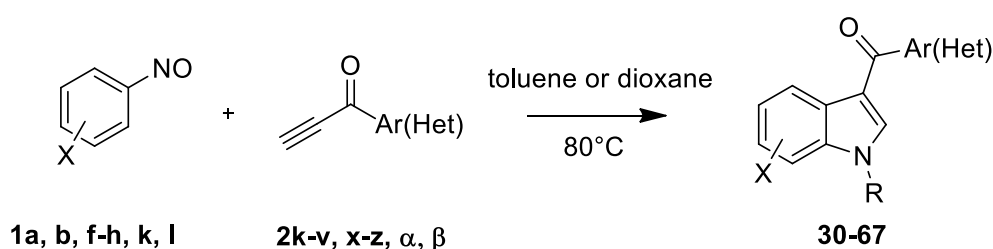
Entry	Nitro-sobenzene	X	Ar(Het) alkynone	Ar(Het)	R	Product	Yield
1	1a	4-NO$_2$	2y		OH	30	57% [a]
2	1b	4-COOH	2y		OH	31	68% [a, b, c]
3	1g	4-CN	2y		OH	32	40% [a]
4	1l	H	2y		OH	33	40% [a]

5	1a	4-NO$_2$	2k		OH	34	47% [a]
6	1b	4-COOH	2k		OH	35	64% [b, d]
7	1a	4-NO$_2$	2l		OH	36	15% [a]
8	1a	4-NO$_2$	2β		OH	37	30% [a]
9	1k	2-NO$_2$	2β		H	38	45% [d]
10	1l	H	2β		H	39	32% [d]
11	1a	4-NO$_2$	2m		OH	40	20% [a]
12	1b	4-COOH	2m		OH	41	64% [a, b, c]
13	1f	2-COOMe	2m		H	42	30% [d]
14	1l	H	2m		H	43	
15	1a	4-NO$_2$	2x		OH	44	65% [a]
16	1b	4-COOH	2x		OH	45	50% [a, b, c]
17	1a	4-NO$_2$	2n		OH	46	50% [a]
18	1a	4-NO$_2$	2o		OH	47	51% [a]
19	1a	4-NO$_2$	2p		OH	48	65% [a]
20	1a	4-NO$_2$	2z		OH	49	36% [a]
21	1g	4-CN	2z		OH	50	29% [a]
22	1b	4-COOH	2z		OH	51	16% [a, b, c]
23	1a	4-NO$_2$	2α		OH	52	22% [a]
24	1a	4-NO$_2$	2q		OH	53	49% [a]
25	1g	4-CN	2q		H	54	39% [a]
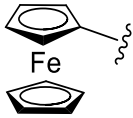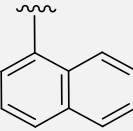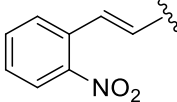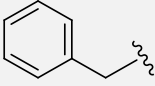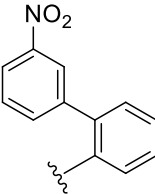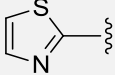
26	1b	4-COOH	2q		H	55	47% [a, b, c]
27	1a	4-NO$_2$	2r		OH	56	68% [a]
28	1g	4-CN	2r		OH	57	30% [a]
29	1h	4-Br	2r		H	58	37% [d]
30	1l	H	2r		OH	59	38% [d]
31	1l	H	2r		H	60	17% [d]
32	1g	4-CN	2s		OH	61	33% [a]
33	1a	4-NO$_2$	2s		OH	62	50% [a]
34	1f	2-COOMe	2s		OH	63	24% [a]
35	1l	H	2s		H	64	53% [d]
36							
37	1a	4-NO$_2$	2t		OH	65	27% [a]
38	1a	4-NO$_2$	2u		OH	66	32% [a]
39	1a	4-NO$_2$	2v		H	67	Not isolated

Table 5: synthesis of *N*-hydroxy-3-aroylindoles and 3-aroylindoles. [a]; product precipitated: [b]; reaction carried in 1,4-dioxane: [c]; product recrystallized: [d]; product chromatographated.

High impact progresses were made in benzotriazole chemistry. Katritzky et al.[112,113] illustrated different major functions of benzotriazole in organic transformations, focusing its activity as leaving group in nucleophilic substitutions, proton activator, cation stabilizer, anion and radical precursor (Scheme 31). Compounds **30**, **31**, **32**, **33** are then good candidates to be furtherly functionalized: investigations will be performed in the next future. Given the lability of the N–OH motif, is preferable to protect the hydroxy function prior to proceed.
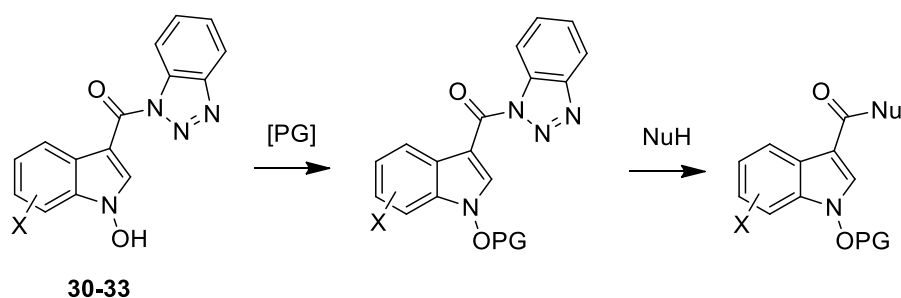
Scheme 31: use of benzotriazole as leaving group for nucleophilic substitution.

After detailed searching in literature for novel bioactive compounds containing the 3-aroylindole or the 3-heteroaroylindole fragment, indothiazinone (1H-indol-3-yl(1,3-thiazol-2-yl)methanone) and related fine chemicals were recurring motifs in naturally occurring sources. Antibiotic properties of indothiazinones were reported.[114] It was tried then to synthetize products containing this moiety with nitrosoarene-alkynone annulation described so far. First step was synthesis of related alkynone **2v**. The latter was immediately employed in annulation reaction in standard conditions (Scheme 32), as it was described in literature low stability of similar compounds.[115]

Formation of two major products was clearly detected. No chromatography separation was possible due to decomposition of indole **67** on stationary phase. The latter showed also a low thermal stability. A recent publication suggests operating at very low temperature to overcome the problem.[116]
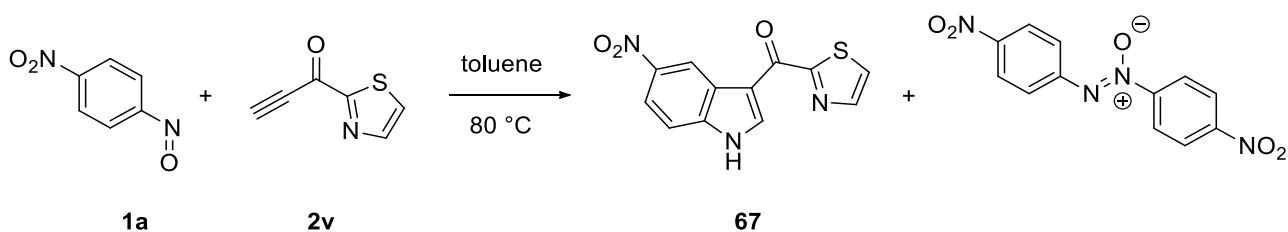
Scheme 32: synthesis of indothiazinone related compound **67**.

Products were finally identified by crude reaction mixture injection in GC-MS. It was found not only target compound **67** but also 4,4'-dinitroazoxybenzene, usual byproduct found in reactions with nitrosoaromatics. Fragmentation patterns of two compounds are reported in Figure 12. Interestingly, mass value for compound **67** is compatible with NH indole, whilst generally 4-nitronitrosobenzene forms *N*-hydroxy compounds.
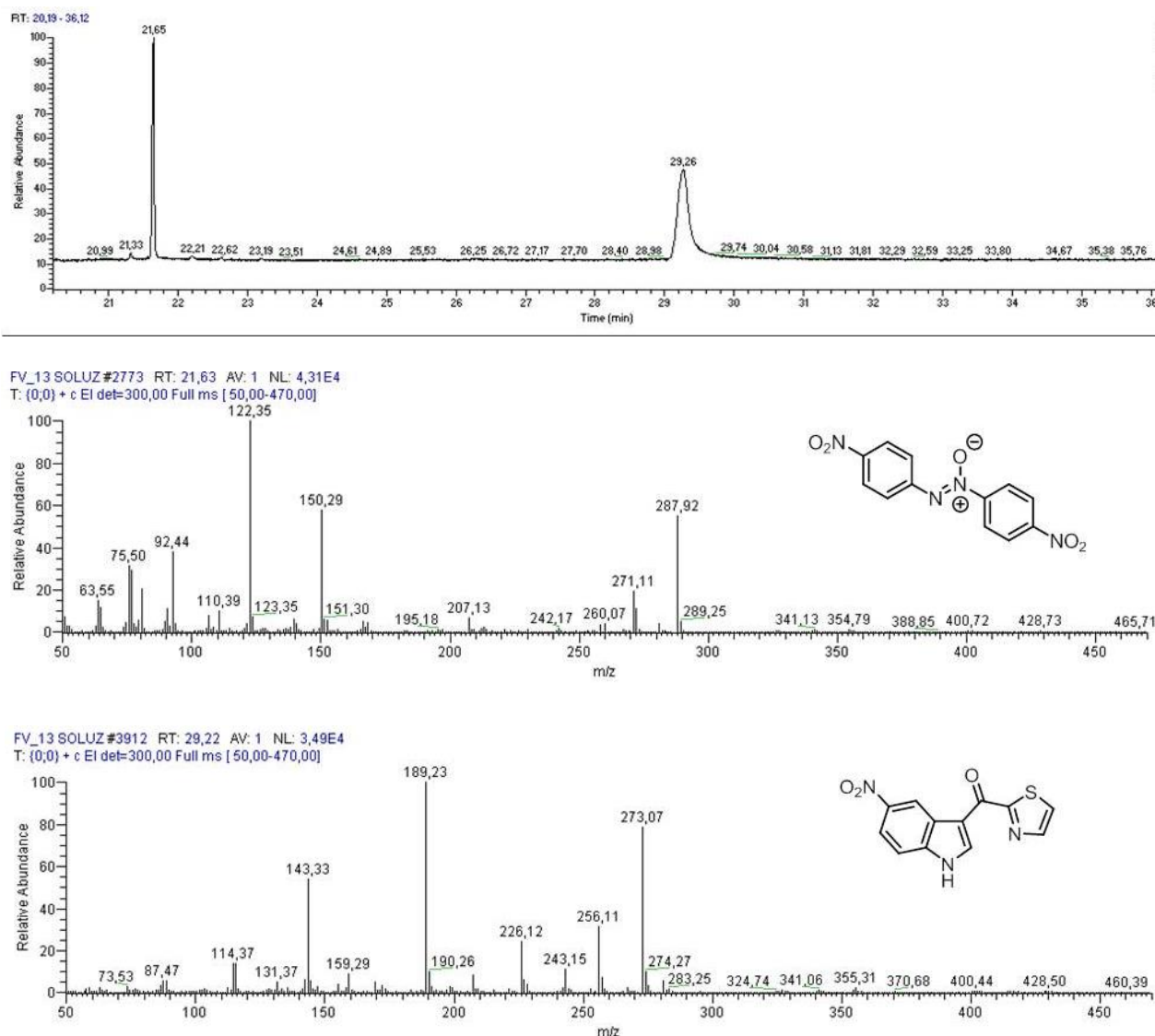
Figure 12: on top: gas chromatography of crude reaction mixture (on top) plot. On bottom: mass analyses of **67** and 4,4'-dinitro-azoxybenzene.

5.4.3.   Annulation between nitrosoarenes and internal alkynones

Reaction scope was extended also to internal alkynones, despite it was already reported by Penoni a lower reactivity of internal phenylacetylenes.[90] High interest was running annulation reaction with 3-bromo-1-phenylprop-2-yn-1-one **2γ.** This way a library of brominated indoles can be achieved and a possibility of further functionalizations on indole compounds by cross coupling reaction can be accomplished. 1-phenylbut-2-yn-1-one **2w** was also employed as internal alkynone. Only one product was isolated by these reactions: it was postulated a coherent 3 regioselectivity for benzoyl group. Experiments of products crystal growing are ongoing to have the definitive molecular structures. Results of cycloaddition reactions are resumed in Table 6.
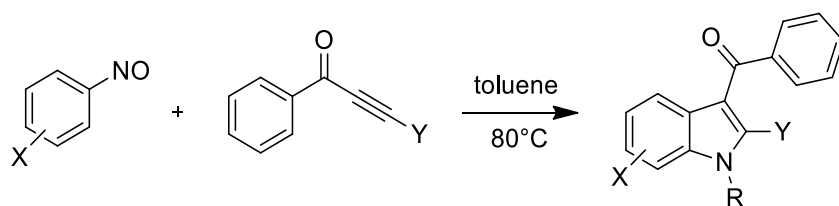
Entry	Nitro-sobenzene	X	Phenyl-alkynone	Y	R	Product	Yield
1	1a	4-NO$_2$	2γ	Br	OH	68	56% [a]
2	1h	4-Br	2γ	Br	H	69	26% [b]
3	1l	H	2γ	Br	H	70	28% [b]
4	1f	2-COOMe	2γ	Br	H	71	57% [b]
5	1l	H	2w	Me	H	72	16% [b]

Table 6: synthesis of *N*-hydroxy-3-aroylindoles and 3-aroylindoles from internal alkynes. [a]; product precipitated: [b]; product chromatographated.

Except for annulation with deactivated nitrosoarenes like 4-nitronitrosoarene **1a** and 2-carbomethoxynitrosobenzene **1f**, lowering yield trend with internal alkynones is confirmed. Product **72** is afforded in particularly low yield. A possibility to improve synthetic route to **72** is split up into three steps as indicated in Scheme 33. Another possibility can come from a metal catalysed nitroarene-alkyne indolization as they are less sensitive on alkynone electronic features, as shown by Ragaini.[117] Studies on this way will be performed in the next future. Importance of compound **72** is underlined as it is precursor for NSAID pravadoline.
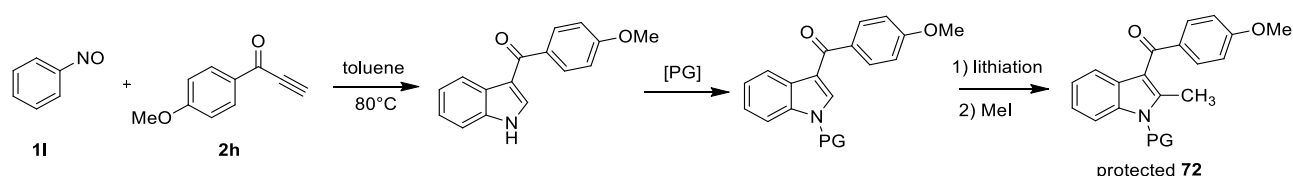
Scheme 33: hypothesis of alternative route to protected **72**.

5.4.4. Annulation between nitrosoarenes and internal alkynones with unconventional methods

In collaboration with prof. Giancarlo Cravotto, a preliminary explorative study was performed to search a more environmental benign approach to the indolization of nitrosoarenes with alkynones. Different techniques like ball-milling and microwaves in solventless conditions were explored. Yields were determined by GC-MS analyses. Annulation between nitrosobenzene **1l** and 1-phenyl-2-propyn-1-one **2a** was studied as they are the simplest reactants. Nitrosobenzene **1l**, the substrate of choice because it is commercially available, gave in standard conditions only moderate yields of indole **18** (25%, entry 15, Table 4). Poor yields were also achieved using mechanochemical activation in a planetary ball-mill (12% of **18** and traces of azobenzene) with large amount of starting materials. An interesting improvement was observed when the reaction was

carried out without any solvent under microwave irradiation (Scheme 34). This last result prompts further studies for the formation of indole derivatives with unconventional methods.
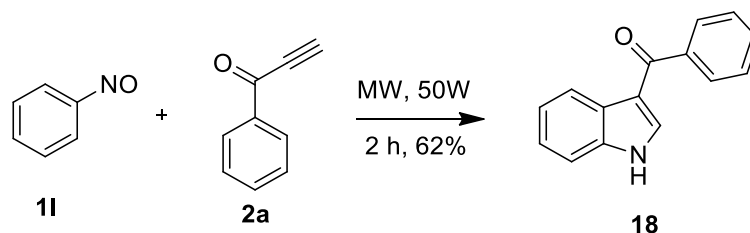
Scheme 34: microwave assisted synthesis of compound **18**.

5.4.5. Reactivity and functionalization of *N*-hydroxy-3-aroylindoles and 3-aroylindoles

5.4.5.1. Alkylation

N-hydroxyindoles can be *O* alkylated under mild basic conditions due to acidity of the *N*-hydroxy moiety. pKa is supposed to be between 7 and 10 depending on the substitution pattern of respective indole. Easy methylation reactions with excellent yields were performed dissolving starting material in methanol with K_2CO_3 and Me_2SO_4 as alkylating agent (Table 7).
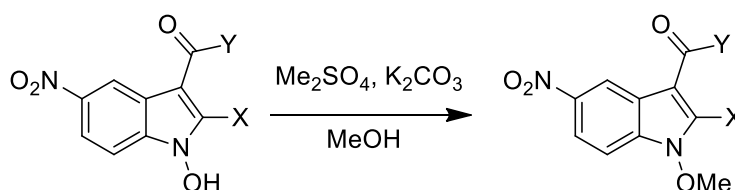
Entry	Y	X	Reactant	Product	Yield
1	Ph	H	4	3	96% [a]
2	Ph	Br	68	73	64% [b, c]
3	2-bromophenyl	H	6	74	96% [a]
4	2-iodophenyl	H	7	75	89% [a]
5	*N*-methyl-3-indolyl	H	34	76	Quant. [a]

Table 7: methylation of *N*-hydroxy-5-nitro-3-aroylindoles. [a]; product precipitated: [b]; product chromatographated: [c]; reaction run with CH_3I instead of Me_2SO_4.

Successful alkylation of compound **72** provided NSAID pravadoline **77** in excellent yield (Scheme 35).
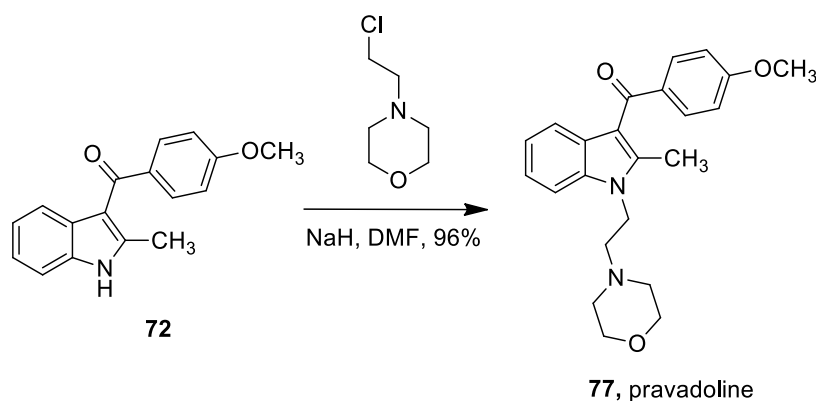
Scheme 35: synthesis of pravadoline **77**.

n-Butyl and *n*-pentyl alkyl chains were introduced on compound **60** (Scheme 36). Alkyl naphtoyl indoles obtained were originally synthetized and studied by Huffman as they show relevant analgesic activity, acting as a full agonist at both the CB1 and CB2 cannabinoid receptors, with some selectivity for CB2.[118] These compounds, known as JWHs, are quite popular in smart drug market as they can replace tetrahydrocannabinol: several states are then planning a permanent ban.
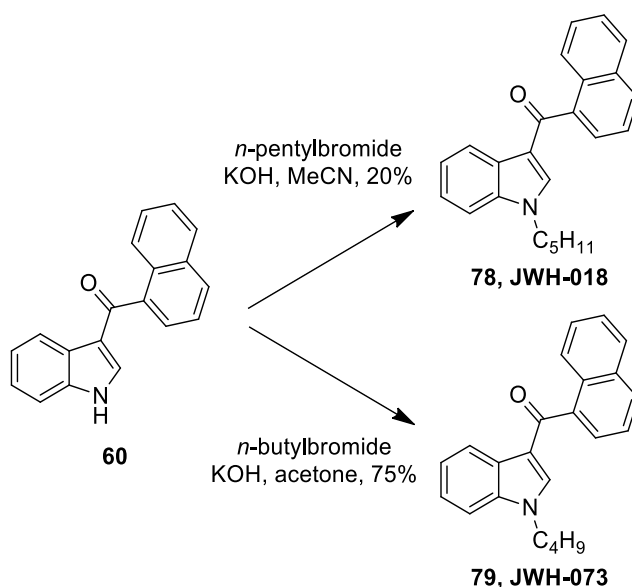
Scheme 36: synthesis of JWH-018 and JWH-073.

Other *O* alkylation reactions can explore reactivity of Michael acceptors. Addition of 1-phenylprop-2-yn-1-one **2a** and methyl propiolate was explored. However, using K_2CO_3 as base products were detected only in traces. Isolation was also difficult due to a high number of byproducts formed. Changing to DABCO in acetonitrile higher yields in minor times were achieved (Table 8). Products were collected as precipitates.

Michael addition product formation was confirmed by ^{1}H-NMR spectrum as olefin protons were detected as classic *AB* systems and with J ≈ 12 Hz. This is consistent with a *trans* coupling constant.
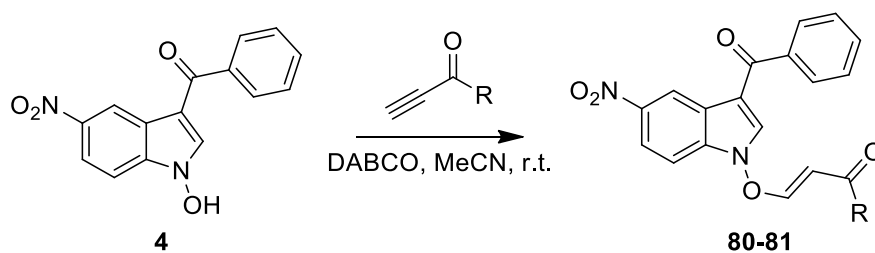
Entry	R	Product	Yield
1	Ph	80	80%
2	OMe	81	85%

Table 8: alkylation by Michael addition.

Compounds obtained by Micheal addition of triple bonds to *N*-hydroxyindoles are reported to show thermal transpositions[119] as indicated in Scheme 37. Transpositions are invoked to pass by [3,3]-sigmatropic rearrangements, whilst rearrangement to amide is supposed to pass through an oxa-aziridinium ring.
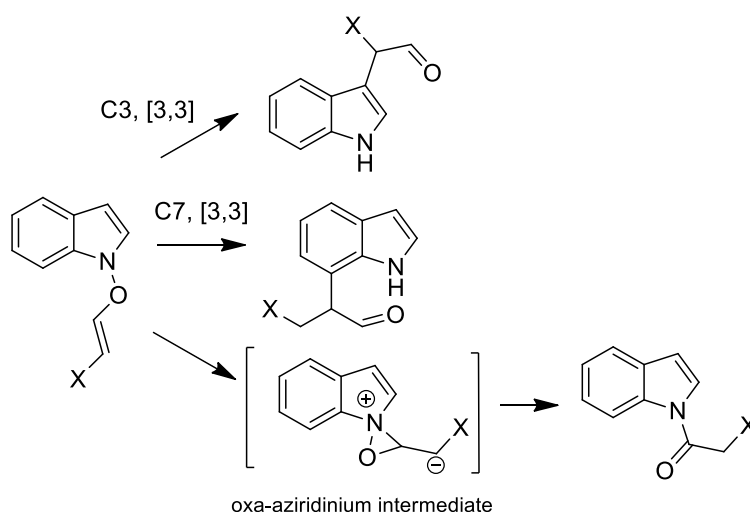
Scheme 37: rearrangements for Michael adducts between *N*-hydroxyindoles and activated triple bonds.

It was tried then a thermal reaction using **81** as substrate. Since C3 is occupied by a benzoyl group, reaction pathway could undergo only by C7 trasposition or by oxa-aziridinium intermediate. It was isolated just only one substance after reaction run (Scheme 38) and its ¹H-NMR spectrum was compatible only with C7 isomerization product.
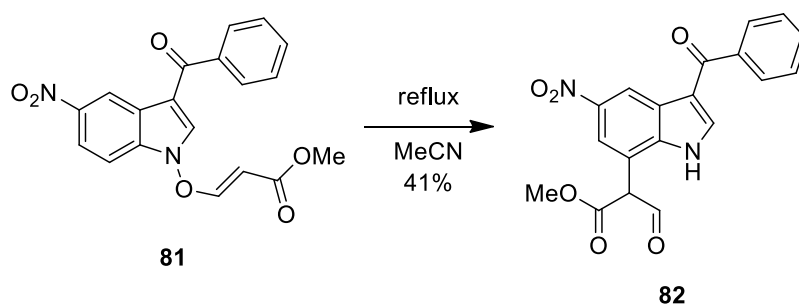
Scheme 38: C7 [3,3]-sigmatropic transposition of **81**.

5.4.5.2. Radical reactions

An interesting indole C2-H functionalization by radical reactivity was explored by Chuang in 1997.[120] A free radical reaction with Mn(OAc)$_3$ and dimethyl malonate is induced on 3-benzoylindoles C2 position to form a new 6-membered ring. Same concept was brought successfully on protected *N*-hydroxy-3-aroylindoles to achieve complex fused structures (Table 9). All products were purified by column chromatography.

3, 76   **83, 84**
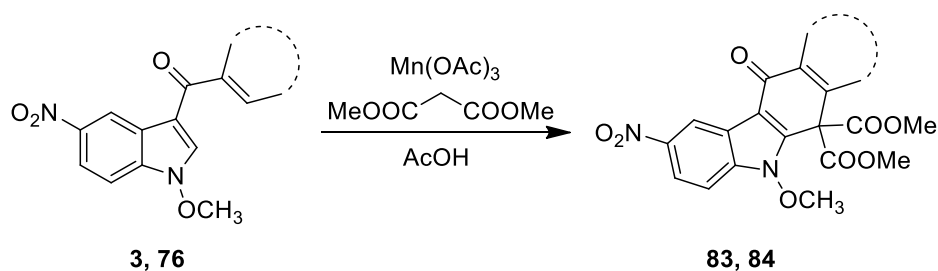
Entry	Substrate	Product	Yield
1	76	83	78%
2	3	84	67%

Table 9: radical C2-H functionalization to achieve fused products **83** and **84**.

5.4.5.3. Reaction with DCC

Reaction between 1-hydroxyindole-3-carboxaldehyde with dicyclohexylcarbodiimide (DCC) was reported by Somei in 1991[56]: In the presence of triethylamine it was produced *N,N'*-dicyclohexyl-(3-formyl-indol-2-yl)urea in 83%. Reduction on N-OH moiety was observed. Unfortunately, reaction conditions were not reported in the cited paper.

Same concept was exploited for compound **4**. It was obtained product **85** in high yield and isolated with no need of column chromatography (Scheme 39).

4   **85**
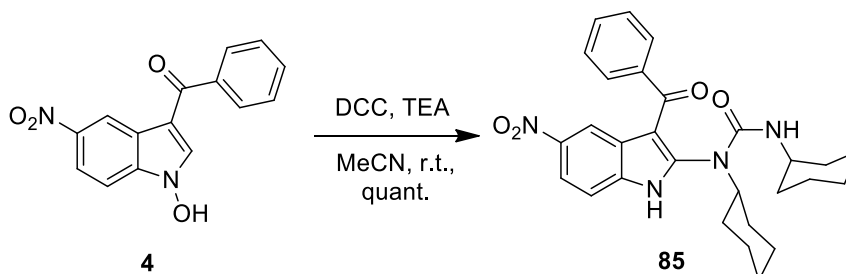
Scheme 39: synthesis of compound **85**.

5.4.5.4. Reduction

An unselective reduction reaction of compound **5** was afforded by Zn mediation in AcOH.[121] Yield of **86** is high but main drawback is reduction not only of *N*-hydroxy moiety but also nitro group is reduced to amine (Scheme 40). C-Cl bond and carbonyl were left untouched.
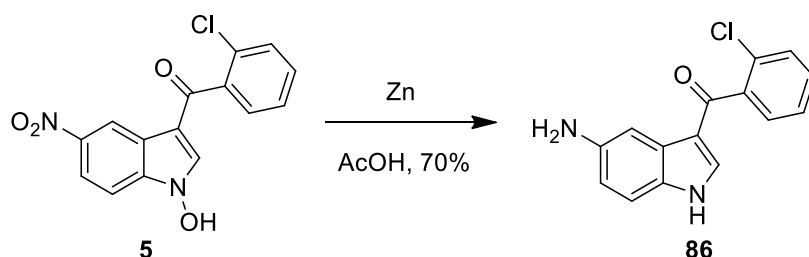
Scheme 40: Zn reduction of **5** to afford **86**.

Aiming for a selective reduction for only *N*-hydroxy motif, some new conditions were tried. Attempts to use nitrosobenzene as reducing agent failed, leaving reactant untouched. Trials with Hantzsch ester failed too. Optimal conditions were found using a mild and facile dihydroxylation with phenacyl bromide and triethylamine (Scheme 41). Protocol was nitro and carbonyl groups respectful. Similar reactions were explored by Somei[54] and more recently by Wojciechowski and Wròbel[62]. The latter reported also ethyl bromoacetate is effective in this transformation, albeit it is slower in reacting and less selective.[122]
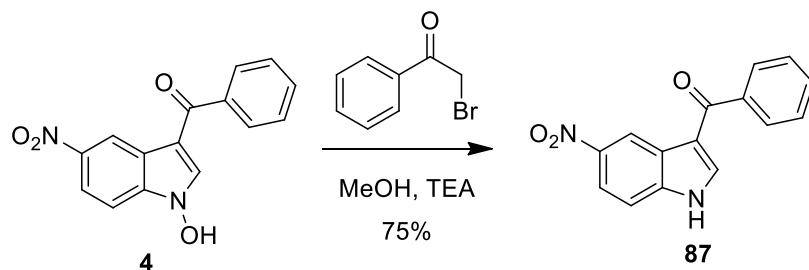
Scheme 41: selective N-OH motif reduction.

5.4.5.5. Cyclization

Indoles **61-64** with 2-nitrochalchone moiety are particularly interesting for further functionalization: for example, they are starting materials for Cadogan-Sundberg indole synthesis.[123] Modifications on the original protocol were introduced during the last decades, using microwave radiation as unconventional heat source[124] or metal catalysts.[125] Successful Cadogan-Sundberg reaction runs were achieved using PPh3 (Table 10) instead of classic P(OEt)3: latter reactant was found to produce a complex mixture of products very hard to separate and identify. Reduction of *N*-hydroxy motif was observed. All products were purified by chromatography. Modest yields were obtained: improvements will be studied in the next future and a wide survey will be carried out.
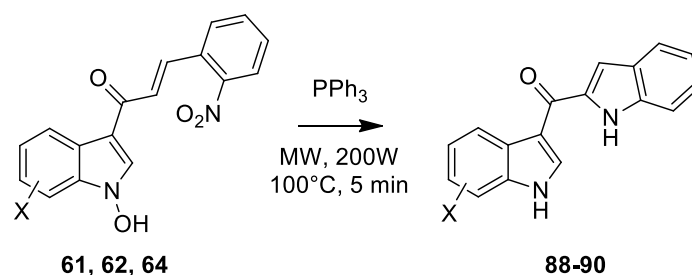
Entry	X	Substrate	Product	Yield
1	5-CN	61	88	25%
2	5-NO$_2$	62	89	36%
3	7-COOMe	64	90	19%

Table 10: Cadogan-Sundberg cyclization.

Banik reported another brilliant cyclization starting off from 2-nitrochalcones and affording quinolines. Reaction is mediated by indium and ammonium chloride.[126] Hot point of this protocol is usage of environmental benign conditions as solvent is EtOH/water. Nitro reduction to aniline is invoked by the authors to explain quinoline ring closure by a condensation process. A successful cyclization was achieved starting from **61** (Scheme 42): product **91** was obtained in modest yield and optimization will be hot topic for the next future and for further compound to be prepared. *N*-hydroxy motif was lost during the reaction. Water was replaced by 1,4-dioxane to improve substrate solubility.
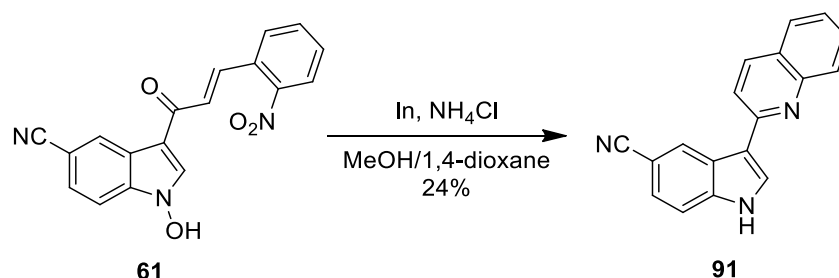
Scheme 42: cyclization reaction to afford **91**.

5.4.5.6. Cross coupling reactions

Indoles **68-71** exhibit a C-Br bond on indole 2 position. Halogenated aromatic compounds are important reactants in cross coupling reactions. Preliminary trials were performed on *O*-protected compound **73**. Reaction partner was phenylboronic acid to have the classic Suzuki-Miyaura coupling. First trial employing Pd(PPh$_3$)$_4$ as catalyst in toluene/EtOH/water was unfruitful, leading to complete reactant recovery. Working with Pd(OAc)$_2$ in refluxing 1,4-dioxane reaction proceeded with quantitative yield (Scheme 43). No addition of any phosphine ligand was necessary. A wide survey of coupling products will be synthetized in the next future exploiting these conditions.
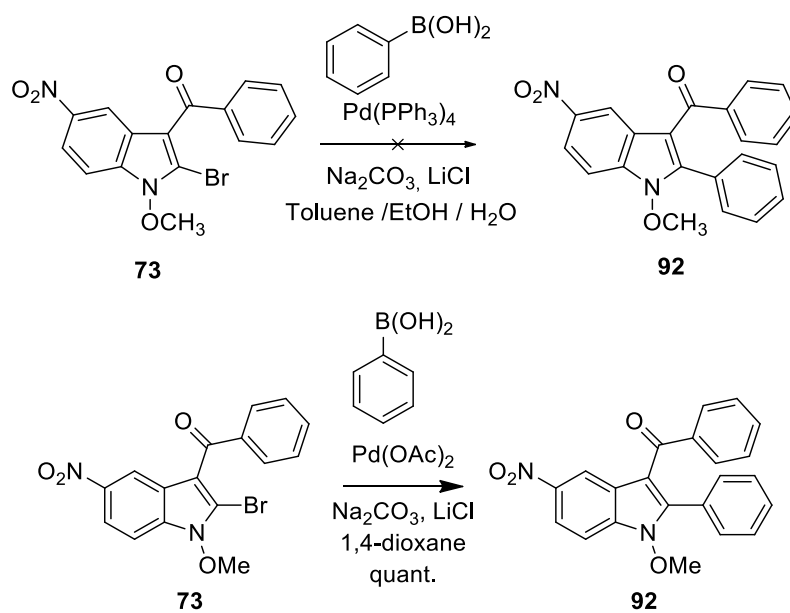
Scheme 43: Suzuki-Miyaura cross coupling reaction affording compound **92**.

6. Conclusions and future developments

In conclusion, a direct methodology for the regioselective synthesis of stable *N*-hydroxy-3-aroylindoles and 3-aroylindoles by cycloaddition of nitrosoarenes with conjugated alkynones in 1:1 ratio was developed. Terminal ynones were used for the first time in similar reactions and were identified as privileged reactants. Reactions of the latter with 4-nitronitrosobenzene can be used as facile and propitious tests to recognize conjugated alkynones through the formation of precipitates of 5-nitro-*N*-hydroxy-3-aroylindoles. Reactions using internal alkynones gave modest yields of indole products, but optimization of the process is currently on study. Yield improving of reactions involving eletron rich nitrosoarenes is scheduled. Indoles produced by this protocol are interesting scaffolds for the preparation of high valuable compounds generally known as analgesic and NSAID drugs as demonstrated by pravadoline and JWHs synthesis.

A detailed mechanistic study is in progress, especially focused on understanding the discrimination step between formation of N–OH indoles and N–H indoles.

Indoles **68-71** exhibiting a brominated C2 position will be the starting materials of a wide survey of Pd catalyzed cross coupling reactions (Scheme 44). Only a preliminary Suzuki-Miyaura reaction with phenylboronic acid was successfully performed but ampliation of the scope is currently work in progress. Different boronic acids are going to be tested to expand library of target compounds.

Particularly interesting are Sonogashira type reactions. Possibility to introduce a triple bond is attracting due to great possibility of further functionalization, like for example Glaser dimerization, alkyne cyclotrimerization, Pauson-Khand reaction and alkyne metathesis.

Brominated *N*-hydroxyindoles are also attractive due to presence in natural molecules. One example is convolutindole A (Figure 13), which synthesis has never been reported and could be an interesting target to achieve for nitrosoarene-alkyne annulation in the next future. Convolutindole A is extracted from *Amanthia convoluta* and has been recently tested as new nematocidal drug[127]: results indicate a higher vermicide potency and broader spectrum activity than commercially available levamisole.[128] Tryptamine subunit is clearly recognizable in convolutindole A structure.
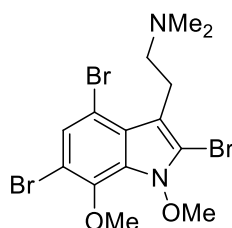
Figure 13: convolutindole A.
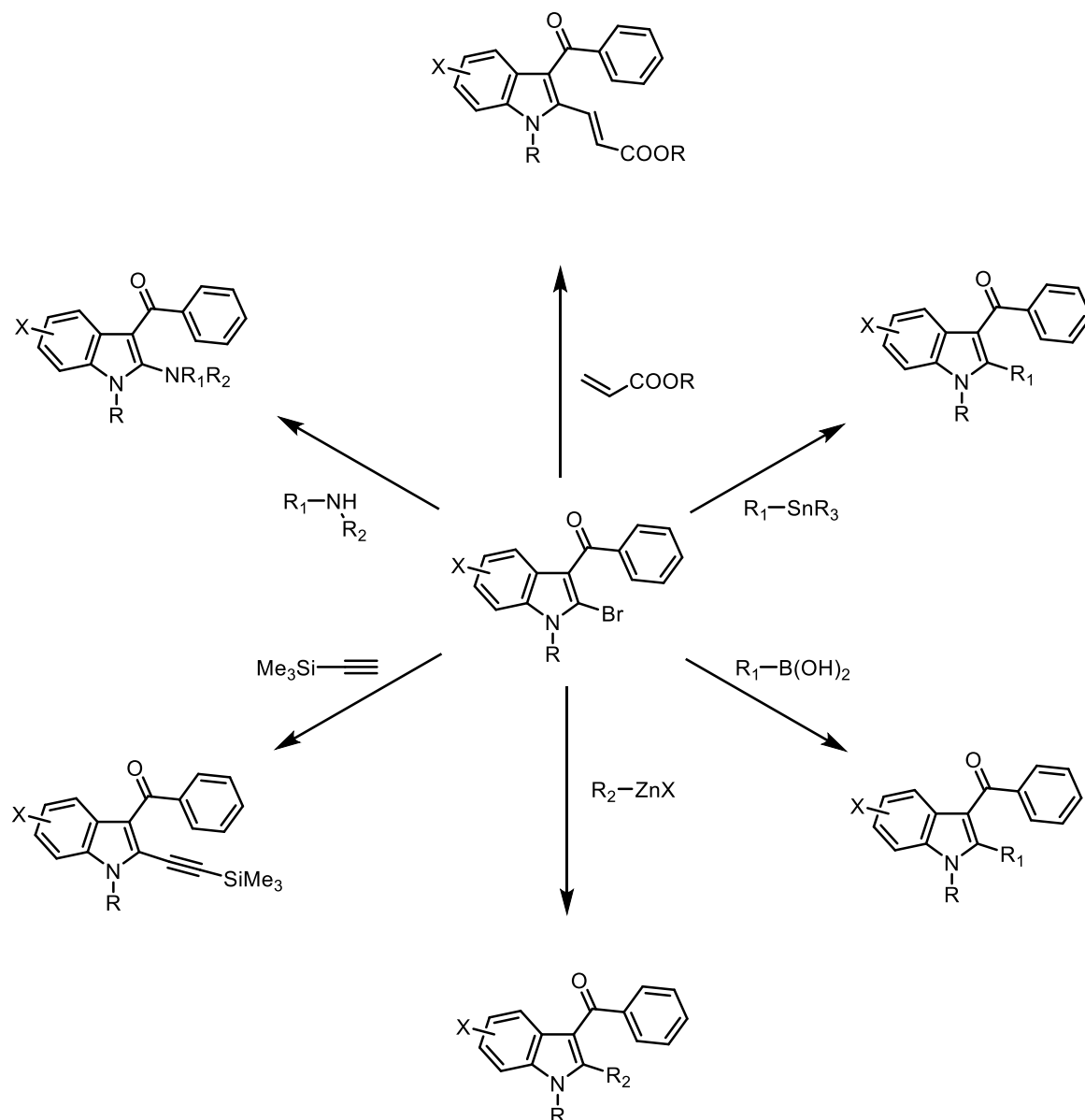
Scheme 44: Pd catalyzed cross coupling reactions on brominated indoles.

Broad expansion scope can come from annulation of nitrosoarenes with dialkynones: modulating condition could be achieved mono- and bicyclization products selectively (Scheme 45). Asymmetric monoannulation product opens space for other transformations based on alkyne triple bond. Interesting aspect would be investigating on possible confirmation of N-OH motif formation with deactivated nitrosoarenes. Experiments in this way are to be done in the next future.
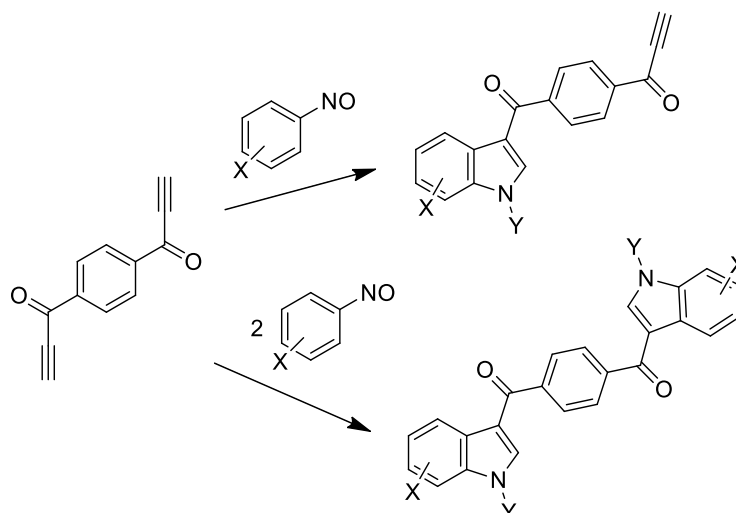
Scheme 45: annulation of a dialkynone.

A possible hypothesis to work on is investigating on intramolecular annulations. Naturally, this approach needs a molecule bearing both nitrosoarene and alkynone moiety. However, since nitrosoaromatics are not commercially available except for few exceptions, it would be easier to start off from nitroarenes. Ragaini recently reported an effective hetero Diels Alder ring closure from nitroarenes using phenyl formate as CO surrogate[129] (Scheme 46). Oxazine products formation is compatible only invoking successful reduction of nitro to nitroso.
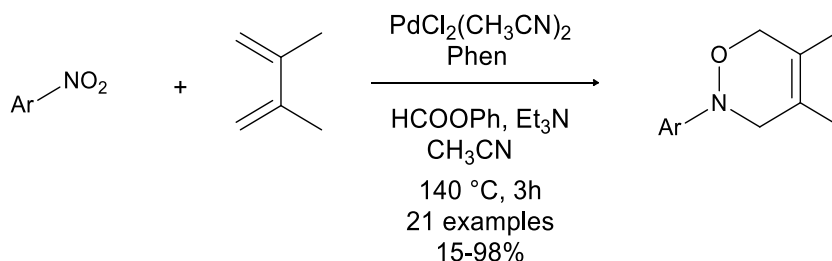
Scheme 46: hetero Diels Alder reaction with diene and nitrosoarene.

This protocol could be inspiration nitrosoarene-alkyne intramolecular annulation (Scheme 47). The latter should be favored according Baldwin rules as it is *5-endo dig* closure. Reduction of eventual N-OH moiety is expected due to reducing reaction environment. Intramolecular cycloaddition can provide a fused tricyclic or tetracyclic system. Strong similarities with ergot alkaloids can be noticed (Figure 14). If successful, this project could lead to these products without starting from preformed indole rings, which is the most common literature approach in their total synthesis. Computational studies will be performed to calculate if indolization is favored or difficult by some molecular strain.
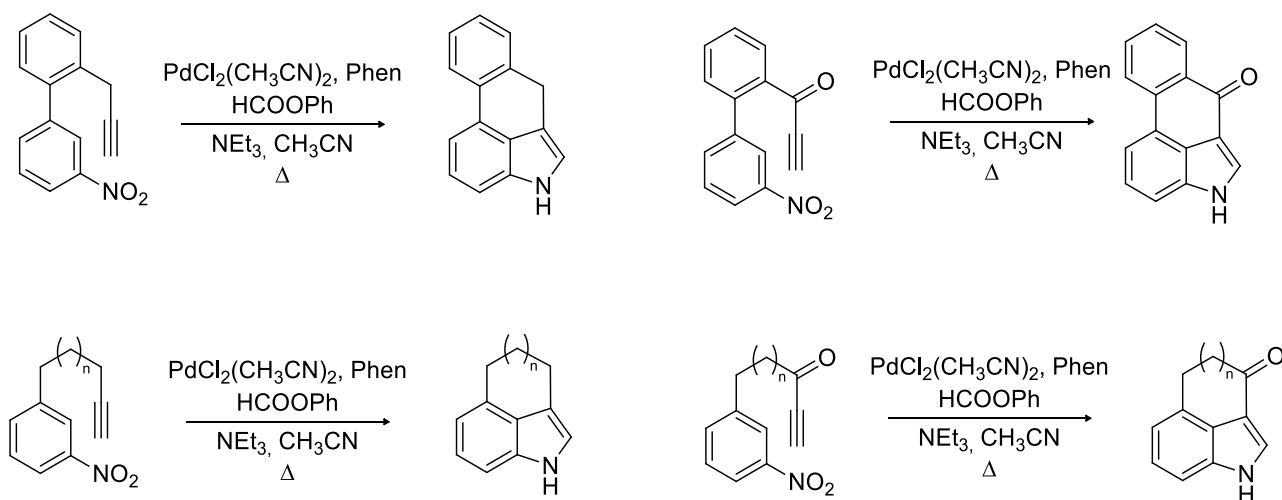
Scheme 47: intramolecular nitroso-alkyne cycloaddition.

| Chuangxinmycin | Lysergic Acid | *cis*-Claviciptic Acid | Aurantioclavine |
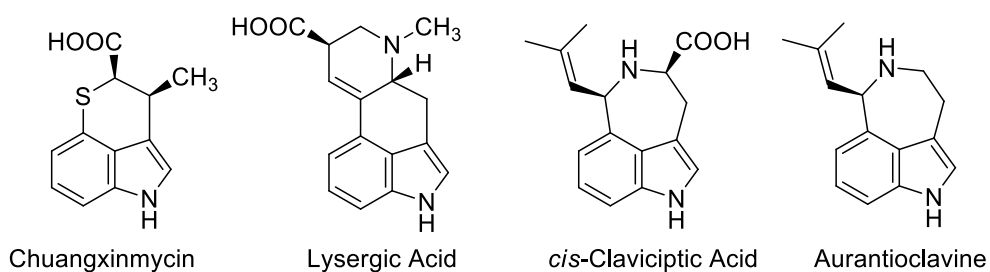
Figure 14: some ergot alkaloids.

- Chapter 2 -

Synthesis of new organic semiconductors based on 2,2'- and 3,3'-biindole backbone

7.   Foreword

In everyday life polymers are commonly seen as *plastics*: compared to metals, they are usually lighter, less robust, show decomposition or burning and, among all, they do not conduct electricity. Heeger, MacDiarmid and Shirakawa in 1977 contributed to change this view showing that an organic polymer like polyacetylene, if treated properly, can conduct electric current.[130] Polyacetylene can be synthesized by Ziegler-Natta polymerization[131] of gaseous acetylene in high yield. Exposure of thin films of polymer to iodine vapours (p-doping) brings the conductivity up to 10^8 times, thus attaining values close to those exhibited by silver metal.[130] Without any treatment, material behaves like a common insulator. This discovery was worth a Nobel Prize assigned to Shirakawa, McDiarmid and Heeger in 2000.[132] Oxidation takes place because the ionization potential of the extensively π conjugated structure is quite low. The σ backbone is left untouched whilst in the π molecular orbitals there are electron vacancies which can travel along the chain due to resonance thus conducting electric current (Figure 15). Analogous result could be obtained using photoexcitation, putting a fundamental basis for organic photovoltaics.[133] Discover of this phenomenon is however antecedent 1977, thanks to Kallmann and Pope studies on anthracene crystals in 1960.[134] Theoretical and experimental works, however, show that one-dimensional conjugated systems are unstable.[135] Doped polyacetylene is not an exception as it is not stable to prolonged exposure to air due to its easy oxidation. It is in addition insoluble and infusible (it cannot be therefore moulded into any shape); introduction of substituents on polymer backbone is then necessary to tune properties, making the polymer more stable but drastically lessening conductivity.[136] For these reasons polyacetylene has nowadays no commercial application, although it has been basic pulse to organic semiconductors (OCSs) further developments. This was the first generation of OSCs.
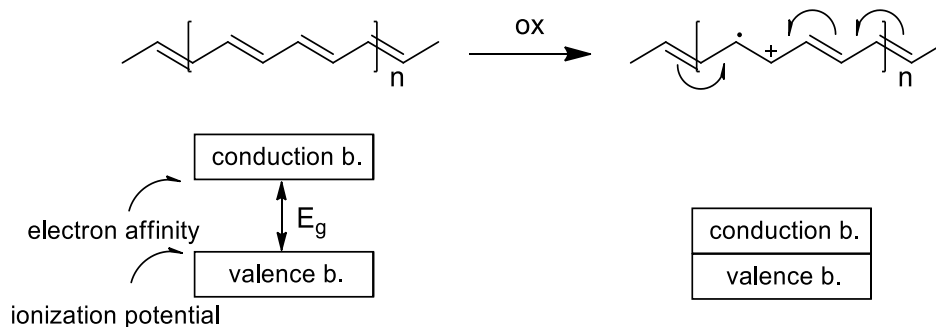
Figure 15: p-doping of polyacetylene by chemical oxidation. *b.* is band abbreviation.

In OSCs second generation (Figure 16) modifications on the polymer backbone are investigated, changing the alkenyl chain in a polyaromatic system (poly-*p*-phenylene, PPP; polyphenylenevinylene, PPV). Stability, charge transport and optoelectronic properties are improved, and functionalisation was made easier by exploitation of classic aromatic rings reactivity, allowing an even finer tuning of the optical and electronic properties.[137] PANI (polyaniline) was the first synthetized second generation OSC, although at that time it was not recognised as such.[138] OSCs based on heteroaromatic rings such as pyrrole, thiophene and 3,4-ethylenedioxythiophene (EDOT) were synthetized successfully as well. [139]
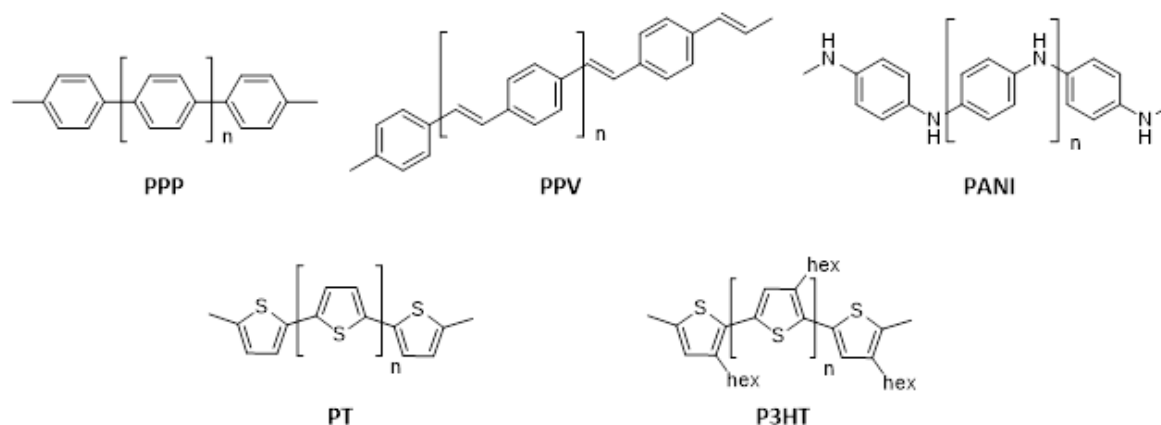
Figure 16: some second generation OSCs.

All second generation OSCs must undergo doping to allow charge transport as at neutral state they are insulator like polyacetylene. Oxidative p-doping can accomplish this result, extracting an electron or two from π orbitals every two or three units and creating the so called polaronic or bipolaronic states[140] (Figure 17).
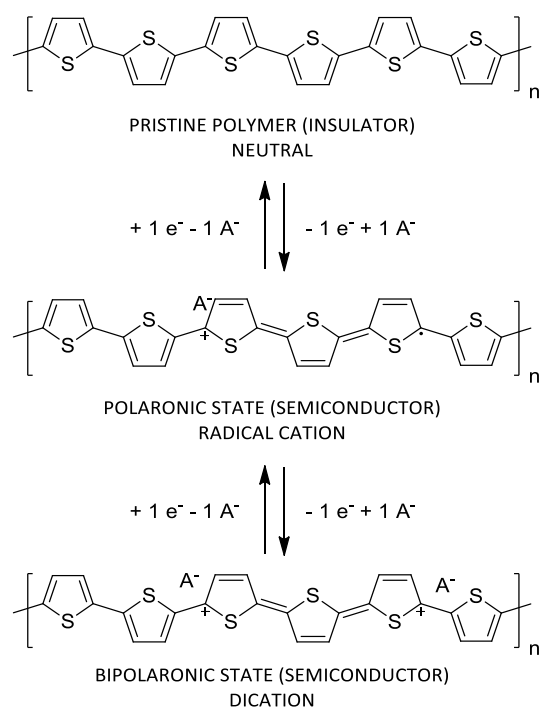
Figure 17: polythiophene (PT) at natural stage and after *p*-doping.

Chemical oxidation is performed using $FeCl_3$ or $(NH_4)_2S_2O_8$ to afford insoluble polymeric powders which can conduct electric current. Counter anions coming from the oxidizing agent (Cl^- or HSO_4^-/SO_4^{2-}) are incorporated in the material to compensate electronic vacancies. When an electrochemical route is chosen instead, a potential is imposed to oxidize monomer and then polymer starts to deposite on the working electrode. Initial stages of the process (formation of the radical cations and aggregation into oligomers) happen in solution; counter anions are attracted too as charge compensators.

The main drawback of these structures is solubility, even when in oligomeric state. The problem can be partially solved by attaching alkyl (as in poly-3-hexylthiophene, PH3T) or alkoxy chains: in this case electronic characteristics, unlike in functionalised polyacetylenes, do no drop as much.

With third generation of OCSs ever more complex structures have started to appear. Key concept is synthesis of donor-acceptor copolymers, which are up to now a very popular research field, with particular attention in bulk heterojunction (BHJs).[141] The latter represent the core concept in the fabrication of organic solar cells to afford clean and renewable energy.[142] Alternating a donor and an acceptor scaffold results in a band-gap lowering in resulting copolymer (Figure 18). Regioregularity is therefore a fundamental parameter which must be considered in synthesis planning.
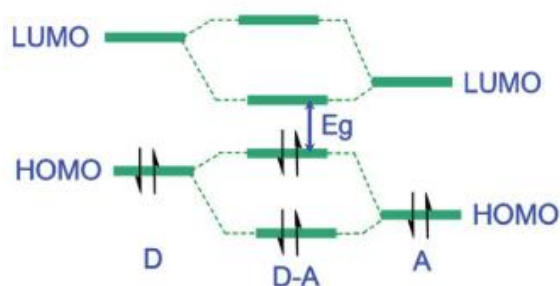
Figure 18: donor (D) and acceptor (A) orbital coupling to afford donor-acceptor (D-A) orbital structure.

Fundamental D units are weak donor benzene, carbazole and fluorene whilst much stronger are thiophene-based structures like thiophene itself, cyclopentadithiophene (CPDT) and dithienopyrrole (DTP). On the other hand, examples of A units are constituted by weak acceptor phthalimide and bithiazole whilst high acceptor power characterized benzochalcogenodiazoles and quinoxalines[141] (Figure 19). Many D/A combinations are therefore possible and huge panorama on possible modifications of fundamental subunits opened by exploiting their chemical properties.

Planarity is an important factor as the higher the planarity, the better the electronic delocalization over π copolymer orbitals. Introduction of side chains is sometimes mandatory to increase solubility since, in solar cell fabrication, the key step is casting a copolymer solution on the assembling device.[143]
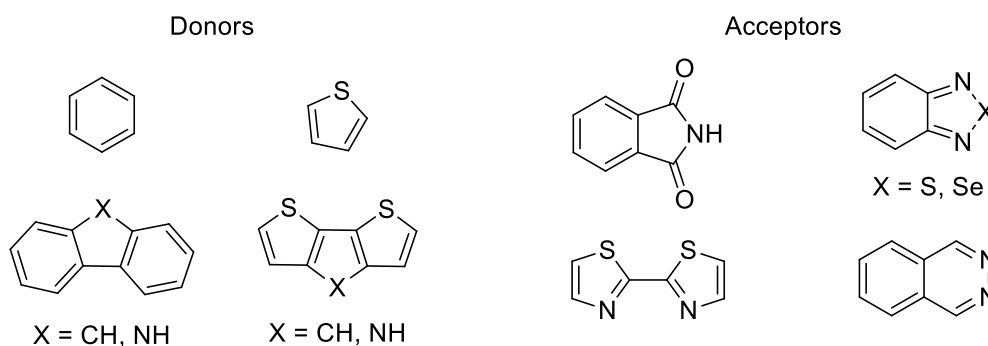
Figure 19: some common donor and acceptor scaffolds.

Synthetic methods generally are based on Stille or Suzuki cross coupling reactions starting from difunctionalized halides and organometallic reagents to afford high polymerization regioregularity.[144] An example is reported in Scheme 48. Brominated P3HT is used as chain terminator.
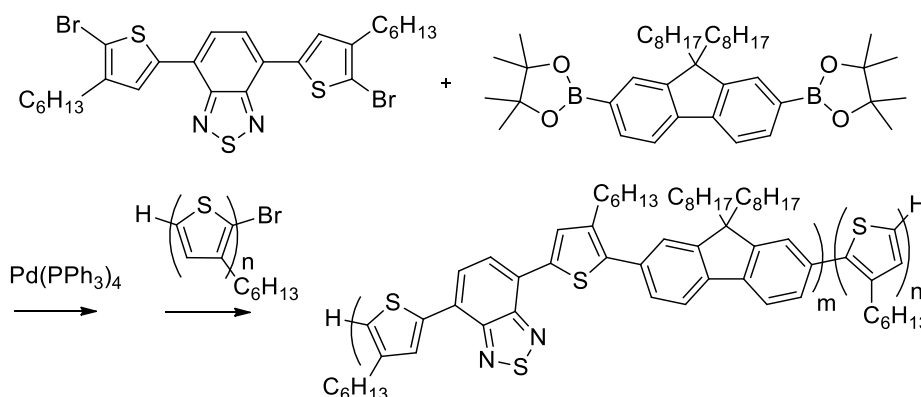
Scheme 48: synthesis of a regioregular D/A copolymer by Suzuki cross coupling reaction.

Third generation OSCs applications go beyond organic photovoltaics as they were applied successfully also as electrochemical biosensors.[145] Their working mechanism is based on analyte interaction directly with the semiconductor material in a redox process. The electrochemical signal is then transduced through the semiconductor material with high sensitivity as limit of detection in reading analyte is $\approx 0.1\ \mu M$ and broad linear range spanning 5 magnitude orders.

Naturally, objective of this foreword is summarizing some fundamental aspects either on OSCs synthesis and practical use with no claim to be complete as a deep description is beyond the aim of this PhD thesis. For further informations on this topic the reader is sent to the literature.[137,142,145–149]

8.   Chiral electroactive materials

Chirality is a fascinating property and a key concept in chemistry. A molecule is chiral when it does not possess any symmetry plane, roto reflection axes or inversion centers. This produces two stereoisomers of the former chiral molecules called enantiomers, which are one the mirror image of the other. An immediate property of enantiomers is their impossibility of superimposition. Chirality is not a feature proper only of molecules but it is present also in macroscopic world: the word *chirality* itself derives from Greek χείρ, meaning *hand*, which are the most immediate chiral objects generally we usually think about (Figure 20).
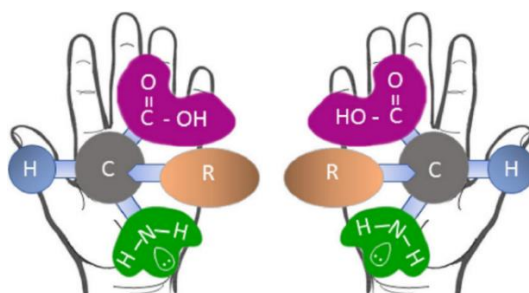
Figure 20: hands and a generic amino acid.

The control of chirality is a fundamental aspect of modern chemical synthesis as almost no natural chiral molecule can be found as racemic mixture but one enantiomer is always preferred. An incredible voluminous literature has been published on enantioselective synthesis and catalysis[150,151] and this research field was awarded by Nobel Prize in 2001 thanks to Knowles, Noyori and Sharpless pioneering work.[152] Parallel to synthesis, characterization methods also are prompted in pursuing enantioselective analyses with ease. Chiral electroactive materials are a relevant topic as their aim is combining in the same OSC material conduction properties with the ability to discriminate between the two enantiomers of a chiral analyte.

Because of their relative ease of synthesis and good environmental stability, polythiophenes (PTs) and polypyrroles (PPs) are the materials of election.[153] Optical activity can be induced in two ways: by incorporating an enantiomerically pure counter ion during oxidation process or by performing the polymerization starting from an enantiomerically pure monomer. While the former strategy works best on polyanilines (PANIs), the latter is more applied for PTs[154] and PPs[155], with polythiophene being the most studied due to its easier functionalization and stability. A huge variety of molecules has been produced (Figure 21), based on the strategy of functionalising 3 or 4 thiophene positions with cheap chiral enantiopure pendants, like monosaccharides and amino acids[142,153,156] bearing a quaternary carbon as a stereocentre.

Synthesis of the polymer is usually carried out with previously described cross coupling reactions: oxidants like $FeCl_3$ are rarely used due to the sensitivity of pendant chiral groups. A further issue with these monomers regards the non-equivalence of thiophene α positions due to their C1-symmetry. Polymers resulting from

oxidation of this kind of monomers may not be constitutionally regular. Quite laborious synthetic pathways are requested to afford regioregularity.[153]
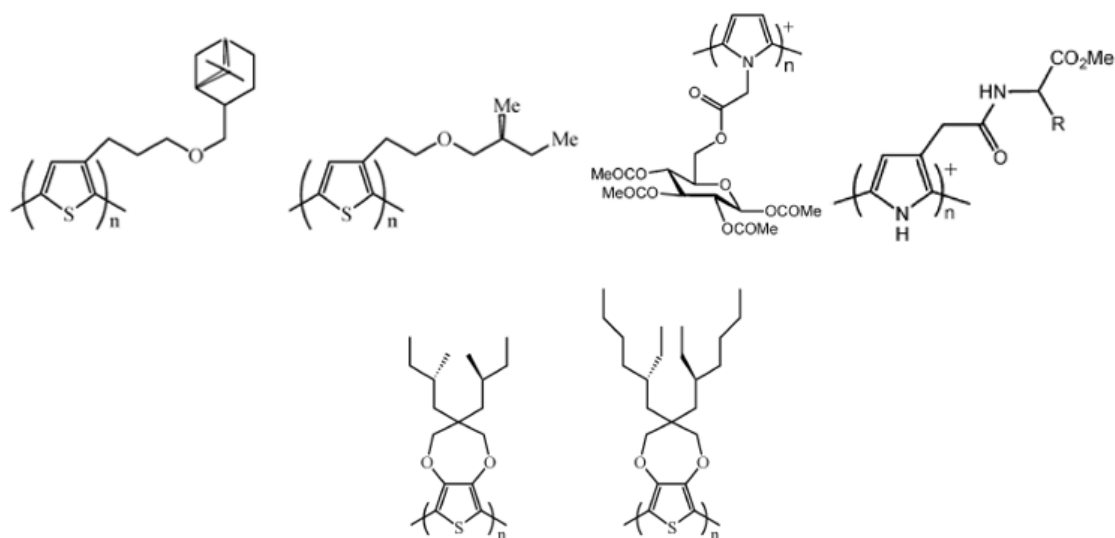
Figure 21: different types of chiral PTs and PPs.

Circular dichroism (CD) data show that chirality at the supramolecular level arises from the adoption of a one-handed helical conformation by the PT main chain, induced by the presence of chiral pendants[154] (Figure 22).
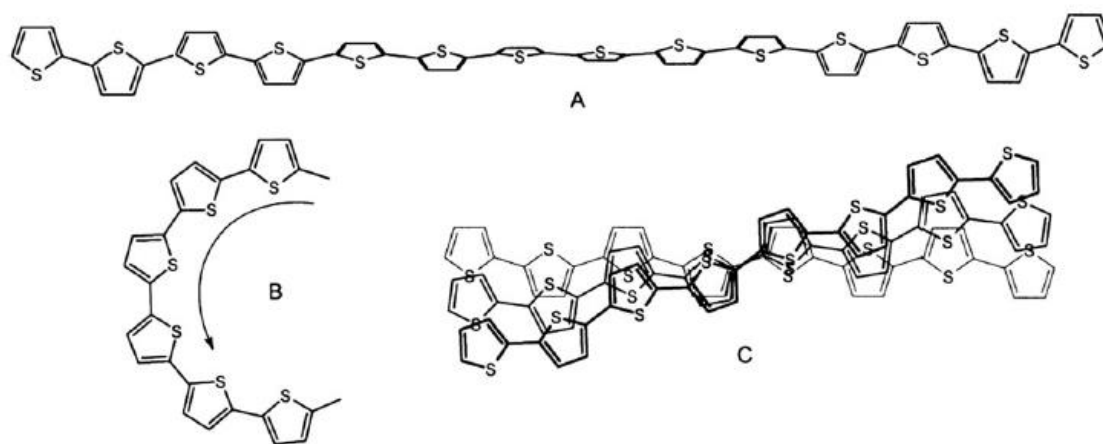
Figure 22: different possible configurations of the chains. **C** is the most probable. Chiral substituents on PT backbone are omitted for clarity.

A general drawback of these kinds of chiral electroactive polymers is that they manifest relevant chiral properties only under very specific experimental conditions and almost nothing elsewhere. In Figure 23 an example of the solvatochromic effect is reported: no CD signal is detectable when the polymer is dissolved in pure CHCl₃ whilst a progressive signal increasing is observed when subsequent amounts of polar solvents, like methanol, are added: explanation of this phenomenon could be that a better supramolecular aggregation is

favoured by polar solvents. Despite the large number of chiral polymers synthetized, few examples of applications are known because chiral manifestations happen quite sporadically and in very specific conditions.
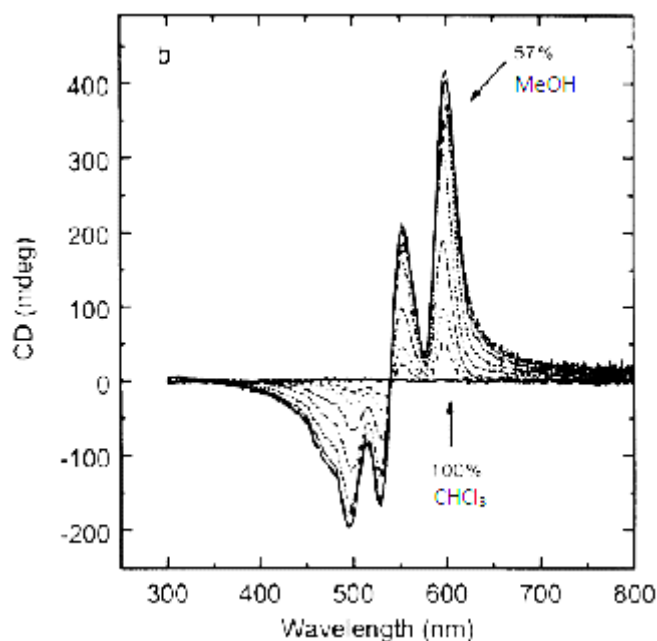
Figure 23: CD profile of a chiral PT with and without MeOH addition.

Since, as stated before, OSCs are particularly investigated as sensors, it's no surprise that chiral polymers too are studied in the field of enantioselective sensors. Basic hypothesis regards chirality of enantiopure conductive material: as it contains a well-defined stereochemical information, it may behave differently in the presence of one or of the other enantiomer of a chiral analyte giving different responses due to diastereoisomeric interactions between polymer itself and analyte.

One notable example was carried out at University of Bari, where chiral polymers were used in a gas sensor and achieved chiral discrimination of molecules in concentrations of 0.1 ppm.[157] The research group built a bilayer organic thin-film transistor (OTFT) employing thiophene-based oligomers decorated with cheap but efficient chiral pendants (Figure 24).
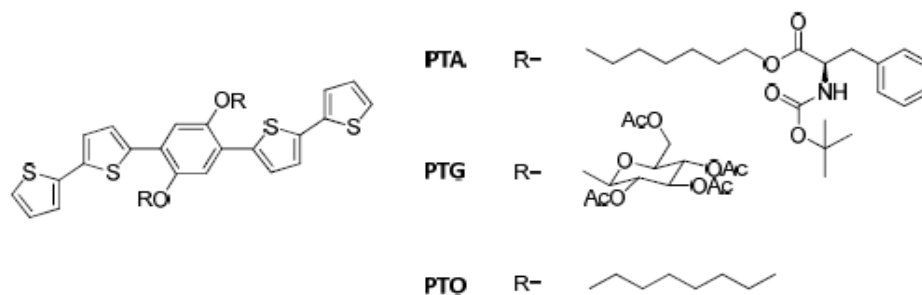
Figure 24: thiophene-based oligomers employed in the OTFT. PTO is achiral.

The alkoxy-substituted phenylene ring acts as a convenient structural subunit that can be properly function-alised by introduction of proper chains on O atoms. The chiral enantiopure functions are commercially accessible and easy to find: L – phenylalanine-N-BOC for PTA and β-D-glucose acetate for PTG. A thicker layer of the achiral PTO (Figure 25) is necessary because PTA or PTG made only OTFTs do not show field-effect amplified current, which is the phenomenon required for these systems to function properly. Probably this is due to the steric hindrance of the amino acid or the glucose molecule. PTA was employed for discriminating the enantiomers of citronellol, PTG for carvone antipodes.
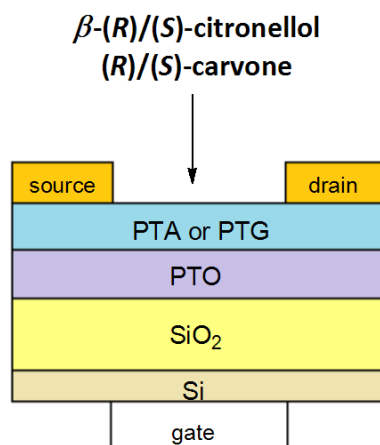
Figure 25: cross-section of the OTFT gas sensor with interaction site.

In Figure 26 the response of the transistor to exposure to different vapour concentrations of (R)-, (S)-citronel-lol and racemic mixture is reported. The device can distinguish between the two enantiomers, having a more sensible response for the (S) enantiomer. Identical behaviour was seen for enantiopure forms of carvone and for its racemic mixture as well.
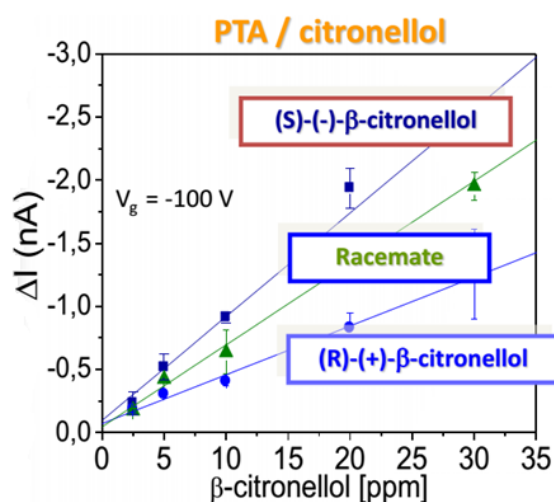
Figure 26: calibration curve of OTFT exposed to (R)- and (S)-citronellol, as well as the racemic mixture.

9. The inherently chiral concept and inherently chiral electroactive materials

9.1. *Inherent chirality* concept

The inherent chirality concept was introduced for the first time by Böhmer in 1994 to describe chirality in calix[4]arenes.[158] Their chemistry started to be an interesting topic due to this feature.[159,160] Calixarenes manifest chirality as they have C1 symmetry although they do not possess any classical stereogenic element but only an unsymmetrical 3D shape (Figure 27). This brought the definition of inherent chirality by Dalla Cort in 2004 as follows: *inherent chirality arises from the introduction of a curvature in an ideal planar structure that is devoid of perpendicular symmetry planes in its bidimensional representation* (Figure 28).[161]
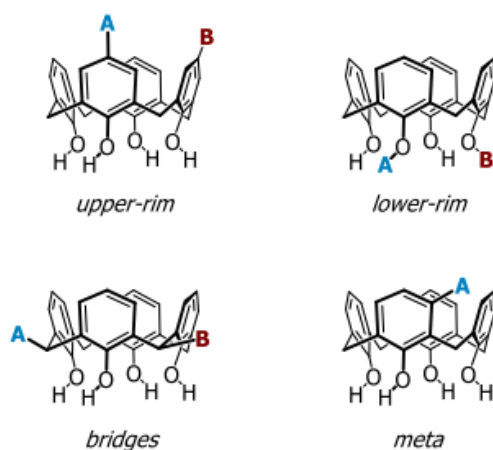
Figure 27: four types of inherently chiral calixarenes.[160]

It's important to notice the previously cited inherently chiral definition is not completely leaving out all classical stereogenic elements like stereogenic planes and axes. Helical chirality is in particular very common in helical shaped molecules known as helicenes.[162]
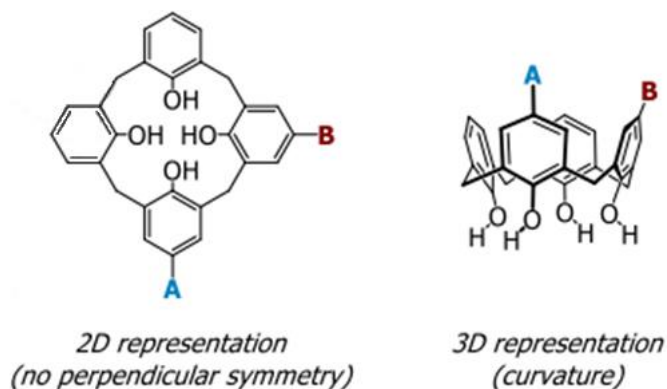
Figure 28: lack of symmetry in an ideal 2D calixarene.

Calixarenes are afforded generally by reaction of phenols with formaldehyde. It is widely known that running reaction in presence of acid leads to formation of a branched polymer known as bakelite.[163] When basic conditions are employed instead, a formation of cyclic tetramers is seen and their 3D structure was recognized in early 1970s by Gutsche[164], who called them calixarenes since their calix shape.

Another definition of inherent chirality was provided by Sannicolò in 2018 concerning functional molecular materials as follows: *in inherently chiral molecular materials the stereogenic element responsible for chirality coincides with the functional group responsible for the material specific property.*[165] This definition implies no restrictions in the possible stereogenic element responsible for chiral properties: this concept was, however, exploited only concerning tailored torsions obtained by stereogenic axes.[166,167] This interpretation of the inherently chiral concept is the one followed during development of the present PhD thesis.

♦♦♦♦♦♦

9.2.   Inherently chiral electroactive materials

The possibility to combine the inherently chiral concept with OSCs sensing performances was explored by Sannicolò in 2010.[168] A new inherently chiral monomer was designed with the generic structure reported in Figure 29.
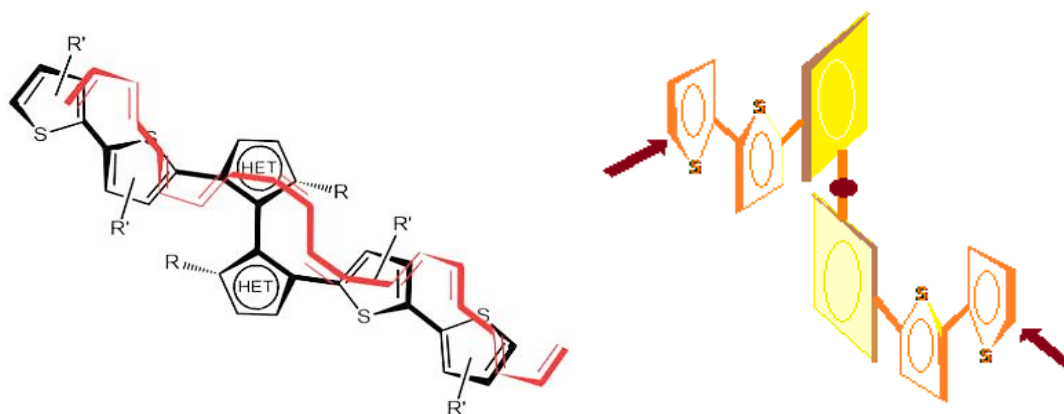
Figure 29: design of new inherently chiral monomer. Conjugated double-bond backbone is highlighted in red and slightly shifted from main drawing (left): 3D shape of inherently chiral monomer; red arrows indicate homotopic positions for oxidative oligomerization (right).

This model scaffold provides an internal torsion in the conjugated backbone, affording 3D shape; the stereogenic element, in this case a stereogenic axis, is embedded in the main frame, not in a pendant away from the conjugated chain, justifying the inherently chiral definition. Substitution of biheteroaromatic base scaffold with bithiophene provides stereogenic axis to be blocked at room or higher temperature: the latter is tailored to interconnect the two main units without interrupting π conjugation.

The advantage of this kind of scaffold over the others seen before is that electrochemical, chiroptical and enantiorecognition properties are strictly correlated and are connected to one another, since the same conjugate system is responsible for both chirality and optoelectronical properties. Last but not least, thanks to C2 symmetry, alpha position of terminal thiophenes are homotopic, giving perfect constitutional regularity to oligomers/polymers.

9.2.1. Inherently chiral electroactive materials based on 3,3'-bithianaphtene

The first intrinsically nonplanar, dissymmetrical, multitiophene – based monomer synthetized was 2,2'-bis[2-(5,2'-bithyenyl)]-3,3'-bithianaphtene (Figure 30), nicknamed BT_2T_4.[168]
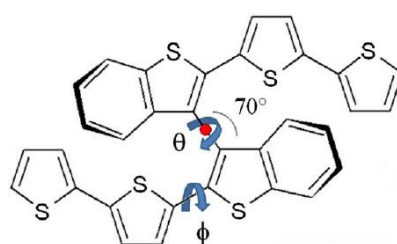
Figure 30: structural formula of BT_2T_4. Dihedral θ angle is calculated around 70°C. Dihedral φ angle permits 360° rotation.

The racemate was separated using HPLC on a chiral stationary phase by Dr. Roberto Cirilli (Istituto Superiore di Sanità, Rome). BT_2T_4 antipodes were characterized from a chiroptical point: the circular dichroism (CD) curves (Figure 31) are perfectly symmetrical and the calculated CD for the (*S*) enantiomer (dashed line) was used to assign the absolute configuration. High optical power (≈ 1000) was noticed for the antipodes, underlining pivotal role of inherently chiral chromophore[169]

$$[\alpha]_D^{20} = +1001 \ (c = 0.1\%, \ CHCl_3)$$
$$[\alpha]_D^{20} = -991 \ (c = 0.1\%, \ CHCl_3)$$
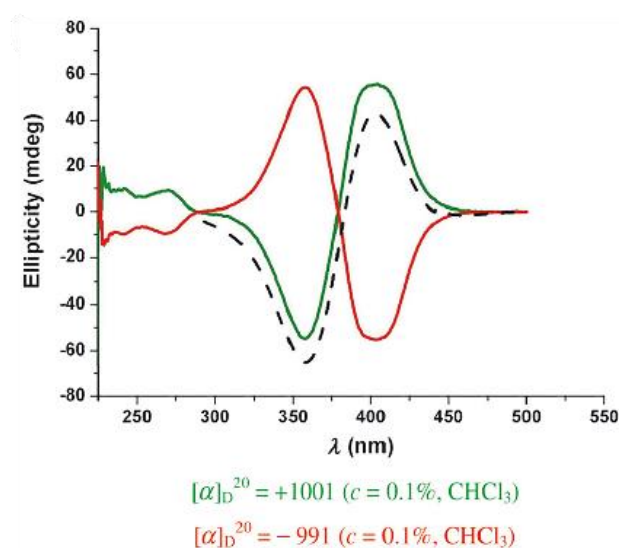
Figure 31: CD curves for the two enantiomers. The dashed line is the calculated CD for (*S*) enantiomer.

Enantiopure BT_2T_4 monomers were electropolymerized by cyclic voltammetry (CV) on electrode surfaces to produce chiral electrodes. Enantiodiscrimination ability of enantiopure film coated electrodes was tested by CV. CV curves for two enantiomers are identical if registered with an achiral electrode but since the electrode was covered with an enantiopure chiral oligomer, a differentiation between analyte enantiomers was seen ($\approx$ 100 mV) and different CV curves were produced (Figure 32). Chosen analyte was *N,N*-dimethyl-1-ferrocenylethylamine due to its high reversible redox peaks. Other chiral and commercially available APIs like DOPA and ofloxacin were tested showing great results in enantiomer discrimination.[170,171]
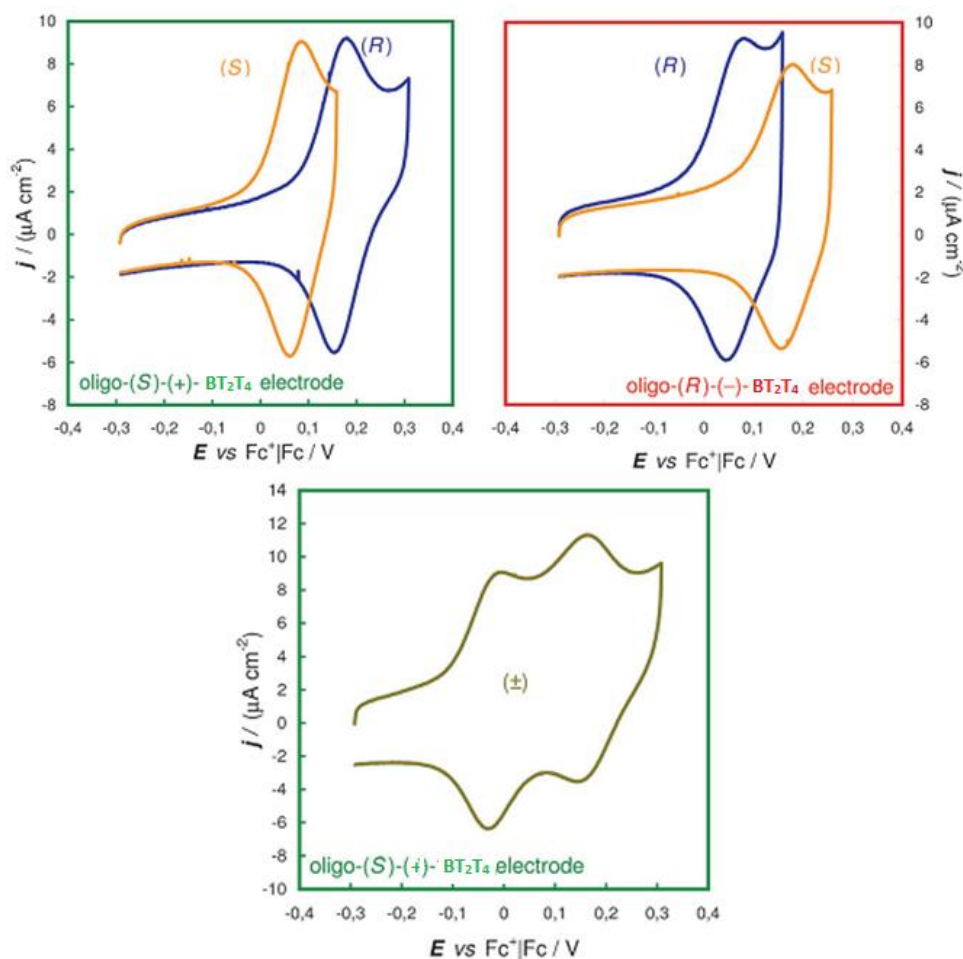
Figure 32: enantiodiscrimination tests on enantiopure oligo-(*S*)- BT_2T_4 (deposited form 36 cycles, 0.5 mM monomer solution in DCM + 0.1 M TBAPF$_6$, 200 mV s^{-1} scan rate) with the enantiopure probes (8 mM) (on top left); enantiodiscrimination tests on enantiopure oligo-(*R*)- BT_2T_4 (deposited as previously described) with the enantiopure probes (8 mM) (on top right); enantiodiscrimination tests with enantiopure oligo-(*S*)- BT_2T_4 and the racemic probe (8 mM) (on bottom).

To fully understand the molecular structure and reasons for such high enantiodiscrimination of the electrode oligomeric coating[171], chemical polymerisation of the racemic mixture of BT_2T_4 and of its enantiomers was carried out by high dilution oxidation with $FeCl_3$ in dry $CHCl_3$. Crude mixture was quenched with hydrazine to reduce radical cations and oxidant excess. Further purification was accomplished by Soxhlet extraction with THF. Samples were analysed with high resolution laser desorption ionization. Surprisingly, it was found that

the polymer is actually a mixture of cyclic oligomers, the most abundant being the dimer and trimer (Figure 33): molecular weights correspond to those of the opened oligomers minus two hydrogen atoms. This result was coherent with integration in NMR spectra. DFT calculations on resulting geometry structure were performed as well.
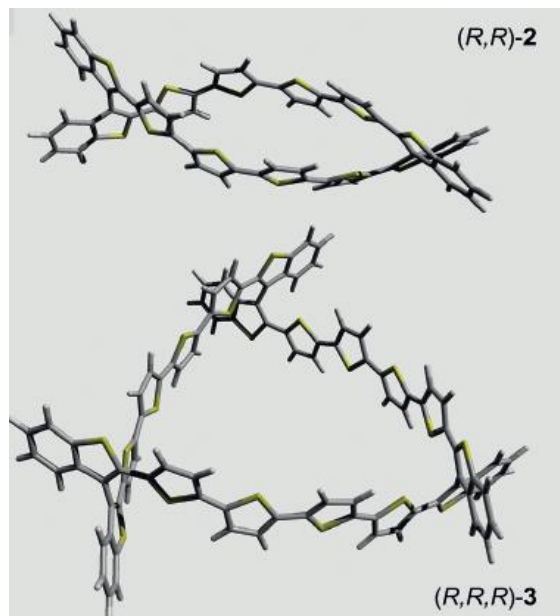
Figure 33: DFT calculations for the structures of cyclic BT_2T_4 dimer (top) and trimer (bottom).

Other inherently chiral systems based on the bithianaphtene core were synthetized and the materials derived from studied and results like those of BT_2T_4 (optical activity, formation of closed-ring oligomers) were obtained (Figure 34). Their chemical oxidation resulted in a mixture of cyclic and open oligomers and showed outstanding chiroptical manifestations as well, confirming the general trend.
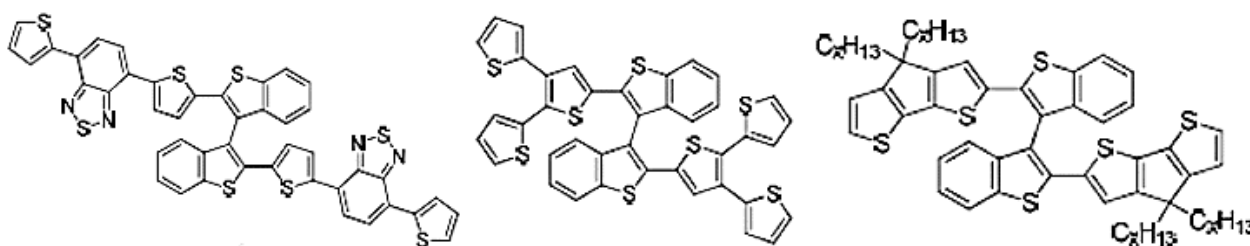
Figure 34: new monomers with bithianaphtenic skeleton. On the left there is BT_2BTD_2.

BT_2BTD_2 is of particular interest: the benzothiadiazole moiety[172] grants the monomer peculiar and very different optical properties: UV-Vis absorption and emission spectra are both 100 nm red-shifted, in comparison to other monomers (Figure 35); quantum yield is 51% (others generally stop at 10-15%) and emission half-life is even 10 times superior. Benzothiadiazole core is actually very popular in materials science: as stated before in the Foreword, it's a great acceptor scaffold with sensible applications in solar cells field. Its chemistry is well explored[173] like its photophysical properties either after a fine tuning of the substituents effects[174–176] or chalcogen atom (O[177], Se[147,178–181], Te[182]) substitution.[183,184]
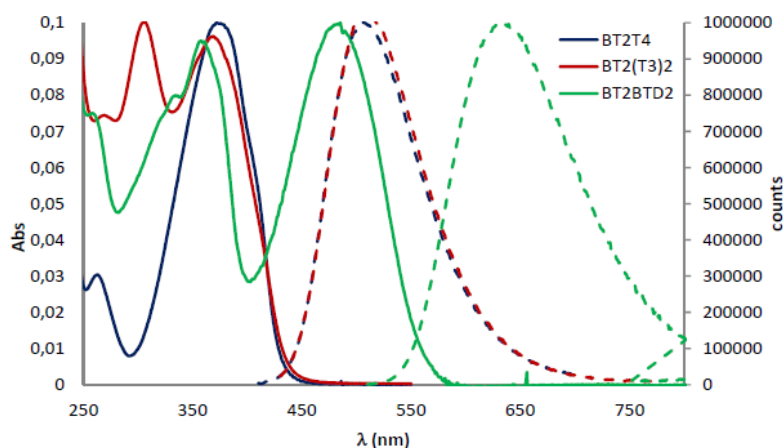
Figure 35: solid state UV-Vis absorption (solid lines) and fluorescence (dashed lines) spectra of BT-functionalised monomers. The green lines come from BT_2BTD_2.

However, the major drawback of these substrates, regardless the substituent, is the very low solubility of monomers and oligomers in most organic solvents, which compromises greatly their synthesis as well as processability making difficult their employment in optoelectronics. Applications on electroanalysis too are quite difficult, as electrodeposition sometimes could be very challenging.

9.2.2. Inherently chiral electroactive materials based on 2,2'-biindole

In order to overcome aforementioned problems connected to 3,3'-bithianaphtene monomers and expand the knowledge on inherently chiral electroactive materials, a different class of inherently chiral compounds based on 2,2'-biindoles has been investigated in the last years by Benincori group.[185] The first synthesised member of this family was 3,3'-bis(2,2'-bithiophen-5-yl)-1,1'-dimethyl-1H,1'H-2,2'-biiindole **93**, nicknamed (N-Me)Ind$_2$T$_4$ (Figure 36).

93
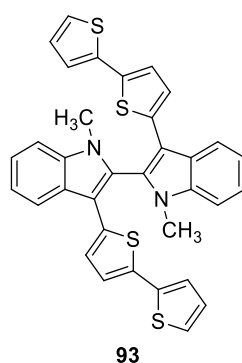
Figure 36: structure of (N-Me)Ind$_2$T$_4$ **93**.

The rationale on which is based the decision to turn to a biindole structure lays on some fundamental reasons. Firstly, indole is a very electron rich system easier to be oxidized than 3,3'-bithianaphtenes are. The first two oxidations happen at a particularly low potential value and are localised on the two halves of the biindolic scaffold. Secondly, indole can be functionalised at N atoms allowing a fine tuning of some important properties like solubility and processability by introduction of proper substituents. In addition, N alkylation

can provide steric hindrance on 2,2' interannular axis free rotation, thus ensuring configurational stability. If a chiral, enantiopure substituent is attached, it could be even possible to isolate the enantiomers via gravimetric column chromatography. Last but not least, either synthesis of the 2,2'-biindole and 3,3' functionalisation can be achieved in one single step via a Pd-catalyzed Larock-like strategy[74] starting from dialkyne **95** with appropriate aromatic halide (i.e. 5-iodo-2,2'-bithiophene **96**), the only missing step to complete the synthesis being the attachment of pendants to the nitrogen atoms (Scheme 49).
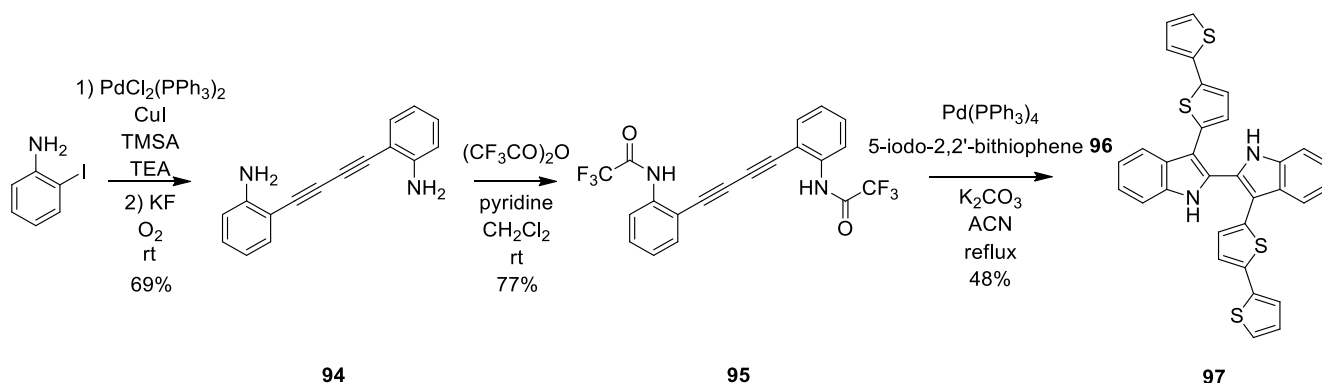
Scheme 49: synthetic scheme for the Ind$_2$T$_4$ scaffold.

Ind$_2$T$_4$ **96** can be easily alkylated in high yield using KOH as base to form the dianion and a generic R-X (X = Br, I) as alkylating agent. Alkylation with iodomethane provided product **93** in 70% yield, whilst 1-bromopropane provided more soluble (*N*-Pr)Ind$_2$T$_4$ **98**.
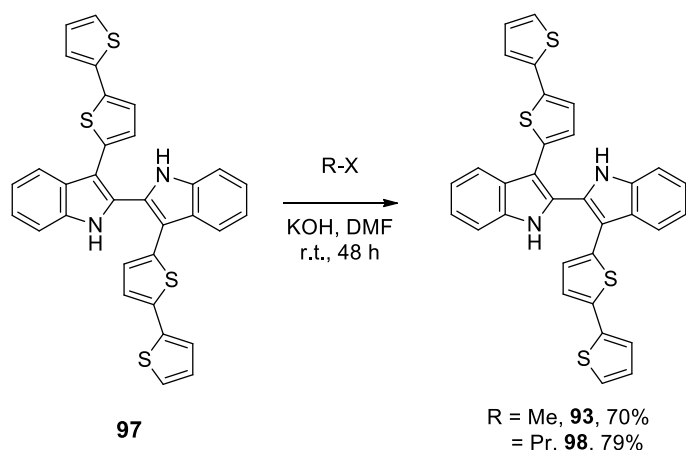
Scheme 50: synthesis of compounds **93** and **98**.

Both the monomers were obtained as racemates and the optical antipodes of product **93** were then separated by chiral HPLC. Enantiomers of **93** were oligomerized by CV on a glassy carbon (GC) electrode from monomer solutions (0.00093 M in DCM + 0.1 M TBAP, tetrabutylammonium perchlorate), by repeated oxidative potential cycling at 0.2 V/s around the monomer last oxidation peak, followed by repeated stability cycles in a monomer free solution (DCM + 0.1 M TBAP). Chiral electrodes were then obtained and they were

employed to discriminate the antipodes of various chiral probes on the basis of the difference of their oxidative potential values.

Figure 36 shows two types of experiments: on the left side, CVs of both enantiomers of a chiral *N,N*-dimethylferrocenylamine were recorded in the presence of a enantiomerically pure (*S*)-(*N*-Me)Ind$_2$T$_4$ **93** coated electrode. An outstanding difference between two oxidation peaks was noticed (≈ 300 mV) thus validating the inherently chiral strategy. On the right side, CV curves of commercially available drug Madopar® (which contains a mix of enantiopure levodopa and benserazide) by using both enantiomeric films are reported. Another time a strong difference in peak detection can be noticed. Performances are superior compared to chiral sensors based on traditional electroactive materials featuring stereogenic centers external to the polyconjugated chain.[186–189]
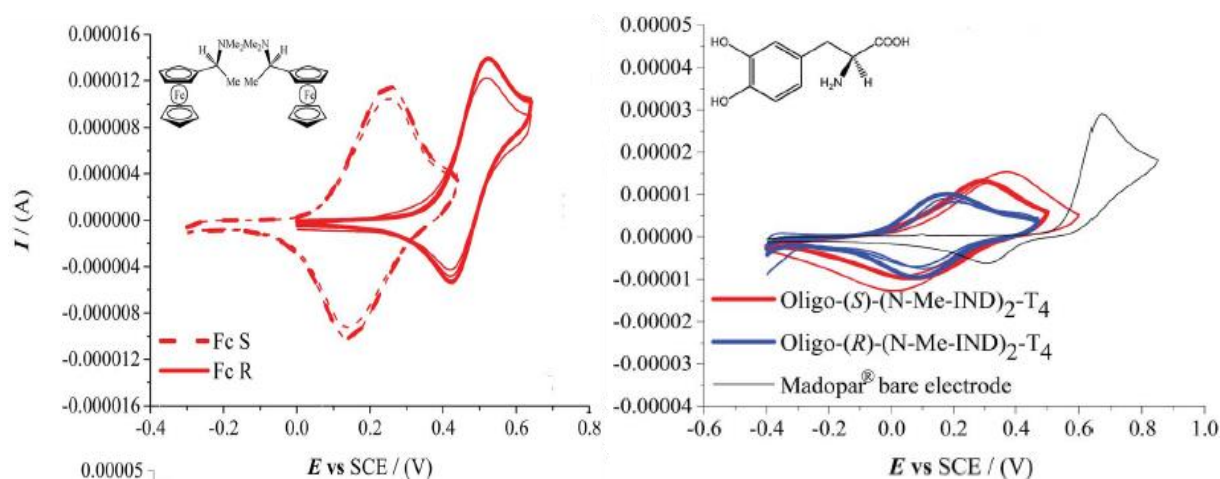
Figure 37: CV with enantiomerically pure (*N*-Me)Ind$_2$T$_4$ **93** polymer-coated electrode; on the left, ferrocenylamine, on the right Madopar®. Experimental conditions are identical to those reported in Figure 31.

The enantiopure electrodeposited films also gave outstanding performances when tested in magnetoelectrochemical experiments as molecular spin filters[185] of potential interest in spintronics: the latter is an emerging technology in which it is not the electron charge, but the electron spin to carry informations. Phenomenon is related to spin-dependent effects arising from the interaction between carrier spin and the magnetic properties of the material.[190] In particular, CV patterns (Figure 37) were recorded for an achiral, reversible Fe(III)/Fe(II) couple in aqueous solution on an ITO (Indium Tin Oxide glass) electrode modified with a very thin film of oligo (*N*-Me)Ind$_2$T$_4$ **93**, under the application of an external magnetic field. A wide shift in the couple redox potential was observed upon flipping the north/south magnet orientation or changing the (*R*)- or (*S*)-enantiopure film configuration; the same striking behaviour was very recently observed on inherently chiral oligo-BT$_2$T$_4$ films.[191]
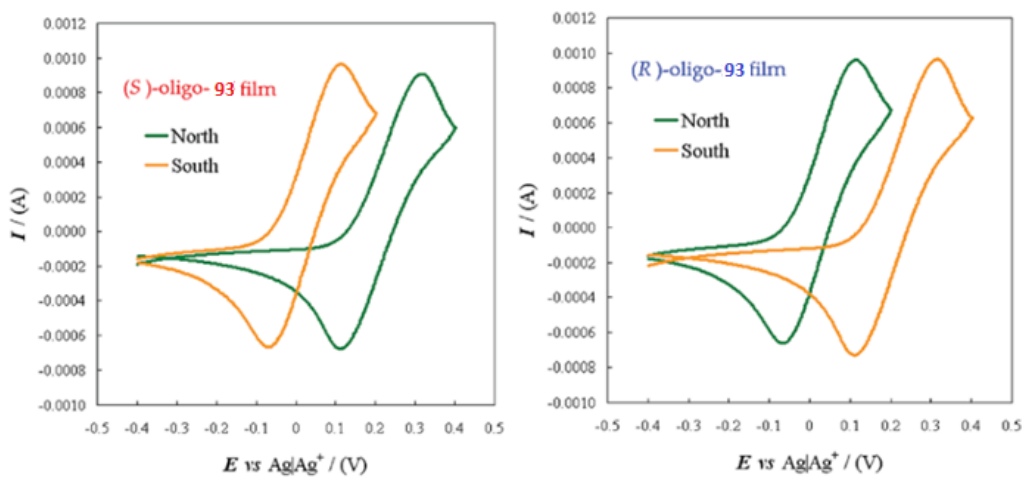
Figure 38: CV patterns for the achiral $Fe(CN)_6^{3-}$ | $Fe(CN)_6^{4-}$ redox couple recorded at 50 mV s^{-1} in aqueous solution on ITO electrodes modified by coating with a thin layer of a enantiopure oligo-**93** film applying an external magnetic field with NS or SN orientation (green or orange lines respectively).

10. Aim of the research project

The results presented above show that oligomers based on the 2,2'-biindole scaffold exhibit notable enantiodiscrimination and optoelectronic properties. It's therefore set as objective to evaluate the possibility to expand the inherently chiral biindole family by modification of 3,3' substituents.

Introduction of a π spacer is nowadays common in designing new molecules for optoelectronics[192] as it is reported to lower the optical band gap[193] and improve charge transport[194]. Introduction of an aromatic linker between biindole framework and bithiophene chain could then lead to interesting modifications of the electrochemical properties of resulting electroactive films due to the elongation of π conjugation. Enantiodiscrimination abilities of chiral films deriving from oligomerization of enantiopure monomers should be affected as well. On the basis of these considerations, two new monomers were designed in which a phenyl and a thienyl group were introduced as spacers between the biindolic core and the bithienylic wings. (Figure 39).
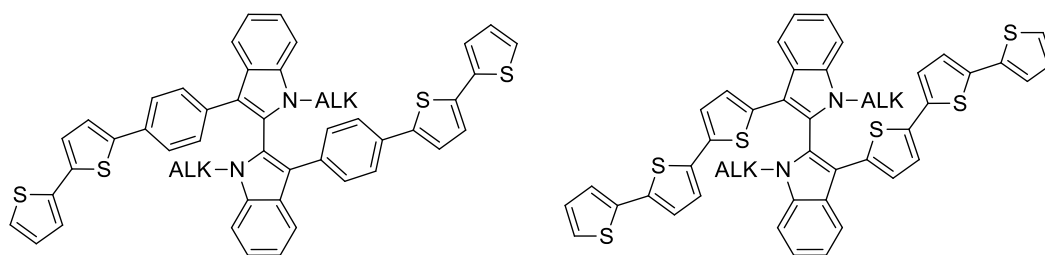
Figure 39: new inherently chiral 2,2'-biindoles with aromatic spacer.

Furthermore, a new family of inherently chiral 2,2'-biindole monomers characterized by 3,3'-substituents featuring a benzochalcogenodiazole chromophore (Figure 40) was investigated. Preliminary results were reported in a previous PhD thesis in the case of benzothiadiazole.[195] However, a full characterization should be carried out. In addition, an interesting objective could be to expand this class by synthesis of the analogous benzoselendiazole derivative. Alkylation of biindole moiety can overcome solubility issues of previously described BT_2BTD_2 which was strongly limiting their applications. Furthermore, a substitution from sulphur to selenium of the atom in the benzochalcogenodiazole molecule should produce interesting effects on absorbance-related behaviour and electronic distribution. Sulphur substitution with selenium is generally reported, for example, to have a strong bathochromic effect.[147]
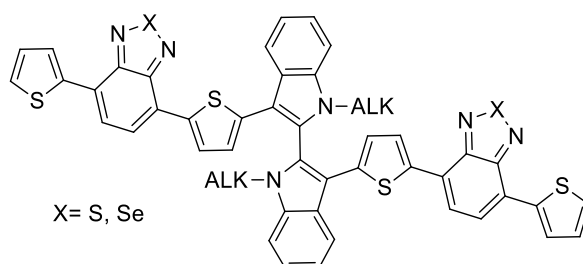
Figure 40: 2,2'-biindoles with chromophore units.

Moreover, the synthesis of analogous 3,3'-biindoles (Figure 41) was planned in order to verify their configurational stability and the possibility to employ them as inherently chiral materials. This topic is actually quite unexplored and very few examples of configurationally stable 3,3'-biindoles are known.[196–198] Their structure is actually very close to BT_2T_4 one. In addition, spacer introduction could be interesting expansion topic as well for previously cited reasons.
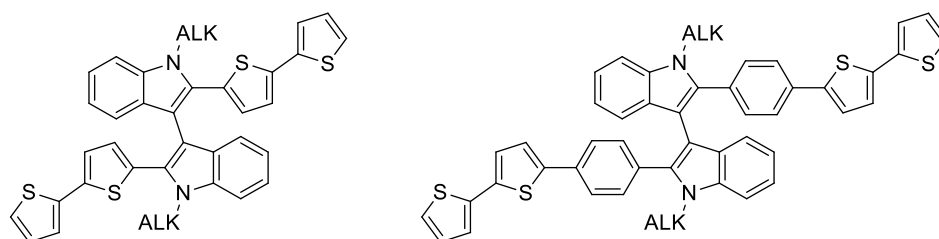
Figure 41: new inherently chiral 3,3'-biindoles.

11. Results and discussion

11.1. 2,2'-Biindole derivatives based on π spacer introduction

11.1.1. Synthesis

As anticipated, the first strategy planned to modify the general structure of (*N*-Me)Ind$_2$T$_4$ **93** was to extend π conjugation of the bithiophene side chains by aromatic spacer introduction, with the aim to study spacer influence on chiral performances and electrochemical properties. Synthesis of compound **101-103** and **106** belonging to nicknamed Ind$_2$Ph$_2$T$_4$ and Ind$_2$T$_6$ families, was planned according to the strategy followed for the preparation of (*N*-Me)Ind$_2$T$_4$ **93**. Key step is convenient and one-pot indolization reaction by Larock-type approach as described by Abbiati in 2006[74] (Scheme 51).
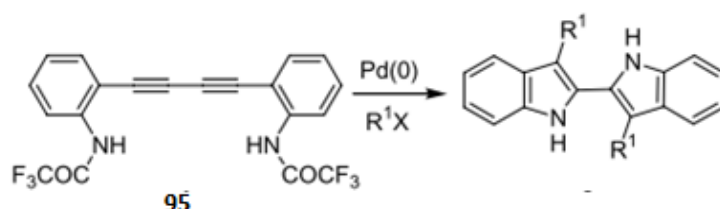
Scheme 51: Larock-like Pd-catalyzed synthesis of 3,3'-disubstituted 2,2'-biindoles.

11.1.1.1. Synthesis of Ind$_2$Ph$_2$T$_4$ compounds

Concerning the synthesis of Ind$_2$Ph$_2$T$_4$ compounds, the coupling partner for **95** in Larock-like ring closure reaction is 5-(4-bromophenyl)-2,2'-bithiophene **99**. Its synthesis was achieved successfully by chemoselective Suzuki-Miyaura cross coupling reaction starting from *p*-iodobromobenzene (Scheme 52). An analogous approach was reported in literature exploiting a Stille coupling method.[199]
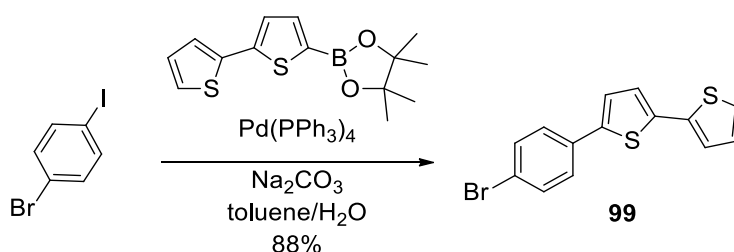
Scheme 52: synthesis of halide **99**.

Trifluoroacetamide **95** on the other hand, was obtained in two steps synthesis starting from commercially available 2-iodoaniline. The latter underwent a Sonogashira Pd-catalyzed reaction in the presence of ethynyltrimethylsilane (TMSA) and copper(I) iodide in TEA as a solvent. Corresponding 2-alkynyl aniline product was not isolated and, after deprotection of the TMS group by action of KF, was subjected to a Glaser coupling by O$_2$ oxidation to afford compound **94**.[185] Acylation of the latter with trifluoroacetic anhydride provided starting material **95**.[200] Trifluoroacetyl group is crucial for the subsequent Larock indolization reaction, since it

reduces aniline nitrogen atoms nucleophilicity directing palladium catalyst to selective alkyne binding to promote both indole rings closure.[74]

The bromoderivative **99** was then involved in Larock cyclization (Scheme 53) with trifluoroacetamide **95**. However, modest yield was detected probably due to scarce reactivity of an aromatic bromide than an aromatic iodide, generally employed in these reactions. This trend was noticed already by Abbiati.[74] Standard MeCN solvent for this reaction has been replaced with DMF for **99** solubility issues: no reaction was in fact detected using MeCN.
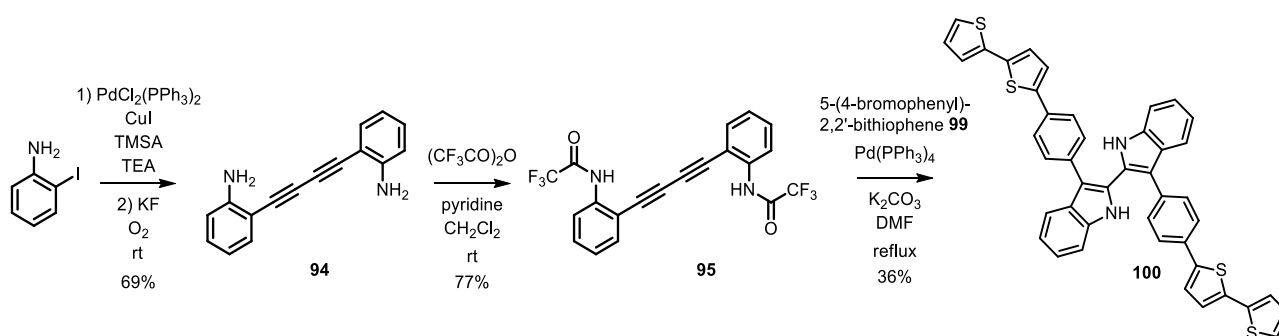
Scheme 53: synthesis of Ind$_2$Ph$_2$T$_4$ **100**.

Once isolated Ind$_2$Ph$_2$T$_4$ **100**, the alkylation step was performed with ease (Scheme 54). Three different compounds **101-103** with different solubility properties have been obtained by varying alkyl chain length. In particular, chirality of **102** and **103** is underlined by ^{1}H-NMR as alkyl protons (N-CH$_2$ portion in particular) show diastereotopic pattern (Figure 42). **101** is slightly soluble in DCM, whilst **102** is completely soluble in DCM and EtOAc. Hexylated compound **103** shows excellent solubility even in diethyl ether.
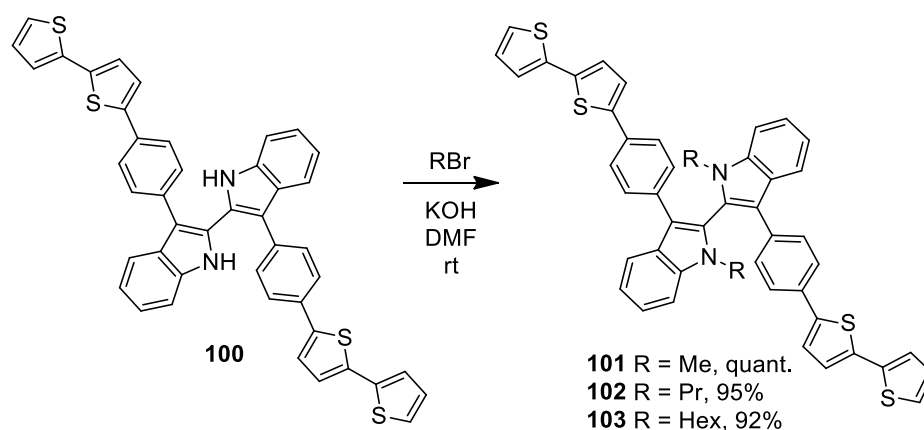
Scheme 54: alkylation of Ind$_2$Ph$_2$T$_4$. (*N*-Me)Ind$_2$Ph$_2$T$_4$ **101** was obtained by alkylation with iodomethane.
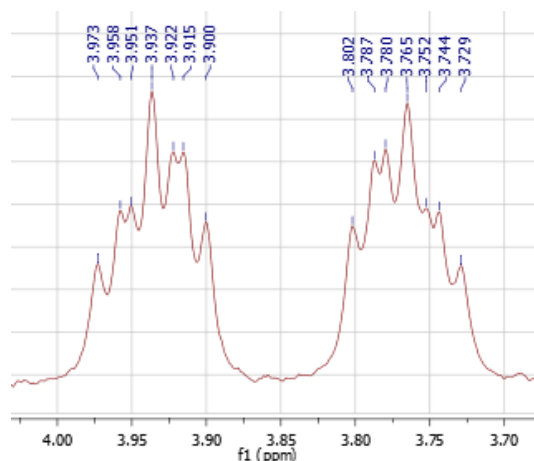
Figure 42: N-CH$_2$ protons pattern for (N-Pr)Ind$_2$Ph$_2$T$_4$ **102**.

11.1.1.2. Synthesis of (N-Pr)Ind$_2$T$_6$ compound

(N-Pr)Ind$_2$T$_6$ compound **106** was afforded with the same synthetic strategy too. Iodide **104** was obtained by classical iodination reaction with NIS in quantitative yield[201] (Scheme 55).
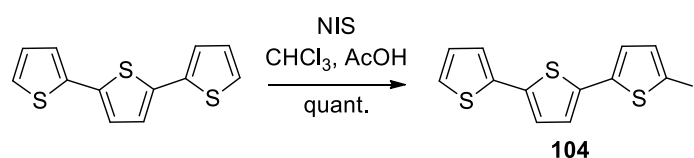
Scheme 55: synthesis of halide **104**.

Employment of heteroaryl iodide **104** was expected to produce better yield in Larock-like cyclization than previously observed for the synthesis of compound **100**. However, either trials with DMF and MeCN didn't show any difference in yielding Ind$_2$T$_6$: compound **105** was afforded in 35% yield in both cases and fully characterized from analytical and spectroscopical point of view. The details of synthetic route to **105** is reported in Scheme 56.
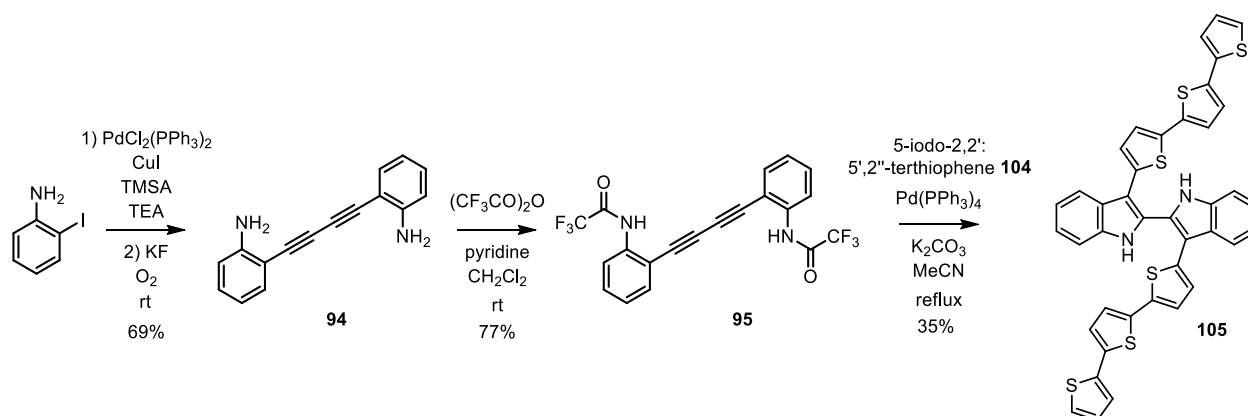
Scheme 56: synthesis of Ind$_2$T$_6$ **105**.

Alkylation with 1-bromopropane of **105** provided with excellent yield compound (*N*-Pr)Ind$_2$T$_6$ **106** (Scheme 57). Its chirality was another time underlined by diastereotopic behaviour of alkyl protons in ^{1}H-NMR spectrum. In this case, only propylation reaction was accomplished as Pr group represents a good solubility compromise between methyl and hexyl, as noticed for Ind$_2$Ph$_2$T$_4$ family.

All the compounds were obtained as racemates and resolved into antipodes by chiral HPLC by Dr. Roberto Cirilli (Istituto Superiore di Sanità, Rome).
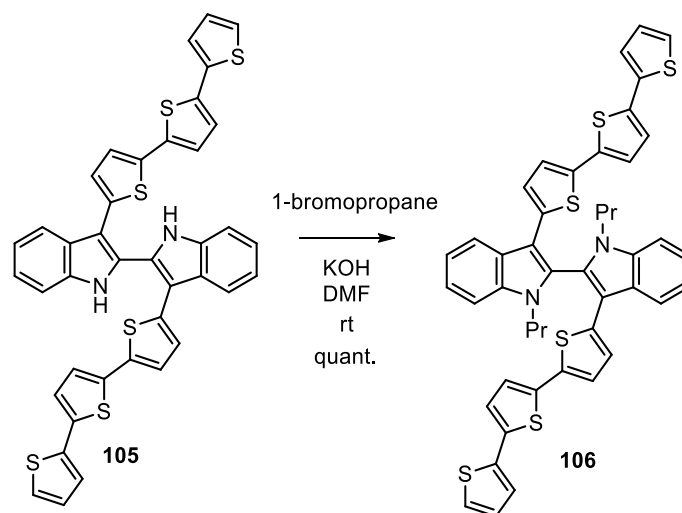
Scheme 57: synthesis of (*N*-Pr)Ind$_2$T$_6$ **106**.

11.1.2. Effects of π spacer introduction on spectral and electrochemical properties of 2,2'-biindole-based electroactive films

All the experiments presented in this section were performed in collaboration with prof. Sabine Ludwigs research group.

11.1.2.1. Monomers characterizations

Racemate compounds **98**, **102** and **106** were chosen for a comparative study of the role of the spacer introduction on 2,2'-biindole based monomers. First, they show the same propyl chain on nitrogen atom for a cleaner comparison; secondly, propyl group affords a good compromise in terms of monomer solubility and oligomeric film adherence on electrode surface. Actually, a too short alkyl chain may provide insoluble monomers difficult to be processed, whilst too long may permit resulting oligomeric film dissolution in any organic solvent.

The absorption spectra of monomer compounds **98**, **102** and **106** are reported in Figure 43; the characteristic λ$_{max}$ and extinction coefficient ε are reported in Table 11. The absorption spectra of compounds **98** and **102** appear very similar in shape with only small variations of the λ$_{max}$. In general, the λ$_{max}$ are comparable with tabulated literature values for π - π* transitions of bithiophene and terthiophene units.[202] More precisely, the observed transitions are intra-molecular charge transfer transition (ICT) from the π system of the pyrrole

ring of the core to the π* of the oligothiophene wing as evidenced by DFT calculation[185]. Considering the modification of the thienyl arms with introduction of different π spacers a systematic red-shift with increase of the conjugation from (N-Pr-Ind)$_2$T$_4$ **98** to (N-Pr-Ind)$_2$T$_6$ **106** is observed (31 nm). The introduction of a phenyl spacer also induces a less drastic increase of the absorption maximum in comparison to the addition of a thienyl unit (9 nm); this is regarded as consequence of a less efficient conjugation of the phenyl unit[203].
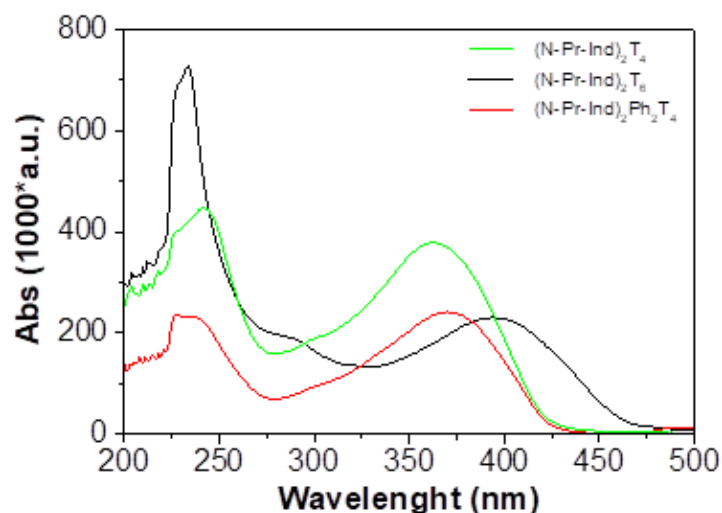
Figure 43: UV-Vis spectra of molecules **98** (N-Pr-Ind)$_2$T$_4$, green curve, **106** (N-Pr-Ind)$_2$T$_6$, black curve, and **102** (N-Pr-Ind)$_2$Ph$_2$T$_4$, red curve.

For all three molecules the cyclic voltammetry pattern are defined by multiple peak-sets as consequence of the molecular structure and particularly, of the molecular symmetry, which results in the presence of two equivalent partially interacting pyrrole (Pyr) oligo-thiophene (T$_2$; PhT$_2$ and T$_3$) redox sites (Figure 44 and Figure 45). Considering the structural differences between the molecules, a first set of two peaks is observed for the first oxidation of the two interacting radical cations of the PyrT$_2$, PyrPhT$_2$ and PyrT$_3$ moieties. Supported by previous calculations, and by the fact that no oligomerization is possible by oxidation around these first set of peaks, the first oxidation should be localized on the more electron-rich pyrrole moiety with only partial delocalization on the oligo-thiophene system. The electrochemical behaviour of this class of molecules is extremely dependent on the nature of the solvent. In a previous work, it was found that the observed peak splitting is strongly dependent on solvent polarity; indeed, the use of a solvent such as CH$_3$CN having a higher dipolar moment (charge screening ability) than CH$_2$Cl$_2$ results in the twin peak merging. This fact, together with the solvatochromism observed in UV-Vis experiments, hints to a charge transfer character of the transitions between the electron-rich biindole core and the thiophene wings[185].

The second set of peaks obtained by polarizing the working electrode (WE) at more positive potentials corresponds to the activation of the thiophenes terminals. This oxidation leads in CH$_2$Cl$_2$ to the deposition of an electroactive film by the coupling of the so generated radical cations, generating oligomers of higher order which nucleate on the electrode surface. Also in this case, the choice of a more polar solvent such as CH$_3$CN

stabilizes the formed charged species and no oligomerization process is observed[204]. Examples of solvent influence on the radical-cation reactivity towards dimerization can be found in the literature[185,205].
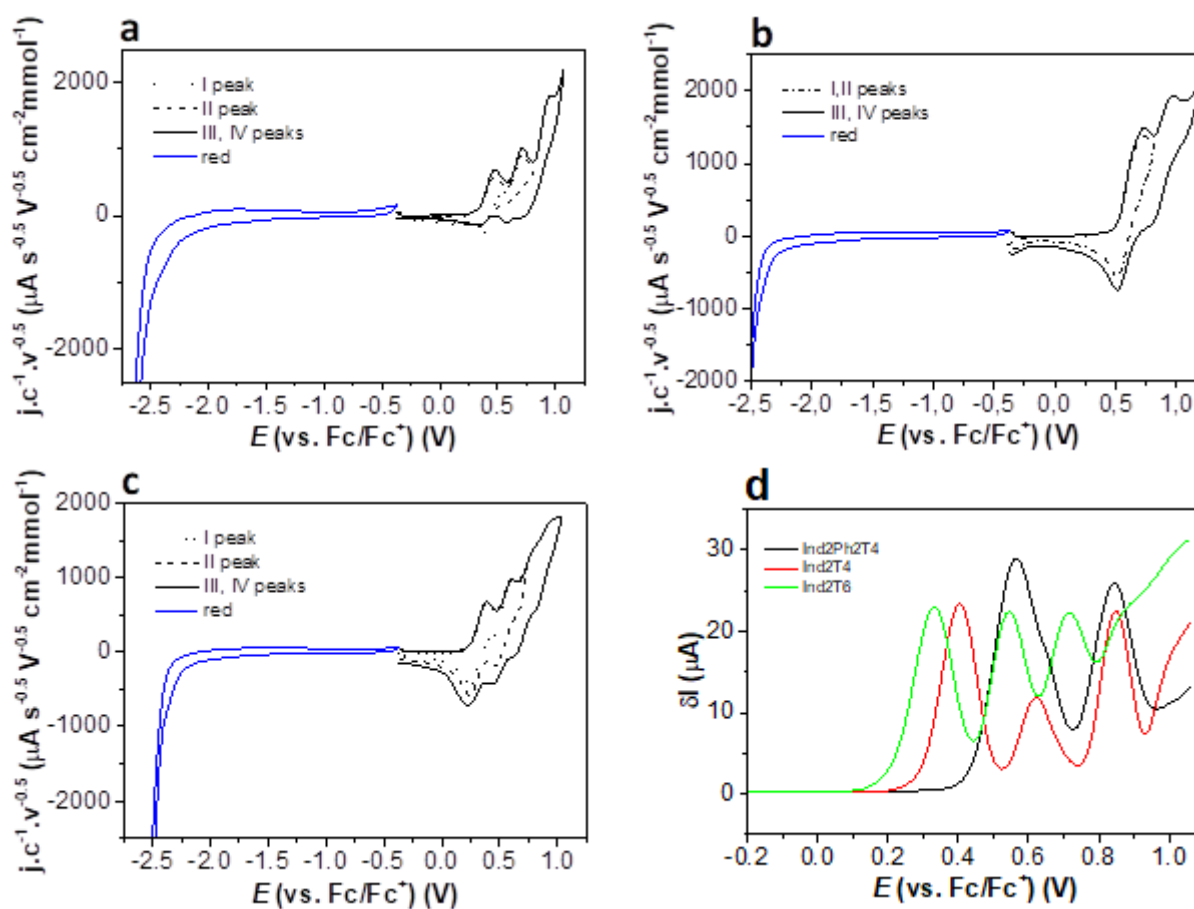
Figure 44: cyclic voltammetry of a) **98**, b) **106** and c) **102** d) different pulse voltammetry (DPV) of the three species in CH$_2$Cl$_2$/NBu$_4$PF$_6$ 0.1M at a scan-rate of 200 mV/s, monomer concentration 0.5 mM, ITO electrode.
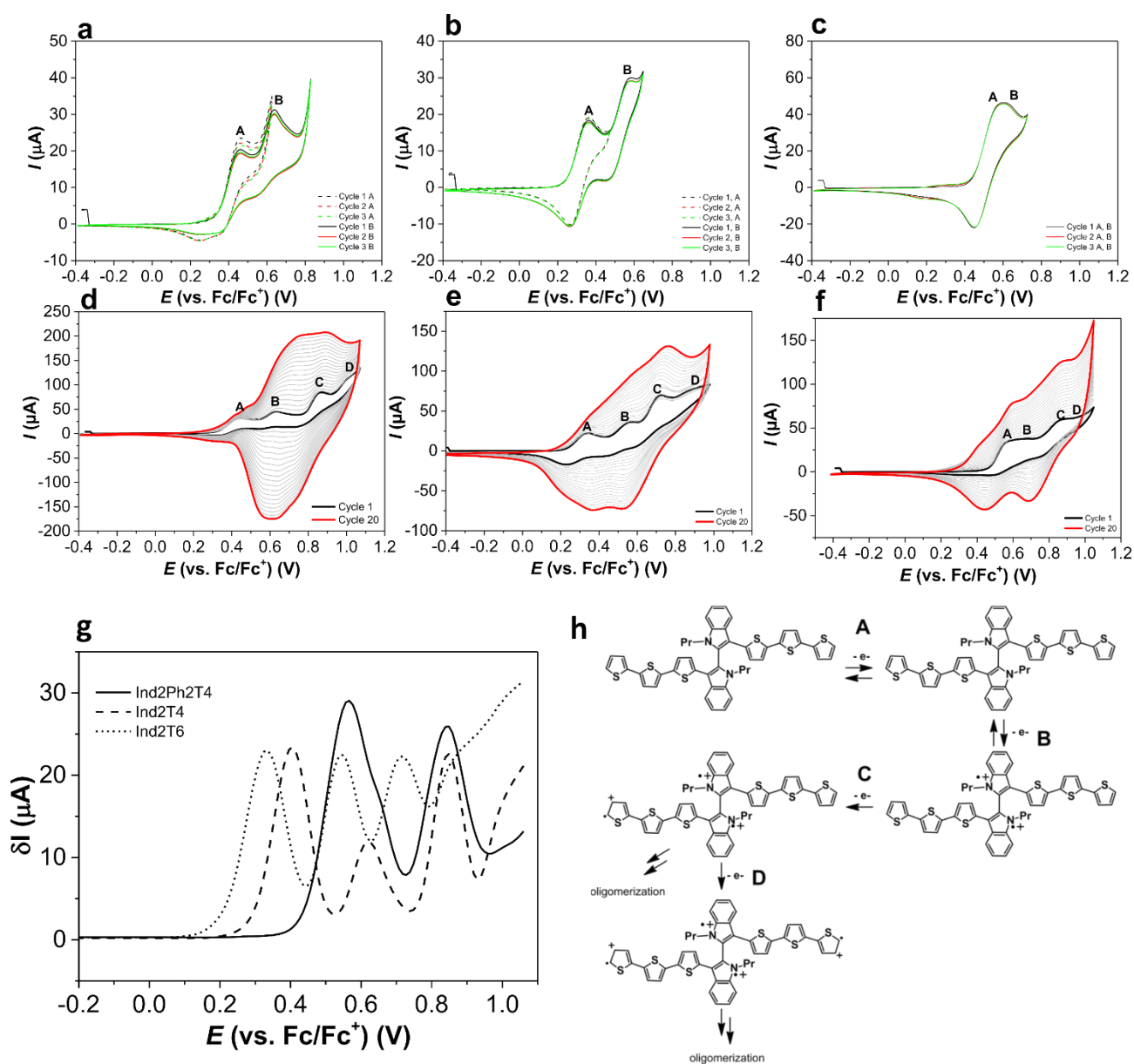
Figure 45: cyclic voltammetry of a) **98**, b) **106** and c) **102** in CH₂Cl₂/NBu₄PF₆ 0.1M at a scan-rate of 20 mV/s; multiple cycles around the first (A) and second (B) peaks of oxidation. Electrodeposition of d) **98**, e) **106** and f) **102** by multiple cycles around the III (C) and IV (D) oxidation peaks. Scan-rate 20 mV/s; monomer concentration 0.5 mM, ITO electrode. g) Different pulse voltammetry (DPV) of the three species in the oxidation sweep at 20 mV/s, voltage amplitude (dE) of 25 mV. h) Oxidation scheme exemplified for compound **106**.

The lower oxidation potential for the oxidation of **106** respect to **102** and **98** good correlates the increasing conjugation of the terthiophene respect to the bithiophene units. The oxidation potentials of **98** and **102** are found to be very similar, indeed for the oxidations localized on the biindole core of **98** (0.40 V, 0.62 V) and **102** (0.56 V, 0.66 V). The oxidation involving the reactive thiophene alpha terminals for **98** is measured at 0.85 V and in the case of **102** at 0.86 V. The IV peak associated to the chemically irreversible activation of the terminal thiophenes can be clearly distinguished in the case of **106**. Data are resumed in Table 11.

Molecule	λ_{max} (nm)	ε (L·mol^{-1}·cm^{-1})	$E^{1/2}$ from DPV (V vs Fc/Fc$^+$)			
			I ox	II ox	III ox	IV ox
98	364	44286	0.40	0.62	0.85	0.98
102	373	36400	0.56	0.66	0.86	1.00
106	395	17958	0.33	0.55	0.72	0.86

Table 11: half wave potential *(*E$^{1/2}$) calculated from previous experiments on ITO electrode.

11.1.2.2. Electrooligomerization

Electrodeposition was performed in CH$_2$Cl$_2$/NBu$_4$PF$_6$ 0.1 M, 0.5 mM racemate monomer solutions by subsequent potentiodynamic cycles around the peaks associated with activation of the thienyl alpha terminals of the molecules (Figure 45). The film growth appears for all the species rather regular with a reversible CV pattern also after a higher number of cycles (Figure 45). The electrodeposition of **98** seems to lead to a steadier growth as higher current densities are measured in comparison with **102** and **106**. This result might be explained by the higher reactivity of the monomer due to its lower conjugation and the fact that higher turning potentials are necessary for the deposition[204].

Due to the presence of the atropoisomeric scaffold the efficient conjugation length between the two symmetric units of the molecule is limited and the electroactive film should be regarded as a redox film[206]. If no oxidation at the terminal thiophene α positions are taking place, the electrodeposited film should be constituted by a series of oligomers with the same conjugation length namely oligo-(*N*-Pr-Ind)$_2$T$_4$; oligo-(*N*-Pr-Ind)$_2$T$_6$ and oligo-(*N*-Pr-Ind)$_2$Ph$_2$T$_4$ in the form of opened and closed oligomers[169,185]. The exact composition of this mixture might variate depending on the deposition conditions (scan-rate, monomer concentration, substrate nature); unfortunately, a direct determination of the latter was not possible but is expected from theoretical calculation similarly to dibenzothiophene atropoisomeric compounds[207]. After electrodeposition, the samples were carefully rinsed with dichloromethane to remove excess of monomer and electrolyte, dried and stored in inert atmosphere[208]. All electrodeposited films present upon cycling a good charge reversibility (> 90%). The electroactive films were subjected to multiple oxidative cycles (100 cycles at a scan-rate of 200 mV/s) showing good stability with almost absent loss of electroactivity after several charge/discharge processes.

11.1.2.3. UV-Vis-NIR spectroelectrochemistry

The UV-Vis NIR spectroelectrochemical characterization of the electrodeposited film has the aim to investigate charged state specification as a function of the working electrode potential. *In situ* UV-Vis-NIR spectroelectrochemical data of oligo-(*N*-Pr-Ind)$_2$T$_4$ are presented in *Figure 46*. The electrodeposited film presents in the neutral state a band with maximum 425 nm with two shoulders at 569 nm and 980 nm. Upon increasing the oxidation potential, the intensity of the neutral band decreases with concurrent increase of a broad band

with three characteristic maxima at 569 nm; 980 nm and 1289 nm. Interestingly, despite the limited conjugation of the material and in contrast to the other analyzed film, no isosbestic points are found for the different states of oxidation.

The *in-situ* absorbance variation at the above max wavelengths was plotted as function of the electrode potential and current (accounted for the black CV curve), in order to monitor the relative distribution of the above states of charge. Although, not necessarily different states of charge of the same material do have similar extinction coefficients. The blue and red curves represent the peak absorption variation for the neutral (425 nm) and oxidized state (569; 980 and 1289 nm) respectively. The potential dependent peak-absorption is characterized by a step-like variation of the absorbances for the neutral (blue line) and oxidized state (red lines) which correlates well with the redox peaks in the CV experiment. A first change of absorption is observed concurrently with the first absorption peak (oxidation localized on the biindolic core) with an onset for the absorption variation at 0.16 V coinciding with the electrochemical onset up to 0.49 V in the forward scan.

In contrast to the other two analyzed systems, oligo-(N-Pr-Ind)$_2$T$_4$ does not present a characteristic transient absorption state with maximum for the radical cation/dication transition for the oligothiophene redox center.

The peak trend also hints to a limited discharging ability of the oligo-(N-Pr-Ind)$_2$T$_4$ in the analyzed electrolyte. Comparing the film absorption before and after the charge/discharge process, the electroactive film does not recover the initial absorption measured for the neutral state resulting partially oxidized indicatively at the level of the first oxidation peak (biindole core oxidation).

Electrodeposited oligo-(N-Pr-Ind)$_2$T$_6$ films (Figure 46) are characterized by an absorption maximum in the neutral state (blue curve) at 452 nm. Upon polarizing the WE to values more positive than 0.14 V, which coincides with the electrochemical onset, the neutral band (452 nm) progressively bleaches with concurrent formation and increase in intensity of two bands at 713 nm and 1278 nm. These bands are assigned to the radical-cation and dication state localized on the T$_6$ moieties of oligo-(N-Pr-Ind)$_2$T$_6$. The middle-energy band with maximum 713 nm reaches an absorption maximum during the forward oxidation scan at ca. 0.6 V, between the second and third couple of redox waves identifiable in the CV signal. Upon potential values superior to the 0.52 V (second redox wave) the low-energy band with maximum 1278 nm broadens, showing absorption also in the spectral region of 750-1000 nm. To follow this variation, absorption was sampled as function of the potential at wavelength of 902 nm. Oligo-(N-Pr-Ind)$_2$T$_6$ film is characterized by different isosbestic points within different states of charge: 539 nm for the N/R$^{+\cdot}$ redox couple, whereas for the redox couple R$^{+\cdot}$/D^{2+} the following isosbestic points are found 512 nm; 629 nm; 763 nm. Oligo-Ind$_2$T$_6$ can be reversibly oxidized over several cycles, without loss of absorption properties.

In situ spectroelectrochemistry of oligo-(N-Pr-Ind)$_2$Ph$_2$T$_4$ in 0.1 M CH$_2$Cl$_2$/NBu$_4$PF$_6$ is presented in *Figure 46*. In the neutral state, the film is characterized by an absorption maximum at 412 nm. Upon increase of the oxidation potential the neutral band (412 nm) bleaches with concurrent formation of two bands at 743 nm and 1122 nm respectively, which are assigned to the radical cation state localized on the Ph-T$_4$-Ph units. Upon further increase of the oxidation potential during the forward scan, the band at 743 nm reaches its maximum of absorption at a potential value of 0.68 V. In correspondence with the third redox wave, the film absorption further changes, showing a broadening of the low-energy band also in the spectral region of 800-1000 nm (λ 929 nm sampled for absorptogram). The potential dependent peak-absorption is analyzed, sampling the maxima for the neutral state (412 nm; blue line), radical cation state (743 nm and 1122 nm; green lines) and dication state (929 nm; red line). The onset for the absorption change is located at 0.22 V, with significant absorption changes only starting at 0.3 V in concurrence with the overlapped oxidation localized on the biindole core and radical cation oxidation on the oligo-thiophenes. The first redox signal observed for oligo-(N-Pr-Ind)$_2$Ph$_2$T$_4$ consists of a small reversible couple of peaks at E$^{1/2}$ 0.14 V. The absorption at 929 nm increases up to 0.68 V during the forward scan of oxidation, this value well matches the simultaneous oxidation of the indoles centers and the Ph-T$_4$-Ph units to their radical cation state at E$^{1/2}$ 0.47 V. The potential value 0.68 V coincides for the forward scan of oxidation with the abrupt increase in absorption of the wavelength 929 nm during the redox event and is associated with the oxidation Ph-T$_4$-Ph units to the dication level. All parameters are resumed in Table 12.

	E$^{1/2}$ vs Fc/Fc$^+$ (V)				λ$_{max}$ (nm)	
	I ox	II ox	III ox	N	R$^{+\bullet}$	D^{2+}
oligo-(N-Pr-Ind)$_2$T$_4$	0.31	0.54	0.75	425	569; 980; 1289 *	
oligo-(N-Pr-Ind)$_2$Ph$_2$T$_4$		0.47	0.74	412	606; 743	545; (929); 1227
oligo-(N-Pr-Ind)$_2$T$_6$	0.20	0.39	0.58	452	713; (826)	575; (902); 1278

Table 12: E$^{1/2}$ from electrochemical doping of the redox films and characteristic wavelengths for different states of charge from spectroelectrochemical experiments.
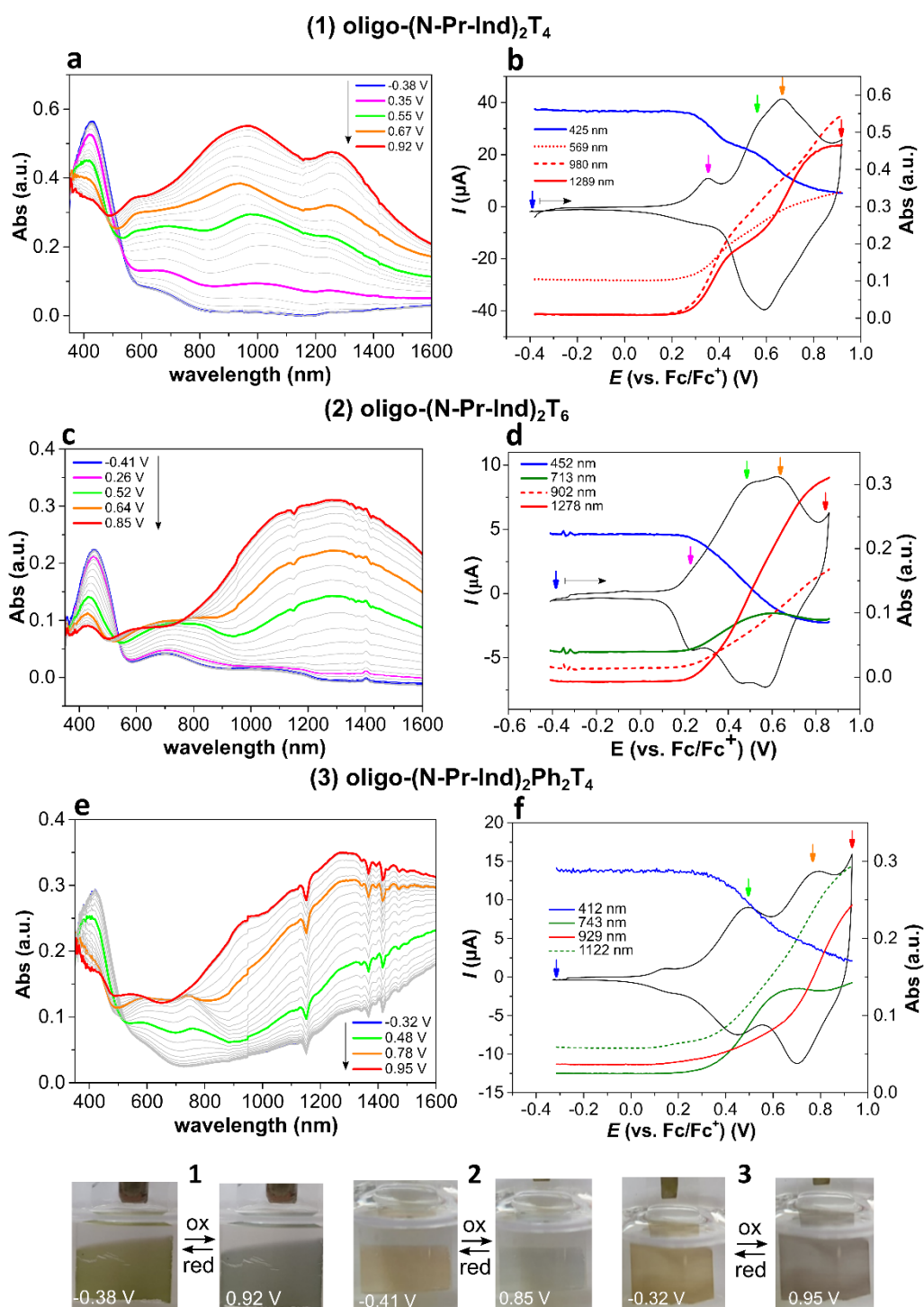
Figure 46: UV-Vis-NIR spectroelectrochemical measurements registered during the forward oxidation cycle at a scan-rate of 20 mVs^{-1} in 0.1 M CH$_2$Cl$_2$/NBu$_4$PF$_6$. Absorption spectra and peak variation of (a, b) oligo-(*N*-Pr-Ind)$_2$T$_4$; (c, d) oligo-(*N*-Pr-Ind)$_2$T$_6$ and (e, f) oligo-(*N*-Pr-Ind)$_2$Ph$_2$T$_4$. Pictures of the redox films in their neutral and charged state are also presented (bottom).

All electrodeposited oligo(*N*-Pr-Ind)$_2$(spacerT$_2$)$_2$ films are characterized at the neutral state after deposition, by similar patterns of absorption (*Figure 46*). The λ$_{max}$ in the case of oligo-(*N*-Pr-Ind)$_2$T$_6$, characterized by the highest conjugation length, was found at 452 nm; while oligo-(*N*-Pr-Ind)$_2$T$_4$ showed maximum at 425 nm and in the case of oligo-(N-Pr-Ind)$_2$Ph$_2$T$_4$ at 412 nm. In all cases, a red-shift was found upon electrodeposition due to the increased conjugation; this red-shift from monomer to electrodeposited film is more pronounced in

the case of oligo-(N-Pr-Ind)$_2$T$_6$ (57 nm) with respect to oligo-(N-Pr-Ind)$_2$Ph$_2$T$_4$ (42 nm). Interestingly, the introduction of the phenyl spacers causes a blue-shift in oligo-(N-Pr-Ind)$_2$Ph$_2$T$_4$ with respect to oligo-(N-Pr-Ind)$_2$T$_4$ variation which becomes even more pronounced for the electrodeposition products. This experimental observation could be a result of the steric hindrance introduced by the phenyl units, limiting planarity and causing a loss in the conjugation efficiency. Torsion along the oligomer backbone is, among others, a parameter influencing conjugation efficiency; a distortion of the conjugated backbone leads to a decrease in the effective conjugation by decrease of the overlap between consecutive rings, causing an increase of the ionization potential[203,209]. In addition to characteristic neutral band, all the samples as obtained after electrodeposition are characterized by two shoulders at 700 and 1100 nm, characteristic for the radical cation absorption. This result hints to a partial oxidation of the film after electrodeposition. The same shoulder remains present, without change in intensity, also upon pre-polarization at negative potentials (-1.0 V vs Ag/AgCl for 60 s). Studies on electropolymerization of indole by Inzelt et al.[210] have revealed that during the electrodeposition a fraction of the polymer and of the monomers are overoxidized leading to non-uniform film deposition. Furthermore, the authors found that even traces of oxygen in the solution containing the monomer could lead to the oxidation of the monomer and electropolymerization.

11.1.2.4. *In situ* conductance

In situ conductance measurements are performed to analyze conductivity changes as function of the redox state of the film with reference to the nature of the π spacer. The measurements are performed using interdigitated electrodes on which the indole-films were electrodeposited. The successful coverage of the interdigitated area after electropolymerization was assured by scanning electron microscopy (SEM, Figure 47).
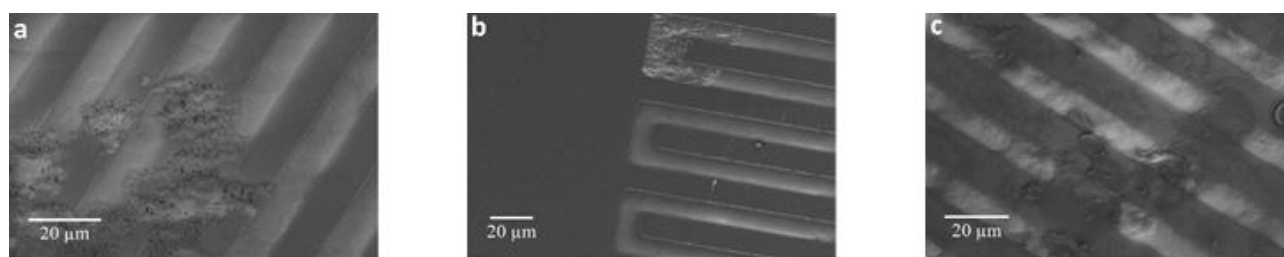
Figure 47: SEM pictures of a) oligo-(N-Pr-Ind)$_2$T$_4$; b) oligo-(N-Pr-Ind)$_2$T$_6$ and c) oligo-(N-Pr-Ind)$_2$Ph$_2$T$_4$ on 10 µm Pt-IDE electrodes. The brighter spots are associated to charging phenomena upon interactions with the electron-beam. EHT 0.6 kV; WD=1.9 mm; InLens. Pictures were obtained from a Gemini SEM500 (Zeiss).

Unfortunately, in the case of oligo-(N-Pr-Ind)$_2$T$_4$ and oligo-(N-Pr -Ind)$_2$Ph$_2$T$_4$ the drain currents from which *in situ* conductance is measured were too low to be distinguished from the background current.

In-situ conductance of electrodeposited oligo-(N-Pr-Ind)$_2$T$_6$ is presented in Figure 48.
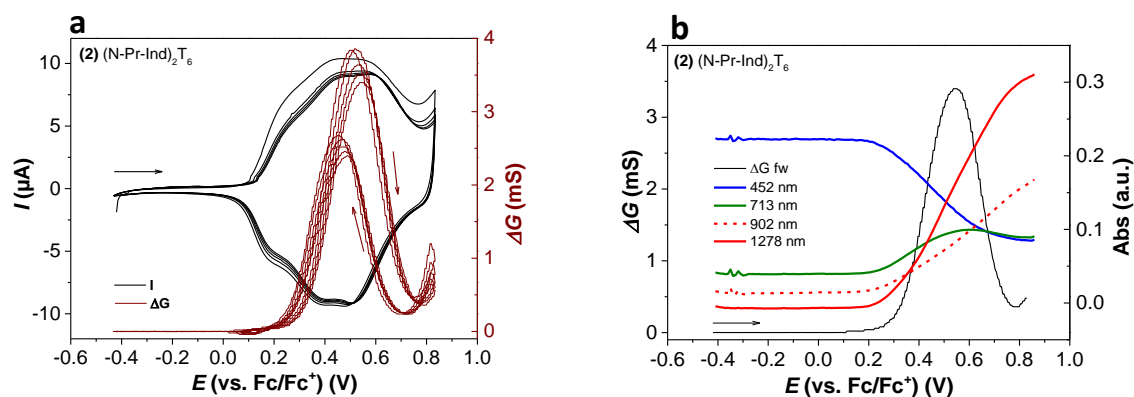
Figure 48: *in-situ* conductance plot for repeated charge/discharge cycle (left side) and overimposition with peak-absorption trend for the neutral (blue), radical cation (green) and dication (red).

The conductance onset is found in correspondence with the electrochemical onset. The main conductance maximum is localized at 0.55 V for the forward scan and 0.50 V in the backward scan of the CV cycle, in proximity of the half-wave potential for the R+• / D++ oxidation of the hexathiophene units. Further, a small conductance peak can be distinguished for the backward scan of at ca. 0.20 V, in correspondence to the oxidation of biindolic cores.

Upon these observations, the *in situ* conductance behaviour of oligo-(N-Pr-Ind)$_2$T$_6$ can also be described in terms of mixed valence conductivity (MVC). In the neutral state as well as for the dication state the films is characterized by a low conductance, whereas for potential values corresponding to the concurrent presence of radical cation and dication species localized on the T$_6$ units, the highest conductance is registered. Several overlapping redox states must be considered: open and closed oligomers (dimers, trimers, tetramers etc.) with slightly different E$^{1/2}$ causing a broadening of the conductance window, in correlation to the CV. The conductance change is mostly associated with the oxidation involving the oligo-thienyl units as the redox change N/R$^{+\cdot}$ on the biindolic unit center (first peak) is characterized only by a small change in conductance in comparison to T$_6$, observable during the discharge cycle.

This might be explained by the fact that the indole units are highly spatially separated resulting in an inefficient centers distribution for electron hopping. Overall, the conductance behaviour observed seems to follow the findings from Zotti et al[211,212]. The results also well correlate the peak-trend variation for the different redox states of the film, which find for hexathiophene units conductance sustained by a hopping mechanism of polarons and bipolarons, as observed here with introduction of further redox centers not modifying this type of behaviour.

11.1.2.5.   Conclusions

The redox behaviour of the molecules endowed with symmetric oligothienyl linked through an internal indole core allowing for a partial conjugation is characteristic of interacting equivalent redox moieties. We found

that the employment of a thienyl unit as π spacer (**106** (*N*-Pr-Ind)$_2$T$_6$) induces a shift to less positive potential values for the oxidation in comparison to **98** (*N*-Pr-Ind)$_2$T$_4$ but identical peak-to-peak separations hinting to the fact that the two molecules have similar residual interactions. In the case of the phenyl substituted molecule (**102** (*N*-Pr-Ind)$_2$Ph$_2$T$_4$), this separation is significantly lower; the results are explained by the less efficient conjugation of a Ph unit in comparison to a thienyl one. All molecules could be successfully electrodeposited; the resulting redox active films are stable upon oxidation. All films are obtained in a partially charged states as suggested by the absorption spectra of pristine films; further, electroactive films of oligo-(*N*-Pr-Ind)$_2$T$_4$ are characterized by charge-trapping upon subsequent cycling which could result from the lower conjugation of the oligomers as well as to the lower size of macrocycle cavities within the film. Overall we find that with exception of oligo-(*N*-Pr-Ind)$_2$T$_4$, the substitution of the dibenzothiophene with biindolic moieties does not induce significant variations in the absorption properties of the electrodeposited film concerning the position and topology of the bands at different states of charge. The analysis of in-situ conductance also hints to the fact that the biindole center covers only a marginal role in determine charge transport within the system; this is in fact taken over by the oligothienyl moieties as a mixed-valence conductivity behaviour between oligothienyl radical cation and dication state, similarly to results from Zotti and al[211,212].

11.1.3. HPLC enantioseparation and computational configurational stability of compounds 101-103

After having deeply elucidated electrochemical features of racemate compound **102**, studies to resolve racemates of compounds **101**-**103** ((*N*-Me)Ind$_2$Ph$_2$T$_4$, (*N*-Pr)Ind$_2$Ph$_2$T$_4$, (*N*-Hex)Ind$_2$Ph$_2$T$_4$ respectively, Scheme 53) were performed by Dr. Roberto Cirilli by chiral HPLC. In order to develop efficient and enantioselective analytical HPLC systems useful to isolate multi milligram amounts of both enantiomers, a deep screening for the optimal eluent was carried out, using the analytical 250 mm x 4.6 mm, 5 μm, Chiralpak IB column.

Different ternary mobile phases containing hexane as a hydrocarbon, an alcohol as polar phase and a solvent capable of solubilizing chiral analytes (dichloromethane, acetone or ethyl acetate) were evaluated. In each elution condition, the column temperature was changed from 5 to 45 °C, in 10 °C increments. The best results in terms of enantioselectivity was obtained using the mixtures *n*-hexane/EtOH/dichloromethane 100:1:5 (v/v/v) at 5°C. Simultaneous resolution of **101-103** obtained on the Chiralpak IB CSP monitoring simultaneously absorption and circular dicroism (CD) during chromatography is showed in Figure 49. Specific rotations of compound **101-103** are reported in Table 10.
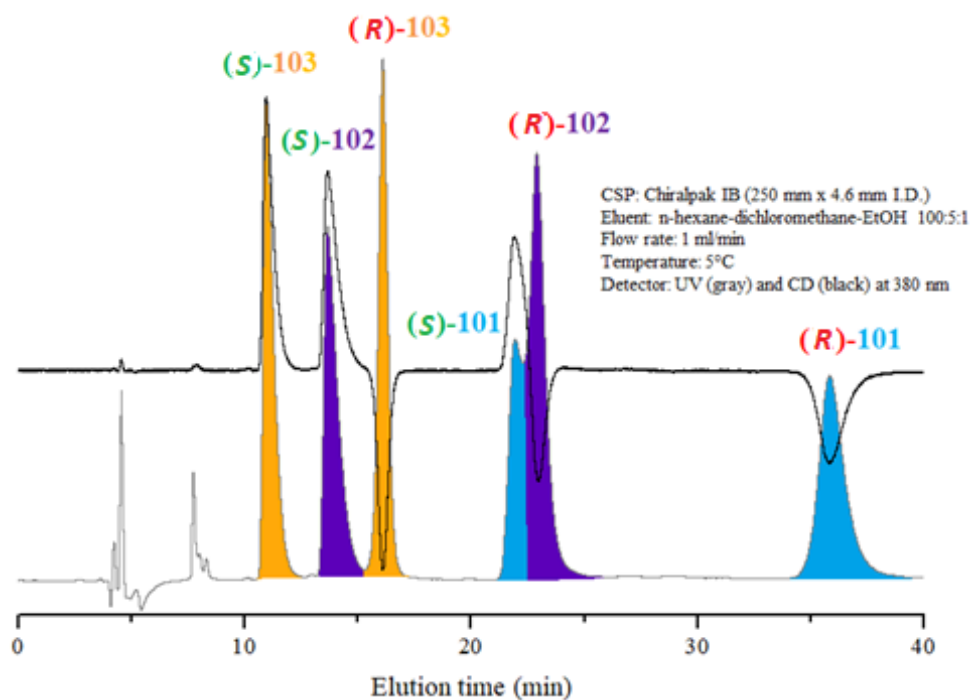
Figure 49: racemate resolution of compounds **101-103** using chiral HPLC.

	(S)-101	(R)-101	(S)-102	(R)-102	(S)-103	(R)-103
$[\alpha]^{20}_{589\,nm}$	1011	-1096	993	-990	970	-968

Table 13: specific rotations of compounds **101-103** in chloroform. Samples concentration: 0.2 mg/100mL.

As highlighted in Figure 49, at 5°C it was noticed that the enantiomer (S) is always eluted before the form (R) and the peak pertinent to the second eluted enantiomer was unusually higher and narrower than of the less retained one. In addition, the retention of the (S)-enantiomer of hexylated chiral analyte **103** was always lower than that of the homologues with a shorter alkyl chain.

After having established separation optimized conditions, next step was to scale-up them on a semipreparative scale using the 250 mm x 10 mm I.D. Chiralpak IB column. The good solubility of biindole compounds **101-103** in the dichloromethane-based mobile phase as well as the high enantiodiscrimination ability of the Chiralpak IB CSP were key factors that made possible to load onto the column mg amounts (from 5 to 10 mg) of racemic sample in a single run and obtain baseline enantioseparations (Figure 50). The enantiomeric excess of the two collected fractions was > 99% for all compounds **101-103** and the yield of the enantiomeric separations ranged between 75% and 90%.

CSP: Chiralpak IB (250 mm x 4.6 mm I.D.)
Eluent: n-hexane-dichloromethane-EtOH 100:5:1
Flow rate: 5.0 ml/min
Temperature: 5°C
Detector: UV at 380 nm
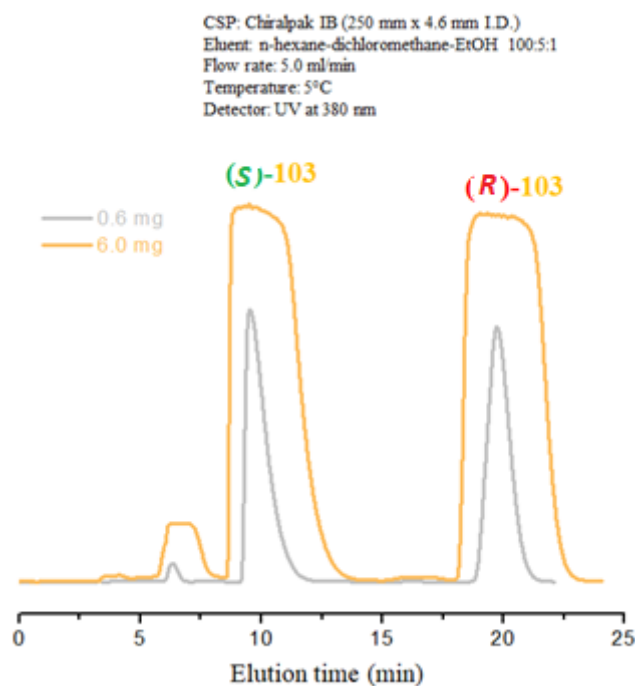
Figure 50: semipreparative separation of compound **103**.

The CD spectra of the isolated enantiomers in chloroform solution between 500 and 230 nm were recorded (Figure 51). As expected, the CD curves of enantiomers, were perfectly specular. In all cases, the first enantiomer eluted (green curves), showed a positive Cotton effect and was dextrorotatory in chloroform solution (Table 13). Same CD profile (Figure 51) and optical activity was recorded for the first eluted enantiomer on the Chiralpak IB CSP of the chiral analogue (*N*-Me-IND)$_2$T$_4$ **98**, devoid of the phenyl portion, whose absolute configuration was already determined as (*S*).[185]
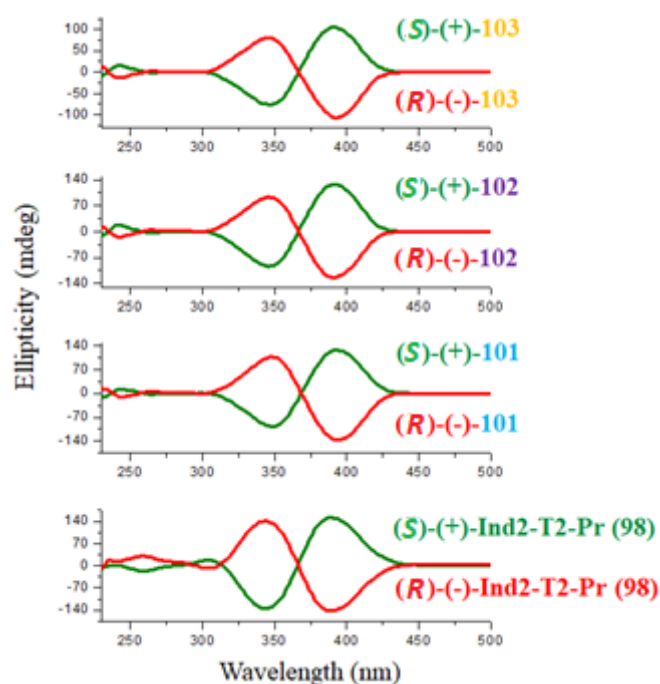
Racemization barriers of (*N*-alkyl)Ind$_2$Ph$_2$T$_4$ **101-103** were determined by DFT calculations by Dr. Sergio Rossi and revealed that the thiophenyl pendant units connected to the 2,2'-bindole scaffold are oriented in a *s*-trans conformation, in an orthogonal arrangement respect to the biindole backbone (Figure 52). Two possible transition states for racemization were located for all the three above mentioned compounds, *i.e.* **TS1**, related to a rotation process in which the two coplanar aromatic pendants face the 2,2'-bindole scaffold in a *s*-trans arrangement and **TS2**, where the two bithiophenyl chains face the biindole backbone in a *s*-cis arrangement. As found, **TS1** is generally more accessible than **TS2** and the torsional barrier around the bond interconnecting the (N-R)-indole rings, calculated by B3LYP/6-311G+(3df,3pd) // B3LYP/6-31G(d,p) level from such ground energy level, range between 24-26 Kcal mol^{-1} (Figure 52). As expected, in each aromatic pendant, the two thiophene rings adopted a *head-to-tail* (HT) configuration, which is usually preferred to a *tail-to-tail* (TT) configuration. However, since in the case of TS2 the two aromatic pendants are faced and closed together, two more transition states have been identified, where the two HT thiophene units can be oriented in a specular (**TS2a**) or in an opposite conformation (**TS2b**). Energies associate to those transition states are reported in Figure 52.

.
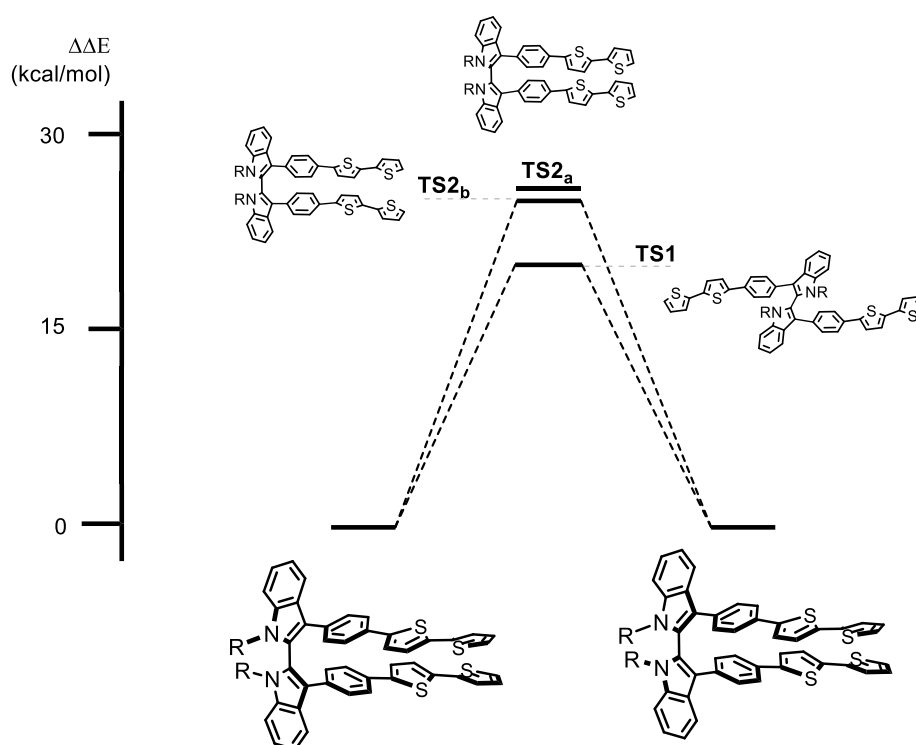
	(*N*-Me-Ind)$_2$Ph$_2$T$_4$ **101** (kcal/mol)	(*N*-Pr-Ind)$_2$Ph$_2$T$_4$ **102** (kcal/mol)	(*N*-Hex-Ind)$_2$Ph$_2$T$_4$ **103** (kcal/mol)
TS1	24.74	26.60	25.23
TS2a	29.08	34.77	33.25

TS2b	29.19	33.52	32.04
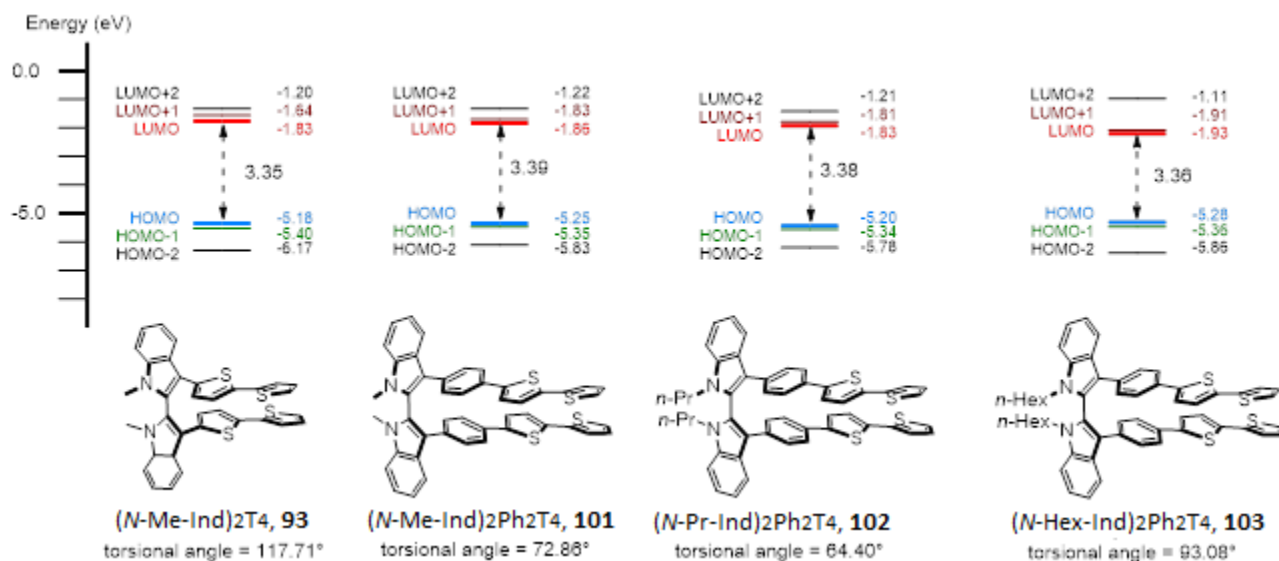
Figure 52: schematic reaction pathway for racemization of (*N*-alkyl)Ind$_2$Ph$_2$T$_4$ **101-103** with computed interconversion energies (up); molecular orbital energy levels of **93** and **101-103** (bottom).

11.1.4. Enantiorecognition tests

The availability of the antipodes of compounds **101-103** allowed the evaluation of their enantiodiscrimination abilities toward different chiral probes after their deposition as oligomeric films over glassy carbon electrode surface (as described in Figure 45). These studies were conducted in collaboration with the prof. Patrizia Mussini research group of the University of Milan. As stated before, the effect of different alkyl chains is very clear (Figure 53). Actually, increasing the length of the alkyl chain on the nitrogen atoms the efficiency of electrodeposition decreases. The monomer with Hex chain does not undergo the electrooligomerization (this could be due to an increase in solubility of the oligomeric film). On the other hand, particularly efficient and very similar is the deposition starting from the (*N*-Me)Ind$_2$Ph$_2$T$_4$ and (*N*-Pr)Ind$_2$Ph$_2$T$_4$ monomers.
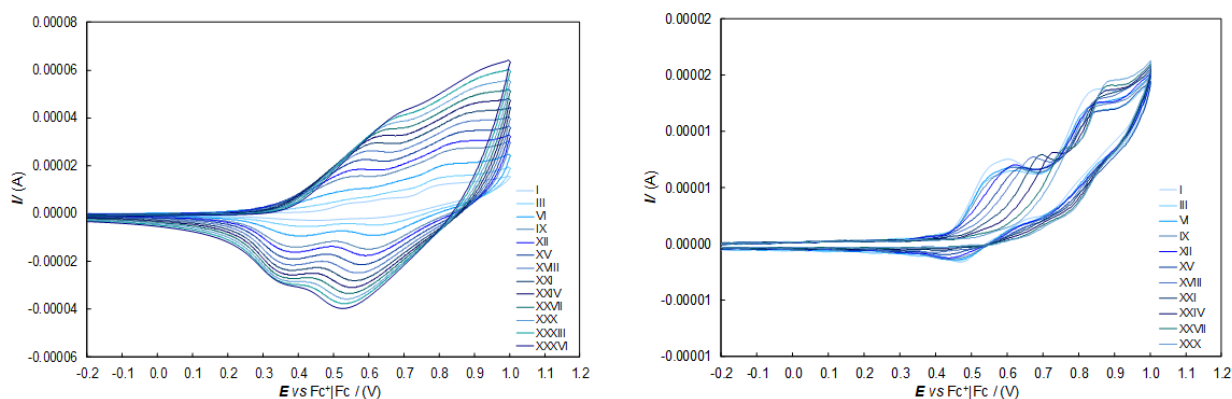
Figure 53: electropolymerization of compound **101** (left) and **103** (right), 50 mV/s, 0.00075 M monomer in CH$_2$Cl$_2$ + 0.1 M TBAPF$_6$. The latter shows no formation of electroactive film on electrode surface as current is not increasing with cycles. Compound **102** electropolymerization has been shown in Figure 45.

The enantiodiscrimination experiments were performed by Differential Pulse Voltammetry (DPV) using as chiral probe a chiral ferrocene (Figure 54), chosen on account of its facile and reversible electron transfer at a mild oxidation potential. Reproducibility tests were performed by repeatedly recording the DPV patterns of model probes on freshly deposited chiral surfaces.

FcR   **FcS**
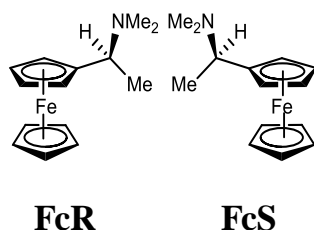
Figure 54: (*R*)-(+)- and (*S*)-(-)-*N,N′*-dimethyl-1-ferrocenylethylamine, FcR and FcS respectively.

As evident in Figure 55 and Figure 56, outstanding enantiodiscrimination in terms of peak potential difference values is obtained, with a separation of ≈ 160 mV for oligo-(*N*-Me)Ind$_2$Ph$_2$T$_4$ and ≈ 80 mV for oligo-(*N*-Pr)Ind$_2$Ph$_2$T$_4$. In fact, two quite different DPV signals, both well defined, are observed, specularly by changing the probe or the selector configurations. Moreover, using as electrode surface the oligo-(*N*-Me)Ind$_2$Ph$_2$T$_4$, we also test the racemic ferrocene, working with a 1:1 solution of FcR and FcS (as reported in Figure 55, panel c) and we obtained in two neatly separated peaks, located at potentials close to the single enantiomer ones. All experiments were performed at 0.05 V s^{-1} scan rate in 0.002 M solutions of the probe in CH$_2$Cl$_2$ + TBAPF$_6$ 0.1 M as supporting electrolyte on a glassy carbon electrode.
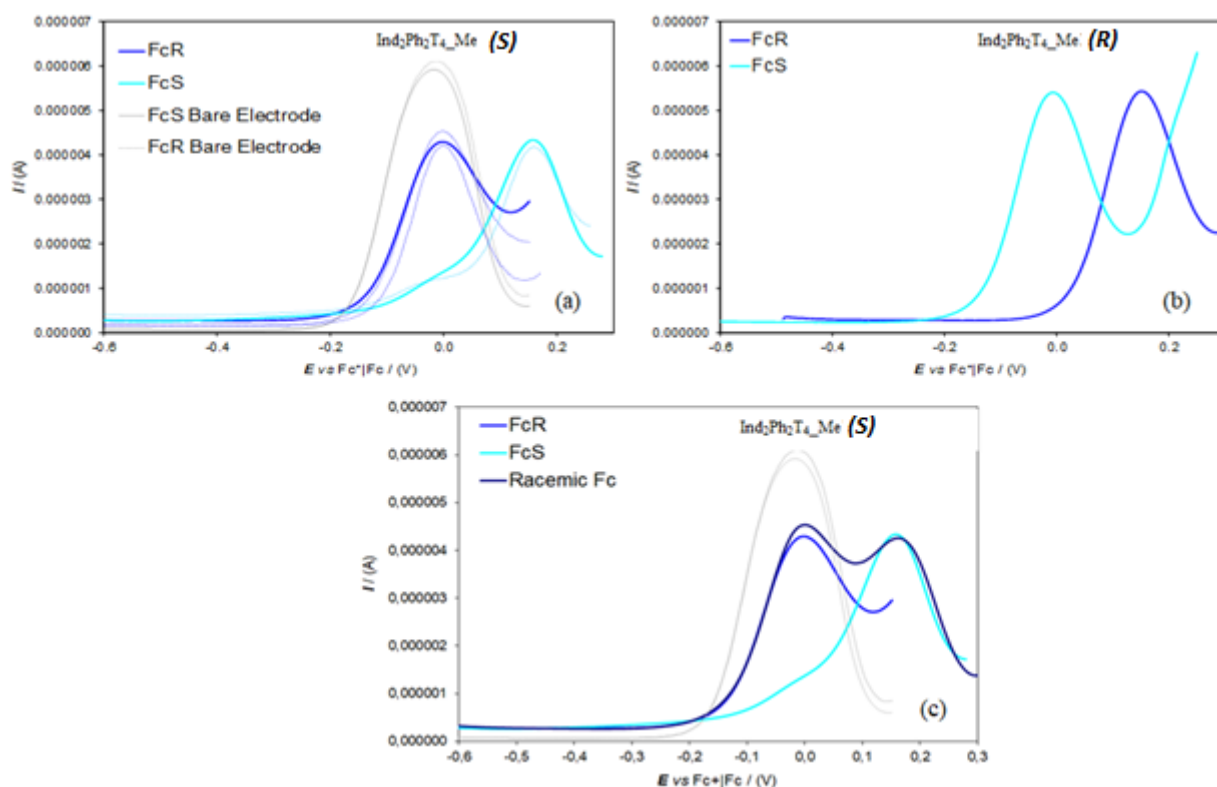
Figure 55: enantioselection performances of enantiopure oligo-(*S*)-(*N*-Me)Ind$_2$Ph$_2$T$_4$ (a) and oligo-(*R*)-(*N*-Me)Ind$_2$Ph$_2$T$_4$ (b) electrode surfaces towards chiral electroactive ferrocenyl probes, named FcR and FcS (in grey are reported the signals of FcR and FcS

recorded on bare glassy carbon (GC) electrode). In (c) is also reported the DPV pattern of racemic ferrocene. DPV patterns were recorded at 0.05 V s^{-1} potential scan rate.
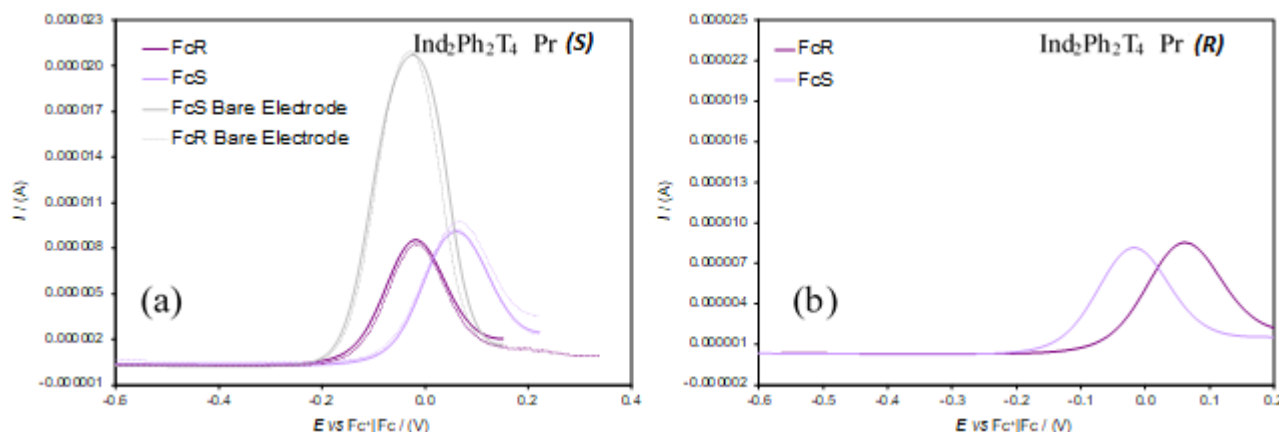
Figure 56: enantioselection performance of enantiopure oligo-(*S*)-(*N*-Pr)Ind$_2$Ph$_2$T$_4$ (a) and oligo-(*R*)-(*N*-Me)Ind$_2$Ph$_2$T$_4$ (b) electrode surfaces towards chiral electroactive ferrocenyl probes, named FcR and FcS (in grey are also reported the signals of FcR and FcS recorded on bare GC electrode). DPV patterns were recorded at 0.05 V s^{-1} potential scan rate.

Experiments were also carried out, using a modified electrode surface with oligo-*(S)-(N*-Me)Ind$_2$Ph$_2$T$_4$**,** with mixed enantiomer solutions in asymmetric ratios (Figure 57); measurements confirmed that the two peaks correspond to the same enantiomers as in the single experiments.
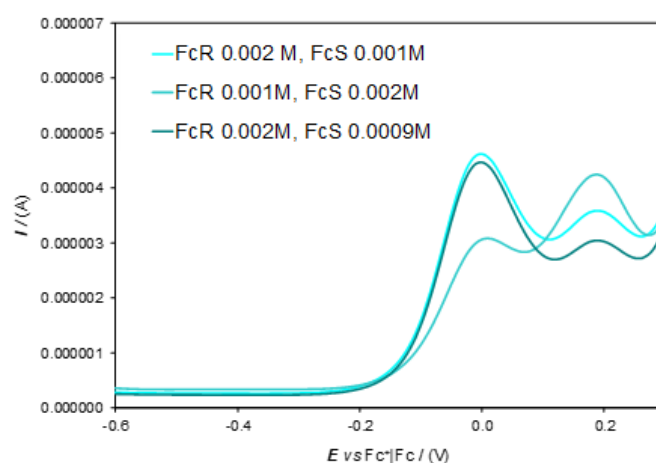
Figure 57: DPV patterns of FcR (0.002-0.001 M) and FcS (0.002-0.0009 M) mixed solutions on GC electrode modified with oligo-(*S*)-(*N*-Me)Ind$_2$Ph$_2$T$_4$.

Enantiodiscrimination experiments were performed also using the enantiomers of terazosin, a probe of pharmacological interest used to treat symptoms of an enlarged prostate and high blood pressure (Figure 58). The enantiodiscrimination tests were performed by CV experiments at 0.05 V s^{-1} scan rate in 0.003 M solutions of the enantiopure chiral probes (Ter (*S*) and Ter (*R*)) in commercial pH 4 buffer (Fluka, prepared with citric acid, NaOH, and NaCl). In this case the optimal conditions to test this probe is to electrooligomerize the enantiopure (*N*-Me)Ind$_2$Ph$_2$T$_4$ or (*N*-Pr)Ind$_2$Ph$_2$T$_4$ performing only 20 CV cycles at 0.2 V s^{-1}. Reproducibility

tests were performed by repeatedly recording the CV patterns of model probes on freshly deposited chiral surfaces.

Preliminary tests were carried out recording CV signals of Ter (*S*) and Ter (*R*) on bare GC electrode in Buffer pH 4 (Figure 58), showing a single first irreversible oxidation peak (E_{pa} ≈ 0.96 V *vs* SCE) and, as expected, they are practically overlapped for the two enantiomers. Instead, modifying the electrode surface with enanti-opure oligo-(*N*-Me)Ind$_2$Ph$_2$T$_4$ or oligo-(*N*-Pr)Ind$_2$Ph$_2$T$_4$ a good peak potential separation was obtained of ≈ 80 mV for oligo-(*N*-Me)Ind$_2$Ph$_2$T$_4$ (Figure 59), with specular results by changing the configuration of the inher-ently chiral monomer, and of ≈ 40 mV for oligo--(*N*-Pr)Ind$_2$Ph$_2$T$_4$ (Figure 59).
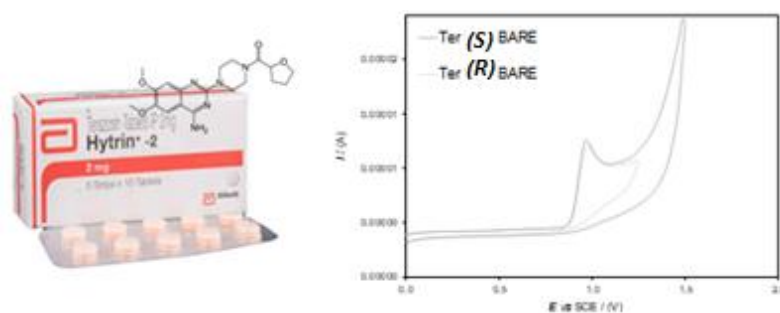
Figure 58: chemical structure of terazosin (left side) and CV signals of the enantiomers of terazosin on bare glassy carbon electrode.
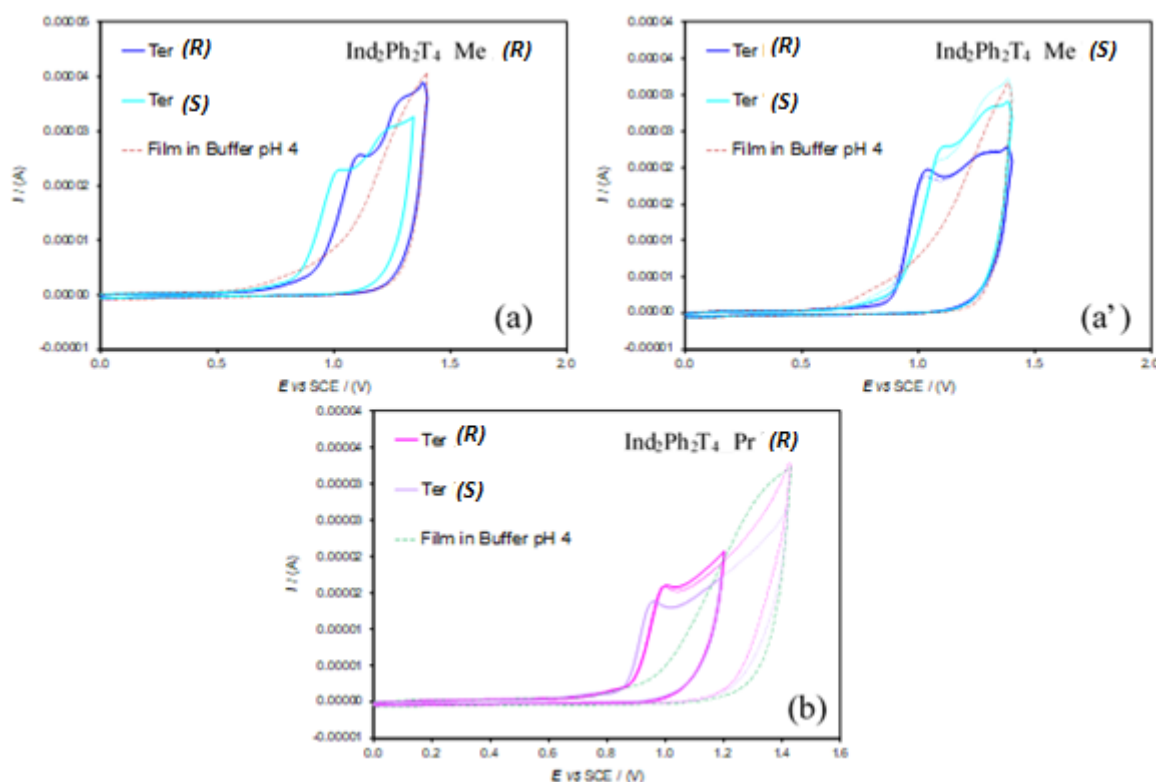
Figure 59: enantioselection performance of enantiopure oligo-(*S*)-(*N*-Me)Ind$_2$Ph$_2$T$_4$ (a) and oligo-(*R*)-(*N*-Me)Ind$_2$Ph$_2$T$_4$ (a') or oligo-(*R*)-(*N*-Pr)Ind$_2$Ph$_2$T$_4$ (b) electrode surfaces towards the enantiomers of terazosin. CVs were recorded at 0.05 V s^{-1} potential scan rate. All the graphs also show the stability cycle of the electrodeposited film in buffer pH = 4.

Considering the film stability CV patterns in Figure 59, at such potential, films should be still uncharged. However, it must be taken into account that probe/film interactions can modify film activation conditions; this points to significant differences in the electron transfer mechanism and follow-up, which could involve film activation too. Concentration calibration plots have also been obtained for the enantiomers of terazosin at pH = 4, by recording CV patterns at increasing probe concentration in the 0.002–0.004 M range (Figure 60) on glassy carbon (GC) electrode modified with oligo-(S)-(N-Me)Ind$_2$Ph$_2$T$_4$ and oligo-(R)-(N-Me)Ind$_2$Ph$_2$T$_4$. Good linearity is observed in all cases.
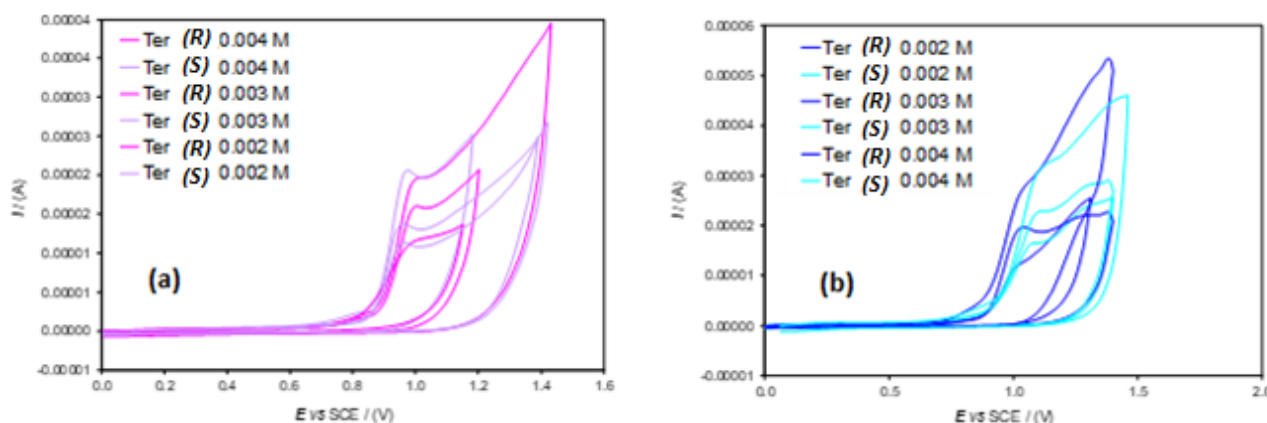
Figure 60: CV patterns of the enantiomers of terazosin (Ter (S) and Ter (R)) at increasing probe concentrations in pH = 4 buffer, recorded at 0.05 V s^{-1} scan rate on GC covered with oligo-(S)-(N-Me)Ind$_2$Ph$_2$T$_4$ (a) and oligo-(R)-(N-Pr)Ind$_2$Ph$_2$T$_4$ (b).

Due to impossibility of coating an electrode by electropolymerizing the very soluble (N-Hex)Ind$_2$Ph$_2$T$_4$ enantiomers, the latter were used as chiral additive in electrochemical cell. Enantioselective analysis was carried out in ionic liquid (1-butyl-3-methylimidazolium bis(trifluoromethylsulfonyl)imide, BMIMTFSI) using a screen-printed electrode (SPE). This experimental setup allows to run the analyses in extremely low quantity of solvent, thus saving enantiopure additive (R)-(N-Hex)Ind$_2$Ph$_2$T$_4$ as well. CV data are resumed in Figure 61 and show very high separation ($\approx$ 230 mV) towards oxidation of enantiomers of FcR and FcS. Of course, when no chiral probe is present, no separation is observed. Further experiments with different chiral probes are planned in the near future.
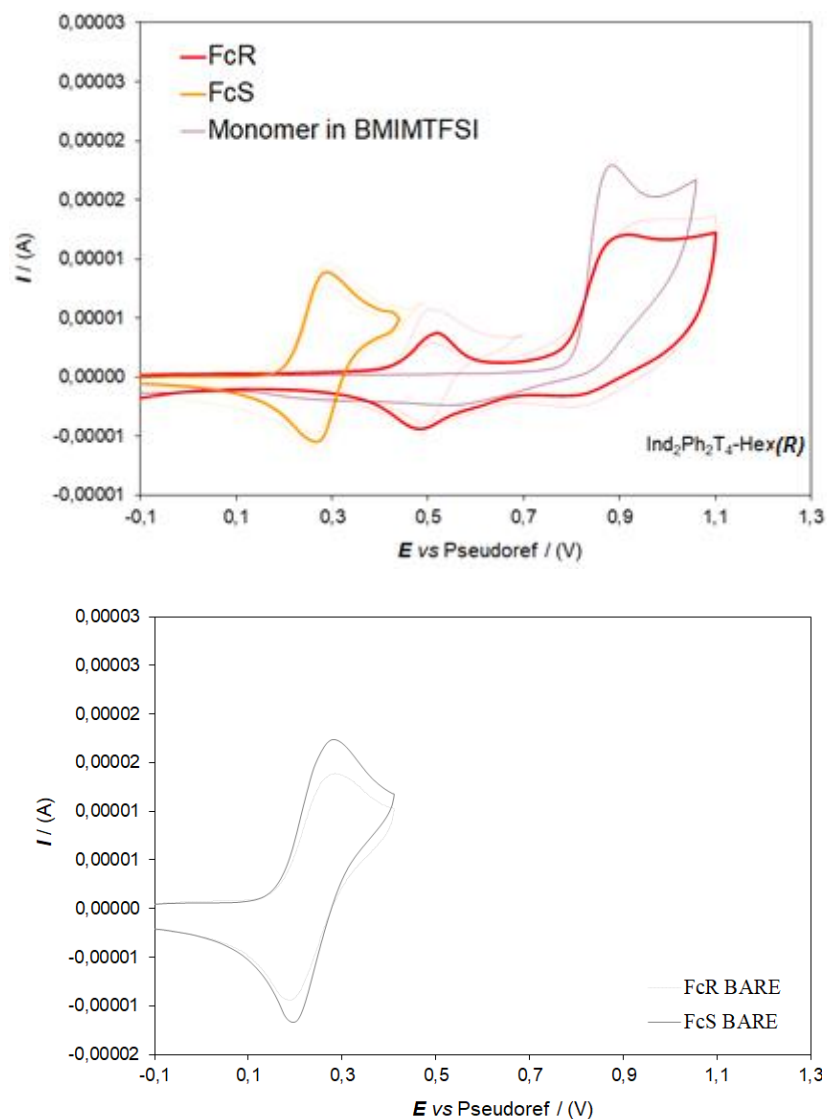
Figure 61: CV patterns of FcR and FcS (both 0.004 M) using enantiopure monomeric (*R*)-(*N*-Hex)Ind$_2$Ph$_2$T$_4$ (0.0074 M) as chiral selector in BMIMTFSI (up); CV patterns of FcR and FcS in absence of any chiral selector (bottom). Scan speed: 50 mV/s.

Concerning (*N*-Pr)Ind$_2$T$_6$ **106**, resolution by chiral HPLC showed an interesting phenomenon since two couples of enantiomers were isolated in different amounts (Figure 62). Curiously, proton NMR spectra of the most and the less abundant chiral compounds are identical, revealing that in HPLC conditions two different chiral conformers are present. An explanation of this phenomenon is currently under investigation through a theoretical approach. A first enantioselectivity DPV test has been carried out towards FcR and FcS. Enantiopure oligomer electrodeposition has been performed in the same conditions as previously exposed for (*N*-alkyl)Ind$_2$Ph$_2$T$_4$. A good enantiodiscrimination in terms of peak potential values, was obtained, with a separation of ≈ 60 mV between FcR and FcS (Figure 63). In fact, two quite different DPV signals, both well defined, were observed, specularly by changing the probe or the selector configurations. Reproducibility tests were performed by repeatedly recording the DPV patterns of model probes on freshly deposited chiral surfaces.

CSP: Chiralpak IB (250 mm x 4.6 mm I.D.)
Eluent: pentane-methanol-dichloromethane 100:1:5
Flow rate: 1 ml/min
Temperature: 5°C
Detector: UV (gray) and CD (blue) at 380 nm
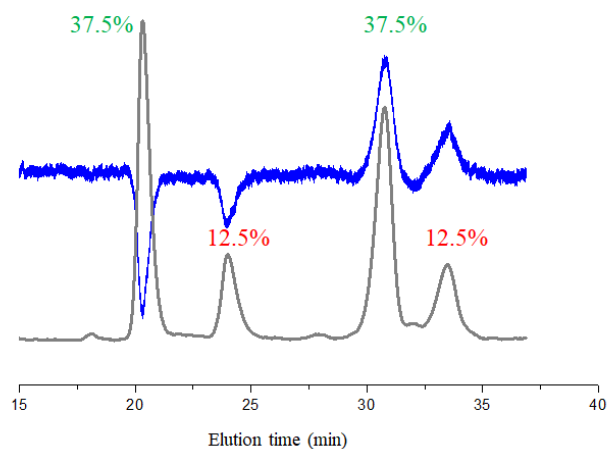
Figure 62: chiral HPLC elution profile of (N-Pr)Ind$_2$T$_6$ monomer **106**.
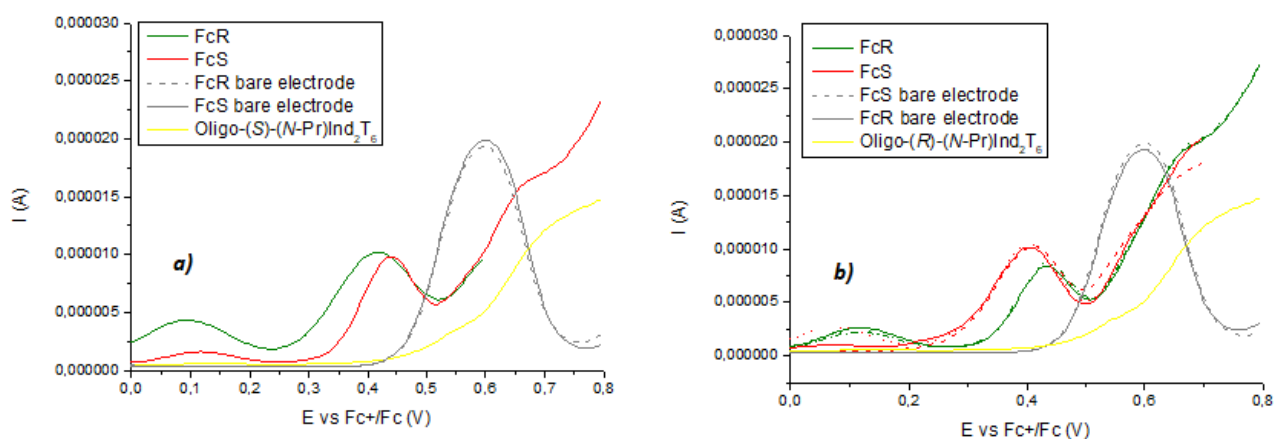
Figure 63: enantioselection performances of enantiopure oligo-(*S*)-(N-Pr-Ind)$_2$T$_6$ (a) and oligo-(*R*)-(N-Pr-Ind)$_2$T$_6$ (b) electrode surfaces towards FcR (green line) and FcS (red line). In grey are also reported the signals of FcR and FcS recorded on bare GC electrode; in orange is reported the DPV pattern of oligo-(*S*)-(N-Pr-Ind)$_2$T$_6$ or oligo-(*R*)-(N-Pr-Ind)$_2$T$_6$.

11.1.4.1. Conclusions

Enantiopure electroactive films of oligo-(*N*-Me)Ind$_2$Ph$_2$T$_4$ and of oligo-(*N*-Pr)Ind$_2$Ph$_2$T$_4$ proved excellent enantioselectivity towards different chiral probes. Even higher performances were obtained using (*N*-Hex)Ind$_2$Ph$_2$T$_4$ enantiopure monomer as chiral additive in electrochemical cell solutions. Concerning (*N*-Pr)Ind$_2$T$_6$ monomer, synthesis of analogues methylated and hexylated compounds is in planning. Prompted by very good enantioselection abilities of enantiopure oligo-(*N*-alkyl)Ind$_2$Ph$_2$T$_4$, a detailed chiral HPLC separation study will be carried out in the near future also on (*N*-alkyl)Ind$_2$T$_6$ family, followed by enantiorecognition tests.

♦ ♦ ♦ ♦ ♦ ♦

11.2. 3,3'-Biindoles

11.2.1. Synthesis

11.2.1.1. Synthesis of 3,3'- (*N*-Me)Ind$_2$T$_4$

A particularly interesting approach to the construction of a 3,3'-biindolyl backbone via Brønsted acid catalysis has been developed by Arcadi in 2014.[213] In this procedure, four new chemical bonds are formed leading to the formation of 2,2'-disubstituted 3,3'-biindole through Brønsted acid catalyzed cascade reaction of 2-[(2-aminophenyl)ethynyl]phenylamine derivatives with aryl(heteroaryl)aldehydes (Scheme 58). Noticeably no use of organometallic chemistry was exploited in this protocol. A detailed mechanism of this process is not completely clear yet.
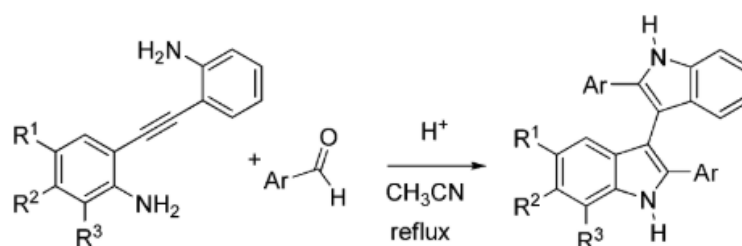
Scheme 58: synthesis of 2,2'-disubstituted-3,3'-biindoles.

A synthetic strategy for 3,3'- Ind$_2$T$_4$ **111** has been developed basing on this approach: key reactants were thus identified in 2,2'-(ethyne-1,2-diyl)dianiline **109** and 2,2'-bithiophene-5-carboxaldehyde **110**. The latter was easily afforded by Vilsmeier formylation from 2,2'-bithiophene[214] (Scheme 59).
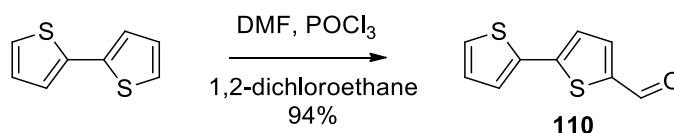
Scheme 59: formylation of 2,2-bithiophene to afford **110**.

Route to **109** starts off from 2-iodoaniline. Like previously cited 2,2'-biindole synthesis, Sonogashira reaction with TMSA on this substrate led to the isolation of compound **107** in quantitative yield.[215] Same yield was detected for KF mediated silicon group removal to afford **108**.[216] Another Sonogashira coupling in usual conditions with 2-iodoaniline provided 2,2'-(ethyne-1,2-diyl)dianiline **109**.[217] Brønsted acid catalyzed indolization reaction was accomplished successfully but, due to some difficulties in affording the purification after repeated chromatographies, subsequent alkylation reaction was performed directly on crude product (Scheme 60) and (*N*-Me)3,3'- Ind$_2$T$_4$ was isolated as racemate in 29% yield.
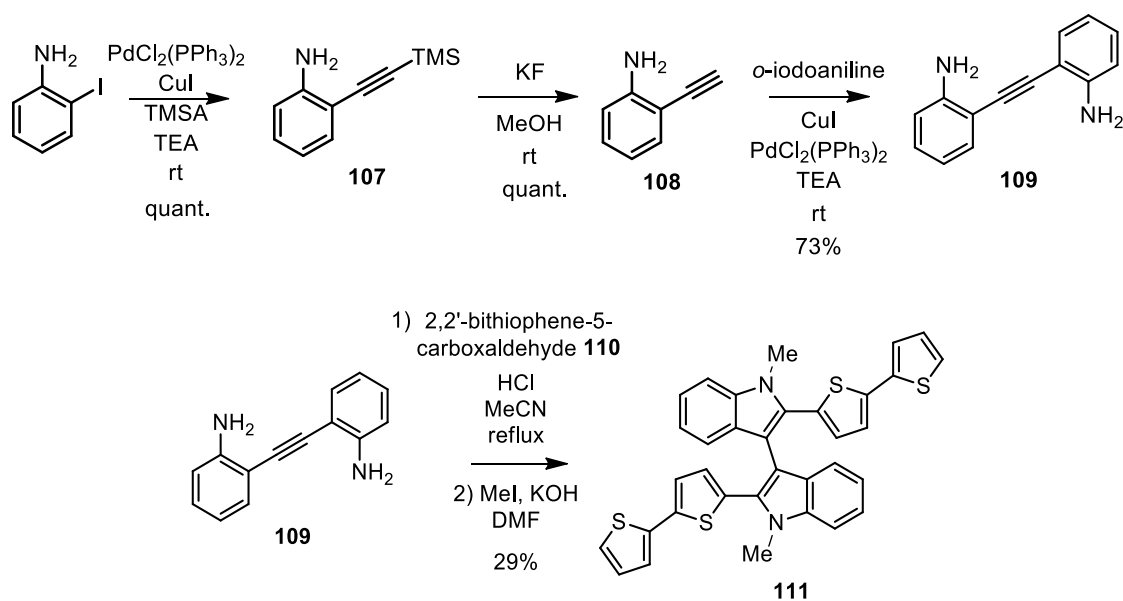
Scheme 60: synthesis of 3,3'-(*N*-Me)-Ind₂T₄ **111**.

11.2.1.2.   Synthesis of 3,3'- (*N*-Hex)Ind₂Ph₂T₄

Since aromatic spacer introduction was aim for 3,3'-biindoles too, synthesis of the alkylated 3,3'- Ind₂Ph₂T₄ compound **115** was planned. Interestingly, pathway does not contemplate biindole ring closure with 2,2' functionalization in same synthetic step as previously exposed biindole compounds. Starting material was identified in *p*-bromoacetophenone which, through a classical Fischer indolization, was converted to product **112**.[218] Formation of 3,3'-biindole backbone was achieved by oxidative radical coupling mediated by iron(III) chloride and oxygen to afford product **113**.[219] The latter was alkylated in high yield to obtain **114a** and **114b**, which were converted to (*N*-Me)3,3'- Ind₂Ph₂T₄ **115a** and (*N*-Hex)3,3'- Ind₂Ph₂T₄ **115b** by Pd-catalyzed Suzuki-Miyaura cross coupling reaction with 2 2'-bithiophene-5-boronic acid pinacol ester (Scheme 61).
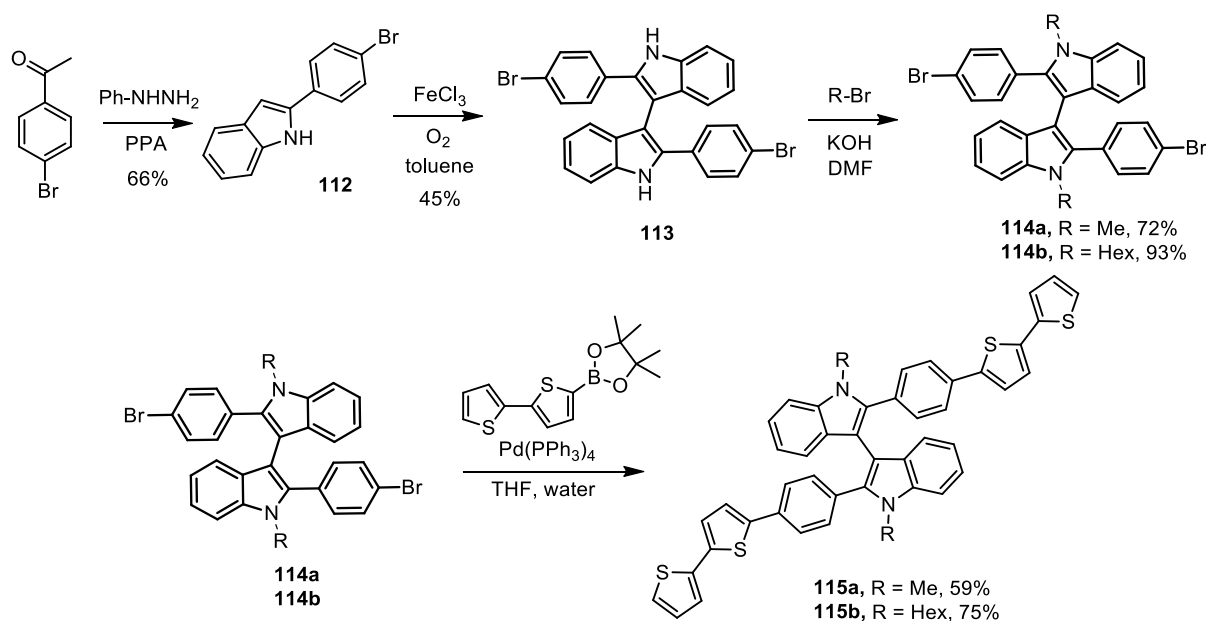
Scheme 61: synthesis of 3,3'-(*N*-Me)Ind$_2$Ph$_2$T$_4$ **115a** and 3,3'-(*N*-Hex)Ind$_2$Ph$_2$T$_4$ **115b**.

Noticeably, N-CH$_2$ protons of compound **115b** do not show a clear diastereotopic behaviour like 2,2'-biindoles. Pattern is much more confused due to signals overlap: on the other hand, diastereotopic pattern is more distinguishable in N-CH$_2$ protons of compound **114b** (Figure 64).
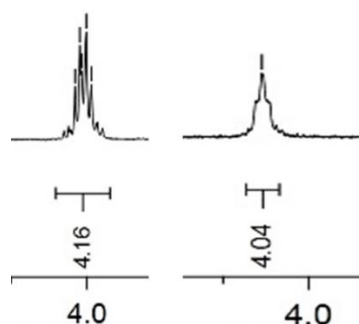
Figure 64: N-CH$_2$ protons pattern for **114b** (right) and 3,3'- (*N*-Hex)Ind$_2$Ph$_2$T$_4$ **115b** (right).

11.2.2. HPLC and DFT configurational stability studies

Despite 3,3'-(*N*-Me)Ind$_2$T$_4$ **111** structure is very close to that of BT$_2$T$_4$ one, chiral HPLC separations conducted at different temperatures by Dr. Roberto Ciriilli showed configurational instability for **111**. Enantiomers peaks start to overlap at 25°C and at 40°C coalescence is almost complete (Figure 65).
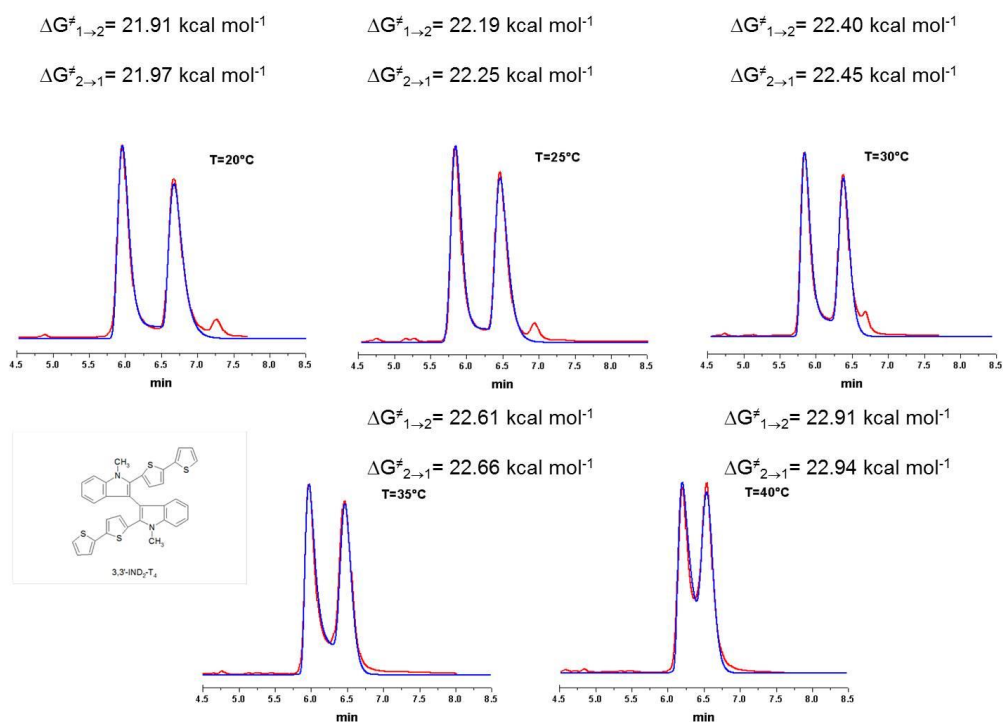
Figure 65: chiral HPLC of compound **111**.

Thermodynamic parameters for racemization processes were DFT computed by prof. Marco Pierini: racemization transition states, which shows flattening of both indole rings on the same plane, were particularly low in energy as racemization ΔG is calculated to be 23.4 kcal/mol (*Figure 66*). Therefore it was not possible to resolve the racemate of compound **111** as it behaves as racemic compound at room temperature, thus being suitable only as achiral starting material for films electrodeposition.

Similar behaviour was noticed for compound **115a**. Introduction of a phenyl spacer did not contribute to configurational stability at room temperature since free rotation on biindole interannular axis requests only 22.7 kcal/mol (Figure 67). Compound **115b** as well, which features the longer hexyl chain, did not show any substantial difference in interconversion thermodynamic parameters (Figure 68). Different temperature chiral HPLC analyses of compound **115b** showed enantiomers peak coalescence already at 35°C (Figure 69).
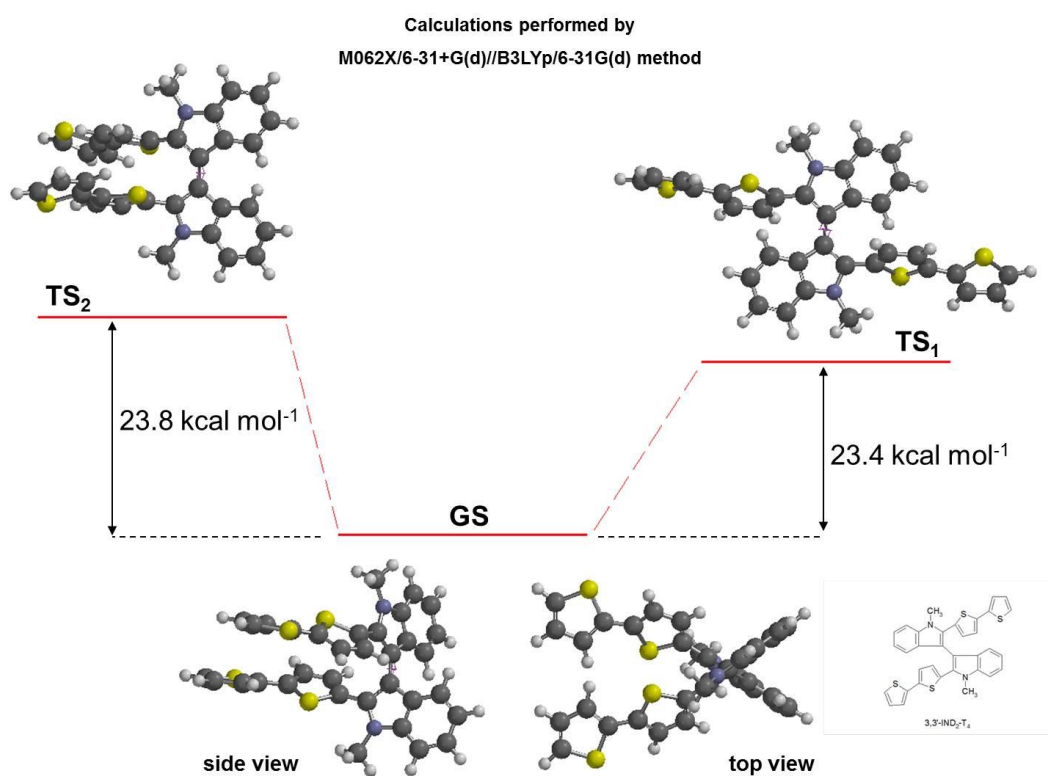
Figure 66: plausible interconversion transition states of compound **111** optical antipodes.
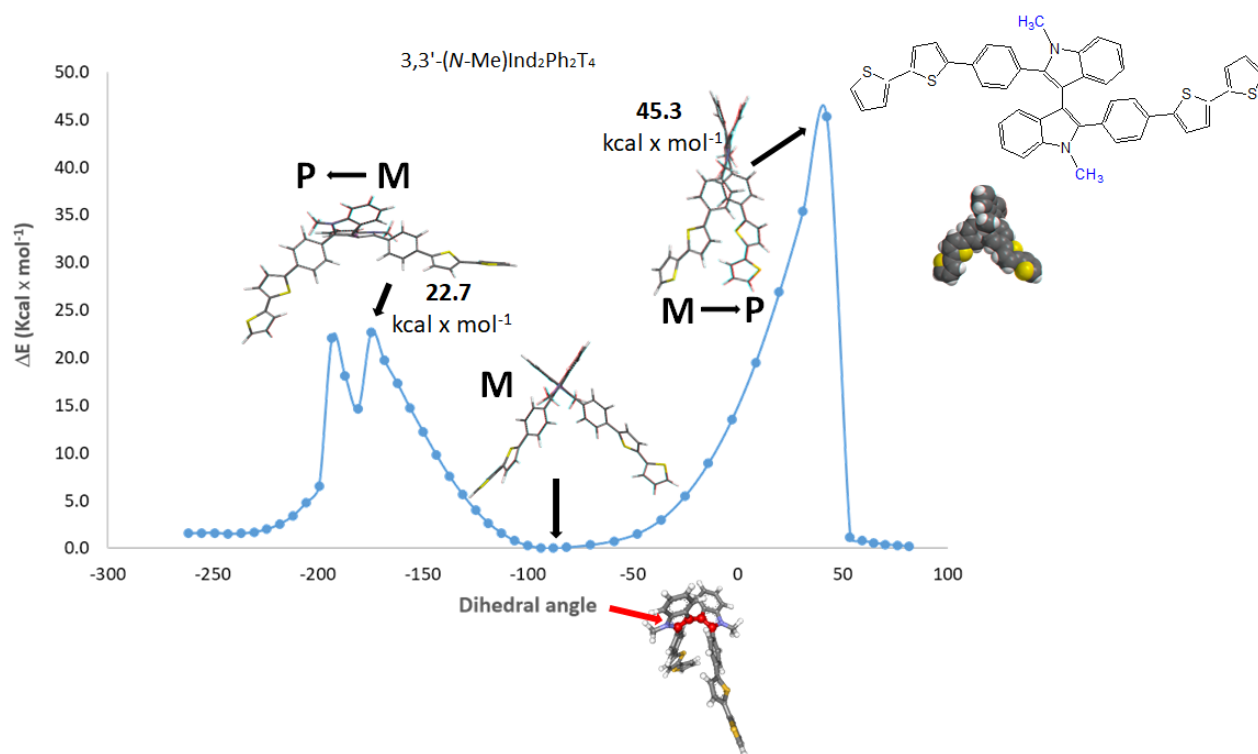
Figure 67: interconversion barriers for enantiopure 3,3'-(N-Me)Ind$_2$Ph$_2$T$_4$ **115a**.
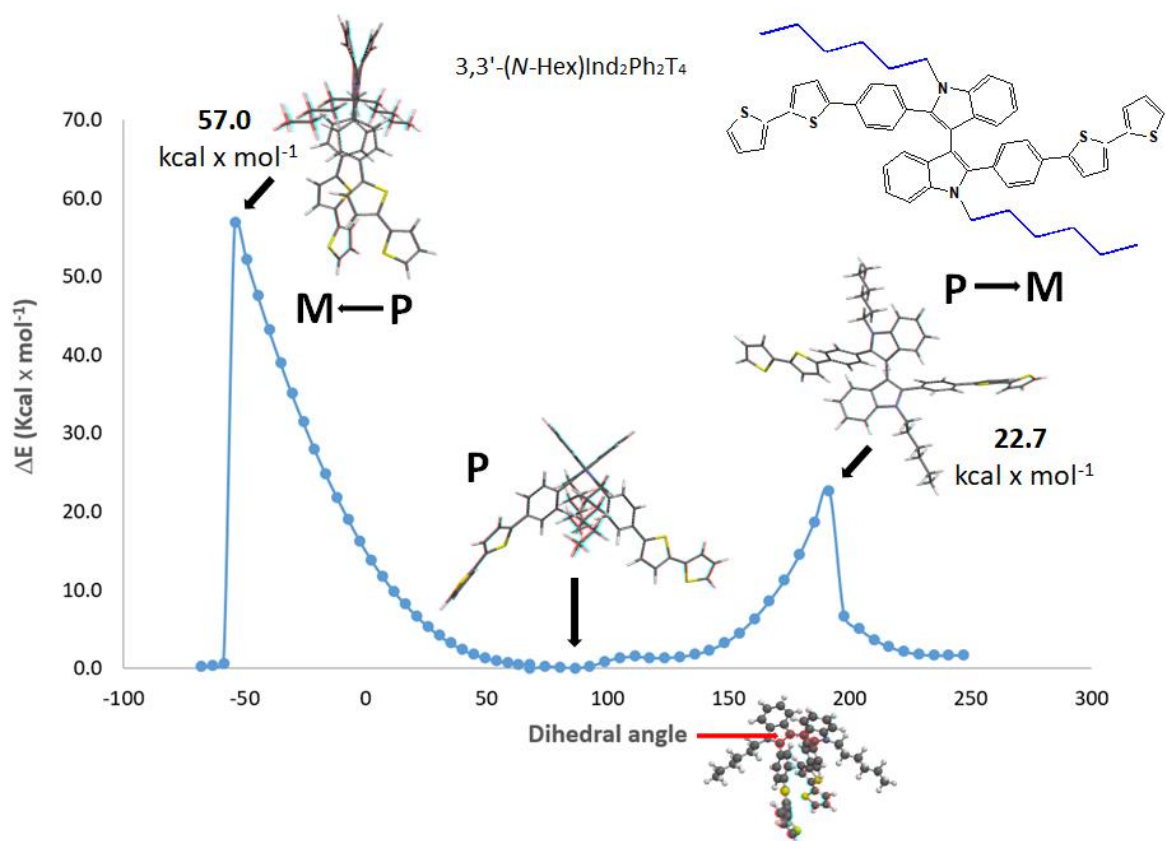
Figure 68: interconversion barriers for enantiopure 3,3'-(N-Me)Ind$_2$Ph$_2$T$_4$ **115b**.
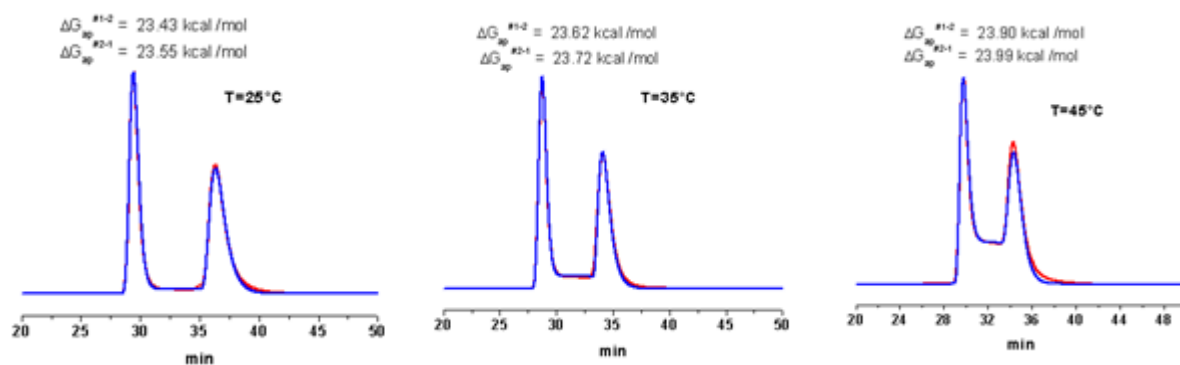
Figure 69: chiral HPLC of compound **115b** at different temperatures.

A detailed DFT analysis showed that this kind of 3,3'-biindoles derivatives could be configurationally stable if substituents causing more steric hindrance were introduced. The most immediate hypothesis is decoration of nitrogen indolic atoms with a very bulky chain, *i.e.* isopropyl or tertbutyl. Theoretical DFT calculations of racemization barriers on the hypothetical 3,3'-(N-iPr)Ind$_2$Ph$_2$T$_4$ and 3,3'-(N-tBu)Ind$_2$Ph$_2$T$_4$ showed configurational stability for the latter (racemization barrier 41.2 kcal/mol, Figure 70), whereas isopropyl chain was not enough to block free 3,3' axis rotation (only 23.1 kcal/mol, Figure 71).
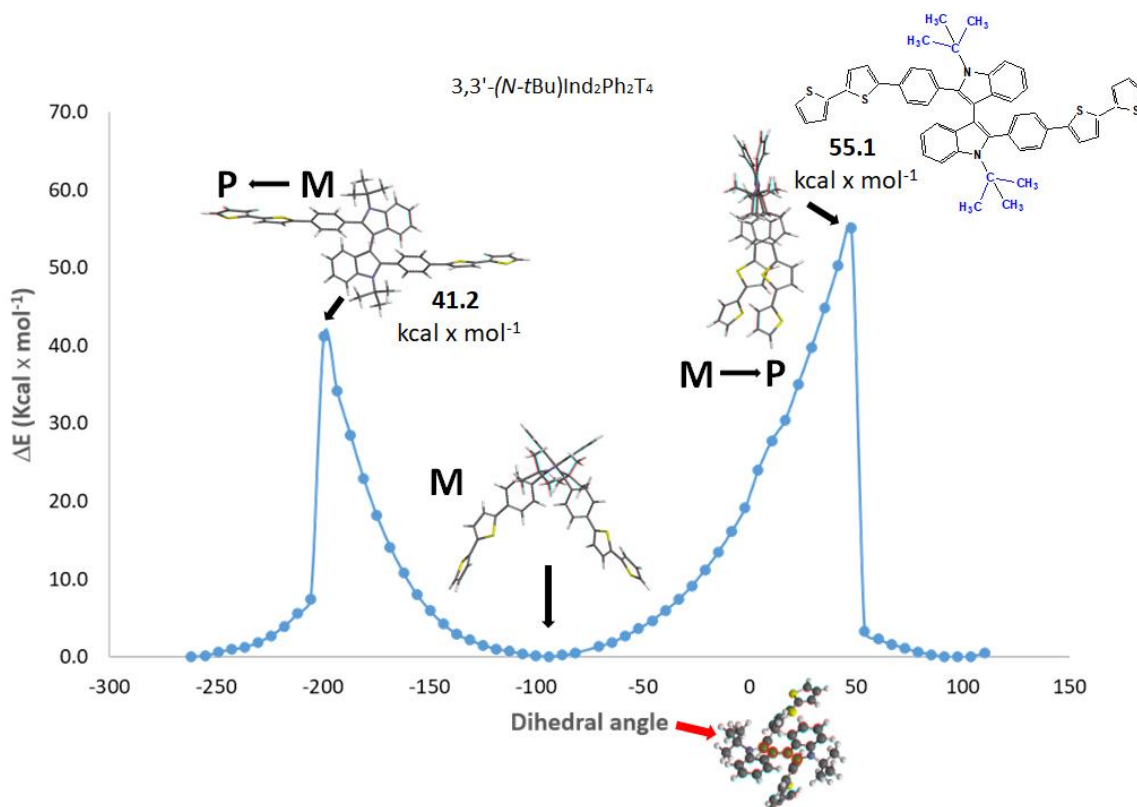
Figure 70: interconversion barriers for 3,3'-(N-tBu)Ind$_2$Ph$_2$T$_4$.
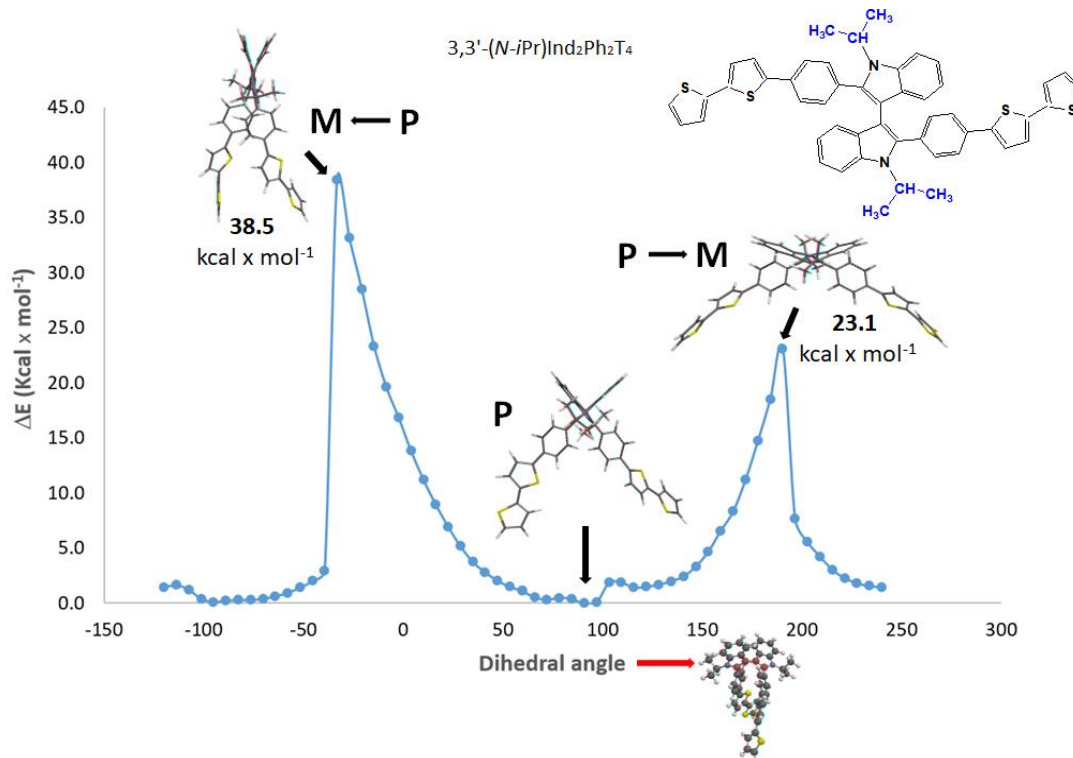
Figure 71: interconversion barriers of 3,3'-(N-iPr)Ind$_2$Ph$_2$T$_4$.

However since the functionalization of nitrogen atoms with t-butyl groups appeared a difficult target from a synthetic point of view, a different axis rotation inhibition was envisaged on modifications of indole benzenoid ring. For example, methyl groups introduction in 4,4' positions forms a room temperature blocked *gear wheel* structure (nicknamed 3,3'-(N-Me)-4,4'-(diMe)Ind$_2$Ph$_2$T$_4$), with high racemization barrier (Figure 72).
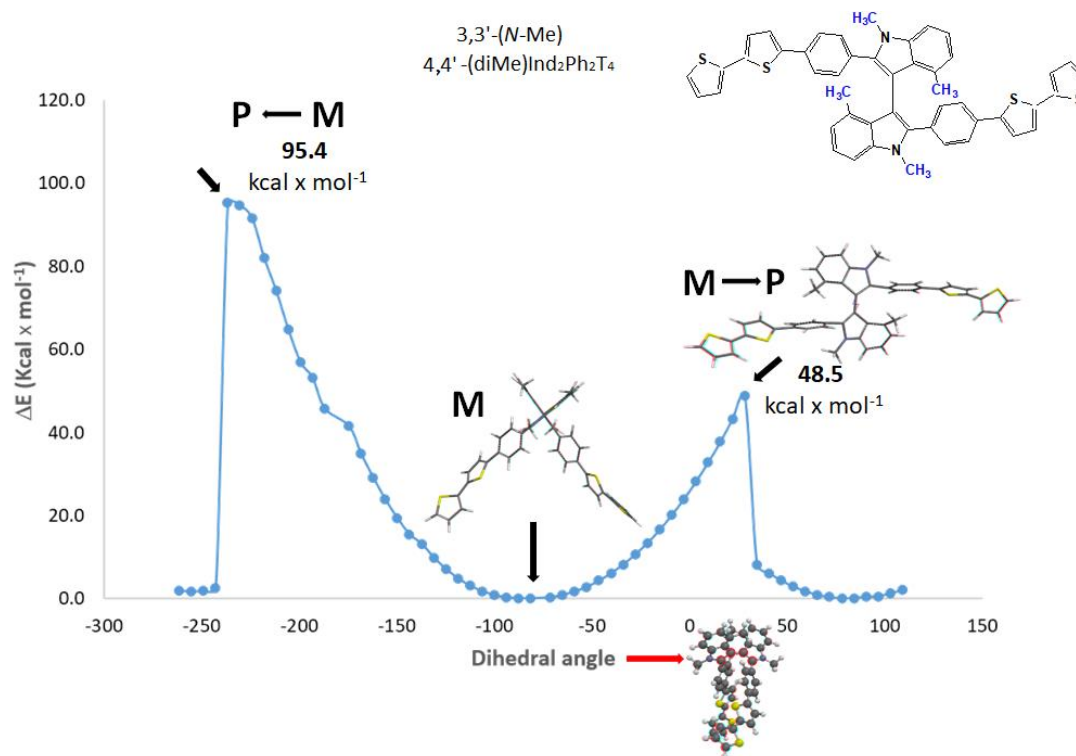
Figure 72: interconversion barriers of 3,3'-(*N*-Me)-4,4'-(diMe)Ind$_2$Ph$_2$T$_4$.

Based on these calculations, the synthesis of 3,3'-(*N*-Me)-4,4'-(diMe)Ind$_2$Ph$_2$T$_4$ is currently under planning and to be will be an objective for the near future.

♦♦♦♦♦♦

11.3. 2,2'-Biindole derivatives based on chromophore introduction

11.3.1. Synthesis

11.3.1.1. Synthesis of (*N*-Hex)Ind$_2$(BTD)$_2$T$_4$ 121

The approach to the synthesis of compound Ind$_2$BTD$_2$T$_4$ **121**, was analogous to that followed for the prepa-ration of other 2,2'-biindoles, showing another time as key point the Larock-like indolization of trifluoroa-cetamide **95** and appropriate halide **119**. 4-([2-Thieno]-5-bromyl)-7-(2-thienyl)-2,1,3-benzothiadiazole **119** was prepared through bromination of benzothiadiazole to afford compound **116** in quantitative yield.[220] Pd-catalyzed Stille cross coupling reaction with 2-tributylstannyl thiophene **117** provided dark red solid **118** in 93% yield.[221] Subsequent halogenation reaction was tried with NIS[222], however even when NIS was slightly sub stoichiometric employed, large amounts of diiodinated by-product were detected. Presence of dihalogenated derivative was of course not desired, as could generate complex oligomerization products when involved in the Larock-like indolization. NBS bromination reaction instead afforded very easily product **119** in good yield, despite heteroaryl bromide are known to produce lower yield in subsequent ring closure

reaction. A simple purification by chromatography was enough to get rid of dibrominated impurity. All reactions are resumed in Scheme 62.
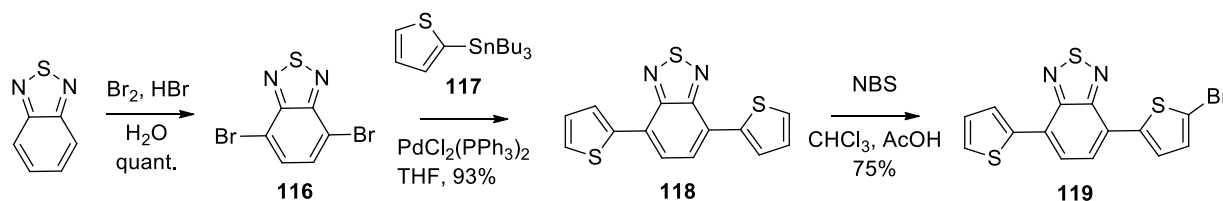
Scheme 62: synthesis of halide **119**.

2-Tributylstannyl-thiophene **117** was synthetized from thiophene direct stannylation with *n*-BuLi and tributyltin chloride (Scheme 63).
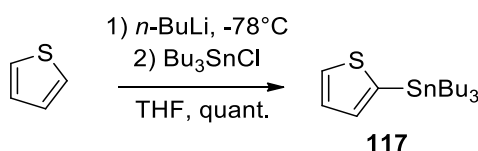
Scheme 63: synthesis of organotin **117**.

The Larock-type indolization reaction between bromide **119** and trifluoroacetylamide **95** afforded Ind$_2$BTD$_2$T$_4$ **120** in mediocre yield even in refluxing DMF. This is probably due not only to lower bromide reactivity but also from difficulties in workup and purification due to very bad solubility of final product **120**. Solubility problem was overcome by hexylation with potassium hydroxide and 1-bromohexane which afforded (*N*-Hex)Ind$_2$(BTD)$_2$T$_4$ **121** as dark red solid. Further studies are ongoing to optimize indolization reaction conditions. Reactions are resumed in Scheme 64.
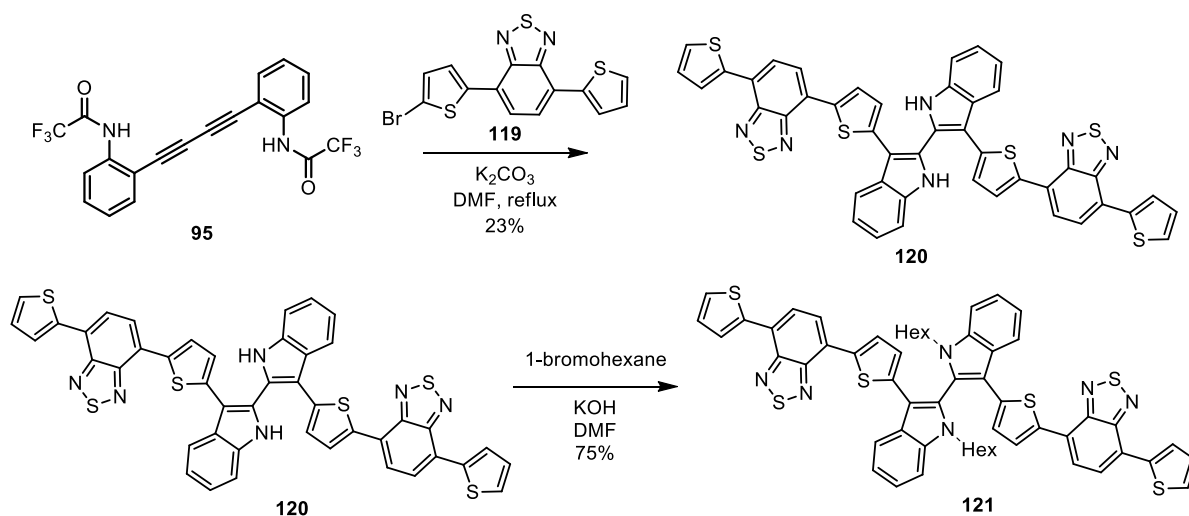
Scheme 64: synthesis of (*N*-Hex)Ind$_2$(BTD)$_2$T$_4$ **121**.

11.3.1.2. Synthesis of (*N*-Hex)Ind$_2$(BSeD)$_2$T$_4$ 127

As stated in the introduction, substitution of S with Se in benzochalcogenodiazole scaffold leads to important red shift in absorbance, showing a bathochromic effect; it generally increases also power conversion efficiencies in D/A copolymers used for solar cells applications.[178] Except for unsatisfactory yield, synthetic approach for (*N*-Hex)Ind$_2$(BTD)$_2$T$_4$ 121 was proven fruitful. Therefore, same Larock-like approach was adopted for the synthesis of the analogous selenium compound, nicknamed (*N*-Hex)Ind$_2$(BSeD)$_2$T$_4$.

Approach to halide 125 started off from compound 116: its reduction with sodium borohydride provided dianiline 122[223] which was converted to benzoselendiazole 123 by reaction with selenium dioxide.[224] The latter was substrate for Stille reaction with 2-tributylstannyl-thiophene 117 to afford 124 as dark red compound.[225] Monoiodination of 124 was unsuccessful for the same reasons described for the synthesis of 118: bromination resulted effective instead and bromoderivative 125 was obtained in good yield. Reactions are resumed in Scheme 65.
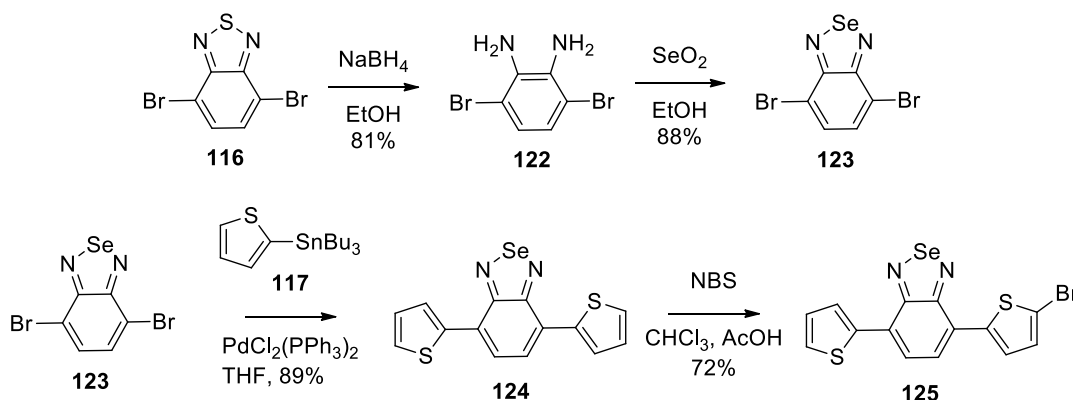
Scheme 65: synthesis of halide 125.

Larock-like cyclization afforded Ind$_2$BSeD$_2$T$_4$ 126 as a purple solid although in modest yield, probably for the same reasons reported above for Ind$_2$(BTD)$_2$T$_4$ 120. The introduction of an hexyl group was again chosen as long alkyl chain allowed to overcome any solubility issue (Scheme 66).
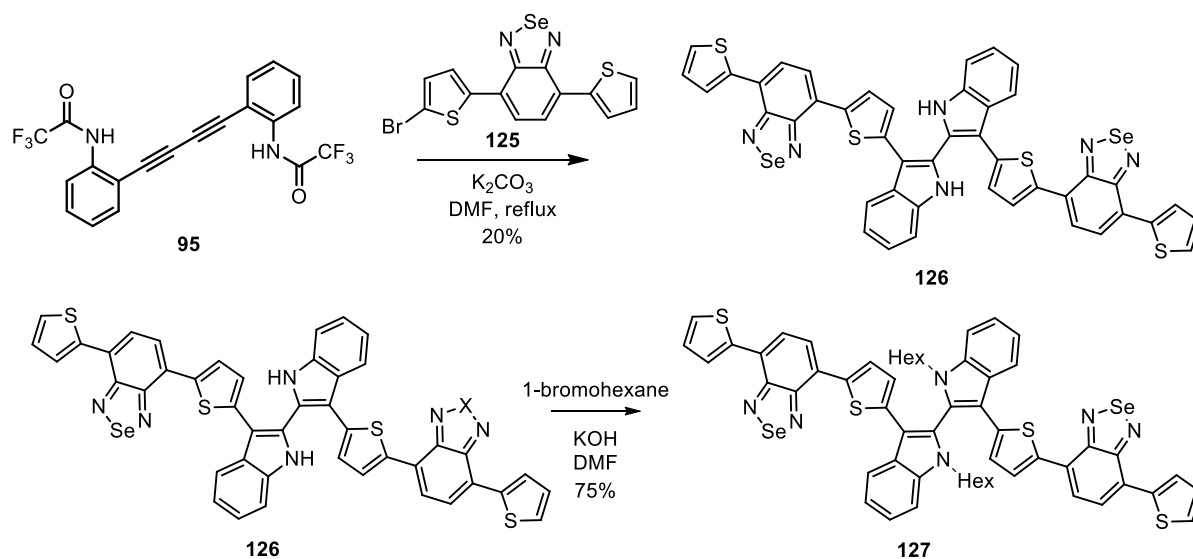
Scheme 66: synthesis of (*N*-Hex)Ind$_2$(BSeD)$_2$T$_4$ **127**.

11.3.2. Effects of chromophore introduction on spectral and electrochemical properties of 2,2'-biindole-based electroactive films

All the studies presented in this section were performed in collaboration with prof. Sabine Ludwigs research group.

11.3.2.1. Monomers characterization

Racemate compounds **121** and **127** were characterized by UV-Vis spectroscopy (Figure 73) to find absorption maxima. As expected, Se atom introduction produced a clear red shift in absorption λ_{max} (503 vs 538 nm). Red shifted emission was observed too (701 vs 770 nm), associated with a lower quantum yield (13% for (*N*-Hex)Ind$_2$(BTD)$_2$T$_4$, 6.5% for (*N*-Hex)Ind$_2$(BSeD)$_2$T$_4$).
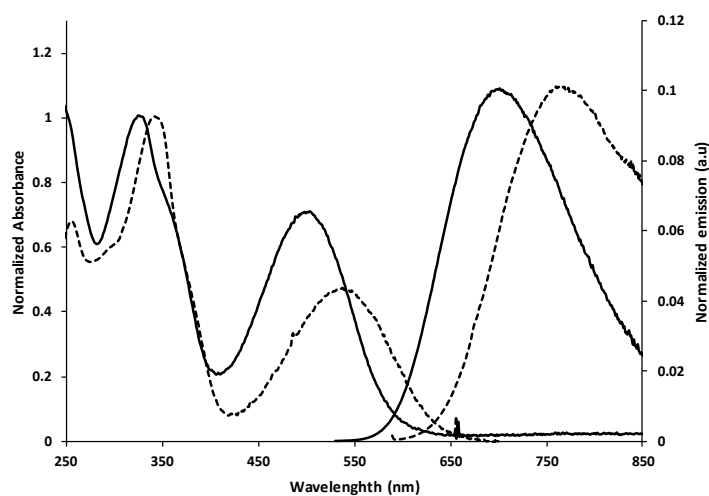
Figure 73: UV-Vis absorption and emission spectra in DCM for (*N*-Hex)Ind$_2$(BSeD)$_2$T$_4$ **127** (dashed line) and (*N*-Hex)Ind$_2$(BTD)$_2$T$_4$ **121** (solid line).

From the electrochemical point of view, **121** and **127** CVs in anodic range presents the same four peaks pattern already observed for π spaced biindoles (see section **11.1.2.1**). Compared to (*N*-Pr)Ind$_2$T$_6$, a delayed first oxidation peak was noticed and imputed to benzochalcogenodiazole presence as electron acceptor moiety.[226]
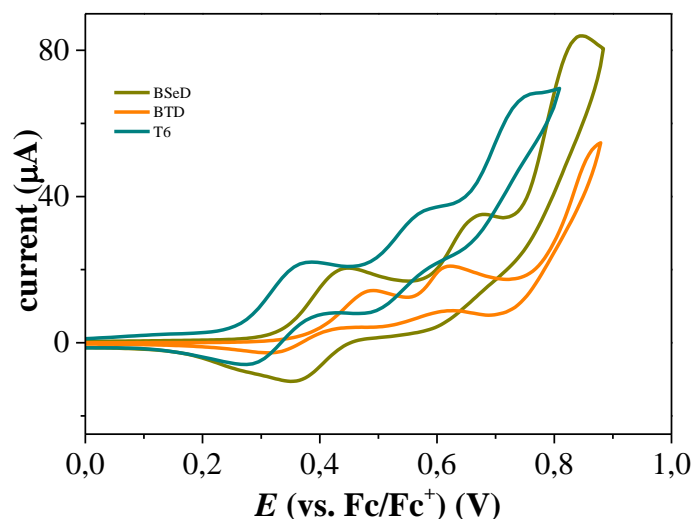
Figure 74: superimposed anodic cyclic voltammograms for (*N*-Pr)Ind$_2$T$_6$ **106** (blue line), (*N*-Hex)Ind$_2$(BTD)$_2$T$_4$ **121** (orange line) and (*N*-Hex)Ind$_2$(BSeD)$_2$T$_4$ **127** (green line); analyses in CH$_2$Cl$_2$/NBu$_4$PF$_6$ 0.1M at a scan-rate of 20 mV/s, monomer concentration 0.5 mM, Au electrode.

11.3.2.2. Electropolymerization

Electrodeposition was performed in CH$_2$Cl$_2$/NBu$_4$PF$_6$ 0.1 M, 0.5 mM racemate monomer solutions by subsequent potentiodynamic cycles (20 mV/s) around the peaks associated with activation of the thienyl alpha terminals of the monomers. As previously indicated for π spaced films (see section **11.1.2**), the electrodeposited film should be constituted by oligomers with the same conjugation length (namely oligo(*N*-Hex)Ind$_2$(BTD)$_2$T$_4$ oligo(*N*-Hex)Ind$_2$(BSeD)$_2$T$_4$) also in these cases.
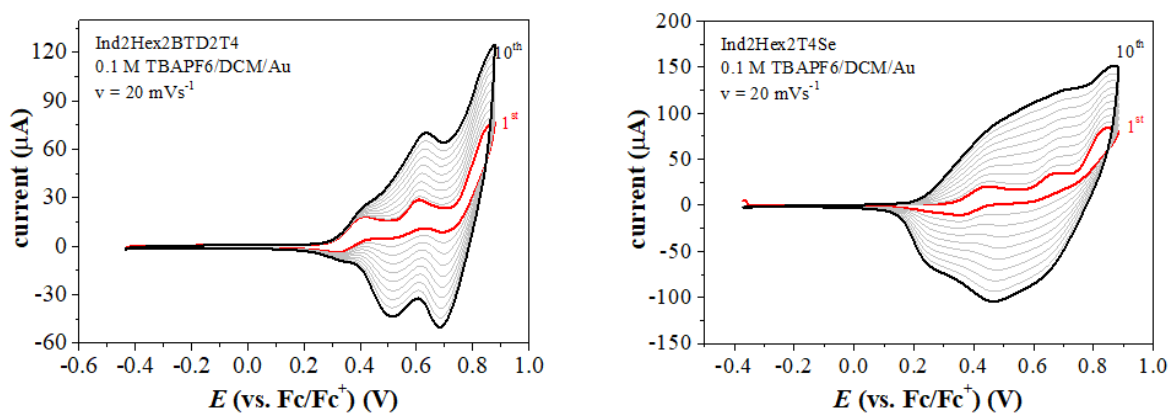
Figure 75: electropolymerization of *(N*-Hex)Ind$_2$(BTD)$_2$T$_4$ **121** (left) and (*N*-Hex)Ind$_2$(BSeD)$_2$T$_4$ **127** (right).

Compared to (N-Pr)Ind$_2$T$_6$ electropolymerization, compound **121** and **127** showed a faster film growth, since only 10 cycles were requested to achieve the same current intensities. Redox peaks at lower potentials appeared as a result of formation and electrodeposition of compounds with extended π conjugation on electrode surface[204], as noticed for π spaced biindoles too (see section **11.1.2**). Electroactive films were subjected several times to cyclic voltammetries in a monomer free DCM solution, proving to be perfectly stable. Interestingly, compound **121** and **127**, featuring a hexyl alkyl pendant, were successfully electrodeposited, whilst (N-Hex)Ind$_2$Ph$_2$T$_4$ was too soluble.

Oligomeric films of **121** and **127** showed also a perfectly reversible and visible peak in cathodic range, in contrast with oligo(Ind$_2$T$_6$) electrodeposited material which shows a very low intensity reduction peak around -1.79 V (Figure 76). Cathodic maxima are probably due to reduction of the strong electron acceptor benzochalcogenodiazole unit.[226] Half wave potentials of all CV peaks were reported in

Table *14*. The difference between potential of first oxidation and first reduction represents a good estimation for the electrochemical band gap.

Au	$E^{1/2}$ V vs Fc/Fc$^+$			
	I ox	II ox	III ox	red
Oligo-(Ind2T6)	0.22	0.41	0.53	-
Oligo-(Ind2(T4-BTD2)	0.50	0.67	-	-1.79
Oligo-(Ind2(T4-BSeD2)	0.21	0.43	0.58	-1.69

Table 14: $E^{1/2}$ for electron transfers in oligomeric electroactive films.
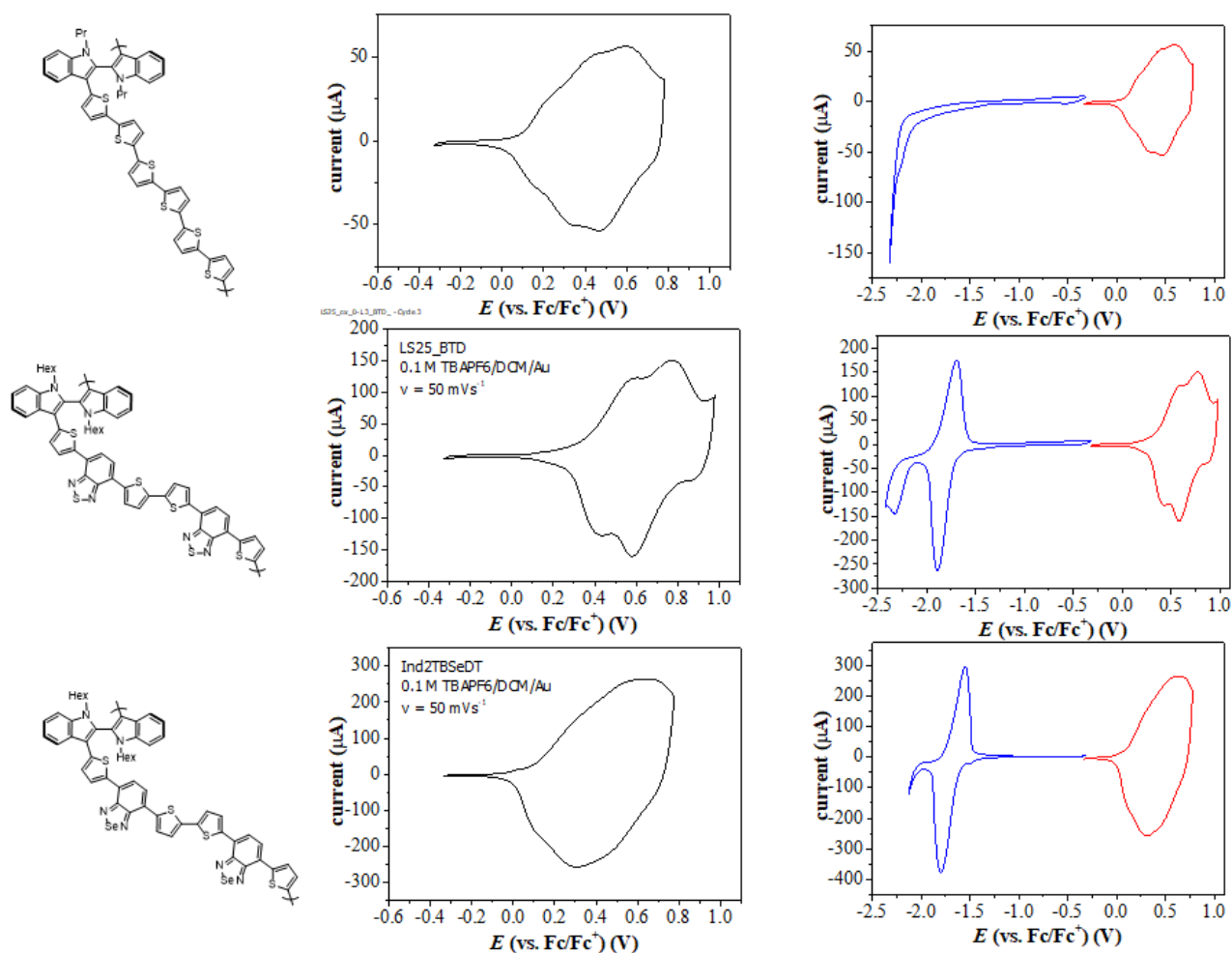
Figure 76: anodic range CVs of electroactive films (left column); anodic and cathodic range CVs of electroactive films (right column).

Parameters concerning UV-Vis absorbance of electroactive films were recorded as well and it is possible to determine the *spectroscopical onset* of the first electronic transition, which can be a good extimation of the optical band gap.[227] This value is usually a more reliable band gap estimation since in electronic excitation, in contrast with electrochemical processes, no net charge is formed.[228]

Oligo-(Ind2T6)	Oligo-(Ind2(T4-BTD2)	Oligo-(Ind2(T4-BSeD2)
565 nm	825 nm	859 nm
2.19 eV	1.50 eV	1.44 eV
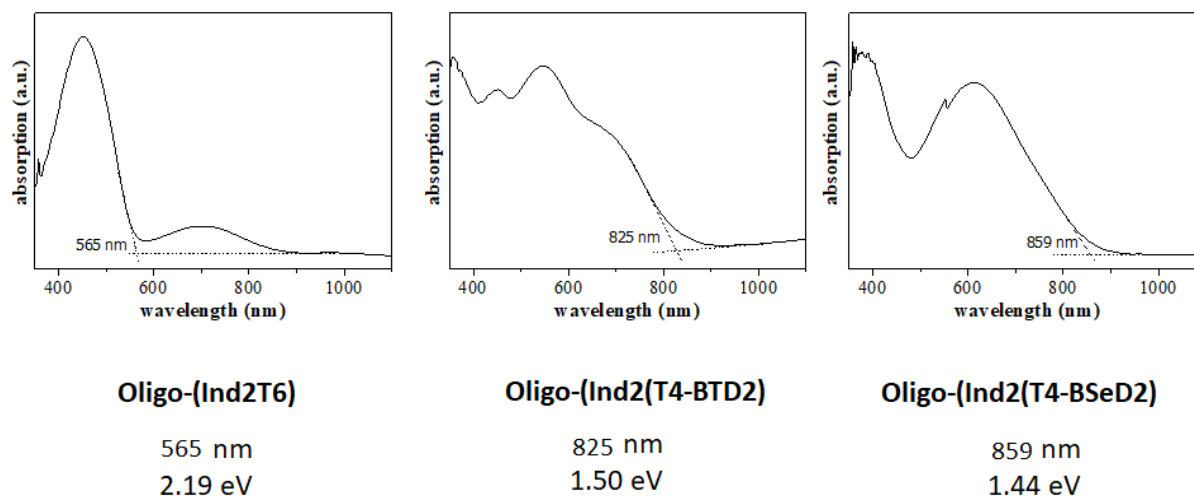
Figure 77: UV-vis spectra of oligomeric films; calculation of electronic transition energy was obtained from the respective λ onset.

Given aforementioned data, spectroscopical and electrochemical band gaps were reported in Table 15. Compared to oligo(*N*-Pr)Ind$_2$T$_6$ structure having no chromophore, the introduction of the donor acceptor moiety in biindole based oligomers strongly reduced HOMO LUMO gap. Bathochromic effect of BTD and BSeD acceptor units (in the order BTD – BSeD) can be observed in the electrochemical and optical HOMO LUMO gaps of the two electrodeposited films.

Oligo-	E onset (V vs Fc/Fc+)		E onset (eV)		Eg (ev) ec	Λonset (nm)	Eg (eV) UV-Vis
	ox	red	HOMO	LUMO	HOMO-LUMO		HOMO-LUMO
Ind2T6	0.11	-1.79	-5.21	-3.31	**1.91**	565	**2.19**
Ind2T4BTD2	0.24	-1.43	-5.34	-3.67	**1.67**	825	**1.50**
Ind2T4BSeD2	0.18	-1.39	-5.28	-3.71	**1.57**	859	**1.44**

Table 15: electrochemical and optical HOMO-LUMO gaps of oligomeric films.

11.3.2.3. UV-Vis-NIR spectroelectrochemistry

As previously indicated in paragraph **11.1.2.3**, spectroelectrochemistry is useful to investigate charged state specification as a function of the working electrode potential. The *in-situ* light absorbance variation at max wavelengths was plotted as function of the electrode potential and current, in order to monitor the relative distribution of the above states of charge. Data for oligo(*N*-Hex)Ind$_2$(BTD)$_2$T$_4$ are resumed in Figure 78. Neutral band was characterized by two peaks located at 448 and 549 nm. They can be assigned to intramolecular charge transfer (ICT) between donor and acceptor units. An ICT band is usually present in D–A conjugated molecules either small or polymeric containing benzochalchogenodiazoles and thiophenes in their structure.[229]

When increasing potential, after first oxidation peak, aforementioned bands decreased and different absorption maxima were individuated (749, 843, 999, 1388 nm) and deputed to formation of a radical cation specie at 0.58 V. At 0.76 V a second oxidation was observed with formation of a dication specie, characterized by broad band in near infrared region (with maximum at 1187 nm). Compared to oligo (*N*-Pr-Ind)$_2$T$_6$, a general red shift for all bands was observed, which seemed more significative in the case of neutral and radical cation state. Lower band gap resulted in almost complete superimposition of bands for radical cation and dication. Low energy gap and broad absorbance are important features in photovoltaic and electrochromic applications.[230,231] Actually, strong electrochromic effect was noticed during charging film since colour switched from violet to dark green. Perfect reversibility was noticed when discharging the film.

λ max (nm)		
N	**R⁺·**	**D²⁺**
448; 549	749; 843; 999; (1388)*	(649); 1187
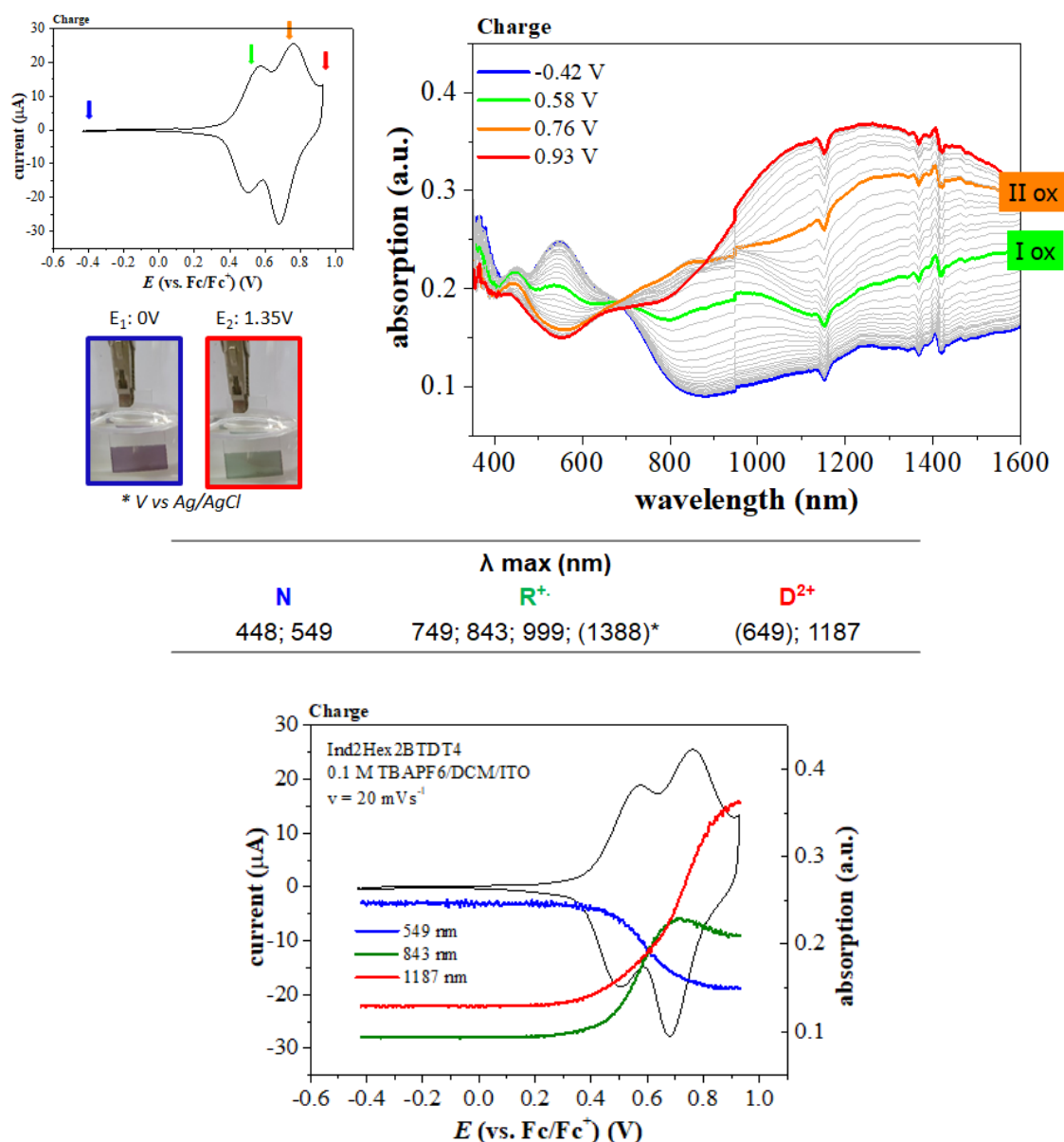
Figure 78: UV-Vis-NIR spectroelectrochemical absorption spectra (up) and peak variation measurements (bottom) for oligo(N-Hex)Ind$_2$(BTD)$_2$T$_4$ registered during the forward oxidation cycle at a scan-rate of 20 mVs^{-1} in 0.1 M CH$_2$Cl$_2$/NBu$_4$PF$_6$. Films were deposited on ITO. Pictures of the redox films in their neutral and charged state are also presented.

Similar behaviour was noticed for oligo(N-Hex)Ind$_2$(BSeD)$_2$T$_4$ (Figure 79). Compared to oligo(N-Hex)Ind$_2$(BTD)$_2$T$_4$, the neutral state was characterized by a red shifted absorption maximum of 613 nm. At 0.36 V, formation of the radical cation specie is noticed at 1042 nm. A NIR broad band was seen to grow when the dication specie was formed (0.72 V, 1187 nm). As noticed for oligo(N-Hex)Ind$_2$(BTD)$_2$T$_4$, radical cation and dication bands appeared overlapped, making difficult to distinguish one from another. Another time electrochromism effect was noticed; charging film the colour changed from blue to dark green with perfect reversibility when discharging.
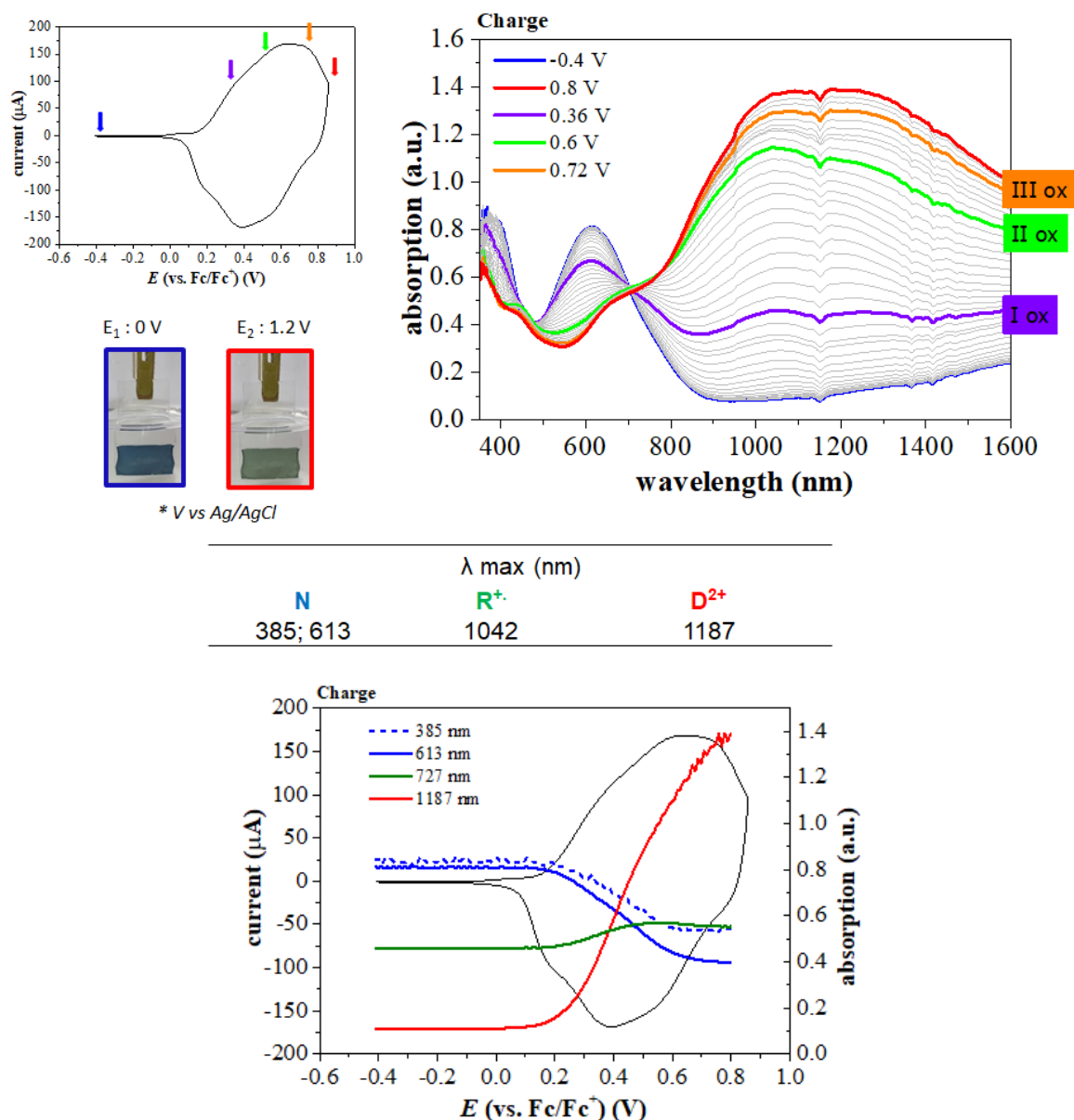
Figure 79: UV-Vis-NIR spectroelectrochemical absorption spectra (up) and peak variation measurements (bottom) for oligo(*N*-Hex)Ind$_2$(BSeD)$_2$T$_4$ registered during the forward oxidation cycle at a scan-rate of 20 mVs^{-1} in 0.1 M CH$_2$Cl$_2$/NBu$_4$PF$_6$. Films were deposited on ITO. Pictures of the redox films in their neutral and charged state are also presented.

The *in situ* conductance experiments are planned for the near future.

♦♦♦♦♦♦

11.4.   A new approach for the synthesis of 3,3'-diheteroaryl-2,2'-biindoles

Despite Larock-like ring closure reaction proved to be effective, its general mediocre yield prompted to investigate new synthetic approach to 2,2'-biindoles. Another strategy could be to consider 3,3'-heteroaryl substitution coming from a Pd-catalyzed cross coupling reaction starting from an already preformed 2,2'-biindole (Figure 80). The latter could behave either as the substrate (retrosynthesis A) or as the organometallic reagent (retrosynthesis B) in the cross coupling reaction.
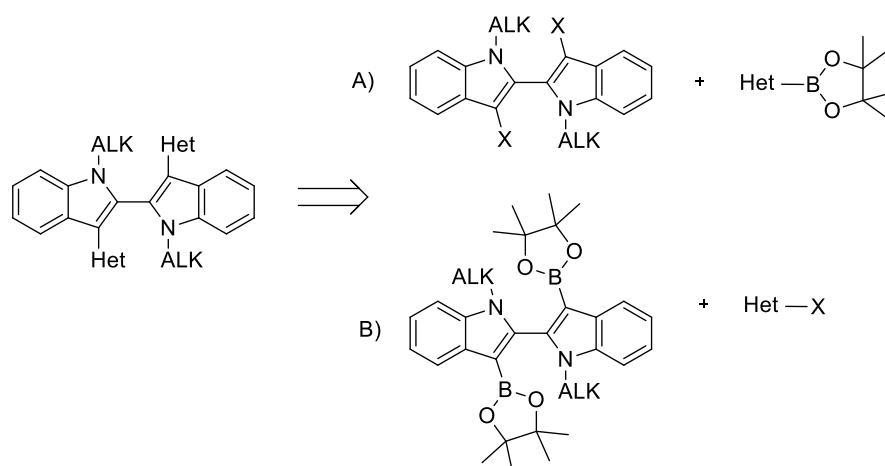
Figure 80: retrosynthetical analysis for 3,3'-diheteroaryl-2,2'-biindoles by a Suzuki-Miyaura approach.

First investigations were performed following approach A) as 3,3'-dihalo-2,2'-biindoles are already known in literature. Moreover, some organoboron reagents, like 2,2'-bithiophene-5-boronic acid pinacol ester are even commercially available and it appears particularly attractive as it can be used to produce the well known (*N*-alkyl)Ind$_2$T$_4$ compounds.[185]

Since organoboron reagent was already available, efforts were focused on the synthesis of 3,3'-diiodo-2,2'-biindole **128a**. A paper published by Arcadi[232] in 2004 described an Au(III) catalysed *5-endo dig* ring closure of dianiline **94** to 2,2'-biindole **128** and subsequent one pot iodination with I$_2$ to directly afford 3,3'-diiodo-2,2'-biindole **128a**. However, when reaction was performed, only 23% of iodinated compound was detected (Scheme 67), resulting in no substantial improvement of Larock-like approach.
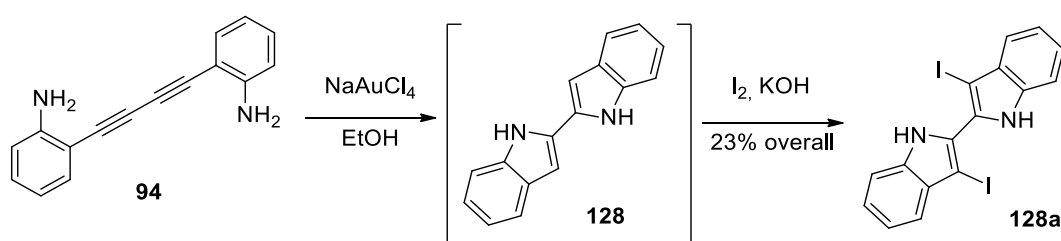
Scheme 67: synthesis of compound **128a**.

Another literature approach starting from **94** was explored by Koradin[233] in 2003: same *5-endo dig* ring closure of dianiline **94** to 2,2'-biindole **128** was accomplished by reaction with KH in NMP (*N*-methyl-2-pyrrolidone). Interestingly, Koradin reported that only potassium and caesium strong bases are effective in this type of transformation. Reaction was performed then with high success using fresh potassium hydride (Scheme 68): however, as KH gets older, reaction efficiency dramatically drops, leading to isolation of mono-closure product **128b**; moreover, even to complete no reaction at all was observed with KH reagent samples older than one month.
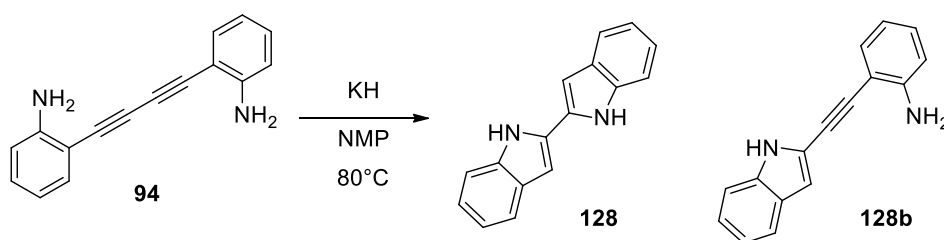
Scheme 68: synthesis of 2,2'-biindole **128**.

Such high dependence on KH batch quality drove to another similar approach: Chang in 2006[234] used copper(I) iodide instead of potassium hydride with excellent results. Same idea was exploited by Lee in 2009 on highly functionalized 1,4-di(2-aminophenyl)-butadiynes to achieve new molecular tweezers.[235] Reaction was repeated successfully and even big batches were accomplished without too much loss in yield. A slight change in the workup must be performed when separating solid CuI from mother liquors by filtration as significant quantity of **128** stayed trapped in solid cake. It can be easily recovered by dissolving solid cake in aqueous NH_3 and extracting with Et_2O. The only disadvantage of this protocol is over stoichiometrical usage of CuI. Alkylation of **128** with 1-bromopropane was easily afforded: subsequent iodination with NIS was successful too and gave product **130** in good yield. After the functionalization of 3,3' positions, **130** showed in its proton NMR spectrum the characteristic diastereotopic pattern of alkyl protons. All reactions are resumed in Scheme 69.
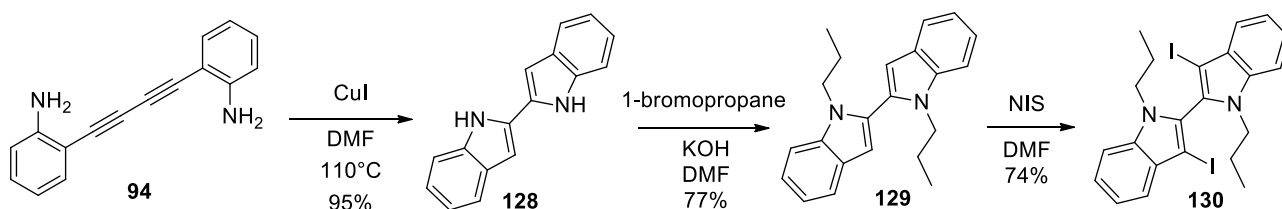
Scheme 69: synthesis of 3,3'-diiodo-2,2'-biindole **130**.

Compound **130** was then made reacting in subsequent Suzuki-Miyaura reaction with 2,2'-bithiophene-5-boronic acid pinacol ester (Scheme 70) producing the expected coupling product (*N*-Pr)Ind₂T₄ **98** in less than an hour with high yield (79%). Best reaction conditions regarded Pd(PPh₃)₄ as catalyst, KOH as base and a ternary mixture of solvents toluene/ethanol/water as solvent.
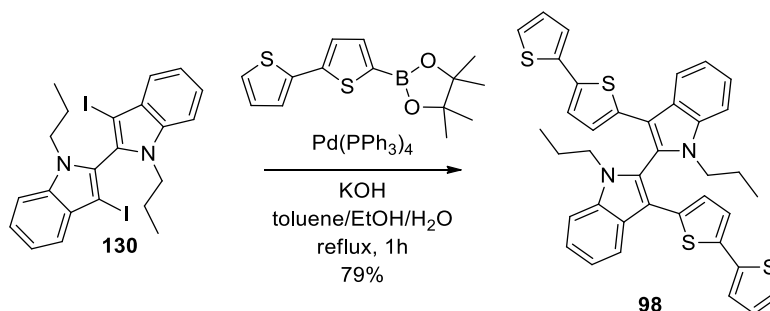
Scheme 70: synthesis of N-Pr)Ind$_2$T$_4$ **98.**

Achievement of this result opens possibility to further expansion of 3,3'-diheteroaryl-2,2'-biindole synthesis for electroactive material applications. Moreover, this pathway can be exploited to surpass previously exposed Larock-type indolizations to achieve biindolic products in higher yield. Hot point is to obtain appropriate boronic acid pinacol ester: this purpose may be accomplished by exploitation of Miyaura borylation[236]. Discovered in 1995, this reaction allows the conversion of aromatic and heteroaromatic halides to the corresponding boronic acid pinacol ester in mild conditions by palladium(II) dichloride diphenylphosphinoferrocene (dppf) catalysis. Reaction is highly tolerant towards several functional groups. Boron source is bis(pinacolato)diboron (B$_2$(pin)$_2$). Commonly accepted mechanism is reported in Scheme 70.
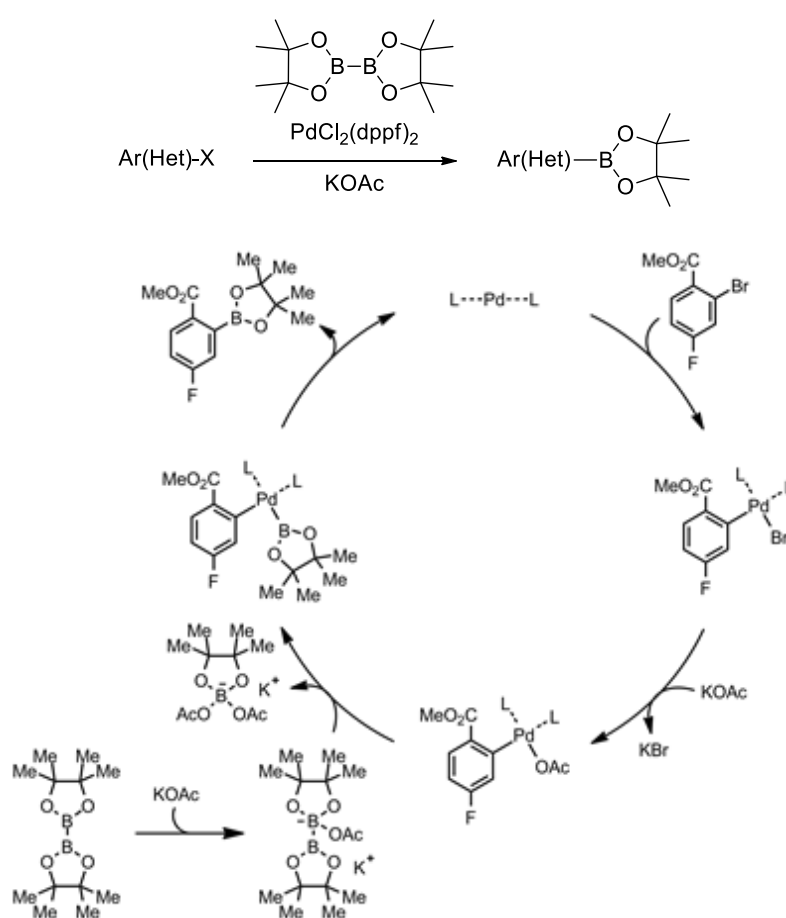
Scheme 71: general reaction and mechanism of Miyaura borylation.

We tried to apply this strategy to the synthesis of compounds **121** and **127,** which were obtained in modest yield through the classical Larock-type approach. Unfortunately, first attempts of borylation of compound **119** did not have success as reactant was always recovered unchanged (Scheme 72), probably because tested conditions were not suitable for catalyst insertion in C-Br bond. Further experiments (especially catalyst survey) are planned to solve the problem.
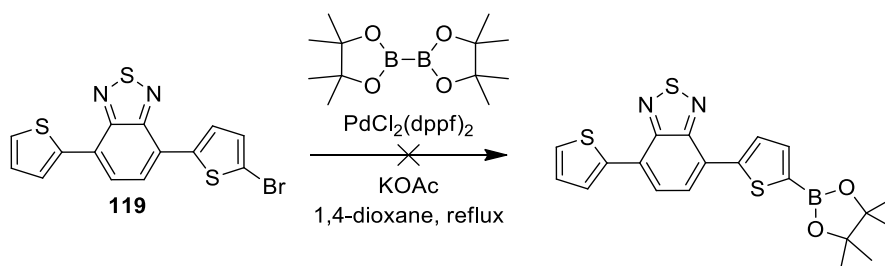
Scheme 72: unsuccessful Miyaura borylation of **119**.

11.4.1. Preliminary chemical oligomerization of compound 98

All biindoles-based oligomeric films are obtained by appropriate 2,2'-biindole monomer *in situ* electrooxidation. As mentioned in previous results, only full electrochemical and spectroelectrochemical characterization on films has been deeply explored. No investigations on *chemical identity* of electroactive film have been carried out yet. Some investigations were conducted over BT_2T_4 oligomeric films[237]: LDI analyses of raw material scratched from working electrodes revealed presence of dimers, trimers and superior oligomers. Interestingly, cyclic dimers and trimers in significant quantities were found too: their role in enantiodiscrimination mechanism is currently under discussion.

To get some insights also on biindole films, LDI investigations using raw film directly scratched from electrodes were tried but gave no result. This was probably due to some positive charge trapping in biindole films after oligomerization. To overcome this problem, some anodic range voltametric cycles to quench positive charges were performed after deposition: however, still no result was found.

Given the new synthetic pathway improving accessibility to compound **98**, some preliminary chemical oxidation experiments of biindole **98** were performed. As previously indicated for 3,3'-bithianaphtene monomers[171,238], oligomerization reactions were run in high dilution in dry chloroform and using $FeCl_3$ as oxidant (Scheme 73). High dilution medium reflected conditions adopted in electrochemical cells for electropolymerization. Partially oxidised products were quenched by adding hydrazine prior to column chromatography purification. High solubility given by propyl group of biindole **98** allowed facile separation by chromatography of some oligomerization products.
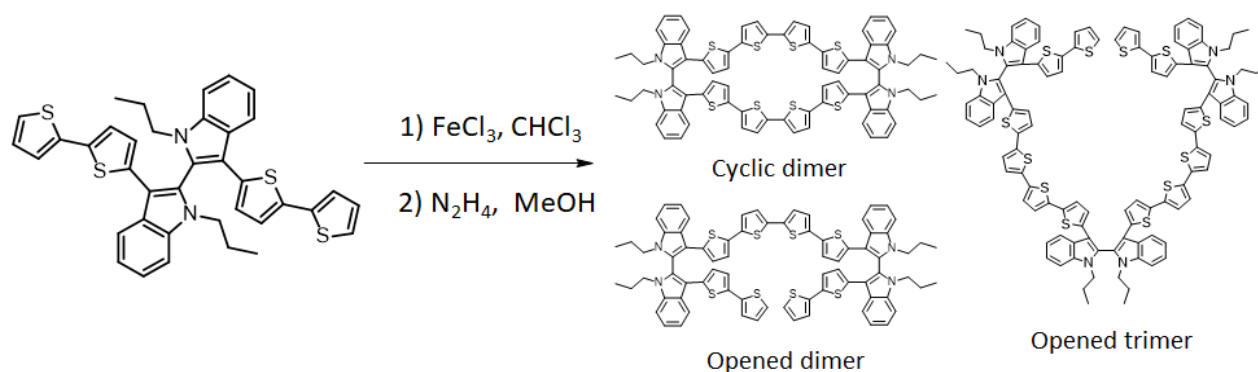
Scheme 73: chemical oligomerization of compound **98**.

As indicated in Scheme 73, three main products were identified after high resolution MALDI analyses (Figure 81). The open dimer was obtained in 38% yield and isolated in pure form. Noticeably, as already reported for bithianaphtene chemical oligomerization, a cyclic dimer was afforded, despite it was not separated from opened trimer. A mixture of unidentified superior oligomers was found too.

Further experiments are planned to isolate and characterize all the oligomerization products, seeking particularly for closed oligomers. Since compound **98** can now be prepared on gram scale, after HPLC resolution, enantiopure oligomers could be afforded by this protocol. It is planned for the near future to deposit them on electrode surface to get new insights on enantiodiscrimination mechanism behind chiral cyclic voltammetry analyses towards different chiral probes.
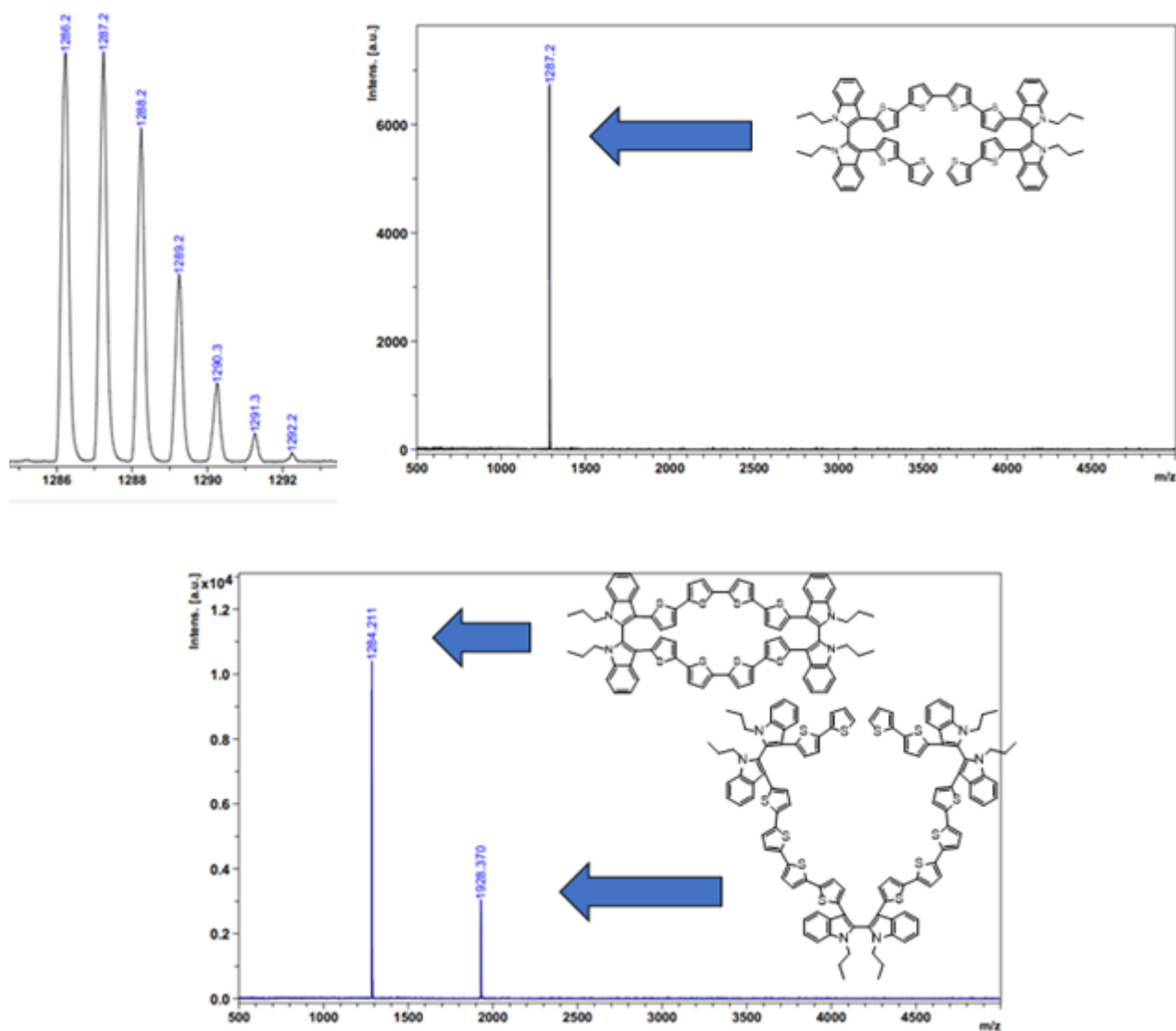
Figure 81: MALDI analyses for opened dimer (up left; calculated mass pattern: up right; found mass value) and closed dimer/opened trimer mixture (bottom).

12. Conclusions and further developments

The synthesis of a family of new π spaced 2,2'-biindoles has been carried out. Their electrochemical behaviour, both for monomers and oligomers, has been deeply discussed. Introduction of a thienyl spacer to modify the classic Ind_2T_4 backbone brought higher conjugation efficiency for $(N\text{-Pr})Ind_2T_6$ rather than adding a phenyl spacer, which originated the $(N\text{-alkyl})Ind_2Ph_2T_4$ family.

$(N\text{-alkyl})Ind_2Ph_2T_4$ racemates were effectively resolved by mean of chiral HPLC in a preparative way. Enantiomers were used as starting material to coat electrodes with electroactive enantiopure films. These films proved an excellent enantiodiscrimination ability towards different chiral probes, some of them being of pharmaceutical interest. In the case of $(N\text{-Hex})Ind_2Ph_2T_4$, electrodeposition was not possible due to its very high solubility. However excellent enantiodiscrimination were obtained by using it as enantiopure additive.

A deep HPLC investigation is ongoing for $(N\text{-Pr})Ind_2T_6$ in order to improve the separation conditions and in order to expand enantioselective electrochemical experiments with different chiral probes.

Compounds showing a 3,3'-biindole moiety were demonstrated to free rotate around interannular bond at room temperature. Therefore, they can be considered only as achiral monomers in electrochemistry applications. Theoretical studies showed the possibility to achieve configurationally stable compounds by introducing methyl groups in 4,4'- positions of indole benzenoid rings. Confirmation of the theoretical data will be achieved by synthetizing the suggested derivative in the near future.

2,2'-Biindoles featuring a benzochalchogenodiazole were successfully synthetized and electrodeposited. Their electroactive films showed a low bandgap due to the donor-acceptor structure. Spectroelectrochemical analyses revealed a strong electrochromic effect. Further experiments like *in situ* conductance are in planning for better understanding of oligomer features: moreover, HPLC study to separate the racemate must be done in the future to combine their optical and chiral properties.

A new synthetic strategy involving Suzuki-Miyaura cross coupling has been studied presenting advantages over the previous Larock-like approach. It uses a common skeleton, namely 3,3'-diiodo-2,2'-biindole **130**, that can be obtained and isolated in high yields and few passages, allowing also functionalisation at nitrogen atom before the coupling reaction. A large number of boronic acids, boronic esters, pinacolborates and boranes is commercially available and suitable for cross coupling reactions. Following this strategy, compound **98** was achieved in high yield, opening path for experiments of chemical oligomerization to get insights on chemical nature of electroactive films.

Unfortunately, synthesis of 4-([2-thieno]-5-pinacolborano)-7-(2-thienyl)-2,1,3-benzothiadiazole by Miyaura borylation of **119** was unsuccessful. Reactant was recovered unreacted, proving that C-Br bond was not

affected by catalyst. A survey of better reaction conditions must be done in order to use this strategy for benzocalchogenodiazole containing biindoles.

An alternative to C-B bond formation on the pendant could be C-B bond formation directly on the biindole skeleton (Figure 42, B), employing Miyaura conditions or other synthetic strategies; an interesting idea could be the borylative cyclisation of *N*-protected 1,4-di(2-aminophenyl)-butadiynes to form directly 2,2'-biindole boronic ester (Scheme 72), without passing through 3,3'-iodination, firstly studied by Harrity in 2010.[239] A further development of this pathway avoiding metal catalyst and poisonous arsenic compounds is the use of boron trichloride (BCl_3), as reported by Lv and coworkers[240] in 2018 (Scheme 74).
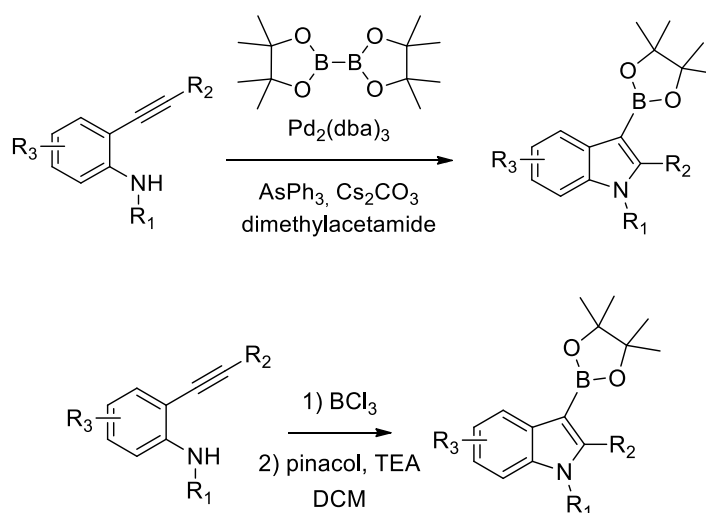
Scheme 74: synthesis of indole 3 boronic acid pinacol esters by Harrity (up) and Lv (bottom) approach.

Noticeably, once a more performant synthetic pathway is identified, possibility to obtain 2,2'-biindoles bigger batches will available. Achieving this is therefore quite important fort subsequent chiral HPLC separation, thus leading to chiral features analysis on enantiomers. In particular, (*N*-Hex)Ind$_2$BTD$_2$T$_4$ **121** and (*N*-Hex)Ind$_2$BSeD$_2$T$_4$ **127**, once separated in optical antipodes, could be interesting substrates to study chiral photoluminescence.

Meanwhile, given interesting properties of (*N*-Hex)Ind$_2$BTD$_2$T$_4$ **121** and (*N*-Hex)Ind$_2$BSeD$_2$T$_4$ **127**, a new study on synthesis of analogous 2,2'-biindole with oxygen substitution in benzochalcogenodiazole moiety (leading to benzoxadiazole) was started, with the aim to better understand chalcogen atom role in physical properties of corresponding biindoles. Synthesis was approached by usual Larock-type ring closure, which, albeit overall low yields, can surely afford target compound. This choice is also justified by ongoing studies on Miyaura borylation on halide **119**.

Requested halide 4-([2-thieno]-5-bromyl)-7-(2-thienyl)-2,1,3-benzoxadiazole **133** was approached starting from benzoxadiazole. Synthetic steps leading to target are similar to those followed for benzothiadiazole.

After bromination[241] and subsequent Stille coupling[183], mono halogenation with NBS was successfully accomplished (Scheme 75).

Scheme 75: synthesis of halide **133**.
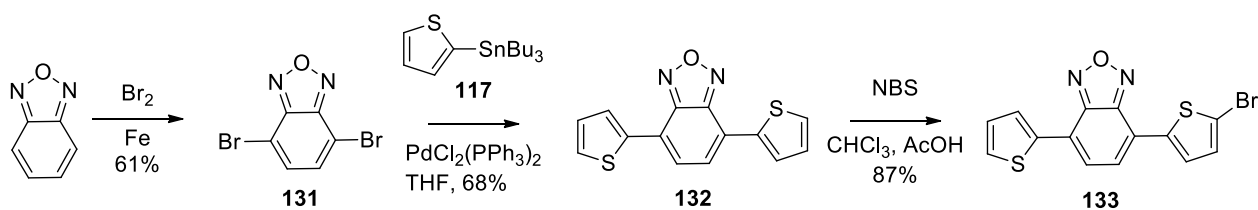
Preliminary attempts of indolization between trifluoroacetamide **95** and halide **133** gave 2,2-biindole **134** in low yield (Scheme 76). No alkylation reaction was attempted due to very small quantity of **134** recovered as intense dark red coloured solid. This result witnesses again the necessity to find alternative synthetic methods with better performances.
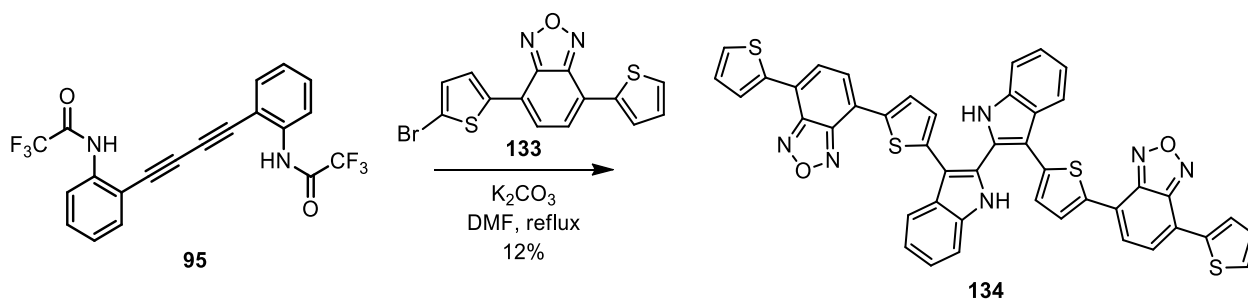
Scheme 76: synthesiis of 2,2'-biindole **134**.

- Appendix -

Synthesis of novel tetrapyrazinoporphyrazines for applications in material science field

13. Introduction on pyrrole containing macrocycles

13.1. Porphyrins

Among pyrrole containing macrocyclic structures a strong predominant role is played by porphyrins. They are constituted by a skeleton of four pyrrole rings interconnected on α positions by methine bridges.[242] These compounds possess 26 π electrons; delocalization of 18 of them in continuous and planar cycle allows porphyrins and related compounds to be aromatic[243] (Figure 82) according to Hückel rule. Due to high extension of conjugation, all pyrrole containing macrocyclic structures show an intense absorbing in visible light region. This is responsible for their intense coloration: it's no surprise then that their name derives from Greek πορφύρα, meaning *purple*.
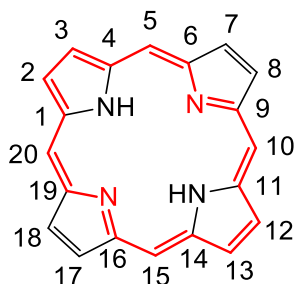
Figure 82: porphin, the simplest pyrrole containing macrocycle and its numbering. Aromatic subunit is red highlighted.

Aromatic nature of porphyrins explains why former double bonds prefer to react by electrophilic aromatic substitution instead of classic additions: nitration[244] and Vilsmeier-Haack formylation[245] are for example well documented.

Porphyrins are useful ligands for metal complexation. Coordinated metal, which generally has +2 or +3 oxidation state, is situated in macrocycle centre.[242] Coordination provides extra stabilization to products. Most majority of natural occurring porphyrins are metal complexes: one of the most famous is Fe(II) complex haem (Figure 83), prosthetic group of haemoglobin protein. The latter is responsible for oxygen transportation in human blood and for its red colour. Haem complex structure is a continuous stimulus for chemists as it never has been synthetized in laboratory from available reagents. Biosynthesis starts off from glycine and succinyl-coenzyme A and follows a complicate pathway[246] (Figure 84). Haem can be oxidized to its analogous Fe(III) complex, haemin.[247] Fischer's haemin synthesis was awarded by a Nobel Prize in 1930.[248]
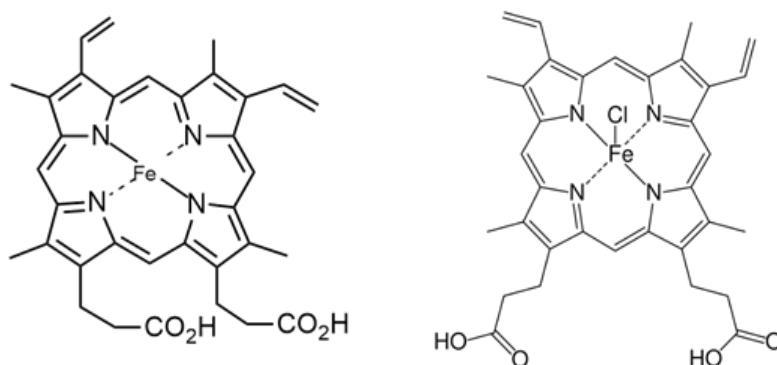
Figure 83: haem (left) and haemin (right).
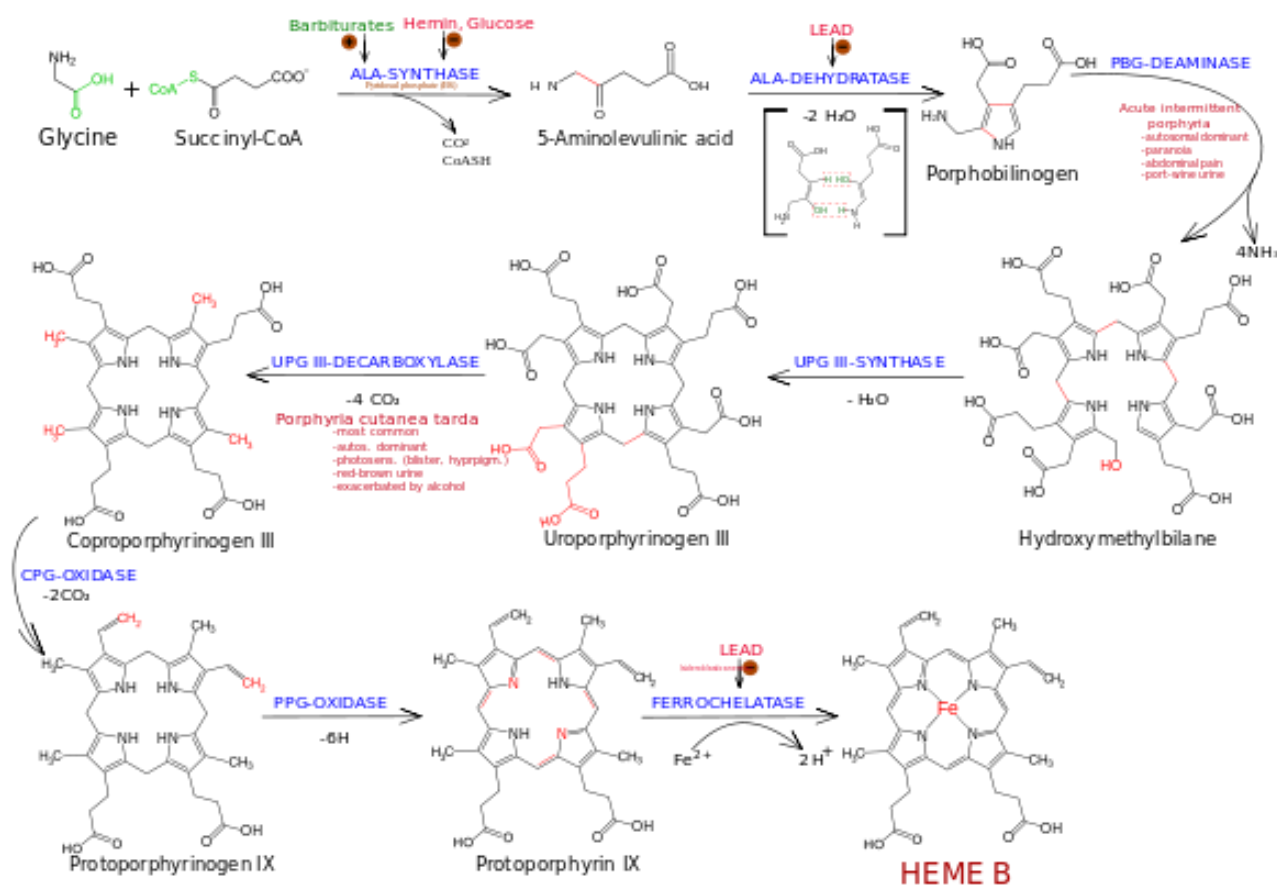
Figure 84: haem group biosynthesis.

Great importance in natural porphyrins is covered by chlorophylls. They are responsible for plants green colour as they are light absorber to promote glucose photosynthesis. Instead of Fe(II), Mg(II) is hosted in their centers. Another difference is saturation 17-18 double bond: however, since it is not involved in 18 electrons delocalization, all chlorophylls maintain aromaticity. 17,18-Diihydroporphyrins are known as chlorines (Figure 85). Traces of chlorophylls and other nickel and vanadium porphyrin complexes in crude oil demonstrated its biological provenience.[249]
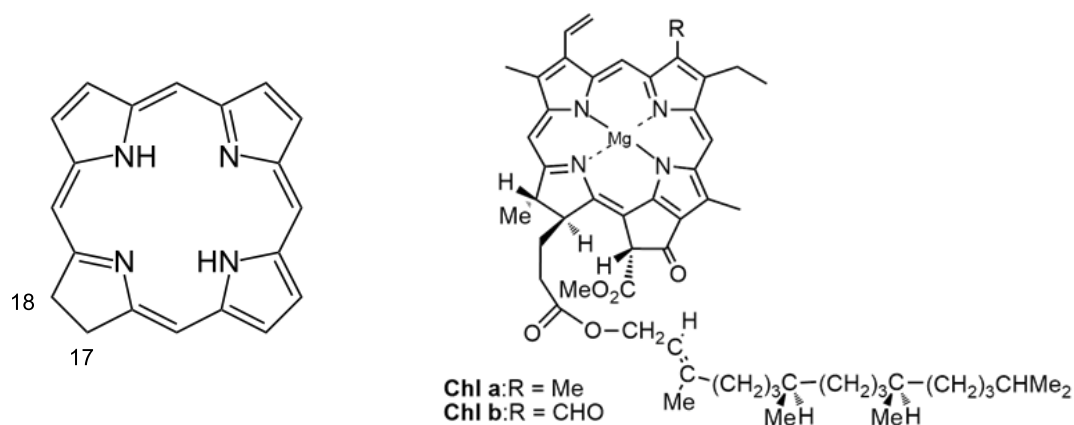
Figure 85: chlorine (right) and chlorophyll A and B (left).

Laboratory porphyrin synthesis started in 1935 with effective macrocyclization published by Rothemund.[250,251] Protocol exploits HCl catalysed hydroxyalkylation of four pyrrole units with four aldehyde fragments in refluxing methanol. Reaction shows great versatility with high number of aldehydes. A later work by Adler optimized protocol by conducting reaction in neat refluxing propionic acid (Scheme 77).[252] Further improvements focused on using catalytic amounts of Brønsted or Lewis acid in non-acidic solvent.[253,254] With progresses in green chemistry, microwave assisted synthesis nowadays represents an excellent alternative.[255]
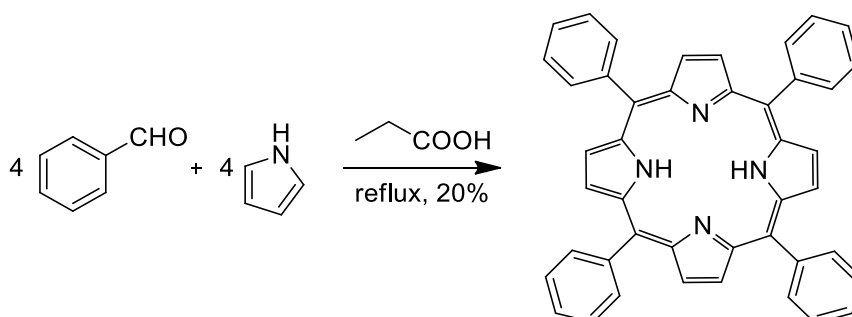
Scheme 77: synthesis of meso-tetraphenylporphyirine.

Given previously cited extended π conjugation in porphyrins, it's no surprise that a lot of research was focused in exploring practical use of their optical properties. Applications as dyes in solar cells[256–258] and activator in photodynamic cancer therapy[259,260] are ones of the most extensively studied. On the other hand, porphyrin metal complexes are often studied as catalysts in oxidation or photo oxidation reactions[261] or as sensors for small molecule substances.[262]

♦ ♦ ♦ ♦ ♦ ♦

13.2. Phthalocyanines

Phthalocyanines (Pcs) are strongly relate to porphyrins structure: instead of having a tetrapyrrole based macrocycle, phthalocyanines are based on a tetraisoindole skeleton (Figure 86). Methine bridge groups are replaced by nitrogen linkers.[263]
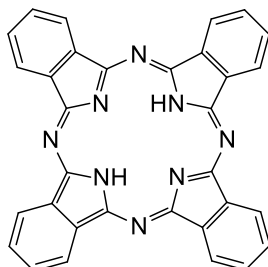
Figure 86: phthalocyanine.

Phthalocyanines were accidentally discovered in 1907 by Braun and Tcherniac at South Metropolitan Gas Company in London during preparation attempts of *o*-cyanobenzamide from phthalimide in refluxing acetic acid.[264] The first phthalocyanine metal complexes was serendipindously prepared in 1927 by refluxing CuCN in pyridine with *o*-dibromobenzene[265] and its structure was elucidated by Robertson in 1937 with X-rays technique.[266]

Phthalocyanine compounds show generally a bad solubility in solvents due to their tendency to aggregate thanks to strong π stacking interactions.[267] Introduction and tuning of peripheral groups can improve solubility in water or organic solvents.[268] Unsubstituted phthalocyanines have broad band absorption light around 600-700 nm thus they appear as green or blue solids.[267] This makes commercial application of phthalocyanines is strongly pointing on their colour properties: around 25% of artificial dyes or pigments is constituted by Pcs.[269] A relevant application is as catalyst in industrial Merox process to oxidize thiols in crude oil to disulfides which can be easily removed by decantation.[270] Other applications are in common with porphyrins.

Pioneering studies on phthalocyanines synthesis were afforded by Linstead in 1930s with the synthesis of iron phthalocyanine.[271–273] Compared to porphyrins, which do not need any metal for their synthesis, phthalocyanines' synthesis must pass through a metal salt template process. Most common synthetic alternatives involve template cyclotrimerization of phthalonitriles in protic high boiling point solvent in presence of a base in catalytic amount.[274] Solvent deprotonation by base generates the nucleophilic catalyst responsible for reaction start (Scheme 78).[275] Another possibility is to start from phthalic acids or anhydrides in presence of urea and a base.[275] Reactions are always conducted at high temperature, usually above 180°C.
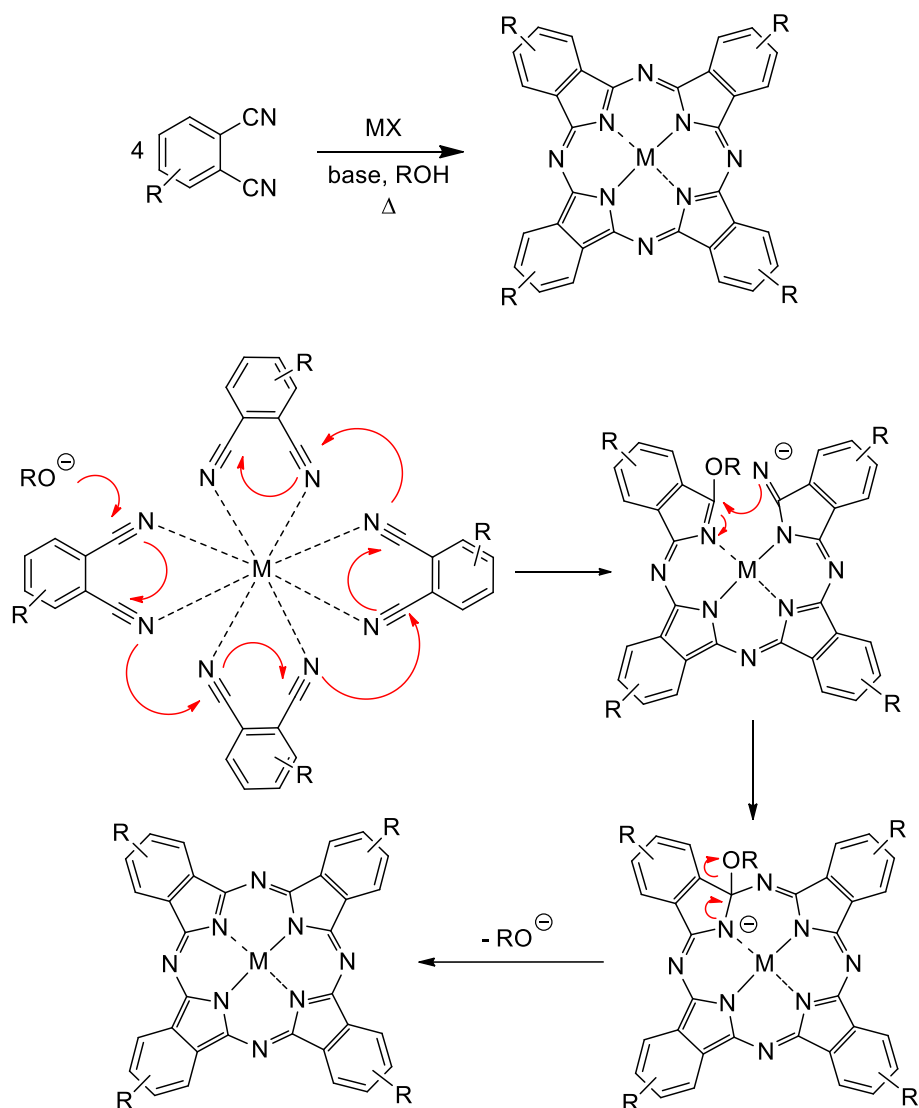
Scheme 78: metal salt (MX) template synthesis of phthalocyanine compound (on top): cyclotetramerization mechanism (on bottom).

♦ ♦ ♦ ♦ ♦ ♦

13.3. Porphyrazines (azaporphyrins)

Porphyrazines (Pzs) structure is very close to porphyrins as the share the same tetrapyrrolic macrocycle. However, in porphyrazines bridges are constituted by aza linkers instead of methine bridges (Figure 87).
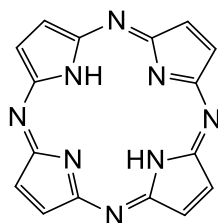
Figure 87: porphyrazine, also known as tetrazaporphyrin.

They were introduced by Linstead in 1937 as natural extension of his works on phthalocyanines.[276] A deep study on their optical and chemical features was carried out in by Stuzhin[277–279] and Lukyanets.[268,280]

Porphyrazines UV-vis absorbance is quite similar to phthalocyanines[281]: diagnostic is presence of high absorption in near UV region (300-400 nm, known as Soret band) and a red shifted band (inferior of 600 nm, known as Q band).[282] Some fluorescence can be detected in visible region due to macrocycle structure rigidity.[283] Optical features make for porphyrazines, like phthalocyanines and porphyrins, possible applications in cancer photodynamic therapy as photosensitizers.[284,285] However, critical point for their usage is extremely low solubility, making difficult synthetizing pure samples.[286]

Appropriate alkyl substitution can partially solve solubility issues. Synthesis of substituted azaporphyrins starts off from maleonitriles, in analogous conditions as phthalocyanines.[280] Major issue is synthesis of maleonitrile as during preparation is possible to afford mixtures with relative fumaronitrile[287]: the latter is not useful in macrocyclization reaction due to *trans* configuration of cyano groups. A photochemical reaction can be applied to convert fumaronitrile into active maleonitrile[287] albeit resulting reaction mixture is sometimes hard to separate (Scheme 79). Nucleophilic substitution on chloromaleonitrile to synthetize more complex dinitriles can avoid fumaronitrile impurities[288] (Scheme 80). Metal salt templating effect is like phthalocyanines fundamental to achieve tetramerization successfully.[279] Cyclization conditions are the same previously cited.
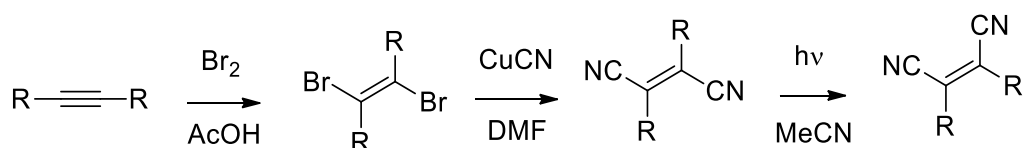
Scheme 79: synthesis of maleonitriles via photochemical conversion of fumaronitriles.
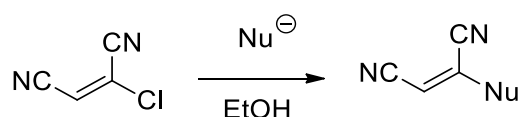
Scheme 80: synthesis of maleonitriles by nucleophilic substitution.

14. Synthesis of tetrapyrazinoporphyrazines (TPyzPzs)

In chemical space of porphyrazines, growing interest have tetrapyrazinoporphyrazines (TPyzPzs)[289,290] (Figure 88). Their success in the last decade is justified by broad application spectrum such as in electrochemical[291] devices, in Langmuir Blodgett films as sensors[292,293] and even as polymers heat stabilizers.[294] Their optical properties, common to previously cited macrocycles, make them suitable as pigments[295], dyes[296] and dye-sensitized solar cells.[297] Not negligible are applications as photoactivators for singlet oxygen production[298–300] and as fluorescence marker for DNA detection.[301]
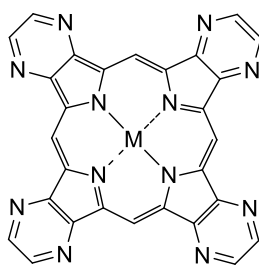
Figure 88: structure of a tetrapyrazinoporphyrazine metal complex.

Retrosynthetic analysis shows that immediate precursors of TPyzPzs are 2,3-dicyanopyrazines, which can be prepared by condensations of an appropriate vicinal diketone with diaminomaleonitrile (DAMN) (Scheme 81). The latter is a very cheap and commercially available, as it's prepared by hydrogen cyanide tetramerization.[302] Availability of DAMN makes it an extremely useful building block in synthesis of many nitrogen containing heterocycles.[303] Condensation between DAMN and diketones usually takes place in high temperature batches in presence of acid catalysis.[304,305] Appropriate tuning of diketone substituents can afford very soluble 2,3-dicyanopyrazines, which can overcome solubility issues of respective tetrapyrazinoporphyrazines in water[306] or organic solvents.[307]
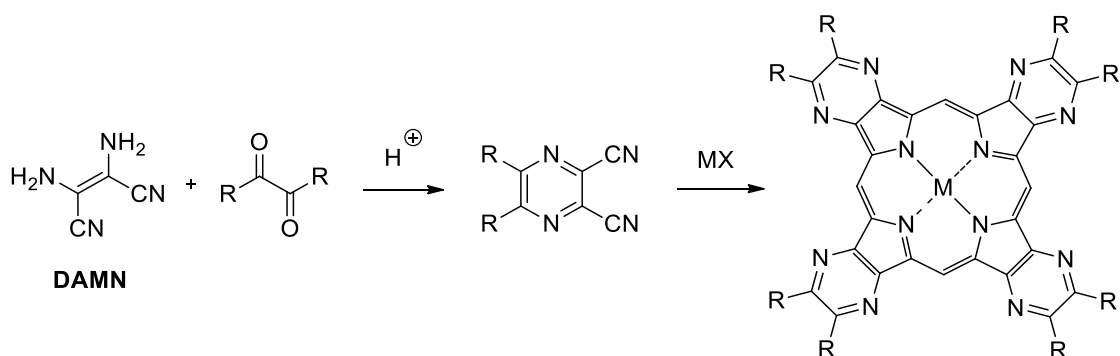
Scheme 81: synthesis of 2,3-dicyanopyrazines from DAMN and 1,2-diketone.

DAMN itself cannot be used as monomer to achieve TPyzPzs. Octaminoporphyrazines can be prepared in a 3 steps sequence by protecting DAMN with selenium dioxide and selenium removal after macrocyclization with H_2S.[308] Octaminoporphyrazines are reported to be unstable as they exhibit high oxidation tendency exposed

to air[308,309] and must be condensed with diketone immediately to afford a tetrapyrazinoporphyrazine (Scheme 82). However, this synthetic pathway is longer and only limited to academic interest.
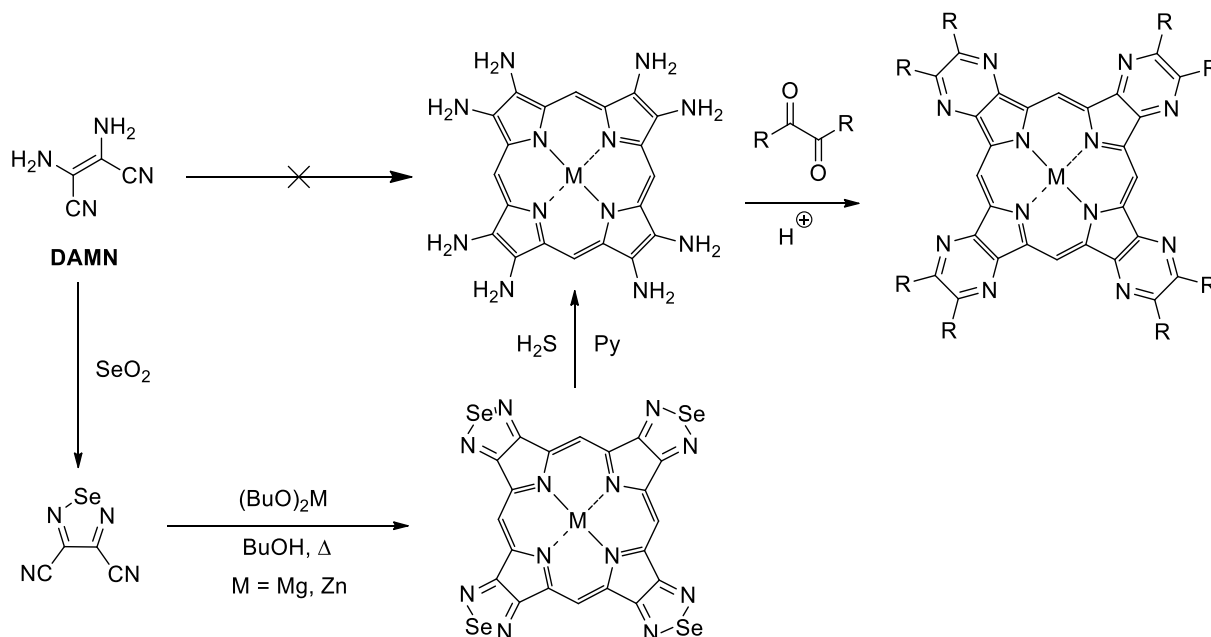
Scheme 82: synthesis of TPyzPzs by octaminoporphyrazine.

Another path to highly functionalized 2,3-dicyanopyrazine monomers comes from commercially available 5,6-dichloropyrazine-2,3-dicarbonitrile. The latter can be prepared by acylation of DAMN with oxalyl chloride and subsequent chlorination with SOCl₂.[310] Its chlorine atoms can be easily substituted by a large amount of nucleophiles[311] or by classic cross coupling reactions[312,313] (Scheme 83).
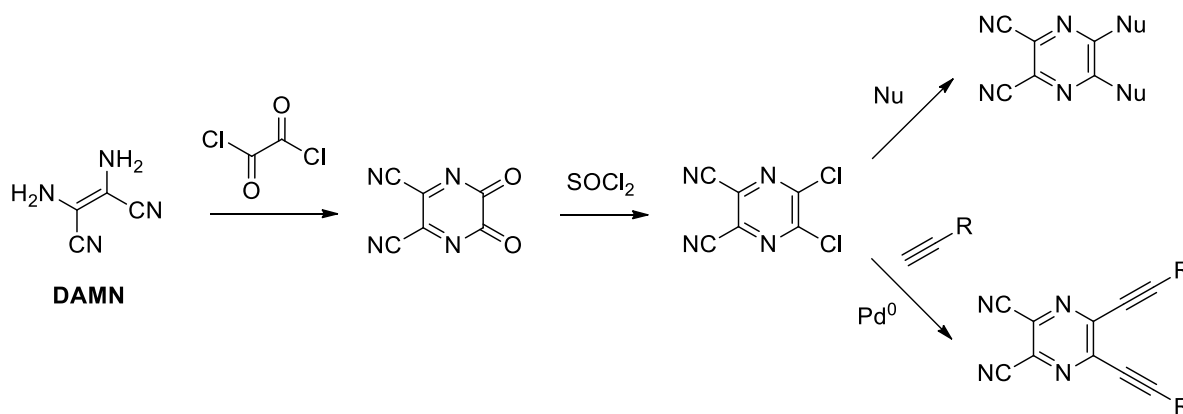
Scheme 83: synthesis of functionalized 2,3-dicyanopyrazine monomers from 5,6-dichloropyrazine-2,3-dicarbonitrile.

15. Aim of the research project

Given high application interest of tetrapyrazinoporphyrazine products, Penoni research group completed successfully synthesis of novel TPyzPzs fused with dibenzo[b,f]azepine units[314] (Figure 89). Palmitoyl chains were introduced to afford better solubility. This metal complex proved to be effective catalyst for cyclopropanation of olefins and α,β-unsaturated ketones with ethyl diazoacetate.

M = Cu(II), Co(II)
R = C$_{15}$H$_{31}$
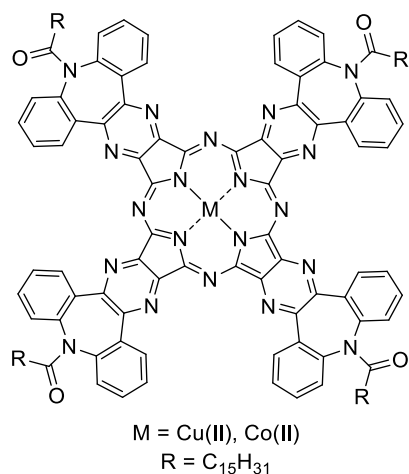
Figure 89: TPyzPz with fused dibenzo[b,f]azepine units.

Research project is therefore focused on synthesis of analogous TPyzPz skeleton but decorated with octyl group (type **A**) instead of previously cited palmitoyl. The rationale of such modification is to avoid the presence in the final complexes palmitoyl chain carbonyl group: it can be a problem both for 3D packing and electronic properties, in order to employ new octyl TPyzPz in organic electronics keeping however high solubility. Furthermore, presence of long alkyl chains makes phthalocyanines and analogues to exhibit thermotropic liquid crystalline behaviour.[315] Aiming for same applications, a new tetrapyrazinoporphyrazine based on thiophenes (type **B**) has been set as target as well (Figure 90). Thiophenes predominant role in organic electronics and photonics is in fact well documented.[139]

M = Cu(II), Zn(II)
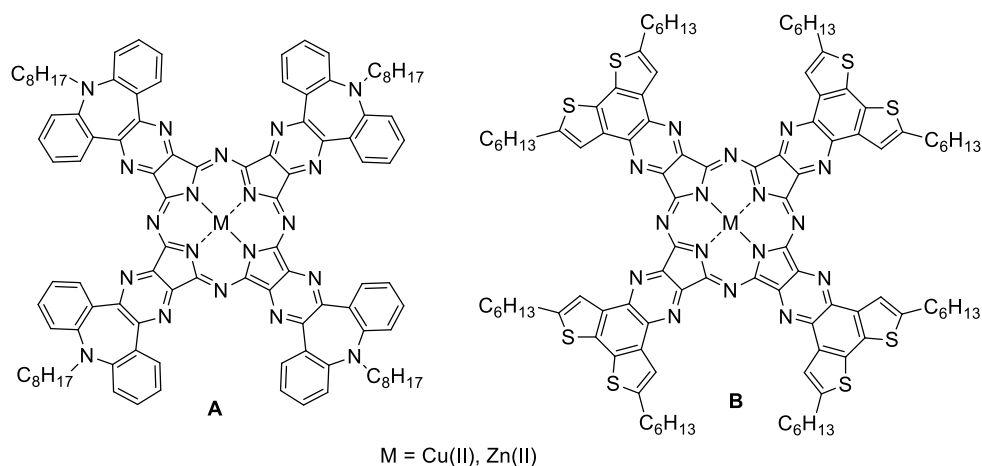
Figure 90: target types **A** and **B** TPyzPzs structures.

16. Results and discussion

16.1. Type A tetrapyrazinoporphyrazine synthesis and characterization

16.1.1. Preliminary results

Key point to achieve type **A** tetrapyrazinoporphyrazine is synthetizing dinitrile **135** (Figure 91), which is suitable monomer for tetracyclization as octyl group increases dramatically solubility.
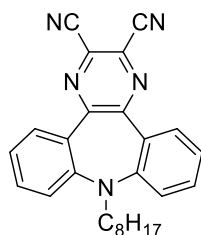
Figure 91: dinitrile **135**.

First approach to **135** was inspired by one previously reported by Penoni[314] and starting material was identified in commercially available oxcarbazepine **136**. This molecule is widely used as antiepileptic drug and is particularly known to treat focal or partial seizures in adults and children.[316] Its chemical properties were deeply studied by Penoni to prepare a wide library of derivatives with possible biological activity.[317] Oxcarbazepine was oxidized by benzeneseleninic anhydride in boiling 1,4-dioxane to diketone **137**. Despite its high cost, benzeneseleninic acid anhydride allow to obtain pure **137**, without selenium impurities, tipically present when SeO_2 is used as oxidating agent. Ureido group removal during this reaction was previously reported[314,317], but mechanism of this side reaction is unknown. Subsequent condensation with DAMN in acetic acid afforded **138** in pure form as precipitate from the reaction mixture in 93% yield. Reactions are resumed in Scheme 84.
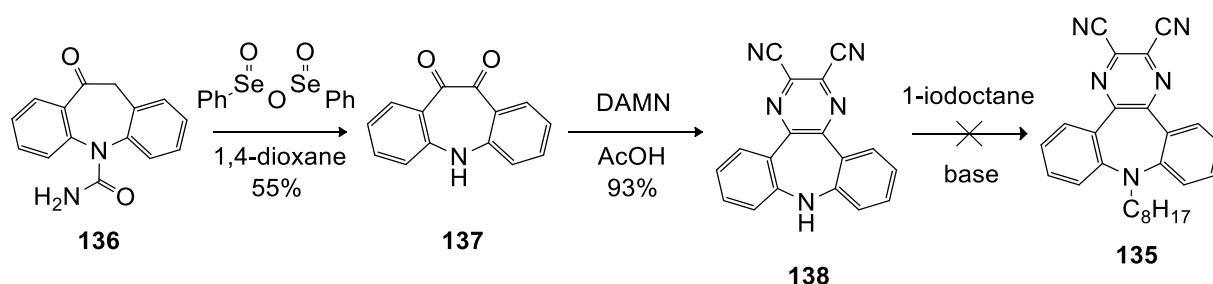
Scheme 84: first unsuccessful approach to dinitrile **135**.

Several alkylation attempts were performed on product **135**, but none was successful due to its extremely low solubility in any solvent. Several bases like NaH, NaOH, Na_2CO_3 and $NaNH_2$ in different solvents and temperature conditions were tested but in all cases reactant **138** was recovered unchanged with no traces of any other products. However, when performing reaction in boiling DMF and K_2CO_3 as base the formation of a

major product was observed. Mass analysis and X-ray crystallography led to assign the structure of this by-product as **139** (Scheme 85). This behaviour of pyrazino-2,3-dicarbonitriles was already reported.[318] Presumably, in this conditions, 1-iodoctane was hydrolyzed to 1-octanol, which in basic condition drove to a nucleophilic aromatic substitution. Compound **139** crystallizes in the centrosymmetric P-1 space group with two independent molecules in the asymmetric unit. Intriguingly, these two molecules, stacked by π-π interaction of ca. 3.37 Å, differ only by the stereochemistry at the terminal torsional angle of the alkyl chain, which is found to be in trans and gauche conformation for the two molecules, respectively.
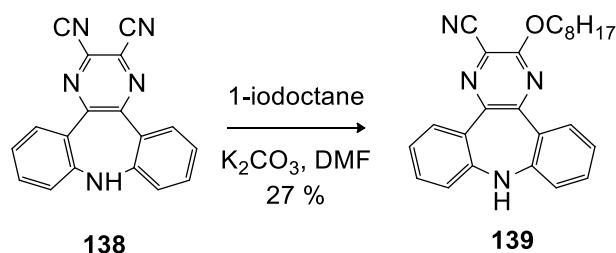
Scheme 85: synthesis of product **139** by nucleophilic aromatic substitution.
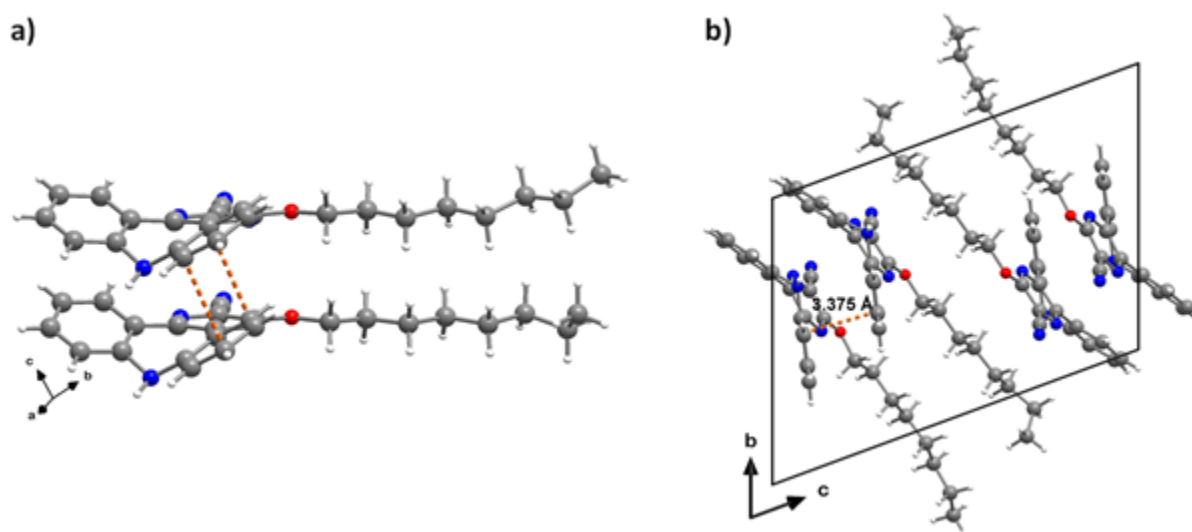
Figure 92: a) asymmetric unit for the crystal structure of **139** highlighting the π-π stacking between the two phenyl rings; b) crystal packing viewed down to the (100) crystallographic direction. Color codes: C, gray; N, blue; O, red; H white. The π-π stacking (3.375 Å) is highlighted with the dashed orange line.

Very low solubility of **137** in any organic solvent and the presence of a free NH group negated the possibility to try directly the macrocyclization with this compound. Octylation of product **136** was also difficult: treating with bases to generate anion is competitive with the known benzylic acid rearrangement, leading to a ring contraction and not to desired *N*-alkylation product.[319]
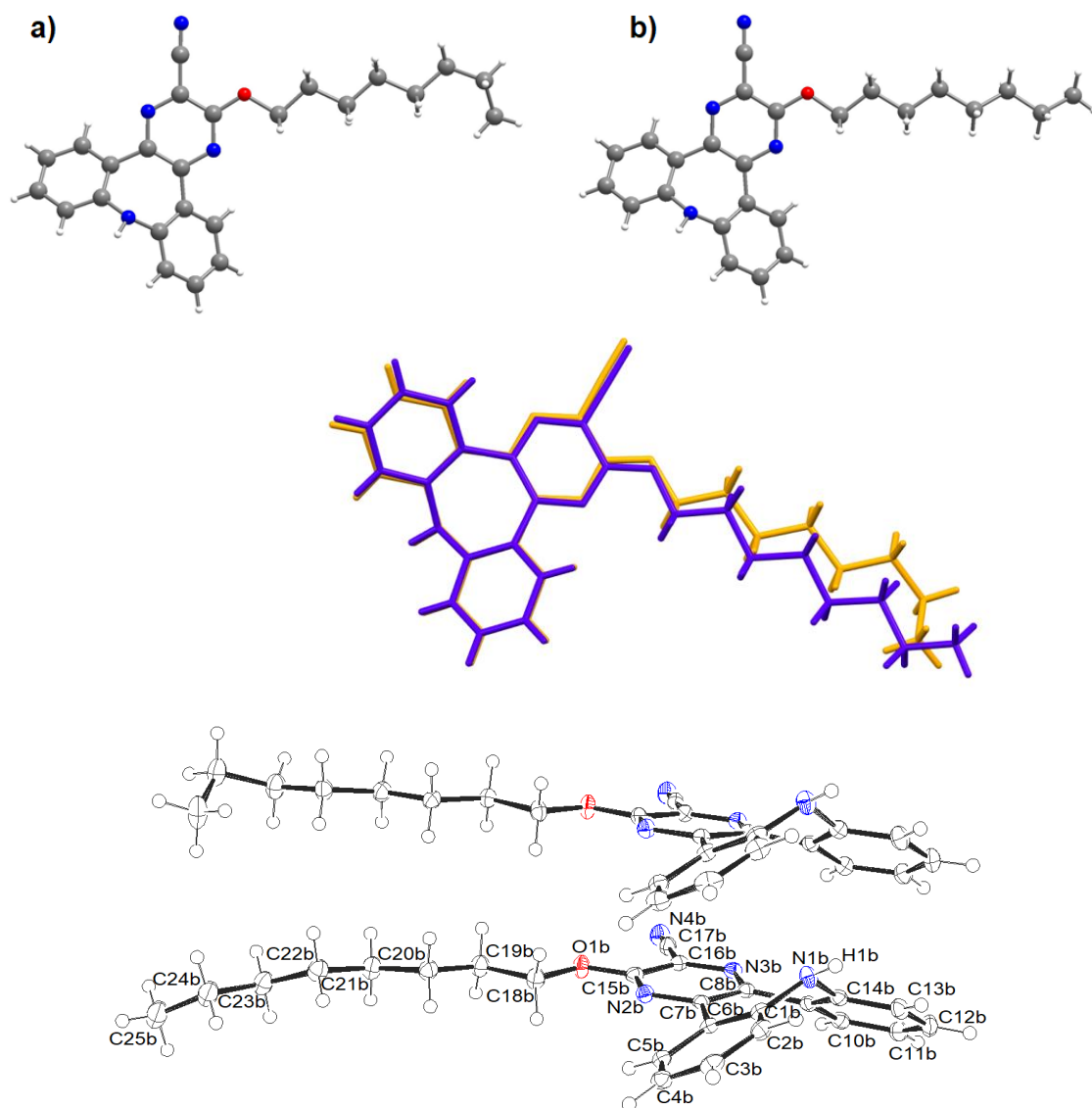
Figure 93: Up; Side comparison between the two molecules of the asymmetric unit, highlighting the different conformation of the alkyl side chain.

Middle; top-view of the two independent molecules of the asymmetric unit (colored in blue and orange for simplicity), highlighting the different conformation of the alkyl side chains.

Bottom; asymmetric unit for the crystal structure of **139**. Labelling scheme is depicted only for one of the two molecules, i.e. molecule **b** (C1b; C2b…), for the sake of simplicity. Same labelling scheme has been used for molecule **a**. Coloring scheme: C, gray; N, blue; O, red; H white. Ellipsoids are depicted at 50% probability.

16.1.2. Synthesis of type A TPyzPzs

Given impossibility to achieve dinitrile **135** by first planned pathway, synthetic approach was then revised. New starting material was individuated in 10-methoxyiminostilbene **140**. First reaction was alkylation: octyl group was introduced by deprotonation with NaH in DMF or MeCN, but best results were obtained exploiting *n*-BuLi in THF and then quenching with 1-iodoctane. This way compound **141** is achieved in a satisfactory 86% yield. Subsequent reaction is vinyl ether hydrolysis by action of a protic acid to afford compound **142**. Oxidation of the α-position to the 1,2-diketone **143** was carried out using selenium dioxide. In this case SeO₂ is a

good choice due to easy removal of selenium traces by simple filtration due the very good solubility of product **143**. It is in addition much cheaper than benzeneseleninic acid anhydride and with analogous oxidizing power. Condensation between **143** and DAMN in boiling acetic acid led finally to achieve dinitrile **135**. All these reactions are resumed in Scheme 86.
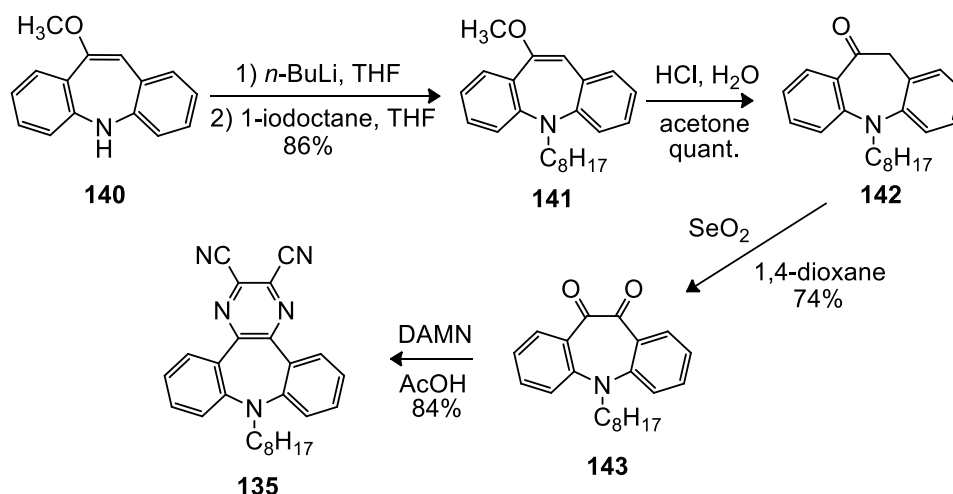
Scheme 86: successful approach to dinitrile **135**.

Dinitrile **135** was then used to perform tetracyclization reaction. Preliminary trials were performed using $(NH_4)_2MoO_4$ as catalyst in boiling *o*-dichlorobenzene[320] but best reaction conditions were found using boiling *N,N*-dimethylaminoethanol (DMAE) as solvent, $Cu(OAc)_2$ or $ZnCl_2$ as a templating agent. In this way synthesis of copper(II) and zinc(II) tetrapyrazinoporphyrazines in 49% and 25% yield respectively was afforded (Scheme 87). Presence of octyl pendants allows a facile chromatography purification.
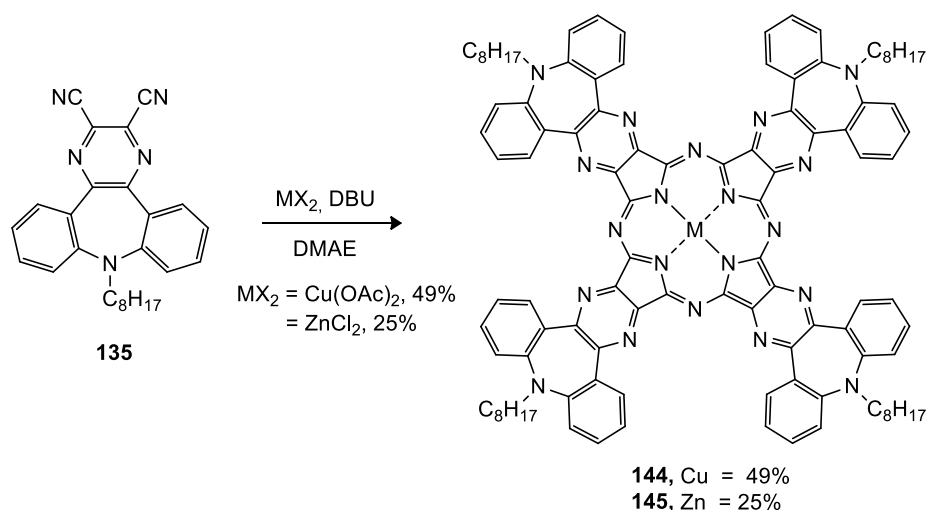
Scheme 87: synthesis of type **A** tetrapyrazinoporphyrazines.

16.1.3. Electrochemical characterization

Compound **144** and **145** were both tested by cyclic voltammetry with the help of prof. Damiano Monticelli to characterize their redox behaviour and measure the electrochemical bandgap (E_g^{EC}). Cyclic voltammograms (CV) for the oxidation and reduction of the two compounds are reported in Figure 94.
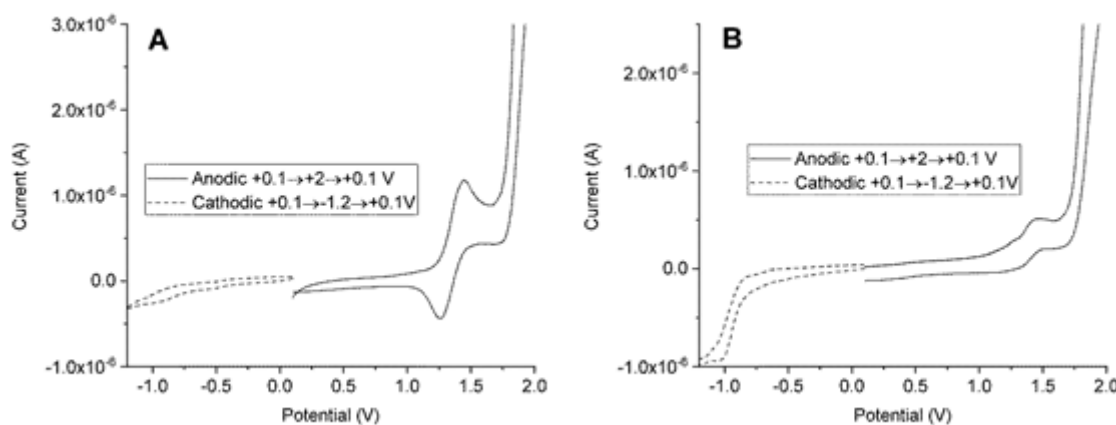
Figure 94: cyclic voltammograms of compounds **144** (A) and **145** (B). Full line: cyclic voltammograms (CV) in the anodic range (starting potential: +0.1 V, vertex potential: +2.0 V, end potential: +0.1 V); dashed line: CV in the cathodic direction (starting potential: +0.1 V, vertex potential: -1.2 V, end potential: +0.1 V). Scan speed 10 mV/s; supporting electrolyte: 0.1 M tetrabutylammonium hexafluorophosphate; concentrations: compound **144**: 0.14 mM; compound **145**: 0.36 mM.

The two compounds showed a similar redox behaviour, with two reduction (-0.5 V and and -1 V) and two oxidation peaks (≈+1.4 V and ≈+1.9 V, not shown in Figure 94), although differences in the peak currents were evident (compare the +1.4 V and the -1 V peaks among the two species). The presence of multiple oxidation and reduction peaks is a common feature of variously substituted porphyrazines[321–323]. As regards the oxidation process, the synthetized complexes showed potential in accordance to the least oxidizable complexes reported in the literature[324], highlighting the poor electron donor ability of the tetrapyrazino moieties. The potentials of the two reduction peaks were in good agreement with literature data[321], notwithstanding different moieties were investigated. The copper complex is slightly more easily reduced than the zinc one, pointing to the participation of *d* orbitals in the LUMO. As a conclusion, the similar electrochemical behaviour of the two complexes suggests the electrochemistry of these species being mainly dictated by the ligand, at least under the present experimental conditions.

16.1.4. Optical characterization

All studies presented in this section were conducted in collaboration with Dr. Luca Nardo.

16.1.4.1. Solid state characterization

In Figure 95 full-scale absorption spectra (panel a) and the UV-Vis absorption and emission spectra (panel b) of **144** (top) and **145** (bottom) in the solid state were reported. Both TPyzPzs compounds exhibit intense

absorption in the whole UV-Vis portion of the spectrum. Namely, a peak in the UV (around 310 nm and 340 nm for **144** and **145**, respectively) and another one in the orange-red (around 590 nm and 600 nm, respectively) dominate the spectrum. The former peak can be attributed to the Soret transition whilst the latter can either be ascribed to absorption in the macrocycle Q-bands or to a metal *d-d* transition. A further peak in the near infrared (800 nm), which appears as a shoulder in compound **144**, denounces another *d-d* transition. Fluorescence was excited by irradiation in correspondence of both the UV and the visible band for both compounds.
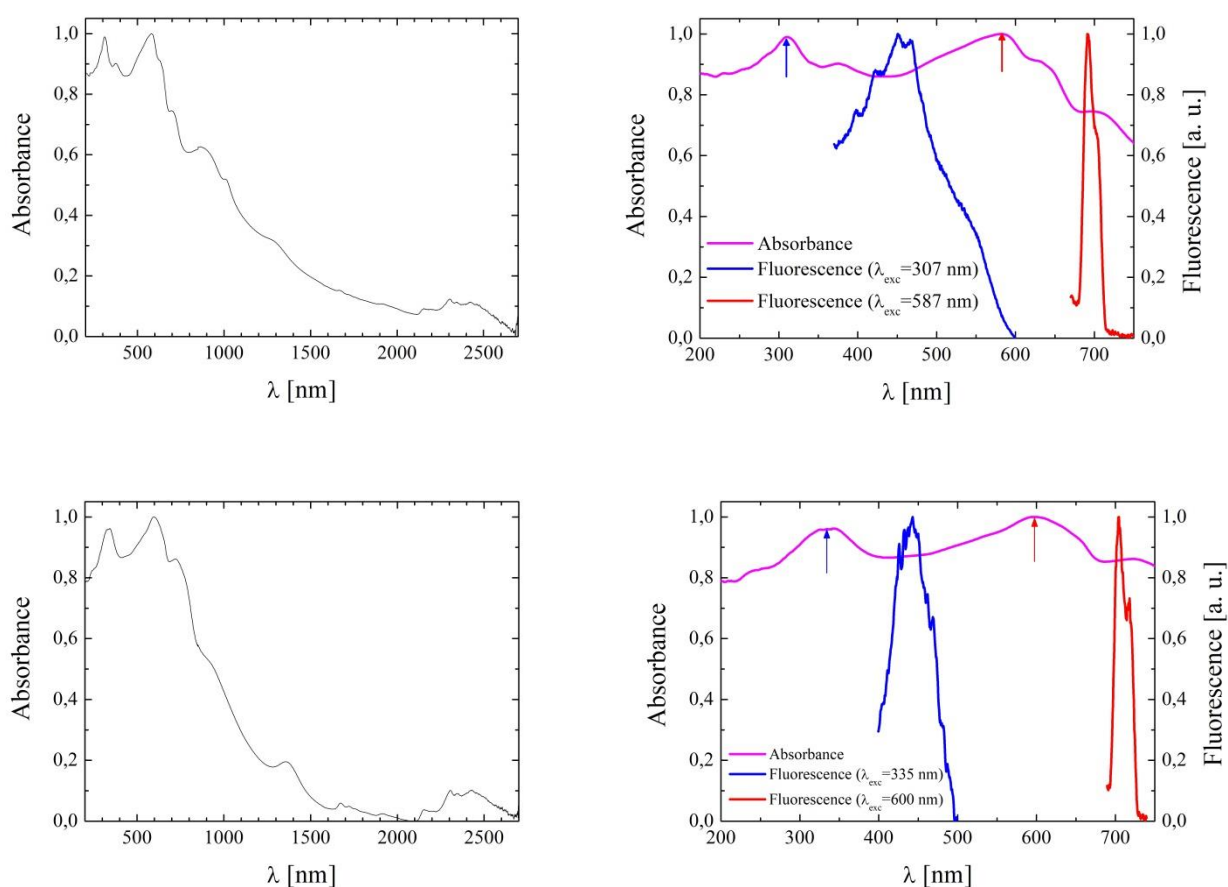
Figure 95: panel a): peak-normalized absorption spectra of **144** (top) and **145** (bottom) in the solid state. Panel b): peak-normalized fluorescence emission spectra obtained upon excitation in the UV (blue line) and visible (red line) absorption peak of the same samples. To improve readability, the spectra are superimposed to the pertaining absorption spectrum in the UV-Vis wavelength range (magenta line), and the excitation wavelengths are indicated by arrows of the same colour as the produced emission spectrum.

16.1.4.2. Compound 144 (Cu) absorption and fluorescence in solution

The peak absorption wavelengths in toluene, DCM, EtOH and DMSO are reported as λ_{abs} in the second column of Table 16. The absorption spectral line-shapes are plotted in Figure 96 a). In Table 16 the molar extinction coefficient value at the Soret band peak, ε_{Soret}, was also reported (third column), as determined through linear fit of absorbance *vs* concentration plots similar to the exemplary one shown in Fig. YYY b).

Figure 96: a) Peak-normalized absorption spectra of **144** in toluene (red), DCM (blue), EtOH (cyan) and DMSO (magenta). b) Exemplary absorbance vs concentration plot used to estimate the molar extinction coefficient at the Soret band peak in the solvent DMSO. c) Fluorescence emission spectra of **144** in the same solvents. Colour codes are conserved. The spectral integral scale as the measured quantum yield values, reported in Table 16.

In all solvents, compound **144** showed two main absorption bands peaked in the UVB (the Soret band) and in the red region (Q-band). The former appears structured, suggesting the superposition of at least two transitions, one below 350 nm and the other around 400 nm. The latter was peaked at ≈ 650 nm, with a pronounced shoulder at ≈ 590 nm, and may be identified with the HOMO-LUMO transition determined by means of cyclic voltammetry studies (λ_{Volt} ≈ 642 nm). Overall, the absorption features significantly depend on the solvent properties. Particularly, the molar extinction coefficient at the Soret band peak exhibited a two-fold increment in shifting the environment from polar non-H-bonding to H-bonding, while it assumed intermediate values in non-polar solvent (Table 16).

Solvent	λ_{abs} [nm]	ε_{Soret} [M^{-1}cm^{-1}]	λ_{fluo} [nm]	Φ_{fluo}
Toluene	328, (374), 612, 660	190000 ± 1300	528	0.0009
DCM	348, 594, 658	239000 ± 5600	561	0.0041
EtOH	359, 619, 666	101000 ± 2900	506	0.0022
DMSO	(333), 372, (600), 657	109400 ± 3500	520, 567	0.0043

Solvent	τ_1 [ps] (f_1)	τ_2 [ps] (f_2)	$\tau_{average}$ [ps]
Toluene	324±33 (0.35±0.04)	4070±97 (0.65±0.04)	2762±435
DCM	581±20 (0.490±0.001)	2811±72 (0.510±0.001)	1709±74
EtOH	596±4 (0.785±0.002)	3657±120 (0.225±0.002)	1283±44
DMSO	368±20 (0.36±0.02)	4026±50 (0.64±0.02)	2693±218

Solvent	k_{fluo} [s^{-1}]	K_{NR} [s^{-1}]
Toluene	3 x 10^5	3.6 x 10^8

DCM	2.4 x 10^6	5.8 x 10^8
EtOH	1.7 x 10^6	7.8 x 10^8
DMSO	1.6 x 10^6	3.7 x 10^8

Table 16: spectroscopic parameters of **144**.

The fluorescence emission spectra recorded in the same solvents upon excitation at the Soret band absorption peak are shown in Figure 96 c). The peak fluorescence wavelengths were reported as λ$_{fluo}$ in the fourth column of Table 16 a). In the fifth column of the same table the fluorescence quantum yield values, Φ$_{fluo}$, determined for the compound in the different solvents by comparison with dimethyl-POPOP dissolved in cyclohexane (Φ$_{fluo}$= 0.95)[325] are reported. The fluorescence emission appears to be notably solvent dependent, and not to obey to trivial polarity-driven solvation effects. Moreover, in any of the tested solvent fluorescence is extremely dim.
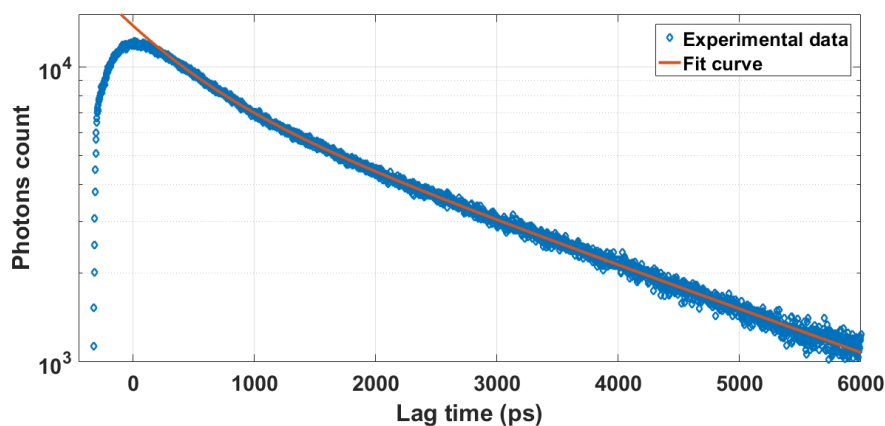
Figure 97: experimental fluorescence decay pattern of the Cu compound **144** in dichloromethane (circles). The solid line represents the best fitting curve to a double-exponential decay function (for details and for fitting parameters, see *Table 16* b)).

To investigate the cause of such a low luminescence, time-resolved fluorescence measurements were performed. The decay was double exponential in all the tested solvents. An exemplary decay pattern is plotted in Figure 97. The best-fitting curve was also shown as solid line. The best fitting parameters in the different solvents were reported in Table 16 b). Neither the values of the decay constants, nor their relative amplitudes seem to exhibit a specific trend with respect to variations in both the polarity and the H-bonding properties of the solvent, suggesting complex decay dynamics, likely influenced by other parameters such as viscosity. For instance, an increase in polarity seemed to enhance deactivation through the pathway associated to the shorter decay component, but DMSO, i.e., the more viscous solvent in the panel, escaped to this rule.

From the decay parameters it was possible to calculate the average excited-state lifetime τ$_{average}$, according to Equation 1:

$$\tau_{average} = \tau_1 f_1 + \tau_2 f_2$$

(1)

Combining the latter parameter with the measured quantum yield value and exploiting Equations 2, the radiative (k_{Fl}) and non-radiative (k_{NR}) decay rates were estimated, whose values are reproduced in Table 16 c).

$$k_{Fl} = \frac{\phi_{Fluo}}{\tau_{average}}; \qquad k_{NR} = \frac{1}{\tau_{average}} - k_{Fl} \qquad \qquad (2)$$

The above calculations suggest that the low luminescence of the Cu TPyzPz is primarily due to a very low radiative decay rate.

16.1.4.3. Compound 145 (Zn) absorption and fluorescence in solution

The same investigations were undertaken also on compound **145**. The steady-state absorption and emission spectra of this compound in the same solvents utilized for the characterization of compound **144** were plotted in Figure 98 a) and b), respectively. Similarly to Cu compound **144**, the absorption spectra in Zn TPyzPz **145** were dominated by the Soret band in the UVB spectral region and by one or more Q-bands in red region. However, the Soret band appeared to be generally red shifted for the Zn with respect to the Cu compound. Moreover, the Q-bands pattern was rather similar to the one observed for **144**. Thus, the slight blue-shift in the HOMO-LUMO transition energy observed by means of cyclic voltammetry was not evidenced in the absorption spectral line-shape. It should be mentioned, however, that the difference in transition energy recorded by electrochemical methods (0.04 eV) was below the instrumental sensitivity of the used cyclic voltammetry apparatus. In Table 17 a) the wavelengths of the Soret and Q-band peaks were reported in column 2. The molar extinction coefficients at the Soret band peak were also determined in the different solvents and are detailed in column 3 of the same Table. Fluorescence emission features were similar to those detected for the Cu compound, with spectra peaking in the green-yellow region and very low quantum yields. These parameters were reported in Table 17 a) columns 4 and 5, respectively.
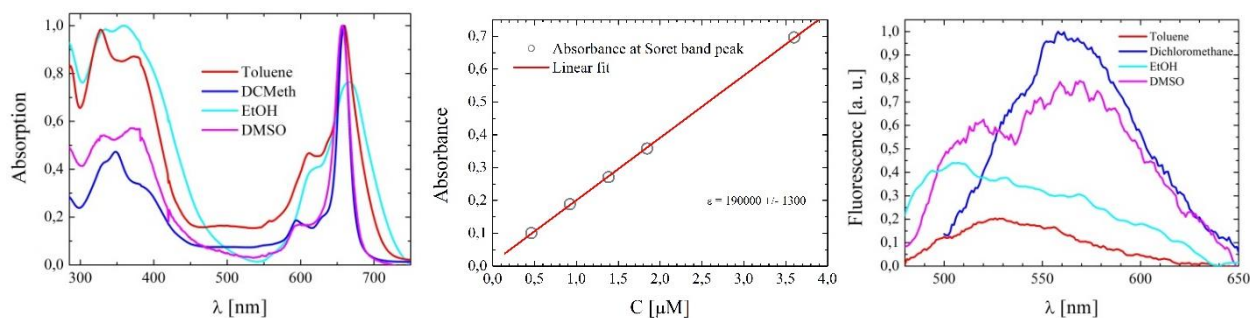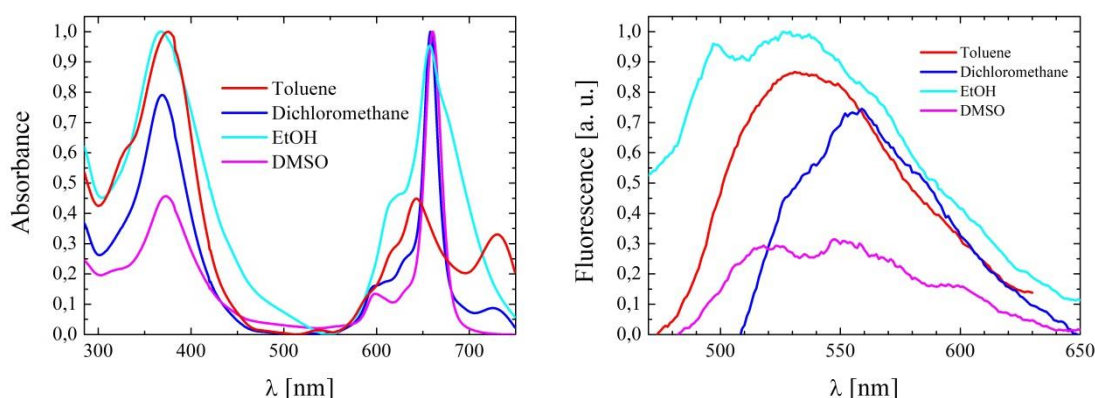

Figure 98: a) Peak-normalized absorption spectra of Zn compound **145** in toluene (red), DCM (blue), EtOH (cyan) and DMSO (magenta). b) Fluorescence emission spectra of the Zn compound **145** in the same solvents. Colour codes are conserved. The spectral integral scale as the measured quantum yield values, reported in Table 17 a.

The decay patterns recorded for **145** were also optimally fitted to a double exponential decay model in all the solvents. The fitting parameters are reported in Table 17 b). The radiative and non-radiative decay constants were estimated as detailed above. The excited state dynamics was similar to compound **144**. In particularly, the low quantum yield seemed to be due to a rather slow radiative decay.

Solvent	λ_{abs} [nm]	ε_{Soret} [M^{-1}cm^{-1}]	λ_{fluo} [nm]	Φ_{fluo}
Toluene	376, 643, 730	152200 ± 540	532	0,0020
DCM	369, (600), 658	97500 ± 3800	559	0,0012
EtOH	368, (620), 657	107400 ± 1900	498, 529	0,0024
DMSO	373, 599, 661	139400 ± 1300	520, 552 (600)	0,0007

Solvent	τ_1 [ps] (f_1)	τ_2 [ps] (f_2)	$\tau_{average}$ [ps]
Toluene	467±25 (0.14±0.01)	1408±5 (0.86±0.01)	1274±85
Dichloromethane	440±4 (0.70±0.01)	1990±25 (0.30±0.01)	910±34
EtOH	572±5 (0.76±0.02)	3586±34 (0.24±0.02)	1293±100
DMSO	323±2 (0.60±0.01)	3411±19 (0.40±0.01)	1571±21

Solvent	k_{fluo} [s^{-1}]	K_{NR} [s^{-1}]
Toluene	1.5×10^6	7.8×10^8
DCM	1.3×10^6	1.1×10^9
EtOH	1.8×10^6	7.7×10^8
DMSO	4×10^5	6.4×10^8

Table 17: a), spectroscopic parameters of the Zn compound **145**.

♦ ♦ ♦ ♦ ♦ ♦

16.2. Type B tetrapyrazinoporphyrazine synthesis approach

Alkylated dinitrile **146** is requested to have a soluble monomer for cyclotetramerization (Figure 99). Hexyl group was chosen due to commercial availability of 2-hexylthiophene **147**, the designed starting material for synthesis.

146
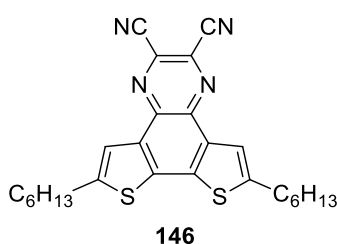
Figure 99: dinitrile **146**.

Compound **146** can be obtained by DAMN condensation with diketone **150** in THF in presence of an acid catalysis. Product **150** was previously synthetized in literature[326] starting from 2-hexylthiophene **147**. After NBS bromination, resulting product **148** was dimerized with CuCl$_2$ passing through LDA mediated deprotonation with bromine atoms transposition. Next step provided diketone **150** synthesis by reaction with *n*-BuLi and diethyl oxalate. All reactions are resumed in Scheme 88.
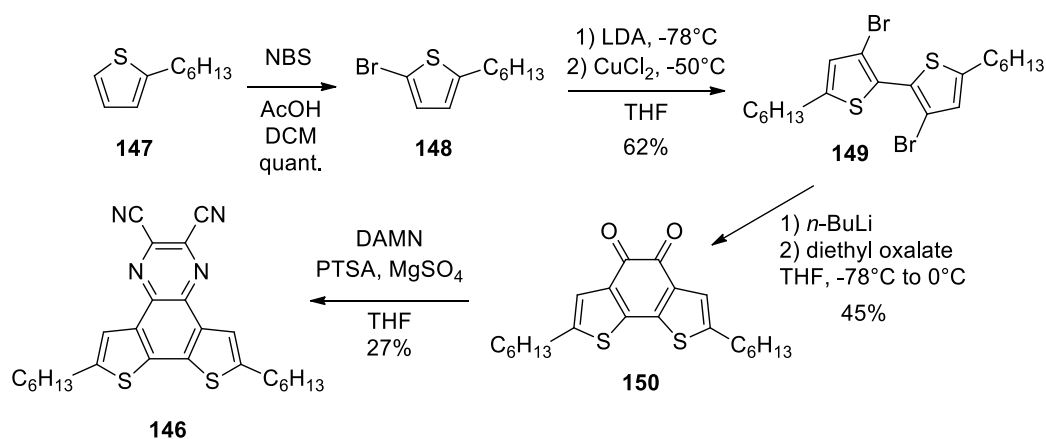
Scheme 88: synthesis of alkylated dinitrile **146**.

Preliminary macrocyclization with dinitrile **146** were tried in boiling DMAE as solvent and ZnCl$_2$ as a templating agent (Scheme 89). However, despite high solubility of starting material, only impure samples were obtained even after careful column chromatographies.
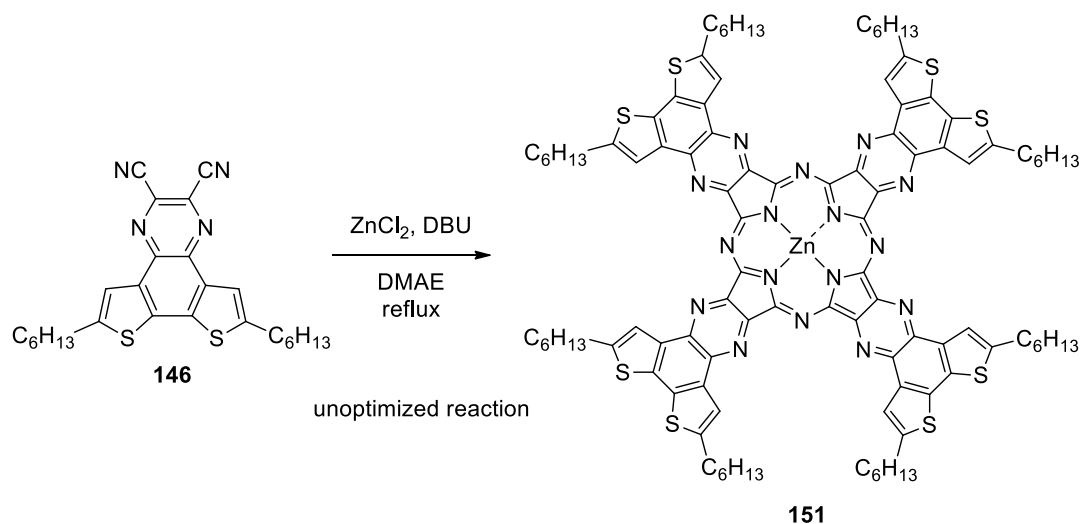
Scheme 89: unoptimized synthesis of type **B** TPyzPz **151**.

Detection of a 718 nm Q band was diagnostic for TPyzPz formation (Figure 100). Studies are currently ongoing to determine best cyclization method and purification. A current hypothesis on bad tetrapyrazinoporphyrazine formation focuses on possible steric hindrance due to hexyl groups pointing each other in final

macrocycle. A possible solution could be a macrocyclization starting from an equimolar mixture of alkylated dinitrile **146** and compound **152** (Scheme 90).
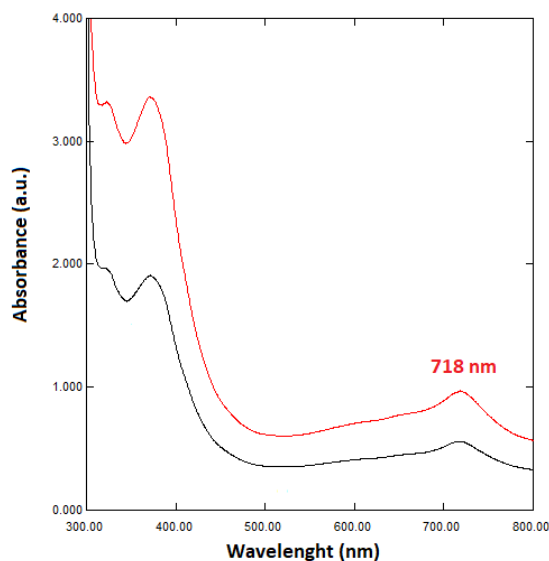
Figure 100: UV-Vis of impure sample of Zn-TPyzPz **151** at two different concentrations. Red line; 10 µM. Black line; 2 µM.
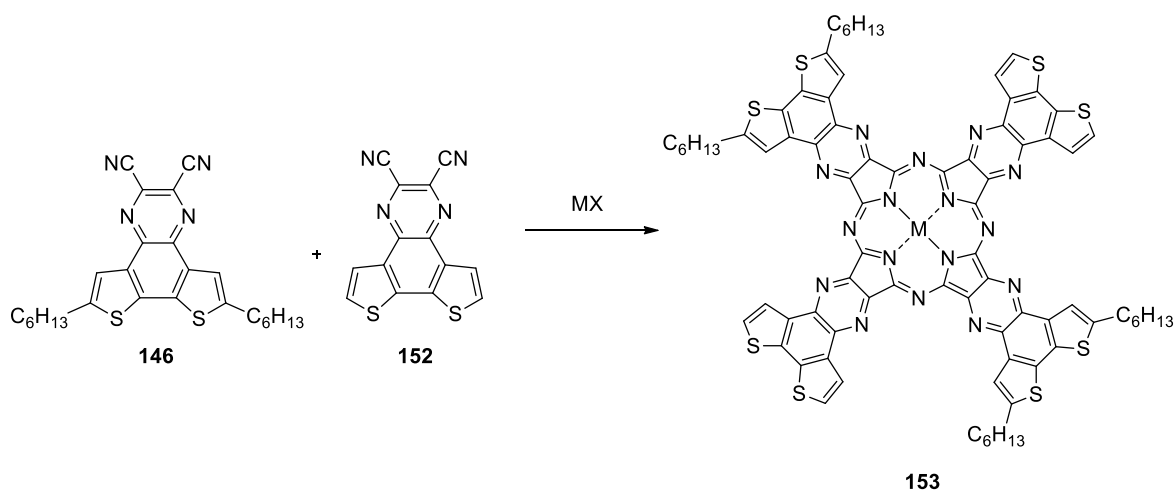
Scheme 90: macrocyclization reaction starting from equimolar mixture of **146** and **152**.

Pointing this new objective, synthesis of dinitrile **152** was approached starting off from 3-thiophenecarbal-dehyde **154** which was subjected to a benzoin condensation catalysed by thiamine hydrochloride to afford product **155** in good yields.[327] The latter was successfully oxidized to 1,2-diketone **156** by $CuSO_4$[238] which can be easily transformed to fused structure **157** by ring closure oxidation mediated by $FeCl_3$. This product shows limited solubility. Some difficulties were found in condensation reaction between the latter and DAMN. Several conditions were tried but it was achieved no more than 16% operating in refluxing 1:1 mixture of DMSO and acetic acid. Reactions are resumed in Scheme 91.

139
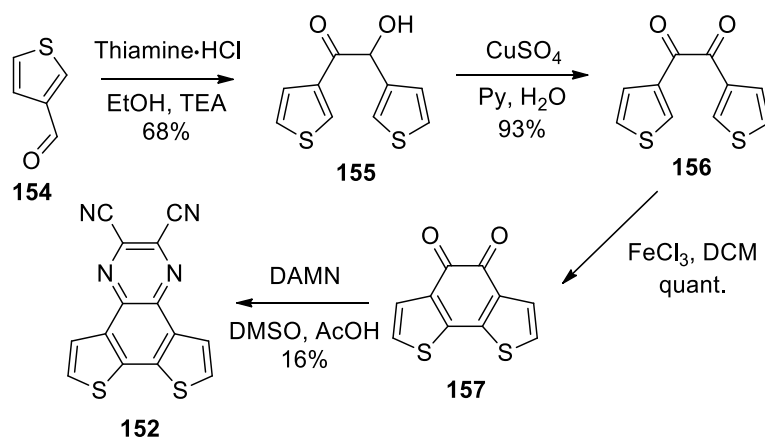
Scheme 91: first approach to dinitrile **152**.

Much higher yields were obtained switching oxidative FeCl$_3$ mediated ring closure and DAMN condensation steps:[328] this way dinitrile **152** can be recovered directly as precipitated solid in last step without any further purification (Scheme 92).
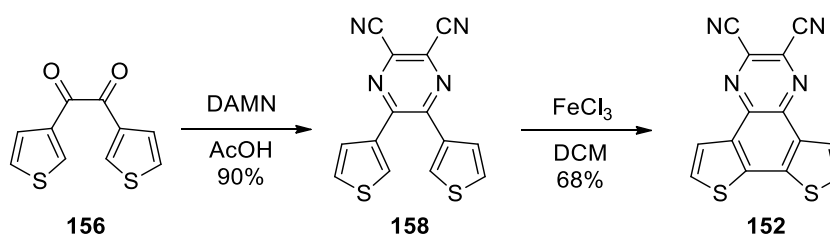
Scheme 92: effective synthesis of dinitrile **152**.

Product **152** showed bad solubility in organic solvents, suggesting its cyclotetramerization reaction wouldn't be successful. A preliminary test was conducted running reaction with equimolar mixture of **152** and **146** in DMAE with ZnCl$_2$: however, albeit total consumption of reagents, same purifications issues were noticed. Raw macrocyclization product showed high solubility in halogenated solvents. Further investigations are currently on planning to achieve pure type **B** tetrapyrazinoporphyrazines.

17. Conclusions and future developments

Synthesis of type **A** tetrapyrazinoporphyrazines was achieved successfully. Computational, optic and electro-chemical characterization was performed as well. The electronic-state transition spectroscopic properties of the two derivatives of type **A** TPyzPzs were probed by solid-state and in-solution UV-Vis absorption, steady-state fluorimetry and time-correlated single-photon counting experiments. The photophysical parameters were not trivially dependent from the environment. The most striking aspect of their excited-state dynamics resulted to be an extremely low fluorescence emission, which was in turn ascribed to very slow radiative decay.

Further developments on this topic are focused on preparation of a wide library of TPyzPzs with different metal centers to explore different applications ranges: experiments as catalysts for cyclopropanation reactions are planned to be done soon. The latter project could be expanded by introducing chiral alkyl pendants on dinitrile monomer to achieve an enantiopure catalyst and measure its stereoselectivity in cyclopropanation reactions. Usage of these type **A** tetrapyrazinoporphyrazine as sensor for small molecules is scheduled for the next future as well.

On the other hand, type **B** tetrapyrazinoporphyrazine needs further investigations on purification method to afford clean product. A survey of different tetramerization conditions will be carried out to find best conditions for reaction outcome. Once isolated, computational, optic and electrochemical characterizations are in plan to understand best application field for these new molecules.

18. Global experimental section

18.1. Experimental details

18.1.1. Synthesis

All reactions were performed with 220°C oven dried laboratory glassware and under nitrogen atmosphere unless otherwise indicated. All reactions were performed under vigorous magnetic stirring. Anhydrous solvents were purchased in sealed bottles provided with crown cap from Sigma Aldrich, Acros Organics and Alfa Aesar. All reactants used were purchased from Sigma Aldrich, Fluorochem and Tokyo Chemical Industry and used as received without any further purification.

Reactions were monitored with thin-layer chromatography (TLC) using TLCs ALUGRAM® Xtra SIL G/UV254 (0.2 mm thin layer depth; Macherey-Nagel). Spots visualization was accomplished with UV lamp (365 nm and/or 254 nm respectively). Gravimetric chromatography columns were performed using silica gel (60 Å, particles size: 0.63-0.2 mm) as stationary phase. Flash chromatography columns were performed using silica gel (60 Å, particle size: 0.063-0.04 mm) as stationary phase, exploiting protocol developed by Still in 1978[329].

^{1}H-NMR spectra were recorded with Bruker AVANCE instrument working at 400.13 MHz. Chemical shifts are reported in ppm (δ) with the solvent reference relative to tetramethylsilane (TMS) employed as the internal standard standard ($CDCl_3$ δ = 7.26 ppm; CD_2Cl_2, δ = 5.32 ppm; DMSO-d_6, δ = 2.50 ppm; acetone-d_6, δ = 2.05 ppm). Spin multiplicity was reported by using some abbreviations: s = singlet, d = doublet, t = triplet, q = quartet, quin = quintet, m = multiplet, br = broad signal, dd = doublet of doublets, td = triplet of doublets, dt = doublet of triplets. Coupling constants are reported in Hz. ^{13}C-NMR spectra were recorded with Bruker AVANCE instrument operating at 100.56 MHz, with complete proton decoupling. Chemical shifts are reported in ppm (δ) with the solvent reference relative to TMS employed as the internal standard ($CDCl_3$, δ = 77.16 ppm; CD_2Cl_2, δ = 54.00 ppm; DMSO-d_6, δ = 39.51 ppm; acetone-d_6, δ = 29.84 ppm, 206.26 ppm).

GC-MS analyses were performed with a Finnigan Trace GC-MS equipped with a quadrupole analyzer and electronic impact (EI) source. Other masses were obtained by VG 7070 EQ mass spectrometer with chemical ionization (CI) source.

IR spectra were recorded with a FT-IR Thermo Scientific Nicolet iS10 Smart iTR equipped with a Smart OMNI Transmission instrument, interfaced with Omnic 9.2.98 software; spectra were recorded either with attenuated total reflection (ATR) technique or KBr disk.

Melting points were obtained with a Stuart Melting Point SMP30 instrument and they are uncorrected.

18.1.2. Cyclic voltammetries, spectroelectochemistry and *in situ* conductance characterizations

Electrochemical measurements on racemate biindole (Chapter 2) compounds were carried at the University of Stuttgart (Germany) and they were performed with an Autolab PGSTAT204 potentiostat (Metrohm) at room temperature and under argon atmosphere. A three-electrode glass cell provided with a Pt plate as counter electrode (CE) and an AgCl-coated silver wire as pseudo reference electrode (RE) were employed. As working electrode (WE) (a) ITO-coated glass slides S ~ 0.4 cm^2 (≤20 Ω/sq, PGO, Germany) or (b) Au (vacuum deposited on glass slides over 3 nm of adhesion Cr layer; 30 nm Au layer) S ~ 0.5 cm^2 slides and (c) Pt inter-digitated electrodes with a 10 μm band width were used. Prior to usage, the ITO electrodes were subjected to a 10 minutes treatment in a plasma chamber. For all the electrochemical measurements a 0.1 M CH_2Cl_2 solution (Sigma Aldrich) with Bu_4NPF_6 as supporting electrolyte (Sigma Aldrich) was employed as received. The electrolyte solution was degassed through Argon bubbling before the measurements. All potentials were referenced to the formal potential of the Fc|Fc$^+$ inter-solvental reference redox couple, measured in the same conditions of the analytes.

Cyclic voltammetry (CV) and Differential Pulse Voltammetry (DPV) experiments on enantiopure biindole compounds (Chapter 2) were carried at the University of Milan (Italy) and they were performed using an Autolab PGSTAT potentiostat (Eco-Chemie, Utrecht, Netherlands), controlled by a PC with the GPES software provided by the same manufacturer. The three-electrode V-shaped minicell (with 3 cm^3 of solution) included a glass-embedded glassy carbon disk (GC, Metrohm, S = 0.033 cm^2) as working electrode, a Pt disk as counter electrode, and an aqueous saturated calomel (SCE) as reference electrode, inserted in a compartment filled with the working medium and ending with a porous frit, to avoid water and KCl leakage into the working solution. The optimized preliminary polishing procedure for the GC disk electrode consisted in treatment with a diamond powder of 1 μm diameter (Aldrich) on a wet DP-Nap cloth (Struers).

Electrodepositions of all biindole compounds were performed under potentiodynamic conditions (20 cycles at a scan rate of 20 mV s^{-1} using a 0.5 mM of the monomer in 0.1 M CH_2Cl_2/ Bu_4NPF_6. After electrodeposition, the films were washed with CH_2Cl_2 to remove residual Bu_4NPF_6 and monomers and the samples were stored under inert atmosphere. Some monomers were also characterized in MeCN solutions.

Thin-film in-situ spectroelectrochemical measurements were performed using an Autolab PGSTAT204 potentiostat (Metrohm) and a Zeiss UV–vis spectrometer endowed with a MCS621 Vis II spectrometer cassette and a CLH600F lamp or a Zeiss UV–vis-NIR spectrometer endowed with a MCS621 Vis II and a MCS611 NIR 2.2μ spectrometer cassette and a CLH600F lamp and through the use of optical fibres (OceanInside). The measurements were conducted in a custom-made three-electrodes quartz cell employing a Pt wire as CE, an AgCl coated Ag wire as (pseudo)reference electrode and the coated ITO slides as WE. The measurements were performed under Ar atmosphere and all the potential values were referenced to the formal potential of the Fc/Fc+ redox couple. In-situ spectroelectrochemical measurements were conducted with a scan rate of 20

mV s^{-1} and potential steps of 10 mV, with simultaneous recording of electrochemical data points and UV-Vis spectra every 0.5 s.

In-situ conductance experiments combined to CV experiments were performed on Pt interdigitated electrodes from DropSens (comb distance = 5 μm) were used as the working electrodes. The CV experiments were performed at room temperature under argon atmosphere using an Autolab PGSTAT204 potentiostat (Metrohm) with a Pt wire as CE and an AgCl-coated Ag wire directly immersed into the electrolyte solution as pseudoreference electrode. A constant bias (Ed) of 10 mV was applied between the combs of the interdigitated electrode using a second potentiostat (μStat400, DropSens) measuring the current (Id) which is flowing between the two combs of the interdigitated electrodes as a function of the potential in the CV measurement. With the help of two resistors (Heka interface), both current signals are separated to allow to conduct both the CV measurements and to measure the in-situ conductance simultaneously. The conductance values G were calculated from the measured current flowing between the combs according to Ohm's law G=1/R=I/V. Electrolyte solutions (0.1 M Bu4NPF6/CH3CN) were deaerated by argon bubbling before use. Conductance values are given as conductance change (ΔG) with respect to the conductance of the materials in the neutral state.

Cyclic voltammograms (CV) for TPyzPzs (Appendix) were acquired using a Metrohm 663 polarograph controlled by an Ecochemie micro III potentiostat. A standard three electrode configuration was used, including a graphite, 2 mm diameter working electrode, a 3M Ag/AgCl reference electrode and a graphite rod counterelectrode. CVs were measured on saturated solution in dichloromethane in the presence of 0.1M tetrabutylammonium hexafluorophosphate as a supporting electrolyte. Oxygen was removed by nitrogen purging for 300 s before the voltage scan and the potential was scanned at a speed of 100 mV/s. Electrochemical HOMO and LUMO energies $E_{H,max}$ e $E_{L,max}$, were calculated according to the following formulas:

$$E_{H,max} = -\left(E_{p,a} - E_{(Fc^+/Fc \ vs. \ Ag \ |AgCl)}\right) - 4.8$$

$$E_{L,max} = -\left(E_{p,c} - E_{(Fc^+/Fc \ vs. \ Ag \ |AgCl)}\right) - 4.8$$

where $E_{(Fc^+/Fc \ vs. \ Ag \ |AgCl)}$ is the ferrocene redox potential under the employed experimental conditions (-0.449 V).

18.1.3. TPyzPzS optical characterizations

The UV-Vis absorption and fluorescence emission spectra of the two compounds were recorded both in the solid state and in a panel of solvents differing as to their polarity and H-bonding properties, namely: toluene, dichloromethane, ethanol, and dimethyl sulfoxide.

The solid-state UV-Vis spectra were acquired with a Jasco V-770 spectrophotometer equipped with an integrating sphere module. The UV-Vis spectra in solution were recorded with a Perkin Elmer Lambda2 spectrophotometer. The fluorescence spectra in the solid state were measured by means of a Jasco FP-8500

spectrofluorimeter equipped with a dedicated sample holder for powdered samples. The powder was submitted to the irradiation beam at the magic angle to optimize the signal-to-excitation stray light collection ratio. The fluorescence spectra in solution were recorded with a PTI fluorescence master system spectrofluorimeter. The instrument was interfaced with the acquisition software Felix 2000, which performed online correction of the data with respect to the excitation lamp spectral radiance and detector spectral quantum efficiency.

The time-resolved fluorescence decay patterns of the compounds in solution were also reconstructed recurring to the time-correlated single-photon counting (TCSPC) technique. The experimental apparatus exploited to this aim is fully described in the literature.[330,331] For the experiments reported hereby, the excitation source was a Nd:VAN cw-mode locked laser (mod. GE-100, Time Bandwidth Product, Zürich, Switzerland) delivering pulses at 113 MHz repetition rate of 9 ps duration at the fundamental wavelength. The samples were excited at 355 nm by generating out of cavity the third harmonic of the beam.[332] The fluorescence photons were detected by means of a MPD50 single-photon avalanche diode with integrated active quenching and cooling circuitry and timed by a single module of an SPC-152 integrated board (Becker & Hickl GmbH, Berlin, Deutschland). The decays were fitted to a double-exponential model function. The data were acquired in triplicate, and the fitting parameters reported below are averaged over the three parallels. The errors are expressed in terms of the pertaining standard deviations.

The fluorescence emission spectra obtained upon excitation at the Soret band peak were also recorded in all the solvents of above and plotted in section **16.1.4** (Figure 96 and Figure 98), where are data are normalized in order to set the peak intensity value in dichloromethane to unit and to preserve the (absorbance-corrected) ratios between the spectral integrals.

18.1.4. Abbreviations and registered trademarks

Ac: acetyl	Et: ethyl
Bu: butyl	h: hours
DAMN: diaminomaleonitrile	Hex: hexyl
DABCO: 1,4-diazacyclo[2.2.2]octane	LDA: lithium diisopropylamide
DBU: 1,8-diazabicyclo[5.4.0]undec-7-ene	Me: methyl
DCM: dichloromethane	NBS: *N*-bromosuccinimide
DCC: dicyclohexylcarbodiimide	NIS: *N*-iodosuccinimide
DMAP: 4-dimethylaminopyridine	NMP: *N*-methyl-2-pyrrolidone
DMAE: *N,N*-dimethylaminoethanol	Ph: phenyl
DMF: *N,N*-dimethylformamide	PTSA: *p*-toluenesulfonic acid
DMSO: dimethylsulfoxide	r.t.: room temperature

TEA: triethylamine

TMSA: (trimethylsilyl)acetylene

TBAB: tetrabutylammonium bromide

Ts: tosyl

TBAF: tetrabutylammonium fluoride

Celite®: 3CaO·Al₂O₃

THF: tetrahydrofuran

Oxone®: 2KHSO₅·KHSO₄·K₂SO₄

♦ ♦ ♦ ♦ ♦ ♦

18.2. Chapter 1 experimental part

18.2.1. Synthesis of nitrosoarenes

18.2.1.1. Synthesis of 4-nitro-nitrosobenzene (1a)
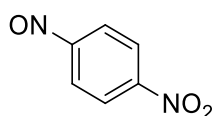
To a solution of Oxone® (32.1 g, 52.13 mmol) in water (300 mL), 4-nitroaniline (7.2 g, 52.13 mmol) was added at 0 °C. The suspension was vigorously stirred at r.t. for 48 h then filtered. Collected solid was recrystallized from methanol to afford 4-nitro-nitrosobenzene as a yellow solid (5.61 g, 71%). ^{1}H-NMR (CDCl₃) δ: 8.52 (d, 2H, J = 8.9 Hz), 8.06 (d, 2H, J = 8.9 Hz) ppm. Other spectral data match the literature.[333–335]

18.2.1.2. Synthesis of 4-nitrosobenzoic acid (1b)
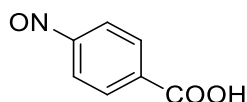
To a solution of 4-aminobenzoic acid (1.0 g, 7.3 mmol) in DCM (12 mL), a solution of Oxone® (8.97 g, 14.6 mmol) in water (45 mL), was added. The suspension was vigorously stirred at r.t. for 1 h. Precipitated solid was isolated by filtration, washed with H₂O and dried under vacuum to afford 4-nitrosobenzoic acid as yellow solid (1.1 g, quantitative yield). ^{1}H-NMR (DMSO-d_6) δ: 13.5 (br, 1H), 8.27 (d, 2H, J = 8.8 Hz), 8.08 (d, 2H, J = 8.8 Hz) ppm. Other spectral data match the literature.[334,336]

18.2.1.3. Synthesis of 4-carbethoxy-nitrosobenzene (1c)
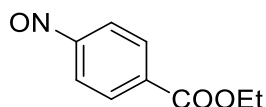
To a solution of benzocaine (4.96 g, 30 mmol) in a mixture of DCM (150 mL) and *n*-pentane (150 mL), sodium tungstate dihydrate (1 g, 3.4 mmol), H₃PO₄ (1.5 mL of a 85% solution, 25.76 mmol), H₂O₂ (30 mL of a 30% solution, 300 mmol) and TBAB (0.30 g, 1 mmol) were added. Reaction mixture is the heated to 40°C for 6 h. The green reaction mixture was then washed with HCl 0.01 M and brine. The reunited organic phases were dried over Na₂SO₄, filtered and evaporated under reduced pressure to afford 4-carbethoxy-nitrosobenzene

as yellow solid (2.02 g, 37%). ^{1}H-NMR (CDCl$_3$) δ: 8.32 (d, 2H, *J* = 8.4 Hz), 7.95 (d, 2H, *J* = 8.4 Hz), 4.45 (q, 2H, *J* = 7.1 Hz), 1.45 (t, 3H, *J* = 7.1Hz) ppm. Other spectral data match the literature.[334,337]

18.2.1.4. Synthesis of 4-nitroso-toluene (1d)
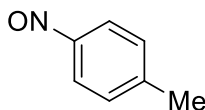
Cis-Mo(O)$_2$(acac)$_2$ (3.26 g, 10 mmol) was suspended in cyclohexane (200 mL) at r.t. and vigorously stirred for 5 min, then 4-methylaniline (10.87 g, 10 mmol) and H$_2$O$_2$ (50 mL of a 30% solution, 500 mmol) were added. Mixture was then vigorously stirred for 1 h and then 200 mL of cyclohexane and 10 g of Na$_2$SO$_4$ were added. After 20 min the mixture was filtered. Organic layers were dried over Na$_2$SO$_4$ and cooled to –5 °C for 2 h. The solution was filtered to afford 4-nitroso-toluene as yellow solid (4.94 g, 41%). ^{1}H-NMR (CDCl$_3$) δ: 7.82 (d, 2H, *J* = 7.8 Hz), 7.40 (d, 2H, *J* = 7.8 Hz), 2.46 (s, 3H) ppm. Other spectral data match the literature.[334,338]

18.2.1.5. Synthesis of 4-methoxy-nitrosobenzene (1e)
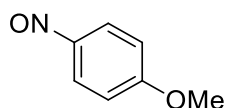
To a solution of NOBF$_4$ (3.25 g, 27.8 mmol) in MeCN (40 mL), anisole (1 mL, 9.20 mmol) was added. The mixture was stirred at r.t. for 0.5 h. Reaction mixture was poured into water and the mixture was extracted with DCM. Reunited organic phases were dried over Na$_2$SO$_4$, filtered and evaporated under reduced pressure. Crude product is purified by gravimetric column chromatography (*n*-hexane/DCM 7:3) to afford 4-methoxynitrosobenzene as green-blue oil (884 mg, 70%). ^{1}H-NMR (CDCl$_3$, 50 °C) δ: 7.93 (d, 2H, *J* = 7.0 Hz), 7.05 (d, 2H, *J* = 7.0 Hz), 3.97 (s, 3H) ppm. GC-MS (EI): *m/z*: 137. Other spectral data match with the literature.[334,339]

18.2.1.6. Synthesis of 2-carbomethoxy-nitrosobenzene (1f)
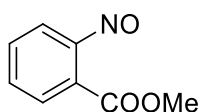
To a solution of methyl antranilate (10.4 mL, 80 mmol) in EtOH (160 mL), H$_3$PO$_4$ (8 mL of 85% solution), sodium tungstate dihydrate (7.92 g, 24 mmol) and H$_2$O$_2$ (80 mL of a 30% solution, 800 mmol) were added. The mixture was stirred at 65 °C overnight. Mixture was then cooled to r.t. and filtered. Collected precipitate was washed with water to afford 2-carbomethoxy-nitrosobenzene as a yellow solid (12.1 g, 92%). ^{1}H-NMR (DMSO-*d$_6$*) δ: 7.93-7.92 (m, 2H), 7.78-7.76 (m, 1H), 7.08-7.06 (m, 1H), 3.96 (s, 3H) ppm. GC-MS (EI): *m/z:* 166 [*M*H+]. Other spectral data match the literature.[334,337]

18.2.1.7. Synthesis of 4-nitroso-benzonitrile (1g)
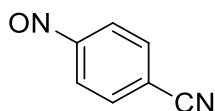
To a solution of 4-amino-benzonitrile (2.36 g, 20 mmol) in DCM (50 mL) and *n*-pentane (50 mL), sodium tungstate dihydrate (0.66 g, 1 mmol), H_3PO_4 (1 mL of a 85% solution, 14.6 mmol), H_2O_2 (20 mL of a 30% solution, 195.82 mmol) and TBAB (0.2 g, 0.62 mmol) were added. Reaction mixture was then stirred at 40 °C for 3 h. Mixture was then washed with HCl 0.01 M and water. Organic phase was dried over Na_2SO_4, filtered and evaporated under reduced pressure. Crude product was recrystallized from *n*-hexane to afford 4-nitroso-benzonitrile as a yellow solid (1.63 g, 62%). ^{1}H-NMR (CDCl$_3$) δ: 7.98 (s, 4H). Other spectral data match the literature.[334,340]

18.2.1.8. Synthesis of 4-bromo-nitrosobenzene (1h)
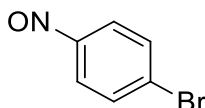
To a solution of 4-bromoaniline (3.44 g, 20 mmol) in DCM (50 mL) and *n*-pentane (50 mL), sodium tungstate dihydrate (0.66 g, 2 mmol), H_3PO_4 (1 mL of a 85% solution 15 mmol), H_2O_2 (20 mL of a 30% solution, 196 mmol) and TBAB (0.2 g, 0.62 mmol) were added. Reaction mixture is then stirred at 40°C for 3 h. Reaction mixture was then washed with HCl 0.01 M and water. Organic phase was dried over Na_2SO_4, filtered and evaporated under reduced pressure. Crude product was recrystallized from *n*-hexane to afford 4-bromo-nitrosobenzene as yellow solid (2.42 g, 65%). ^{1}H-NMR (CDCl$_3$) δ: 8.00 (d, 2H, *J* = 8.7 Hz), 7.89 (d, 2H, *J* = 8.7 Hz) ppm. Other spectral data match the literature.[337,341]

18.2.1.9. Synthesis of 4-trifluoromethyl-nitrosobenzene (1i)
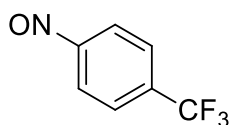
To a solution of 4-(trifluoromethyl)aniline (1.5 g, 9.3 mmol) in DCM (20 mL), a solution of Oxone® (11.5 g, 18.7 mmol) in water (20 mL), was added and the mixture was vigorously stirred at r.t. for 6 h. The aqueous phase was separated and washed with DCM. The combined organic phases were reunited and washed with HCl 1M, aqueous saturated NaHCO$_3$, and brine. Collected organic phases were dried over Na_2SO_4, filtered and evaporated under reduced pressure to afford 4-trifluoromethyl-nitrosobenzene as a brown solid (1.08 g, 66%). ^{1}H-NMR (CDCl$_3$) δ: 8.02 (d, 2H, *J* = 8.2 Hz), 7.92 (d, 2H, *J* = 8.2 Hz) ppm. Other spectral data match with literature.[341,342]

18.2.1.10. Synthesis of 4-chloro-nitrosobenzene (1j)
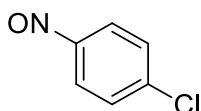
Cis-Mo(O)$_2$(acac)$_2$ (0.978 g, 3 mmol) was suspended in cyclohexane (60 mL) at r.t. and vigorously stirred for 5 min, then 4-chloro-aniline (3.261 g, 30 mmol) and H$_2$O$_2$ (15 mL, 150 mmol) were added. Reaction mixture was stirred at r.t. for 1 h to the mixture and then additional 60 mL of cyclohexane and about 3 g of Na$_2$SO$_4$ were added. After 20 min mixture was filtered. Organic phase was dried over Na$_2$SO$_4$ and cooled to -5 °C for 2 h and then filtered to afford 4-chloro-nitrosobenzene as yellow solid (1.695 g, 40%). ^{1}H-NMR (CDCl$_3$) δ: 7.87 (d, 2H, J = 8.6 Hz), 7.62 (d, 2H, J = 8.6 Hz) ppm. Other spectral data match the literature.[337,341]

18.2.1.11. Synthesis of 2-nitro-nitrosobenzene (1k)
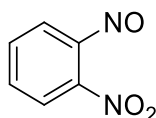
To a solution of 2-nitroaniline (1.4 g, 10.14 mmol) in ethanol (20 mL), H$_3$PO$_4$ (1 mL of a 85% solution, 15 mmol), sodium tungstatedihydrate (1.0 g, 3 mmol) and H$_2$O$_2$ (10 mL of a 30% solution, 98 mmol) were added. The mixture was stirred at 65 °C overnight. Reaction mixture was then filtered and solid washed with water to afford 2-nitro-nitrosobenzene (1.07 g, 70%) as a yellow solid. ^{1}H-NMR (CDCl$_3$) δ: 8.17 (d, J = 8.0 Hz, 1H), 7.96 (t, J = 8.0 Hz, 1H), 7.77 (t, J = 8.0 Hz, 1H), 6.63 (d, J = 8.0 Hz, 1H). Other spectral data match the literature.[337,343]

Nitrosobenzene (1l) was purchased as it is a commercial product.

♦ ♦ ♦ ♦ ♦ ♦

18.2.2. Synthesis of alkynones

18.2.2.1. Synthesis of 1-phenylprop-2-yn-1-one (2a)
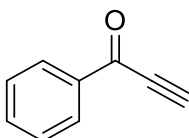
To a 0°C solution of 1-phenylprop-2-yn-1-ol (2.34 g, 20 mmol) in acetone (150 ml), Jones reagent was added dropwise to persistent orange color. Excess of Jones reagent was quenched adding isopropanol dropwise to persistent green color. Reaction mixture was filtered through Celite® and organic solution was evaporated under reduced pressure. Crude residue was dissolved in DCM and washed with saturated aqueous Na$_2$HCO$_3$ and brine. Organic phase was then dried over Na$_2$SO$_4$, filtered and the solvent removed under reduced pressure to afford 1-phenylprop-2-yn-1-one as yellow solid (2.6 g, quantitative yield) without any further

purification. ^{1}H-NMR (CDCl$_3$) δ: 8.19 (d, 2H, J = 7.5 Hz), 7.66 (t, 1H, J = 7.5 Hz), 7.53 (t, 2H, J = 7.5 Hz), 3.45 (s, 1H). Other spectral data match the literature.[334,335,344]

18.2.2.2. Synthesis of 1-(2-chlorophenyl)prop-2-yn-1-ol
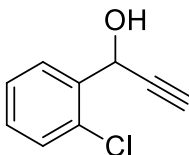
A solution of ethynylmagnesium bromide 0.5 M in THF (39.6 mL, 17.07 mmol) was added dropwise to a 0°C solution of 2-chloro-benzaldehyde (2 g, 14.22 mmol) in THF (35 mL). Reaction mixture is then allowed to warm up to r.t. and stirred overnight. Reaction mixture was quenched with saturated aqueous solution of NH$_4$Cl and the aqueous phase was extracted with EtOAc. The combined organic phases were washed with H$_2$O and brine, dried over Na$_2$SO$_4$ and the solvent removed under reduced pressure to afford 1-(2-chlorophenyl)prop-2-yn-1-ol as a brown oil (2.3 g, quantitative yield) without any further purification. ^{1}H-NMR (CDCl$_3$) δ: 7.80 (dd, 1H, J = 7.5 Hz, 1.8 Hz), 7.41 (dd, 1H, J = 7.5 Hz, 1.3 Hz), 7.35 (td, 1H, J = 7.5 Hz, 1.3 Hz), 7.31 (td, 1H, J = 7.5 Hz, 1.8 Hz), 5.86 (d, 1H, J = 2.1 Hz), 2.68 (d, 1H, J = 2.1 Hz), 2.49 (br, 1H) ppm. ^{13}C-NMR (CDCl$_3$) δ: 137.4, 132.5, 129.6, 129.5, 128.1, 127.1, 82.4, 74.6, 61.3 ppm. Other spectral data match the literature.[334,345]

18.2.2.3. Synthesis of 1-(2-chlorophenyl)prop-2-yn-1-one (2b)
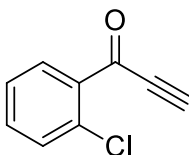
To a 0°C solution of 1-(2-chlorophenyl)prop-2-yn-1-ol (2.2 g, 13.22 mmol) in acetone (110 ml), Jones reagent was added dropwise to persistent orange color. Excess of Jones reagent was quenched adding isopropanol dropwise to persistent green color. Reaction mixture was filtered through Celite® and organic solution was evaporated under reduced pressure. Crude residue was dissolved in DCM and washed with saturated aqueous Na$_2$HCO$_3$ and brine. Organic phase was then dried over Na$_2$SO$_4$, filtered and the solvent removed under reduced pressure to afford 1-(2-chlorophenyl)-2-propyn-1-one as a yellow solid (1.99 g, 90%), without any further purification. ^{1}H-NMR (CDCl$_3$) δ: 8.13 (d, 1H, J = 8.0 Hz), 7.54 – 7.49 (m, 2H), 7.44 – 7.40 (m, 1H), 3.49 (s, 1H) ppm. Other spectral data match the literature.[334,345]

18.2.2.4. Synthesis of 1-(2-bromophenyl)prop-2-yn-1-ol

A solution of ethynylmagnesium bromide 0.5 M in THF (22 mL, 10.81 mmol) was added dropwise to a 0°C solution of 2-bromobenzaldehyde (2 g, 10.81 mmol) in THF (55 mL). Reaction mixture is then allowed to warm up to r.t. and stirred overnight. Reaction mixture was quenched with saturated aqueous solution of NH_4Cl and the aqueous phase was extracted with EtOAc. The combined organic phases were washed with H_2O and brine, dried over Na_2SO_4 and the solvent removed under reduced pressure to afford 1-(2-bromophenyl)prop-2-yn-1-ol (1.78 g, 78%) as a yellow oil without any further purification. ^{1}H NMR (CDCl$_3$) δ: 7.72 (d, J = 7.6 Hz, 1H), 7.50 (d, J = 8.0 Hz, 1H), 7.30 (t, J = 7.6 Hz, 1H), 7.14 (t, J = 7.6 Hz, 1H), 5.74 (s, 1H), 3.46 (d, J = 3.6 Hz, 1H), 2.62 (s, 1H). Other spectral data match the literature.[334,346]

18.2.2.5. Synthesis of 1-(2-bromophenyl)prop-2-yn-1-one (2c)

To a 0°C solution of 1-(2-bromophenyl)prop-2-yn-1-ol (1.78 g, 8.44 mmol)) in acetone (100 ml), Jones reagent was added dropwise to persistent orange color. Excess of Jones reagent was quenched adding isopropanol dropwise to persistent green color. Reaction mixture was filtered through Celite® and organic solution was evaporated under reduced pressure. Crude residue was dissolved in DCM and washed with saturated aqueous Na_2HCO_3 and brine. Organic phase was then dried over Na_2SO_4, filtered and the solvent removed under reduced pressure to afford 1-(2-bromophenyl)-2-propyn-1-one as a yellow-orange solid (1.64 g, 93%) without any further purification. ^{1}H NMR (CDCl$_3$) δ: 8.11 (d, J = 7.2 Hz, 1H), 7.70 (d, J = 7.6 Hz, 1H), 7.50-7.35 (m, 2H), 3.49 (s, 1H). Other spectral data match the literature.[334,346]
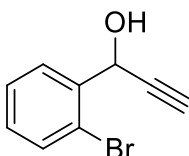
18.2.2.6. Synthesis of 1-(2-iodophenyl)prop-2-yn-1-ol

A solution of ethynylmagnesium bromide 0.5 M in THF (36 mL, 18 mmol) was added dropwise to a 0°C solution of 2-iodobenzaldehyde (4.00 g, 17.24 mmol) in THF (100 mL). Reaction mixture is then allowed to warm up to r.t. and stirred 3 h. Reaction mixture was quenched with saturated aqueous solution of NH_4Cl and the aqueous phase was extracted with EtOAc. The combined organic phases were washed with H_2O and brine, dried over Na_2SO_4 and the solvent removed under reduced pressure to afford to afford 1-(2-iodophenyl)prop-2-yn-1-ol (1.78 g, 78%) as yellow oil without any further purification. ^{1}H-NMR (CDCl$_3$) δ: 7.87 (d, 1H, J = 7.6 Hz), 7.80 (dd, 1H, J = 7.6 Hz, 1.6 Hz), 7.43 (td, 1H, J = 7.6 Hz, 1.6 Hz), 7.06 (td, 1H, J = 7.6 Hz, 1.6 Hz), 5.69 (dd, 1H, J = 5.2 Hz, 2.2 Hz), 2.70 (d, 1H, J = 2.2 Hz), 2.50 (d, 1H, J = 5.2 Hz) ppm. Other spectral data matchthe literature.[341,347]

18.2.2.7. Synthesis of 1-(2-iodophenyl)prop-2-yn-1-one (2d)
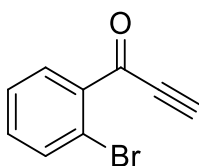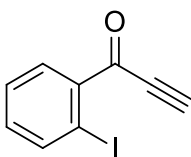

To a 0°C solution of 1-(2-iodophenyl)prop-2-yn-1-ol (2.00 g, 7.75 mmol) in acetone (90 ml), Jones reagent was added dropwise to persistent orange color. Excess of Jones reagent was quenched adding isopropanol dropwise to persistent green color. Reaction mixture was filtered through Celite® and organic solution was evaporated under reduced pressure. Crude residue was dissolved in DCM and washed with saturated aqueous Na_2HCO_3 and brine. Organic phase was then dried over Na_2SO_4, filtered and the solvent removed under reduced pressure to afford 1-(2-iodophenyl)-2-propyn-1-one (1.64 g, 93%) as a yellow oil without any further purification. ^{1}H-NMR (CDCl$_3$) δ: 8.20 (dd, 1H, J = 7.6 Hz, 1.6 Hz), 8.08 (dd, 1H, J = 7.6 Hz, 1.6 Hz), 7.52 (td, 1H, J = 7.6 Hz, 1.6 Hz), 7.24 (td, 1H, J = 7.6 Hz, 1.6 Hz), 3.49 (s, 1H) ppm.[341]

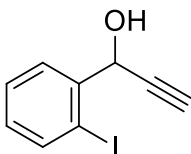### 18.2.2.8. Synthesis of 1-(2-nitrophenyl)prop-2-yn-1-ol

A solution of ethynylmagnesium bromide 0.5 M in THF (36 mL, 18 mmol) was added dropwise to a 0°C solution of 2-nitrobenzaldehyde (2.50 g, 16.5 mmol) in THF (80 mL). Reaction mixture is then allowed to warm up to r.t. and stirred 3 h. Reaction mixture was quenched with saturated aqueous solution of NH$_4$Cl and the aqueous phase was extracted with EtOAc. The combined organic phases were washed with H$_2$O and brine, dried over Na$_2$SO$_4$ and the solvent removed under reduced pressure to afford to afford 1-(3-nitrophenyl)prop-2-yn-1-ol (2.68 g, 92%) as brown oil without any further purification. ^{1}H-NMR (CDCl$_3$) δ: 8.13 (s, 1H), 7.65 (s, 1H), 7.51 (d, J = 2.9 Hz, 2H), 6.10 (s, 1H), 2.34 (s, 1H), 1.19 (s, 1H). Other spectral data match the literature.[341,348]

18.2.2.9. Synthesis of 1-(2-nitrophenyl)prop-2-yn-1-one (2e)
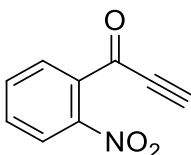
Dess-Martin periodinane (2.4 g, 5.6 mmol) was added to a r.t solution of 1-(3-nitrophenyl)prop-2-yn-1-ol (1 g, 5.6 mmol) in DCM (60 mL). Reaction mixture was stirred for 1 h. Et$_2$O and aqueous NaOH 1M were the added and the mixture was stirred for 0.5 h. Aqueous phase was the extracted with Et$_2$O and the reunited organic layers were washed with H$_2$O., dried over Na$_2$SO$_4$ and the solvent removed under reduced pressure

to afford 1-(3-nitrophenyl)prop-2-yn-1-one (990 mg, quantitative yield) as a brown solid with no further purification. ^{1}H-NMR (CDCl$_3$) δ: 7.95 (dd, 1H, J = 7.6, 1.3 Hz), 7.84 (dd, 1H, J = 7.6, 1.8 Hz), 7.77-7.69 (m, 2H), 3.48 (s, 1H). ^{13}C-NMR (CDCl$_3$) δ: 175.3; 147.9; 133.3; 133.2; 132.8; 130.1; 124.3; 82.1; 79.9. MS (CI): m/z = 176 [M]+. IR (film): ν (cm^{-1}) = 3271, 2097, 1677, 1528, 1348, 1241, 855, 790, 702. m.p.: 94-96 °C.[341]

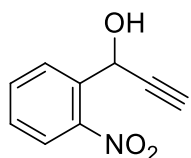### 18.2.2.10. Synthesis of 1-(3-nitrophenyl)prop-2-yn-1-ol

A solution of ethynylmagnesium bromide 0.5 M in THF (26.5 mL, 13.23 mmol) was added dropwise to a 0°C solution of 3-nitrobenzaldehyde (2 g, 13.23 mmol) in THF (65 mL). Reaction mixture is then allowed to warm up to r.t. and stirred overnight. Reaction mixture was quenched with saturated aqueous solution of NH$_4$Cl and the aqueous phase was extracted with EtOAc. The combined organic phases were washed with H$_2$O and brine, dried over Na$_2$SO$_4$ and the solvent removed under reduced pressure. Crude product is purified by flash column chromatography (*n*-hexane/EtOAc 8:2) to afford 1-(3-nitrophenyl)prop-2-yn-1-ol as a yellow oil (1.43 g, 61%). ^{1}H-NMR (CDCl$_3$) δ: 8.47 (s, 1H), 8.23 (dd, 1H, J = 8.0, 1.4 Hz), 7.92 (d, 1H, J = 8.0 Hz), 7.60 (t, 1H, J = 8.0 Hz), 5.60 (d, 1H, J = 2.2 Hz), 2.77 (d, 1H, J = 2.2 Hz).[334]

18.2.2.11. Synthesis of 1-(3-nitrophenyl)prop-2-yn-1-one (2f)
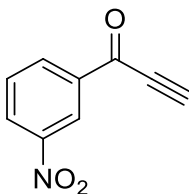
To a 0°C solution of 1-(3-nitrophenyl)prop-2-yn-1-ol (1.65 g, 9.32 mmol) in acetone (70 ml), Jones reagent was added dropwise to persistent orange color. Excess of Jones reagent was quenched adding isopropanol dropwise to persistent green color. Reaction mixture was filtered through Celite® and organic solution was evaporated under reduced pressure. Crude residue was dissolved in DCM and washed with saturated aqueous Na$_2$HCO$_3$ and brine. Organic phase was then dried over Na$_2$SO$_4$, filtered and the solvent removed under reduced pressure. Crude product was purified by flash column chromatography (petroleum ether/EtOAc 8:2) to afford 1-(3-nitrophenyl)prop-2-yn-1-one as a yellow solid (1.05 g, 64%). ^{1}H-NMR (CDCl$_3$) δ: 9.00 (s, 1H), 8.51 (dd, 1H, J = 7.8, 1.4 Hz), 8.50 (d, 1H, J = 7.8 Hz), 7.75 (t, 1H, J = 7.8 Hz), 3.62 (s, 1H). Other spectral data match the literature.[334,349]

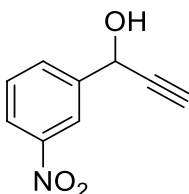### 18.2.2.12. Synthesis of 1-(4-nitrophenyl)prop-2-yn-1-ol

A solution of ethynylmagnesium bromide 0.5 M in THF (26.5 mL, 13.23 mmol) was added dropwise to a 0°C solution of 4-nitrobenzaldehyde (2 g, 13.23 mmol) in THF (65 mL). Reaction mixture is then allowed to warm up to r.t. and stirred overnight. Reaction mixture was quenched with saturated aqueous solution of NH_4Cl and the aqueous phase was extracted with EtOAc. The combined organic phases were washed with H_2O and brine, dried over Na_2SO_4 and the solvent removed under reduced pressure. Crude product is purified by flash column chromatography (petroleum ether/EtOAc 6:4) to afford 1-(4-nitrophenyl)prop-2-yn-1-ol as a yellow oil (1.28 g, 55%). ^{1}H-NMR (CDCl$_3$) δ: 8.27 (d, 2H, J = 8.6 Hz), 7.76 (d, 2H, J = 8.6 Hz), 5.60 (d, 1H, J = 2.2Hz), 2.76 (d, 1H, J =2.2 Hz) ppm. Other spectral data match the literature.[334,350]

18.2.2.13. Synthesis of 1-(4-nitrophenyl)prop-2-yn-1-one (2g)
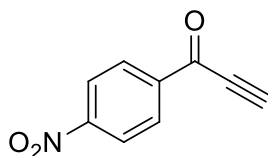
To a 0°C solution of 1-(4-nitrophenyl)prop-2-yn-1-ol (1.28 g, 7.23 mmol) in acetone (70 ml), Jones reagent was added dropwise to persistent orange color. Excess of Jones reagent was quenched adding isopropanol dropwise to persistent green color. Reaction mixture was filtered through Celite® and organic solution was evaporated under reduced pressure. Crude residue was dissolved in DCM and washed with saturated aqueous Na_2HCO_3 and brine. Organic phase was then dried over Na_2SO_4, filtered and the solvent removed under reduced pressure. Crude product was purified by flash column chromatography (petroleum ether/EtOAc 8:2) to afford 1-(3-nitrophenyl)prop-2-yn-1-one as a yellow solid (810 mg, 64%). ^{1}H-NMR (CDCl$_3$) δ: 8.37 (d, 2H, J = 9.1Hz), 8.34 (d, 2H, J = 9.1Hz), 3.63 (s, 1H) ppm. Other spectral data match the literature.[334,351]

18.2.2.14. Synthesis of 1-(4-methoxyphenyl)prop-2-yn-1-ol
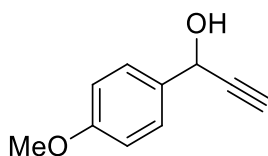
A solution of ethynylmagnesium bromide 0.5 M in THF (44 mL, 22.03 mmol) was added dropwise to a 0°C solution of 4-methoxybenzaldehyde (3 g, 22.03 mmol) in THF (110 mL). Reaction mixture is then allowed to warm up to r.t. and stirred overnight. Reaction mixture was quenched with saturated aqueous solution of NH_4Cl and the aqueous phase was extracted with EtOAc. The combined organic phases were washed with

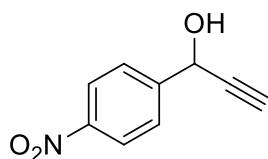H$_2$O and brine, dried over Na$_2$SO$_4$ and the solvent removed under reduced pressure. Crude product is purified by flash column chromatography (*n*-hexane/EtOAc 8:2) to afford 1-(4-methoxyphenyl)prop-2-yn-1-ol (2.1 g, 59%) as a yellow oil. ^{1}H-NMR (CDCl$_3$) δ: 7.42 (d, 2H, *J* = 6.4 Hz), 6.88 (d, 2H, *J* = 6.4 Hz), 5.37 (s, 1H), 3.77 (s, 3H), 2.60 (s, 1H), 2.59 (br s, 1H). Other spectral data match the literature.[334,352]

18.2.2.15. Synthesis of 1-(4-methoxyphenyl)prop-2-yn-1-one (2h)
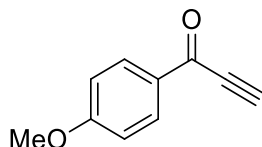

To a 0°C solution of 1-(4-methoxyphenyl)prop-2-yn-1-ol (1.57 g, 9.69 mmol) in acetone (80 ml), Jones reagent was added dropwise to persistent orange color. Excess of Jones reagent was quenched adding isopropanol dropwise to persistent green color. Reaction mixture was filtered through Celite® and organic solution was evaporated under reduced pressure. Crude residue was dissolved in DCM and washed with saturated aqueous Na$_2$HCO$_3$ and brine. Organic phase was then dried over Na$_2$SO$_4$, filtered and the solvent removed under reduced pressure to afford 1-(4-methoxyphenyl)prop-2-yn-1-one (1.19 g, 77%) as white solid without any further purification. ^{1}H-NMR (CDCl$_3$) δ: 8.16 (d, 2H, *J* = 8.8 Hz); 6.99 (d, 2H, *J* = 8.8 Hz); 3.92 (s, 3H); 3.39 (s, 1H). Other spectral data match the literature.[334,353]

18.2.2.16. Synthesis of 1-(4-formylphenyl)prop-2-yn-1-ol
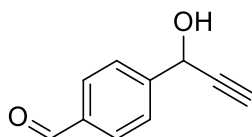
TMSA (118 mg, 1.2 mmol) was added to THF (50 mL) and cooled to −70 °C. *n*-Butyllithium 1.6 M in THF (0.75 mL, 1.2 mmol) was added dropwise over 30 min at −70 °C. After 1 h, a solution of terephthalaldehyde (134 mg, 1 mmol) in THF (5 mL) was added at −70 °C. Rection mixture was stirred for 1 h and slowly warmed to r.t. and stirred for extra 30 min. Reaction mixture was then quenched with saturated NH$_4$Cl aqueous solution at 0 °C and aqueous phase was extracted with Et$_2$O. Combined organic phases were washed with water and brine, dried over Na$_2$SO$_4$, filtered and evaporated under reduced pressure. The crude product was subsequently used for next step with no further purification. Methanol (15 mL) and K$_2$CO$_3$ (345.5 mg, 2.5 mmol) were added to the crude residue. Reaction mixture was stirred under an argon atmosphere at r.t. overnight. Reaction mixture was diluted with EtOAc and washed with water and brine. Organic phases were separated, dried over Na$_2$SO$_4$, filtered and solvent removed under reduced pressure to afford 1-(4-formylphenyl) prop-2-yn-1-ol (141 mg, 88%) as a pale yellow solid. ^{1}H-NMR (CDCl$_3$) δ: 9.93 (s, 1H), 7.83 (d, *J* = 8.1 Hz, 2H), 7.67 (d, *J* = 8.1 Hz, 2H), 5.51 (d, *J* = 1.8 Hz, 1H), 3.66 (bs, 1H), 2.69 (d, *J* = 2.4 Hz, 1H); ^{13}C-NMR (CDCl$_3$) δ: 192.3, 146.6, 135.9, 130.0, 127.0, 82.8, 75.4, 63.5. Other spectral data match the literature.[334,354]

18.2.2.17. Synthesis of 1-(4-formylphenyl)prop-2-yn-1-one (2i)
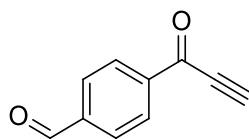
To a r.t. solution of 1-(4-formylphenyl)prop-2-yn-1-ol (400 mg, 2.50 mmol) in DCM (30 mL), MnO_2 (2.8 g, 32.21 mmol) was added. After 4 h, reaction mixture was filtered through Celite®. Solvent was then removed by rotary evaporation to afford 1-(4-formylphenyl)prop-2-yn-1-one (261 mg, 63%) as an orange solid without any further purification. ^{1}H-NMR (CDCl$_3$) δ: 10.15 (s, 1H), 8.34 (d, 2H, J = 2 Hz), 8.03 (d, 2H, J = 2Hz), 3.55 (s, 1H) ppm.[334]

18.2.2.18. Synthesis of 1-(benzo[d][1,3]dioxol-5-yl)prop-2-yn-1-ol
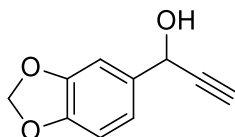
A solution of ethynylmagnesium bromide 0.5 M in THF (100.5 mL, 50 mmol) was added dropwise to a 0°C solution of piperonal (2.5 g, 16.65 mmol) in THF (60 mL). Reaction mixture is then allowed to warm up to r.t. and stirred 5 h. Reaction mixture was quenched with saturated aqueous solution of NH_4Cl and the aqueous phase was extracted with EtOAc. The combined organic phases were washed with H_2O and brine, dried over Na_2SO_4 and the solvent removed under reduced pressure. Crude product is purified by flash column chromatography (*n*-hexane/EtOAc 4:1) to afford 1-(benzo[d][1,3]dioxol-5-yl)prop-2-yn-1-ol (2.29 g, 78%) as a yellow oil. ^{1}H-NMR (CDCl$_3$) δ: 7.00 (d, *J* = 1.8 Hz, 1H), 6.96 (dd, *J* = 8.0, 1.8 Hz, 1H), 6.75 (d, *J* = 8.0 Hz, 1H), 5.92 (s, 2H), 5.31 (d, *J* = 2.0 Hz, 1H), 3.28 (br, 1H), 2.66 (d, *J* = 2.0 Hz, 1H); ^{13}C NMR (CDCl$_3$) δ: 147.78, 147.65, 134.17, 120.41, 108.16, 107.43, 101.24, 83.66, 74.82, 63.98. Other spectral data match the literature.[334,353]

18.2.2.19. Synthesis of 1-(benzo[d][1,3]dioxol-5-yl)prop-2-yn-1-one (2j)
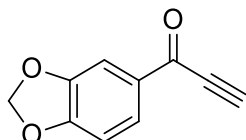
To a solution of 1-(benzo[d][1,3]dioxol-5-yl)prop-2-yn-1-ol (1.2 g, 6.82 mmol), MnO_2 (7.73 g, 88.66 mmol) was added. After 4 h, reaction mixture was filtered through Celite®. Solvent was then removed under reduced pressure to obtain 1-(benzo[d][1,3]dioxol-5-yl)prop-2-yn-1-one (1.05 g, 89%) as yellow solid with no further purification. ^{1}H-NMR (CDCl$_3$) δ: 7.81 (d, *J* = 8.2 Hz, 1H), 7.52 (s, 1H), 6.87 (d, *J* = 8.2 Hz, 1H), 6.06 (s, 2H), 3.38 (s, 1H); ^{13}C-NMR (CDCl$_3$) δ: 175.6, 153.4, 148.4, 131.5, 127.8, 108.3, 108.2, 102.3, 80.3, 80.3. Other spectral data match the literature.[334,355]

18.2.2.20. Synthesis of 1-(1-methyl-1H-indol-3-yl)prop-2-yn-1-one (2k)
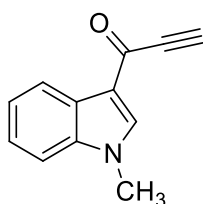
To a 0°C solution of 1-methyl-1*H*-indole-3-carbaldehyde (1.50 g, 9.44 mmol) in THF (30 mL), ethynylmagnesium bromide 0.5 M in THF (38 mL, 18.87 mmol) was added dropwise. Reaction mixture is then allowed to warm up to r.t. and stirred 16 h. Reaction mixture was quenched with saturated aqueous solution of NH_4Cl and the aqueous phase was extracted with $CHCl_3$. The combined organic phases were washed with H_2O and brine, dried over Na_2SO_4 and the solvent reduced under reduced pressure to around 30 mL. To this solution, MnO_2 (3.7 g, 41.56 mmol) was added and the mixture was refluxed for 1 h. After cooling to r.t., reaction mixture was filtered through Celite®. The solvent was removed under reduced pressure. Crude product was purified by gravimetric column chromatography (petroleum ether/EtOAc 6:4) to afford 1-(1-methyl-1*H*-indol-3-yl)prop-2-yn-1-one (895 mg, 52%) as a yellow solid. ^{1}H-NMR (CDCl$_3$) δ: 8.40 – 8.37 (m, 1H), 7.94 (s, 1H), 7.44 – 7.37 (m, 3H), 3.88 (s, 3H), 3.18 (s, 1H) ppm. Other spectral data match the literature.[334,356]

18.2.2.21. Synthesis of 1-(1-tosyl-1H-indol-3-yl)prop-2-yn-1-ol
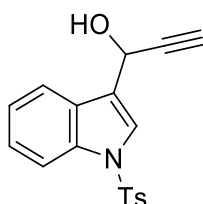
A solution of ethynylmagnesium bromide 0.5 M in THF (8 mL, 4 mmol) was added dropwise to a 0°C solution of N-tosyl-3-indolcarbaldehyde (1 g, 3.3 mmol) in THF (35 mL). Reaction mixture is then allowed to warm up to r.t. and stirred 5 h. Reaction mixture was quenched with saturated aqueous solution of NH_4Cl and the aqueous phase was extracted with $CHCl_3$. The combined organic phases were washed with H_2O and brine, dried over Na_2SO_4 and the solvent removed under reduced pressure to afford 1-(1-tosyl-1H-indol-3-yl)prop-2-yn-1-ol (1 g, quantitative yield) as brown oil with no further purification. ^{1}H-NMR (CDCl$_3$) δ: 7.96 (d, J = 8.3 Hz, 1H), 7.76 (d, J = 8.3 Hz, 1H), 7.74 (s, 1H), 7.24 (t, J = 2.4 Hz, 1H), 7.22 (d, J = 8.2 Hz, 1H), 7.17 (d, J = 8.2 Hz, 1H), 5.64 (s, 1H), 3.35 (s, 1H), 2.66 (s, 1H), 2.29 (s, 1H). Other spectral data match the literature.[341]

18.2.2.22. Synthesis of 1-(1-tosyl-1H-indol-3-yl)prop-2-yn-1-one (2l)
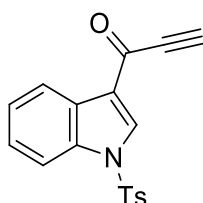
To a solution of 1-(1-tosyl-1H-indol-3-yl)prop-2-yn-1-ol (1100 mg, 3.4 mmol) in CHCl$_3$ (30 mL), MnO$_2$ (1.76 g, 20.3 mmol) was added. Mixture was stirred and refluxed for 4 h. Reaction mixture was then filtered through Celite®. Solvent was then removed under reduced pressure to afford 1-(1-tosyl-1H-indol-3-yl)prop-2-yn-1-one (601 mg, 76%) as brown solid without any further purification. ^{1}H-NMR (CDCl$_3$) δ: 8.46 (s, 1H), 8.30 (d, J = 8.6 Hz, 1H), 7.93 (d, J = 8.5 Hz, 1H), 7.87 (d, J = 8.4 Hz), 7.42 − 7.35 (m, 2H), 3.32 (s, 1H), 2.39 (s, 1H). Other spectral data match the literature.[341,357]

18.2.2.23. Synthesis of 1-(1-methyl-1H-indol-2-yl)prop-2-yn-1-ol

A solution of ethynylmagnesium bromide 0.5 M in THF (19 mL, 9.30 mmol) was added dropwise to a 0°C solution of 1-methyl-1H-indole-2-carbaldehyde (1.48 g, 9.30 mmol) in THF (55 mL). Reaction mixture is then allowed to warm up to r.t. and stirred 5 h. Reaction mixture was quenched with saturated aqueous solution of NH$_4$Cl and the aqueous phase was extracted with EtOAc. The combined organic phases were washed with H$_2$O and brine, dried over Na$_2$SO$_4$ and the solvent removed under reduced pressure. Crude product is purified by flash column chromatography (n-hexane/EtOAc 4:1) to afford 1-(1-methyl-1H-indol-2-yl)prop-2-yn-1-ol (1.29 g, 75%) as a brown oil. ^{1}H-NMR (CDCl$_3$) δ: 7.50 (d, 1H, J = 8 Hz), 7.19 (m, 2H), 7.01 (t, 1H, J = 7.6 Hz), 6.56 (s, 1H), 5.50 (d, 1H, J = 5.2 Hz), 3.68 (s, 3H), 2.58 (d, 1H, J = 2.4 Hz), 2.35 (d, 1H. J = 6.8 Hz) ppm. ^{13}C-NMR (CDCl$_3$) δ: 138.5, 137.4, 126.7, 122.5, 121.2, 119.8, 109.3, 101.6, 81.7, 74.8, 58.2, 31.2 ppm.[334]

18.2.2.24. Synthesis of 1-(1-methyl-1H-indol-2-yl)prop-2-yn-1-one (2m)
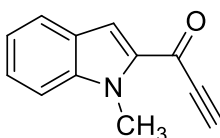
To a solution of 1-(1-methyl-1H-indol-2-yl)prop-2-yn-1-ol (1.3 g, 6.9 mmol) in CHCl$_3$ (60 mL), MnO$_2$ (3.57 g, 42 mmol) was added and the mixture was heated to reflux for 1h. Then, reaction mixture was filtered through Celite®. The solvent was removed under reduced pressure to afford 1-(1-methyl-1H-indol-2-yl)prop-2-yn-1-one (986 mg, 78%) as a brown solid without any further purification. ^{1}H-NMR (CDCl$_3$) δ: 7.63 (d, 1H, J = 8 Hz), 7.53 (s 1H), 7.34 (t, 1H), J = 7.2 Hz), 7.28 (d, 1H, J = 8.4 Hz), 7.08 (t, 1H, J = 7.2 Hz), 3.99 (s, 3H), 3.20 (s, 1H) ppm. ^{13}C-NMR (CDCl$_3$) δ: 168.7, 141.2, 135.5, 127.3, 125.9, 123.5, 121.2, 117.5, 110.5, 81.3, 77.4, 32.1 ppm.[334]
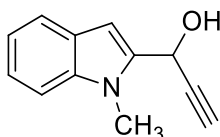
18.2.2.25. Synthesis of 1-(1-methyl-1*H*-pyrrol-2-yl)prop-2-yn-1-ol
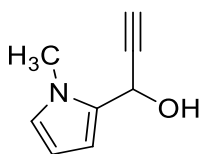
A solution of ethynylmagnesium bromide 0.5 M in THF (4 mL, 2 mmol) was added dropwise to a 0°C solution of *N*-methyl-2-pyrrolecarboxaldehyde (160 mg, 1.47 mmol) in THF (8 mL). Reaction mixture is then allowed to warm up to r.t. and stirred 5 h. Reaction mixture was quenched with saturated aqueous solution of NH_4Cl and the aqueous phase was extracted with EtOAc. The combined organic phases were washed with H_2O and brine, dried over Na_2SO_4 and the solvent removed under reduced pressure. Crude product is purified byflash column chromatography (*n*-hexane /EtOAc 7:3) to afford 1-(1-methyl-1*H*-pyrrol-2-yl)prop-2-yn-1-ol (151 mg, 76 %) as a yellow oil. ^{1}H-NMR (CDCl$_3$) δ: 2.12 (br, 1H), 2.60 (d, *J* = 2.3 Hz, 1H), 3.79 (s, 3H), 5.45 (d, *J* = 3.2 Hz, 1H), 6.03 (m, 1H), 6.30 (m, 1H), 6.61 (m, 1H). ^{13}C-NMR (CDCl$_3$) δ: 132.0, 124.4, 108.8, 106.6, 82.1, 73.7, 57.5, 34.1.[334]

18.2.2.26. Synthesis of 1-(1-methyl-1*H*-pyrrol-2-yl)prop-2-yn-1-one (2n)
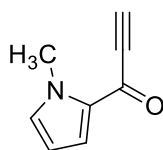
To a solution of 1-(1-methyl-1*H*-pyrrol-2-yl)prop-2-yn-1-ol (135 mg, 1 mmol) in CHCl$_3$ (10 mL), MnO$_2$ (255 mg, 2.93 mmol) was added. Reaction mixture was heated to reflux for 1 h. Then, extra MnO$_2$ (255 mg, 2.93 mmol) was added and the mixture was refluxed for 1 extra h. After cooling to r.t., reaction mixture is filtered through Celite®. The solvent was then removed under reduce pressure. Crude product is purified by flash column chromatography (petroleum ether/ EtOAc 8:2) to afford 1-(1-methyl-1*H*-pyrrol-2-yl)prop-2-yn-1-one (98 mg, 75%) as a yellow solid. ^{1}H-NMR (CDCl$_3$) δ: 7.24 (dd, 1H, *J$_1$* = 4.1 Hz, *J$_2$* = 1.6 Hz), 6.89 (d, 1H, *J* = 4.1 Hz), 6.19 (dd, 1H, *J$_1$* = 4.1 Hz, *J$_2$* = 2.4 Hz), 3.96 (s, 3H), 3.14 (s, 1H) ppm.[334]

18.2.2.27. Synthesis of 1-(furan-2-yl)prop-2-yn-1-ol
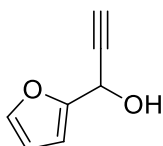
A solution of ethynylmagnesium bromide 0.5 M in THF (2.5 mL, 1.25 mmol) was added dropwise to a 0°C solution of furfural (96 mg, 1 mmol) in THF (5 mL). Reaction mixture is then allowed to warm up to r.t. and stirred 5 h. Reaction mixture was quenched with saturated aqueous solution of NH_4Cl and the aqueous phase was extracted with EtOAc. The combined organic phases were washed with H_2O and brine, dried over Na_2SO_4 and the solvent removed under reduced pressure. Crude product is purified by flash column chromatography

(*n*-hexane /EtOAc 8:2) to afford 1-(furan-2-yl)prop-2-yn-1-ol (64 mg, 52 %) as a yellow oil.^{1}H-NMR (CDCl$_3$) δ: 7.37 (s, 1H), 6.42 (d, 1H, *J* = 2.9 Hz), 6.31 (d, 1H, *J* = 1.8 Hz), 5.40 (d, 1H, *J* = 4.2 Hz), 3.00 (br, 1H), 2.57 (d, 1H, *J* = 1.8 Hz) ppm. Other spectral data match the literature.[334,358]

18.2.2.28. Synthesis of 1-(furan-2-yl)prop-2-yn-1-one (2o)
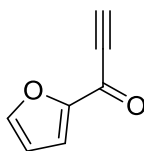
To a solution of 1-(furan-2-yl)prop-2-yn-1-ol (350 mg, 2.87 mmol) in CHCl$_3$ (15 mL), MnO$_2$ (1.09 g, 12.54 mmol) was added. Reaction mixture was heated to reflux for 1 h. Then, extra MnO$_2$ (1.09 g, 12.54 mmol) was added and the mixture was refluxed for 1 extra h. After cooling to r.t., reaction mixture is filtered through Celite®. The solvent was then removed under reduce pressure. Crude product is purified by flash column chromatography (petroleum ether/ EtOAc 7:3) to afford 1-(furan-2-yl)prop-2-yn-1-one (225 mg, 65%) as a yellow solid. ^{1}H-NMR (CDCl$_3$) δ: 7.68 (s, 1H), 7.40 (d, 1H, J = 3.6 Hz), 6.59 (d, 1H, J = 3.6 Hz), 3.38 (s, 1H) ppm. Other spectral data match the literature.[334,351]

18.2.2.29. Synthesis of 1-(pyren-1-yl)-3-(trimethylsilyl)prop-2-yn-1-ol
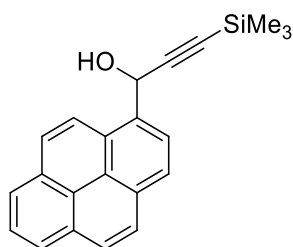
A solution 1.6 M of *n*-BuLi in hexanes (8 mL, 13 mmol) were added to a -78°C solution of TMSA (1.83 ml, 13 mmol) in Et$_2$O (30 mL). After 0.5 h, a solution of pyrene-1-carboxaldehyde (2.3 g, 10 mmol) in Et$_2$O (20 mL) was added dropwise. Reaction mixture was the allowed to reach r.t. and stirred overnight. Reaction mixture was quenched with saturated aqueous solution of NH$_4$Cl and the aqueous phase was extracted with EtOAc. The combined organic phases were washed with H$_2$O and brine, dried over Na$_2$SO$_4$ and the solvent removed under reduced pressure to afford 1-(pyren-1-yl)-3-(trimethylsilyl)prop-2-yn-1-ol (279 mg, 85%) as a yellow solid without any further purification. ^{1}H-NMR (CDCl$_3$) δ: 8.51 (d, *J* = 9.3 Hz, 1H), 8.36 (d, *J* = 7.9 Hz, 1H), 8.16 (m, 4H), 8.04 (m, 3H), 6.40 (d, *J* = 5.7 Hz, 1H), 2.37 (d, *J* = 5.7 Hz, 1H), 0.20 (s, 9H). Other spectral data match the literature.[334,359]

18.2.2.30. Synthesis of 1-(pyren-1-yl)prop-2-yn-1-ol
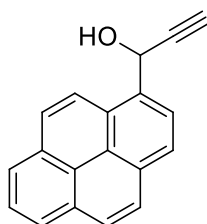
To a 0°C solution of 1-(pyren-1-yl)-3-(trimethylsilyl)prop-2-yn-1-ol (328 mg, 1 mmol) in water (10 mL), a solution of TBAF (340 mg, 1.3 mmol) in THF (10 mL) was added. After 4 h, water is added to reaction mixture and aqueous phase was then extracted with Et$_2$O. Reunited organic phases were then washed with brine, dried with MgSO$_4$, filtered and solvents removed under reduced pressure. Crude product was then purified by gravimetric column chromatography (DCM/hexane 6:4) to afford 1-(pyren-1-yl)prop-2-yn-1-ol (200 mg, 78%) as a yellow solid. ^{1}H-NMR (DMSO-d_6) δ: 8.59 (d, J = 10.0 Hz, 1H), 8.35–8.29 (m, 4H), 8.26 (d, J = 10.0 Hz, 1H), 8.20–8.16 (m, 2H), 8.09 (t, 1H, J = 7.5 Hz), 6.41–6.39 (d, J = 5.0 Hz, 1H), 6.34–6.31 (dd, J = 5.0 Hz, 2.5 Hz, 1H), 3.60 (d, J = 2.5 Hz, 1H) ppm; ^{13}C-NMR (DMSO-d_6) δ: 135.0, 130.7, 130.5, 130.1, 127.3, 127.3, 127.3, 127.2, 126.2, 125.3, 125.2, 124.6, 124.6, 124.1, 123.8, 123.7, 85.5, 76.6, 60.8 ppm. Other spectral data match the literature.[334,360]

18.2.2.31. Synthesis of 1-(pyren-1-yl)prop-2-yn-1-one (2p)
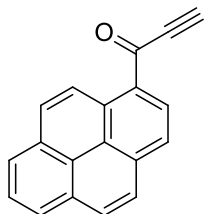
To a solution of 1-(pyren-1-yl)prop-2-yn-1-ol (256 mg, 1 mmol) in DCM (30 mL), MnO$_2$ (2.61 g, 30 mmol) was added. Mixture was refluxed for 24 h. Then, after cooling to r.t., reaction mixture was filtered through Celite®. The solvent was removed under reduced pressure to afford 1-(pyren-1-yl)prop-2-yn-1-one (252 mg, quantitative yield) as yellow solid without further purification. ^{1}H-NMR (CDCl$_3$) δ: 9.48 (d, J = 10.0 Hz, 1H), 8.94 (d, J = 8.0 Hz, 1H), 8.28–8.23 (m, 3H), 8.19–8.14 (m, 2H), 8.07–8.02 (m, 2H), 3.53 (s, 1H); ^{13}C-NMR (CDCl$_3$) δ: 179.3, 135.8, 132.2, 131.31, 131.25, 131.14, 131.05, 130.6, 128.4, 127.35, 127.29, 127.1, 126.8, 124.97, 124.96, 124.95, 124.2, 124.1, 82.6, 80.1. Other spectral data match the literature.[334,360]

18.2.2.32. Synthesis of 1-(ferrocene)prop-2-yn-1-ol
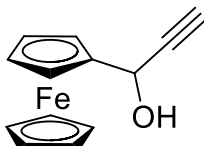
A solution of ethynylmagnesium bromide 0.5 M in THF (10 mL, 5 mmol) was added dropwise to a 0°C solution of ferrocene carboxaldehyde (1.00 g, 4.67 mmol) in THF (45 mL). Reaction mixture is then allowed to warm up to r.t. and stirred overnight. Reaction mixture was quenched with saturated aqueous solution of NH_4Cl and the aqueous phase was extracted with EtOAc. The combined organic phases were washed with H_2O and brine, dried over Na_2SO_4 and the solvent removed under reduced pressure. Crude product is purified by flash column chromatography (DCM/*n*-hexane 8:2) to afford 1-(ferrocene)prop-2-yn-1-ol (908 mg, 81%) as yellow solid. ^{1}H-NMR (CDCl$_3$) δ: 5.18 – 5.16 (dd, 1H, J_1 = 7.7 Hz, J_2 = 2.1 Hz), 4.40 – 4.37 (m, 2H), 4.25 (s, 5H), 4.22 – 4.25 (m, 2H), 2.62 – 2.61 (d, 1H, J = 2.1 Hz), 2.15 – 2.13 (d, 1H, *J* = 7.7 Hz) ppm. Other spectral data match the literature.[334,361]

### 18.2.2.33. Synthesis of 1-(ferrocene)prop-2-yn-1-one (2q)
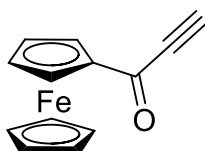
To a solution of 1-(ferrocene)prop-2-yn-1-ol (480 mg, 2 mmol) in DCM (30 mL), MnO_2 (5.22 g, 60 mmol) was added and the mixture was stirred for 15 minutes at r.t.. Then, reaction mixture was filtered through Celite®. The solvent was removed under reduced pressure to afford 1-(ferrocene)prop-2-yn-1-one (480 mg, quantitative yield) as a dark red solid without any further purification. ^{1}H-NMR (CDCl$_3$) δ: 4.97 (s, 2H), 4.65 (s, 2H), 4.30 (s, 5H), 3.27 (s, 2H) ppm. Other spectral data match the literature.[334,361]

18.2.2.34. Synthesis of 1-(naphthalen-1-yl)prop-2-yn-1-ol

A solution of ethynylmagnesium bromide 0.5 M in THF (20 mL, 10 mmol) was added dropwise to a 0°C solution of 1-naphthaldehyde (1.5 g, 9.61 mmol) in THF (60 mL). Reaction mixture is then allowed to warm up to r.t. and stirred overnight. Reaction mixture was quenched with saturated aqueous solution of NH_4Cl and the aqueous phase was extracted with EtOAc. The combined organic phases were washed with H_2O and brine, dried over Na_2SO_4 and the solvent removed under reduced pressure. Crude product is purified by flash column chromatography (*n*-hexane/EtOAc 8:2) to afford 1-(naphthalen-1-yl)prop-2-yn-1-ol (1.45 g, 83%) as a yellow oil. ^{1}H-NMR (CDCl$_3$) δ: 8.30 (d, 1H, *J* = 8.4 Hz), 7.89 - 7.80 (m, 3H), 7.59 - 7.49 (m, 3H), 6.11 (d, 1H, *J* = 2.0 Hz), 3.11 (br, 1H), 2.73 (d, 1H, *J* = 2.0 Hz) ppm. Other spectral data match the literature.[334,362]

18.2.2.35. Synthesis of 1-(naphthalen-1-yl)prop-2-yn-1-one (2r)
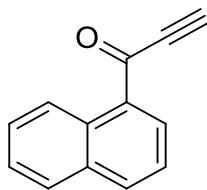
To a 0°C solution of 1-(naphthalen-1-yl)prop-2-yn-1-ol (1.38 g, 7.58 mmol) in acetone (60 ml), Jones reagent was added dropwise to persistent orange color. Excess of Jones reagent was quenched adding isopropanol dropwise to persistent green color. Reaction mixture was filtered through Celite® and organic solution was evaporated under reduced pressure. Crude residue was dissolved in DCM and washed with saturated aqueous Na_2HCO_3 and brine. Organic phase was then dried over Na_2SO_4, filtered and the solvent removed under reduced pressure to afford 1-(naphthalen-1-yl)prop-2-yn-1-one (1.23 g, 90%) as yellow solid with no further purification. ^{1}H-NMR (CDCl$_3$) δ: 9.22 (d, 1H, J = 8.7 Hz), 8.63 (dd, 1H, J_1 = 7.2 Hz, J_2 = 0.8 Hz), 8.11 (d, 1H, J = 8.1 Hz), 7.92 (d, 1H, J = 8.1 Hz), 7.69 (td, 1H, J_1 = 7.8 Hz, J_2 = 1.2 Hz), 7.59 (t, 2H, J = 7.8 Hz), 3.45 (s, 1H) ppm. Other spectral data match the literature.[334,344]

18.2.2.36. Synthesis of (*E*)-1-(2-nitrophenyl)pent-1-en-4-yn-3-ol
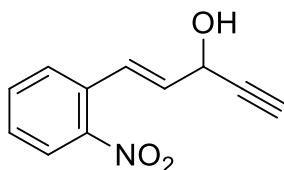
A solution of ethynylmagnesium bromide 0.5 M in THF (20 mL, 10 mmol) was added dropwise to a 0°C solution of (*E*)-2-nitrocinnamaldehyde (1.68 g, 9.5 mmol) in THF (70 mL). Reaction mixture is then allowed to warm up to r.t. and stirred 5 h. Reaction mixture was quenched with saturated aqueous solution of NH$_4$Cl and the aqueous phase was extracted with EtOAc. The combined organic phases were washed with H$_2$O and brine, dried over Na_2SO_4 and the solvent removed under reduced pressure. Crude product is purified by flash column chromatography (n-hexane/DCM 8:2) to afford (*E*)-1-(2-nitrophenyl)pent-1-en-4-yn-3-ol (1.93 g, quantitative yield) as brown oil. ^{1}H-NMR (CDCl$_3$) δ: 7.96 (d, 1H, J = 7.9 Hz), 7.63-7.57 (m, 2H), 7.43 (m, 1H), 7.30 (dd, 1H, J = 15.6, 1.1 Hz), 6.27 (dd, 1H, J = 15.6, 5.6 Hz), 5.11 (m, 1H), 2.66 (d, 1H, J = 2.2 Hz), 2.67 (br s, 1H). Other spectral data match the literature.[334,363]

18.2.2.37. Synthesis of (*E*)-1-(2-nitrophenyl)pent-1-en-4-yn-3-one (2s)
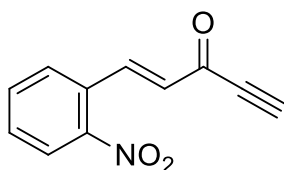
Dess-Martin periodinane (2.4 g, 5.6 mmol) was added to a solution of (E)-1-(2-nitrophenyl)pent-1-en-4-yn-3-ol (1.14 g, 5.6 mmol) in DCM (60 ml) and the mixture was stirred for 1 h at r.t.. Et_2O and an aqueous NaOH 1M were added and the mixture was stirred for 0.5 h. Aqueous phase was extracted with Et_2O and the reunited organic phases were washed with H_2O, dried over Na_2SO_4 and the solvent removed under reduced pressure to afford (E)-1-(2-nitrophenyl)pent-1-en-4-yn-3-one as a brown solid (844 mg, 75 %) with no further purification. ^{1}H-NMR (DMSO-d_6) δ: 8.25 (d, 1H, J = 16 Hz), 8.13 (dd, 1H, J = 8.1, 1.2 Hz), 7.98 (dd, 1H, J = 7.8, 1.3 Hz), 7.81 (td, 1H, J = 7.4, 0.8 Hz), 7.73 (td, 1H, J = 7.8, 1.4 Hz), 6.96 (d, 1H, J = 16 Hz), 4.99 (s, 1H). ^{13}C-NMR (DMSO-d_6) δ: 177.7, 148.8, 144.9, 134.5, 132.2, 131.9, 130.0, 129.3, 125.4, 84.7, 80.3. MS (CI): m/z = 202 [M]$^{+}$. IR (KBr disk): ν (cm^{-1}) = 3255, 3105, 2099, 1645, 1518, 1347, 1238, 970, 787, 741. m.p.: 102-104 °C.[334]

18.2.2.38. Synthesis of 4-phenylbut-1-yn-3-ol
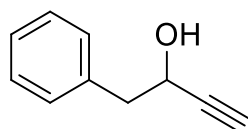
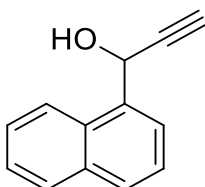A solution of ethynylmagnesium bromide 0.5 M in THF (36 mL, 18 mmol) was added dropwise to a 0°C solution of phenylacetaldehyde (1.8 g, 15 mmol) in THF (50 mL). Reaction mixture is then allowed to warm up to r.t. and stirred overnight. Reaction mixture was quenched with saturated aqueous solution of NH_4Cl and the aqueous phase was extracted with EtOAc. The combined organic phases were washed with H_2O and brine, dried over Na_2SO_4 and the solvent removed under reduced pressure. Crude product was purified by flash column chromatography (n-hexane/EtOAc 5:1) to afford 4-phenylbut-1-yn-3-ol (1.5 g, 70%) as yellow oil. ^{1}H-NMR (CDCl$_3$) δ: 7.38 – 7.30 (m, 5H), 4.61 (m, 1H), 3.08 (dd, J = 13.4, 6.5. 1H), 3.03 (dd, J = 13.6, 6.5 Hz, 1H), 2.52 (d, J = 2.1 Hz, 1H), 2.11 (d, J = 5.5 Hz, 1H). ^{13}C-NMR (CDCl$_3$) δ: 136.2, 129.7, 128.4, 127.0, 84.1, 73.8, 62.9, 43.8. Other spectral data match the literature.[334,364]

18.2.2.39. Synthesis of 4-phenylbut-1-yn-3-one (2t)
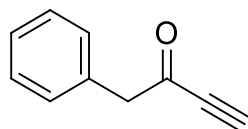
To a 0°C solution of 4-phenylbut-1-yn-3-ol (1.8 g, 12.33 mmol) in acetone (70 ml), Jones reagent was added dropwise to persistent orange color. Excess of Jones reagent was quenched adding isopropanol dropwise to persistent green color. Reaction mixture was filtered through Celite® and organic solution was evaporated under reduced pressure. Crude residue was dissolved in DCM and washed with saturated aqueous Na_2HCO_3 and brine. Organic phase was then dried over Na_2SO_4, filtered and the solvent removed under reduced pressure to afford 4-phenylbut-1-yn-3-one (1.6 g, 90%) as yellow solid with no further purification. ^{1}H-NMR (CDCl$_3$) δ: 7.41 – 7.21 (m, 5H), 3.87 (s, 2H), 3.23 (s, 1H) ppm; ^{13}C-NMR (CDCl$_3$) δ: 184.5, 132.4, 129.9, 128.9, 127.7, 81.3, 80.3, 52.10 ppm. Other spectral data match the literature.[334,365]

18.2.2.40. Synthesis of 3'-nitro-[1,1'-biphenyl]-2-carbaldehyde
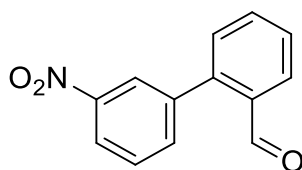
To a r.t. solution of 1-iodo-3-nitrobenzene (2 g, 8 mmol) in DMSO (40 mL), 2-formylphenylboronic acid (1.3 g, 8.9 mmol) and Pd(PPh$_3$)$_2$Cl$_2$ (281 mg, 0.4 mmol) were added. Reaction mixture was further deoxygenated via N$_2$ bubbling for additional 15 minutes before an aqueous solution of Na$_2$CO$_3$ 2M (8 ml, 16 mmol) was added. The mixture was heated to 80°C and stirred 24 h. Reaction mixture is then diluted with ice and water. The resulting emulsion was extracted with EtOAc and the reunited organic phases washed with saturated aqueous NH$_4$Cl, dried over Na$_2$SO$_4$ and the solvent removed under reduced pressure to afford 3'-nitro-[1,1'-biphenyl]-2-carbaldehyde (1.8 g, quantitative yield) as a brown solid without any further purification. ^{1}H-NMR (CDCl$_3$) δ: 9.99 (s, 1H), 8.34-8.31 (m, 1H), 8.30-8.29 (m, 1H), 8.08 (dd, 1H, J = 7.7, 1 Hz), 7.74-7.61 (m, 3H), 7.47-7.45 (m, 1H). ^{13}C-NMR (CDCl$_3$) δ: 191.1, 148.2, 142.7, 139.8, 135.9, 134.0, 133.6, 130.9, 129.4, 129.0, 128.9, 124.4, 123.0. MS (CI): m/z = 229 [M]+. IR (film): ν (cm^{-1}) = 2862, 1689, 1530, 1349. m.p. 113-115°C.[341]

18.2.2.41. Synthesis of 1-(3'-nitro-[1,1'-biphenyl]-2-yl)prop-2-yn-1-ol
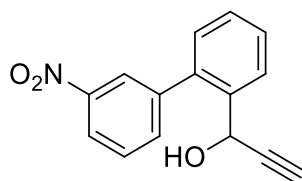
A solution of ethynylmagnesium bromide 0.5 M in THF (3 mL, 1.5 mmol) was added dropwise to a 0°C solution of 3'-nitro-[1,1'-biphenyl]-2-carbaldehyde (227 mg, 1 mmol) in THF (10 mL). Reaction mixture is then allowed to warm up to r.t. and stirred overnight. Reaction mixture was quenched with saturated aqueous solution of NH$_4$Cl and the aqueous phase was extracted with DCM. The combined organic phases were washed with H$_2$O and brine, dried over Na$_2$SO$_4$ and the solvent removed under reduced pressure. Crude product is purified by flash column chromatography (*n*-hexane/EtOAc 7:3) to afford 1-(3'-nitro-[1,1'-biphenyl]-2-yl)prop-2-yn-1-ol (225 mg, 89%) as yellow oil. ^{1}H-NMR (CDCl$_3$) δ: 8.35-8.34 (m, 1H), 8.28-8.25 (m, 1H), 7.93 (dd, 1H, J = 7.8, 0.8 Hz), 7.82-7.79 (m, 1H), 7.63 (t, 1H, J = 7.9 Hz), 7.53 (td, 1H, J = 7.7, 1.2 Hz), 7.48-7.44 (m, 1H), 7.31-7.27 (m, 1H), 5.35 (d, 1H, J = 1.6 Hz), 2.66 (d, 1H, J = 1.6 Hz), 2.29 (br s, 1H). ^{13}C-NMR (CDCl$_3$) δ: 148.1, 141.8, 138.5, 137.7, 135.6, 130.1, 129.2, 129.1, 128.8, 127.7, 124.4, 122.5, 83.7, 75.2, 61.4. MS (CI): m/z = 255 [M]+. IR (film): ν (cm^{-1}) = 3240, 2093, 1682, 1515, 1348, 1229, 1113, 980, 740.[341]

18.2.2.42. Synthesis of 1-(3'-nitro-[1,1'-biphenyl]-2-yl)prop-2-yn-1-one (2u)
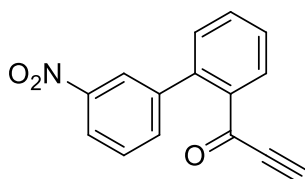
Dess-Martin periodinane (2.4 g, 5.6 mmol) was added to a solution of 1-(3'-nitro-[1,1'-biphenyl]-2-yl)prop-2-yn-1-ol (1.4 g, 5.6 mmol) in DCM (65 mL) and the mixture was stirred for 1 h at r.t.. Then Et_2O and aqueous NaOH 1M were added and the mixture was stirred for 0.5 h. Aqueous phase was extracted with Et_2O and the reunited organic phases were washed with H_2O, dried over Na_2SO_4 and the solvent removed under reduced pressure to afford 1-(3'-nitro-[1,1'-biphenyl]-2-yl)prop-2-yn-1-one (1.4 g, quantitative yield) as a brown solid without any further purification. ^{1}H-NMR (CDCl$_3$) δ: 8.26 (dt, 1H, J = 7.9, 1.8 Hz), 8.23-8.19 (m, 2H), 7.68 (td, 1H, J = 7.5, 1.3 Hz), 7.63-7.55 (m, 3H), 7.38 (d, 1H, J = 7.6 Hz), 3.28 (s, 1H). ^{13}C-NMR (CDCl$_3$) δ: 178.1, 148.1, 142.3, 140.5, 135.6, 135.2, 133.2, 132.2, 131.4, 129.0, 128.6, 123.8, 122.5, 81.3. MS (CI): m/z = 253 [M]+. IR (film): ν (cm^{-1}) = 3256, 2089, 1645, 1520, 1345, 1229, 994, 725.[341]

18.2.2.43. Synthesis of thiazole-2-carbaldehyde
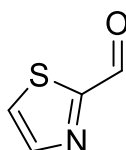
To a -78°C cooled solution of 2-bromothiazole (10 g, 61 mmol) in 30 mL of Et_2O, *n*-BuLi 1.6 M in hexanes is added dropwise (46 mL, 73 mmol). After adding, reaction is stirred for 0.5 h. A solution of DMF (8 mL, 109 mmol) in Et_2O (15 mL) is then added. Reaction mixture was allowed to reach -40°C and then quenched with a 0°C HCl solution 4M (50 mL). Organic phase in then washed with HCl 4M whilst aqueous phases are extracted with Et_2O. Reunited organic phases are dried with $MgSO_4$, filtered and evaporated under reduced pressure to afford thazole-2-carbaldehyde (3.84 g, 55%) as a yellow oil. ^{1}H NMR (CDCl$_3$) δ: 7.79 (d, 1 H, J = 3.2 Hz), 8.15 (d, 1 H, J = 3.2 Hz), 10.03 (s, 1 H); ^{13}C NMR (CDCl$_3$) δ: 126.3, 145.5, 165.8, 183.7. Other spectral data match the literature.[366]

### 18.2.2.44. Synthesis of 1-(thiazol-2-yl)prop-2-yn-1-ol
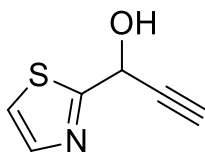
A solution of ethynylmagnesium bromide 0.5 M in THF (46 mL, 23 mmol) was added dropwise to a 0°C solution of thiazole-2-carbaldehyde (2.32 g, 20.5 mmol) in THF (100 mL). Reaction mixture is then allowed to warm up to r.t. and stirred overnight. Reaction mixture was quenched with saturated aqueous solution of

NH$_4$Cl and the aqueous phase was extracted with DCM. The combined organic phases were washed with H$_2$O and brine, dried over Na$_2$SO$_4$ and the solvent removed under reduced pressure to afford 1-(thiazol-2-yl)prop-2-yn-1-ol (2.33 g, 82%) as brown solid. ^{1}H-NMR (CDCl$_3$) δ: 7.70 (d, 1H, J = 3.2 Hz), 7.29 (d, 1H, J = 3.2 Hz), 5.72 (d, 1H, J = 1.2 Hz), 4.65 (br, 1H), 2.62 (d, 1H, J = 2 Hz) ppm. Other spectral data match the literature.[367]

18.2.2.45. Synthesis of 1-(thiazol-2-yl)prop-2-yn-1-one (2v)
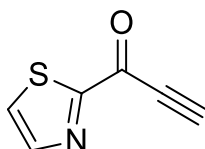
To a r.t. solution of 1-(thiazol-2-yl)prop-2-yn-1-ol (500 mg, 3.6 mmol) in DCM (20 mL), Dess-Martin periodinane is added (1.6 g, 3.7 mmol). Reaction is then stirred for 2 h. Then aqueous saturated NaHCO$_3$ and Et$_2$O were added. Aqueous phase is extracted with Et$_2$O and reunited organic phases are washed with brine, separated, dried with MgSO$_4$ and evaporated under inert atmosphere. Raw product is used immediately for next reaction due to high instability of target compound 1-(thiazol-2-yl)prop-2-yn-1-one. Other spectral data match the literature.[367]

18.2.2.46. Synthesis of 1-(4-methoxyphenyl)but-2-yn-1-ol
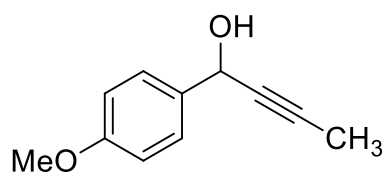
To a 0°C solution of 4-methoxybenzaldehyde (3.0 g, 22.03 mmol) in THF (90 mL), prop-1-ynylmagnesium bromide (57 mL of a 0.5 M solution in THF, 28.64 mmol) was added dropwise. After addition reaction mixture was allowed to reach r.t. and was stirred for 16 h. Solvent was removed under reduced pressure. Crude product was dissolved in DCM and washed with saturated NH$_4$Cl and brine. Reunited organic phases were dried over Na$_2$SO$_4$, filtered and evaporated under reduced pressure to afford 1-(4-methoxyphenyl)but-2-yn-1-ol (3.86 g, quantitative yield) as a pale yellow oil with no further purification. ^{1}H-NMR (CDCl$_3$) δ: 7.46 (d, 2H, J = 8.7 Hz), 6.90 (d, 2H, J = 8.7 Hz), 5.38 (s, 1H), 3.82 (s, 3H), 2.42 (d, 1H, J = 5.1 Hz), 1.91 (d, 3H, J = 2.2. Hz) ppm. GC-MS (EI): m/z: 176, 175, 161, 159, 145, 109, 67. Other spectral data match the literature.[368]

18.2.2.47. Synthesis of 1-(4-methoxyphenyl)but-2-yn-1-one (2w)
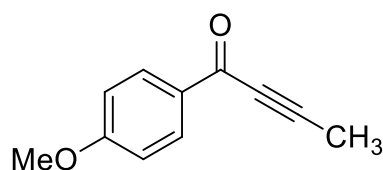
To a 0°C solution of 1-(4-methoxyphenyl)but-2-yn-1-ol (3.50 g, 20 mmol) in acetone (130 mL), Jones reagent was added dropwise to persistent orange color. Excess of Jones reagent was quenched adding isopropanol dropwise to persistent green color. Reaction mixture was filtered through Celite® and organic solution was evaporated under reduced pressure. Crude residue was dissolved in DCM and washed with saturated aqueous Na_2HCO_3 and brine. Organic phase was then dried over Na_2SO_4, filtered and the solvent removed under reduced pressure to afford 1-(4-methoxyphenyl)but-2-yn-1-one (3.01 g, 87%) as a pale yellow solid without any further purification. ^{1}H-NMR (CDCl$_3$) δ: 8.13 (d, 2H, J = 8.8 Hz), 6.96 (d, 2H, J = 8.8 Hz), 3.91 (s, 3H), 2.16 (s, 3H). Other spectral data match the literature.[369]

18.2.2.48. Synthesis of (*E*)-1-phenylpent-1-en-4-yn-3-one (2x)
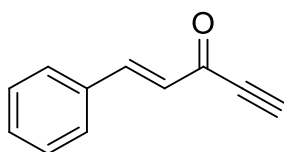
To a -40°C solution of AlCl$_3$ (267 mg, 2 mmol) in DCM (20 mL), a solution of cinnamoyl chloride (333 mg, 2 mmol) and TMSA (340 µL, 2.4 mmol) in DCM (30 mL) were added dropwise in 0.5 h. Reaction mixture was stirred at −40 °C for 1 h, then temperature was increased to −10 °C and stirred for extra 4 h. Then ice was added to reaction mixture. Reaction mixture was washed with aqueous 10% HCl and aqueous saturated NaHCO$_3$. Organic phase was dried over Na$_2$SO$_4$, filtered and solvents removed under reduced pressure. Crude product was purified by gravimetric column chromatography (petroleum ether/EtOAc 9:1) to afford (E)-1-phenylpent-1-en-4-yn-3-one (162 mg, 52%) as yellow solid. ^{1}H-NMR (CDCl$_3$) δ: 7.89 (d, *J* = 16.0 Hz, 1H), 7.65-7.53 (m, 2H), 7.51-7.36 (m, 3H), 6.81 (d, J=16.0 Hz, 1H), 3.33 ppm (s, 1H). ^{13}C-NMR (CDCl$_3$) δ: 177.6, 149.7, 133.9, 131.4, 129.1, 128.8, 128.0, 80.0, 79.3 ppm. Other spectral data match the literature.[334,370]

18.2.2.49. Synthesis of 1-(1*H*-benzotriazol-1-yl)prop-2-yn-1-one (2y)
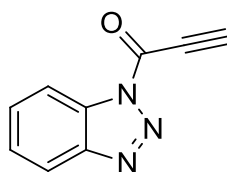
Thionyl chloride (3.6 g, 30 mmol) was added to a r.t solution in DCM (150 mL) of 1H-benzotriazole (14.4 g, 120 mmol). After 0.5 h, propiolic acid (2.1 g, 30 mmol) was added and reaction stirred overnight. Reaction mixture was filtered and precipitate was washed with DCM. The solution obtained was washed with NaOH 2M, dried with MgSO$_4$, filtered and then solvent removed under reduced pressure. Crude product was then purified by gravimetric column chromatography (toluene/DCM 7:3) to afford 1-(1*H*-benzotriazol-1-yl)prop-2-yn-1-one (2.57 g, 50%) as grey solid. ^{1}H-NMR δ: 8.24 (d, *J* = 8.2 Hz, 1 H), 8.16 (d, *J* = 8.4 Hz, 1 H), 7.74–7.68 (m, 1 H), 7.56 (td, *J* = 8.2, 1.0 Hz, 1 H), 3.72 (s, 1 H). ^{13}C-NMR δ: 149.2, 146.2, 130.9,130.6, 126.9, 120.5, 114.1, 83.9, 74.5. Other spectral data match the literature.[109,334]

18.2.2.50. Synthesis of *N*-phenylpropiolamide (2z)
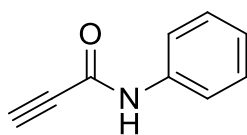
A solution of *n*-BuLi 2.5 M in hexane (1.44 mL, 10.2 mmol) was added dropwise to a 0°C solution of TMSA (1.4 mL, 10.2 mmol) in THF (100 mL). The reaction mixture was stirred at 0°C for 1 h, then phenyl isocyanate (1.1 mL, 10.2 mmol) was added dropwise and reaction stirred overnight. Then a saturated aqueous solution of NH_4Cl was added and the water phase extracted with DCM. Reunited organic phases were dried over Na_2SO_4 and the solvent removed under reduced pressure. Crude product was dissolved in THF (100 ml) at 0°C and TBAF (2.6 g, 10.2 mmol) was added. The reaction mixture was stirred at 0°C for 5 h, then quenched with H_2O. The water phase was then extracted with Et_2O. Reunited organic phases were dried over Na_2SO_4 and the solvent removed under reduced pressure. Crude product was purified by flash column chromatography (*n*-hexane/EtOAc 7:3) afforded *N*-phenylpropiolamide (845 mg, 57%) as a brown oil. ^{1}H-NMR (CDCl$_3$) δ: 8.01 (br s, 1H), 7.54 (d, 2H, *J* = 8 Hz), 7.32 (2H, t, *J* = 8 Hz), 7.14 (1H, t, *J* = 8 Hz), 2.92 (s, 1H). Other spectral data match the literature.[110,334]

18.2.2.51. Synthesis of *N*-(2-iodophenyl)propiolamide (2α)
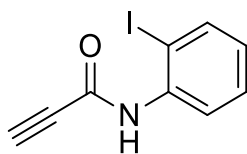
A solution of *n*-BuLi 2.5 M in hexane (1.6 mL, 4 mmol) was added dropwise at 0°C to a solution of TMSA (575 µL, 4 mmol) in THF (40 mL). The mixture was stirred at 0°C for 1h, then 2-iodophenylisocyanate (529 µl, 4 mmol) was added and the solution stirred at 0°C for 4 h. Reaction mixture was quenched adding saturated aqueous solution NH_4Cl and the water phase was extracted with DCM. The reunited organic phases were dried over Na_2SO_4 and the solvent removed under reduced pressure. The crude material was dissolved in THF, cooled at 0°C, TBAF was added (1 g, 4 mmol) and reaction was stirred for 2 h. The solvent was removed under reduced pressure and crude product was purified by flash column chromatography (DCM) to afford *N*-(2-iodophenyl)propiolamide (650 mg, 60%) as a yellow solid. ^{1}H-NMR (CDCl$_3$) δ: 8.19 (d, 1H, *J* = 8.1 Hz), 7.80 (d, 1H, *J* = 7.6 Hz), 7.27 (br s, 1H), 7.36 (td, 1H, *J* = 8.6, 1.1 Hz), 6.88 (t, 1H, *J* = 7.4 Hz), 3.01 (s, 1H). Other spectral data match the literature.[341,371]

18.2.2.52. Synthesis of 2,4,6-tri(pyridin-3-yl)-1,3,5,2,4,6-trioxatriborinane
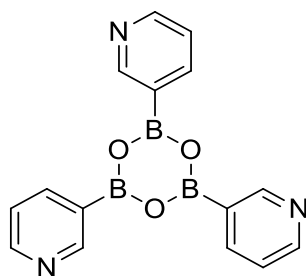
To a -40°C solution of toluene (320 ml), THF (80 mL), triisopropyl borate (55.4 mL, 240 mmol) and 3-bromopyridine (19.3 mL, 200 mmol), a *n*-BuLi solution 2.5M in hexanes (96 mL, 240 mmol) was added dropwise over 1 h. The reaction mixture was stirred for an additional 30 minutes at -40°C, then warmed to -r.t. and aqueous HCl 2M (200 mL, 400 mmol) was added. Aqueous layer was separated and the an aqueous NaOH 5M was added dropwise up to pH 7.6-7.7 (precipitation of a white solid was observed around pH 7). The mixture was then extracted with THF. Combined organic phases were dried over Na_2SO_4 and the solvent removed under reduced pressure. The solid residue was recrystallized from MeCN to afford 2,4,6-tri(pyridin-3-yl)-1,3,5,2,4,6-trioxatriborinane (17.6 g, 28%) as a pale yellow solid. ^{1}H-NMR (CD_3OD) δ: 8.61 (s, 3H); 8.54 (dd, 3H, *J* = 5.4, 1.6 Hz); 8.33 (d, 3H, *J* = 7.5 Hz); 7.6 (t, 3H, *J* = 6 Hz). Other spectral data match the literature.[372]

18.2.2.53. Synthesis of 2-(pyridin-3-yl)aniline
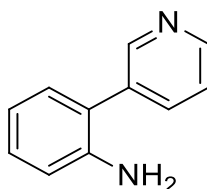
A solution of 2,4,6-tri(pyridin-3-yl)-1,3,5,2,4,6-trioxatriborinane (4.8 g, 15.2 mmol), *2*-bromoaniline (8 g, 50 mmol) and Pd(PPh$_3$)Cl$_2$ (1.4 g, 2 mmol) in 1,4-dioxane (100ml) was stirred at r.t for 0.5 h. Then aqueous Na$_2$CO$_3$ 1M was added and the reaction mixture was heated to reflux overnight. Solvent was then removed under reduced pressure. EtOAc was added and organic phase with aqueous HCl 0.1 M. The aqueous phase was neutralized with aqueous NaOH 0.1 M, then extracted with EtOAc. Reunited organic phase was dried over MgSO$_4$, filtered and the solvent removed under reduced pressure. Crude product was purified by gravimetric column chromatography (EtOAc/*n*-hexane 4:1) to afford 2-(3-pyridyl)aniline (7.1 g, 83%) as a violet oil. ^{1}H-NMR (CDCl$_3$) δ: 8.69 (s, 1H), 8.56 (d, *J* = 2.68 Hz, 1H), 7.78 (d, *J* = 7.52 Hz, 1H), 7.34 (t, *J* = 6.56 Hz, 1H), 7.17 (t, *J* = 7.36 Hz, 1H), 7.07 (d, *J* = 7.20 Hz, 1H), 6.83 (t, *J* = 7.24 Hz, 1H), 6.76 (d, *J* = 7.84 Hz, 1H), 3.72 (s, 2H). Other spectral data match the literature.[111]

18.2.2.54. Synthesis of (*E*)-3-(1H-indol-3-yl)acrylaldehyde
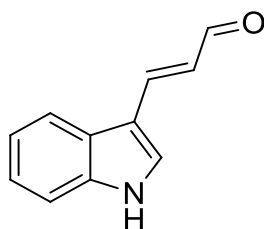
To a 40°C solution of 2-(pyridin-3-yl)aniline (5 g, 29 mmol) in EtOH (275 mL) , a solution of BrCN (6.2 g, 59 mmol) in EtOH (30 mL) was added. After 0.5 h, aqueous 10% NH_4Cl (100 mL) was added and the mixture stirred at 40°C for 3 extra h. The reaction was concentrated under reduced pressure to around 30 mL: residue was taken up in EtOAc (70 mL), washed with an aqueous saturated $NaHCO_3$, dried over Na_2SO_4 and the solvent removed under reduced pressure. Crude product is purified by flash column chromatography (petroleum ethere/EtOAc 6:4) to afford (*E*)-3-(1H-indol-3-yl)acrylaldehyde (1.5 g, 30%) as a brown oil. ^{1}H-NMR (CDCl$_3$) δ: 9.66 (d, 1H, *J* = 7.9 Hz), 8.89 (br s, 1H), 7.91 (d, 1H, *J* = 7.1 Hz), 7.72 (d, 1H, *J* = 15.8 Hz), 7.61 (d, 1H, *J* = 2.8 Hz), 7.47 (dd, 1H, *J* = 7.1, 1.6 Hz), 7.34-7.30 (m, 2H), 6.80 (dd, 1H, *J* = 15.8, 7.9 Hz). Other spectral data match the literature.[111]

18.2.2.55. Synthesis of (*E*)-3-(1-tosyl-1H-indol-3-yl)acrylaldehyde
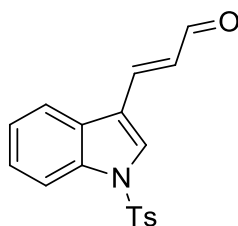
To a r.t. solution of (*E*)-3-(1H-indol-3-yl)acrylaldehyde (1.5 g, 8.6 mmol) in DCM (80 mL), DMAP (105 mg, 0.86 mmol), Et$_3$N (1.9 ml, 13.8 mmol) and 4-toluenesulfonyl chloride (1.6 g, 8.6 mmol) were added. Reaction mixture was stirred for 2 h. at rt. Reaction mixture was then washed with water and brine, dried over Na_2SO_4 and the solvent removed under reduced pressure to afford (*E*)-3-(1-tosyl-1H-indol-3-yl)acrylaldehyde (2.6 g, 91%) as brown solid without any further purification. ^{1}H-NMR (CDCl$_3$) δ: 9.68 (d, 1H, *J* = 7.6 Hz), 8.02 (d, 1H, *J* = 8.2 Hz), 7.95 (s, 1H), 7.84-7.80 (m, 3H), 7.59 (d, 1H, *J* = 16.1 Hz), 7.42 (td, 1H, *J* = 7.7, 1.2Hz), 7.36 (td, 1H, *J* = 7.6, 1.2 Hz), 7.28 (d, 2H, *J* = 7.5 Hz), 6.81 (dd, 1H, *J* = 16.1, 7.6 Hz), 2.37 (s, 3H). Other spectral data match with literature.[373]

18.2.2.56. Synthesis of (*E*)-1-(1-tosyl-1H-indol-3-yl)pent-1-en-4-yn-3-ol
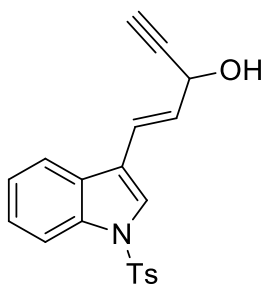
A solution of ethynylmagnesium bromide 0.5 M in THF (11 mL, 5.5 mmol) was added dropwise to a 0°C solution of (*E*)-3-(1-tosyl-1H-indol-3-yl)acrylaldehyde (1.00 g, 4.67 mmol) in THF (50 mL). Reaction mixture is then allowed to warm up to r.t. and stirred overnight. Reaction mixture was quenched with saturated aqueous solution of NH_4Cl and the aqueous phase was extracted with DCM. The combined organic phases were washed with H_2O and brine, dried over Na_2SO_4 and the solvent removed under reduced pressure to afford (*E*)-1-(1-tosyl-1H-indol-3-yl)pent-1-en-4-yn-3-ol (1.6 g, quantitative yield) without any further purification. ^{1}H-NMR (CDCl$_3$) δ: 8.00 (d, 1H, *J* = 8.2 Hz), 7.78-7.74 (m, 3H), 7.65 (s, 1H), 7.36 (t, 1H, *J* = 7.6 Hz), 7.29 (t, 1H, *J* = 7.1 Hz), 7.23 (d, 2H, *J* = 8.4 Hz), 6.89 (dd, 1H, *J* = 16.0, 0.6 Hz), 6.40 (dd, 1H, *J* = 16.0, 5.9 Hz), 5.10 (d, 1H, *J* = 0.8 Hz), 2.67 (d, 1H, *J* = 2.2 Hz), 2.35 (s, 3H), 2.09 (br s, 1H). ^{13}C-NMR (CDCl$_3$) δ: 145.2, 135.5, 134.9, 129.9, 128.8, 128.7, 126.8, 125.1, 124.9, 123.6, 122.8, 120.4, 119.3, 113.8, 82.5, 74.7, 62.8, 21.5. MS (CI): *m/z* = 352 [M]+. IR (film): ν (cm^{-1}) = 3291, 3056, 2924, 1598, 1447, 1368, 1265, 1173, 745, 665.[341]

18.2.2.57. Synthesis of (*E*)-1-(1-tosyl-1H-indol-3-yl)pent-1-en-4-yn-3-one (2β)
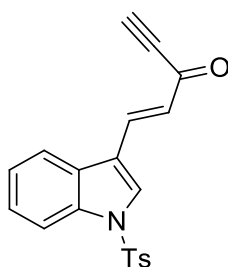
To a r.t. solution of (*E*)-1-(1-tosyl-1H-indol-3-yl)pent-1-en-4-yn-3-ol (363 mg, 1 mmol) in DCM (10 mL), Dess-Martin periodinane (424 mg, 1 mmol) was added and the mixture was stirred for 1 h. Et$_2$O (20 mL) and aqueous NaOH 1M (40 mL) were added and the mixture was stirred for 0.5 h. Aqueous phase was extracted with Et$_2$O and the reunited organic phases were washed with water, dried over MgSO$_4$ and the solvent removed under reduced pressure. Crude product was recrystallized from *n*-hexane/EtOAc 1:1 to afford (*E*)-1-(1-tosyl-1H-indol-3-yl)pent-1-en-4-yn-3-one (263 mg, 75%) as a brown solid. ^{1}H-NMR (DMSO-*d$_6$*) δ: 8.67 (s, 1H), 8.08 (d, 1H, *J* = 16.3 Hz), 7.98 (d, 2H, *J* = 8.7 Hz), 7.94 (d, 2H, *J* = 8.7 Hz), 7.44 (dt, 1H, *J* = 7.3, 1.0 Hz), 7.42 (d, 2H, *J* = 8.7 Hz), 7.37 (dt, 1H, *J* = 7.3, 1.0 Hz), 7.01 (d, 1H, *J* = 16.3 Hz), 4.90 (s, 1H), 2.32 (s, 3H). ^{13}C-NMR (CDCl$_3$) δ: 177.5, 145.8, 140.8, 135.7, 134.6, 130.2, 128.0, 127.6, 127.1,

125.9, 124.4, 120.8, 117.8, 113.9, 79.8, 79.5, 29.7, 21.6. MS (CI): m/z = 350 [M]+. IR (film): ν (cm^{-1}) = 2098, 1625, 1172. m.p.: degradation > 170°C.[341]

18.2.2.58. Synthesis of 3-bromo-1-phenylprop-2-yn-1-one (2γ)
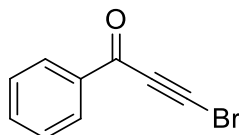
To a shielded from light solution of 1-phenylprop-2-yn-1-one (2.5 g, 19.21 mmol) in acetone (50 mL), AgNO$_3$ (346 mg, 2 mmol) and NBS (3.78 g, 21.24 mmol) were added. Reaction mixture was then r.t. stirred overnight. Mixture was filtered through Celite® and organic solution was evaporated under reduced pressure. Crude product was purified by gravimetric column chromatography (n-hexane/DCM 1:1) to afford 3-bromo-1-phe-nylprop-2-yn-1-one (3.68 g, 92%) as pale yellow solid. ^{1}H-NMR (CDCl$_3$) δ: 8.06 (d, 2H; J = 7.2 Hz), 7.58 (t, J = 7.2 Hz, 1H), 7.44 (t, J = 7.6 Hz, 2H) ppm. Other spectral data match the literature.[374]

♦ ♦ ♦ ♦ ♦ ♦

18.2.3. Synthesis of 3-aroylindoles and *N*-hydroxy-3-aroylindoles

18.2.3.1. Synthesis of 3-benzoyl-1-hydroxy-5-nitro-1*H*-indole (4)
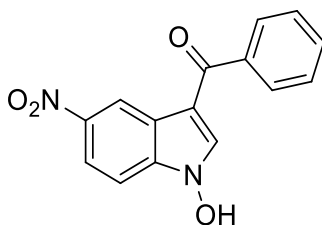
A 80°C solution of 4-nitro-nitrosobenzene (500 mg, 3.29 mmol) and 1-phenyl-2-propyn-1-one (428 mg, 3.29 mmol) in toluene (30 mL) was stirred for 5.5 h. Precipitation of the desired product was observed during the reaction. After cooling to r.t, 3-benzoyl-1-hydroxy-5-nitro-1*H*-indole was isolated by filtration (490 mg of a yellow solid, yield = 54%) as a yellow solid without any further purification. ^{1}H-NMR (DMSO-d_6) δ: 12.67 (s, 1H), 9.16 (d, 1H, J = 2.3 Hz), 8.34 (s, 1H), 8.22 (dd, 1H, J_1 = 9 Hz, J_2 = 2.3 Hz), 7.85 (d, 2H, J = 7.5 Hz), 7.75 (d, 1H, J = 9 Hz), 7.67 (t, 1H, J = 8 Hz), 7.58 (t, 2H, J = 8 Hz) ppm. ^{13}C-NMR (DMSO-d_6) δ: 189.0, 143.3, 139.4, 136.7, 136.5, 131.9, 128.7, 128.6, 122.1, 118.9, 118.3, 111.0, 110.4 ppm. FT-IR (KBr disk): 1619, 1560, 1518, 1336, 850, 817, 740, 700 cm^{-1}. m.p.: 239.5°C. MS (CI): m/z: 283 [M+1]. Elemental Analysis for C$_{15}$H$_{10}$N$_2$O$_4$: calcd. (%) C 63.83, H 3.57, N 9.93; found (%) C 63.92, H 3.68, N 9.87.[334,335]

18.2.3.2. Synthesis of 3-(2-chlorobenzoyl)-1-hydroxy-5-nitro-1*H*-indole (5)
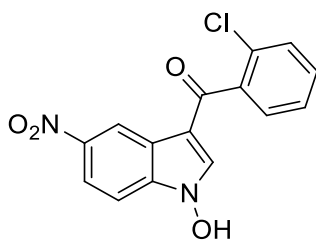
A 80°C solution of 4-nitro-nitrosobenzene (100 mg, 0.66 mmol) and 1-(2-chlorophenyl)-2-propyn-1-one (108 mg, 0.66 mmol) in toluene (10 mL) was stirred for 4.5 h. Precipitation of the desired product was observed during the reaction. After cooling to r.t., 3-(2-chlorobenzoyl)-1-hydroxy-5-nitro-1*H*-indole was isolated by filtration (146 mg, 70%) as pale yellow solid without any further purification. ^{1}H-NMR (DMSO-d_6) δ: 12.75 (s, 1H), 9.03 (d, 1H, J = 1.6 Hz), 8.23 (dd, 1H, J_1 = 9 Hz, J_2 = 1.6 Hz), 8.14 (s, 1H), 7.75 (d, 1H, J = 9 Hz), 7.63 - 7.57 (m, 3H), 7.5 (t, 1H, J = 7.1 Hz) ppm. ^{13}C-NMR (DMSO-d_6) δ: 187.7, 139.6, 139.2, 137.7, 137.2, 131.4, 130.0, 129.6, 128.9, 127.4, 121.3, 119.1, 117.8, 112.1, 110.6 ppm. FT-IR (KBr disk): 1620, 1581, 1518, 1338, 763, 746 cm^{-1}. m.p.: decomposition from 207°C. MS (CI): *m/z*: 319/317 [M+1 (^{37}Cl/^{35}Cl)]. Elemental Analysis for $C_{15}H_9ClN_2O_4$: calcd. (%) C 56.89, H 2.86, N 8.85; found (%) C 56.95, H 2.91, N 8.97.[334]

18.2.3.3. Synthesis of 3-(2-bromobenzoyl)-1-hydroxy-5-nitro-1*H*-indole (6)

A 80°C solution of 4-nitro-nitrosobenzene (100 mg, 0.66 mmol) and 1-(2-bromophenyl)-2-propyn-1-one (138 mg, 0.66 mmol) in toluene (10 mL) was stirred for 4.5 h. Precipitation of the desired product was observed during the reaction. After cooling to r.t., 3-(2-bromobenzoyl)-1-hydroxy-5-nitro-1*H*-indole was isolated by filtration (124 mg, 52%) as a pale yellow solid without any further purification. ^{1}H-NMR (DMSO-d_6) δ: 12.73 (s, 1H), 9.02 (d, 1H, J = 2.1 Hz), 8.24 (dd, 1H, J_1 = 9 Hz, J_2 = 2.1 Hz), 8.13 (s, 1H), 7.77 (d, 2H, J = 7.6 Hz), 7.75 (d, 1H, J = 9 Hz), 7.55-7.31 (m, 2H) ppm. ^{13}C-NMR (DMSO-d_6) δ: 188.5, 143.6, 141.2, 137.7, 136.9, 133.5, 131.5, 128.8, 127.8, 121.3, 119.1, 118.5, 117.8, 111.7, 110.6 ppm. FT-IR (KBr disk): 1602, 1583, 1518, 1338, 761, 744 cm^{-1}. MS (CI): *m/z*: 362 [M+1]. Elemental Analysis for $C_{15}H_9BrN_2O_4$: calcd. (%) C 49.89, H 2.51, N, 7.76; found (%) C 50.01, H 2.63, N 7.84.[334]

18.2.3.4. Synthesis of 3-(2-iodobenzoyl)-1-hydroxy-5-nitro-1*H*-indole (7)

A 80°C solution of 4-nitro-nitrosobenzene (435 mg, 2.87 mmol) and 1-(2-iodophenyl)-2-propyn-1-one (1.10 g,4.3 mmol) in toluene (35 mL) was stirred for 2.5 h. After cooling to r.t., solvent was removed under reduced pressure. Crude product was purified by gravimetric column chromatography (petroleum ether/EtOAc 1:1) to afford 1-hydroxy-3-(2-iodobenzoyl)-5-nitro-1*H*-indole (382 mg, 37%) as a yellow solid. ^{1}H-NMR (DMSO-d_6) δ: 12.71 (s, 1H), 9.03 (d, 1H, J = 2.0 Hz), 8.18 (dd, 1H, ^3J = 9.0 Hz, ^4J = 2.0 Hz), 7.99 (d, 1H, J = 7.5 Hz), 7.92 (s, 1H), 7.73 (d, 1H, J = 9.0 Hz), 7.56 (t, 1H, J = 7.5 Hz), 7.50 (d, 1H, J = 7.5 Hz), 7.30 (t, 1H, J = 7.5 Hz) ppm. ^{13}C-NMR (DMSO-d_6) δ: 192.1, 146.1, 143.9, 141.2, 140.1, 132.0, 129.0, 128.8, 125.5, 119.6, 118.4, 117.3, 114.3, 93.8, 87.2 ppm. MS (CI): *m/z:* 408 [*M*+1]. FT-IR (KBr disk): 1632, 1589, 1519, 1383, 1336, 745 cm^{-1}.[334]

18.2.3.5. Synthesis of 3-(2-nitrobenzoyl)-1-hydroxy-5-nitro-1*H*-indole (8)
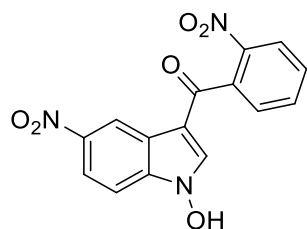
A 80° solution of 1-(2-nitrophenyl)prop-2-yn-1-one (175 mg, 1 mmol) and 4-nitro-nitroso-benzene (152 mg, 1 mmol) was stirred in toluene (10 mL) for 5 h. Reaction mixture was then dried under reduced pressure. Crude product was purified by flash column chromatography (toluene/EtOAc 5:5) and subsequent recrystallization from EtOAc/*n*-hexane 1:1 to afford 3-(2-nitrobenzoyl)-1-hydroxy-5-nitro-1*H*-indole (157 mg, 48%) as a brown solid. ^{1}H NMR (DMSO-d$_6$) δ: 9.02 (d, 1H, J = 2.3 Hz); 8.22 (dd, 1H, J = 8.2, 1.0 Hz); 8.18 (dd, 1H, J = 9.0; 2.3 Hz); 8.07 (s, 1H); 7.91 (td, 1H, J = 7.5, 1.2 Hz); 7.82 (td, 1H, J = 7.9, 1.5 Hz); 7.76 (dd, 1H, J = 7.4, 1.4 Hz); 7.72 (d, 1H, J = 9.0 Hz). ^{13}C-NMR (DMSO-d$_6$) δ: 187.6, 147.2, 143.5, 140.6, 140.0, 136.2, 134.8, 131.6, 129.7, 125.3, 125.2, 119.3, 117.9, 117.3, 113.9. MS (CI): *m/z* = 312 [M]+. IR (film): ν (cm^{-1}) = 2725; 1616; 1526; 1461; 1377; 1112; 722. m.p.: 206°C.[334]
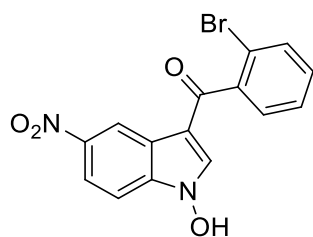
18.2.3.6. Synthesis of 3-(3-nitrobenzoyl)-1-hydroxy-5-nitro-1*H*-indole (9)
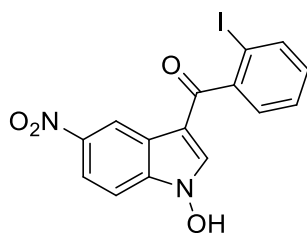

A 80°C solution of 4-nitro-nitrosobenzene (100 mg, 0.66 mmol) and 1-(3-nitrophenyl)-2-propyn-1-one (115 mg, 0.66 mmol) in toluene (10 mL) was stirred C for 8 h. Precipitation of the desired product was observed during the reaction. After cooling to r.t., 3-(3-nitrobenzoyl)-1-hydroxy-5-nitro-1*H*-indole was isolated by filtration (149 mg, 69%) as a yellow solid without any further purification. ^{1}H-NMR (DMSO-d_6) δ: 12.83 (br, 1H), 9.14 (s, 1H), 8.62 (s, 1H), 8.54 (s, 1H), 8.47 (d, 1H, *J* = 8.1 Hz), 8.27 -8.25 (m, 2H), 7.87 (t, 1H, *J* = 7.8 Hz), 7.78 (d, 1H, *J* = 9 Hz) ppm. ^{13}C-NMR (DMSO-d_6) δ: 186.9, 147.9, 143.6, 113.3, 137.6, 136.8, 134.8, 130.6, 126.2, 123.4, 122.1, 119.2, 118.2, 110.7, 110.5 ppm. FT-IR (KBr disk): 1620, 1589, 1568, 1533, 1338, 714 cm^{-1}. m.p.: decomposition from 263°C. MS (CI): *m/z*: 328 [M+1]. Elemental Analysis for $C_{15}H_9N_3O_6$: calcd. (%) C 55.05, H 2.77, N 12.84; found (%) C 55.01, H 2.82, N 12.69.[334]

### 18.2.3.7. Synthesis of 3-(4-nitrobenzoyl)-1-hydroxy-5-nitro-1*H*-indole (10)
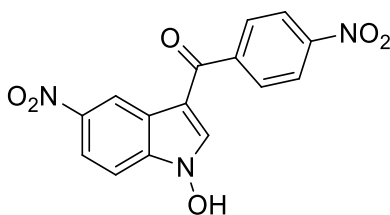
A 80°C solution of 4-nitro-nitrosobenzene (100 mg, 0.66 mmol) and 1-(4-nitrophenyl)-2-propyn-1-one (115 mg, 0.66 mmol) in toluene (10 mL) was stirred at 80 °C for 7 h. Precipitation of the desired product was observed during the reaction. After cooling to r.t, 1-hydroxy-5-nitro-3-(4-nitrobenzoyl)-1*H*-indole was isolated by filtration (134 mg, 62%) as a brown solid without any further purification. ^{1}H-NMR (DMSO-d_6) δ: 12.73 (br, 1H), 9.15 (d, 1H, *J* = 2.2 Hz), 8.46 (s, 1H), 8.37 (dd, 2H, , J_1 = 8.7 Hz, J_2 = 1.9 Hz), 8.23 (dd, 1H, , J_1 = 9 Hz, J_2 = 2.2 Hz), 8.05 (dd, 2H, , J_1 = 8.7 Hz, J_2 = 1.9 Hz), 7.76 (d, 1H, 9 Hz) ppm. ^{13}C-NMR (DMSO-d_6) δ: 187.5, 149.1, 145.5, 143.5, 137.4, 136.7, 129.8, 123.8, 122.0, 119.2, 118.1, 110.8, 110.5 ppm. FT-IR (KBr disk): 1618, 1597, 1521, 1346, 837 cm^{-1}. m.p.: decomposition from 247°C. MS (CI): *m/z*: 328 [M+1], 301. Elemental Analysis for $C_{15}H_9N_3O_6$: calcd. (%) C 55.05, H 2.77, N 12.84; found (%) C 55.09, H 2.68, N 12.99.[334]

18.2.3.8. Synthesis of 3-(4-methoxybenzoyl)-1-hydroxy-5-nitro-1*H*-indole (11)
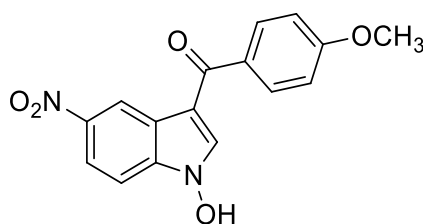
A 80°C solution of 4-nitro-nitrosobenzene (100 mg, 0.66 mmol) and 1-(4-methoxyphenyl)-2-propyn-1-one (106 mg, 0.66 mmol) in toluene (25 mL) was stirred 2.5 h. Precipitation of the desired product was observed during the reaction. After cooling to r.t., 1-hydroxy-3-(4-methoxybenzoyl)-5-nitro-1*H*-indole was isolated by filtration (77 mg, 37%) without any further purification. ^{1}H-NMR (DMSO-d_6) δ: 12.6 (s, 1H), 9.14 (s, 1H), 8.39 (s, 1H), 8.21 (d, 1H, J = 9 Hz), 7.87 (d, 2H, J = 8.4 Hz), 7.73 (d, 1H, J = 9 Hz), 7.11 (d, 2H, J = 8.4 Hz), 3.88 (s, 3H) ppm. ^{13}C-NMR (DMSO-d_6) δ: 188.5, 163.2, 144.0, 137.2, 136.8, 132.5, 131.8, 123.1, 119.6, 119.2, 114.8, 112.0, 111.0, 56.4 ppm. FT-IR (KBr disk): 1604, 1572, 1521, 1473, 1367, 1331, 1176, 841 cm^{-1}. m.p.: decomposition from 223°C. MS (CI): *m/z*: 313 [M+1]. Elemental Analysis for $C_{16}H_{12}N_2O_5$: calcd. (%) C 61.54, H, 3.87, N 8.97; found (%) C 61.46, H 3.92, N 9.01.[334]
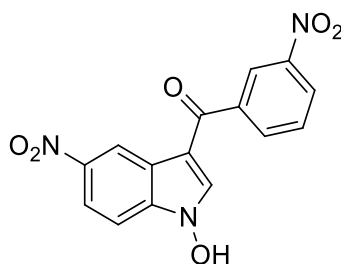
18.2.3.9. Synthesis of 3-(4-formylbenzoyl)-1-hydroxy-5-nitro-1*H*-indole (12)
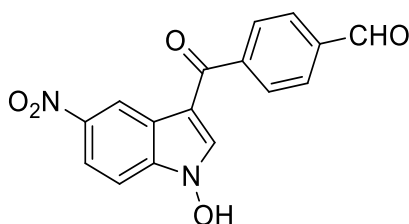
A 80°C solution of 4-nitro-nitrosobenzene (100 mg, 0.66 mmol) and 1-(4-formylphenyl)prop-2-yn-1-one (106 mg, 0.66 mmol) in toluene (10 mL) was stirred for 2.5 h. Precipitation of the desired product was observed during the reaction. After cooling to r.t., 3-(4-formylbenzoyl)-1-hydroxy-5-nitro-1*H*-indole was isolated by filtration (64.5 mg, 31%) as brown solid without any further purification. ^{1}H-NMR (DMSO-d_6) δ: 12.73 (s, 1H), 10.15 (s, 1H), 9.15 (d, 1H, J = 1 Hz) 8.34 (s, 1H), 8.23 (td, 1H, J_1 = 9.2 Hz, J_2 = 1 Hz), 8.08 (d, 2H, J = 8 Hz), 8.02 (d, 2H J = 8 Hz), 7.76 (d, 1H, J = 9.2 Hz) ppm. ^{13}C-NMR (DMSO-d_6) δ: 193.6, 188.8, 144.4, 143.9, 138.4, 137.7, 137.0, 130.2, 129.6, 122.4, 119.5, 118.6, 111.3, 110.9 ppm. FT-IR (ATR): 3118, 1705, 1626, 1582, 1516, 1448, 1365, 1335, 1208, 745 cm^{-1}. m.p.: decomposition from 193°C. MS (CI): *m/z*: 311 [M+1]. Elemental Analysis for $C_{16}H_{10}N_2O_5$: calcd. (%) C 61.94, H 3.25, N 9.03; found (%) C 61.87, H 3.28, N 9.52.[334]

18.2.3.10. Synthesis of 3-(benzo[d][1,3]dioxol-5-yl)-1-hydroxy-5-nitro-1*H*-indole (13)
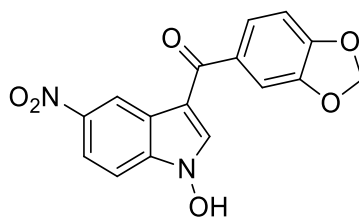
A 80°C solution of 4-nitro-nitrosobenzene (100 mg, 0.66 mmol) and 1-(benzo[d][1,3]dioxol-5-yl)prop-2-yn-1-one (115 mg, 0.66 mmol) in toluene (10 mL) was stirred for 2.5 h. Precipitation of the desired product was observed during the reaction. After cooling to r.t., 3-(benzo[d][1,3]dioxol-5-yl)-1-hydroxy-5-nitro-1*H*-indole was isolated by filtration (131 mg, 61%) as a brown solid without any further purification. ^{1}H-NMR (DMSO-d_6) δ: 12.58 (s, 1H), 9.12 (d, 1H, J = 2 Hz), 8.43 (s, 1H), 8.21 (dd, 1H, J_1 = 9.2 Hz, J_2 = 2 Hz), 7.73 (d, 1H, J = 2.4 Hz), 7.47 (d, 1H, J = 7.2 Hz), 7.38 (s, 1H), 7.08 (d, 1H, J = 8 Hz), 6.17 (s, 2H) ppm. ^{13}C-NMR (DMSO-d_6) δ: 187.2, 150.5, 147.6, 143.1, 136.2, 136.0, 133.4, 124.5, 122.1, 118.7, 118.3, 110.9, 110.1, 108.5, 108.0, 101.8 ppm. FT-IR (ATR): 3132, 2553, 1519, 1334, 1254, 1090, 768, 744 cm^{-1}. m.p.: decomposition from 244°C. MS (CI): m/z: 327 [M+1]. Elemental Analysis for $C_{16}H_{10}N_2O_6$: calcd. (%) C 58.90, H 3.09, N 8.59; found (%) C 59.01, H 3.05, N 8.61.[334]

### 18.2.3.11. Synthesis of 3-(2-chlorobenzoyl)-1-hydroxy-1*H*-indole-5-carboxylic acid (14)
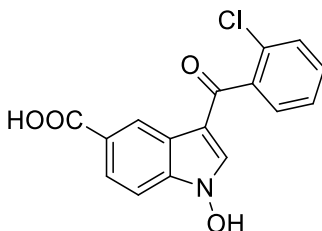
A 80°C solution of 4-nitro-nitrosobenzene (100 mg, 0.66 mmol) and 1-(benzo[d][1,3]dioxol-5-yl)prop-2-yn-1-one (115 mg, 0.66 mmol) in toluene (10 mL) was stirred for 2.5 h. Precipitation of the desired product was observed during the reaction. After cooling to r.t., 3-(benzo[d][1,3]dioxol-5-yl)-1-hydroxy-5-nitro-1*H*-indole was isolated by filtration (131 mg, 61%) as brown without any further purification. ^{1}H-NMR (DMSO-d_6) δ: 12.58 (s, 1H), 9.12 (d, 1H, J = 2 Hz), 8.43 (s, 1H), 8.21 (dd, 1H, J_1 = 9.2 Hz, J_2 = 2 Hz), 7.73 (d, 1H, J = 2.4 Hz), 7.47 (d, 1H, J = 7.2 Hz), 7.38 (s, 1H), 7.08 (d, 1H, J = 8 Hz), 6.17 (s, 2H) ppm. ^{13}C-NMR (DMSO-d_6) δ: 187.2, 150.5, 147.6, 143.1, 136.2, 136.0, 133.4, 124.5, 122.1, 118.7, 118.3, 110.9, 110.1, 108.5, 108.0, 101.8 ppm. FT-IR (ATR): 3132, 2553, 1519, 1334, 1254, 1090, 768, 744 cm^{-1}. m.p.: decomposition from 244°C. MS (CI): m/z: 327 [M+1]. Elemental Analysis for $C_{16}H_{10}N_2O_6$: calcd. (%) C 58.90, H 3.09, N 8.59; found (%) C 59.01, H 3.05, N 8.61.[334]

18.2.3.12. Synthesis of 3-(2-bromobenzoyl)-1-hydroxy-1*H*-indole-5-carboxylic acid (15)
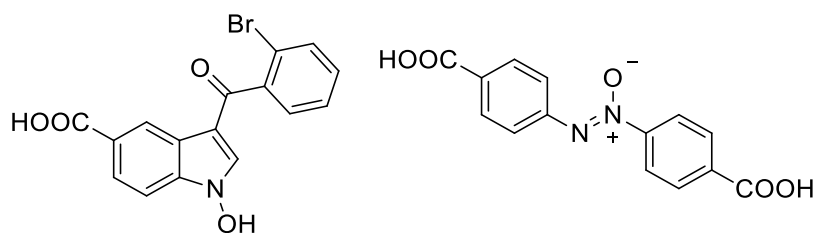
4-nitrosobenzoic acid (100 mg, 0.66 mmol) was suspended in 1,4-dioxane (10 mL). Mixture is then heated to complete solid dissolving. 1-(2-bromophenyl)-2-propyn-1-one (138 mg, 0.66 mmol) was then added and the mixture was refluxed for 7 h. During the reaction, precipitation of azoxybenzene-4,4'-dicarboxylic acid as byproduct was observed. After cooling to r.t., reaction mixture was filtered to remove solid byproduct (25 mg). Mother liquors were dried under reduced pressure. Crude product was purified by gravimetric column chromatography (DCM/MeOH 95:5) to afford 3-(2-bromobenzoyl)-1-hydroxy-1*H*-indole-5-carboxylic acid as (120 mg, 50%) as orange solid. ^{1}H-NMR (DMSO-d_6) δ: 12.36 (br, 1H), 8.81 (d, 1H, J = 1.6 Hz), 7.94 (dd, 1H, ^3J = 8.6 Hz, ^4J = 1.6 Hz), 7.86 (s, 1H), 7.73 (td, 1H, ^3J = 7.7 Hz, ^4J = 0.7 Hz), 7.60 (dd, 1H, ^3J = 8.6 Hz, ^5J = 0.7 Hz), 7.52 - 7.50 (m, 2H), 7.48 - 7.43 (m, 1H) ppm. ^{13}C-NMR (DMSO-d_6) δ: 188.6, 167.8, 141.7, 136.4, 135.9, 133.0, 131.2, 128.7, 127.8, 125.5, 124.9, 123.8, 121.8, 118.6, 111.1, 109.6 ppm. MS (CI): *m/z*: 360 [*M*+1]. FT-IR (KBr disk): 1686, 1588, 1504, 751, 687 cm^{-1}.[341]

18.2.3.13. Synthesis of 3-(3-nitrobenzoyl)-1-hydroxy-1*H*-indole-5-carboxylic acid (16)
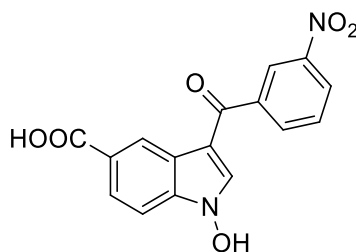
4-nitrosobenzoic acid (100 mg, 0.66 mmol) was suspended in 1,4-dioxane (10 mL). Reaction mixture was heated to complete solid dissolving. 1-(3-nitrophenyl)-2-propyn-1-one (116 mg, 0.66 mmol) was then added and the mixture was refluxed for 7 h. After cooling to r.t., 3-(3-nitrobenzoyl)-1-hydroxy-1*H*-indole-5-carbox-ylic acid was isolated by filtration (183 mg, 84%) as yellow solid without any further purification. ^{1}H-NMR (DMSO-d_6) δ: 12.40 (br, 1H), 8.96 (dd, 1H, ^4J = 1.6 Hz, ^5J = 0.6 Hz), 8.50 (t, 1H, J = 1.8 Hz), 8.47 (ddd, 1H, ^3J = 8.6 Hz, ^4J =1.6 Hz, 5J = 0.6 Hz), 8.40 (s, 1H), 8.22 (dt, 1H, ^3J =8.1 Hz, ^4J =1.8 Hz), 7.97 (dd., 1H, ^3J =8.6 Hz, ^4J =1.6 Hz), 7.85 (t, 1H, J =7.8 Hz), 7.63 (dd, 1H, ^3J = 8.6 Hz, ^5J = 0.6 Hz) ppm. ^{13}C-NMR (DMSO-d_6) δ: 186.9 (+), 167.9, 147.8, 140.9, 136.3, 136.0, 134.7, 130.5, 125.9, 125.5 (+), 125.0 (-), 124.1 (-), 123.3 (-), 122.5 (-), 109.9, 109.5 ppm. MS (CI): *m/z*: 327 [*M*+1]. FT-IR (KBr disk): 1695, 1599, 1566, 1532, 1350, 1220, 709 cm^{-1}.[341]

### 18.2.3.14. Synthesis of 3-(4-nitrobenzoyl)-1-hydroxy-1*H*-indole-5-carboxylic acid (17)
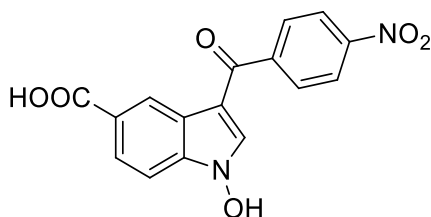
A 80°C solution of 4-nitro-nitrosobenzene (100 mg, 0.66 mmol) and 1-(4-nitrophenyl)-2-propyn-1-one (115 mg, 0.66 mmol) in toluene (10 mL) was stirred for 7 h. Precipitation of the desired product was observed during the reaction. After cooling to r.t, 1-hydroxy-5-nitro-3-(4-nitrobenzoyl)-1*H*-indole-5-carboxylic acid was isolated by filtration (144 mg, 67%) as a brown solid without any further purification. ^{1}H-NMR (DMSO-d_6) δ: 12.83 (br, 1H), 12.43 (br, 1H), 8.96 (d, 1H, J = 1.6 Hz), 8.36 (d, 2H, J = 8.8 Hz), 8.26 (s, 1H), 8.02 (d, 2H, J = 8.8 Hz), 7.96 (dd, 1H, J_1 = 8.6 Hz, J_2 = 1.6 Hz), 7.63 (d, 1H, J = 8.6 Hz) ppm. ^{13}C-NMR (DMSO-d_6) δ: 187.5, 167.8, 148.9, 145.2, 136.3, 131.1, 129.8, 125.6, 125.0, 124.1, 123.8, 122.4, 110.1, 109.5 ppm. FT-IR (KBr disk): 1697, 1591, 1517, 1345, 719 cm^{-1}. m.p.: decomposition from 293°C. MS (CI): *m/z*: 327 [M+1]. Elemental Analysis for $C_{16}H_{10}N_2O_6$: calcd. (%) C 58.90, H 3.09, N 8.59; found (%) C 59.03, H 3.02, N 8.62.[334]

18.2.3.15. Synthesis of 3-benzoyl-1*H*-indole (18)
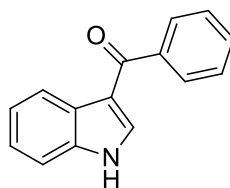
A 80°C solution of nitrosobenzene (100 mg, 0.93 mmol) and 1-phenylprop-2-yn-1-one (121 mg, 0.93 mmol) in toluene (10 mL) was stirred for 3 h. Solvent was removed under reduced pressure. Crude product was purified by gravimetric column chromatography (petroleum ether/EtOAc 7:3) to afford 3-benzoyl-1H-indole (52 mg, 25%) as an orange solid. ^{1}H-NMR (DMSO-d_6) δ: 12.06 (s, 1H), 8.26 (d, 1H, J = 7 Hz), 7.93 (d, 1H, J = 3 Hz), 7.79 (d, 2H, J = 7 Hz), 7.61 – 7.52 (m, 4H), 7.29-7.22 (m, 2H) ppm. Other spectral data match the literature.[334,375]

18.2.3.16. Synthesis of 3-benzoyl-1*H*-indole by unconventional methods

Planetary ball milling: nitrosobenzene (20 mg, 0.187 mmol) and 1-phenyl-2-propyn-1-one (24.3 mg, 0.187 mmol) were placed inside a grinding jar with 40 balls (4 mm ⌀). Reaction was conducted solventless. The grinding duration was 2 h with 450 rpm speed. Every 5 minutes rotation direction was reversed for better reaction homogeneity and to avoid excessive heating. Estimated temperature (45-55 °C) was not monitored. 12% of 3-benzoyl-1H-indole, traces of azobenzene and strong presence of the two starting reagents was detected. Data were obtained by GC-MS analysis.

Microwaves: nitrosobenzene (20 mg, 0.187 mmol) and 1-phenyl-2-propyn-1-one (24.3 mg, 0.187 mmol) were placed inside a flask and irradiated with 50W fixed power microwaves of 50W for 2 h. Reaction was conducted solventless. Followed program foresaw 5 minutes of treatment followed by 1 minute break until reaching an effective reaction time of 2 h. 62% of 3-benzoyl-1H-indole, 7% of azobenzene, 12% of nitrosobenzene and 19% of 1-phenyl-2-propyn-1-one were afforded at the end of the reaction. Data were obtained by GC-MS analysis.

18.2.3.17. Synthesis of 3-benzoyl-5-carboethoxy-1*H*-indole (19)

A 80° solution of 4-carboethoxy-nitrosobenzene (150 mg, 0.84 mmol) and 1-phenylprop-2-yn-1-one (109 mg, 0.84 mmol) in toluene (10 mL) was stirred for 6 h. Solvent was removed under reduced pressure. Crude product was purified by gravimetric column chromatography (petroleum ether/EtOAc = 55:45) to afford 3-benzoyl-5-carboethoxy-1*H*-indole (66 mg, 27%) an orange solid. ^{1}H-NMR (CDCl$_3$) δ: 8.96 (br, 1H), 8.73 (s, 1H), 8.40 (d, 1H, *J* = 1.6 Hz), 7.92 (d, 2H, *J* = 7.8 Hz), 7.85 (dd, 1H, *J* = 9.0 Hz, *J* = 1.6 Hz), 7.73 (t, 1H, *J* = 7.8 Hz), 7.67 - 7.61 (m, 3H), 4.39 (q, 2H, *J* = 7.1 Hz), 1.42 (t, 3H, *J* = 7.1 Hz) ppm. Other spectral data match the literature.[334,376]

18.2.3.18. Synthesis of 3-benzoyl-5-methyl-1*H*-indole (20)
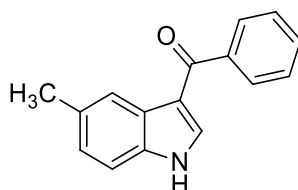
A 80°C solution of 4-nitrosotoluene (150 mg, 1.24 mmol) and 1-phenylprop-2-yn-1-one (161 mg, 1.24 mmol) in toluene (12 mL) was stirred for 6 h. Solvent was then removed under reduced pressure. Crude product was purified by gravimetric column chromatography (petroleum ether/EtOAc 55:45) to afford 3-benzoyl-5-methyl-1*H*-indole (58 mg, 20%) as a yellow solid. ^{1}H-NMR (CDCl$_3$) δ: 12.42 (br, 1H), 8.75 (d, 1H, J = 1.8 Hz), 8.2 (s, 1H), 7.87 (d, 2H, J = 8.6 Hz), 7.79 (d, 1H, J = 9 Hz), 7.75 − 7.72 (m, 2H), 7.67 (t, 2H, J = 8.6 Hz), 2.35 (s, 3H) ppm. Other spectral data match the literature.[334,377]

18.2.3.19. Synthesis of 3-benzoyl-5-methoxy-1*H*-indole (21)
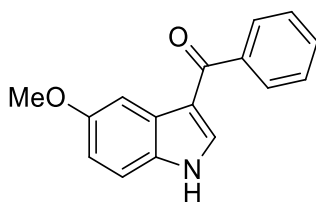
A 80°C solution of 4-methoxy-nitrosobenzene (137 mg, 1 mmol) and 1-phenylprop-2-yn-1-one (130 mg, 1 mmol) in toluene (10 mL) was stirred for 6 h. Solvent was then evaporated under reduced pressure. Crude product was purified by gravimetric column chromatography (petroleum ether/EtOAc 55:45) to afford 3-benzoyl-5-methoxy-1*H*-indole (75.3 mg, 30%) as yellow solid. 1H-NMR (DMSO-d_6) δ: 11.87 (s, 1H), 8.11 (d, *J* = 9 Hz, 1H), 7.80-7.76 (m, 3H), 7.60 (t, *J* = 7.0 Hz, 1H), 7.53 (dd, J_1 = 7, J_2 =7 Hz, 2H), 7.00 (s, 1H), 6.88 (d, *J* = 8 Hz, 1H), 3.80 (s, 3H). Other spectral data match the literature.[334,377]

18.2.3.20. Synthesis of 3-benzoyl-5-cyano-1*H*-indole (22)
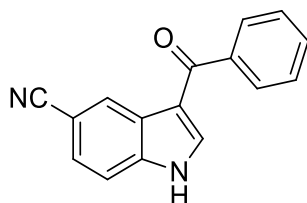
A 80°C solution of 4-cyano-nitrosobenzene (100 mg, 0.76 mmol) and 1-phenylprop-2-yn-1-one (493 mg, 3.76 mmol) in toluene (12 mL) was stirred for 2 h. Solvent was then removed under reduced pressure. Crude product was purified by gravimetric column chromatography (petroleum ether/EtOAc 6:4) to afford 3-benzoyl-5-cyano-1*H*-indole (86 mg, 41%) as brown solid. ^{1}H-NMR (DMSO-d_6) δ: 12.56 (s, 1H), 8.62 (d, 1H, *J* = 2.0 Hz), 8.20 (d, 1H, *J* = 3.0 Hz), 7.83 (dd, 2H, 3*J* = 7.6 Hz, 4*J* = 1.4 Hz), 7.72 (d, 1H, *J* = 8.5 Hz), 7.65 (dd, 1H, 3*J* = 8.5 Hz, 4*J* = 2.0 Hz), 7.57 (t, 3H, *J* = 7.6 Hz) ppm. ^{13}C-NMR (DMSO-d_6) δ: 190.7, 140.6, 139.5, 138.8, 134.3, 132.5, 130.1, 129.4, 129.3, 127.4, 127.0, 121.0, 120.2, 116.0, 114.7, 105.0 ppm. MS (CI): *m/z*: 247 [*M*+1].[341]

18.2.3.21. Synthesis of 3-benzoyl-5-chloro-1-hydroxy-1*H*-indole (23) and 3-benzoyl-5-chloro-1*H*-indole (24)
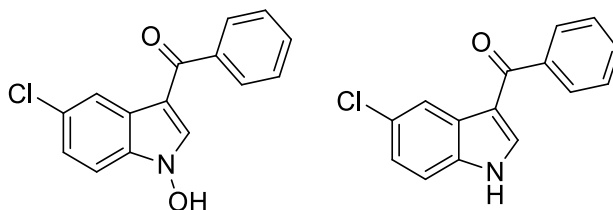
A 80°C solution of 4-chloro-nitrosobenzene (150 mg, 1.06 mmol) and 1-phenylprop-2-yn-1-one (138 mg, 1.06 mmol) in toluene (12 mL) was stirred for 4.5 hours. Solvent was removed under reduced pressure. Crude product was purified by gravimetric column chromatography (petroleum ether/EtOAc 55:45) to afford 3-benzoyl-5-chloro-1*H*-indole (92 mg, 36%) and 3-benzoyl-5-chloro-1-hydroxy-1*H*-indole (40 mg, 15%) as

yellow solids. **3-benzoyl-5-chloro-1-hydroxy-1*H*-indole:** ^{1}H-NMR (CDCl₃) δ: 11.00 (br, 1H), 8.33 (d, 1H, J = 1.9 Hz), 7.65 (dd, 1H, ^3J =9.0 Hz, ^4J = 1.9 Hz), 7.38 (d, 1H, J = 9.0 Hz), 7.33 - 7.29 (m, 2H), 7.30 (s, 1H), 7-14 - 7.10 (m, 2H) ppm. MS (CI): m/z: 274 / 272 [M+1 (^{37}Cl / ^{35}Cl)]. **3-benzoyl-5-chloro-1*H*-indole**: ^{1}H-NMR (CDCl₃) δ: 9.33 (br, 1H), 8.23 (d, 1H, J = 1.6 Hz), 7.54 (d, 1H, J = 3.0 Hz), 7.32 (dd, 1H, ^3J = 9.0 Hz, ^4J = 1.6 Hz), 7.22 - 7.19 (m, 3H), 7.14 (d, 1H, J = 9.0 Hz), 7.12 (t, 2H, J = 7.7 Hz) ppm. MS (CI): m/z: 258 / 256 [M+1 (^{37}Cl / ^{35}Cl)]. Other spectral data match the literature.[103]

18.2.3.22. Synthesis of 3-benzoyl-5-bromo-1-hydroxy-1*H*-indole (25) and 3-benzoyl-5-bromo-1*H*-indole (26)
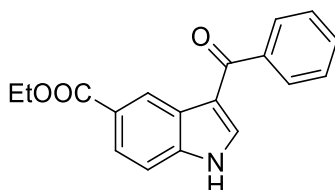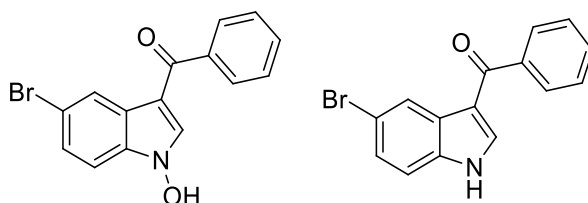

A 80°C solution of 4-bromo-nitrosobenzene (150 mg, 0.8 mmol) and 1-phenylprop-2-yn-1-one (105 mg, 0.8 mmol) in toluene (12 mL) was stirred for 4.5 h. Solvent was removed under reduced pressure. Crude material was purified by gravimetric column chromatography (petroleum ether/EtOAc 55:45). 3-benzoyl-5-bromo-1*H*-indole (82 mg, 35%) and 3-benzoyl-5- bromo-1-hydroxy-1*H*-indole (38 mg, 15%) were isolated as yellow-orange solids. **3-benzoyl-5-bromo-1-hydroxy-1*H*-indole:** ^{1}H-NMR (CDCl₃) δ: 10.46 (br, 1H), 8.59 (d, 1H, J = 1.6 Hz), 7.77 (d, 1H, J = 9.0 Hz), 7.49 (d, 2H, J = 7.7 Hz), 7.41 (s, 1H), 7.38 (d, 1H, J = 9.0 Hz), 7.21 (t, 3H, J = 7.7 Hz) ppm. MS (CI): m/z: 317 [M+1]. **3-benzoyl-5-bromo-1*H*-indole:** ^{1}H-NMR (CDCl₃) δ: 9.20 (br, 1H), 8.41 (d, 1H, J = 1.6 Hz), 7.38 - 7.34 (m, 2H), 7.29 - 7.25 (m, 3H), 7.18 - 7.15 (m, 3H) ppm. MS (CI): m/z: 301 [M+1]. Other spectral data match the literature.[377]

18.2.3.23. Synthesis of 3-benzoyl-5-trifluoromethyl-1-hydroxy-1*H*-indole (27)
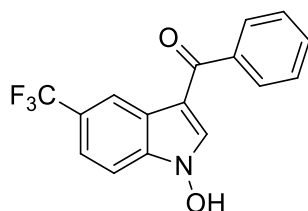
A 80°C solution of 4-(trifluoromethyl)-nitrosobenzene (200 mg, 1.14 mmol) and 1-phenylprop-2-yn-1-one (148 mg, 1.14 mmol) in toluene (15 mL) was stirred for 7 h. After cooling to r.t., 3-benzoyl-1-hydroxy-5-(trifluoromethyl)-1*H*-indole was isolated by filtration (47 mg). Extra 68 mg were isolated after purification of the dried mother liquors by gravimetric column chromatography (DCM/petroleum ether 8:2) as yellow solid (115 mg, 33%). ^{1}H-NMR (DMSO-d_6) δ: 12.46 (s, 1H), 8.59 (d, 1H, J = 1.8 Hz), 8.17 (d, 1H, J = 2.8 Hz), 7.82 (dd, 2H, ^3J = 8.3 Hz, ^4J = 1.5 Hz), 7.73 (d, 1H, J = 8.6 Hz), 7.63 (tt, 1H, ^3J = 7.5 Hz, ^4J = 1.5 Hz), 7.57 (dd, 1H, ^3J = 8.6 Hz, ^4J = 1.8 Hz), 7.56 (tt, 2H, ^3J = 7.5 Hz, ^4J = 1.5 Hz) ppm. ^{13}C-NMR (DMSO-d_6) δ: 190.0, 139.9, 138.4, 137.8, 131.5,

128.6, 128.5, 125.8, 122.7 (q, J = 31.0 Hz), 122.6 (q, J = 269.3 Hz), 119.7, 118.8 , 115.3, 113.3 ppm. MS (CI): m/z: 290 [M+1]. FT-IR (KBr disk): 1603, 1432, 1325, 1156, 1109, 722 cm^{-1}.[341]

18.2.3.24. Synthesis of 3-benzoyl-7-nitro-1-hydroxy-1H-indole (28)
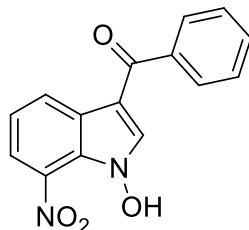
A 80°C solution of 2-nitro-nitrosobenzene (150 mg, 0.98 mmol) and 1-phenyl-2-propyn-1-one (129 mg, 0.98 mmol) in toluene (12 mL) was stirred 7 h. Solvent was then removed under reduced pressure. Crude product was purified by gravimetric column chromatography (*n*-hexane/EtOAc 8:2) to afford 3-benzoyl-1-hydroxy-7-nitro-1H-indole (128 mg, 46%) as orange solid. ^{1}H-NMR (CDCl$_3$) δ: 13.52 (s, 1H), 9.91 (s, 1H), 8.93 (d, 1H, J = 7.9 Hz), 8.28 (d, 2H, J = 8.5 Hz), 8.19 (d, 1H, J = 7.9 Hz), 7.64 (t, 1H, J = 8.5 Hz), 7.46 (t, 1H, J = 7.9 Hz), 7.12 (t, 2H, J = 8.5 Hz) ppm. ^{13}C-NMR (CDCl$_3$) δ: 190.2, 143.1, 139.5, 138.4, 138.0, 136.6, 136.5, 132.6, 132.1, 129.0, 126.6, 124.3, 122.6, 122.1, 117.1 ppm. MS (CI): m/z: 283 [M+1], 267.[341]

### 18.2.3.25. Synthesis of 3-benzoyl-7-carbomethoxy-1-hydroxy-1H-indole (29)
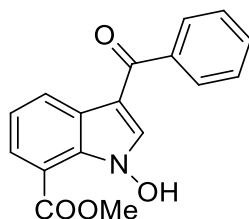
A 80°C solution of 2-carbomethoxy-nitrosobenzene (100 mg, 0.61 mmol) and 1-phenylprop-2-yn-1-one (79 mg, 0.61 mmol) in toluene (8 mL) was stirred for 2.5 h. Solvent was evaporated then evaporated under reduced pressure. Crude material was purified by gravimetric column chromatography (petroleum ether/EtOAc 8:2) to afford 3-benzoyl-7-carbomethoxy-1-hydroxy-1H-indole (60 mg, 34%) as an orange solid. ^{1}H-NMR (CDCl$_3$) δ: 12.94 (s, 1H), 8.85 (d, 1H, J = 7.8 Hz), 8.07 (d, 1H, J = 7.8 Hz); 7.85 (d, 2H, J = 7 Hz), 7.77 (s, 1H), 7.59 (t, 1H, J = 7 Hz), 7.52 (7, 2H, J = 7 Hz), 7.37 (t, 1H, J = 7.8 Hz), 4.10 (s, 3H) ppm. ^{13}C-NMR (CDCl$_3$) δ: 190.6, 170.7, 140.7, 135.2, 131.9, 131.8, 130.4, 129.1, 128.8, 128.5, 126.3, 122.3, 112.8, 111.2, 54.1 ppm. FT-IR (KBr disk): 1666, 1631, 1601, 1520, 1440, 1385, 750, 700 cm^{-1}. m.p.: 113°C. MS (CI): m/z: 296 [M+1], 280. Elemental Analysis for C$_{17}$H$_{13}$NO$_4$: calcd. (%) C 69.15, H 4.44, N 4.74; found (%) C 69.21, H 4.41, N 4.82.[334]

18.2.3.26. Synthesis of 3-(1H-benzo[d][1,2,3]triazole-1-carbonyl)-5-nitro-1-hydroxy-1H-indole (30)
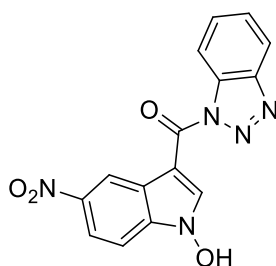
A 80° solution of 4-nitro-nitrosobenzene (100 mg, 0.66 mmol) and 1-(1*H*-benzo[*d*][1,2,3]triazol-1-yl)prop-2-yn-1-one (113 mg, 0.66 mmol) in toluene (10 mL) was stirred for 4 h. Precipitation of desired product was observed. After cooling to r.t., 3-(1H-benzo[d][1,2,3]triazole-1-carbonyl)-5-nitro-1-hydroxy-1H-indole was collected by filtration (122 mg, 57%) as a yellow solid without any further purification. ^{1}H-NMR (DMSO-d_6) δ: 13.02 (br, 1H), 9.24 (d, 1H, J = 2.2 Hz), 9.10 (s, 1H), 8.42 (dt, 1H, J_1 = 8.2 Hz, J_2 = 0.8 Hz), 8.30 (dt, 1H, J_1 = 8.2 Hz, J_2 = 0.8 Hz), 8.28 (dd, 1H, J_1 = 8.9 Hz, J_2 = 2.2 Hz), 7.85 (d, 1H, J = 8.9 Hz), 7.82 (td, 1H, J_1 = 8.2 Hz, J_2 = 0.8 Hz), 7.64 (td, 1H, J_1 = 8.2 Hz, J_2 = 0.8 Hz) ppm. ^{13}C-NMR (DMSO-d_6) δ: 160.1, 145.1, 143.7, 138.0, 136.0, 131.7, 130.7, 126.4, 123.4, 120.0, 119.2, 117.7, 114.5, 110.9, 102.6 ppm. FT-IR (KBr disk): 1689, 1527, 1450, 1364, 1339, 1288, 1106, 1025, 744 cm^{-1}. MS (CI): *m/z*: 324 [M+1]. Elemental Analysis for $C_{15}H_9N_5O_4$: calcd. (%) C 55.73, H 2.81, N 21.66; found (%) C 55.82, H 2.91, N 21.57.[334]

18.2.3.27. Synthesis of 3-(1H-benzo[d][1,2,3]triazole-1-carbonyl)-1-hydroxy-1H-indole-5-carboxylic acid (31)
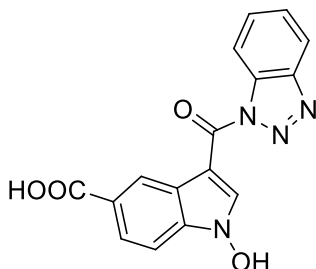
4-nitrosobenzoic acid (181 mg, 1.20 mmol) was suspended in 1,4-dioxane (15 mL): Mixture is then heated to complete solid dissolving. Then 1-(1*H*-benzo[*d*][1,2,3]triazol-1-yl)prop-2-yn-1-one (205 mg, 1.20 mmol) was added and the mixture was refluxed for 5 h. Precipitation of desired product was observed. After cooling to r.t., 3-(1*H*-benzo[*d*][1,2,3]triazol-1-oyl)-1-hydroxy-1*H*-indole-5-carboxylic acid was isolated by filtration (261 mg, 68%) as a yellow solid without any further purification. ^{1}H-NMR (DMSO-d_6) δ: 12.79 (s, 1H), 9.03 (d, 1H, J = 1.4 Hz), 8.94 (s, 1H), 8.39 (d, 1H, J = 8.2 Hz), 7.26 (d, 1H, J = 8.2 Hz), 7.98 (dd, 1H, J_1 = 8.6 Hz, J_2 = 1.4 Hz), 7.79 (t, 1H, J = 8.2 Hz), 7.69 (d, 1H, J = 8.6 Hz), 7.61 (t, 1H, J = 8.2 Hz) ppm. ^{13}C-NMR (DMSO-d_6) δ: 167.9, 160.3, 145.2, 136.4, 135.7, 131.9, 130.6, 126.4, 125.8, 125.1, 123.9, 123.6, 120.1, 114.6, 110.0, 101.7 ppm. FT-IR (KBr disk): 1695, 1608, 1448, 1362, 1292, 1105, 1031, 815, 750 cm^{-1}. MS (CI): *m/z*: 323 [M+1]. Elemental Analysis for $C_{16}H_{10}N_4O_4$: calcd. (%) C 59.63, H 3.13, N 17.38; found (%) C 59.39, H 3.22, N 17.33.[334]

18.2.3.28. Synthesis of 3-(1H-benzo[d][1,2,3]triazole-1-carbonyl)-1-hydroxy-1H-indole-5-carbonitrile (32)
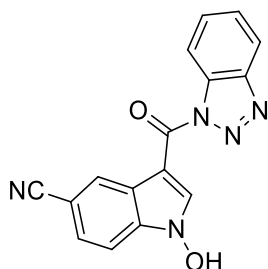
A 80°C solution of 4-cyano-nitrosobenzene (158 mg, 1.20) and 1-(1*H*-benzo[*d*][1,2,3]triazol-1-yl)prop-2-yn-1-one (205 mg, 1.20 mmol) in toluene (15 mL) was stirred for 4 h. Precipitation of desired product was observed. After cooling to r.t., 3-(1H-benzo[d][1,2,3]triazole-1-carbonyl)-1-hydroxy-1H-indole-5-carbonitrile was collected by filtration (145 mg, 40%) as a pale yellow solid without any further purification. ^{1}H-NMR (DMSO-d_6) δ: 12.55 (br, 1H), 9.04 (s, 1H), 8.74 (dd, 1H, J1 = 1.4 Hz, J2 = 0.8 Hz), 8.39 (dt, 1H, J_1 = 8.3 Hz, J_2 = 0.9 Hz), 8.28 (dt, 1H, J_1 = 8.3 Hz, J_2 = 0.9 Hz), 7.84 – 7.80 (m, 2H), 7.80 (td, 1H, J_1 = 8.3 Hz, J_2 = 0.9 Hz), 7.63 (td, 1H, J_1 = 8.3 Hz, J_2 = 0.9 Hz) ppm. ^{13}C-NMR (DMSO-d_6) δ: 160.1, 145.2, 135.1, 132.6, 131.8, 130.7, 126.9, 126.5, 126.3, 123.8, 120.1, 119.8, 114.5, 111.5, 105.6, 101.5 ppm. FT-IR (KBr disk): 2228, 1700, 1448, 1353, 1288, 1102, 1031, 756 cm^{-1}. MS (CI): *m/z*: 304 [M+1]. Elemental Analysis for $C_{16}H_9N_5O_2$: calcd. (%) C 63.37, H 2.99, N 23.09; found (%) C 63.42, H 2.88, N 23.12.[334]

18.2.3.29. Synthesis of 3-(1H-benzo[d][1,2,3]triazole-1-carbonyl)-1-hydroxy-1H-indole (33)

A 80°C solution of nitrosobenzene (128 mg, 1.20 mmol) and 1-(1*H*-benzo[*d*][1,2,3]triazol-1-yl)prop-2-yn-1-one (205 mg, 1.20 mmol) in toluene (15 mL) was stirred 4 h. Precipitation of desired product was observed. After cooling to r.t., 3-(1H-benzo[d][1,2,3]triazole-1-carbonyl)-1-hydroxy-1H-indole was isolated by filtration as a yellow solid (63 mg). Purification of mother liquors by gravimetric column chromatography (*n*-hexane/EtOAc 8:2) afforded extra 70 mg of product (133 mg, 40%). ^{1}H-NMR (DMSO-d_6) δ: 2.49 (s, 1H), 8.86 (s, 1H), 8.38 (dt, 1H, J_1 = 8.3 Hz, J_2 = 1.0 Hz), 8.36 (dd, 1H, J_1 = 8.6 Hz, J_2 = 1.4 Hz), 8.26 (dt, 1H, J_1 = 8.3 Hz, J_2 = 1.0 Hz), 7.78 (tt, 1H, J_1 = 8.3 Hz, J_2 = 1.0 Hz), 7.63 (dd, 1H, J_1 = 8.6 Hz, J_2 = 1.4 Hz), 7.61 (tt, 1H, J_1 = 8.3 Hz, J_2 = 1.0 Hz), 7.42 (dd, 1H, J_1 = 8.6 Hz, J_2 = 1.4 Hz), 7.40 (dd, 1H, J_1 = 8.6 Hz, J_2 = 1.4 Hz) ppm. ^{13}C-NMR (DMSO-d_6) δ: 160.2, 145.1, 134.6, 133.5, 131.8, 130.3, 126.1, 124.3, 124.0, 123.4, 121.0, 119.9, 114.4, 109.9, 100.3 ppm. MS (CI): *m/z*: 279 [*M*+1]. FT-IR (KBr disk): 1690, 1447, 1360, 1288, 1099, 1037, 761, 735 cm^{-1}. Elemental Analysis for $C_{15}H_{10}N_4O_2$: calcd. (%) C 64.74, H 3.62, N 20.13; found (%) C 64.68, H 3.71, N 19.98.[334]

18.2.3.30. Synthesis of (1-hydroxy-5-nitro-1H-indol-3-yl)(1-methyl-1H-indol-3-yl)methanone (34)
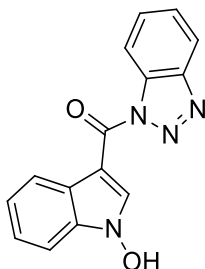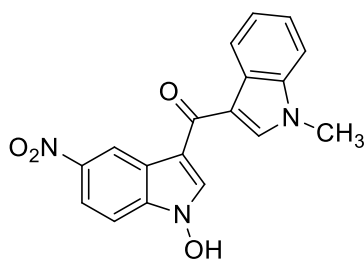

A 80°C solution of 4-nitro-nitrosobenzene (100 mg, 0.66 mmol) and 1-(1-methyl-1*H*-indol-3-yl)prop-2-yn-1-one (121 mg, 0.66 mmol) in toluene (10 mL) was stirred 3 h. Precipitation of desired product was observed. After cooling to r.t., (1-hydroxy-5-nitro-1H-indol-3-yl)(1-methyl-1H-indol-3-yl)methanone was collected by filtration (104 mg, 47%) as a yellow solid without any further purification. ^{1}H-NMR (DMSO-d_6) δ: 12.50 (s, 1H), 9.23 (d, 1H, J = 2.2 Hz), 8.67 (s, 1H), 8.38 (s, 1H), 8.32 (d, 1H, J = 7.5 Hz), 8.18 (dd, 1H, J_1 = 9 Hz, J_2 = 2.2 Hz), 7.71 (d, 1H, J = 9 Hz), 7.58 (d, 1H, J = 7.5 Hz), 7.32 (t, 1H, J = 7.5 Hz), 7.27 (t, 1H, J = 7.5 Hz), 3.92 (s, 3H) ppm. ^{13}C-NMR (DMSO-d_6) δ: 183.2, 143.4, 138.0, 137.6, 136.9, 134.3, 127.7, 123.8, 123.0, 122.7, 122.5, 119.5, 119.1, 115.5, 113.7, 111.3, 110.7, 34.0 ppm. FT-IR (KBr disk): 1620, 1562, 1523, 1458, 1381, 1329, 821, 742 cm^{-1}. m.p.: > 300°C. MS (CI): *m/z*: 336 [M+1]. Elemental Analysis for $C_{18}H_{13}N_3O_4$: calcd. (%) C 64.48, H 3.91, N 12.53; found (%) C 64.41, H 3.92, N 12.32.[334]

18.2.3.31. Synthesis of 1-hydroxy-3-(1-methyl-1*H*-indole-3-carbonyl)-1*H*-indole-5-carboxylic acid (35)
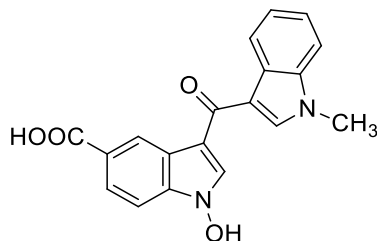
Under nitrogen atmosphere, 4-nitrosobenzoic acid (100 mg, 0.66 mmol) was suspended in dioxane (10 mL) and heated until the solid was completely dissolved. Then 1-(1-methyl-1*H*-indol-3-yl)prop-2-yn-1-one (122 mg, 0.66 mmol) was added and the mixture was refluxed for 7.5 h. During the reaction, precipitation of the desired product together with the azoxy-derivative was observed. When the reaction was complete, the mixture was cooled to r.t.. Solid collected by filtration and the washings concentrated under reduced pressure. Crude product was recrystallized from EtOAc to afford 1-hydroxy-3-(1-methyl-1*H*-indole-3-carbonyl)-1*H*-indole-5-carboxylic acid as a yellow solid (142 mg, 64%). ^{1}H-NMR (DMSO-d_6) δ: 12.15 (br, 1H), 8.99 (dd, 1H, ^4J = 1.6 Hz, ^5J = 0.6 Hz), 8.47 (s, 1H), 8.30 (s, 1H), 8.29 (d, 1H, J = 8.0 Hz), 7.89 (dd, 1H, ^3J = 8.6 Hz, ^4J = 1.6 Hz), 7.57 (dd, 1H, ^3J = 8.6 Hz, ^5J = 0.6 Hz), 7.55 (d, 1H, J = 8.0 Hz), 7.30 (dd, 1H, ^3J = 8.0 Hz, ^4J = 0.8 Hz), 7.24 (dd, 1H, ^3J = 8.0 Hz, ^4J = 0.8 Hz), 3.91 (s, 3H) ppm. ^{13}C-NMR (DMSO-d_6) δ: 182.9, 168.1, 137.1, 136.4, 135.7, 131.8, 126.9, 124.5, 124.0, 122.5, 121.7, 112.6, 115.0, 112.1, 110.4, 108.9, 33.1 ppm. MS (CI): *m/z*: 335 [*M*+1]. FT-IR (KBr disk): 1685, 1603, 1517, 1463, 771 cm^{-1}.

18.2.3.32. Synthesis of (1-hydroxy-5-nitro-1H-indol-3-yl)(1-tosyl-1H-indol-2-yl)methanone (36)
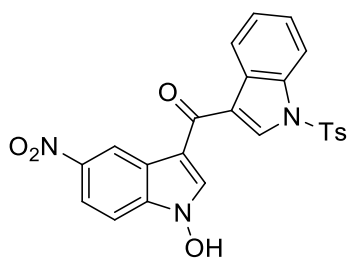
A 80°C solution of 3-(*N*-tosyl-3-indolyl)-propyn-3-one (327 mg, 1 mmol) and 4-nitro-nitrosobenzene (175 mg, 1 mmol) was stirred for 24 h. Reaction mixture is filtered and obtained solid is purified by gravimetric column chromatography (*n*-hexane/EtOAc 1:1) to afford (1-hydroxy-5-nitro-1H-indol-3-yl)(1-tosyl-1H-indol-2-yl)methanone as brown solid (64.5 mg, 15%). ^{1}H-NMR (CDCl$_3$): δ 12.64 (1H, s), 9.13 (d, 1H, *J* = 2.3 Hz), 8.62 (d, 1H, *J* = 2.9 Hz), 8.55 (s, 1H), 8.19-8.14 (m, 2H), 7.98 (d, 1H, *J* = 8 Hz), 7.75 (d, 1H, *J* = 8.99 Hz), 7.47-7.37 (m, 3H), 2.33 (s, 3H).[341]

18.2.3.33. Synthesis of (*E*)-1-(5-nitro-1-hydroxy-1H-indol-3-yl)-3-(1-tosyl-1H-indol-3-yl)prop-2-en-1-one (37)
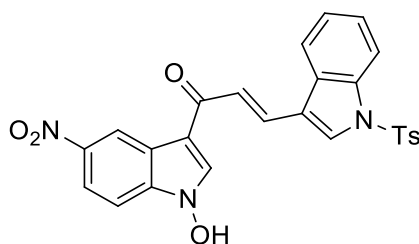
A 80°C solution containing (*E*)-1-(1-tosyl-1H-indol-3-yl)pent-1-en-4-yn-3-one (349 mg, 1.0 mmol) and 4-nitro-nitrosobenzene (152 mg, 1.0 mmol) in toluene (10 mL) was stirred overnight. Reaction mixture was then dried under reduced pressure. Crude product was purified by flash column chromatography (toluene/EtOAc 8:2) to afford (*E*)-1-(5-nitro-1-hydroxy-1H-indol-3-yl)-3-(1-tosyl-1H-indol-3-yl)prop-2-en-1-one (150 mg, 30%) as a brown solid. ^{1}H-NMR (acetone-d_6) δ: 11.64 (br s, 1H), 9.43 (d, 1H, *J* = 2.4 Hz), 8.83 (d, 1H, *J* = 2.8 Hz), 8.36 (s, 1H), 8.20 (dd, 1H, *J* = 8.8, 2.0 Hz), 8.14 (d, 1H, *J* = 8.4 Hz), 8.09 (d, 1H, *J* = 8.4 Hz), 8.00 (d, 1H, *J* = 15.8 Hz), 7.97 (d, 2H, *J* = 8.8 Hz), 7.87 (d, 1H, *J* = 15.8 Hz), 7.76 (d, 2H, *J* = 9.2), 7.47 (td, 1H, *J* = 7.6, 1.2 Hz), 7.43-7.38 (m, 2H), 2.37 (s, 3H). ^{13}C-NMR (acetone-d_6) δ: 182.3, 146.0, 136.1, 134.7, 134.5, 131.9, 130.3; 130.2, 129.0, 127.2, 127.1, 125.4, 124.5, 124.2, 124.1, 123.8, 121.0, 119.1, 119.0, 118.8, 118.6, 113.7, 112.5, 20.5. MS (CI): *m/z* = 486 [M]+. IR (ATR): ν (cm^{-1}) = 3583, 3184, 2921, 1721, 1640, 1525, 1376, 1337, 1261, 800, 634. m.p.: degradation from 128 °C.[341]

18.2.3.34. Synthesis of (*E*)-1-(7-nitro-1H-indol-3-yl)-3-(1-tosyl-1H-indol-3-yl)prop-2-en-1-one (38)
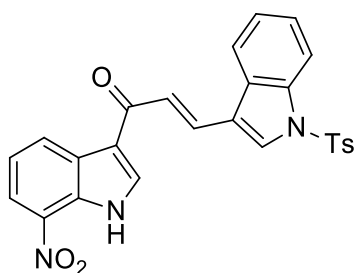
A 80°C solution containing (*E*)-1-(1-tosyl-1H-indol-3-yl)pent-1-en-4-yn-3-one (349 mg, 1.0 mmol) and 2-nitro-nitrosobenzene (152 mg, 1.0 mmol) in toluene (10 mL) was stirred overnight. Reaction mixture was dried under reduced pressure. Crude product was purified by flash column chromatography (*n*-hexane/EtOAc 1:1) to afford (*E*)-1-(7-nitro-1H-indol-3-yl)-3-(1-tosyl-1H-indol-3-yl)prop-2-en-1-one (218 mg, 45%) as a brown oil. ^{1}H-NMR (DMSO-*d$_6$*) δ: 9.15 (s, 1H), 7.40 (d, 1H, *J* = 7.4 Hz), 8.57 (s, 1H), 8.19 (d, 1H, *J* = 7.6 Hz), 7.97 (d, 1H, *J* = 8.1 Hz), 7.92 (d, 2H, *J* = 8.4 Hz), 7.87 (d, 1H, *J* = 15.6 Hz), 7.85 (d, 1H, *J* = 7.9 Hz), 7.80 (d, 1H, *J* = 15.6 Hz), 7.42 (m, 5H), 2.32 (s, 3H). ^{13}C-NMR (DMSO-*d$_6$*) δ: 183.5, 146-5, 136.6, 136.0, 135.2, 134.2, 132.1, 130.9, 129.9, 128.5, 127.5, 127.3, 126.1, 126.7, 124.1, 122.4, 121.8, 120.2, 119.0, 113.8, 113.0, 21.5. MS (CI): *m/z* = 486 [M]+. IR (ATR): ν (cm^{-1}) = 3579, 3190, 2903, 1719, 1640, 1527, 1374, 1335, 126, 806.[341]

18.2.3.35. Synthesis of (*E*)-1-(1H-indol-3-yl)-3-(1-tosyl-1H-indol-3-yl)prop-2-en-1-one (39)

A 80°C solution containing (*E*)-1-(1-tosyl-1H-indol-3-yl)pent-1-en-4-yn-3-one (349 mg, 1mmol) and 4-nitro-sobenzene (107 mg, 1.0 mmol) in toluene (10 mL) was stirred overnight. Reaction mixture was dried under reduced pressure. Crude product was then purified by flash column chromatography (toluene/EtOAc 9:1) to afford (*E*)-1-(1H-indol-3-yl)-3-(1-tosyl-1H-indol-3-yl)prop-2-en-1-one (141 mg, 32%) as a brown solid. ^{1}H-NMR (DMSO-*d$_6$*) δ: 12.10 (br s, 1H); 8.74 (d, 1H, *J* = 2.8 Hz); 8.53 (s, 1H), 8.34 (dd, 1H, *J* = 7.2, 2.4 Hz), 8.14 (dd, 1H, *J* = 7.2, 1.2 Hz), 7.98 (dd, 1H, *J* = 7.6, 1.2 Hz), 7.92 (d, 2H, *J* = 8.4 Hz), 7.84 (d, 1H, *J* = 15.6 Hz), 7.79 (d, 1H, *J* = 15.6 Hz), 7.51 (dd, 1H, *J* = 6.8, 1.2 Hz), 7.48-7.33 (m, 4H), 7.29-7.17 (m, 2H), 2.32 (s, 3H). ^{13}C NMR (DMSO-*d$_6$*) δ: 182.1, 137.3, 135.3, 135.2, 134.2, 130.9, 130.6, 129.3, 129.2, 127.5, 127.3, 127.2, 126.0, 125.0, 124.7, 123.6, 122.4, 122.3, 122.2, 121.6, 119.2, 113.8, 112.6, 21.5. MS (CI): *m/z* = 441 [M]+. IR (film): ν (cm^{-1}) = 3360; 2918; 1642; 1527; 739. m.p.: 176°C.[341]

### 18.2.3.36. Synthesis of (1-hydroxy-5-nitro-1H-indol-3-yl)(1-methyl-1H-indol-2-yl)methanone (40)
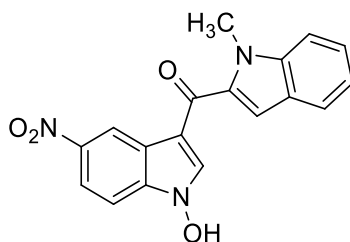
A 80°C solution of 4-nitro-nitrosobenzene (152 mg, 1 mmol) and 1-(1-methyl-1H-indol-2-yl)prop-2-yn-1-one (183 mg, 1 mmol) in toluene (10 mL) was stirred for 3 h. Precipitation of desired product was observed. After cooling to r.t., (1-hydroxy-5-nitro-1H-indol-3-yl)(1-methyl-1H-indol-2-yl)methanone was collected by filtration (94 mg, 20%) as an orange-solid without any further purification. ^{1}H-NMR (DMSO-d_6) δ: 12.68 (br, 1H), 9.20 (d, 1H, J = 2 Hz), 8.61 (s, 1H), 8.23 (dd, 1H, J_1 = 1.6 Hz, J_2 = 8.8 Hz), 7.75 (t, 2H, J = 9.2 Hz), 7.63 (d, 1H, J = 8.4 Hz), 7.39 (t, 1H, J = 7.2 Hz), 7.29 (s, 1H), 7.17 (t, 1H, J = 7.2 Hz), 4.02 (s, 3H) ppm. ^{13}C-NMR (DMSO-d_6) δ: 180.7, 143.1, 139.4, 136.35, 136.1, 135.8, 125.7, 124.9, 122.5, 121.9, 120.4, 118.8, 118.2, 112.4, 110.7, 110.5, 110.2, 31.5 ppm. FT-IR (ATR): 1553, 1518, 1493, 1452, 1424, 1332, 1210, 1154, 1109, 925, 736 cm^{-1} m.p.: decomposition from 230°C. MS (CI): m/z: 336 [M+1]. Elemental Analysis for $C_{18}H_{13}N_3O_4$: calcd. (%) C 64.48, H 3.91, N 12.53; found (%) C 64.59, H 3.88, N 12.64.[334]

### 18.2.3.37. Synthesis of 1-hydroxy-3-(1-methyl-1H-indole-2-carbonyl)-1H-indole-5-carboxylic acid (41)
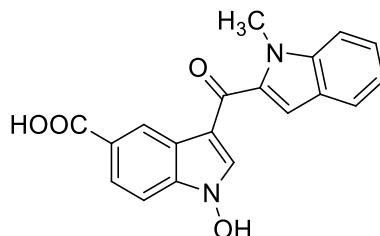
4-nitrosobenzoic acid (100 mg, 0.66 mmol) was suspended in 1,4-dioxane (10 mL) and heated to complete solid dissolving. 1-(1-methyl-1H-indol-3-yl)prop-2-yn-1-one (122 mg, 0.66 mmol) was then added and the mixture was refluxed for 7.5 h. After cooling to r.t., the precipitated solid was collected by filtration and recrystallized from EtOAc to afford 1-hydroxy-3-(1-methyl-1H-indole-3-carbonyl)-1H-indole-5-carboxylic acid (142 mg, 64%) as a yellow solid. ^{1}H-NMR (DMSO-d_6) δ: 12.15 (br, 1H), 8.99 (dd, 1H, ^4J = 1.6 Hz, ^5J = 0.6 Hz), 8.47 (s, 1H), 8.30 (s, 1H), 8.29 (d, 1H, J = 8.0 Hz), 7.89 (dd, 1H, ^3J = 8.6 Hz, ^4J = 1.6 Hz), 7.57 (dd, 1H, ^3J = 8.6 Hz, ^5J = 0.6 Hz), 7.55 (d, 1H, J = 8.0 Hz), 7.30 (dd, 1H, ^3J = 8.0 Hz, ^4J = 0.8 Hz), 7.24 (dd, 1H, ^3J = 8.0 Hz, ^4J = 0.8 Hz), 3.91 (s, 3H) ppm. ^{13}C-NMR (DMSO-d_6) δ: 182.9, 168.1, 137.1, 136.4, 135.7, 131.8, 126.9, 124.5, 124.0, 122.5, 121.7, 112.6, 115.0, 112.1, 110.4, 108.9, 33.1 ppm. MS (CI): m/z: 335 [M+1]. FT-IR (KBr disk): 1685, 1603, 1517, 1463, 771 cm^{-1}.[341]

18.2.3.38. Synthesis of 3-(1-methyl-1H-indole-2-carbonyl)-7-carbomethoxy-1H-indole-7-carboxylate (42)
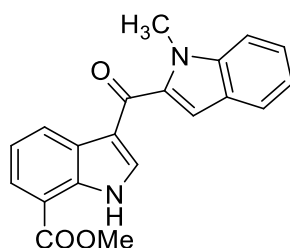
A 80°C solution of 2-carbomethoxy-nitrosobenzene (165 mg, 1 mmol) and 1-(1-methyl-1H-indol-2-yl)prop-2-yn-1-one (183 mg, 1 mmol) in toluene (10 mL) was stirred at 80 °C for 4 h. reaction mixture was then dried under reduced pressure. Crude product was purified by gravimetric column chromatography (DCM/toluene 6:4) to afford methyl 3-(1-methyl-1H-indole-2-carbonyl)-1H-indole-7-carboxylate (100 mg, 30%) as a brown solid. ^{1}H-NMR (CDCl$_3$) δ: 12.85 (s, 1H), 8.75 (d, 1H, J = 8 Hz), 7.99 (d, 1H, J = 7.6 Hz), 7.94 (s, 1H), 7.62 (d, 1H, J = 15.2 Hz), 7.38 (d, 1H, J = 8 Hz), 7.28 (m, 2H), 7.12 (t, 1H, J = 7.2 Hz), 7.03 (s, 1H), 4.02 (s, 3H), 4.00 (s, 3H) ppm. ^{13}C-NMR (CDCl$_3$) δ: 181.7, 170.3, 139.8, 136.8, 130.9, 130.7, 129.7, 128.1, 126.2, 124.9, 125.8, 124.9, 122.5, 121.8, 120.57, 112.34, 110.59, 110.2, 53.7, 31.3 ppm. FT-IR (ATR): 2915, 2848, 1590, 1516, 1437, 1424, 1264, 1202, 1143, 1094, 1051, 918, 855, 762, 746 cm^1. m.p.: 176.5°C. GC-MS (EI): m/z: 332 [M$^+$]. Elemental Analysis for C$_{20}$H$_{16}$N$_2$O$_3$: calcd. (%) C 72.28, H 4.85, N 8.43; found (%) C 72.35, H 4.80, N 8.44.[334]

18.2.3.39. Synthesis of (1H-indol-3-yl)(1-methyl-1H-indol-2-yl)methanone (43)


A 80°C solution of (*E*)-1-(1-tosyl-1H-indol-3-yl)pent-1-en-4-yn-3-one (349 mg, 1 mmol) and 4-nitrosobenzene (107 mg, 1 mmol) in toluene (10 mL) was stirred overnight. Reaction mixture was dried under reduced pressure. Crude material was purified by flash column chromatography (toluene/EtOAc 9:1) to afford (*E*)-1-(1H-indol-3-yl)-3-(1-tosyl-1H-indol-3-yl)prop-2-en-1-one (141 mg, 32%) as a brown solid. ^{1}H-NMR (DMSO-d_6) δ: 12.10 (br s, 1H), 8.74 (d, 1H, J = 2.8 Hz), 8.53 (s, 1H), 8.34 (dd, 1H, J = 7.2, 2.4 Hz), 8.14 (dd, 1H, J = 7.2, 1.2 Hz), 7.98 (dd, 1H, J = 7.6, 1.2 Hz), 7.92 (d, 2H, J = 8.4 Hz), 7.84 (d, 1H, J = 15.6 Hz), 7.79 (d, 1H, J = 15.6 Hz), 7.51 (dd, 1H, J = 6.8, 1.2 Hz), 7.48-7.33 (m, 4H), 7.29-7.17 (m, 2H), 2.32 (s, 3H). ^{13}C NMR (DMSO-d_6) δ: 182.1, 137.3, 135.3, 135.2, 134.2, 130.9, 130.6, 129.3, 129.2, 127.5, 127.3, 127.2, 126.0, 125.0, 124.7, 123.6, 122.4, 122.3, 122.2, 121.6, 119.2, 113.8, 112.6, 21.5. MS (CI): m/z = 441 [M]+. IR (film): ν (cm^{-1}) = 3360, 2918, 1642, 1527, 739. m.p.: 176°C.[341]

18.2.3.40. Synthesis of 3-cinnamoyl-5-nitro-1-hydroxy-1H-indole (44)
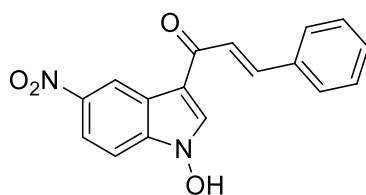
A 80°C mixture of 4-nitro-nitrosobenzene (100 mg, 0.66 mmol) and (*E*)-1-phenylpent-1-en-4-yn-3-one (103 mg, 0.66 mmol), in toluene (8 mL) was stirred for 2 h. Precipitation of the desired product was observed during the reaction. After cooling to r.t., the solid was collected by filtration to afford 3-cinnamoyl-5-nitro-1-hydroxy-1H-indole as a yellow solid (132 mg, 65%) without any further purification. ^{1}H-NMR (DMSO-d_6) δ: 12.67 (s, 1H), 9.24 (d, 1H, *J* = 2.2 Hz), 9.23 (s, 1H), 8.21 (dd, 1H, J^1 = 9 Hz, J^2 = 2.2 Hz), 7.90 (dd, 2H, J^1 = 7.9 Hz, J^2 = 1.6 Hz), 7.86 (d, 1H, *J* = 15.7 Hz), 7.75 (d, 1H, 9 Hz), 7.71 (d, 1H, *J* = 15.7 Hz), 7.51 – 7.45 (m, 3H) ppm. ^{13}C-NMR (DMSO-d_6) δ: 183.9, 144.1, 142.2, 137.2, 135.2, 134.0, 130.5, 129.2, 128.6, 123.5, 122.4, 120.0, 119.2, 114.5, 109.8 ppm. FT-IR (KBr disk): 1630, 1575, 1525, 1313, 974, 744, 680 cm^{-1}. m.p.: decomposition from 270°C. MS (CI): *m/z*: 309 [M+1], 293. Elemental Analysis for $C_{17}H_{12}N_2O_4$: calcd. (%) C 66.23, H 3.92, N 9.09; found (%) C 66.17, H 3.99, N 9.13.[334]

18.2.3.41. Synthesis of 3-cinnamoyl-1-hydroxy-1H-indole-5-carboxylic acid (45)
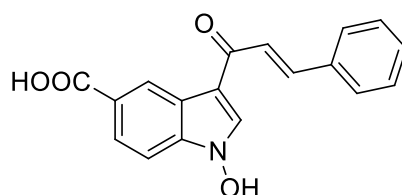
4-nitrosobenzoic acid (100 mg, 0.66 mmol) was suspended in 1,4-dioxane (10 mL) and heated to complete solid dissolving. Then (*E*)-1-phenylpent-1-en-4-yn-3-one (104 mg, 0.66 mmol) was added and the mixture was refluxed for 7.5 h. After cooling to r.t., the precipitated solid was collected by filtration and recrystallized from DCM to afford 3-cinnamoyl-1-hydroxy-1H-indole-5-carboxylic acid (102 mg, 50%) as a yellow solid. ^{1}H-NMR (DMSO-d_6) δ: 12.85 (br, 1H), 12.31 (br, 1H), 9.05 (s, 1H), 9.02 (dd, 1H, ^4J = 1.6 Hz, ^5J = 0.6 Hz), 7.91 (dd, 1H, ^3J = 8.6 Hz, ^4J = 1.6 Hz), 7.87 (dd, 2H, ^3J = 8.0 Hz, ^4J = 1.6 Hz), 7.82 (d, 1H, *J* = 15.6 Hz), 7.65 (d, 1H, *J* = 15.6 Hz), 7.59 (dd, 1H, ^3J = 8.0 Hz, ^5J =0.4 Hz), 7.47 - 7.44 (m, 3H) ppm. ^{13}C-NMR (DMSO-d_6) δ: 183.1, 168.0, 140.4, 136.4, 135.1, 136.6, 131.3, 130.1, 128.9, 128.6, 124.7, 124.5, 124.3, 122.1, 113.3, 109.3 ppm. MS (CI): *m/z*: 308 [*M*+1]. FT-IR (KBr disk): 1686, 1631, 1513, 973, 766 cm^{-1}.

18.2.3.42. Synthesis of (1-hydroxy-5-nitro-1H-indol-3-yl)(1-methyl-1H-pyrrol-2-yl)methanone (46)
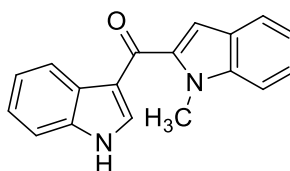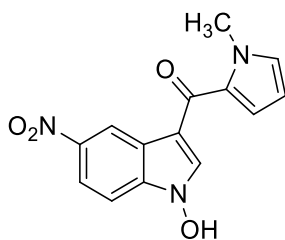

A 80°C solution of 4-nitro-nitrosobenzene (100 mg, 0.66 mmol) and 1-(1-methyl-1*H*-pyrrol-2-yl)prop-2-yn-1-one (88 mg, 0.66 mmol) in toluene (8 mL) was stirred for 7.5 h. Precipitation of desired product was observed. After cooling to r.t., (1-hydroxy-5-nitro-1H-indol-3-yl)(1-methyl-1H-pyrrol-2-yl)methanone was isolated by filtration (94 mg, 50%) as brown solid without any further purification. ^{1}H-NMR (DMSO-d_6) δ: 12.51 (s, 1H, 9.11 (d, 1H, J = 2.2 Hz), 8.42 (s, 1H), 8.17 (dd, 1H, J_1 = 9 Hz, J_2 = 2.2 Hz), 7.96 (d, 1H, J = 9 Hz), 7.15 (d, 1H, J = 4 Hz), 6.97 (dd, 1H, J_1 = 4 Hz, J_2 = 1.7 Hz), 6.18 (dd, 1H, J_1 = 4 Hz, J_2 = 2.5 Hz), 3.92 (s. 3H) ppm. ^{13}C-NMR (DMSO-d_6) δ: 178.5, 142.8, 136.1, 134.2, 131.1, 130.5, 122.1, 119.1, 118.5, 118.4, 112.3, 110.0, 108.0, 36.5 ppm. FT-IR (KBr disk): 2947, 1617, 1557, 1531, 1455, 1378, 1332, 1215, 743 cm^{-1} m.p.: decomposition from 254°C. MS (CI): *m/z*: 286 [M+1]. Elemental Analysis for $C_{14}H_{11}N_3O_4$: calcd. (%) C 58.95, H 3.89, N 14.73; found (%) C 58.82, H 3.96, N 14.88.[334]

18.2.3.43. Synthesis of furan-2-yl(1-hydroxy-5-nitro-1H-indol-3-yl)methanone (47)
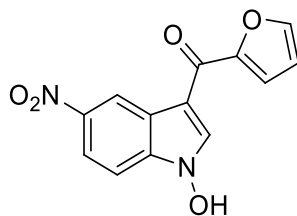
A 80°C solution of 4-nitro-nitrosobenzene (100 mg, 0.66 mmol) and 1-(furan-2-yl)prop-2-yn-1-one (79 mg, 0.66 mmol) in toluene (8 mL) was stirred for 6.5 h. Precipitation of desired product was observed. After cooling to r.t., furan-2-yl(1-hydroxy-5-nitro-1H-indol-3-yl)methanone was collected by filtration (92 mg, 51%) as yellow solid without any further purification. ^{1}H-NMR (DMSO-d_6) δ: 12.70 (br, 1H), 9.20 (d, 1H, J = 2.3 Hz),, 8.83 (s, 1H), 8.20 (dd, 1H, J_1 = 9 Hz, J_2 = 2.3 Hz), 8.03 (dd, 1H, J_1 = 1.7 Hz, J_2 = 0.7 Hz), 7.73 (d, 1H, J = 9 Hz), 7.47 (dd, 1H, J_1 = 3.6 Hz, J_2 = 0.7 Hz), 6.77 (dd, 1H, J_1 = 3.6 Hz, J_2 = 1.7 Hz) ppm. ^{13}C-NMR (DMSO-d_6) δ: 174.6, 152.4, 147.0, 143.3, 136.1, 135.6, 122.3, 118.9, 118.3, 117.5, 112.6, 110.3, 109.9 ppm. FT-IR (KBr disk): 1633, 1577, 1519, 1453, 1367, 1336, 825, 746 cm^{-1}. m.p.: decomposition from 267°C. MS (CI): *m/z*: 273 [M+1]. Elemental Analysis for $C_{13}H_8N_2O_5$: calcd. (%) C 57.36, H 2.96, N 10.29; found (%) C 57.09, H 2.86, N 10.37.[334]

18.2.3.44. Synthesis of (1-hydroxy-5-nitro-1H-indol-3-yl)(pyren-1-yl)methanone (48)
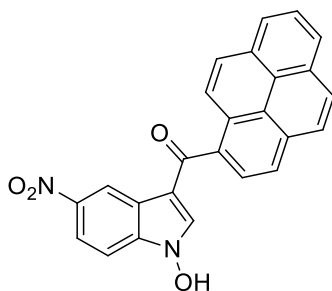
A 80°C solution of 4-nitro-nitrosobenzene (152 mg, 1 mmol) and 1-(pyren-1-yl)prop-2-yn-1-one (254 mg, 1 mmol) in toluene (12 mL) was stirred for 8 h. Precipitation of desired product was observed. After cooling to r.t., (1-hydroxy-5-nitro-1H-indol-3-yl)(pyren-1-yl)methanone was collected by filtration (264 mg, 65%) as yellow solid without any further purification. ^{1}H-NMR (DMSO-d_6) δ: 12.60 (br, 1H), 9.46 (d, 1H, J = 2.2 Hz), 8.45 (d, 1H, J = 9.3 Hz), 8.22–8.41 (m, 7H), 8.31–8.33 (m, 1H), 8.12 − 8. 16 (t, 1H, J = 7.6 Hz), 8.06 (s, 1H), 7.80 − 7.83 (d, 1H, J = 9 Hz) ppm. ^{13}C-NMR (DMSO-d_6) δ: 191.4, 143.9, 138.4, 137.2, 135.0, 132.5, 131.2, 130.7, 129.1, 128.9, 128.6, 127.8, 127.2, 126.5, 126.4, 126.3, 124.9, 124.8, 124.5, 124.2, 122.2, 119.5, 118.7, 113.9, 110.9 ppm FT-IR (ATR): 3135, 1594, 1526, 1506, 1376, 1333, 1215, 923, 831 cm^{-1}. m.p.: decomposition from 273°C. MS (CI): m/z: 407 [M+1]. Elemental Analysis for $C_{25}H_{14}N_2O_4$: calcd. (%) C 73.89, H 3.47, N 6.89; found (%) C 73.96, H 3.45, N 6.78.[334]

18.2.3.45. Synthesis of 1-hydroxy-5-nitro-*N*-phenyl-1H-indole-3-carboxamide (49)
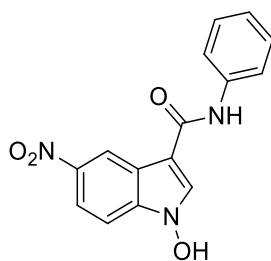
A 80° solution of 4-nitro-nitrosobenzene (152 mg, 1 mmol) and *N*-phenylpropiolamide (145 mg, 1 mmol) in toluene (10 mL) was stirred for 8 h. Precipitation of desired product was observed. After cooling to r.t., 1-hydroxy-5-nitro-*N*-phenyl-1H-indole-3-carboxamide was collected by filtration (107 mg, 36%) as pale yellow solid without any further purification. ^{1}H-NMR (DMSO-d_6) δ: 9.87 (br, 1H), 9.16 (dd, 1H, J_1 = 2 Hz, J_2 = 0.4 Hz), 8.67 (s, 1H), 8.13 (dd, 1H, J_1 = 9.2 Hz, J_2 = 2.4 Hz), 7.76 (dd, 2H, J_1 = 8.4 Hz, J_2 = 0.8 Hz), 7.67 (d, 1H, J = 8.8 Hz), 7.35 (t, 2H, J = 8 Hz), 7.08 (t, 1H, J = 7.4 Hz) ppm. ^{13}C-NMR (DMSO-d_6) δ: 162.0, 142.7, 139.6, 136.2, 131.4, 129.1, 123.7, 122.4, 120.4, 118.7, 118.4, 110.3, 107.7 ppm. FT-IR (KBr disk): 2682, 1635, 1601, 1541, 1513, 1442, 1374, 1323, 1293, 746, 686 cm^{-1}. m.p.: 270-274°C. MS (CI): m/z: 298 [M$^+$]. Elemental Analysis for $C_{15}H_{11}N_3O_4$: calcd. (%) C 60.61, H 3.73, N 14.14; found (%) C 60.34, H 3.86, N 14.28.[334]

18.2.3.46. Synthesis of 5-cyano-1-hydroxy-*N*-phenyl-1H-indole-3-carboxamide (50)
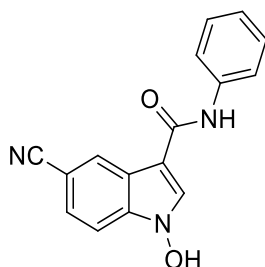
A 80°C solution of 4-cyano-nitrosobenzene (132 mg, 1 mmol) and *N*-phenylpropiolamide (145 mg, 1 mmol) in toluene (10 mL) was stirred for 8 h. Precipitation of desired product was observed. After cooling to r.t., 5-cyano-1-hydroxy-*N*-phenyl-1H-indole-3-carboxamide was collected by filtration (80.3 mg, 29%) as brown solid without any further purification. ^{1}H-NMR (DMSO-d_6) δ: 12.36 (br, 1H), 9.83 (s, 1H), 8.63 (s, 2H), 7.75 (d, 2H, *J* = 7.6 Hz), 7.67 (d, 1H, *J* = 8.5 Hz), 7.62 (dd, 1H, J_1 = 8.5 Hz, J_2 = 1.4 Hz), 7.35 (t, 2H, *J* = 7.9 Hz), 7.07 (t, 1H, *J* = 7.3 Hz) ppm. ^{13}C-NMR (DMSO-d_6) δ: 162.3, 139.7, 135.1, 130.4, 129.1, 127.1, 125.8, 123.6, 122.9, 120.6, 120.4, 111.0, 106.3, 103.9 ppm. FT-IR (KBr disk): 3340, 2217, 1629, 1538 cm^{-1}. m.p.: 278-280°C. MS (CI): *m/z*: 278 [M$^+$]. Elemental Analysis for $C_{16}H_{11}N_3O_2$: calcd. (%) C 69.31, H 4.00, N 15.15; found (%) C 69.46, H 4.09, N 15.11.[334]

18.2.3.47. Synthesis of 1-hydroxy-3-(phenylcarbamoyl)-1H-indole-5-carboxylic acid (51)
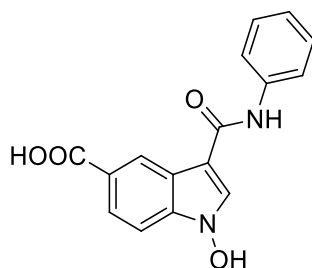
A 80°C solution containing *N*-phenylpropiolamide (145 mg, 1 mmol) and 4-nitrosobenzoic acid (151 mg, 1 mmol) in 1,4-dioxane (10 mL) was stirred overnight. Solvent is then removed under reduced pressure. Crude product is then purified by gravimetric column chromatography to afford 1-hydroxy-3-(phenylcarbamoyl)-1H-indole-5-carboxylic acid (petroleum ether/EtOAc 1:1) as brown oil (48 mg, 16%) as a brown oil. ^{1}H-NMR (DMSO-d_6) δ: 10.48 (br s, 1H), 9.76 (s, 1H), 8.95 (d, 1H, *J* = 0.4 Hz), 8.11 (s, 1H), 7.86 (dd, 1H, *J* = 8.5, 1.4 Hz), 7.75 (d, 2H, *J* = 8.2 Hz), 7.54 (d, 1H, *J* = 8.5 Hz), 7.34 (t, 2H, *J* = 7.6 Hz), 7.05 (t, 1H, *J* = 7.5 Hz). ^{13}C-NMR (DMSO-d_6) δ: 168.5, 166.6, 146.9, 139.9, 131.8, 129.1, 125.4, 124.5, 124.2, 123.4, 122.1, 120.3, 109.3, 106.6. MS (CI): *m/z* = 297 [M]+. IR (ATR): ν (cm^{-1}) = 2553, 1700, 1603, 1564, 1312, 1295, 1267, 1121, 935, 871, 774, 690.[341]

18.2.3.48. Synthesis of 1-hydroxy-N-(2-iodophenyl)-5-nitro-1H-indole-3-carboxamide (52)
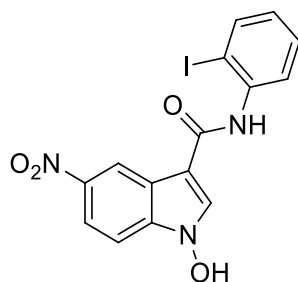
A 80°C solution containing 1-hydroxy-N-(2-iodophenyl)-5-nitro-1H-indole-3-carboxamide (271 mg, 1.0 mmol) and 4-nitro-nitrosobenzene (152 mg, 1.0 mmol) in toluene (10 mL) was stirred for 10 h. Precipitation of desired product was observed. After cooling to r.t., 1-hydroxy-N-(2-iodophenyl)-5-nitro-1H-indole-3-carboxamide was isolated by filtration (93 mg, 22 %) as a brown solid with no further purification. ^{1}H-NMR (DMSO-d_6) δ: 12.47 (bs, 1H), 9.71 (s, 1H), 9.11 (d, 1H, J = 2.3 Hz), 8.63 (s, 1H), 8.15 (dd, 1H, J = 9.1, 2.3 Hz), 7.94 (dd, 1H, J = 7.8, 1.1 Hz), 7.70 (d, 1H, J = 9.1 Hz), 7.51-7.43 (m, 2H), 7.06 (td, 1H, J = 7.6, 1.8 Hz) ppm.[341]

### 18.2.3.49. Synthesis of (5-nitro-1-hydroxy-3-indolyl)(1-ferrocenyl)methanone (53)
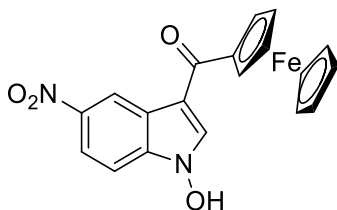
A 80°C solution of 4-nitro-nitrosobenzene (96 mg, 0.63 mmol) and 1-(ferrocene)prop-2-yn-1-one (150 mg, 0.63 mmol) in toluene (10 mL) was stirred for 24 h. Solvent is then removed under reduced pressure. Crude product is then purified by gravimetric column chromatography (*n*-hexane/EtOAc 6:4) to afford (5-nitro-1-hydroxy-3-indolyl)(1-ferrocenyl)methanone (115.5 mg, 49%) as a red solid. ^{1}H-NMR (DMSO-d_6) δ: 12.68 (br, 1H), 9.15 (s, 1H), 8.66 (s, 1H), 8.13 (dd, 1H, J_1 = 8Hz, J_2 = 2.3 Hz), 7.70 (d, 1H, J = 8 Hz), 5.05 (s, 2H), 4.64 (s, 2H), 4.24 (s, 5H) ppm. ^{13}C-NMR (DMSO-d_6) δ: 191.7, 142.9, 139.8, 136.1, 126.3, 118.7, 118.6, 117.5, 113.3, 80.8, 72.0, 70.7, 70.3 ppm. FT-IR (ATR): 3121, 1572, 1528, 1453, 1335, 1107, 1059, 815, 749 cm^{-1}. m.p.: > 300°C. MS (CI): *m/z*: 375 [M+1]. Elemental Analysis for $C_{19}H_{14}FeN_2O_3$: calcd. (%) C 60.99, H 3.77, N 7.49; found (%) C 61.05, H 3.88, N 7.41.[334]

18.2.3.50. Synthesis of 3-(ferrocene-1-carbonyl)-5-cyano-1H-indole (54)
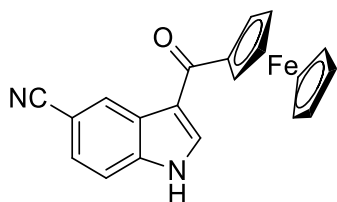
A 80° solution containing 1-(ferrocene)prop-2-yn-1-one (119 mg, 0.5 mmol) and 4-nitrosobenzonitrile (132 mg, 0.5 mmol) in toluene (10 mL) was stirred overnight. Reaction mixture was then filtered and mother liquors were dried under reduced pressure. Crude product was purified by flash column chromatography (DCM/*n*-hexane 8:2) to afford 3-(ferrocene-1-carbonyl)-5-cyano-1H-indole (80.5 mg, 69%) as dark red solid. ^{1}H-NMR (CDCl$_3$): δ 8.84 (s, 1H), 8.78 (br, 1H), 8.17-8.16 (d, J = 2.4 Hz, 1H), 7.58-7.56 (dd, J^1 = 8.4 Hz, J^2 = 2.3 Hz, 1H), 7.53-7.51 (d, J = 8.4 Hz, 1H), 4.99-4.98 (m, 2H), 4.57-4.58 (m, 2H), 4.23 (s, 5H).[341]

18.2.3.51. Synthesis of 3-(ferrocene-1-carbonyl)-1H-indole-5-carboxylic acid (55)
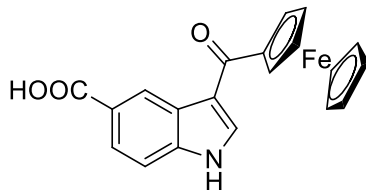
A 80°C solution containing 1-(ferrocene)prop-2-yn-1-one (110 mg, 0.46 mmol) and 4-nitrosobenzoic acid (151 mg, 1.0 mmol) in toluene (12 mL) was stirred overnight. Reaction mixture was then filtered and mother liquors were dried under reduced pressure. Crude product was purified by flash column chromatography to afford 3-(ferrocene-1-carbonyl)-1H-indole-5-carboxylic acid as dark red solid (80.5 mg, 47%) as dark red solid). ^{1}H-NMR (DMSO-d$_6$) δ: 12.8 (br, 1H), 8.97-8.96 (d, J = 2.1 Hz, 1H), 8.56 (s, 1H), 7.91-7.88 (dd, J^1 = 8.1 Hz, J^2 = 2.1 Hz), 7.57-7.55 (d, J = 8.1 Hz, 1H), 5.03 (s, 2H), 4.60 (s, 2H), 4.21 (s, 5H). MS (CI): *m/z* = 374 [M]+1.[341]

18.2.3.52. Synthesis of (1-hydroxy-5- nitro-1H-indol-3-yl)(naphthalen-1-yl)methanone (56)
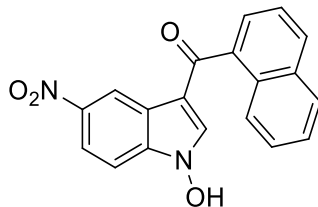

A 80°C solution of 4-nitro-nitrosobenzene (100 mg, 0.66 mmol) and 1-(naphthalen-1-yl)prop-2-yn-1-one (119 mg, 0.66 mmol) in toluene (10 mL) was stirred for 7.5 h. Precipitation of desired product was observed. After cooling to r.t., (1-hydroxy-5-nitro-1H-indol-3-yl)(naphthalen-1-yl)methanone was isolated by filtration (149 mg, 68%) as a dark yellow solid without any further purification. ^{1}H-NMR (DMSO-*d$_6$*) δ: 12.60 (br, 1H), 9.19 (d, 1H, J = 2.3 Hz), 8.24 (dd, 1H, J_1 = 9 Hz, J_2 = 2.3 Hz), 8.13 (d, 1H, J = 7 Hz), 8.11 (s, 1H), 8.06 (dd, 1H, J_1 = 7.9 Hz, J_2 = 0.7 Hz), 8.04 (d, 1H, J = 7.9 Hz), 7.77 (dd, 1H, J_1 = 7 Hz, J_2 = 1 Hz), 7.74 (d, 1H, J = 9 Hz), 7.63 (td, 1H, J_1 = 7 Hz, J_2 = 1 Hz), 7.59 (td, 1H, J_1 = 7.9 Hz, J_2 = 1.3 Hz), 7.55 (td, 1H, J_1 = 7.9 Hz, J_2 = 1.3 Hz) ppm. ^{13}C-NMR (DMSO-*d$_6$*) δ: 190.6, 143.6, 137.5, 137.2, 136.8, 133.4, 130.6, 130.0, 128.5, 127.1, 126.6, 126.5, 125.2, 125.0, 121.8, 119.0, 118.2, 113.1, 110.5 ppm. FT-IR (KBr disk): 1602, 1578, 1517, 1334, 775 cm^{-1}. m.p.: decomposition from 261°C. MS (CI): *m/z*: 333 [M+1]. Elemental Analysis for C$_{19}$H$_{12}$N$_2$O$_4$: calcd. (%) C 68.67, H 3.64, N 8.43; found (%) C 68.56, H 3.61, N 8.49.[334]

18.2.3.53. Synthesis of 3-(1-naphthoyl)-1-hydroxy-1H-indole-5-carbonitrile (57)
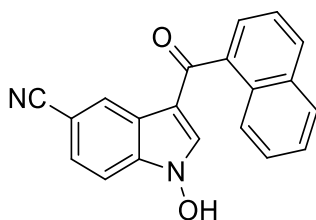
A 80°C solution of 4-cyano-nitrosobenzene (132 mg, 1 mmol) and 1-(naphthalen-1-yl)prop-2-yn-1-one (180 mg, 1 mmol) in toluene (10 mL) was stirred overnight. Precipitation of desired product was observed. After cooling to r.t., 3-(1-naphthoyl)-1-hydroxy-1H-indole-5-carbonitrile was collected by filtration (95 mg, 30%) as an orange solid without any further purification. ^{1}H-NMR (DMSO-d_6) δ: 12.54 (br, 1H), 8.66 (d, 1H, J = 1 Hz), 8.12 (d, 1H, J = 8.2 Hz), 8.04 (s, 1H), 8.03 (d, 2H, J = 8 Hz), 7.74 (dd, 1H, J_1 = 8 Hz, J_2 = 1 Hz), 7.73 – 7.72 (m, 2H), 7.63 (dd, 1H, J_1 = 8.2 Hz, J_2 = 1 Hz), 7.58 (td, 1H, J_1 = 8 Hz, J_2 = 1.4 Hz), 7.53 (td, 1H, J_1 = 8 Hz, J_2 = 1.4 Hz) ppm. ^{13}C-NMR (DMSO-d_6) δ: 190.6, 137.4, 136.5, 135.7, 133.5, 130.5, 130.0, 128.5, 127.1, 126.8, 126.6, 126.5, 125.2, 125.1, 122.3, 120.0, 112.0, 111.2, 105.2 ppm. FT-IR (KBr disk): 2221, 1571, 1509, 1364, 1341, 1225, 775 cm^{-1}. m.p.: 226 – 228°C. MS (CI): m/z: 313 [M+1]. Elemental Analysis for $C_{20}H_{12}N_2O_2$: calcd. (%) C 76.91, H 3.87, N 8.97; found (%) C 77.02, H 3.75, N 9.06.[334]

18.2.3.54. Synthesis of 5-bromo-1-hydroxy-3-(1-naphthoyl)-1*H*-indole (58)
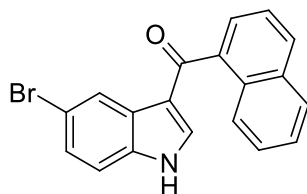
A 80°C solution of 4-bromo-nitrosobenzene (223 mg, 1.2 mmol) and 1-(naphthalen-1-yl)prop-2-yn-1-one (216 mg, 1.2 mmol) in toluene (12 mL) was stirred for 14 h. Precipitation of desired product was observed. After cooling to r.t., 5-bromo-1-hydroxy-3-(1-naphthoyl)-1*H*-indole was collected by filtration as a red–brown solid (130 mg, 37%) without any further purification. ^{1}H-NMR (DMSO-d_6) δ: 12.23 (s, 1H), 8.43 (d, 1H, J = 1.8 Hz), 8.09 (d, 1H, J = 8.1 Hz), 8.02 (d, 1H, J = 8.1 Hz), 7.99 (d, 1H, J = 8.1 Hz), 7.73 (d, 1H, J = 3.1 Hz), 7.69 (dd, 1H, ^3J = 8.1 Hz, ^4J = 1.3 Hz), 7.61 (t, 1H, J = 8.1 Hz), 7.57 (td, 1H, ^3J = 8.1 Hz, ^4J = 1.3 Hz), 7.54 (td, 1H, ^3J = 8.1 Hz, ^4J = 1.3 Hz), 7.50 (d, 1H, J = 8.5 Hz), 7.42 (dd, 1H, ^3J = 8.5 Hz, ^4J = 1.8 Hz) ppm. ^{13}C-NMR (DMSO-d_6) δ: 191.5, 138.1, 138.0, 135.8, 133.4, 130.1, 129.0, 128.5, 128.3, 127.7, 127.0, 126.5, 125.4, 125.3, 125.1, 123.7, 116.7, 115.1, 114.7 ppm. MS (CI): m/z: 351 [M+1]. FT-IR (KBr disk): 1599, 1510, 1413, 1223, 787 cm^{-1}.[341]

18.2.3.55. Synthesis of (1-hydroxy-1H-indol-3-yl)(naphthalen-1-yl)methanone (59) and 3-(1-naphthoyl)-1*H*-indole (60)
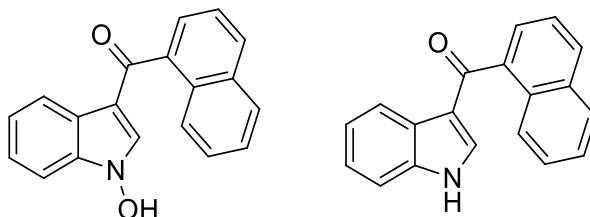
A 80°C mixture of nitrosobenzene (214 mg, 2 mmol) and 1-(naphthalen-1-yl)prop-2-yn-1-one (360 mg, 2 mmol) in toluene (16 mL) was stirred for 24 h. Reaction mixture was then removed under reduced pressure. Crude product was purified by gravimetric column chromatography (*n*-hexane/EtOAc 7:3), (1-hydroxy-1H-indol-3-yl)(naphthalen-1-yl)methanone (154 mg, 38%) and 1-hydroxy-3-(1-naphthoyl)-1*H*-indole (65 mg, 17%) were collected as dark orange solids. **(1-hydroxy-1H-indol-3-yl)(naphthalen-1-yl)methanone:** ^{1}H-NMR (DMSO-d_6) δ: 12.17 (br, 1H), 8.25 (dd, 1H, J_1 = 7.3 Hz, J_2 = 0.9 Hz), 8.08 (d, 1H, J = 8.1 Hz), 8.00 (td, 2H, J_1 = 7.3 Hz, J_2 = 0.9 Hz), 7.73 (s, 1H), 7.68 (dd, 1H, J_1 = 7 Hz, J_2 = 1.3 Hz), 7.61 (d, 1H, J = 8.1 Hz), 7.60 (t, 1H, J = 8.1 Hz), 7.57 − 7.49 (m, 2H), 7.35 (td, 1H, J_1 = 8 Hz, J_2 = 1.3 Hz), 7.30 (td, 1H, J_1 = 8 Hz, J_2 = 1.3 Hz) ppm. ^{13}C-NMR (DMSO-d_6) δ: 190.7, 138.4, 134.3, 134.0, 133.4, 130.1, 130.0, 128.5, 126.9, 126.4, 125.9, 123.3, 125.1, 123.8, 123.1, 122.7, 121.6, 111.6, 109.8 ppm. FT-IR (KBr disk): 1594, 1503, 1364, 1318, 1224, 787, 746 cm^{-1}. m.p.: 102.5°C. MS (CI): *m/z*: 288 [M+1]. Elemental Analysis for $C_{19}H_{13}NO_2$: calcd. (%) C 79.43, H 4.56, N 4.88; found (%) C 79.36, H 4.68, N 4.96.[334] **3-(1-naphthoyl)-1*H*-indole:** ^{1}H-NMR (CDCl₃): δ 11.52 (br, 1H), 8.14 (m, 1H), 7.90-8.02 (m, 3H), 7.79 (m, 1H), 7.49-7.60 (m, 2H), 7.24 (m, 1H), 7.12 (t, 1H, J = 7.7 Hz), 6.99 (m, 1H), 6.89 (m, 1H), 6.64 (t, 1H, J = 7.0 Hz). Other spectral data match the literature.[378]

18.2.3.56. Synthesis of (*E*)-1-hydroxy-3-(3-(2-nitrophenyl)acryloyl)-1H-indole-5-carbonitrile (61)

A 80°C solution of 4-cyano-nitrosobenzene (132 mg, 1 mmol) and (*E*)-1-(2-nitrophenyl)pent-1-en-4-yn-3-one (201 mg, 1 mmol) in toluene (11 mL) was stirred for 8 h. Precipitation of desired product was observed. After cooling to r.t., (*E*)-1-hydroxy-3-(3-(2-nitrophenyl)acryloyl)-1*H*-indole-5-carbonitrile was collected by filtration (110 mg, 33%) as dark yellow solid without any further purification. ^{1}H-NMR (acetone-d_6) δ: 11.53 (br, 1H), 8.89 (s, 1H), 8.83 (dd, 1H, J_1 = 1.4 Hz, J_2 = 0.7 Hz), 8.14 − 8.08 (m, 3H), 7.82 (td, 1H, J_1 = 7.6 Hz, J_2 = 0.8 Hz), 7.77 − 7.66 (m, 4H) ppm. ^{13}C-NMR (acetone-d_6) δ: 182.5, 149.3, 135.9, 135.7, 134.3, 133.4, 130.5, 130.4, 129.1, 128.1, 127.4, 126.6, 124.6, 122.7, 119.5, 112.8, 110.5, 105.9 ppm. FT-IR (KBr disk): 2924, 2854, 2225, 1643, 1603, 1514, 1452, 1345, 1205, 1069, 973, 740 cm^{-1}. m.p.: degradation from 270°C. MS (CI): *m/z*: 334

[M$^+$]. Elemental Analysis for $C_{18}H_{11}N_3O_4$: calcd. (%) C 64.87, H 3.33, N 12.61; found (%) C 65.01, H 3.19, N 12.74.[334]

18.2.3.57. Synthesis of (*E*)-1-(1-hydroxy-5-nitro-1H-indol-3-yl)-3-(2-nitrophenyl)prop-2-en-1-one (62)
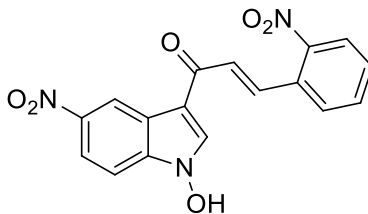
A 80°C solution of (*E*)-1-phenylpent-1-en-4-yn-3-one (201 mg, 1 mmol) and 4-nitro-nitrosobenzene (152 mg, 1.0 mmol) in toluene (10 mL) was stirred overnight. Precipitation of desired product was observed. (*E*)-1-(1-hydroxy-5-nitro-1H-indol 3-yl)-3-(2-nitrophenyl)prop-2-en-1-one was isolated by filtration (176 mg, 50%) as a brown solid. ^{1}H-NMR (DMSO-*d$_6$*) δ: 12.68 (br s, 1H), 9.21-9.20 (m, 2H), 8.22-8.19 (m, 2H), 8.08 (dd, 1H, *J* = 8.1, 1 Hz), 7.95 (d, 1H, *J* = 15.4 Hz), 7.86-7.82 (m, 2H), 7.74 (d, 1H, *J* = 9 Hz), 7.70 (dt, 1H, *J* = 8.3, 1.3 Hz). ^{13}C-NMR (DMSO-*d$_6$*) δ: 182.9, 149.3, 143.9, 137.2, 137.1, 135.8, 134.0, 131.2, 130.2, 129.7, 128.6, 125.1, 122.1, 119.5, 118.8, 113.8, 110.8. MS (CI): *m/z* = 354 [M]+. FT-IR (ATR): ν (cm^{-1}) = 1580, 1568, 1510, 1342, 1314, 1153, 1055, 969, 784. m.p.: decomp. > 300°C.[341]

18.2.3.58. Synthesis of (*E*)-1-(1H-indol-3-yl)-3-(2-nitrophenyl)prop-2-en-1-one (63)
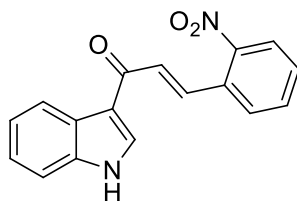
A 80°C solution containing (*E*)-1-phenylpent-1-en-4-yn-3-one (201 mg, 1 mmol) and nitrosobenzene (107 mg, 1.0 mmol) in toluene (10 mL) was stirred overnight. Reaction mixture was dried under reduced pressure. Crude product was then purified by flash column chromatography (*n*-hexane/EtOAc 7:3) to afford (*E*)-1-(1H-indol-3-yl)-3-(2-nitrophenyl)prop-2-en-1-one (155 mg, 53%) as a brown solid. ^{1}H-NMR (acetone-*d$_6$*) δ: 11.20 (br s, 1H), 8.58 (d, 1H, *J* = 3.2 Hz), 8.49-8.46 (m, 1H), 8.13-8.06 (m, 3H), 7.80 (td, 1H, *J* = 7.3, 1.3 Hz), 7.75 (d, 1H, *J* = 15.4 Hz), 7.68 (td, 1H, *J* = 8.5, 1.4 Hz), 7.55-7.53 (m, 1H), 7.29-7.26 (m, 2H). ^{13}C-NMR (acetone-*d$_6$*) δ: 183.0, 149.3, 137.2, 134.4, 133.8, 133.3, 130.8, 130.1, 129.0, 128.9, 126.3, 126.5, 124.5, 122.3, 122.1, 118.3, 111.9. MS (CI): *m/z* = 293 [M]+. FT-IR (ATR): ν (cm^{-1}) = 3359, 2953, 2924, 2854, 1691, 1642, 1521, 1343, 1153, 972, 854, 747. m.p.: 194-196°C.[341]

18.2.3.59. Synthesis of (*E*)-methyl 1-hydroxy-3-(3-(2-nitrophenyl)acryloyl)-1H-indole-7-carboxylate (64)
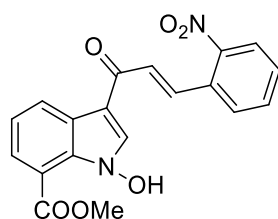
A 80°C solution containing (*E*)-1-phenylpent-1-en-4-yn-3-one (201 mg, 1 mmol) and 4-carbomethoxy-nitrosobenzene (165 mg, 1.0 mmol) in toluene (12 mL) was stirred for 24 h. Precipitation of desired product was observed. (*E*)-methyl 1-hydroxy-3-(3-(2-nitrophenyl)acryloyl)-1H-indole-7-carboxylate was isolated by filtration (88 mg, 24%) as a brown solid. ^{1}H-NMR (acetone-d_6) δ: 12.66 (bs, 1H), 8.85 (d, 1H, *J* = 7.6 Hz), 8.74 (s, 1H), 8.17 (d, 1H, J = 7.6 Hz), 8.12-8.07 (m, 2H), 8.02 (d, 1H, J = 7.9 Hz), 7.84-7.77 (m, 2H), 7.70 (m, 1H), 7.42 (t, 1H, J = 7.9 Hz), 4.10 (s, 3H).^{13}C-NMR (acetone-d_6) δ: 182.3, 169.6, 166.0, 149.4, 139.6, 135.2, 133.3, 131.3, 130.3, 129.1, 128.9, 128.5, 127.6, 125.3; 124.6, 123.1, 122.0, 112.7, 53.2. MS (CI): m/z = 367 [M]+. IR (film): ν (cm^{-1}) = 3447, 1684, 1654, 1559, 1521, 1507, 1437, 1340, 1266, 1199, 1143, 756. m.p.: 202-205°C.[341]

18.2.3.60. Synthesis of 1-(1-hydroxy-5-nitro-1H-indol-3-yl)-2-phenylethanone (65)
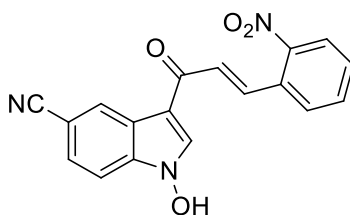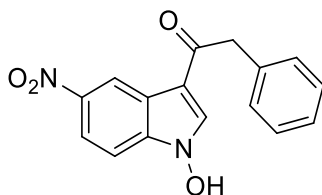

A 80°C solution of 4-nitro-nitrosobenzene (152 mg, 1 mmol) and 1-phenylbut-3-yn-2-one (144 mg, 1 mmol) in toluene (10 mL) was stirred for 8 h. Precipitation of desired product was observed. After cooling to r.t., 1-(1-hydroxy-5-nitro-1*H*-indol-3-yl)-2-phenylethanone was collected by filtration (35 mg, 27%) as yellow solid without any further purification. ^{1}H-NMR (DMSO-d_6) δ: 12.62 (br, 1H), 9.04 (s, 1H), 8.98 (s, 1H), 8.15 (d, 1H, 8 Hz), 7.68 (d, 1H, *J* = 8 Hz), 7.30 (m, 5H), 4.18 (s, 2H) ppm. ^{13}C-NMR (DMSO-d_6) δ: 192.8, 143.6, 137.0, 136.7, 136.2, 129.9, 128.7, 126.9, 121.8, 119.1, 118.5, 112.4, 110.6, 46.1 ppm. MS (CI): *m/z*: 297 [M$^+$]. Elemental Analysis for $C_{16}H_{12}N_2O_4$: calcd. (%) C 64.86, H 4.08, N 9.46; found (%) C 64.72, H 4.11, N 9.56.[334]

18.2.3.61. Synthesis of (1-hydroxy-5-nitro-1H-indol-3-yl)(3'-nitro-[1,1'-biphenyl]-2-yl)methanone (66)
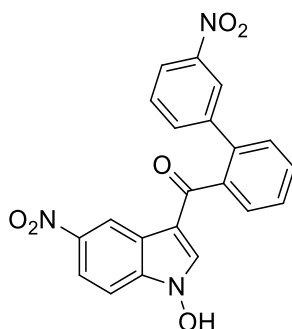
A 80°C solution containing 1-(3'-nitro-[1,1'-biphenyl]-2-yl)prop-2-yn-1-one (251 mg, 1 mmol) and 4-nitro-nitrosobenzene (152 mg, 1.0 mmol) in toluene (11 mL) was stirred 10 h. Precipitation of desired product was observed. After cooling to r.t., (1-hydroxy-5 nitro-1H-indol-3-yl)(2'-nitro-[1,1'-biphenyl]-2-yl)methanone is isolated by filtration and subsequent recrystallization from ethanol as a brown solid (129 mg, 32%). ^{1}H-NMR (DMSO-d_6) δ: 14.78 (br s, 1H), 9.71 (s, 1H), 9.52 (d, 1H, J = 1.8 Hz), 8.94 (d, 1H, J = 8.3 Hz), 8.56 (d, 1H, J = 8.0 Hz), 8.49-8.36 (m, 5H), 8.35 (dd, 1H, J = 9, 1.8 Hz), 7.96 (t, 1H, J = 7.2 Hz), 7.83 (t, 1H, J = 7.4 Hz). ^{13}C-NMR (DMSO-d_6) δ: 166.2, 157.2, 148.7, 148.3, 145.3, 144.8, 136.5, 133.4, 132.8, 129.2, 128.4, 126.2, 125.6, 125.4, 125.2, 124.2, 123.9, 122.4, 121.9, 119.6, 112.8. MS (CI): m/z = 404 [M]+. FT-IR (ATR): ν (cm^{-1}) = 1663, 1568, 1532, 1342, 1338, 1125, 969, 800.[341]

18.2.3.62. Synthesis of (5-nitro-1H-indol-3-yl)(thiazol-2-yl)methanone (67)
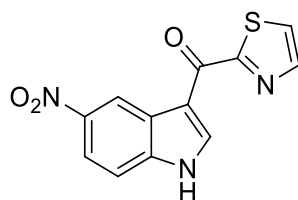
To a 80°C solution of raw 1-(thiazol-2-yl)prop-2-yn-1-one (0.214 g, 1.57 mmol) in toluene (10 mL), a solution of 4-nitro-nitrosobenzene (0.229 g, 1.57 mmol) in toluene (10 mL) was added dropwise. Reaction mixture was stirred at 80°C for 3 h. Reaction mixture was then filtered and mother liquors were dried under reduced pressure and inert atmosphere. Isolated brown oil was immediately analyzed through GC-MS.

18.2.3.63. Synthesis of 3-benzoyl-2-bromo-1-hydroxy-5-nitro-1*H*-indole (68)
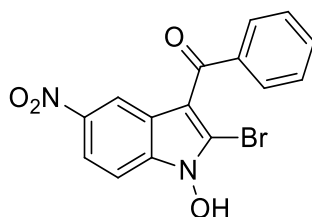
A 80°C solution of 4-nitro-nitrosobenzene (152 mg, 1 mmol) and 3-bromo-1-phenyl-2-propyn-1-one (209 mg, 1 mmol) in toluene (8 mL) was stirred overnight. Precipitation of desired product was observed. After cooling to r.t., 3-benzoyl-2-bromo-1-hydroxy-5-nitro-1*H*-indole was isolated by filtration (183 mg, 56%) as light brown solid with no further purification. ^{1}H-NMR (DMSO-d_6) δ: 12.87 (br, 1H), 8.50 (d, 1H, J = 1.6 Hz), 8.17 (dd, 1H, J_1 = 9.2 Hz, J_2 = 1.6 Hz), 7.74 (m, 3H), 7.68 (t, 1H, J = 7.6 Hz), 7.56 (t, 2H, J = 7.6 Hz) ppm. ^{13}C-NMR (DMSO-d_6) δ: 189.7, 142.8, 138.8, 135.9, 132.5, 128.95, 128.55, 122.3, 121.9, 118.6, 116.7, 116.6, 111.9, 110.0 ppm. FT-IR (ATR): 3123, 2571, 1599, 1558, 1520, 1357, 1333, 1213, 736 cm^{-1}. m.p.: 224°C. Elemental Analysis for C$_{15}$H$_9$BrN$_2$O$_4$: calcd. (%) C 49.89, H 2.51, N 7.76; found (%) C 50.19, H 2.62, N 7.39.

18.2.3.64. Synthesis of 3-benzoyl-2,5-dibromo-1*H*-indole (69)
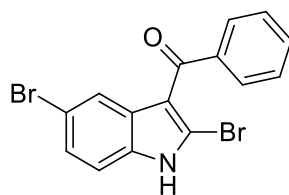
A 80°C solution of 4-bromo-nitrosobenzene (186 mg, 1 mmol) and 3-bromo-1-phenylprop-2-yn-1-one (105 mg, 0.8 mmol) in toluene (8 mL) was stirred for 24 h. Solvent was removed under reduced pressure. Crude material was purified by gravimetric column chromatography (*n*-hexane/EtOAc 3:1) to afford 3-benzoyl-2,5-dibromo-1*H*-indole (98 mg, 26%) as brown solid. : ^{1}H-NMR (CDCl$_3$) δ: 8.59 (br, 1H), 7.78 (s, 1H), 7.78 (s, 1H), 7.72 (d, 2H, *J* = 7.6 Hz), 7.52 (t, 1H, *J* = 7.2 Hz), 7.42 (m, 3H), 7.29 (d, 1H, J = 7.6 Hz), 7.16 (m, 2H) ppm.

18.2.3.65. Synthesis of 3-benzoyl-2-bromo-1*H*-indole (70)
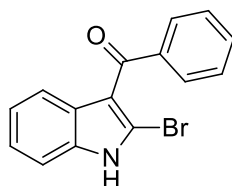
A 80°C solution of nitrosobenzene (106 mg, 1 mmol) and 3-bromo-1-phenylprop-2-yn-1-one (209 mg, 1 mmol) in toluene (8 mL) was stirred for 24 h. Solvent was removed under reduced pressure. Crude product was purified by gravimetric column chromatography (*n*-hexane/EtOAc 5:1) to afford 3-benzoyl-2-bromo-1*H*-indole (82 mg, 28%) as a brown solid. ^{1}H-NMR (CDCl$_3$) δ: 8.74 (br, 1H), 7.82 (d, 2H, *J* = 8 Hz), 7.62 (d, 1H, *J* = 8 Hz), 7.57 (d, 1H, *J* = 8 Hz), 7.47 (t, 2H, *J* = 8 Hz), 7.36 (d, 1H, *J* = 8 Hz), 7.25 (m, 1H), 7.16 (t, 1H, *J* = 8 Hz) ppm.

18.2.3.66. Synthesis of methyl 3-benzoyl-2-bromo-1H-indole-7-carboxylate (71)
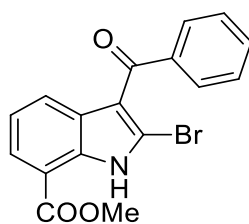
A 80°C solution of 2-carbomethoxy-nitrosobenzene (165 mg, 1 mmol) and 3-bromo-1-phenylprop-2-yn-1-one (209 mg, 1 mmol) in toluene (8 mL) was stirred for 24 h. Solvent was evaporated then evaporated under reduced pressure. Crude material was purified by gravimetric column chromatography (DCM/*n*-hexane 3:1) to afford methyl 3-benzoyl-2-bromo-1H-indole-7-carboxylate (196 mg, 57%) as a yellow solid. ^{1}H-NMR (CDCl$_3$) δ: 12.26 (br, 1H), 7.81 (d, 1H, *J* = 8 Hz), 7.76 (d, 2H, *J* = 7.6 Hz), 7.58 (m, 3H), 7.30 (t, 1H, *J* = 7.6 Hz), 3.96 (s, 3H) ppm.

18.2.3.67. Synthesis of 3-(4-methoxybenzoyl)-2-methyl-5-nitro-1*H*-indole (72)
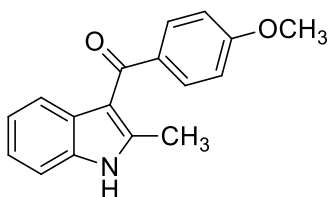
A 80° solution of nitrosobenzene (428 mg) and 1-(4-methoxyphenyl)but-2-yn-1-one (697 mg) in toluene (20 mL) was stirred for 48 h. Solvent was then removed under reduced pressure. Crude product was purified by gravimetric column chromatography (n-hexane/EtOAc 1:1) to afford 3-(4-methoxybenzoyl)-2-methyl-5-nitro-1*H*-indole (170 mg, 16%) as brown solid. ^{1}H-NMR (DMSO-d_6) δ: 11.84 (s, 1H); 7.61 (dd, 2H, ^3J = 8.7 Hz, ^4J = 2.1 Hz), 7.36 (d, 1H, J = 8.0 Hz), 7.32 (d, 1H, J = 8.0 Hz), 7.09 (td, 1H, ^3J = 8.0 Hz, ^4J = 1.2 Hz), 7.02 (dd, 2H, ^3J = 8.7 Hz, ^4J = 2.1 Hz), 6.97 (td, 1H, ^3J = 8.0 Hz, ^4J = 1.2 Hz), 3.83 (s, 3H), 2.40 (s, 3H) ppm. ^{13}C-NMR (DMSO-d_6) δ: 189.8, 162.0, 143.5, 135.0, 133.7, 129.9, 127.3, 121.8, 120.9, 120.0, 113.7, 112.8, 111.4, 55.5, 14.2. MS (CI): *m/z*: 266 [*M*+1].[341]

♦ ♦ ♦ ♦ ♦ ♦

18.2.4. Reactivity and functionalization of *N*-hydroxy-3-aroylindoles and 3-aroylindoles

18.2.4.1.   Synthesis of 3-benzoyl-1-methoxy-5-nitro-1*H*-indole (3)
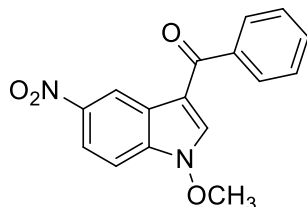
To a r.t. solution of 3-benzoyl-1-hydroxy-5-nitro-1*H*-indole (100 mg, 0.35 mmol) in MeOH (15 mL), K$_2$CO$_3$ (294 mg, 2.13 mmol) and Me$_2$SO$_4$ (270 µL, 2.85 mmol) were added. Reaction mixture was then r.t. stirred for 24 h. Then extra Me$_2$SO$_4$ (270 µL, 2.85 mmol) was added. After extra 24 h reaction mixture was filtered. Liquid phases were evaporated under reduced pressure, dissolved in DCM and washed with water. Organic phases were dried over Na$_2$SO$_4$, filtered and evaporated under reduced pressure to afford 3-benzoyl-1-methoxy-5-nitro-1*H*-indole (101 mg, 96%) as dark yellow solid without any further purification. ^{1}H-NMR (DMSO-d_6) δ: 9.17 (d, 1H, J = 2.4 Hz), 8.71 (s, 1H), 8.27 (dd, 1H, J$_1$ = 8.8 Hz, J$_2$ = 2.4 Hz), 7.88 (m, 3H), 7.69 (t, 1H, J = 8 Hz), 7.59 (t, 2H, J = 8 Hz), 4.24 (s, 3H) ppm. ^{13}C-NMR (DMSO-d_6) δ: 189.5, 144.1, 139.4, 136.1, 135.3, 132.5, 129.2, 129.1, 122.6, 119.8, 118.9, 112.3, 110.4, 67.9 ppm. FT-IR (KBr disk): 1631, 1519, 1449, 1382, 1334, 706 cm^{-1}. m.p.: 245°C. MS (CI): *m/z*: 297 [M+1]. Elemental Analysis for C$_{16}$H$_{12}$N$_2$O$_4$: calcd. (%) C 64.86, H 4.08, N 9.46; found (%) C 64.67, H 4.11, N 9.52.[334]

18.2.4.2. Synthesis of 3-benzoyl-2-bromo-1-methoxy-5-nitro-1*H*-indole (73)
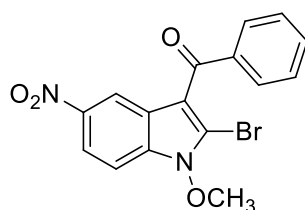
To a r.t. solution of 3-benzoyl-3-bromo-1-hydroxy-5-nitro-1*H*-indole (250 mg, 0.69 mmol) and CH$_3$I (172 µL, 2.76 mmol) in MeOH (10 mL), NEt$_3$ (220 µL, 1.6 mmol) was added and reaction mixture was stirred 72 h. Solvent was then removed under reduced pressure. Crude product was purified by gravimetric column chromatography (*n*-hexane/DCM 1:1) to afford 3-benzoyl-2-bromo-1-methoxy-5-nitro-1*H*-indole (165 mg, 64%) as white solid. ^{1}H-NMR (DMSO-d_6) δ: 8.58 (d, 1H, J = 1.6 Hz), 8.30 (dd, 1H, J = 8.8, 1.6 Hz), 7.97 (d, 1H, J = 8.8 Hz), 7.85 (d, 2H, J = 9.2 Hz), 7.76 (t, 1H, J = 9.2 Hz), 7.63 (t, 2H, J = 9.2 Hz), 4.30 (s, 3H) ppm. ^{13}C-NMR (CDCl$_3$) δ: 189.3, 143.2, 134.1, 132.4, 128.9, 128.1, 122.3, 118.8, 118.6, 117.1, 113, 108.8, 66.5 ppm. m.p.: 174°C. Elemental Analysis for C$_{16}$H$_{11}$BrN$_2$O$_4$: calcd. (%) C 51.22, H 2.96, N 7.47; found (%) C 50.67, H 3.22, N 7.56. FT-IR (ATR): 3113, 1632, 1520, 1328, 900, 739 cm^{-1}.

18.2.4.3. Synthesis of 3-(2-bromobenzoyl)-1-methoxy-5-nitro-1*H*-indole (74)
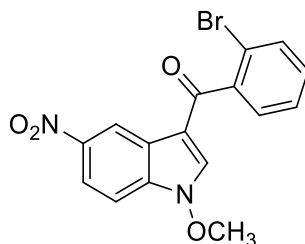
To a r.t. solution of 3-(2-bromobenzoyl)-1-hydroxy-5-nitro-1*H*-indole (40 mg, 0.11 mmol) in MeOH (10 mL), K$_2$CO$_3$ (92 mg, 0.66 mmol) and Me$_2$SO$_4$ (63 µL, 0.66 mml) were added. Reaction mixture was then r.t. stirred 24 h and filtered. Mother liquors were dried under reduced pressure, dissolved in DCM and washed with water. Organic phases were dried over Na$_2$SO$_4$, filtered and evaporated under reduced pressure to afford 3-(2-bromobenzoyl)-1-methoxy-5-nitro-1*H*-indole (40 mg, 96%) as a yellow solid without any further purification. ^{1}H-NMR (CDCl$_3$) δ: 9.30 (d, 1H, ^4J = 2.0 Hz), 8.30 (dd, 1H, ^3J = 9.0 Hz, ^4J = 2.0 Hz), 7.70 (d, 1H, J = 7.8 Hz), 7.67 (s, 1H), 7.58 (d, 1H, J = 9.0 Hz), 7.42 − 7.49 (m, 2H), 7.37 − 7.40 (m, 1H), 4.22 (s, 3H) ppm. ^{13}C-NMR (CDCl$_3$) δ: 188.9, 144.7, 141.2, 135.2, 134.0, 133.5, 131.3, 128.6, 127.4, 121.9, 120.0 , 119.9, 113.9, 109.0, 67.4 ppm. FT-IR (KBr disk): 1639, 1583, 1523, 1454, 1365, 1340, 744 cm^{-1}.[341]

18.2.4.4. Synthesis of 3-(2-iodobenzoyl)-1-methoxy-5-nitro-1*H*-indole (75)
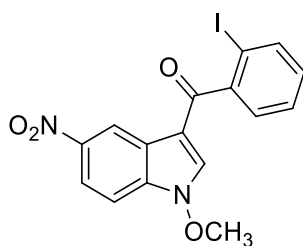
To a r.t. solution of 3-(2-iodobenzoyl)-1-hydroxy-5-nitro-1*H*-indole (25 mg, 0.06 mmol) in MeOH (10 mL), K_2CO_3 (51 mg, 0.37 mmol) and Me_2SO_4 (35 µL, 0.37 mmol) were added. Reaction mixture was r.t. stirred 24 h then filtered. Mother liquors were dried under reduced pressure, dissolved in DCM and washed with water. Organic phases were dried over Na_2SO_4, filtered and evaporated under reduced pressure to afford 3-(2-iodo-benzoyl)-1-methoxy-5-nitro-1*H*-indole as yellow solid (23 mg, 89%) characterized without any further purification. ^{1}H-NMR (CDCl$_3$) δ: 9.29 (d, 1H, ^4J = 2.2 Hz), 8.29 (dd, 1H, ^3J = 9.0 Hz, ^4J = 2.2 Hz), 7.98 (dd, 1H, ^3J = 8.0 Hz, ^4J = 1.0 Hz), 7.48 (dd, 1H, ^3J = 8.0 Hz, ^4J = 1.0 Hz), 7.47 (d, 1H, J = 9.0 Hz), 7.45 (s, 1H), 7.42 (td, 1H, ^3J = 7.5 Hz, ^4J = 1.8 Hz), 7.22 (td, 1H, ^3J = 7.5 Hz, ^4J = 1.8 Hz), 3.91 (s, 3H) ppm. ^{1}H-NMR (DMSO-d_6) δ: 9.02 (d, 1H, J = 1.8 Hz), 8.23 (dd, 1H, 3J = 9.0 Hz, 4J = 1.8 Hz), 7.99 (d, 1H, J = 7.4 Hz), 7.98 (s, 1H), 7.82 (d, 1H, J = 9.0 Hz), 7.55 (t, 1H, J = 7.4 Hz), 7.48 (d, 1H, J = 7.3 Hz), 7.30 (t, 1H, J = 7.4 Hz), 3.92 (s, 3H) ppm. ^{13}C-NMR (DMSO-d_6) δ: 190.8, 145.1, 143.6, 143.4, 140.7, 139.3, 131.3, 128.1, 128.0, 125.2, 118.6, 117.5, 115.3, 112.2, 93.0, 33.8 ppm. FT-IR (KBr disk): 1611, 1583, 1522, 1464, 1379, 1334, 739 cm^{-1}.[341]

18.2.4.5. Synthesis of (1-methoxy-5-nitro-1H-indol-3-yl)(1-methyl-1H-indol-3-yl)methanone (76)
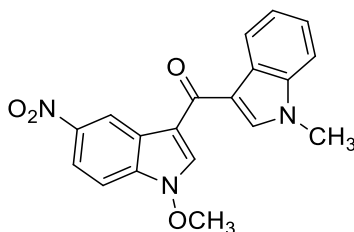
To a suspension of -(1-methyl-1*H*-indol-3-yl)prop-2-yn-1-one (72 mg, 0.23 mmol) in MeOH (3 mL), K_2CO_3 was added (189 mg, 1.38 mmol). Then Me_2SO_4 (35 µL, 0.37 mmol) was added. Reaction mixture was stirred for 20 h. DCM was added and organic phase is washed with water, then dried with $MgSO_4$, filtered and dried under reduced pressure to afford (1-methoxy-5-nitro-1H-indol-3-yl)(1-methyl-1H-indol-3-yl)methanone (80 mg, quantitative yield) as brown solid. ^{1}H-NMR (CDCl$_3$): δ 9.29 (d, J = 2.1 Hz, 1H), 8.39 (d, J = 8.1 Hz, 1H), 8.25 (dd, J = 2.2 Hz, J = 9 Hz, 1H), 7.99 (s, 1H), 7.69 (s, 1H), 7.55 (dd, J = 9.6 Hz, J = 0.3 Hz, 1H), 7.41-7.35 (m, 3H), 4.23 (s, 1H), 3.90 (s, 1H).[341]

18.2.4.6. Synthesis of pravadoline (77)
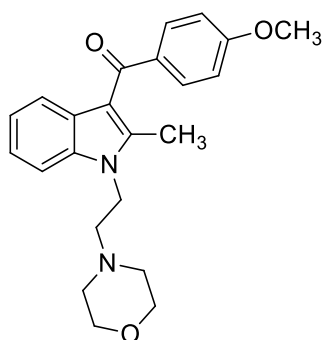
3-(4-methoxybenzoyl)-2-methyl-5-nitro-1*H*-indole (132.5 mg, 0.5 mmol) was dissolved in anhydrous DMF and solution was cooled to 0 °C. NaH 60% dispersion in paraffin (22 mg, 0.55 mmol) was added in small portions over a period of 15 min. Then reaction mixture was stirred at 0 °C for 0.5 h before 4-(2-bromo-ethyl)morpholine (97 mg, 0.5 mmol) was added. Reaction was then stirred r.t. for 48 h. Then mixture was quenched with water, extracted with diethylether, washed with water, brine, dried over MgSO₄ and filtered. Organic phase was dried under reduced pressure. Crude product was purified by gravimetric column chromatography (petroleum ether/EtOAc 5:1) to afford pravadoline (181 mg, 96%) as white solid[379]. ¹H-NMR (CDCl₃) δ: 7.78 (d, J = 8.7 Hz, 2H), 7.40 – 7.30 (m, 2H), 7.20 (t, *J* = 7.3 Hz, 1H), 7.07 (t, *J* = 7.5 Hz, 1H), 6.93 (d, *J* = 8.7 Hz, 2H), 4.27 (t, *J* = 6.9 Hz, 2H), 3.88 (s, 3H), 3.80 – 3.66 (m, 4H), 2.71 (t, *J* = 7.0 Hz, 2H), 2.61 (s, 3H), 2.53 (s, 4H). Other spectral data match the literature.[379]

18.2.4.7. Synthesis of naphthalen-1-yl(1-pentyl-1H-indol-3-yl)methanone (JWH-018) (78)
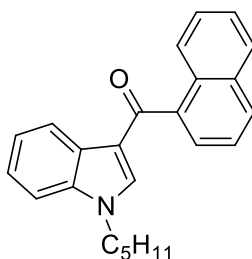
A r.t mixture of 1-hydroxy-3-(1-naphthoyl)-1*H*-indole (211 mg, 0.73 mmol), *n*-pentyl bromide (293 mg, 1.94 mmol), KOH (108.6 mg, 1.94 mmol) in MeCN (10 mL) was stirred for 24 h. Solvent was removed under reduced pressure. Crude product was diluted in DCM and washed with aqueous 5% NaOH. Reunited organic phases were dried with MgSO₄, filtered and solvent removed under reduced pressure. Crude product was then purified by gravimetric column chromatography (*n*-hexane/DCM 4:6) to afford JWH-018 (53 mg, 20%) as a brown solid. ¹H-NMR (CDCl₃) d 8.49 (m, 1H), 8.19 (d, 1H, *J* = 8.4 Hz), 7.97 (d, 1H, *J* = 8.2 Hz), 7.91 (d, 1H, *J* = 8.1 Hz), 7.66 (d, 1H, J = 6.9 Hz), 7.53 (t, 1H, *J* = 7.5 Hz), 7.52 (t, 1H, *J* ¼=7.1 Hz), 7.47 (t, 1H, *J* = 7.6 Hz), 7.41-7.35 (m, 4H), 4.07 (t, 2H, *J* = 7.3 Hz), 1.81 (quin, 2H, *J* = 7.4 Hz), 1.28 (m, 4H), 0.85 (t, 3H, *J* = 7.0 Hz).[334] Other spectral data match the literature.[380]

18.2.4.8. Synthesis of naphthalen-1-yl(1-butyl-1H-indol-3-yl)methanone (JWH-073) (79)
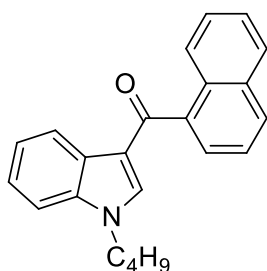
A r.t mixture of 1-hydroxy-3-(1-naphthoyl)-1*H*-indole (211 mg, 0.73 mmol), *n*-butyl bromide (264 mg, 1.94 mmol), KOH (108.6 mg, 1.94 mmol) in acetone (10 mL) was stirred for 24 h. Solvent was removed under reduced pressure. Crude product was diluted in DCM and washed with aqueous 5% NaOH. Reunited organic phases were dried with $MgSO_4$, filtered and solvent removed under reduced pressure. Crude product was then purified by gravimetric column chromatography (*n*-hexane/DCM 4:6) to afford JWH-073 (179 mg, 75%) as a brown solid. ^{1}H-NMR (CDCl₃) δ: 8.48 (m, 1H), 8.18 (d, **J** = 8.4 Hz, 1H), 7.97 (d, *J* = 8.0 Hz, 1H), 7.90 (d, *J* = 7.6 Hz, 1H), 7.65 (dd, *J* = 1.2 Hz, 1H), 7.54-7.44 (m, 3H), 7.40-7.33 (m, 4H), 4.06 (t, *J* = 7.2 Hz, 2H), 1.82-1.75 (q, 2H), 1.33-1.25 (q, 2H), 0.91-0.88 (t, *J* = 7.2 Hz, J = 7.6 Hz, 3H). Other spectral data match the literature.[381]

18.2.4.9. Synthesis of (*E*)-3-((3-benzoyl-5-nitro-1H-indol-1-yl)oxy)-1-phenylprop-2-en-1-one (80)
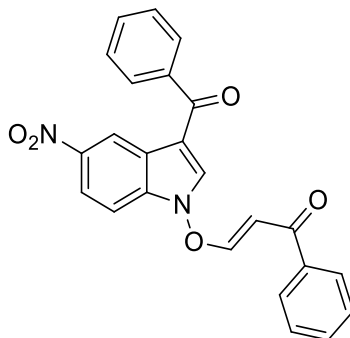
To a r.t. solution of 3-benzoyl-1-hydroxy-5-nitro-1*H*-indole (10 mg, 35 µmol) in MeCN (2 mL), DABCO (5 mg, 39 µmol) and 1-phenylprop-2-yn-1-one (6 mg, 42 µmol) were added. Mixture was stirred for 5 minutes, then evaporated under reduced pressure with no heating. Crude product was dissolved in EtOAc and washed with water and brine. Organic phases were dried over Na_2SO_4, filtered and evaporated under reduced pressure with no heating to afford (*E*)-3-(5-nitro-3-(phenylcarbonyl)-1*H*indol-1-yloxy)-1-phenylprop-2-en-1-one (13 mg, 80%) as orange solid without any further purification. ^{1}H-NMR (CDCl₃) δ: 9.44 (d, 1H, *J* = 2.0 Hz), 8.36 (dd, 1H, ^3J =9.0 Hz, ^4J =2.0 Hz), 8.01 (d, 1H, *J* = 11.9 Hz), 7.95 (s, 1H), 7.89 (dd, 2H, ^3J = 7.2 Hz, ^4J = 1.2 Hz), 7.77 (d, 2H, *J* = 7.2Hz), 7.64 – 7.69 (m, 2H), 7.58 (d, 1H, *J* =9.0 Hz), 7.56 – 7.57 (m, 2H), 7.45 (t, 2H, *J* = 7.6Hz), 6.45 (d, 1H, *J* = 11.9 Hz) ppm. MS (CI): *m/z*: 413 [*M*+1].[341]

18.2.4.10. Synthesis of (*E*)-methyl 3-((3-benzoyl-5-nitro-1H-indol-1-yl)oxy)acrylate (81)
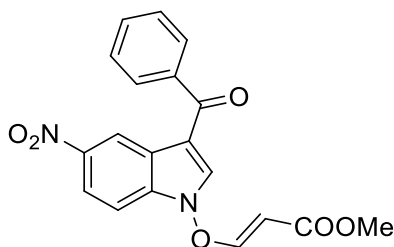
To a r.t. solution of 3-benzoyl-1-hydroxy-5-nitro-1*H*-indole (200 mg, 0.71 mmol) in MeCN (30 mL), DABCO (88 mg, 0.78 mmol) and methylpropiolate (76 μL, 0.85 mmol) were added. Mixture was stirred at r.t. for 5 minutes, then evaporated under reduced pressure with no heating. Crude product was dissolved in EtOAc and washed with water and brine. Organic layers were dried over Na_2SO_4, filtered and evaporated under reduced pressure with no heating to afford (*E*)-methyl 3-((3-benzoyl-5-nitro-1H-indol-1-yl)oxy)acrylate (220 mg, 85%) as an orange solid without any further purification. ^{1}H-NMR (CDCl$_3$) δ: 9.36 (d, 1H, *J* = 2.1 Hz), 8.29 (dd, 1H, ^3J = 9.0 Hz, ^4J = 2.1 Hz), 7.89 (d, 1H, *J* = 12.3 Hz), 7.88 (s, 1H), 7.84 (dd, 1H, 3*J* = 7.3 Hz, 4*J* = 1.3 Hz), 7.60 – 7.62 (m, 1H), 7.53 (t, 1H, *J* = 7.3 Hz), 7.47 (d, 1H, *J* = 9.0 Hz), 5.30 (d, 1H, *J* = 12.3 Hz), 3.72 (s, 3H) ppm. ^{13}C-NMR (CDCl$_3$) δ: 186.4, 165.3, 160.5, 144.9, 138.9, 135.0, 132.4, 128.8, 128.7, 122.6, 120.7, 120.2, 114.6, 109.0, 101.5, 52.2 ppm. MS (CI): *m/z*: 367 [*M*+1]. FT-IR (KBr disk): 1720, 1634, 1526, 1443, 1380, 1335, 1089 cm^{-1}.[341]

18.2.4.11. Synthesis of methyl 2-(3-benzoyl-5-nitro-1H-indol-7-yl)-3-oxopropanoate (82)
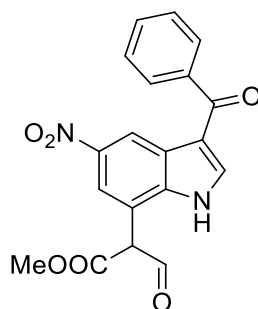
(*E*)-methyl 3-((3-benzoyl-5-nitro-1H-indol-1-yl)oxy)acrylate (150 mg, 0.41 mmol) was dissolved in MeCN (15 mL) and reaction mixture was refluxed for 2 h. Solvent was then removed under reduced pressure. Crude product was purified by gravimetric column chromatography (*n*-hexane/EtOAc 6:4) to afford methyl 2-(3-benzoyl-5-nitro-1H-indol-7-yl)-3-oxopropanoate (61 mg, 41%) as yellow solid. ^{1}H-NMR (CDCl$_3$) δ: 8.92 (br, 1H), 8.86 (s, 1H), 8.54 (d, 1H, *J* = 1.9 Hz), 8.17 (d, 1H, *J* = 1.9 Hz), 7.84 (d, 2H, *J* = 8.0 Hz), 7.63 (d, 1H, *J* = 2.4 Hz), 7.60 (t, 1H, *J* = 8.0 Hz), 7.33 (t, 2H, *J* = 8.0 Hz), 3.91 (s, 3H) ppm. MS (CI): *m/z*: 366 [*M*+1]. FT-IR (KBr disk): 1721, 1636, 1436, 1383, 1100 cm^{-1}.[341]

18.2.4.12. Synthesis of dimethyl 5-methoxy-7-methyl-2-nitro-12-oxo-7,12-dihydroindolo[2,3-b]carbazole-6,6(5*H*)-dicarboxylate (83)
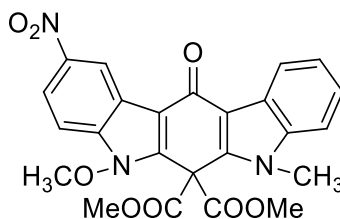
To a solution of (1-methoxy-5-nitro-1H-indol-3-yl)(1-methyl-1H-indol-3-yl)methanone (50 mg, 0.15 mmol) in AcOH (5 mL), dimethylmalonate (71 μL, 0.623 mmol) and Mn(OAc)$_3$ trihydrate (237 mg, 0.885 mmol) were added and mixture was stirred 16 h. EtOAc was then added and organic phase was washed with aqueous sodium bisulfite and brine, dried with MgSO$_4$, filtered and evaporated under reduced pressure. Crude product was purified by gravimetric column chromatography to afford dimethyl 5-methoxy-7-methyl-2-nitro-12-oxo-7,12-dihydroindolo[2,3-b]carbazole-6,6(5*H*)-dicarboxylate (56 mg, 78%) as brown solid. ^{1}H-NMR (CDCl$_3$): δ 9.47 (d, 1H, *J* = 2.1 Hz), 8.54 (d, *J* = 6.6 Hz, 1H), 8.29 (dd, *J* = 9 Hz, *J* = 2.2 Hz, 1H), 7.58 (d, *J* = 9 Hz, 1H), 7.44-7.39 (m, 3H), 4.31 (s, 1H), 3.96 (s, 1H), 3.82 (s, 1H).[341]

18.2.4.13. Synthesis of dimethyl 5-methoxy-2-nitro-11-oxo-5H-benzo[b]carbazole-6,6(11H)-dicarboxylate (84)
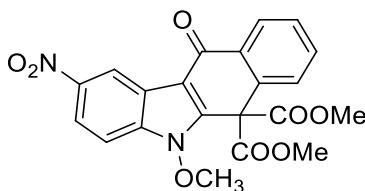
To a solution of 3-benzoyl-1-methoxy-5-nitro-1*H*-indole (50 mg, 0.17 mmol) in AcOH (5 mL) under nitrogen, dimethylmalonate (79 μL, 0.623 mmol) and Mn(OAc)$_3$ trihydrate (267 mg, 1 mmol) were added. Reaction mixture was then heated to 80°C and stirred 24 h. Reaction mixture was then poured onto 10 mL EtOAc and washed with aqueous sodium bisulfite. Organic phase was then washed with brine, dried with MgSO$_4$ and evaporated under reduced pressure. Crude product was then purified by gravimetric column chromatography (*n*-hexane/EtOAc 3:7) to afford final product as a brown solid (48 mg, 67%). ^{1}H-NMR (CDCl$_3$) δ: 9.42 (d, 1H, *J* = 2.1 Hz), 8.42 (dd, 1 Hz, *J$_1$* = 7.4 Hz, *J$_2$* = 1.6 Hz), 8.34 (dd, 1H, *J$_1$*= 2.2 Hz, *J$_2$*= 9 Hz), 7.84 (dd, *J$_1$* = 7.5 Hz, *J$_2$* = 1.6 Hz), 7-69-7.65 (m, 2H), 7.62 (d, 1H, *J* = 8.8 Hz), 4.30 (s, 1H), 3.75 (s, 1H).[341]

18.2.4.14. Synthesis of 1-(3-benzoyl-5-nitro-1H-indol-2-yl)-1,3-dicyclohexylurea (85)
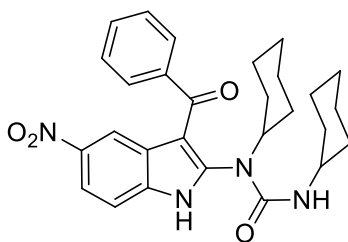
To a r.t. stirred suspension of 3-benzoyl-1-hydroxy-5-nitro-1*H*-indole (50 mg, 0.177 mmol) in MeOH (5 mL), Et$_3$N (30 µL, 0.211 mmol) and DCC (55 mg, 0.266 mmol) were added and reaction mixture was stirred at r.t. for 24 h. Solvent was removed under reduced pressure and water was added. Aqueous layers were extracted with EtOAc. Organic phase was washed with water, dried over Na$_2$SO$_4$, filtered and evaporated under reduced pressure to afford 1-(3-benzoyl-5-nitro-1H-indol-2-yl)-1,3-dicyclohexylurea as yellow solid (yield = quant.). ^{1}H-NMR (CDCl$_3$) δ: 12.55 (br, 1H), 8.41 (d, 1H, J = 2.3 Hz), 8.10 (dd, 1H, ^3J = 9.0 Hz, ^4J = 2.3 Hz), 7.76 (dd, 2H, ^3J = 7.6 Hz, ^4J = 1.3 Hz), 7.62 (tt, 1H, ^3J = 7.6 Hz, ^4J = 1.3 Hz), 7.60 (d, 1H, J = 9.0 Hz), 7.46 (t, 2H, J = 7.6 Hz), 6.17 (d, 1H, J = 7.5 Hz), 1.82 - 0.80 (m, 22H) ppm. MS (CI): *m/z*: 489 [*M*+1].[341]

18.2.4.15. Synthesis of 3-(2-chlorobenzoyl)-5-amino-1*H*-indole (86)
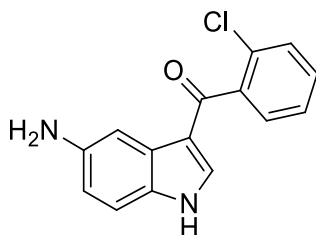
To a r.t. solution of 3-(2-chlorobenzoyl)-1-hydroxy-5-nitro-1*H*-indole (63 mg, 0.20 mmol) in MeOH (15 mL), zinc powder (131 mg, 2 mmol) and AcOH (100 µL) were added and mixture is stirred for 3 h. Reaction mixture was then filtered and mother liquors were evaporated under reduced pressure to afford 5-amino-3-(2-chlorobenzoyl)-1*H*-indole (38 mg, 70%) as a green–yellow solid without any further purification. ^{1}H-NMR (DMSO-*d*$_6$) δ: 11.70 (br, 1H), 7.53 (td, 1H, J_1 = 8.0 Hz, J_2 = 0.6 Hz), 7.50 - 7.48 (m, 1H), 7.46 - 7.42 (m, 3H), 7.34 (s, 1H), 7.18 (d, 1H, J = 8.7 Hz), 6.67 (dd, 1H, J_1 = 8.7 Hz, J_2 = 2.1 Hz), 5.20 (br, 2H) ppm. ^{13}C-NMR (DMSO-*d*$_6$) δ: 186.7, 145.6, 140.4, 132.3, 130.5, 129.7, 129.6, 128.6, 127.6, 127.0, 123.9, 113.3, 109.9, 109.0, 104.1. GC-MS (EI): *m/z*: 272 / 270 [*M*+(^{37}Cl / ^{35}Cl)], 241, 240, 239. Elemental Analysis for C$_{15}$H$_{11}$ClN$_2$O: calcd. (%) C 66.55, H 4.10, N 10.35; found (%) C 66.51, H 4.15, N 10.42.[334]

18.2.4.16. Synthesis of 3-benzoyl-5-nitro-1*H*-indole (87)
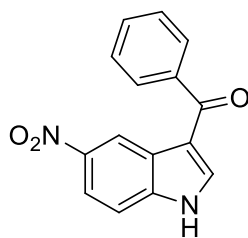
To a r.t. solution of 3-benzoyl-1-hydroxy-5-nitro-1*H*-indole (78 mg, 0.277 mmol) in MeOH (5 mL), 2-bromo-1-acetophenone (56 mg, 0.28 mmol) was added. Reaction mixture was stirred for 5 min, then NEt$_3$ (89 µL, 0.64 mmol) was added and mixture was r.t. stirred for 72 h. Solvent was then removed under reduced pressure. Crude product was purified by gravimetric column chromatography (toluene/EtOAc 1:1) to afford 3-benzoyl-5-nitro-1*H*-indole (55 mg, 75%) as yellow solid. ^{1}H-NMR (DMSO-d_6) δ: 12.68 (1H, br). 9.14 (1H, d, *J* = 2.0 Hz) 8.27 (1H, d, *J* = 3.3 Hz), 8.18 (1H, dd, *J* = 8.9, 2.3 Hz), 7.49 - 8.02 (6H, m). Other spectral data match the literature.[377]

18.2.4.17. Synthesis of 3-(1*H*-indole-2-carbonyl)-1*H*-indole-5-carbonitrile (88)
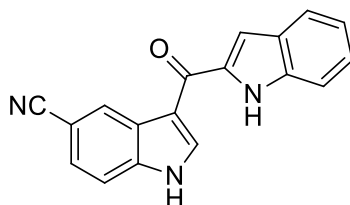
(*E*)-1-hydroxy-3-(3-(2-nitrophenyl)acryloyl)-1H-indole-5-carbonitrile (333 mg, 1 mmol) and PPh$_3$ (1.05 g, 4 mmol) were stirred under microwaves irradiation for 5 minutes at 200 W and 100°C. Reaction mixture was then diluted with acetone, filtered and the solvent removed under reduced pressure. Crude product was purified by flash column chromatography (*n*-hexane/EtOAc 1:1) to afford 3-(1H-indole-2-carbonyl)-1H-indole-5-carbonitrile (72 mg, 25%) as a brown solid. ^{1}H-NMR (acetone-d_6) δ: 11.61 (br, 1H), 10.99 (br, 1H), 8.77 (dd, 1H, *J* = 1.6, 0.7 Hz), 8.68 (s, 1H), 7.77 (dd, 1H, *J* = 8.5, 0.7 Hz), 7.72 (dd, 1H, *J* = 9.0, 0.9 Hz), 7.63-7.60 (m, 2H), 7.43 (dd, 1H, *J* = 2.2, 0.9 Hz), 7.32 (td, 1H, *J* = 7.6, 1.1 Hz), 7.12 (td, 1H, *J* = 7.5, 1.0 Hz) ppm. ^{13}C-NMR (acetone-d_6) δ: 180.2, 138.6, 137.6, 135.9, 134.8, 127.9, 127.1, 126.7, 126.0, 125.0, 122.5, 120.3, 119.8, 116.1, 113.4, 112.4, 107.9, 105.0 ppm. FT-IR (KBr disk): 3314, 2922, 2226, 1718, 1602, 1521, 1438, 1343, 1225, 1129, 874, 804 cm^{-1}. m.p.: degradation from 265°C. MS (CI): *m/z* = 286 [M$^+$]. Elemental Analysis for C$_{18}$H$_{11}$N$_3$O: calcd. (%) C 75.78, H 3.89, N 14.73; found (%) C 75.69, H 3.96, N 14.57.[334]

18.2.4.18. Synthesis of 3-(1*H*-indole-2-carbonyl)-5-nitro-1*H*-indole (89)
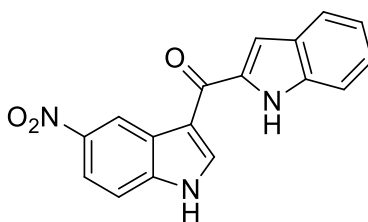
(*E*)-1-(1-hydroxy-5-nitro-1H-indol 3-yl)-3-(2-nitrophenyl)prop-2-en-1-one (50 mg, 0.16 mmol) and PPh$_3$ (168 mg, 0.64 mmol) were stirred under microwaves irradiation for 5 minutes at 200 W and 100°C. Reaction mixture was then diluted with acetone, filtered and the solvent removed under reduced pressure. Crude product was purified by flash column chromatography (petroleum ether/EtOAc 1:1) to afford 3-(1*H*-indole-2-carbonyl)-5-nitro-1*H*-indole (18 mg, 36%) as a brown solid. ^{1}H-NMR (DMSO-d_6) δ: 9.12 (d, 1H, *J* = 2.2 Hz); 8.60 (s, 1H), 8.24 (dd, 1H, *J* = 8.2, 1.2 Hz), 8.01 (dd, 1H, *J* = 8.2, 1.1 Hz), 7.89 (dd, 1H, *J* = 9, 2.4 Hz), 7.78 (td, 1H, *J* = 7.6, 1.2 Hz), 7.75 (s, 1H), 7.62 (td, 1H, *J* = 7, 1.3 Hz), 7.57 (d, 1H, *J* = 7.5 Hz). ^{13}C-NMR (DMSO-d_6) δ: 178.7, 175.3, 149.3, 142.5, 139.7, 136.3, 133.8, 132.5, 132.0, 130.6, 129.4, 124.8, 123.0, 118.6, 116.0, 112.2, 110.5. MS (CI): *m/z* = 322 [M]+. IR (film): ν (cm^{-1}) = 3419, 1641, 1557, 1416, 1374, 1336, 1199, 1113, 1023, 869, 800. m.p.: 298-300°C.[341]s

18.2.4.19. Synthesis of 3-(1H-indole-2-carbonyl)-1H-indole-7-carboxylate (90)
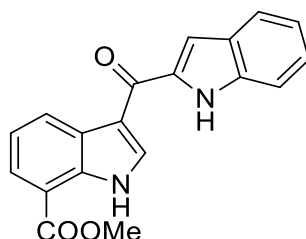
(*E*)-methyl 1-hydroxy-3-(3-(2-nitrophenyl)acryloyl)-1H-indole-7-carboxylate (88 mg, 0.24 mmol) and PPh$_3$ (252 mg, 0.96 mmol) were stirred under microwaves irradiation for 5 minutes at 200 W and 100°C. Reaction mixture was then diluted with acetone, filtered and the solvent removed under reduced pressure. Crude product was purified by flash column chromatography (petroleum ether/EtOAc 4:6) to afford methyl 3-(1H-indole-2-carbonyl)-1H-indole-7-carboxylate as brown solid (14.5 mg, 19%). ^{1}H-NMR (acetone-d_6) δ: 11.40 (br s, 1H), 10.95 (br s), 8.66 (dd, 1H, J = 7.4, 1.0 Hz), 8.49 (d, 1H, J = 3.0 Hz), 7.99 (dd, 1H, J = 7.6, 1.0 Hz), 7.74 (dd, 1H, J = 8.0, 0.9 Hz), 7.62 (dd, 1H, J = 8.3, 0.9 Hz), 7.41-7.37 (m, 2H), 7.31 (td, 1H, J = 7.6, 1.1 Hz), 7.13 (td, 1H, J = 7.5, 1.0 Hz), 4.01 (s, 3H). ^{13}C-NMR (acetone-d_6) δ: 180.5, 166.6, 137.5, 136.3, 135.6, 133.7, 128.2, 127.9, 127.6, 125.6, 124.8, 122.5, 121.4, 120.2, 116.0, 113.7, 112.4, 107.7, 51.5. MS (CI): *m/z* = 319 [M]+. IR (film): ν (cm^{-1}) = 3326, 3294, 1692, 1591, 1524, 1278, 1094, 801.[341]

18.2.4.20. Synthesis of 3-(quinolin-2-yl)-1H-indole-5-carbonitrile (91)
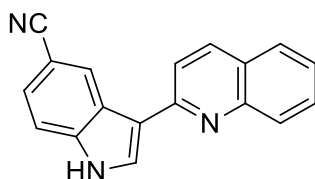
(*E*)-1-hydroxy-3-(3-(2-nitrophenyl)acryloyl)-1H-indole-5-carbonitrile (102 mg, 0.31 mmol) was dissolved in a solution of MeOH (6 ml) and 1,4-dioxane (2 ml). A saturated solution of NH_4Cl (15 ml) and indium powder (175 mg, 1.53 mmol) were added to the solution. Reaction mixture was then refluxed for 12 h. Solvents were then evaporated under reduced pressure. Crude residue was purified by flash chromatography (toluene/EtOAc 7:3) to afford 3-(quinolin-2-yl)-1H-indole-5-carbonitrile (11 mg, 24%) as a brown solid. ^{1}H-NMR (acetone-d_6) δ: 11.28 (br s, 1H), 9.47 (dd, 1H, *J* = 1.6, 0.7 Hz), 8.45 (d, 1H, *J* = 2.8 Hz), 8.27 (dd, 1H, *J* = 8.7, 0.4 Hz), 8.18 (dd, 1H, *J* = 8.4, 1.0 Hz), 8.04 (d, 1H, *J* = 8.7 Hz), 7.89 (dd, 1H, *J* = 8.1, 1.4 Hz), 7.76 (td, 1H, *J* = 7.7, 1.4 Hz), 7.71 (dd, 1H, *J* = 8.4, 0.7 Hz), 7.56-7.51 (m, 2H).^{13}C-NMR (acetone-d_6) δ: 154.7, 148.3, 139.3, 136.0, 129.5, 129.0, 128.9, 128.6, 127.6, 126.5, 126.0, 125.4, 125.1, 120.4, 118.9, 117.1, 112.9, 103.6. MS (CI): *m/z* = 270 [M]$^+$. IR (KBr disk): ν (cm^{-1}) = 3386, 2923, 2854, 2224, 1600, 1572, 1440, 1261, 1093, 803. m.p.: 250°C. Elemental Analysis for $C_{19}H_{11}N_3$: calcd. (%) C 80.28, H 4.12, N 15.60; found (%) C 80.32, H 3.81, N 15.47.[334]

18.2.4.21. Synthesis of (1-methoxy-5-nitro-2-phenyl-1H-indol-3-yl)(phenyl)methanone (92)
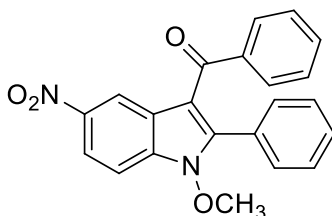
To a solution of 3-benzoyl-2-bromo-1-methoxy-5-nitro-1*H*-indole (80 mg, 0.21 mmol) in 1,4-dioxane (8 mL), phenylboronic acid (33 mg, 0.27 mmol), LiCl (18 mg, 0.42 mmol) and Na_2CO_3 (56 mg, 0.53 mmol) were added. Reaction mixture was then purged with nitrogen for 0.5 h. Pd(OAc)$_2$ (9 mg, 0.04 mmol) was then added and reaction mixture was heated to 80°C and stirred for 24 h. Solvent was then removed under reduced pressure. Crude product was purified through gravimetric column chromatography (DCM/*n*-hexane 1:5 and 3:1) to afford (1-methoxy-5-nitro-2-phenyl-1H-indol-3-yl)(phenyl)methanone (78 mg, quantitative yield) as white solid. ^{1}H-NMR (DMSO-d_6) δ: 8.91 (s, 1H), 8.35 (dd, 1H, *J* = 8.8 Hz, 2 Hz), 7.99 (d, 1H, *J* = 8.8 Hz), 7.56 (d, 2H, *J* = 7.2 Hz), 7.49 (d, 1H, *J* = 6.8 Hz), 7.36 (m, 4H), 7.22 (t, 2H, *J* = 7.6 Hz) ppm. FT-IR (ATR): 3109, 1608, 1516, 1444, 1337, 794, 723 cm^{-1}.

♦ ♦ ♦ ♦ ♦ ♦

18.3. Chapter 2 experimental part

18.3.1. Synthesis of 2-[-4-(2-aminophenyl)-1,3-butadiynyl]-phenylamine (94)
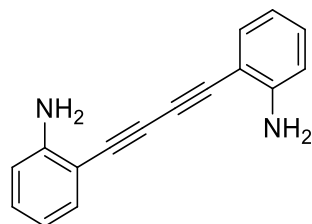
To a r.t. solution of 2-iodoaniline (11.945 g, 54.54 mmol) in TEA (230 mL), PdCl$_2$(PPh$_3$)$_2$ (383 mg, 0.55 mmol) and CuI (0.02 eq., 207 mg, 1.09 mmol) were added. TMSA (10 ml, 70.91 mmol) was then added and the mixture was r.t. stirred for 2 h. A solution of KF (6.327 g, 109.08 mmol) in methanol (150 ml) was then added and the reaction was air opened and r.t. stirred overnight. Reaction mixture was filtered on Celite® and the solvents were evaporated under reduced pressure. Crude product was purified by gravimetric column chromatography (*n*-hexane/DCM 4:6) to afford 2-[-4-(2-aminophenyl)-1,3-butadiynyl]-phenylamine as yellow (4.83 g, 76%). ^{1}H NMR (400 MHz, CD$_2$Cl$_2$): δ 7.36 (dd, *J* = 7.5, 1.2 Hz, 2H), 7.18 (dt, *J* = 8.7, 1.5 Hz, 2H), 6.74 (m, 4H) ppm. Other spectral data match the literature.[382]

18.3.2. Synthesis of 2,2,2-trifluoro-*N*-(2-[-4-(2-(2,2,2-trifluoroacetylamino)-phenyl)-1,3-butadiynyl]-phenylacetamide (95)
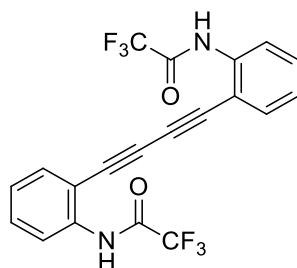
Trifluoroacetic anhydride (6 ml, 58.7 mmol) was added dropwise to a r.t. solution of 2[-4-(2-aminophenyl)-1,3-butadiynyl]-phenylamine (2.782 g, 11.9 mmol) in DCM (45 mL) and pyridine (5 mL). Reaction was stirred overnight. Precipitated solid was filtered, washed with a small amount of DCM and dried under vacuum to afford 2,2,2-trifluoro-*N*-(2-[-4-(2-(2,2,2-trifluoroacetylamino)-phenyl)-1,3-butadiynyl]-phenylacetamide (3.88 g, 77%) as pale pink solid. ^{1}H NMR (400 MHz, DMSO-*d$_6$*): δ (ppm) = 11.39 (s, 2H), 7.74 (d, *J* = 7.8 Hz, 2H), 7.57 (t, *J* = 7.8 Hz, 2H), 7.45 (m, 4H). Other spectral data match the literature.[200]

18.3.3. Synthesis of 5-iodo-2,2'-bithiophene (96)
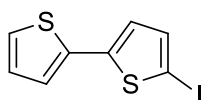
To a r.t. shielded from light solution of 2,2'-bithiophene (4.53 g, 27.2 mmol) in CHCl$_3$ (110 mL) and AcOH (110 mL), NIS (6.74 g, 29.9 mmol) was added one pot. The reaction mixture was stirred at room temperature for

24 h. Mixture was then filtered and the solvent was removed under reduced pressure. Crude residue was diluted with DCM and the solution was washed with aqueous saturate NaHCO$_3$ and water. Collected organic phases were dried with magnesium sulfate, filtered and solvents removed under reduced pressure. Crude product was dissolved in a 1:1 mixture of CHCl$_3$ and AcOH, cooled to 0°C and the precipitate, corresponding to 5,5'-diiodo-2,2'-bithiophene, was removed by filtration. Mother liquors were dried under reduced pressure to afford 5-iodo-2,2'-bithiophene (4.43 g, 56%) as a grey solid. ^{1}H NMR (CDCl$_3$): δ 7.24 (dd, J = 4.8 Hz, J = 0.8 Hz, 1H), 7.18 (d, J = 4 Hz, 1H), 7.14 (dd, J = 3.6 Hz, J = 1.2 Hz, 1H), 7.03 (dd, J = 4.8 Hz, J = 3.6 Hz, 1H), 6.87 (d, J = 4.0 Hz, 1H) ppm. Other spectral data match the literature.[201]

18.3.4. Synthesis of 3,3'-di([2,2'-bithiophen]-5-yl)-1H,1'H-2,2'-biindole (97)
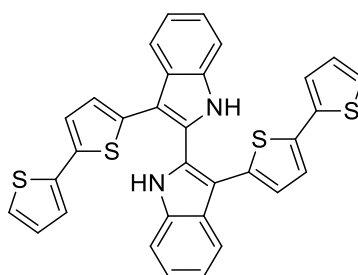
To a stirred solution of 2,2,2-trifluoro-N-(2-(4-[2,2,2- trifluoro-acetylamino-phenyl]-buta-1,3-diynyl)-phenyl)-acetamide (1.99 g, 4.7mmol) in MeCN (100 mL), 5-iodo-2,2'-bithiophene (5.9 g, 20.3 mmol), Pd(PPh$_3$)$_4$ (544 mg, 0.47 mmol) and K$_2$CO$_3$ (3.2 g, 23.5 mmol) were added. The reaction mixture was then refluxed for 24 h. Mixture was dried under reduced pressure and the crude residue was diluted with EtOAc and the organic phase was washed with water. The organic phases were dried over MgSO$_4$, filtered and the solvent was removed under reduced pressure. Crude product was purified by column chromatography (n-hexane/DCM 4:6) to afford 3,3'-di([2,2'-bithiophen]-5-yl)-1H,1'H-2,2'-biindole (1.8 g, 45%) as a yellow solid. ^{1}H-NMR (DMSO-d6): δ 11.95 (s, 2H), 7.99 (d, J = 7.6 Hz, 2H), 7.48 (d, J = 8.0 Hz, 2H), 7.40 (d, J = 4.4 Hz, 2H), 7.29 (t, J = 5.2 Hz, 2H), 7.23 (t, J = 5.2 Hz, 2H), 7.12 (d, J = 3.6 Hz, 2H), 7.09 (d, J = 3.6 Hz, 2H), 7.00 (dd, J = 5.2 Hz, J = 4.0 Hz, 2H), 6.88 (d, J = 4.0 Hz, 2H) ppm. Other spectral data match the literature.[185]

18.3.5. Synthesis of 3,3'-di([2,2'-bithiophen]-5-yl)-1,1'-dimethyl-1H,1'H-2,2'-biindole (93)
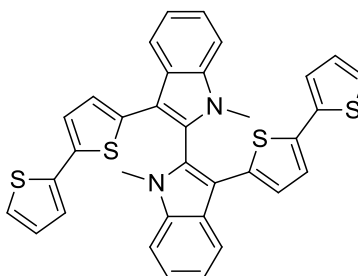
To a r.t. solution of 3,3'-di([2,2'-bithiophen]-5- yl)-1H,1'H-2,2'-biindole (310 mg, 0.55 mmol) in dry DMF (3 mL) KOH (200 mg, 3.56 mmol) was added and the solution was stirred for 0.5 h. Methyl iodide (300 µL, 5.53 mmol) was then added and reaction mixture was stirred at room temperature for 36 h. Solvent was removed

under reduced pressure and the residue was dissolved into DCM. Organic phase was washed with water and brine, then dried over MgSO$_4$, filtered and the solvent was removed under reduced pressure. Crude product was purified by column chromatography (*n*-hexane/DCM 8:2) to afford 3,3'-di([2,2'-bithiophen]-5-yl)-1,1'-dimethyl-1H,1'H-2,2'-biindole as a yellow solid (228 mg, 70 %). ^{1}H-NMR (CDCl$_3$) δ 8.19 (d, *J* = 7.8 Hz, 2H), 7.45-7.32 (m, 6H), 7.14 (d, *J* = 5.1 Hz, 2H), 7.03 -7.01 (m, 4H), 6.97-6.95 (m, 2H), 6.81 (d, *J* = 3.9, 2H), 3.48 (s, 6H) ppm. Other spectral data match the literature.[185]

18.3.6. Synthesis of 3,3'-di([2,2'-bithiophen]-5-yl)-1,1'-dipropyl-1H,1'H-2,2'-biindole (98)
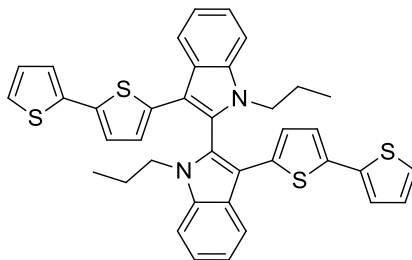
To a solution of 3,3'-di([2,2'-bithiophen]-5-yl)-1H,1'H-2,2'-biindole (135 mg, 0.24 mmol) in DMF (3 mL), KOH (67 mg, 1.2 mmol) was added and the solution was stirred at that temperature for 0.5 h. Then 1-bromopropane (71 μL, 0.72 mmol) was added and reaction mixture was stirred at room temperature for 36 hours. Solvent was removed under reduced pressure and the obtained residue was dissolved into DCM. Organic phase was washed with water and brine, then dried over MgSO$_4$, filtered and the solvent was removed under reduced pressure. Crude product was purified by gravimetric column chromatography (*n*-hexane/DCM 8:2) to afford 3,3'-di([2,2'-bithiophen]-5-yl)-1,1'-dipropyl-1H,1'H-2,2'-biindole (120 mg, 79%) as a yellow solid. ^{1}H-NMR (CDCl$_3$): δ 8.21 (d, *J* = 7.8 Hz, 2H), 7.46-7.31 (m, 6H), 7.14 (d, *J* = 5.1 Hz, 2H), 7.02-6.94 (m, 4H), 6.82 (d, *J* = 3.9 Hz, 4H), 3.86-3.73 (m, 4H), 1.37-1.29 (m, 4H), 0.75 (t, *J* = 7.2 Hz, 6H) ppm. ^{13}C-NMR (CDCl$_3$): δ 137.7, 137.1, 135.9, 135.3, 127.7, 126.5, 125.9, 124.4, 124.2, 123.8, 123.4, 123.2, 120.7, 120.6, 113.3, 110.6, 46.14, 23.0, 11.5 ppm. MS (EI): *m/z*: 644.1 [M$^+$]. Elemental Analysis for C$_{38}$H$_{32}$N$_2$S$_4$: calcd. (%) C 70.77, H 5.00, N 4.34; found (%) C 70.45, H 5.22, N 4.31.

18.3.7. Synthesis of 5-(4-bromophenyl)-2,2'-bithiophene (99)
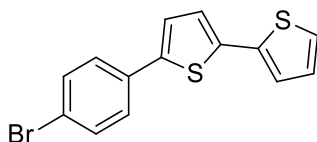
To shielded from light solution of *p*-bromoiodobenzene (407 mg, 1.43 mmol) in toluene (8 mL) and water (4 mL), sodium carbonate (188 mg, 1.77 mmol), was added. Then to this solution, a degassed solution of Pd(PPh$_3$)$_4$ (88 mg, 0.08 mmol) and 2-([2,2'-bithiophen]-5-yl)-4,4,5,5-tetramethyl-1,3,2-dioxaborolane (501 mg, 1.72 mmol) in THF (4 mL) was added. Reaction mixture was then refluxed for 4 h. Mixture was dried under reduced pressure and crude product was purified by gravimetric column chromatography (*n*-

hexane/DCM 9:1) to afford 5-(4-bromophenyl)-2,2'-bithiophene (406 mg, 88%) as yellow solid. ^{1}H-NMR (CDCl$_3$) δ: 7.51–7.49 (d, J = 8.4 Hz, 2H), 7.47–7.45 (d, J = 8.4 Hz, 2H), 7.24–7.23 (d, J = 5.2 Hz, 1H), 7.22–7.20 (m, 2H), 7.144–7.135 (d, J = 3.6 Hz, 1H), 7.04–7.02 (m, 1H). Other spectral data match the literature.[383]

18.3.8. Synthesis of 3,3'-bis(4-([2,2'-bithiophen]-5-yl)phenyl)-1H,1'H-2,2'-biindole (100)
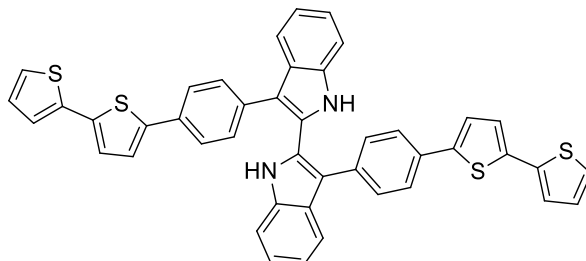
To a r.t. solution of 2,2,2-trifluoro-N-(2-[-4-(2-(2,2,2-trifluoroacetylamino)-phenyl]-1,3-butadiynyl]-phenyla-cetamide (82 mg, 0.193 mmol) in MeCN (7 mL), 5-(4-bromophenyl)-2,2'-bithiophene (200 mg, 0.623 mmol), potassium carbonate (133 mg, 0.965 mmol) and Pd(PPh$_3$)$_4$ (22 mg, 0.019 mmol) were added. Reaction mixture was then refluxed for 3 h. Mixture was then diluted with water and extracted with DCM. Reunited organic phases were dried over MgSO$_4$, filtered and dried under reduced pressure. Crude product was then purified by gravimetric column chromatography (DCM/n-hexane 2:1) to afford 3,3'-bis(4-([2,2'-bithiophen]-5-yl)phenyl)-1H,1'H-2,2'-biindole (50 mg, 36%) as yellow solid. ^{1}H NMR (DMSO-d_6) δ: 11.69 (s, 2H), 7.70 (d, J = 8 Hz, 2H), 7.52 (d, J = 4 Hz, 2H), 7.46-7.44 (m, 4H), 7.38 (d, J = 4 Hz, 2H), 7.31 (d, J = 4 Hz, 2H), 7.28 (d, J = 4 Hz, 2H), 7.24-7.19 (m, 6H), 7.14-7.09 (m, 6H) ppm. ^{13}C NMR (DMSO-d_6) δ: 142.3, 136.5, 136.4, 135.2, 134.4, 130.4, 129.0, 128.3, 126.9, 126.4, 125.4, 125.0, 125.0, 124.0, 123.8, 122.3, 118.9, 115.3, 111.8 ppm. FT-IR (ATR), v (cm^{-1}): 3402, 1500, 1452, 1344, 1096, 835, 803, 745, 641. MS (EI): 712 [M$^+$]. m.p.: 299°C (decomposition). Elemental Analysis for C$_{44}$H$_{28}$N$_2$S$_4$: calcd (%) C 74.12, H 3.96, N 3.93; found (%) C 73.97, H 4.03, N 3.80.

18.3.9. Synthesis of 3,3'-bis(4-([2,2'-bithiophen]-5-yl)phenyl)-1,1'-dimethyl-1H,1'H-2,2'-biindole (101)
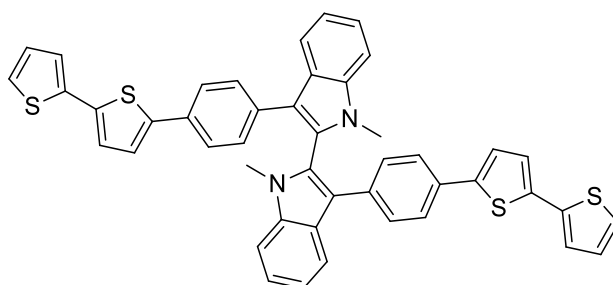
To a solution of 3,3'-bis(4-([2,2'-bithiophen]-5-yl)phenyl)-1H,1'H-2,2'-biindole (114 mg, 0.16 mmol) in DMF (5 mL), KOH (45 mg, 0.8 mmol) was added and reaction mixture was r.t. stirred for 0.5 h. Then iodomethane (342 mg, 2.4 mmol) was added and mixture stirred for 48 h. Solvent was removed under reduced pressure. Crude product was purified by gravimetric column chromatography (n-hexane/AcOEt 8:2) to afford 3,3'-bis(4-([2,2'-bithiophen]-5-yl)phenyl)-1,1'-dimethyl-1H,1'H-2,2'-biindole (118 mg, quant.) as yellow solid. ^{1}H-NMR (DMSO-d_6): 7.93 (d, J = 8 Hz, 2H), 7.65 (d, J = 8 Hz, 6H), 7.56 (d, J = 4 Hz, 2H), 7.51 (d, J = 4 Hz, 2H), 7-39-7.33

(m, 10H), 7.32 (t, J = 8 Hz, 2H), 7.16 (t, J = 4 Hz, 2H), 3.48 (s, 6H). ^{13}C-NMR has not been registered due to poor solubility of compound **101**. Elemental Analysis for $C_{46}H_{32}N_2S_4$: calcd (%) C 74.56, H 4.35, N 3.78; found (%) C 74.92, H 4.44, N 3.67.

18.3.10. Synthesis of 3,3'-bis(4-([2,2'-bithiophen]-5-yl)phenyl)-1,1'-dipropyl-1H,1'H-2,2'-biindole (102)
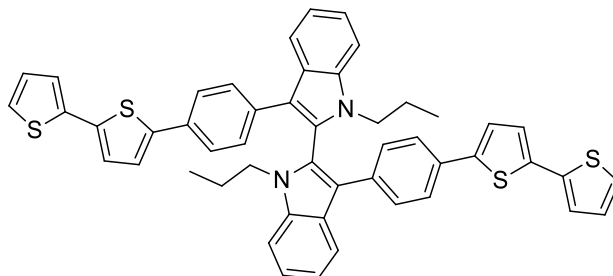
To a solution of 3,3'-bis(4-([2,2'-bithiophen]-5-yl)phenyl)-1H,1'H-2,2'-biindole (114 mg, 0.16 mmol) in DMF (5 mL), KOH (45 mg, 0.8 mmol) was added and reaction mixture was r.t. stirred for 0.5 h. Then 1-bromopropane (295 mg, 2.4 mmol) was added and mixture stirred for 48 h. Solvent was removed under reduced pressure. Crude product was purified by gravimetric column chromatography (*n*-hexane/AcOEt 8:2) to afford 3,3'-bis(4-([2,2'-bithiophen]-5-yl)phenyl)-1,1'-dipropyl-1H,1'H-2,2'-biindole (109 mg, 95%) as yellow solid. ^{1}H-NMR (CDCl$_3$) δ: 7.94 (d, J = 8 Hz, 2H), 7.42 (d, J = 8 Hz, 4H), 7.36 (d, J = 8 Hz, 4H), 7.28 (d, J = 8 Hz, 2H), 7.25 (t, J = 8 Hz, 2H), 7.21 (m, 2H), 7.14 (d, J = 4 Hz, 2H), 7.10 (m, 4H), 7.04 (d, J = 4 Hz, 2H), 6.94 (t, J = 4 Hz, 2H), 3.72 – 3.65 (m, 2H), 3.69 – 3.59 (m, 2H), 1.19 – 1.04 (m, 4H), 0.60 (t, J = 8 Hz, 6H) ppm. ^{13}C NMR (CDCl$_3$) δ: 143.1, 137.5, 137.1, 136.3, 134.5, 131.5, 128.6, 128.9, 127.1, 126.4, 125.8, 124.6, 124.3, 123.5, 123.3, 122.7, 120.4, 120.2, 117.7, 110.7, 45.8, 22.7, 11.5 ppm. m.p.: 105-109°C. MS (EI): 797 [M$^+$], 798 [M+1]. FT-IR (ATR), ν (cm^{-1}): 2960.72, 2924,40, 2870.68, 1733.30, 1531.87, 1500.95, 1456.21, 1358.14, 1328.97, 1224.08, 1094.49, 835.63, 794.57, 730.06. Elemental Analysis for $C_{50}H_{40}N_2S_4$: calcd (%) C 75.34, H 5.06, N 3.51; found (%) C 74.89, H 5.36, N 3.44.

18.3.11. Synthesis of 3,3'-bis(4-([2,2'-bithiophen]-5-yl)phenyl)-1,1'-dihexyl-1H,1'H-2,2'-biindole (103)
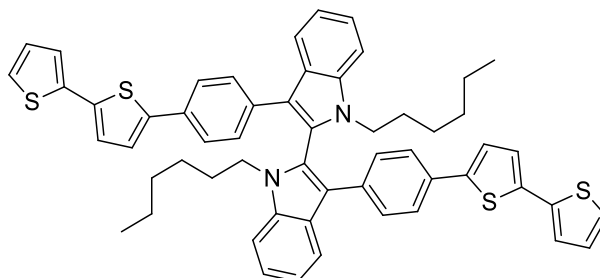
To a solution of 3,3'-bis(4-([2,2'-bithiophen]-5-yl)phenyl)-1H,1'H-2,2'-biindole (114 mg, 0.16 mmol) in DMF (5 mL), KOH (45 mg, 0.8 mmol) was added and reaction mixture was r.t. stirred for 0.5 h. Then 1-bromohexane (396 mg, 2.4 mmol) was added and mixture stirred for 48 h. Solvent was removed under reduced pressure. Crude product was purified by gravimetric column chromatography (*n*-hexane/AcOEt 8:2) to afford 3,3'-bis(4-([2,2'-bithiophen]-5-yl)phenyl)-1,1'-dihexyl-1H,1'H-2,2'-biindole (130 mg, 92%) as yellow solid. ^{1}H-NMR

(DMSO-d_6) δ: 7.96 (d, J = 8 Hz, 2H), 7.93 (d, J = 8 Hz, 4H), 7.57 (d, J = 8 Hz, 2H), 7.52-7.44 (m, 8H), 7.31-7.23 (m, 8H), 7.10 (t, J = 8 Hz, 2H), 3.85-3.71 (m, 4H), 1.22 (br, 2H), 1.00-0.85 (m, 14H), 0.64 (t, J = 8 Hz, 6H). ^{13}C NMR (CDCl$_3$) δ: 143.1, 137.6, 137.1, 136.3, 134.5, 131.5, 128.6, 127.9, 127.2, 126.4, 125.9, 124.6, 124.3, 123.5, 123.3, 122.7, 120.4, 120.2, 117.8, 110.7, 44.2, 31.1, 29.4, 26.7, 22.4, 13.9. FT-IR (ATR), ν (cm^{-1}): 2923, 2852, 1531, 1501, 1456, 1359, 1239, 1104, 836, 794, 741, 687. MS (EI): 881 (M+1). m.p.: 104-105°C. . Elemental Analysis for C$_{56}$H$_{52}$N$_2$S$_4$: calcd (%) C 76.32, H 5.95, N 3.18; found (%) C 76.82, H 6.01, N 3.09.

18.3.12. Synthesis of 5-iodo-2,2':5',2''-terthiophene (104)
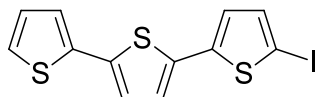
To a r.t. shielded from light solution of 5-iodo-2,2':5',2''-terthiophene (202 mg, 0.81 mmol) in chloroform (10 mL) and acetic acid (10 mL), NIS (210 mg, 0.93 mmol) was added and reaction mixture stirred 24 h. Reaction was quenched with aqueous NaOH 1M was added and product extracted with DCM. Organic phase was washed with aqueous 1M NaOH then brine, dried with sodium sulphate, filtered and solvents removed under reduced pressure to afford 5-iodo-2,2':5',2''-terthiophene (301 mg, quant.) as yellow solid without any further purification. ^{1}H-NMR (acetone-d_6) δ: 7.06 (d, J = 3.8 Hz, 1H), 7.12 (dd, J = 4.9 Hz, J = 1.4 Hz, 1H), 7.24 (d+d, J = 3.8 Hz, J = 3.8 Hz, 2H), 7.34 (d+dd, J = 3.6 Hz, J = 3.6 Hz, J = 1.1 Hz, 2H), 7.48 (dd, J = 4.9 Hz, J = 1.1 Hz, 1H) ppm. Other spectral data match the literature.[222]

18.3.13. Synthesis of 3,3'-di([2,2':5',2''-terthiophen]-5-yl)-1H,1'H-2,2'-biindole (105)
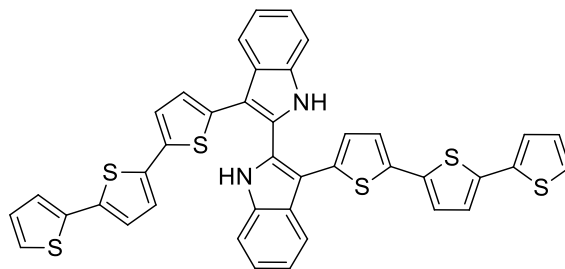
To a solution of 2,2,2-trifluoro-N-(2-[-4-(2-(2,2,2-trifluoroacetylamino)-phenyl)-1,3-butadiynyl]-phenylacetamide (1500 mg, 3.54 mmol) in MeCN (50 mL), 5-iodo-2,2':5',2''-terthiophene (4.5 g, 12 mmol), K$_2$CO$_3$ (2.4 g, 17.7 mmol) and Pd(PPh$_3$)$_4$ (410 mg, 0.35 mmol) were added. Reaction was heated to reflux and stirred 24 h. Reaction mixture was then evaporated under reduced pressure. Crude product was dissolved in DCM and washed with water. Organic phase was dried with Na$_2$SO$_4$, filtered and dried under reduced pressure. Crude product was purified by gravimetric column chromatography (toluene/n-hexane 3:1 then EtOAC) to afford 3,3'-di([2,2':5',2''-terthiophen]-5-yl)-1H,1'H-2,2'-biindole (898 mg, 35%) as yellow solid. ^{1}H-NMR (DMSO-d_6) δ: 12.02 (s, 2H), 8.05 (d, J = 8 Hz, 2H), 7.54 (t, J = 8 Hz, 4H), 7.36 – 7.26 (m, 6H), 7.23 – 7.20 (m, 4H), 7.12 (m, 4H), 6.91 (d, J = 4 Hz, 2H) ppm. ^{13}C-NMR (DMSO-d_6) δ: 136.4, 136.3, 136.0, 135.4, 134.7, 133.4, 128.3, 126.5, 125.5, 125.4, 124.8, 124.5, 124.4, 124.1, 124.0, 122.9, 120.5, 119.5, 112.0, 110.2 ppm. MS (ESI): 724 [M$^{+\bullet}$].

m.p.: 286 (decomp.). Elemental Analysis for $C_{40}H_{24}N_2S_6$: calcd (%) C 66.26, H 3.34, N 3.86; found (%) C 66.52, H 3.18, N 3.88.

18.3.14. Synthesis of 3,3'-di([2,2':5',2''-terthiophen]-5-yl)-1,1'-dipropyl-1H,1'H-2,2'-biindole (106)
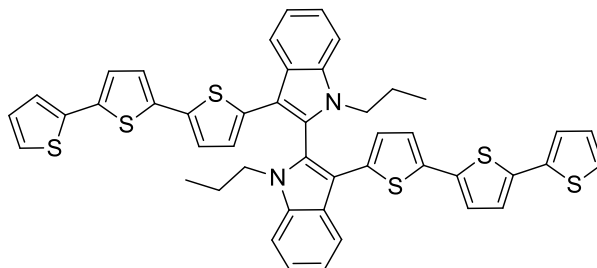
To a r.t. solution of 3,3'-di([2,2':5',2''-terthiophen]-5-yl)-1H,1'H-2,2'-biindole (200 mg, 0.28 mmol) in DMF (10 mL), freshly powdered KOH (79 mg, 1.4 mmol) was added. Reaction mixture was then stirred 1 h then 1-bromopropane (172 mg, 1.4 mmol) was added. Reaction mixture was stirred 24 h. Solvent was removed under reduced pressure and crude product was dissolved in DCM and washed with water. Organic phase was dried with MgSO₄, filtered and solvent removed under reduced pressure. Crude product was purified by gravimetric column chromatography (*n*-hexane/EtOAc 8:2) to afford 3,3'-di([2,2':5',2''-terthiophen]-5-yl)-1,1'-dipropyl-1H,1'H-2,2'-biindole (226 mg, quant.) as yellow solid. ¹H-NMR (DMSO-d_6) δ: 8.12 (d, *J* = 8 Hz, 2H), 7.70 (d, *J* = 8 Hz, 2H), 7.50 (d, *J* = 4 Hz, 2H), 7.40 (t, *J* = 8 Hz, 2H), 7.32 (t, *J* = 8 Hz, 2H), 7.28 (d, *J* = 4 Hz, 2H), 7-08 – 7.05 (m, 4H), 6.90 (d, *J* = 4 Hz, 2H), 3.99 – 3.92 (m, 2H), 3.81 - 3.74 (m, 2H), 0.86 (t, *J* = 8 Hz, 4H), 0.68 (t, *J* = 8 Hz, 6H) ppm. ¹³C-NMR (CDCl₃) δ: 137.3, 137.1, 136.5, 136.1, 135.6, 135.0, 127.8, 126.5, 125.8, 124.5, 124.3, 124.2, 124.1, 123.7, 123.5, 123.3, 120.8, 120.7, 113.2, 110.7, 46.2, 23.0, 11.5 ppm. MS (ESI) 808 [M⁺•]. m.p.: 92.5°C. Elemental Analysis for $C_{46}H_{36}N_2S_6$: calcd (%) C 68.28, H 4.48, N 3.46; found (%) C 68.20, H 4.50, N 3.51.

18.3.15. Synthesis of 2-((trimethylsilyl)ethynyl)aniline (107)
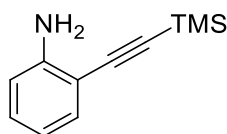
To a solution of 2-iodoaniline (9 g, 41 mmol) in TEA (150 mL), CuI (160 mg, 0.84 mmol) and PdCl₂(PPh₃)₂ (292 mg, 0.41 mmol) were added. Then ethynyltrimetylsylane (7 mL, 49 mmol) was added dropwise. Reaction mixture was r.t. stirred for 3 h. Mixture was then filtered and mother liquors dried under reduced pressure. Crude product was purified through gravimetric column chromatography (*n*-hexane/DCM 1:1) to afford 2-((trimethylsilyl)ethynyl)aniline as yellow solid (7.7 g, quantitative yield). ¹H NMR (CDCl₃) δ: 7.27-7.30 (m, 1H), 7.09-7.13 (m, 1H), 6.63-6.69 (m, 2H), 4.22 (br, 2H), 0.26 (s, 9H) ppm. Other spectral data match the literature.[215]

18.3.16. Synthesis of 2-ethynylaniline (108)
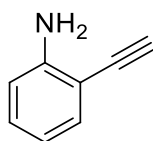
To a r.t. solution of 2-((trimethylsilyl)ethynyl)aniline (7.7 g, 41 mmol) in MeOH (130 mL), KF (7.7 g, 130 mmol) was added and mixture was stirred 24 h. Reaction mixture was dried under reduced pressure: water was added and mixture was extracted with diethylether. Separated organic phases were dried over MgSO$_4$, filtered and solvents removed under reduced pressure to afford 2-ethynylaniline (4.8 g, quantitative yield) as yellow solid without any further purification. ^{1}H NMR (CDCl$_3$): δ 7.35 (dd, J = 7.6, 1.6 Hz, 1H), 7.17 (td, J = 7.8, 1.6 Hz, 1H), 6.79-6.64 (m, 2H), 4.27 (s, 2H), 3.41 (s, 1H) ppm. Other spectral data match the literature.[216]

18.3.17. Synthesis of 2,2'-(ethyne-1,2-diyl)dianiline (109)
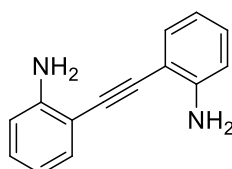
To a r.t. solution of 2-ethynylaniline (3 g, 25.6 mmol) and 2-iodoaniline (4.73 g, 21.6 mol), CuI (34 mg, 0.17 mmol) and PdCl$_2$(PPh$_3$)$_2$ (240 mg, 0.34 mmol) were added. Mixture was r.t. stirred 24 h. Reaction mixture was then filtered and mother liquors dried under reduced pressure. Crude product was purified by gravimetric column chromatography (DCM) to afford 2,2'-(ethyne-1,2-diyl)dianiline (2.88 g, 73%) as yellow solid. ^{1}H NMR (CDCl$_3$) δ: 7.42 − 7.34 (m, 2H), 7.17 (m, J = 8.2, 7.3, 1.6, 2H), 6.80 − 6.69 (m, 4H), 4.29 (s, 4H) ppm. Other spectral data match the literature.[217]

18.3.18. Synthesis of 2,2'-bithiophene-5-carboxaldehyde (110)
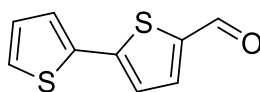
To a 0°C stirred solution of 2,2'-bithiophene (4 g, 24 mmol) in 1,2-dichloroethane (100 mL), DMF (1.8 g, 25.2 mmol) was added and then POCl$_3$ (2.4 g, 19.8 mmol) was added dropwise. Reaction was refluxed overnight. Once cooled to rt, reaction mixture was poured in 200 mL of 1 M aqueous NaOAc solution and stirred for 1 h. Organic phase was separated and dried over MgSO$_4$. Solvents were removed under reduced pressure and residue was purified by flash column chromatography (DCM) to afford 2,2'-bithiophene-5-carboxaldehyde as yellow solid (4.4 g, 94%).[214] ^{1}H-NMR (CDCl$_3$) δ: 9.86 (s, 1H), 7.66 (d, J = 4 Hz, 1H), 7.36 (m, 2H), 7.25 (d, J = 4 Hz, 1H), 7.08 (t, J = 4 Hz, 1H) ppm. Other spectral data match the literature.[384]

18.3.19. Synthesis of 2,2'-di([2,2'-bithiophen]-5-yl)-1,1'-dimethyl-1H,1'H-3,3'-biindole (111)
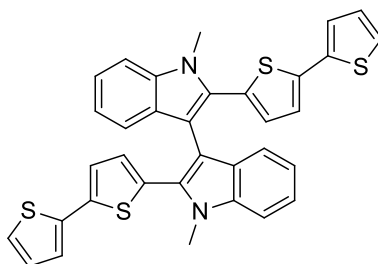
To a solution of 2,2'-(ethyne-1,2-diyl)dianiline (120 mg, 0.577 mmol) in MeCN (8 mL), 2,2'-bithiophene-5-carboxaldehyde (455 mg, 2.35 mmol) and a catalytic amount of HCl 37% were added. Reaction mixture was then refluxed 5 h. Solvent was removed under reduced pressure. Crude product was dissolved in DCM and washed with saturated aqueous sodium bicarbonate. Collected organic phase were dried over MgSO$_4$, filtered and solvent removed under reduced pressure. Raw 2,2'-di([2,2'-bithiophen]-5-yl)-1H,1'H-3,3'-biindole was immediately used for next step without any further purification. Raw product was dissolved in DMF (5 mL) and then KOH (86 mg, 1.52 mmol) was added at r.t. Mixture was stirred 0.5 h then iodomethane (270 mg, 1.9 mmol) was added and mixture stirred for 48 h. Solvent was removed under reduced pressure. Crude product was purified by gravimetric column chromatography (*n*-hexane/AcOEt 8:2) to afford 2,2'-di([2,2'-bithiophen]-5-yl)-1,1'-dimethyl-1H,1'H-3,3'-biindole (98 mg, 29%) as yellow solid. ^{1}H NMR (CDCl$_3$) δ 7.48 (d, *J* = 7.9 Hz, 2H), 7.40 (d, *J* = 8.2 Hz, 2H), 7.30 (d, *J* = 8 Hz, 2H), 7.17 (d, *J* = 5.0 Hz, 2H), 7.11 (t, *J* = 7.3 Hz, 2H), 6.96 (ddd, *J* = 14.3, 9.0, 3.1 Hz, 6H), 6.52 (d, *J* = 3.7 Hz, 2H), 3.81 (s, 6H) ppm. ^{13}C NMR (CDCl$_3$) δ: 138.9, 137.8, 138.3, 131.6, 131.2, 129.1, 128.8, 127.8, 124.2, 123.6, 123.5, 122.3, 120.8, 119.7, 109.4, 109.3, 31.2 ppm. MS (ESI): 588 (M$^{+\bullet}$). Elemental Analysis for C$_{34}$H$_{24}$N$_2$S$_4$: calcd (%) C 69.35, H 4.11, N 4.76; found (%) C 68.97, H 4.18, N. 7.68.

18.3.20. Synthesis of 2-(4-bromophenyl)-1H-indole (112)
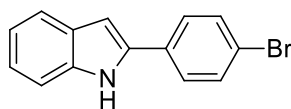
To a solution of *p*-bromo-acetophenone (6.9 g, 34.7 mmol) in polyphosphoric acid (40 g), phenylhydrazine (3.4 mL, 31.5 mmol) was added. Mixture was heated to 110°C and stirred until red colour appeared. Reaction mixture was then poured into a mixture ice/water and stirred 2 h. Mixture was then filtered and washed thoroughly with water. Crude product was recrystallized from EtOH to afford 2-(4-bromophenyl)-1H-indole (6.7 g, 66%) as yellowish solid.[218] ^{1}H NMR (DMSO-*d$_6$*) δ: 11.58 (s, 1H), 7.81 (d, *J* = 8 Hz, 2H), 7.65 (d, *J* = 8 Hz, 2H), 7.53 (d, *J* = 8 Hz, 1H), 7.39 (d, *J* = 8 Hz, 1H), 7.11 (ddd, J = 8, 5, 1 Hz, 1H), 7.00 (ddd, *J* = 10, 5, 1 Hz, 1H), 6.94 (d, *J* = 1.5 Hz, 1H) ppm. Other spectral data match the literature.[219]

18.3.21. Synthesis of 2,2'-bis(4-bromophenyl)-1H,1'H-3,3'-biindole (113)
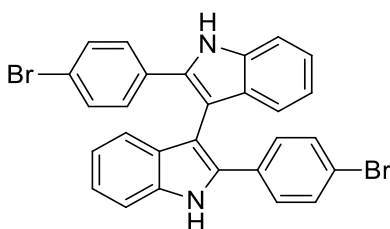
To an open air solution of 2-(4-bromophenyl)-1H-indole (1.63 g, 5.99 mmol) in toluene (35 mL), $FeCl_3$ (100 mg, 0.62 mmol) was added and mixture was heated to 90°C and stirred 24 h. Reaction mixture was then filtered through Celite® and mother liquors were dried under reduced pressure. Crude product was purified by gravimetric column chromatography (toluene/n-hexane 7:3) to afford of 2,2'-bis(4-bromophenyl)-1H,1'H-3,3'-biindole as light brown solid (740 mg, 45%). ^{1}H NMR (DMSO-d_6) δ: 11.6 (s, 2H), 7.46 (d, J = 8 Hz, 2H), 7.42-7.34 (m, 8H), 7.12 (td, J = 8, 1 Hz, 2H), 6.92 (d, J = 8 Hz, 2H), 6.85 (td, J = 8, 4 Hz, 2H) ppm. Other spectral data match the literature.[385]

18.3.22. Synthesis of 2,2'-bis(4-bromophenyl)-1,1'-dimethyl-1H,1'H-3,3'-biindole (114a)
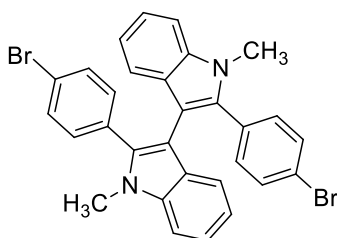
To a solution of 2,2'-bis(4-bromophenyl)-1H,1'H-3,3'-biindole (542 mg, 1 mmol) in DMF (10 mL), KOH (280 mg, 5 mmol) was added and mixture was stirred for 0.5 h. Then iodomethane (1.4 g, 10 mmol) was added and the mixture stirred for 48 h. The solvent was removed under reduced pressure and the residue was purified by gravimetric column chromatography (n-hexane/AcOEt 8:2) to afford 2,2'-bis(4-bromophenyl)-1,1'-dimethyl-1H,1'H-3,3'-biindole (470 mg, 72%) as yellow solid. ^{1}H NMR (400 MHz, DMSO-d_6) δ 7.52 (d, J = 8.3 Hz, 1H), 7.36 (d, J = 8.5 Hz, 2H), 7.26–7.13 (m, 2H), 6.99 (t, J = 7.4 Hz, 1H), 6.84 (d, J = 8.5 Hz, 2H), 3.62 (s, 3H). ^{13}C NMR (101 MHz, DMSO-d_6) δ 137.8, 137.3, 132.2, 131.4, 131.2, 128.2, 122.2, 121.3, 120.1, 119.9, 110.7, 107.1, 31.5; m.p.: 265°C. MS (EI): m/z = 570 [M]$^+$. Elemental Analysis for $C_{30}H_{22}Br_2N_2$: calcd (%) C 63.18, H 3.89, N 4.91; found (%) C 64.21, H 3.95, N 4.79.

18.3.23. Synthesis of 2,2'-bis(4-bromophenyl)-1,1'-dihexyl-1H,1'H-3,3'-biindole (114b)
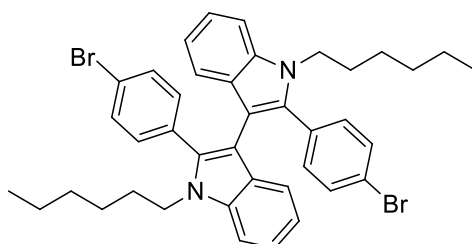
To a solution of 2,2'-bis(4-bromophenyl)-1H,1'H-3,3'-biindole (542 mg, 1 mmol) in DMF (10 mL), KOH (280 mg, 5 mmol) was added and reaction mixture was stirred 0.5 h. Then 1-bromohexane (1.6 g, 10 mmol) was added and mixture stirred for 48 h. Solvent was removed under reduced pressure. Crude product was purified by gravimetric column chromatography (*n*-hexane/AcOEt 8:2) to afford 2,2'-bis(4-bromophenyl)-1,1'-dihexyl-1H,1'H-3,3'-biindole (660 mg, 93%) as yellow solid. ^{1}H NMR (CDCl$_3$) δ: 7.57 (d, *J* = 7.8 Hz, 2H), 7.43 (d, *J* = 8.2 Hz, 2H), 7.30 (t, *J* = 7.6 Hz, 2H), 7.20 (d, *J* = 8.4 Hz, 4H), 7.14 (t, *J* = 7.4 Hz, 2H), 6.55 (d, *J* = 8.4 Hz, 4H), 4.08–3.94 (m, 4H), 1.77–0.99 (m, 16H), 0.79 (t, *J* = 7.0 Hz, 6H) ppm. ^{13}C NMR (CDCl$_3$) δ: 137.0, 137.0, 131.6, 131.4, 131.0, 129.1, 121.8, 121.1, 121.0, 119.4, 110.0, 107.9, 44.0, 31.2, 29.7, 26.3, 22.4, 13.9 ppm. MS (ESI): 708 [M$^{+\bullet}$]. m.p.: 127°C. Elemental Analysis for C$_{40}$H$_{42}$Br$_2$N$_2$: calcd (%) C 67.61, H 5.96, N, 3.94; found C 67.98, H 5.95, N 4.02.

18.3.24. Synthesis of 2,2'-bis(4-([2,2'-bithiophen]-5-yl)phenyl)-1,1'-dimethyl-1H,1'H-3,3'-biindole (115a)
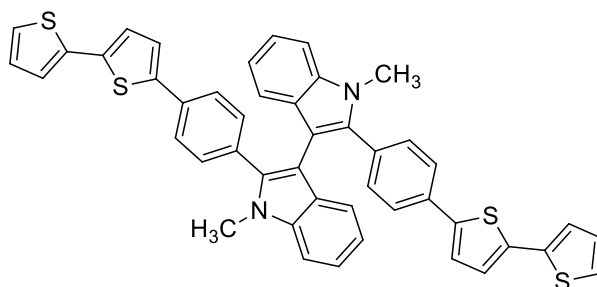
To a solution of 2,2'-bis(4-bromophenyl)-1,1'-dimethyl-1H,1'H-3,3'-biindole (2.16 mmol) in THF (150 mL) and water (15 mL), 5-(4,4,5,5)-Tetramethyl-1,3,2-dioxaborolan-2-yl)-2,2'-bithiophene (1.78 g, 6.1 mmol), Pd(PPh$_3$)$_4$ (380 mg, 0.33 mmol) and potassium carbonate (3 g, 21.7 mmol) were added). The reaction mixture was refluxed for 20 h and the solvent removed under reduced pressure. The residue was dissolved in DCM and washed with water; the organic phase was dried over MgSO$_4$ and dried under reduced pressure. Crude product was purified by gravimetric column chromatography (DCM/*n*-hexane 1:9) to afford 2,2'-bis(4-([2,2'-bithiophen]-5-yl)phenyl)-1,1'-dimethyl-1H,1'H-3,3'-biindole (59%) as yellow solid. ^{1}H-NMR (400 MHz, DMSO-*d*$_6$): 7.56-7.53 (m, 2H), 7.48-7.43 (m, 2H), 7.36-7.33 (m, 2H), 7.25 (t, 1H, J = 8 Hz), 7.21 (t, 1H, J = 8 Hz), 7.12 (t, 1H, J = 8 Hz), 7.01 (m, 1H), 6.96 (d, 2H, J = 8 Hz), 6.86 (d, 1H, J = 8 Hz), 3.67 (s, 3H). ^{13}C NMR spectrum was not recorded due to the insolubility of the compound. m.p..: > 275°C.

18.3.25. Synthesis of 2,2'-bis(4-([2,2'-bithiophen]-5-yl)phenyl)-1,1'-dihexyl-1H,1'H-3,3'-biindole (115b)
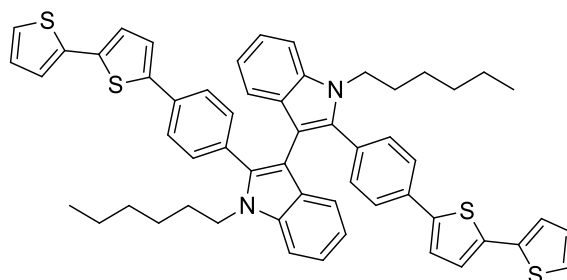
To a solution of 2,2'-bis(4-bromophenyl)-1,1'-dihexyl-1H,1'H-3,3'-biindole (1.54 g, 2.16 mmol) in THF (150 mL) and water (15 mL), 5-(4,4,5,5-tetramethyl-1,3,2-dioxaborolan-2-yl)-2,2'-bithiophene (1.78 g, 6.1 mmol), Pd(PPh$_3$)$_4$ (380 mg, 0.33 mmol) and potassium carbonate (3 g, 21.7 mmol) were added. Reaction mixture was then refluxed 20 h and solvent removed under reduced pressure. Crude mixture was dissolved in DCM and washed with water. Separated organic phase was dried with MgSO$_4$, filtered and dried under vacuum. Crude product was purified by gravimetric column chromatography (DCM/n-hexane 1:9) to afford 2,2'-bis(4-([2,2'-bithiophen]-5-yl)phenyl)-1,1'-dihexyl-1H,1'H-3,3'-biindole (1.4 g, 75%) as yellow solid. ^{1}H NMR (DMSO-d_6) δ: 7.58–7.51 (m, 4H), 7.45 (dd, J = 8.2, 6.1 Hz, 6H), 7.36–7.31 (m, 4H), 7.25–7.15 (m, 4H), 7.11 (dd, J = 5.1, 3.6 Hz, 2H), 6.99 (t, J = 7.2 Hz, 2H), 6.91 (d, J = 8.4 Hz, 4H), 4.21–4.07 (m, 4H), 1.58–1.41 (m, 4H), 1.09–0.88 (m, 12H), 0.65 (t, J = 7.0 Hz, 6H) ppm. ^{13}C NMR (DMSO-d_6) δ: 142.1, 138.3, 137.1, 136.8, 136.5, 132.4, 131.8, 130.7, 129.1, 128.9, 126.1, 125.7, 125.3, 125.2, 124.6, 122.1, 120.1, 119.8, 111.0, 107.7, 43.6, 31.0, 29.5, 25.9, 22.3, 14.1 ppm. MS (ESI) 881 [M+1]. Elemental Analysis for C$_{56}$H$_{52}$S$_4$N$_2$: calcd (%) C 76.32, H 5.95, N 3.18; found (%) C 76.43, N 6.21, N 3.02.

18.3.26. Synthesis of 4,7-dibromo-2,1,3-benzothiadiazole (116)
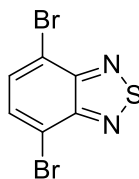
To a stirred solution of 2,1,3-benzothiadiazole (5 g, 36.72 mmol) in water (50 mL) Br$_2$ (5.63 mL, 109.19 mmol) in 48% HBr (57 mL) was added dropwise at rt. The reaction mixture was heated to reflux for 5 h and quenched with Na$_2$SO$_3$ after cooling. Mixture was filtered to afford 4,7-dibromo-2,1,3-benzothiadiazole (10.7 g, quant.) as yellow solid without any further purification. ^{1}H-NMR (CDCl$_3$) δ 7.72 (s, 2H) ppm. Other spectral data match the literature.[386]

18.3.27. Synthesis of 2-tributylstannyl-thiophene (117)
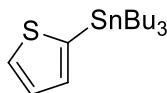
To a -78°C solution of thiophene (4.8 g, 59.2 mmol) in THF (100 mL), n-BuLi 2.5 M (24 mL, 60 mmol) in hexanes was added dropwise. Reaction mixture was stirred for 1 h then tributyltin chloride (19.4 g, 60 mmol) was added dropwise and reaction mixture stirred 1 h at -78°C. Then reaction mixture was allowed to reach slowly r.t. and was stirred r.t. overnight. Reaction mixture was quenched with water and extracted with diethyl ether. Reunited organic phases were dried with MgSO$_4$, filtered and evaporated under reduced pressure to afford 2-tributylstannyl-thiophene (22 g, quant.) as transparent oil without any further purification. ^{1}H-NMR (CDCl$_3$): δ 7.56 (d, J = 4.7 Hz, 1H), 7.18 (dd, J = 4.6, 3.2 Hz, 1H), 7.12 (d, J = 3.1 Hz, 1H), 1.53-1.43 (m, 6H), 1.31-1.21 (m, 6H), 1.05-1.01 (m, 6H) and 0.82 (t, J = 7.3 Hz, 9H) ppm. Other spectral data match the literature.[387]

18.3.28. Synthesis of 4,7-di-2-thienyl-2,1,3-benzothiadiazole (118)
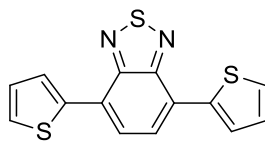
To a solution of 4,7-dibromo-2,1,3-benzothiadiazole (3.9 g, 13.2 mmol) in THF (100 mL), 2-(tributylstannyl)thiophene (11.75 g, 31.5 mmol) and $PdCl_2(PPh_3)_2$ (184 mg, 0.26 mmmol) were added. Reaction was refluxed overnight. Solvents were then evaporated under reduced pressure. MeOH (50 mL) was added and mixture was filtered. Resulting solid was washed exhaustively with MeOH. Product was collected as a red solid (3.6 g, 93%) with no further purifications. ^{1}H-NMR ($CDCl_3$): 8.15 (dd, J_1 = 2.5, J_2 = 1 Hz, 2H), 7.90 (s, 2H), 7.49 (dd, J = 5, J = 2.5 Hz, 2H). 7.25 (dd, J = 5, J = 4 Hz, 2H) ppm. Other spectral data match the literature.[388]

To a solution of 4,7-dibromo-2,1,3-benzothiadiazole (5 g, 17 mmol) in *N,N*-dimethylacetamide (150 mL), potassium acetate (5 g, 51 mmol), thiophene (13.6 ml, 51 mmol) and $Pd(OAc)_2$ (191 mg, 0.85 mmol) were added. Mixture was heated to 130°C and stirred for 4 h. After cooling to r.t., the reaction mixture was poured into brine and extracted with ethyl acetate. Reunited organic phases was dried over anhydrous Na_2SO_4 and evaporated under reduced pressure. Crude product was then suspended in methanol, filtered and washed again several times with methanol to afford 4,7-di-2-thienyl-2,1,3-benzothiadiazole (2.23 g, 45%) as red solid with no further purification.[389]

18.3.29. Synthesis of 4-([2-thieno]-5-bromyl)-7-(2-thienyl)-2,1,3-benzothiadiazole (119)
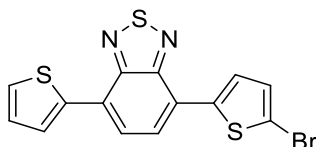
To r.t. shielded from light solution of 4,7-di(2-thienyl)-benzothiadiazole (2.19 g, 7.3 mmol) in DCM (200 mL) and acetic acid (200 mL), NBS (1.428 g, 8.03 mmol) was added slowly over ½ hour while stirring. Reaction mixture was stirred for 24 h at rt. Then aqueous 1M NaOH was added until neutralization of AcOH. Organic phase was separated and washed again with NaOH 1M solution and brine, dried with Na_2SO_4 and evaporated under reduced pressure. Crude product was purified by gravimetric column chromatography (*n*-hexane/DCM 9:1) to afford 4-([2-thieno]-5-bromyl)-7-(2-thienyl)-2,1,3-benzothiadiazole (2.34 g, 75%) as a dark red solid. ^{1}H NMR ($CDCl_3$): δ 8.13 (d, *J* = 3.6 Hz, 1H), 7.88-7.79 (m, 3H), 7.47 (d, *J* = 4.4 Hz, 1H), 7.21 (dd, *J* = 4.6, 4 Hz, 1H), 7.15 (d, *J* = 4 Hz, 1H) ppm. Other spectral data match the literature.[390]

18.3.30. Synthesis of 3,3'-bis-(5-(7-(thiophen-2-yl)-benzo-[c]-[1,2,5]-thiadiazol-4-yl)-thiophen-2-yl)-1H,1'H-2,2'-biindole (120)
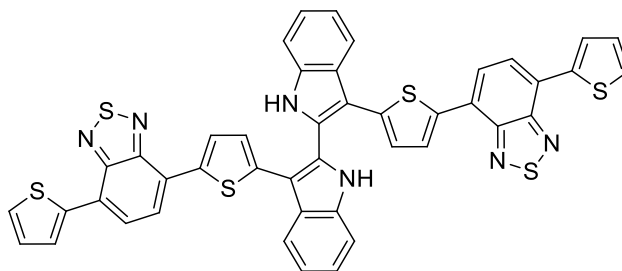
To a solution of 2,2,2-trifluoro-*N*-(2[-4-(2-(2,2,2-trifluoroacetylamino)-phenyl)-1,3-butadiynyl]-phenylacetamide (551 mg, 1.3 mmol) in DMF (33 mL), 4-([2-thieno]-5-bromyl)-7-(2-thienyl)-2,1,3-benzothiadiazole (1.97 g, 5.19 mmol), Pd(PPh$_3$)$_4$ (149 mg, 0.13 mmol), and K$_2$CO$_3$ (897 mg, 6.5 mmol) were added. Reaction was refluxed for 24 h. The solvent was then evaporated under reduced pressure and the crude product was washed 3 times with brine and extracted several times with ethyl acetate. Organic layer was dried with Na$_2$SO$_4$, filtered and evaporated under reduced pressure. Crude product was purified by flash column chromatography (hexane/DCM 3:7) to afford 3,3'-bis-(5-(7-(thiophen-2-yl)-benzo-[c]-[1,2,5]-thiadiazol-4-yl)-thiophen-2-yl)-1H,1'H-2,2'-biindole (170 mg, 23%) as a purple solid. ^{1}H-NMR (DMSO-d_6) δ 12.14 (s, 2H), 8.11 (m, 2H), 8.02 (d, *J* = 4.0 Hz, 2H), 7.97 (d, *J* = 7.6 Hz, 2H), 7.85 (d, *J* = 7.6 Hz, 2H), 7.77 (d, *J* = 4.8 Hz, 2H), 7.60 (d, *J* = 8.0 Hz, 2H), 7.39 (t, *J* = 7.6 Hz, 2H), 7.33 (t, *J* = 7.6 Hz, 2H), 7.28 (t, *J* = 4.0 Hz, 2H), 7.03 (d, *J* = 4.0 Hz, 2H) ppm; ^{13}C-NMR-APT (DMSO-d_6) δ 151.5, 151.4, 139.1, 138.4, 128.0, 127.9, 127.8, 127.1, 126.9, 125.8, 125.7, 125.1, 124.5, 124.1, 123.0, 120.5, 119.6, 112.0, 110.4 ppm; m.p.: 268°C; MS (ESI): 828 [M$^{+\bullet}$]. Elemental Analysis for C$_{44}$H$_{24}$N$_6$S$_6$: calcd (%) C 63.76, H 2.92, N 10.14; found (%) C 64.01, H 2.87, N 10.58.

18.3.31. Synthesis of 7,7'-(5,5'-(1,1'-dihexyl-1H,1'H-[2,2'-biindole]-3,3'-diyl)bis(thiophene-5,2-diyl))bis(4-(thiophen-2-yl)benzo[c][1,2,5]thiadiazole) (121)
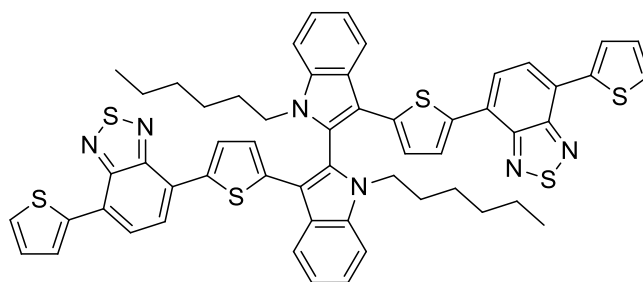
To a solution of 3,3'-bis-(5-(7-(thiophen-2-yl)-benzo-[c]-[1,2,5]-thiadiazol-4-yl)-thiophen-2-yl)-1H,1'H-2,2'-biindole (414 mg, 0.5 mmol) in DMF (10 mL), freshly powdered KOH (280 mg, 5 mmol) was added and reaction mixture was stirred 0.5 h. A colour change to green was noticed. Then 1-bromohexane (825 mg, 5 mmol) was added and reaction mixture was stirred for 48 h. Solvent was then evaporated under reduced pressure and the crude product was suspended in water with water and extracted with DCM. Organic layer was dried with Na$_2$SO$_4$, filtered and the solvent evaporated under reduced pressure. Crude product was purified by

gravimetric column chromatography (*n*-hexane/DCM 7:3) to afford 7,7'-(5,5'-(1,1'-dihexyl-1H,1'H-[2,2'-biindole]-3,3'-diyl)bis(thiophene-5,2-diyl))bis(4-(thiophen-2-yl)benzo[c][1,2,5]thiadiazole) (373 mg, 75%) as dark red solid. ^{1}H-NMR (CD$_2$Cl$_2$): δ 8.21 (d*, J* = 7.6 Hz, 2H), 7.98 (d, *J* = 3.2 Hz, 2H), 7.91 (d, *J* = 4.0 Hz, 2H), 7.71 (d, *J* = 7.6 Hz, 2H), 7.62 (d, *J* = 7.6 Hz, 2H), 7.42 (d, *J* = 8.0 Hz, 2H), 7.36-7.26 (m, 6H), 7.10 (dd, *J* = 5.2 Hz, *J* = 3.6 Hz, 2H), 6.98 (d, *J* = 3.6 Hz, 2H), 3.89 (m, 2H), 3.74 (m, 2H), 1.50 (m, 4H), 1.21 (m, 4H), 0.98 (m, 8H), 0.54 (t, J = 6.4 Hz, 6H) ppm; ^{13}C-NMR (CDCl$_3$) δ 151.5, 151.4, 138.5, 137.5, 136.2, 136.1, 126.9, 126.1, 124.8, 123.9, 123.9, 122.3, 119.8, 112.5, 109.7, 43.6, 30.3, 28.7, 25.7, 21.3, 12.8 ppm; MS (ESI): 996 [M$^{+\bullet}$]. Elemental Analysis for C$_{56}$H$_{48}$N$_6$S$_6$: calcd. (%) C 67.43, H 4.85, N 8.43; found (%) C 66.99, H 4.79, N 8.49.

18.3.32. Synthesis of 3,6-dibromobenzene-1,2-diamine (122)
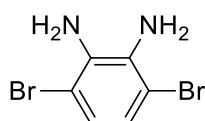
4,7-Dibromobenzothiadiazole (5.609 g, 19.08 mmol) was dissolved open air in ethanol (150 mL) and the solution was cooled to 0°C. NaBH$_4$ (10.826 g, 286.19 mmol) was added slowly under stirring, keeping the temperature at 0°C.The mixture was stirred overnight, allowing it to warm at r.t.. Ethanol was added, the solid was filtered and rinsed with ethanol. Solvent was evaporated under reduced pressure. Crude product was purified by gravimetric column chromatography (*n*-hexane/DCM 3:2) to afford 3,6-dibromo-1,2-benzenediamine (4.1 g, 81%) as a yellow-orange solid. ^{1}H-NMR (CDCl$_3$): δ (ppm) = 6.84 (s, 2H), 3.71 (s, 2H) ppm. Other spectral data match the literature.[391]

18.3.33. Synthesis of 4,7-dibromobenzo[c][1,2,5]selenadiazole (123)
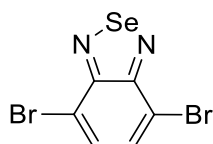
To a solution 3,6-dibromo-1,2-benzenediamine (4.108 g, 15.45 mmol) in ethanol (100 ml), SeO$_2$ (2.057 g, 18.53 mmol) was added. The reaction mixture was stirred for 3 h at 60°C. Obtained orange solid was filtered on short silica gel pad and washed multiple times with EtOH and the organic phase was evaporated to afford 4,7-dibromobenzo[c][1,2,5]selenadiazole (4.656 g, 88%) as bright yellow solid. ^{1}H NMR (DMSO-*d$_6$*): δ 7.83 (s, 2H) ppm. Other spectral data match the literature.[392]

18.3.34. Synthesis of afford 4,7-di(2-thienyl)-2,1,3-benzoselenodiazole (124)
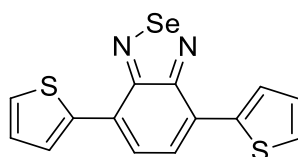
To a solution of 4,7-dibromo-benzoselendiazole (1.362 g, 3.99 mmol) in DMF (20 mL), 2-thienyl-tributylstannane (3.878 g, 10.39 mmol) and PdCl$_2$(PPh$_3$)$_2$ (140 mg, 0.19 mmol) were added and the mixture was stirred at 85°C for 6 h. Solvent was then evaporated under reduced pressure. Crude product was purified by gravimetric column chromatography (n-hexane/DCM 7:3 then n-hexane/DCM 1:1) to afford 4,7-di(2-thienyl)-2,1,3-benzoselenodiazole (1.238 g, 89%) as a dark red solid. ^{1}H-NMR (CDCl$_3$): δ 8.38 (dd, J = 1.2, 4 Hz, 2H), 7.82 (s, 2H), 7.49 (d, J = 1.2, 5.2 Hz, 2H), 7.22 (d, J = 1.2 Hz, 2H) ppm. Other spectral data match literature.[393]

18.3.35. Synthesis of 4-([2-thieno]-5-bromyl)-7-(2-thienyl)-2,1,3-benzoselenodiazole (125)
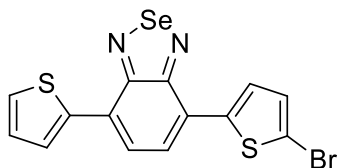
In a shielded from light r.t. solution of 4,7-di(2-thienyl)-2,1,3benzoselenodiazole (1.24 g, 3.57 mmol) in DCM (80 mL) and AcOH (80 mL), NBS (698.5 mg, 3.92 mmol) was added slowly over ½ hour. Reaction was stirred for 24 h, then aqueous NaOH 1M solution was added until neutralization of AcOH. Organic phase was separated and washed with aqueous 1M NaOH and brine, dried with Na$_2$SO$_4$, filtered and solvent removed under reduced pressure. Crude product was purified by flash column chromatography (n-hexane/DCM 9:1) to afford 4-([2-thieno]-5-bromyl)-7-(2-thienyl)-2,1,3-benzoselenodiazole (1.085 g, 72%) of a dark red solid. ^{1}H-NMR (CDCl$_3$): δ 7.96 (d, J = 3.7 Hz, 1H), 7.72 (d, J = 8.0 Hz, 1H), 7.67 (d, J = 7.6 Hz, 1H), 7.63 (d, J = 4.0 Hz, 1H), 7.40 (d, J = 4.5 Hz, 1H), 7.15 − 7.11 (m, 1H), 7.07 (d, J = 4.0 Hz, 1H) ppm. ^{13}C-NMR (CDCl$_3$) δ 158.0, 157.8, 141.0, 139.5, 130.3, 127.8, 127.6, 127.3, 126.7, 126.5, 126.1, 125.9, 125.3, 115.1 ppm. m.p.: 135°C. MS (GC-MS) 426 [M+1, ^{79}Br], 428 [M+1, ^{81}Br]. Elemental Analysis for C$_{14}$H$_7$BrN$_2$S$_2$Se; calcd (%) C 39.45, H 1.66, N 6.57; found C 38.97, H 1.71, N 6.42.

18.3.36. Synthesis of 3,3'-bis(5-(7-(thiophen-2-yl)benzo[c][1,2,5]selenadiazol-4-yl)thiophen-2-yl)-1H,1'H-2,2'-biindole (126)
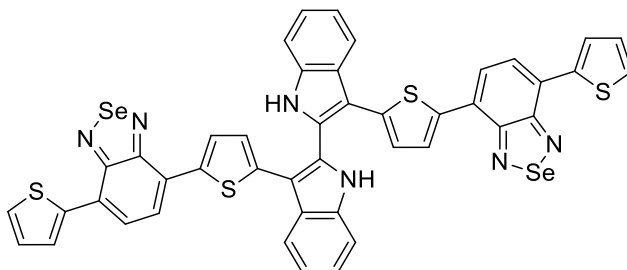
To a solution of 2,2,2-trifluoro-N-(2[-4-(2-(2,2,2-trifluoroacetylamino)-phenyl)-1,3-butadiynyl]-phenylacetamide (360 mg, 0.85 mmol) in DMF (30 ml), 4-([2-thieno]-5-bromyl)-7-(2-thienyl)-2,1,3-benzoselenodiazole (1.085 g, 2.54 mmol), Pd(PPh$_3$)$_4$ (92 mg, 0.08 mmol), and K$_2$CO$_3$ (586 mg, 4.24 mmol) were added. The reaction was heated to reflux and stirred for 24 h. Solvent was evaporated under reduced pressure and the crude product was washed 3 times with brine and extracted several times with ethyl acetate. Organic layer

was dried with Na_2SO_4 and evaporated under reduced pressure. Crude product was purified by gravimetric column chromatography (*n*-hexane/DCM 3:7) to afford 3,3'-bis(5-(7-(thiophen-2-yl)benzo[c][1,2,5]selenadi-azol-4-yl)thiophen-2-yl)-1H,1'H-2,2'-biindole (166 mg, 20%) as a dark violet solid. ^{1}H-NMR (DMSO-*d₆*) δ 12.04 (s, 2H), 8.09 (d, *J* = 8.0 Hz, 2H), 8.01 (d, *J* = 3.3 Hz, 2H), 7.93 (d, *J* = 3.9 Hz, 2H), 7.83 (d, *J* = 7.6 Hz, 2H), 7.71 (d, *J* = 7.6 Hz, 2H), 7.68 (d, *J* = 4.9 Hz, 2H), 7.53 (d, *J* = 8.1 Hz, 2H), 7.35-7,26 (m, 4H), 7.20 (t, J = 4 Hz), 6.95 (d, *J* = 3.9 Hz, 1H). ^{13}C-NMR not recorded due to product low solubility. m.p.: 266°C. MS (EI): 924 [M⁺•]. Elemental Analysis for $C_{44}H_{24}N_6S_4Se_2$: calcd (%) C 57.26, H 2.62, N 9.11; found (%) C 57.31, H 2.58, N 9.15.

18.3.37. Synthesis of 7,7'-(5,5'-(1,1'-dihexyl-1H,1'H-[2,2'-biindole]-3,3'-diyl)bis(thiophene-5,2-diyl))bis(4-(thiophen-2-yl)benzo[c][1,2,5]selenadiazole) (127)
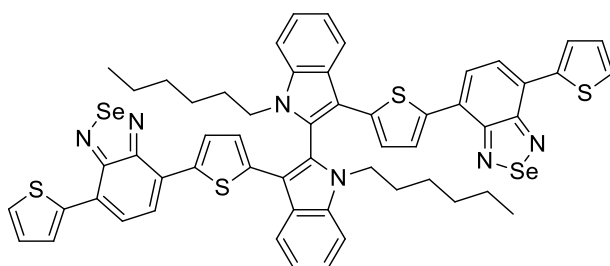
To a solution of 3,3'-bis(5-(7-(thiophen-2-yl)benzo[c][1,2,5]selenadiazol-4-yl)thiophen-2-yl)-1H,1'H-2,2'-biindole (41.5 mg, 0.05 mmol) in DMF (5 mL), freshly powdered KOH (14 mg, 0.24 mmol) was added. Solution was stirred for 1 h. A colour change to green was noticed. Then 1-bromohexane (0.054 mL, 0.4 mmol) was added. The reaction was stirred for 48 h. Solvent was evaporated under reduced pressure and the crude product was washed with water and extracted with DCM. Organic layer was dried with Na_2SO_4, filtered and the solvent removed under reduced pressure. Crude product was purified by gravimetric column chromatography to afford 7,7'-(5,5'-(1,1'-dihexyl-1H,1'H-[2,2'-biindole]-3,3'-diyl)bis(thiophene-5,2-diyl))bis(4-(thiophen-2-yl)benzo[c][1,2,5]selenadiazole) (35 mg, 75%) as a dark violet solid. ^{1}H-NMR (400 MHz, CDCl₃): δ (ppm) = 8.25 (d, *J* = 7.7 Hz, 2H), 7.83 (d, *J* = 3.3 Hz, 2H), 7.77 (d, *J* = 3.8 Hz, 2H), 7.54 (d, *J* = 7.5 Hz, 2H), 7.46 (d, *J* = 7.5 Hz, 2H), 7.38 (d, *J* = 7.6 Hz, 2H), 7.34 – 7.26 (m, 6H), 7.08 – 7.01 (m, 2H), 6.94 (d, *J* = 3.8 Hz, 2H), 3.92 – 3.79 (m, 2H), 3.79 - 3.73 (m, 2H), 1.35 – 0.74 (m, 16H), 0.54 (t, *J* = 6.4 Hz, 6H) ppm. ^{13}C-NMR (CDCl₃) δ 157.1, 157.0, 138.8, 137.9, 136.6, 136.2, 128.0, 127.8, 127.5, 127.3, 126.6, 126.5, 126.4, 126.0, 125.9, 125.7, 125.5, 125.1, 124.9, 124.5, 123.8, 123.6, 122.2, 120.0, 119,7, 112.6, 109.7, 43.6, 30.3, 28.7, 28.6, 25.7, 21.3, 12.8 ppm. m.p.: 112°C. MS (ESI) 1092 [M⁺•]. Elemental Analysis for $C_{56}H_{48}N_6S_4Se_2$; calcd (%) C 61.64, H 4.43, N 7.70; found (%) C 61,92, H 4.40, N, 7.49.

18.3.38. Synthesis of 2,2'-biindole (128)
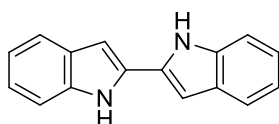
A mixture of fresh KH from an immediately opened flask (830 mg, 20.7 mmol) in distilled *N*-methyl-pyrrolidone (100 mL) was stirred and heated to 80°C. A solution of 2-[-4-(2-aminophenyl)-1,3-butadienyl]-phenylamine (2 g, 8.62 mmol) in NMP (50 mL) was added dropwise. The reaction proceeded for 20 h, then it was quenched with water and extracted with Et_2O. The organic phase was dried over Na_2SO_4 and evaporated under reduced pressure to afford 2,2'-biindole (1.92 g, quant.) without any further purification.

However reaction is heavily dependent from quality of used KH as stated in Chapter 2: Results and Discussion; as it gets older after bottle opening, reaction efficiency drops and 2,2'-biindole yield is gradually substituted by 2-((1H-indol-2-yl)ethynyl)aniline **128b**. With very old KH (> 1 month after flask opening) no reaction occurs. 2-((1H-indol-2-yl)ethynyl)aniline **128b** was fully characterized.
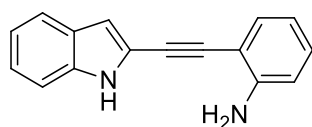
^{1}H-NMR ($CDCl_3$): δ 8.24 (s, 1H), 7.60 (d, J = 12 Hz), 7.38 – 7.24 (m, 2H), 7.23 (d, J = 8 Hz), 7.19 - 7.12 (m, 2H), 6.83 (s, 1H), 6.75 – 6.72 (m, 2H), 4.29 (s, 1H) ppm; ^{13}C NMR ($CDCl_3$): δ 147.96, 136.19, 132.19, 130.17, 127.84, 123.53, 120.83, 120.54, 118.78, 118.11, 114.5, 110.73, 108.68, 107.23, 89.13, 86.84 ppm. m.p.: 171°C. MS (GC-MS) 233 [M+1]. Elemental Analysis for $C_{16}H_{12}N_2$: calcd (%) C 82.73, H 5.21, N 12.06; found (%) 82.90, H 5.19, N 12.05.

To a solution of 2-[-4-(2-aminophenyl)-1,3-butadienyl]-phenylamine (100 mg, 0.431 mmol) in DMF (4 mL), CuI (333 mg, 1.724 mmol) was added and reaction mixture was stirred at 110°C overnight. After completion, the reaction mixture was quenched in water, filtered over Büchner funnel and solid washed two times with Et_2O. Liquid phase was washed with water, extracted with Et_2O, dried over Na_2SO_4 and evaporated under reduced pressure to afford 2,2'-biindole (90.2 mg, 95%) as a brown solid. ^{1}H NMR (DMSO-d_6): δ 11.52 (s, 1H), 7.56 (d, *J* = 7.8 Hz, 1H), 7.40 (d, *J* = 8.0 Hz, 1H), 7.11 (t, *J* = 7.4 Hz, 1H), 7.01 (t, *J* = 7.3 Hz, 1H), 6.92 (s, 1H) ppm. Other spectral data match the literature.[394] On big batches (2-[-4-(2-aminophenyl)-1,3-butadienyl]-phenylamine > 1 g), some 2,2'-biindole stays trapped in solid cake after filtration. Dissolution of the latter with 1M aqueous ammonia and extraction with diethyl ether helps to recover extra product. When reaction was performed on 4000 mg of 2-[-4-(2-aminophenyl)-1,3-butadienyl]-phenylamine, 81% yield was reached with this workup.

18.3.39. Synthesis of 1,1'-dipropyl-2,2'-biindole (129)
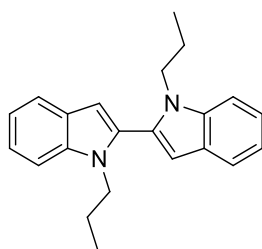
To a r.t. solution of 2,2'-biindole (500 mg, 2.15 mmol) in DMF (15 mL), KOH (603 mg, 10.77 mmol) was added and solution was stirred for 1 h. Then 1-bromopropane (1.3 g, 10.77 mmol) was added and reaction mixture was r.t. stirred 48 h. Solvent was removed under reduced pressure. Crude residue was dissolved in DCM and washed with water. Organic phase was dried with $MgSO_4$, filtered and solvent was evaporated under reduced pressure. Crude product was purified by gravimetric column chromatography (n-hexane to clean up 1-bromohexane residues then n-hexane/EtOAc 8:2) to afford 1,1'-dipropyl-2,2'-biindole (520 mg, 77%) as brown solid. ^{1}H NMR (CDCl$_3$): δ 7.60 (d, J = 8 Hz, 2H), 7.31 (d, J = 8 Hz, 2H), 7.19 (t, J = 8 Hz, 2H), 7.08 (t, J = 8 Hz, 2H), 6.54 (s, 2H), 3.97 (t, J = 8 Hz, 4H), 1.62 (m, 2H), 0.69 (t, J = 8 Hz, 3H) ppm. Other spectral data match the literature.[395]

18.3.40. Synthesis of 3,3'-diiodo-1,1'-dipropyl-2,2'-biindole (130)
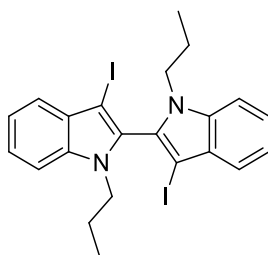
To a 0°C shielded from light solution of 1,1'dipropyl-1H,1'H-2,2'-biindole (1.141 g, 3.61 mmol) in DMF (20 ml), N-iodo-succinimide (2.029 g, 9.02 mmol) was added slowly over 1 h. The reaction was stirred for 36 h. Aqueous 1M NaOH was added and the mixture was extracted with Et$_2$O. Organic phase was washed with water, dried over Na_2SO_4, filtered and solvent was evaporated under reduced pressure. Crude product was purified by flash column chromatography (n-hexane/DCM 8:2) to afford 3,3'-diiodo-1,1'-dipropyl-2,2'-biindole (1.515 g, 74%) as an off-white solid. ^{1}H-NMR (DMSO-d_6): δ 7.71 (d, J = 8.3 Hz, 2H), 7.49 (d, J = 7.8 Hz, 2H), 7.41 (t, J = 7.7 Hz, 2H), 7.30 (t, J = 7.4 Hz, 2H), 4.27 (m, 2H), 3.77 (m, 2H), 1.61 (m, 2H), 0.76 (t, J = 7.4 Hz, 6H) ppm. ^{13}C NMR (CDCl$_3$): δ 137.2, 132.4, 130.4, 132.7, 122.0, 120.7, 110.5, 65.3, 47.3, 23.6, 11.6 ppm. Elemental Analysis for $C_{22}H_{22}I_2N_2$: calcd (%) C 46.50, H 3.90, N 4.93; found (%) C 46.38, H 3.97, N 4.82.

18.3.41. Synthesis of 3,3'-di([2,2'-bithiophen]-5-yl)-1,1'-dipropyl-1H,1'H-2,2'-biindole (98)
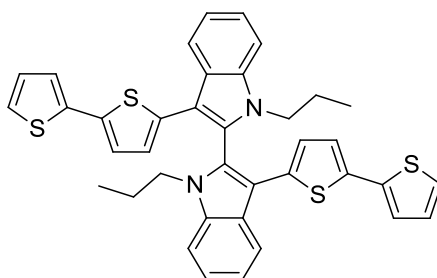
3,3'-diiodo-*N*,*N*'-dipropyl-2,2'-bisindole (1 eq., 100 mg, 0.17 mmol), (2,2'-bitiophen-5-yl)-pinacolborane (3 eq., 154 mg, 0.51 mmol), Pd(PPh₃)₄ (0.1 eq., 20 mg, 0.017 mmol) and KOH (8 eq., 79 mg, 1.36 mmol) were added to a 5:1 solution of toluene/ethanol (1 mL EtOH, 5 mL toluene) and 3 drops of water. The reaction was heated to 90°C and stirred for 2 h. The solvents were evaporated under reduced pressure and the residue was purified by gravimetric column chromatography (*n*-hexane/DCM 8:2) to afford 3,3'-di([2,2'-bithiophen]-5-yl)-1,1'-dipropyl-1H,1'H-2,2'-biindole (84.4 mg, 79%) of the desired product as a yellow powder. For characterizations see paragraph **16.3.6**.

18.3.42. Chemical oxidation of 3,3'-di([2,2'-bithiophen]-5-yl)-1,1'-dipropyl-1H,1'H-2,2'-biindole (98): synthesis of opened dimer
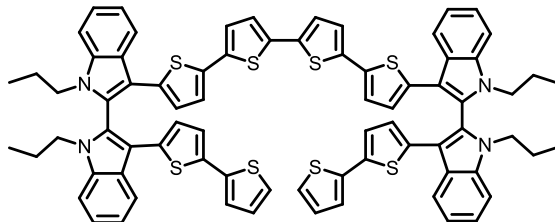
To r.t. solution of iron trichloride (99 mg, 0.61 mmol) in dry chloroform (150 mL), a solution of 3,3'-di([2,2'-bithiophen]-5-yl)-1,1'-dipropyl-1H,1'H-2,2'-biindole (100 mg, 0.155 mmol) in chloroform (50 mL) is added slowly dropwise. Dark green reaction mixture was stirred overnight at r.t., then solvent was removed under reduced pressure. Obtained solid was suspended in methanol (30 mL), then 10 drops of hydrazine were added. Reaction mixture turned from dark green to orange and then stirred for 1 h. Solvent was then dried under reduced pressure and obtained solid was extracted with Soxhlet apparatus with THF (70 mL). Organic phase was dried under reduced pressure and crude product was purified by column chromatography to afford the opened dimer as orange solid (76 mg, 38%) as firstly eluted product. Other fractions contained closed dimer, opened trimer and superior oligomers. ¹H-NMR opened dimer (CDCl₃, 400MHz): δ (ppm) = 8.19 (1H, d, J = 7.6Hz), 7.43 (1H, d, J = 8.0Hz), 7.37 (1H, t, J = 8Hz), 7.32 (1H, t, J = 7.2Hz), 7.12 (1H, d, J = 4.8Hz), 6.95 (3H, m), 6.79 (1H, d, J = 3.6Hz), 3.83 (1H, m), 3.71 (1H, m), 0.73 (3H, t, J = 7.2Hz). MS (MALDI-TOF): opened dimer 1287, closed dimer 1284, opened trimer 1928.

18.3.43. Synthesis of 4,7-dibromo-2,1,3-benzoxadiazole (131)
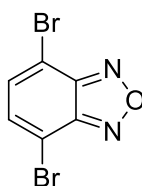
2,1,3-benzoxadiazole (500 mg, 4.16 mmol) and Fe dust (46 mg, 0.83 mmol) were heated to 90°C solventless. Bromine (0.64 mL, 12.48 mmol) was then added dropwise slowly through 2 h. The mixture was stirred for additional 2 h and then cooled to r.t.. Aqueous saturated Na_2SO_3 and ethyl acetate were added. The organic layer was separated, washed with brine, dried with $MgSO_4$ and evaporated under reduced pressure. Crude product was purified by gravimetric column chromatography (*n*-hexane/EtOAc 10:1) to afford 4,7-dibromo-2,1,3-benzoxadiazole (700 mg, 61%) as an orange solid. ^{1}H-NMR (CDCl$_3$): δ = 7.52 (s, 2H) ppm. Other spectral data match with the literature.[241]

18.3.44. Synthesis of 4,7-di(2-thienyl)-2,1,3-benzoxadiazole (132)
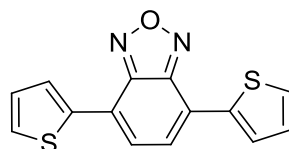
To a solution of 4,7-dibromo-2,1,3-benzoxadiazole (3.301 g, 11.87 mmol) in THF (25 mL), tributyl-2-thienyl-stannane (5.1 ml, 15.8 mmol) and PdCl$_2$(PPh$_3$)$_2$ (185 mg, 0.26 mmol) were added and reaction was refluxed and stirred overnight. Solvent was then evaporated under reduced pressure. Crude product was purified by gravimetric column chromatography (*n*-hexane/chloroform 10:1). Recrystallization from ethanol afforded 4,7-di(2-thienyl)-2,1,3-benzoxadiazole (1.01 g, 68%) as a bright orange solid. ^{1}H NMR (400 MHz CDCl$_3$): δ 8.12 (dd, *J* = 3.8, 1 Hz, 2H), 7.62 (s, 2H), 7.45 (dd, *J* = 5, 1 Hz, 2H), 7.21 (dd, *J* = 3.8, 5 Hz, 2H) ppm. Other spectral data match the literature.[396]

18.3.45. Synthesis of 4-([2-thieno]-5-bromyl)-7-(2-thienyl)-2,1,3-benzoxadiazole (133)
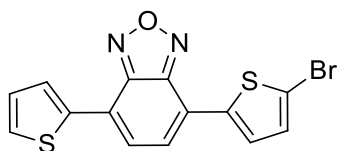
To a r.t. shielded from light solution of 4,7-di(2-thienyl)-2,1,3-benzoxadiazole (358 mg, 1.26 mmol) in chloroform (100 mL) and AcOH (100 mL), NBS (247 g, 1.39 mmol) was added slowly over 1 h. The reaction was stirred for 24 h. Solvents were evaporated under reduced pressure. Aqueous NaOH 1M solution and DCM were added. Organic phase was then separated and washed with brine, dried over Na_2SO_4, filtered and evaporated under reduced pressure. Crude product was purified by gravimetric column chromatography (hexane/DCM 9:1) to afford 4-([2-thieno]-5-bromyl)-7-(2-thienyl)-2,1,3-benzoxadiazole (424 mg, 87%) of a dark

red solid. ^{1}H NMR (CDCl$_3$): δ (ppm) = 8.05 (d, *J* = 3.3 Hz, 1H), 7.78 (d, *J* = 3.7 Hz, 2H), 7.55 (m, 1H), 7.46 – 7.36 (m, 3H), 7.17 – 7.12 (m, 1H), 7.09 (d, *J* = 3.9 Hz, 1H). ^{13}C NMR (DMSO-*d$_6$*): δ (ppm) = 147.42, 147.22, 138.62, 136.92, 131.95, 128.99, 128.77, 128.55, 128.43, 127.65, 127.29, 121.36, 119.61, 114.3. m.p.: 141°C. Elemental Analysis for C$_{14}$H$_7$BrN$_2$OS$_2$: calcd (%) C 46.29, H 1.94, N, 7.71; found (%) C 46.33, H 2.01, N, 7.65.

18.3.46. Synthesis of 3,3'-bis-(5-(7-(thiophen-2-yl)-benzo-[c]-[1,2,5]-oxadiazol-4-yl)-thiophen-2-yl)-1H,1'H-2,2'-biindole (134)
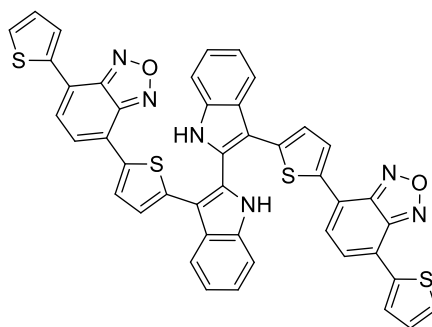
To a solution of 2,2,2-trifluoro-*N*-(2[-4-(2-(2,2,2-trifluoroacetylamino)-phenyl)-1,3-butadiynyl]-phenyla-cetamide (85 mg, 0.2 mmol) in DMF (12 ml), 4-([2-thieno]-5-bromyl)-7-(2-thienyl)-2,1,3-benzoxadiazole (230 mg, 0.63 mmol), Pd(PPh$_3$)$_4$ (46 mg, 0.04 mmol), and K$_2$CO$_3$ (136 mg, 0.9 mmol) were added. The reaction was set to 100°C and stirred for 24 h. The solvent was evaporated in vacuo and the crude product was washed with brine and extracted with ethyl acetate. Organic layer was dried with Na$_2$SO$_4$, filtered and evaporated under reduced pressure. Crude product was purified by flash column chromatography (*n*-hexane/DCM 3:7 – *n*-hexane/DCM 1:2) to afford 3,3'-bis-(5-(7-(thiophen-2-yl)-benzo-[c]-[1,2,5]-oxadiazol-4-yl)-thiophen-2-yl)-1H,1'H-2,2'-biindole (20 mg, 12%) of a red solid. ^{1}H NMR (DMSO-*d$_6$*): δ 12.05 (s, 2H), 7.95 (d, *J* = 8.0 Hz, 2H), 7.85 (d, *J* = 3.6 Hz, 2H), 7.78 (d, *J* = 3.9 Hz, 2H), 7.67 (d, *J* = 5.0 Hz, 2H), 7.62 (d, *J* = 7.5 Hz, 2H), 7.47 (t, *J* = 7.8 Hz, 2H), 7.26 (t, *J* = 7.3 Hz, 2H), 7.23 – 7.13 (m, 4H), 6.92 (d, *J* = 3.9 Hz, 2H), 6.87 (t, *J* = 3.9 Hz, 2H) ppm.

♦ ♦ ♦ ♦ ♦ ♦

18.4. Appendix experimental part

18.4.1. Synthesis of 5H-dibenzo[b,f]azepine-10,11-dione (137)
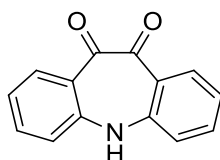
To an open-air solution of oxcarbazepine (5.04 g, 20 mmol) in 1,4-dioxane (120 mL), benzeneseleninic acid anhydride (14.4 g, 40 mmol) was added). The mixture was heated to reflux for 8 hours. The precipitate was then filtered and washed with *n*-hexane to afford 5H-dibenzo[b,f]azepine-10,11-dione as orange solid (2.48

g, 55%) without any further purification. ^{1}H-NMR (DMSO-d_6): δ 10.85 (s, 1H), 7.95 (d, J = 8 Hz, 2H), 7.80 (t, J = 8 Hz, 2H), 7.65 (d, J = 8 Hz, 2H), 7.30 (t, J = 8 Hz, 2H) ppm. Other spectral data match the literature.[397]

18.4.2. Synthesis of 9H-dibenzo[b,f]pyrazino[2,3-d]azepine-2,3-dicarbonitrile (138)
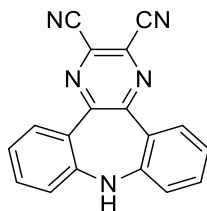
To an open-air solution of 5H-dibenzo[b,f]azepine-10,11-dione (2.48 g, 11 mmol) in acetic acid (100 mL), diaminomaleonitrile (3.60 g, 33 mmol) was added. Reaction mixture was refluxed open-air for 12 hours, then filtered and precipitate was washed with *n*-hexane to afford 9H-dibenzo[b,f]pyrazino[2,3-d]azepine-2,3-di-carbonitrile as a dark brown solid (3.022 g, 93%) without any further purification. ^{1}H-NMR (DMSO-d_6): δ 8.33 (s, 1H), 7.77 (d, J = 8 Hz), 7.23 (t, J = 8 Hz, 2H), 7.20 (d, J = 8 Hz, 2H) ppm. Other spectral data match the literature.[317]

18.4.3. Synthesis of 3-(octyloxy)-9H-dibenzo[b,f]pyrazino[2,3-d]azepine-2-carbonitrile (139)
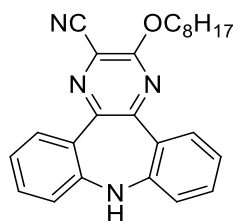
1-iodoctane (1000 mg, 4.16 mmol) was added to a solution of 9H-dibenzo[b,f]pyrazino[2,3-d]azepine-2,3-dicarbonitrile (1400 mg, 1.36 mmol) and K_2CO_3 (1.3 eq., 246 mg, 1.78 mmol) in DMF (10 mL). Reaction mixture was refluxed open-air overnigh, then DMF was removed under reduced pressure. Crude product was then purified by gravimetric column cromatography (DCM/*n*-hexane 8:2) to afford 3-(octyloxy)-9H-dibenzo[b,f]pyrazino[2,3-d]azepine-2-carbonitrile (146 mg, 27%) as an orange solid. ^{1}H NMR (DMSO-d_6,): δ 7.91 (s, 1H), 7.85 (d, J = 7.2 Hz, 1H), 7.64 (d, J = 7.6 Hz), 7.45 (t, J = 7.6 Hz, 1H), 3.38 (t, J = 7.2 Hz, 1H), 7.15 (m, 4H), 4.59 (t, J = 7.2 Hz, 2H), 1.86 (q, J = 6.4 Hz, 2H), 1.16 -1.07 (m, 10H), 0.90 (t, J = 6.8 Hz, 3H) ppm; ^{13}C NMR (CDCl$_3$) 158.41, 151.78, 150.24, 148.48, 144.43, 131.06, 130.67, 129.97, 129.45, 127.16, 127.17, 123.36, 122.90, 119.17, 118.76, 115.28, 113.71, 67.02, 30.65, 28.23, 28.15, 27.66, 24.85, 21.62, 13.08 ppm; m.p.: 108-109 °C; MS (EI, *m/z*): 398 [M$^{+\bullet}$], 286; FT-IR (λ, cm^{-1}): 3333.25, 2922.63, 2852.30, 2236.21, 1534.20, 1395.41, 1175.01, 746.88. Elemental analysis for $C_{25}H_{26}N_4O$: calcd. (%) C 75.35, H 6.58, N 14.06; found (%) C 75.36, H 6.63, N 13.97.

18.4.4. Synthesis of 10-methoxy-5-octyl-5H-dibenzo[b,f]azepine (141)
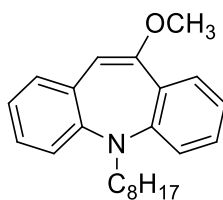
A solution of 10-methoxyiminostilbene (2 g, 9.08 mmol) was cooled to -30°C. Then *n*-Buli 2.5 M in *n*-hexane (4.2 mL, 10.6 mmol) was added dropwise. Reaction mixture quickly became dark red. When reaction reached -20°C degrees, a solution of 1-iodoctane (2.54 g, 10.6 mmol) in dry THF (4 mL) was added dropwise. Reaction was then allowed to reach r.t. and stirred overnight. Mixture was then quenched with water and extracted with Et$_2$O. Collected organic phases were dried with MgSO$_4$, filtered and solvent removed under reduced pressure. Crude product was then purified by gravimetric column chromatography (DCM/*n*-hexane 4:6) to afford 10-methoxy-5-octyl-5H-dibenzo[b,f]azepine as a pale yellow solid (2.60 g, 86%). ^{1}H NMR (DMSO-*d$_6$*): δ 7.39-7.32 (m, 2H), 7.17-7-09 (m, 3H), 7.06-7.01 (m, 2H), 6.53 (t, J = 8 Hz, 1H), 6.11 (s, 1H), 3.81 (s, 3H), 3.66 (m, 2H), 1.45 (m, 2H), 1.30 (m, 2H), 1.23-1.12 (m, 8H), 0.82 (t, J = 8 Hz, 3H) ppm; ^{13}C NMR (DMSO-*d$_6$*) δ 156.09, 151.01, 148.74, 132.25, 131.11, 129.75, 128.63, 126.55, 126.37, 122.86, 122.84, 119.77, 119.41, 103.24, 55.20, 49.09, 31.04, 28.61, 28.47, 26.88, 26.16, 22.03, 13.86 ppm; MS (EI, *m/z):* 335 [M+1], 320, 236, 204, 179; m.p.: 44.7°C. FT-IR (λ, cm^{-1}): 2924.44, 2842.45, 1636.36, 1222.96, 776.32; Elemental analysis for C$_{23}$H$_{29}$NO: calcd. (%) C 82.34, H 8.71, N 4.18; found (%) C 82.03, H 8.85, N 4.35.

18.4.5. Synthesis of 10-methoxy-5-octyl-5H-dibenzo[b,f]azepine (142)
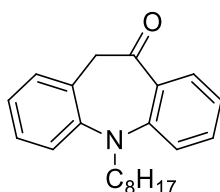
Aqueous HCl 37% (123 mg, 1.24 mmol) was added dropwise to an open-air r.t solution of 10-methoxy-5-octyl-5H-dibenzo[b,f]azepine (2.60 g, 7.78 mmol) in acetone (10 mL). Reaction mixture was then stirred for 4 h, H$_2$O was added (150 mL) and mixture was extracted with DCM. Collected organic phases were dried with MgSO$_4$, filtered and solvent removed under reduced pressure. Crude product was then purified by gravimetric column chromatography (DCM/*n*-hexane 4:6) to afford 10-methoxy-5-octyl-5H-dibenzo[b,f]azepine as a yellow oil (2.11 g, quant. yield). ^{1}H NMR (DMSO-*d$_6$*): δ 7.95 (dd, J$_1$ = 8 Hz, J$_2$ = 1 Hz, 1H), 7.58 (t, J = 8 Hz, 1H), 7.44 (d, J = 8 Hz, 1H), 7.32 (t, J = 8 Hz, 2H), 7.26 (t, J = 8 Hz, 1H), 7.18 (t, J = 8 Hz, 1H), 6.99 (t, J = 8 Hz, 1H), 3.99 (s, 2H), 3.88 (s, 2H), 1.55 (m, 2H), 1.17 (m, 10H), 0.80 (t, J = 8 Hz, 3H) ppm; ^{13}C NMR (DMSO-*d$_6$*) δ 189.80, 149.69, 146.91, 134.05, 130.32, 130.11, 128.31, 127.19, 125.65, 125.20, 122.31, 119.86, 118.42, 50.39, 48.42, 39.97, 31.08, 28.46, 27.51, 26.26, 21.96, 21.48, 13.85 ppm; MS (EI, *m/z*): 321 [M$^{+\bullet}$], 222, 194, 180; FT-IR (λ,

cm^{-1}): 2923.33, 2852.92, 1666.84, 760.96. Elemental analysis for $C_{22}H_{27}NO$: calcd. (%) C 82.20; H 8.47; N 4.36; found (%) C 82.28, H 8.45, N 4.30.

18.4.6. Synthesis of 5-octyl-5H-dibenzo[b,f]azepine-10,11-dione (143)
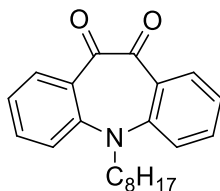
Selenium dioxide (1.83 g, 16.6 mmol) was added to an open-air solution of 10-methoxy-5-octyl-5H-dibenzo[b,f]azepine (2.11 g, 6.6 mmol) in 1,4-dioxane (40 mL). Reaction was then refluxed for 6 h. Reaction mixture was then filtered and precipitate was washed with DCM. Organic solution was then concentrated under reduced pressure. Crude product was then purified by gravimetric column chromatography (DCM/n-hexane 8:2) to afford 5-octyl-5H-dibenzo[b,f]azepine-10,11-dione as a red oil. ^{1}H NMR (CDCl$_3$): δ 7.81 (d, J = 8 Hz, 2H), 7.45 (td, J$_1$ = 8 Hz, J$_2$ = 1 Hz), 7.23 (d, J = 8 Hz, 2H), 7.86 (t, J = 8 Hz, 2H), 3.80 (t, J = 8 Hz), 1.34 (m, 2H), 1.79-1.09 (m, 10H), 0.75 (t, J = 8 Hz, 3H) ppm; ^{13}C NMR (CDCl$_3$) δ 188.38, 147.93, 133.23, 131.05, 129.80, 121.72, 120.19, 50.40, 30.74, 28.00, 27.98, 26.76, 25.87, 21.52, 13.00 ppm; MS (EI, m/z): 335 [M$^{+\bullet}$], 208; FT-IR (λ, cm^{-1}): 2924.11, 2853.48, 1698.54, 1652.25, 1592.92, 923.45, 766.43; VIS (CH$_2$Cl$_2$, λ, nm): 565, 419.60. Elemental analysis for $C_{22}H_{25}NO_2$: calcd. (%) C 78.77, H, 7.51 N 4.18; found (%) C 78.69, H 7.52, N 4.26.

18.4.7. Synthesis of 9-octyl-9H-dibenzo[b,f]pyrazino[2,3-d]azepine-2,3-dicarbonitrile (135)
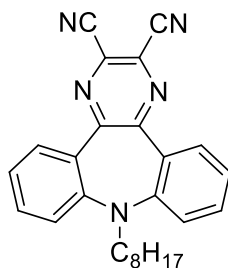
DAMN (2.37 g, 22 mmol) was added to an open-air solution of 5-octyl-5H-dibenzo[b,f]azepine-10,11-dione (2.45 g, 7.31 mmol) in acetic acid (85 mL). Mixture was refluxed for 3 h. Solvent was then removed under reduced pressure and crude product was purified by gravimetric column chromatography (DCM/n-hexane 6:4) to afford 9-octyl-9H-dibenzo[b,f]pyrazino[2,3-d]azepine-2,3-dicarbonitrile as an orange solid (2.60 g, 84%). ^{1}H NMR (DMSO-d_6): δ (ppm) = 7.77 (d, J = 8 Hz, 2H), 7.67 (t, J = 8 Hz, 2H), 7.46 (d, J = 8 Hz, 2H), 7.36 (t, J = 8Hz, 2H), 3.81 (t, J = 8 Hz, 2H), 1.46 (m, 2H), 1.30-1.18 (m, 10H), 0.85 (t, J = 8 Hz, 3H); ^{13}C NMR (CDCl$_3$) δ (ppm) = 154.59, 154.11, 132.60, 131.42, 150.05, 124.75, 120.45, 114.27, 48.38, 30.98, 28.33, 26.78, 25.97, 21.99, 13.85; MS (EI, m/z): 407 [M$^{+\bullet}$], 308; m.p.: 140.7°C; FT-IR (λ, cm^{-1}): 2924.01, 2853.81, 2239.20, 774.90; VIS (CH$_2$Cl$_2$, λ, nm): 431.80. Elemental analysis for $C_{26}H_{25}N_5$: calcd (%) C 76.63, H 6.18, N 17.19; found (%) C 76.92, H 6.03, N 17.33.

18.4.8. Synthesis of type A copper(II) tetrapyrazinoporphyrazine (144)
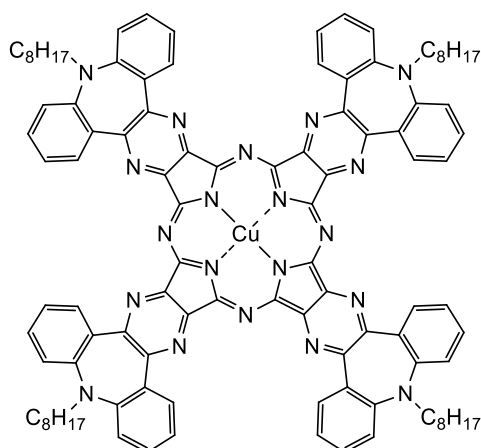
Cu(OAc)$_2$ (89 mg, 0.49 mmol) and DBU (catalytic amount) were added to a solution of 9-octyl-9H-dibenzo[b,f]pyrazino[2,3-d]azepine-2,3-dicarbonitrile (500 mg, 1.23 mmol) in DMAE (10 mL). Mixture was then refluxed 3 h. Reaction mixture was quenched with aqueous HCl 1 M (15 mL), filtered and precipitate was washed with water and methanol. Crude product was purified with gravimetric column chromatography (DCM) to afford copper(II) tetrapyrazinoporphyrazine **144** as a deep green solid (248 mg, 49%). MS (MALDI-TOF, *m/z*) 1714.7 [(M+Na)$^{+\bullet}$] m.p.: 301°C; FT-IR (λ, cm^{-1}): 2919.80, 2849.84, 1542.11, 1496.48, 1449.40, 1350.75, 1250.18, 1117.27, 953.76, 745.83, 704.34; VIS (THF, λ, nm): 655, 592.5, 363. Elemental analysis for C$_{104}$H$_{100}$N$_{20}$Cu: calcd. (%) C 73.76, H 5.95, N 16.54; found (%) C 74.01, H 5.89, N 16.38.

18.4.9. Synthesis of type A zinc(II) tetrapyrazinoporphyrazine (145)
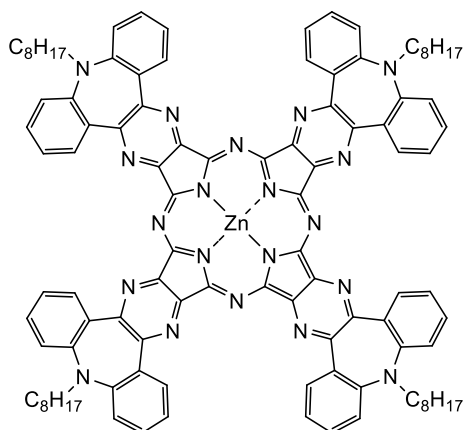
ZnCl$_2$ (53.4 mg, 0.392 mmol) and DBU (catalytic amount) were added to a solution of 9-octyl-9H-dibenzo[b,f]pyrazino[2,3-d]azepine-2,3-dicarbonitrile (397 mg, 0.98 mmol) in DMAE (8 mL). Mixture was then refluxed 3 h. Reaction mixture was quenched with aqueous HCl 1 M (15 mL), filtered and precipitate was washed with water and methanol. Crude product was purified by gravimetric column chromatography (DCM) to afford copper(II) tetrapyrazinoporphyrazine **145** as a deep green solid (104 mg, 25%). MS (MALDI-TOF, *m/z*) 1695.8 [M$^{+\bullet}$]; m.p.: 231°C; FT-IR (λ, cm^{-1}): 2923, 2851, 1741, 1596, 1450, 1350, 1244, 1104, 742, 701;

VIS (THF, λ, nm): 655, 595, 367. Elemental analysis for $C_{104}H_{100}N_{20}Zn$: calcd. (%) C 73.68, H 5.95, N 16.52; found (%) C 73.67, H 5.98, N 16.57.

18.4.10. Synthesis of 2-bromo-5-hexylthiophene (148)
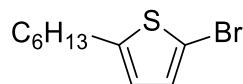
To an open-air and shielded for light solution of 2-hexylthiophene (7 g, 41.6 mmol) in chloroform (135 mL) and acetic acid (65 mL), NBS (7.7 g, 43.3 mmol) was slowly added. Reaction mixture was then stirred 18 h and washed with aqueous 1M NaOH several times. Organic phase was then dried with $MgSO_4$, filtered and solvent removed under reduced pressure to afford 2-bromo-5-hexylthiophene (10.6 g, quant.) as yellow oil without any further purification. ^{1}H NMR (CDCl$_3$) δ 6.84 (d, J = 3.6 Hz, 1 H), 6.53 (d, J = 3.5 Hz, 1 H), 2.74 (t, J = 7.6 Hz, 2 H), 1.68-1.58 (m, 2 H), 1.42-1.22 (m, 6 H), 0.99-0.82 (m, 3H) ppm. Other spectral data match with the literature.[398]

18.4.11. Synthesis of 3,3'-dibromo-5,5'-dihexyl-2,2'-bithiophene (149)
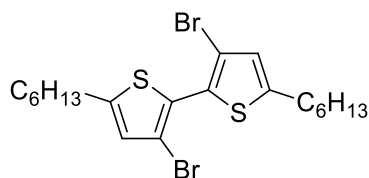
LDA 1.36 M in THF/hexanes (8 mL, 10.85 mmol) was added dropwise to a -78°C solution of 2-bromo-5-hexylthiophene (2 g, 7.23 mmol) in THF (15 mL) and stirred 1 h. Mixture was then allowed to reach -50°C and anhydrous $CuCl_2$ (1.18 g, 8.8 mmol) was added. Reaction mixture was then allowed to reach r.t. and stirred overnight: subsequently it was quenched with aqueous 1M HCl and extracted with Et_2O. Reunited organic phases were with $MgSO_4$, filtered and solvent removed under reduced pressure. Raw product was dissolved in MeOH/EtOAc 2:1, solution cooled down to -20°C and filtered to afford 3,3'-dibromo-5,5'-dihexyl-2,2'-bi-thiophene as pale solid without any further purification. After drying mother liquors, raw product was puri-fied by gravimetric column chromatography (n-hexane) to afford extra product (1.2 g, 62%). ^{1}H-NMR (CDCl$_3$): δ 6.71 (2H, s), 2.76–2.72 (4H, t, J = 8 Hz), 1.69–1.62 (4H, m), 1.40–1.28 (12H, m), 0.89–0.87 (t, J = 8 Hz, 6H) ppm. Other spectral data match the literature.[326]

18.4.12. Synthesis of 2,7-dihexylbenzo[1,2-b:6,5-b']dithiophene-4,5-dione (150)
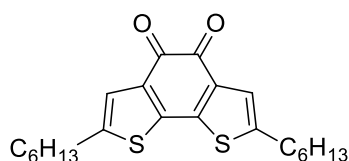
To a -78°C solution of 3,3'-dibromo-5,5'-dihexyl-2,2'-bithiophene (10 g, 18.3 mmol), 2.5 M n-BuLi in hexanes (16 mL, 40 mmol) was added dropwise. Reaction mixture was stirred 1 h at -78°C and then diethyloxalate

(3.7 mL, 25.6 mmol) was added. After 2 h stirring at -78°C, reaction mixture was slowly rised up to 0°C. Mixture was then quenched with saturated aqueous NH_4Cl, extracted with Et_2O and the combined organic layers were dried over Na_2SO_4. The filtered organic phases were dried under reduced pressure. Crude product was purified by gravimetric column chromatography (*n*-hexane/EtOAc 10:1) to afford 2,7-dihexylbenzo[1,2-b:6,5-b']dithiophene-4,5-dione (4 g, 52%) as black solid. ^{1}H-NMR (CDCl$_3$): δ 7.12 (2H, s), 2.78–2.74 (4H, t, J = 8 Hz), 1.69–1.62 (4H, m), 1.38–1.31 (12H, m), 0.91–0.88 (6H, t, J = 7 Hz) ppm. Other spectral data match the literature.[326]

18.4.13. Synthesis of 6,9-dihexyldithieno[3,2-f:2',3'-h]quinoxaline-2,3-dicarbonitrile (146)
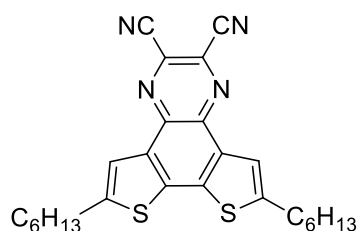
To a r.t. solution of 2,7-dihexylbenzo[1,2-b:6,5-b']dithiophene-4,5-dione (4 g, 9.5 mmol) in THF (120 mL), MgSO$_4$ (1.25 g, 23.7 mmol), PTSA (326 mg, 1.9 mmol) and DAMN (3.1 g, 28.5 mmol) were added and reaction mixture stirred overnight. Mixture was dried under reduced pressure. Crude product was then purified by gravimetric column chromatography (*n*-hexane/EtOAc 10:1) to afford 6,9-dihexyldithieno[3,2-f:2',3'-h]quinoxaline-2,3-dicarbonitrile (1.27 g, 27%) as dark red solid. ^{1}H-NMR (CDCl$_3$): δ 7.94 (s, 2H), 3.05 (t, J = 8 Hz, 4H), 1.84 (m, 4H), 1.46-1.25 (m, 12H), 0.90 (t, J = 8 Hz, 6H) ppm; ^{13}C-NMR (CDCl$_3$): δ 148.5, 138.8, 137.0, 132.7, 127.9, 120.8, 114.1, 31.5, 31.2, 30.7, 28.7, 22.5, 14.1 ppm; m.p.: 111.5°C; MS (CI): *m/z* = 460; FT-IR (λ, cm^{-1}): 2954.09, 2923.57, 2851.37, 2238.45, 1749.68, 1514.33, 1458.97, 1420.43, 1302.66, 1213.21, 1076.85, 837.25, 665.69; $^{+•}$calcd. (%) C 67.79, H, 6.13, N, 12.16; found (%) C 66.41, H 5.99, N 13.39.

18.4.14. Synthesis of 2-hydroxy-1,2-di(thiophen-3-yl)ethenone (155)
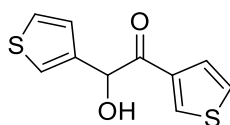
To a r.t. solution of thiamine hydrochloride (1.6 g, 5 mmol) in EtOH (30 mL), TEA (3 g, 30 mmol) was added. After 15 min stirring, 3-thiophenecarbaldehyde (11.2 g, 100 mmol) was added and reaction was stirred 24 h. Reaction mixture was then filtered and collected precipitated 2-hydroxy-1,2-di(thiophen-3-yl)ethenone was washed with col isopropanol. Mother liquors were dried, dissolved in DCM and washed with water. Organic phases were dried with MgSO$_4$, filtered and evaporated under reduced pressure. After addition of cold isopropanol mixture was filtered to afford extra 2-hydroxy-1,2-di(thiophen-3-yl)ethenone (7.63 g, 68%) as white solid. ^{1}H-NMR (CDCl$_3$) δ 8.05 (s, 1H), 7.52 (d, J = 4 Hz, 1H), 7.33 (s, 1H), 7.31-7.29 (m, 2H), 7.00 (d, J = 4 Hz, 1H), 5.84 (d, J = 8 Hz, 1H), 4.32 (d, J = 8 Hz, 1H) ppm. Other data match the literature.[327]

18.4.15. Synthesis of 1,2-di(thiophen-3-yl)ethane-1,2-dione (156)
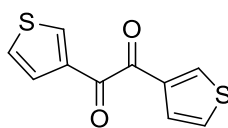
To a 60°C open-air solution of CuSO$_4$ pentahydrate (19.5 g, 78.34 mmol) in pyridine (23 mL) and water (14 mL), 2-hydroxy-1,2-di(thiophen-3-yl)ethenone (7.26 g, 34 mmol) was added. Mixture was then heated to 80°C and stirred 4 h. 10% aqueous HCl was added until solution reaction mixture colour to green, then it was extracted with EtOAc. Reunited organic phases were dried with MgSO$_4$, filtered and evaporated under reduced pressure to afford 1,2-di(thiophen-3-yl)ethane-1,2-dione (7 g, 93%) as yellow solid. ^{1}H-NMR (CDCl$_3$) δ 8.36 (s, 2H), 7.70 (d, J = 4 Hz, 2H), 7.40-7.38 (m, 2H) ppm. Other spectral data match the literature.[327]

18.4.16. Synthesis of benzo[1,2-b:6,5-b']dithiophene-4,5-dione (157)
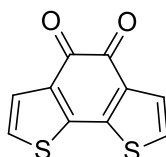
To a r.t. solution of 1,2-di(thiophen-3-yl)ethane-1,2-dione (3.6 g, 16.4 mmol) in DCM (100 mL), anhydrous FeCl$_3$ (7.98 g, 49.2 mmol) was added and reaction mixture stirred 2 h. Reaction mixture was then quenched with cold water and organic solvent removed under reduced pressure. Resulting mixture was then filtered and collected solid was washed thoroughly with water to afford benzo[1,2-b:6,5-b']dithiophene-4,5-dione (3.6 g, quant.) as dark solid. ^{1}H-NMR (DMSO-d_6) δ 7.65 (d, J = 8 Hz, 2H), 7.44 (d, J = 8 Hz, 2H) ppm. Other spectral data match the literature.[399]

18.4.17. Synthesis of 5,6-di(thiophen-3-yl)pyrazine-2,3-dicarbonitrile (158)
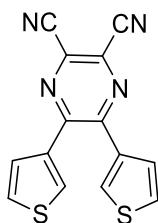
To an open-air solution of 1,2-di(thiophen-3-yl)ethane-1,2-dione (200 mg, 0.9 mmol) in acetic acid (7 mL), DAMN (290 mg, 1.6 mmol) was added. Reaction was then refluxed 2 h. Solvents were dried under reduced pressure. Crude product was purified by gravimetric column chromatography (DCM/n-hexane 2:1) to afford 5,6-di(thiophen-3-yl)pyrazine-2,3-dicarbonitrile (235 mg, 90%) as yellow solid. ^{1}H-NMR (CDCl$_3$) δ 7.83 (s, 2H), 7.38-7.36 (m, 2H), 7.24 (d, J = 5 Hz, 2H). Other spectral data match the literature.[328]

18.4.18. Synthesis of 5,6-di(thiophen-3-yl)pyrazine-2,3-dicarbonitrile (152)
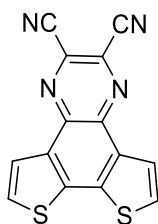
To a r.t. solution of anhydrous $FeCl_3$ (833 mg, 5.1 mmol) in DCM (21 mL), 5,6-di(thiophen-3-yl)pyrazine-2,3-dicarbonitrile (500 mg, 1.7 mmol) was added. Reaction mixture became a red slurry. After 4 h, mixture is quenched with water and filtered. Collected precipitated solid was washed with few cold MeOH and thoroughly with Et_2O to afford 5,6-di(thiophen-3-yl)pyrazine-2,3-dicarbonitrile (340 mg, 68%) as yellow solid without any further purification. . ^{1}H-NMR (DMSO-d_6) δ 8.36 (d, J = 8 Hz, 2H), 8.20 (d, J = 8 Hz, 2H) ppm; ^{13}C-NMR (DMSO-d_6) δ 138.8, 137.3, 132.9, 129.5, 126.4, 124.1, 114.8 ppm; MS (EI): m/z = 292 [M$^{+\bullet}$]; FT-IR (λ, cm^{-1}): 2918.32, 2236.60, 1419.89, 1309.27, 1209.61, 906.67, 738.50, 683.38, 653.23; Elemental Analysis for $C_{14}H_4N_4S_2$: calcd. (%) C 57.52, H 1.38, N 19.17; found (%) C 58.34, H 1.27, N 19.21.

19. References

[1]   R. J. Sundberg, *The Chemistry of Indoles*, New York, **1970**.

[2]   V. Sharma, P. Kumar, D. Pathak, *J. Heterocycl. Chem.* **2010**, *47*, 491–502.

[3]   T. C. Barden, *Peptides* **2011**, *26*, 31–46.

[4]   W. I. Taylor, *Indole Alkaloids: An Introduction to Enamine Chemistry of Natural Products*, Pergamon Press, **1966**.

[5]   M. Bandini, A. Eichholzer, *Angew. Chemie - Int. Ed.* **2009**, *48*, 9608–9644.

[6]   M. Bandini, *Org. Biomol. Chem.* **2013**, *11*, 5206–5212.

[7]   R. Dalpozzo, *Chem. Soc. Rev.* **2015**, *44*, 742–778.

[8]   S. Lakhdar, M. Westermaier, F. Terrier, R. Goumont, T. Boubaker, A. R. Ofial, H. Mayr, *J. Org. Chem.* **2006**, *71*, 9088–9095.

[9]   A. Baeyer, *Justus Liebis Ann. der Chemie* **1866**, *140*, 295–296.

[10]   A. Baeyer, A. Emmerling, *Berichte der Dtsch. Chem. Gesellschaft* **1869**, *2*, 679–682.

[11]   D. F. Taber, P. K. Tirunahari, *Tetrahedron* **2011**, *67*, 7195–7210.

[12]   E. Fischer, F. Jourdan, *Berichte der Dtsch. Chem. Gesellschaft* **1883**, *16*, 2241–2245.

[13]   B. Robinson, *Chem. Rev.* **1963**, *63*, 373–401.

[14]   B. Robinson, *Chem. Rev.* **1969**, *69*, 227–250.

[15]   C. F. H. Allen, C. V. Wilson, *J. Am. Chem. Soc.* **1943**, *65*, 611–612.

[16]   S. Wagaw, B. H. Yang, S. L. Buchwald, *J. Am. Chem. Soc.* **1998**, *120*, 6621–6622.

[17]   H. Harry Szmant, C. Mcginnis, *J. Am. Chem. Soc.* **1950**, *72*, 2890–2892.

[18]   F. D. Hart, P. L. Boardman, *Br. Med. J.* **1963**, *2*, 965–970.

[19]   T. Y. Shen, R. L. Ellis, T. B. Windholz, A. R. Matzuk, A. Rosegay, S. Lucas, B. E. Witzel, C. H. Stammer, A. N. Wilson, F. W. Holly, et al., *J. Am. Chem. Soc.* **1963**, *85*, 488–489.

[20]   T. Y. Shen, *Alpha-(1-Aroyl-3-Indolyl)Alkanoic Acids*, **1964**, 3161654.

[21]   K. R. Campos, J. C. S. Woo, S. Lee, R. D. Tillyer, *Org. Lett.* **2004**, *6*, 79–82.

[22]   F. Antonaci, N. Ghiotto, S. Wu, E. Pucci, A. Costa, *Springerplus* **2016**, *5*, 1–14.

[23]   J. M. Padfield, I. K. Winterborn, A. J. Phillips, *Sumatriptan Claim*, **1992**.

[24]   C. D. Nenitzescu, *Bull. Soc. Chim. Rom.* **1929**, *11*, 37–43.

[25]   D. Katkevica, P. Trapencieris, A. Boman, I. Kalvins, T. Lundstedt, *J. Chemom.* **2004**, *18*, 183–187.

[26]   G. R. Allen, M. J. Weiss, *J. Org. Chem.* **1968**, *33*, 198–200.

[27]   D. M. Ketcha, L. J. Wilson, D. E. Portlock, *Tetrahedron Lett.* **2000**, *41*, 6253–6257.

[28]   Y. S. Huang, W. Q. Zhang, X. Zhang, J. Z. Wang, *Res. Chem. Intermed.* **2010**, *36*, 975–983.

[29]   L. W. Schenck, K. Kuna, W. Frank, A. Albert, C. Asche, U. Kucklaender, *Bioorganic Med. Chem.* **2006**, *14*, 3599–3614.

[30]   M. Rönn, Q. McCubbin, S. Winter, M. K. Veige, N. Grimster, T. Alorati, L. Plamondon, *Org. Process Res. Dev.* **2007**, *11*, 241–245.

[31]   C. Zhao, Y. Zhao, H. Chai, P. Gong, *Bioorganic Med. Chem.* **2006**, *14*, 2552–2558.

[32]   S. Cacchi, G. Fabrizi, *Chem. Rev.* **2005**, *105*, 2873–2920.

[33]   S. Song, M. Huang, W. Li, X. Zhu, Y. Wan, *Tetrahedron* **2015**, *71*, 451–456.

[34]   S. Patil, R. Patil, *Curr. Org. Synth.* **2007**, *4*, 201–222.

[35]   G. Abbiati, F. Marinelli, E. Rossi, A. Arcadi, *Isr. J. Chem.* **2013**, *53*, 856–868.

[36]   J. E. Perea-Buceta, T. Wirtanen, O. V. Laukkanen, M. K. Mäkelä, M. Nieger, M. Melchionna, N. Huittinen, J. A. Lopez-Sanchez, J. Helaja, *Angew. Chemie - Int. Ed.* **2013**, *52*, 11835–11839.

[37]   S. J. Kaldas, A. Cannillo, T. McCallum, L. Barriault, *Org. Lett.* **2015**, *17*, 2864–2866.

[38]   R. C. Larock, E. K. Yum, *J. Am. Chem. Soc.* **1991**, *113*, 6689–6690.

[39]   R. C. Larock, E. K. Yum, M. D. Refvik, *J. Org. Chem.* **1998**, *63*, 7652–7662.

[40]   N. Gathergood, P. J. Scammells, *Org. Lett.* **2003**, *5*, 921–923.

[41]   N. Sutou, K. Kato, H. Akita, *Tetrahedron Asymmetry* **2008**, *19*, 1833–1838.

[42]   G. Xia, X. Han, X. Lu, *Org. Lett.* **2014**, *16*, 2058–2061.

[43]   G. W. Gribble, *Indole Ring Synthesis: From Natural Products to Drug Discovery*, Wiley, **2016**.

[44]   M. L. Huggins, *J. Am. Chem. Soc.* **1953**, *15*, 4123–4126.

[45]   M. Somei, *Heterocycles* **1999**, *50*, 1157–1211.

[46]   J. Iball, W. D. S. Motherwell, J. C. Barnes, W. Golnazarians, *Acta Crystallogr.* **1986**, *C42*, 239–241.

[47]   M. Belley, D. Beaudoin, P. Duspara, E. Sauer, G. St-Pierre, L. A. Trimble, *Synlett* **2007**, 2991–2994.

[48]   R. M. Acheson, *Adv. Heterocycl. Chem.* **1990**, *51*, 105–175.

[49]   K. C. Nicolaou, H. L. Sang, A. A. Estrada, M. Zak, *Angew. Chemie - Int. Ed.* **2005**, *44*, 3736–3740.

[50]   S. Urban, J. W. Blunt, M. H. G. Munro, *J. Nat. Prod.* **2002**, *65*, 1371–1373.

[51]   R. Rani, V. Kumar, *J. Med. Chem.* **2016**, *59*, 487–496.

[52]   C. Escolano, *Angew. Chemie - Int. Ed.* **2005**, *44*, 7670–7673.

[53]   M. Somei, T. Shoda, *Heterocycles* **1981**, *16*, 1523–1525.

[54]   M. Somei, M. Tsuchiya, *Chem. Pharm. Bull.* **1981**, *50*, 3145.

[55]   M. Somei, Y. Karasawa, T. Shoda, C. Kaneko, *Chem. Pharm. Bull.* **1981**, *29*, 249–253.

[56]   T. Kawasaki, A. Kodama, T. Nishida, K. Shimizu, M. Somei, *Heterocycles* **1991**, *32*, 221–227.

[57]   F. Yamada, Y. Fukui, D. Shinmyo, M. Somei, *Heterocycles* **1993**, *35*, 99–104.

[58]   F. Yamada, S. Daisuke, M. Somei, *Heterocycles* **1994**, *38*, 273–276.

[59]   M. Somei, K. Kobayashi, K. Tanii, T. Mochizuki, Y. Kawada, Y. Fukui, *Heterocycles* **1995**, *40*, 119–122.

[60]   A. Reissert, *Berichte der Dtsch. Chem. Gesellschaft* **1897**, *30*, 1030–1053.

[61]   A. Wong, J. T. Kuethe, I. W. Davies, *J. Org. Chem.* **2003**, *68*, 9865–9866.

[62]   R. Bujok, Z. Wrbel, K. Wojciechowski, *Synlett* **2012**, *23*, 1315–1320.

[63]   Y. Du, J. Chang, J. Reiner, K. Zhao, *J. Org. Chem.* **2008**, *73*, 2007–2010.

[64]   W. Yu, Y. Du, K. Zhao, *Org. Lett.* **2009**, *11*, 2417–2420.

[65]   A. Baeyer, *Chem. Ber.* **1874**, *7*, 1638–1640.

[66]   S. Carosso, M. J. Miller, *Org. Biomol. Chem.* **2014**, *12*, 7445–7468.

[67]   W. Adam, O. Krebs, *Chem. Rev.* **2003**, *103*, 4131–4146.

[68]   N. Momiyama, H. Yamamoto, *J. Am. Chem. Soc.* **2004**, *126*, 5360–5361.

[69]   H. Yamamoto, N. Momiyama, *Chem. Commun.* **2005**, 3514–3525.

[70]   Y.-R. Luo, *Comprehensive Handbook of Bond Energies*, Boca Raton, USA, **2007**.

[71]   P. Zuman, B. Shah, *Chem. Rev.* **1994**, *94*, 1621–1641.

[72]   S. Cacchi, V. Carnicelli, F. Marinelli, *J. Organomet. Chem.* **1994**, *475*, 289–296.

[73]   A. Arcadi, S. Cacchi, F. Marinelli, *Tetrahedron Lett.* **1989**, *30*, 2581–2584.

[74]   G. Abbiati, A. Arcadi, E. Beccalli, G. Bianchi, F. Marinelli, E. Rossi, *Tetrahedron* **2006**, *62*, 3033–3039.

[75]   R. R. Singh, R. S. Liu, *Chem. Commun.* **2014**, *50*, 15864–15866.

[76]   S. Murru, A. A. Gallo, R. S. Srivastava, *ACS Catal.* **2011**, *1*, 29–31.

[77]   S. Murru, A. A. Gallo, R. S. Srivastava, *European J. Org. Chem.* **2011**, 2035–2038.

[78]   A. A. Lamar, K. M. Nicholas, *Tetrahedron* **2009**, *65*, 3829–3833.

[79]   S. Manna, R. Narayan, C. Golz, C. Strohmann, A. P. Antonchick, *Chem. Commun.* **2015**, *51*, 6119–6122.

[80]   S. Cenini, F. Ragaini, *Carbonylative Reduction of Organic Nitrocompounds*, Dordrecht, Netherlands, **1997**.

[81]   J. Huang, L. Yu, L. He, Y. M. Liu, Y. Cao, K. N. Fan, *Green Chem.* **2011**, *13*, 2672–2677.

[82]   M. Orlandi, D. Brenna, R. Harms, S. Jost, M. Benaglia, *Org. Process Res. Dev.* **2018**, *22*, 430–445.

[83]   J. B. Peng, H. Q. Geng, D. Li, X. Qi, J. Ying, X. F. Wu, *Org. Lett.* **2018**, *20*, 4988–4993.

[84]   S. Cenini, F. Ragaini, S. Tollari, D. Paone, *J. Am. Chem. Soc.* **1996**, *118*, 11964–11965.

[85]   R. S. Srivastava, K. M. Nicholas, **1998**, 2705–2706.

[86]   A. Penoni, K. M. Nicholas, *Chem. Commun.* **2002**, *2*, 484–485.

[87]   A. Penoni, J. Volkmann, K. M. Nicholas, *Org. Lett.* **2002**, *4*, 699–701.

[88]   K. F. Johnson, R. Van Zeeland, L. M. Stanley, *Org. Lett.* **2013**, *15*, 2798–2801.

[89]   A. Penoni, G. Palmisano, G. Broggini, A. Kadowaki, K. M. Nicholas, *J. Org. Chem.* **2006**, *71*, 823–825.

[90]   G. Ieronimo, A. Mondelli, F. Tibiletti, A. Maspero, G. Palmisano, S. Galli, S. Tollari, N. Masciocchi, K. M. Nicholas, S. Tagliapietra, et al., *Tetrahedron* **2013**, *69*, 10906–10920.

[91]   E. Morera, G. Ortar, *Synlett* **1997**, 1403–1405.

[92]   F. Tibiletti, M. Simonetti, K. M. Nicholas, G. Palmisano, M. Parravicini, F. Imbesi, S. Tollari, A. Penoni,

Tetrahedron **2010**, *66*, 1280–1288.

[93]   A. M. Seldes, M. F. R. Brasco, L. H. Franco, J. A. Palermo, *Nat. Prod. Res.* **2007**, *21*, 555–563.

[94]   S. R. Walker, E. J. Carter, B. C. Huff, J. C. Morris, *Chem. Rev.* **2009**, *109*, 3080–3098.

[95]   K. Bettayeb, O. M. Tirado, S. Marionneau-Lambot, Y. Ferandin, O. Lozach, J. C. Morris, S. Mateo-Lozano, P. Drueckes, C. Schächtele, M. H. G. Kubbutat, et al., *Cancer Res.* **2007**, *67*, 8325–8334.

[96]   A. S. Karpov, E. Merkul, F. Rominger, T. J. J. Müller, *Angew. Chemie - Int. Ed.* **2005**, *44*, 6951–6956.

[97]   E. Merkul, T. Oeser, T. J. J. Müller, *Chem. - A Eur. J.* **2009**, *15*, 5006–5011.

[98]   L. H. Franco, J. A. Palermo, *Chem. Pharm. Bull.* **2003**, *51*, 975–977.

[99]   A. Penoni, G. Palmisano, Y. Zhao, K. N. Houk, J. Volkman, K. M. Nicholas, *J. Am. Chem. Soc.* **2009**, *131*, 653–661.

[100]   D. G. Zhao, J. Chen, Y. R. Du, Y. Y. Ma, Y. X. Chen, K. Gao, B. R. Hu, *J. Med. Chem.* **2013**, *56*, 1467–1477.

[101]   S. J. Yao, Z. H. Ren, Z. H. Guan, *Tetrahedron Lett.* **2016**, *57*, 3892–3901.

[102]   C. C. Kuo, H. P. Hsieh, W. Y. Pan, C. P. Chen, J. P. Liou, S. J. Lee, Y. L. Chang, L. T. Chen, C. T. Chen, J. Y. Chang, *Cancer Res.* **2004**, *64*, 4621–4628.

[103]   Y. Ma, J. You, F. Song, *Chem. - A Eur. J.* **2013**, *19*, 1189–1193.

[104]   E. Kianmehr, S. Kazemi, A. Foroumadi, *Tetrahedron* **2014**, *70*, 349–354.

[105]   Q. Xing, P. Li, H. Lv, R. Lang, C. Xia, F. Li, *Chem. Commun.* **2014**, *50*, 12181–12184.

[106]   P. Kutschy, M. Dzurilla, M. Takasugi, M. Török, I. Achbergerová, R. Homzová, M. Rácová, *Tetrahedron* **1998**, *54*, 3549–3566.

[107]   E. A. Merritt, M. C. Bagley, *Synlett* **2007**, *1*, 954–958.

[108]   R. D. Miller, O. Reiser, *J. Heterocycl. Chem.* **1993**, *30*, 755.

[109]   A. R. Katritzky, Y. Zhang, S. K. Singh, *Synthesis (Stuttg).* **2003**, *6*, 2795–2798.

[110]   G. M. Coppola, R. E. Damon, *Synth. Commun.* **1993**, *23*, 2003–2010.

[111]   A. M. Kearney, C. D. Vanderwal, *Angew. Chemie - Int. Ed.* **2006**, *45*, 7803–7806.

[112]   A. R. Katritzky, S. Rachwal, *Chem. Rev.* **2010**, *110*, 1564–1610.

[113]   A. R. Katritzky, S. Rachwal, *Chem. Rev.* **2011**, *111*, 7063–7120.

[114]   J. S. Park, S. Yabe, K. Shin-Ya, M. Nishiyama, T. Kuzuyama, *J. Antibiot. (Tokyo).* **2015**, *68*, 60–62.

[115]   M. C. Bagley, X. Xiong, *Org. Lett.* **2004**, *6*, 3401–3404.

[116]   S. Kwon, Y. T. Han, J. W. Jung, *Synth. Commun.* **2015**, *45*, 1662–1668.

[117]   F. Ragaini, F. Ventriglia, M. Hagar, S. Fantauzzi, S. Cenini, *European J. Org. Chem.* **2009**, 2185–2189.

[118]   J. L. Wiley, D. R. Compton, D. Dai, J. A. H. Lainton, M. Phillips, J. W. Huffman, B. R. Martin, *J. Pharmacol. Exp. Ther.* **1998**, *285*, 995–1004.

[119]   M. P. Duarte, R. F. Mendonça, S. Prabhakar, A. M. Lobo, *Tetrahedron Lett.* **2006**, *47*, 1173–1176.

[120]   S.-F. Wang, C.-P. Chuang, *Heterocycles* **1997**, *45*, 347–359.

[121] A. Bartsch, M. Bross, P. Spiteller, M. Spiteller, W. Steglich, *Angew. Chemie - Int. Ed.* **2005**, *44*, 2957–2959.

[122] A. Korda, Z. Wróbel, *Synlett* **2003**, 1465–1466.

[123] J. I. G. Cadogan, M. Cameron Wood, *Proc. Soc. Chem.* **1962**, 361.

[124] E. C. Creencia, M. Kosaka, T. Muramatsu, M. Kobayashi, T. Iizuka, T. Horaguchi, *J. Heterocycl. Chem.* **2009**, *46*, 1309.

[125] S. W. Dantale, B. C. G. Söderberg, *Tetrahedron* **2003**, *59*, 5507–5514.

[126] B. K. Banik, I. Banik, L. Hackfeld, F. F. Becker, *Heterocycles* **2002**, *56*, 467–470.

[127] C. K. Narkowicz, A. J. Blackman, E. Lacey, J. H. Gill, K. Heiland, *J. Nat. Prod.* **2002**, *65*, 938–941.

[128] D. Thienpont, O. F. J. Vanparijs, A. H. M. Raeymaekers, J. Vandeberk, P. J. A. Demoen, F. T. N. Allewijn, R. P. H. Marsboom, C. J. E. Niemegeers, K. H. L. Schellekens, P. A. J. Janssen, *Nature* **1966**, *209*, 1084–1086.

[129] M. A. EL-Atawy, D. Formenti, F. Ferretti, F. Ragaini, *ChemCatChem* **2018**, *10*, 4707–4717.

[130] H. Shirakawa, E. J. Louis, A. G. MacDiarmid, C. K. Chiang, A. J. Heeger, *J. Chem. Soc. Chem. Commun.* **1977**, 578–580.

[131] K. Akagi, M. Suezaki, H. Shirakawa, H. Kyotani, M. Shimomura, Y. Tanabe, *Synth. Met.* **1989**, *28*, D1.

[132] A. J. Heeger, *Curr. Appl. Phys.* **2001**, *1*, 247–267.

[133] J. Nelson, *Mater. Today* **2011**, *14*, 462–470.

[134] H. Kallmann, M. Pope, *Nature* **1960**, *186*, 31–33.

[135] R. E. Perierl, *Quantum Theory of Solids*, Oxford University Press, London, **1956**.

[136] J. Liu, J. W. Y. Lam, B. Z. Tang, *Acetylenic Polymers: Syntheses, Structures, and Functions*, **2009**.

[137] A. J. Heeger, *Chem. Soc. Rev.* **2010**, *39*, 2354–2371.

[138] A. G. MacDiarmid, A. J. Epstein, *Makromol. Chemie. Macromol. Symp.* **1991**, *51*, 11–28.

[139] I. F. Perepichka, D. F. Perepichka, *Handbook of Thiophene-Based Materials: Applications in Organic Electronics and Photonics*, Wiley, **2009**.

[140] R. D. McCullough, S. Tristram-Nagle, *J. Am. Chem. Soc.* **1993**, *115*, 4910–4911.

[141] Z. G. Zhang, J. Wang, *J. Mater. Chem.* **2012**, *22*, 4178–4187.

[142] G. Yu, J. Gao, J. C. Hummelen, F. Wudl, A. J. Heeger, *Science (80-.).* **1995**, *270*, 1789–1791.

[143] F. C. Krebs, *Sol. Energy Mater. Sol. Cells* **2009**, *93*, 394–412.

[144] K. Nakabayashi, H. Mori, *Materials (Basel).* **2014**, *7*, 3274–3290.

[145] J. Hopkins, K. Fidanovski, A. Lauto, D. Mawad, *Front. Bioeng. Biotechnol.* **2019**, *7*, 1–8.

[146] E. D. Głowacki, G. Voss, L. Leonat, M. Irimia-Vladu, S. Bauer, N. S. Sariciftci, *Isr. J. Chem.* **2012**, *52*, 540–551.

[147] J. Dhar, K. Swathi, D. P. Karothu, K. S. Narayan, S. Patil, *ACS Appl. Mater. Interfaces* **2015**, *7*, 670–681.

[148] X. Qian, H. H. Gao, Y. Z. Zhu, L. Lu, J. Y. Zheng, *RSC Adv.* **2015**, *5*, 4368–4375.

[149] C. Groves, *Reports Prog. Phys.* **2017**, *80*, DOI 10.1088/1361-6633/80/2/026502.

[150] Y. Gnas, F. Glorius, *Synthesis (Stuttg).* **2006**, 1899–1930.

[151] M. Heitbaum, F. Glorius, I. Escher, *Angew. Chemie - Int. Ed.* **2006**, *45*, 4732–4762.

[152] "The Nobel Prize in Chemistry," can be found under
https://www.nobelprize.org/prizes/chemistry/2001/summary/, **2001**.

[153] L. A. P. Kane-Maguire, G. G. Wallace, *Chem. Soc. Rev.* **2010**, *39*, 2545–2576.

[154] B. M. W. Langeveld-Voss, R. A. J. Lanssen, E. W. Meijer, *J. Mol. Struct.* **2000**, *521*, 1–17.

[155] S. Pleus, M. Schwientek, *Synth. Met* **1998**, *95*, 233–238.

[156] K. Watanabe, I. Osaka, S. Yorozuya, K. Akagi, *Chem. Mater.* **2012**, *24*, 1011–1024.

[157] L. Torsi, G. M. Farinola, F. Marinelli, M. C. Tanese, O. H. Omar, L. Valli, F. Babudri, F. Palmisano, P. G. Zambonin, F. Naso, *Nat. Mater.* **2008**, *7*, 412–417.

[158] V. Böhmer, D. Kraft, M. Tabatabai, *J. Incl. Phenom. Mol. Recognit. Chem.* **1994**, *19*, 17.

[159] Y.-S. Zhang, J. Luo, *J. Incl. Phenom. Macrocycl. Chem.* **2011**, *71*, 35.

[160] G. E. Arnott, *Chem. - A Eur. J.* **2018**, *24*, 1744–1754.

[161] A. D. Cort, L. Mandolini, C. Pasquini, L. Schiaffino, D. Chimica, U. La Sapienza, B. Roma, *New J. Chem.* **2004**, *28*, 1198–1199.

[162] Y. Shen, C. Chen, *Chem. Rev.* **2012**, *112*, 1463–1535.

[163] L. H. Baekeland, *J. Ind. Eng. Chem.* **1909**, *1*, 149–161.

[164] C. D. Gutsche, *Calixarenes: An Introduction*, RSCPublishing, **2008**.

[165] S. Arnaboldi, S. Grecchi, M. Magni, P. Mussini, *Curr. Opin. Electrochem.* **2018**, *7*, 188–199.

[166] S. Rizzo, S. Arnaboldi, V. Mihali, R. Cirilli, A. Forni, A. Gennaro, A. A. Isse, M. Pierini, P. R. Mussini, F. Sannicolò, *Angew. Chemie* **2017**, *129*, 2111–2114.

[167] S. Rizzo, S. Arnaboldi, R. Cirilli, A. Gennaro, A. A. Isse, F. Sannicolò, P. R. Mussini, *Electrochem. commun.* **2018**, *89*, 57–61.

[168] F. Sannicolò, S. Rizzo, T. Benincori, W. Kutner, K. Noworyta, J. W. Sobczak, V. Bonometti, L. Falciola, P. R. Mussini, M. Pierini, *Electrochim. Acta* **2010**, *55*, 8352–8364.

[169] F. Sannicolò, S. Arnaboldi, T. Benincori, V. Bonometti, R. Cirilli, L. Dunsch, W. Kutner, G. Longhi, P. R. Mussini, M. Panigati, et al., *Angew. Chemie - Int. Ed.* **2014**, *53*, 2623–2627.

[170] S. Arnaboldi, T. Benincori, R. Cirilli, W. Kutner, M. Magni, P. R. Mussini, K. Noworyta, F. Sannicolò, *Chem. Sci.* **2015**, *6*, 1706–1711.

[171] F. Sannicolò, P. R. Mussini, T. Benincori, R. Cirilli, S. Abbate, S. Arnaboldi, S. Casolo, E. Castiglioni, G. Longhi, R. Martinazzo, et al., *Chem. - A Eur. J.* **2014**, *20*, 15298–15302.

[172] J. C. Li, S. J. Kim, S. H. Lee, Y. S. Lee, K. Zong, S. C. Yu, *Macromol. Res.* **2009**, *17*, 356–360.

[173] B. A. D. Neto, A. A. M. Lapis, E. N. Da Silva Júnior, J. Dupont, *European J. Org. Chem.* **2013**, 228–255.

[174] S. Ming, S. Zhen, K. Lin, L. Zhao, J. Xu, B. Lu, *ACS Appl. Mater. Interfaces* **2015**, *7*, 11089–11098.

[175] R. Sen, S. P. Singh, P. Johari, *J. Phys. Chem. A* **2018**, *122*, 492–504.

[176] F. Paquin, J. Rivnay, A. Salleo, N. Stingelin, C. Silva, *J. Mater. Chem. C* **2015**, *3*, 10715–10722.

[177] S. Ghosh, P. B. Pati, S. S. Zade, *J. Lumin.* **2018**, *194*, 164–169.

[178] X. He, B. Cao, T. C. Hauger, M. Kang, S. Gusarov, E. J. Luber, J. M. Buriak, *ACS Appl. Mater. Interfaces* **2015**, *7*, 8188–8199.

[179] B. Lu, S. Ming, K. Lin, S. Zhen, H. Liu, H. Gu, S. Chen, Y. Li, Z. Zhu, J. Xu, *New J. Chem.* **2016**, *40*, 8316–8323.

[180] S. Wood, J. H. Kim, J. Wade, J. B. Park, D. H. Hwang, J. S. Kim, *J. Mater. Chem. C* **2016**, *4*, 7966–7978.

[181] R. Acharya, S. Cekli, C. J. Zeman, R. M. Altamimi, K. S. Schanze, *J. Phys. Chem. Lett.* **2016**, *7*, 693–697.

[182] E. I. Carrera, D. S. Seferos, *Macromolecules* **2015**, *48*, 297–308.

[183] P. B. Pati, *Org. Electron.* **2016**, *38*, 97–106.

[184] G. L. Gibson, T. M. McCormick, D. S. Seferos, *J. Phys. Chem. C* **2013**, *117*, 16606–16615.

[185] S. Arnaboldi, T. Benincori, A. Penoni, L. Vaghi, R. Cirilli, S. Abbate, G. Longhi, G. Mazzeo, S. Grecchi, M. Panigati, et al., *Chem. Sci.* **2019**, *10*, 2708–2717.

[186] N. Muskal, I. Turyan, A. Shurky, D. Mandler, *J. Am. Chem. Soc.* **1995**, *117*, 1147–1148.

[187] T. Nakanishi, M. Matsunaga, M. Nagasaka, T. Asahi, T. Osaka, *J. Am. Chem. Soc.* **2006**, *128*, 13322–13323.

[188] Q. Han, Q. Chen, Y. Wang, J. Zhou, Y. Fu, *Electroanalysis* **2012**, *24*, 332–337.

[189] R. Nie, X. Bo, H. Wang, L. Zeng, L. Guo, *Electrochem. commun.* **2013**, *27*, 112–115.

[190] S. A. Wolf, D. D. Awschalom, R. A. Buhrman, J. M. Daughton, S. Von Molnár, M. L. Roukes, A. Y. Chtchelkanova, D. M. Treger, *Science (80-.).* **2001**, *294*, 1488–1495.

[191] T. Benincori, S. Arnaboldi, M. Magni, S. Grecchi, R. Cirilli, C. Fontanesi, P. R. Mussini, *Chem. Sci.* **2019**, *10*, 2750–2757.

[192] D. Casanova, *ChemPhysChem* **2011**, *12*, 2979–2988.

[193] S. P. Singh, M. S. Roy, A. Thomas, K. Bhanuprakash, G. D. Sharma, *Org. Electron.* **2012**, *13*, 3108–3117.

[194] T. M. S. K. Pathiranage, H. D. Magurudeniya, M. C. Biewer, M. C. Stefan, *J. Polym. Sci. Part A Polym. Chem.* **2017**, *55*, 3942–3948.

[195] G. Appoloni, *Axial Stereogenicity for Designing Inherently Chiral Organic Semiconductors*, **2017**.

[196] U. Berens, J. M. Brown, J. Long, R. Selke, *Tetrahedron Asimmetry* **1996**, *7*, 285–292.

[197] T. R. Li, M. M. Zhang, B. C. Wang, L. Q. Lu, W. J. Xiao, *Org. Lett.* **2018**, *20*, 3237–3240.

[198] C. Ma, F. Jiang, F. T. Sheng, Y. Jiao, G. J. Mei, F. Shi, *Angew. Chemie - Int. Ed.* **2019**, *58*, 3014–3020.

[199] Y. S. Kwon, J. Lim, I. Song, I. Y. Song, W. S. Shin, S. J. Moon, T. Park, *J. Mater. Chem.* **2012**, *22*, 8641–8648.

[200] M. G. Saulnier, D. B. Frennesson, M. S. Deshpande, D. M. Vyas, *Tetrahedron Lett.* **1995**, *36*, 7841–7844.

[201] B. R. Kim, E. J. Kim, G. H. Sung, J. J. Kim, D. S. Shin, S. G. Lee, Y. J. Yoon, *European J. Org. Chem.* **2013**, 2788–2791.

[202] R. S. Becker, J. De Seixas Mélo, A. L. Maçanita, F. Eliseil, *J. Phys. Chem.* **1996**, *100*, 18683–18695.

[203] M. I. Nan, E. Lakatos, G. I. Giurgi, L. Szolga, R. Po, A. Terec, S. Jungsuttiwong, I. Grosu, J. Roncali, *Dye. Pigment.* **2020**, *181*, 108527.

[204] J. Heinze, B. A. Frontana-Uribe, S. Ludwigs, *Chem. Rev.* **2010**, *110*, 4724–4771.

[205] C. Malacrida, A. H. Habibi, S. Gámez-Valenzuela, I. Lenko, P. S. Marqués, A. Labrunie, J. Grolleau, J. T. López Navarrete, M. C. Ruiz Delgado, C. Cabanetos, et al., *ChemElectroChem* **2019**, *6*, 4215–4228.

[206] T. M. Swager, *Macromolecules* **2017**, *50*, 4867–4886.

[207] T. Benincori, S. Gámez-Valenzuela, M. Goll, K. Bruchlos, C. Malacrida, S. Arnaboldi, P. R. Mussini, M. Panigati, J. T. López Navarrete, M. C. Ruiz Delgado, et al., *Electrochim. Acta* **2018**, *284*, 513–525.

[208] M. Iyoda, H. Shimizu, *Chem. Soc. Rev.* **2015**, *44*, 6411–6424.

[209] L. Zhang, N. S. Colella, B. P. Cherniawski, S. C. B. Mannsfeld, A. L. Briseno, *ACS Appl. Mater. Interfaces* **2014**, *6*, 5327–5343.

[210] B. B. Berkes, A. S. Bandarenka, G. Inzelt, *J. Phys. Chem. C* **2015**, *119*, 1996–2003.

[211] B. G. Zotti, G. Schiavon, A. Berlin, G. Pagani, *Adv. Mater.* **1993**, *5*, 551–554.

[212] G. Zotti, G. Schiavon, A. Berlin, G. Pagani, *Synth. Met.* **1993**, *61*, 81–87.

[213] A. Arcadi, M. Chiarini, G. D'Anniballe, F. Marinelli, E. Pietropaolo, *Org. Lett.* **2014**, *16*, 1736–1739.

[214] J. M. Raimundo, P. Blanchard, N. Gallego-Planas, N. Mercier, I. Ledoux-Rak, R. Hierle, J. Roncali, *J. Org. Chem.* **2002**, *67*, 205–218.

[215] Á. González-Gómez, L. Añorbe, A. Poblador, G. Domínguez, J. Pérez-Castells, *European J. Org. Chem.* **2008**, 1370–1377.

[216] Z. Li, L. Hong, R. Liu, J. Shen, X. Zhou, *Tetrahedron Lett.* **2011**, *52*, 1343–1347.

[217] C. P. Tüllmann, Y. Chen, R. J. Schuster, P. Knochel, *Org. Lett.* **2018**, *20*, 1–50.

[218] T. P. Homes, F. Mattner, P. A. Keller, A. Katsifis, *Bioorganic Med. Chem.* **2006**, *14*, 3938–3946.

[219] O. Moncea, D. Poinsot, A. A. Fokin, P. R. Schreiner, J. C. Hierso, *ChemCatChem* **2018**, *10*, 2915–2922.

[220] A. Nowakowska-Oleksy, J. Cabaj, K. Olech, J. Sołoducho, S. Roszak, *J. Fluoresc.* **2011**, *21*, 1625–1633.

[221] M. Hemgesberg, D. M. Ohlmann, Y. Schmitt, M. R. Wolfe, M. K. Müller, B. Erb, Y. Sun, L. J. Gooßen, M. Gerhards, W. R. Thiel, *European J. Org. Chem.* **2012**, 2142–2151.

[222] U. Boas, A. Dhanabalan, D. R. Greve, E. W. Meijer, *Synlett* **2001**, 634–636.

[223] F. S. Mancilha, B. A. DaSilveira Neto, A. S. Lopes, P. F. Moreira, F. H. Quina, R. S. Gonçalves, J. Dupont, *European J. Org. Chem.* **2006**, 4924–4933.

[224] X. Sun, X. Lei, Y. Hu, *Asian J. Chem.* **2015**, *27*, 2427–2430.

[225] I. H. Jung, H. Kim, M. J. Park, B. Kim, J. H. Park, E. Jeong, H. J. Woo, S. Yoo, H. K. Shim, *J. Polym. Sci. Part A Polym. Chem.* **2010**, *48*, 1973–1978.

[226] P. Ledwon, N. Thomson, E. Angioni, N. J. Findlay, P. J. Skabara, W. Domagala, *RSC Adv.* **2015**, *5*, 77303–77315.

[227] A. A. Tsegaye, T. T. Waryo, P. G. Baker, E. I. Iwuoha, *Mater. Chem. Phys.* **2016**, *171*, 57–62.

[228] R. Holze, *Organometallics* **2014**, *33*, 5033–5042.

[229]   A. Mirloup, N. Leclerc, S. Rihn, T. Bura, R. Bechara, A. Hébraud, P. Lévêque, T. Heiser, R. Ziessel, *New J. Chem.* **2014**, *38*, 3644–3653.

[230]   J. Tsutsumi, H. Matsuzaki, N. Kanai, T. Yamada, T. Hasegawa, *J. Phys. Chem. C* **2013**, *117*, 16769–16773.

[231]   C. Deibe, T. Strobe, V. Dyakonov, *Adv. Mater.* **2010**, *22*, 4097–4111.

[232]   A. Arcadi, G. Bianchi, F. Marinelli, *Synthesis (Stuttg).* **2004**, 610–618.

[233]   C. Koradin, W. Dohle, A. L. Rodriguez, B. Schmid, P. Knochel, *Tetrahedron* **2003**, *59*, 1571–1587.

[234]   K. J. Chang, M. K. Chae, C. Lee, J. Y. Lee, K. S. Jeong, *Tetrahedron Lett.* **2006**, *47*, 6385–6388.

[235]   C. H. Lee, H. Yoon, W. D. Jang, *Chem. - A Eur. J.* **2009**, *15*, 9972–9976.

[236]   T. Ishiyama, M. Murata, N. Miyaura, *J. Org. Chem.* **1995**, *60*, 7508–7510.

[237]   E. Quartapelle Procopio, T. Benincori, G. Appoloni, P. R. Mussini, S. Arnaboldi, C. Carbonera, R. Cirilli, A. Cominetti, L. Longo, R. Martinazzo, et al., *New J. Chem.* **2017**, *41*, 10009–10019.

[238]   T. Benincori, G. Appoloni, P. R. Mussini, S. Arnaboldi, R. Cirilli, E. Quartapelle Procopio, M. Panigati, S. Abbate, G. Mazzeo, G. Longhi, *Chem. - A Eur. J.* **2018**, *24*, 11082–11093.

[239]   J. Huang, S. J. F. MacDonald, J. P. A. Harrity, *Chem. Commun.* **2010**, *46*, 8770–8772.

[240]   J. Lv, B. Zhao, L. Liu, Y. Han, Y. Yuan, Z. Shi, *Adv. Synth. Catal.* **2018**, *360*, 4054–4059.

[241]   B. A. Coombs, B. D. Lindner, R. M. Edkins, F. Rominger, A. Beeby, U. H. F. Bunz, *New J. Chem.* **2012**, *36*, 550–553.

[242]   K. M. Kadish, K. M. Smith, R. Guilard, *The Porphyrin Handbook*, Academic Press, **2000**.

[243]   T. D. Lash, *J. Porphyr. Phthalocyanines* **2011**, *15*, 1093–1115.

[244]   K. M. Shea, L. Jaquinod, K. M. Smith, *J. Org. Chem.* **1998**, *63*, 7013–7021.

[245]   N. M. M. Moura, M. A. F. Faustino, M. G. P. M. S. Neves, A. C. Duarte, J. A. S. Cavaleiro, *J. Porphyr. Phthalocyanines* **2011**, *15*, 652–658.

[246]   I. J. Schultz, C. Chen, B. H. Paw, I. Hamza, *J. Biol. Chem.* **2010**, *285*, 26753–26759.

[247]   M. P. Richards, *Antioxidants Redox Signal.* **2013**, *18*, 2342–2351.

[248]   H. Fischer, *Nobel Lect. Chem. 1922-1941* **1930**, 165.

[249]   T. Muniyappan, *J. Chem. Educ.* **1955**, *32*, 277–279.

[250]   P. Rothemund, *J. Am. Chem. Soc.* **1935**, *57*, 2010–2011.

[251]   P. Rothemund, *J. Am. Chem. Soc* **1936**, *157*, 625–627.

[252]   A. D. Adler, F. R. Longo, J. D. Finarelli, J. Goldmacher, J. Assour, L. Korsakoff, *J. Org. Chem.* **1967**, *32*, 476.

[253]   M. J. Crossley, P. Thordarson, J. P. Bannerman, P. J. Maynard, *J. Porphyr. Phthalocyanines* **1998**, *2*, 511–516.

[254]   S. Shimizu, J. Y. Shin, H. Furuta, R. Ismael, A. Osuka, *Angew. Chemie - Int. Ed.* **2003**, *42*, 78–82.

[255]   M. Pineiro, *Curr. Org. Synth.* **2014**, *11*, 89–109.

[256]   W. M. Campbell, A. K. Burrell, D. L. Officer, K. W. Jolley, *Coord. Chem. Rev.* **2004**, *248*, 1363–1379.

[257] M. G. Walter, A. B. Rudine, C. C. Wamser, *J. Porphyr. Phthalocyanines* **2010**, *14*, 759–792.

[258] L. L. Li, E. W. G. Diau, *Chem. Soc. Rev.* **2013**, *42*, 291–304.

[259] S. K. Pushpan, S. Venkatraman, V. G. Anand, J. Sankar, D. Parmeswaran, S. Ganesan, T. K. Chandrashekar, *Curr. Med. Chem. - Anti-Cancer Agents* **2002**, *2*, 187–207.

[260] M. Ethirajan, Y. Chen, P. Joshi, R. K. Pandey, *Chem. Soc. Rev.* **2011**, *40*, 340–362.

[261] E. A. Lissi, M. V. Encinas, E. Lemp, M. A. Rubio, *Chem. Rev.* **1993**, *93*, 699–723.

[262] C. Di Natale, D. Monti, R. Paolesse, *Mater. Today* **2010**, *13*, 46–52.

[263] C. C. Leznoff, A. B. Lever, *Phthalocyanines: Properties and Applications*, Wiley, **1989**.

[264] K. Sakamoto, in *Voltammetry*, **2018**, pp. 1–26.

[265] H. de Diesbach, E. von der Weid, *Helv. Chim. Acta* **1927**, *10*, 886–888.

[266] J. M. Robertson, I. Woodward, *J. Chem. Soc.* **1937**, 219.

[267] F. Ghani, J. Kristen, H. Riegler, *J. Chem. Eng. Data* **2012**, *57*, 439–449.

[268] V. N. Nemykina, E. A. Lukyanets, *Arkivoc* **2010**, *1*, 136–208.

[269] D. Wöhrle, G. Schnurpfeil, S. G. Makarov, A. Kazarin, O. N. Suvorova, *Macroheterocycles* **2012**, *5*, 191–202.

[270] B. Basu, S. Satapathy, A. K. Bhatnagar, **2006**, 37–41.

[271] R. P. J. Linstead, *Chem. Soc.* **1934**, 1022.

[272] C. E. Dent, R. P. J. Linstead, A. R. J. Lowe, *Chem. Soc.* **1934**, 1033.

[273] J. M. Robertson, R. P. Linstead, C. E. Dent, *Nature* **1935**, *135*, 506–507.

[274] K. Sakamoto, E. Ohno-Okumura, *Materials (Basel).* **2009**, *2*, 1127–1179.

[275] G. Löbbert, *Phthalocyanines*, **2012**.

[276] R. P. Linstead, E. G. Noble, J. M. Wright, *J. Chem. Soc.* **1937**, 911–921.

[277] P. A. Stuzhin, O. G. Khelevina, *Coord. Chem. Rev.* **1996**, *147*, 41–86.

[278] P. A. Stuzhin, *J. Porphyr. Phthalocyanines* **1999**, *3*, 500–513.

[279] M. S. Rodríguez-Morgade, P. A. Stuzhin, *J. Porphyr. Phthalocyanines* **2004**, *8*, 1129–1165.

[280] E. A. Lukyanets, V. N. Nemykin, *J. Porphyr. Phthalocyanines* **2010**, *14*, 1–40.

[281] N. Kobayashi, H. Konami, *Phthalocyanines Prop. Appl.* **1996**, *4*, 343–404.

[282] H. Miwa, K. Ishii, N. Kobayashi, *Chem. - A Eur. J.* **2004**, *10*, 4422–4435.

[283] I. K. Shushkevich, P. P. Pershukevich, A. P. Stupak, K. N. Solov'ev, *J. Appl. Spectrosc.* **2005**, *72*, 767–770.

[284] K. Schiwon, H. D. Brauer, B. Gerlach, C. M. Müller, F. P. Montforts, *J. Photochem. Photobiol. B Biol.* **1994**, *23*, 239–243.

[285] A. A. Trabanco, A. G. Montalban, G. Rumbles, A. G. M. Barrett, B. M. Hoffman, *Synlett* **2000**, 1010–1012.

[286] J. P. Fitzgerald, B. S. Haggerty, I. A. L. Rheingold, L. May, G. A. Brewers, **2006**, 2006–2013.

[287] J. P. Fitzgerald, W. Taylor, H. Owen, *Synthesis (Stuttg).* **1991**, 686–688.

[288] Kopranenkov. V. N., L. S. Goncharova, E. A. Lukyanets, *Zh. Org. Khim.* **1979**, *15*, 1076.

[289] M. P. Donzello, C. Ercolani, V. Novakova, P. Zimcik, P. A. Stuzhin, *Coord. Chem. Rev.* **2016**, *309*, 107–179.

[290] V. Novakova, M. P. Donzello, C. Ercolani, P. Zimcik, P. A. Stuzhin, *Coord. Chem. Rev.* **2018**, *361*, 1–73.

[291] J. N. Lekitima, K. I. Ozoemena, C. J. Jafta, N. Kobayashi, Y. Song, D. Tong, S. Chen, M. Oyama, *J. Mater. Chem. A* **2013**, *1*, 2821–2826.

[292] S. R. Kim, J. D. Kim, K. H. Choi, Y. H. Chang, *Sensors Actuators, B Chem.* **1997**, *40*, 39–45.

[293] J. Kim, J. Y. Jaung, H. Ahn, *Macromol. Res.* **2008**, *16*, 367–372.

[294] L. V. Markova, G. N. Smirnova, A. B. Korzhenevskii, O. I. Koifman, *Izv. Vyss. Uchebn. Zaved., Khim. Khim. Tekhnol.* **1992**, *35*, 98–102.

[295] S. V. Kudrevich, J. E. Van Lier, *Coord. Chem. Rev.* **1996**, *156*, 163–182.

[296] P. Zimcik, A. Malkova, L. Hruba, M. Miletin, V. Novakova, *Dye. Pigment.* **2017**, *136*, 715–723.

[297] A. Hagfeldt, G. Boschloo, L. Sun, L. Kloo, H. Pettersson, *Chem. Rev.* **2010**, *110*, 6595–6663.

[298] F. Mitzel, S. FitzGerald, A. Beeby, R. Faust, *European J. Org. Chem.* **2004**, 1136–1142.

[299] P. Zimcik, V. Novakova, M. Miletin, K. Kopecky, *Macroheterocycles* **2008**, *1*, 21–29.

[300] M. P. Donzello, D. Vittori, E. Viola, I. Manet, L. Mannina, L. Cellai, S. Monti, C. Ercolani, *Inorg. Chem.* **2011**, *50*, 7391–7402.

[301] I. Manet, F. Manoli, M. P. Donzello, C. Ercolani, D. Vittori, L. Cellai, A. Masi, S. Monti, *Inorg. Chem.* **2011**, *50*, 7403–7411.

[302] L. E. Hinkel, G. O. Richards, O. Thomas, *J. Chem. Soc.* **1937**, 1432–1437.

[303] A. Al-Azmi, A. Z. A. Elassar, B. L. Booth, *Tetrahedron* **2003**, *59*, 2749–2763.

[304] Y. Ohtsuka, E. Tohma, S. Kojima, N. Tomita, *J. Org. Chem.* **1979**, *44*, 4871–4876.

[305] Y. Kubota, T. Shibata, E. Babamoto-Horiguchi, J. Uehara, K. Funabiki, S. Matsumoto, M. Ebihara, M. Matsui, *Tetrahedron* **2009**, *65*, 2506–2511.

[306] M. MacHacek, J. Kollár, M. Miletin, R. Kučera, P. Kubát, T. Simunek, V. Novakova, P. Zimcik, *RSC Adv.* **2016**, *6*, 10064–10077.

[307] K. J. Chun, H. K. Song, K. L. Do, J. Y. Jaung, *Bull. Korean Chem. Soc.* **2008**, *29*, 1665–1666.

[308] A. V. Kozlov, P. A. Stuzhin, *Macroheterocycles* **2014**, *7*, 170–173.

[309] A. V. Kozlov, P. A. Stuzhin, *Russ. J. Org. Chem.* **2013**, *49*, 913–921.

[310] T. Suzuki, Y. Nagae, K. Mitsuhashi, *J. Heterocycl. Chem.* **1986**, *23*, 1419–1421.

[311] P. Zimcik, M. Miletin, M. Kostka, J. Schwarz, Z. Musil, K. Kopecky, *J. Photochem. Photobiol. A Chem.* **2004**, *163*, 21–28.

[312] F. Bureš, H. Čermáková, J. Kulhánek, M. Ludwig, W. Kuznik, I. V. Kityk, T. Mikysek, A. Růžička, *European J. Org. Chem.* **2012**, 529–538.

[313] H. Ali, J. E. Van Lier, *Tetrahedron Lett.* **2012**, *53*, 4824–4827.

[314] M. Parravicini, L. Vaghi, G. Cravotto, N. Masciocchi, A. Maspero, G. Palmisano, A. Penoni, *Arkivoc* **2014**, *2014*, 72–85.

[315] C. Piechocki, J. Simon, A. Skoulios, D. Guillon, P. Weber, *J. Am. Chem. Soc.* **1982**, *104*, 5245–5247.

[316] S. Shorvon, *Seizure* **2000**, *9*, 75–79.

[317] L. Vaghi, E. C. Gaudino, G. Cravotto, G. Palmisano, A. Penoni, *Molecules* **2013**, *18*, 13705–13722.

[318] T. Kojima, F. Nagasaki, *J. Heterocycl. Chem.* **1980**, *17*, 455.

[319] S. Selman, J. F. Eastham, *Q. Rev. Chem. Soc.* **1960**, *14*, 221–235.

[320] W. Freyer, *J. für Prakt. Chmie* **1994**, *336*, 690–692.

[321] M. P. Donzello, D. Dini, G. D'Arcangelo, C. Ercolani, R. Zhan, Z. Ou, P. A. Stuzhin, K. M. Kadish, *J. Am. Chem. Soc.* **2003**, *125*, 14190–14204.

[322] A. Erdoğmuş, A. Koca, U. Avcata, A. Gül, *Zeitschrift fur Anorg. und Allg. Chemie* **2008**, *634*, 2649–2654.

[323] S. Tuncer, A. Koca, A. Gül, U. Avcata, *Dye. Pigment.* **2012**, *92*, 610–618.

[324] A. Koca, Y. Arslanoğlu, E. Hamuryudan, *J. Electroanal. Chem.* **2008**, *616*, 107–116.

[325] B. Berelman, *Handbook of Fluorescence Spectra of Aromatic Molecules*, Academic Press, **1971**.

[326] Y. Xie, T. Fujimoto, S. Dalgleish, Y. Shuku, M. M. Matsushita, K. Awaga, *J. Mater. Chem. C* **2013**, *1*, 3467–3481.

[327] M. C. Fragnelli, P. Hoyos, D. Romano, R. Gandolfi, A. R. Alcántara, F. Molinari, *Tetrahedron* **2012**, *68*, 523–528.

[328] P. Zimcik, E. H. Mørkved, T. Andreassen, J. Lenco, V. Novakova, *Polyhedron* **2008**, *27*, 1368–1374.

[329] W. C. Still, M. Kahn, A. Mitra, *J. Org. Chem.* **1978**, *43*, 2923–2925.

[330] L. Nardo, M. Lamperti, D. Salerno, V. Cassina, N. Missana, M. Bondani, A. Tempestini, F. Mantegazza, *Nucleic Acids Res.* **2015**, *43*, 10722–10733.

[331] L. Nardo, F. Re, S. Brioschi, E. Cazzaniga, A. Orlando, S. Minniti, M. Lamperti, M. Gregori, V. Cassina, D. Brogioli, et al., *Biochim. Biophys. Acta - Gen. Subj.* **2016**, *1860*, 746–756.

[332] A. Maspero, G. B. Giovenzana, N. Masciocchi, G. Palmisano, A. Comotti, P. Sozzani, I. Bassanetti, L. Nardo, *Cryst. Growth Des.* **2013**, *13*, 4948–4956.

[333] N. L. Mutter, J. Volarić, W. Szymanski, B. L. Feringa, G. Maglia, *J. Am. Chem. Soc.* **2019**, *141*, 14356–14363.

[334] G. Ieronimo, G. Palmisano, A. Maspero, A. Marzorati, L. Scapinello, N. Masciocchi, G. Cravotto, A. Barge, M. Simonetti, K. L. Ameta, et al., *Org. Biomol. Chem.* **2018**, *16*, 6853–6859.

[335] L. Scapinello, A. Maspero, S. Tollari, G. Palmisano, K. M. Nicholas, A. Penoni, *J. Vis. Exp.* **2020**, *155*, 1–12.

[336] B. Priewisch, K. Rück-Braun, *J. Org. Chem.* **2005**, *70*, 2350–2352.

[337] E. B. Mel'nikov, G. A. Suboch, E. Y. Belyaev, *Russ. J. Org. Chem.* **1995**, *31*, 1640.

[338] F. Porta, L. Prati, *J. Mol. Catal. A Chem.* **2000**, *157*, 123–129.

[339] E. Bosch, J. K. Kochi, *J. Org. Chem.* **1994**, *59*, 5573–5586.

[340] G. A. Molander, L. N. Cavalcanti, *J. Org. Chem.* **2012**, *77*, 4402–4413.

[341] L. Scapinello, F. Vavassori, G. Ieronimo, K. L. Ameta, G. Cravotto, M. Simonetti, S. Tollari, G. Palmisano, A. Maspero, K. M. Nicholas, et al., *Manuscript in Preparation*, **2020**.

[342] H. Oubaha, N. Demitri, J. Rault-Berthelot, P. Dubois, O. Coulembier, D. Bonifazi, *J. Org. Chem.* **2019**, *84*, 9101–9116.

[343] S. Bellotto, R. Reuter, C. Heinis, H. A. Wegner, *J. Org. Chem.* **2011**, *76*, 9826–9834.

[344] K. C. Weerasiri, A. E. V. Gorden, *European J. Org. Chem.* **2013**, 1546–1550.

[345] Y. Maeda, N. Kakiuchi, S. Matsumura, T. Nishimura, T. Kawamura, S. Uemura, *J. Org. Chem.* **2002**, *67*, 6718–6724.

[346] W. R. Yang, Y. S. Choi, J. H. Jeong, *Org. Biomol. Chem.* **2017**, *15*, 3074–3083.

[347] C. Hempel, C. Maichle-Mössmer, M. A. Pericàs, B. J. Nachtsheim, *Adv. Synth. Catal.* **2017**, *359*, 2931–2941.

[348] U. Kazmaier, S. Lucas, M. Klein, *J. Org. Chem.* **2006**, *71*, 2429–2433.

[349] F. C. Pigge, F. Ghasedi, Z. Zheng, N. P. Rath, G. Nichols, J. S. Chickos, *J. Chem. Soc. Perkin Trans. 2* **2000**, 2458–2464.

[350] M. P. Kumar, R. S. Liu, *J. Org. Chem.* **2006**, *71*, 4951–4955.

[351] F. Shi, S. W. Luo, Z. L. Tao, L. He, J. Yu, S. J. Tu, L. Z. Gong, *Org. Lett.* **2011**, *13*, 4680–4683.

[352] A. Kolarovič, Z. Fáberová, *J. Org. Chem.* **2009**, *74*, 7199–7202.

[353] S. Park, J. M. Joo, E. J. Cho, *European J. Org. Chem.* **2015**, *2015*, 4093–4097.

[354] M. Bhanuchandra, M. R. Kuram, A. K. Sahoo, *J. Org. Chem.* **2013**, *78*, 11824–11834.

[355] J. S. Oakdale, R. K. Sit, V. V. Fokin, *Chem. - A Eur. J.* **2014**, *20*, 11101–11110.

[356] X. Liu, L. Yu, M. Luo, J. Zhu, W. Wei, *Chem. - A Eur. J.* **2015**, *21*, 8745–8749.

[357] B. S. Chinta, B. Baire, *Tetrahedron* **2016**, *72*, 8106–8116.

[358] D. S. P. Ferreira, J. G. Ferreira, E. F. S. Filho, J. L. Princival, *J. Mol. Catal. B Enzym.* **2016**, *126*, 37–45.

[359] A. L. K. Shi Shun, E. T. Chernick, S. Eisler, R. R. Tykwinski, *J. Org. Chem.* **2003**, *68*, 1339–1347.

[360] S. P. Sau, P. J. Hrdlicka, *J. Org. Chem.* **2012**, *77*, 5–16.

[361] S. Barriga, C. F. Marcos, *Tetrahedron* **2002**, *58*, 9785–9792.

[362] L. Burroughs, L. Eccleshare, J. Ritchie, O. Kulkarni, B. Lygo, S. Woodward, W. Lewis, *Angew. Chemie - Int. Ed.* **2015**, *54*, 10648–10651.

[363] H. Salgado-Zamora, J. Hernandez, M. E. Campos, R. Jimenez, H. Cervantes-Cuevas, E. Mojica, *J. Prakt. Chemie* **1999**, *341*, 461.

[364] L. J. Cheng, C. J. Cordier, *Angew. Chemie - Int. Ed.* **2015**, *54*, 13734–13738.

[365] Z. Wang, L. Li, Y. Huang, *J. Am. Chem. Soc.* **2014**, *136*, 12233–12236.

[366] A. Dondoni, D. Perrone, *J. Org. Chem.* **1995**, *60*, 4749–4754.

[367] C. F. Yeung, L. H. Chung, S. W. Ng, H. L. Shek, S. Y. Tse, S. C. Chan, M. K. Tse, S. M. Yiu, C. Y. Wong, *Chem. - A Eur. J.* **2019**, *25*, 9159–9163.

[368] M. Egi, M. Umemura, T. Kawai, S. Akai, *Angew. Chemie - Int. Ed.* **2011**, *50*, 12197–12200.

[369] M. Głodek, A. Makal, D. Plazuk, *J. Org. Chem.* **2018**, *83*, 14165–14174.

[370] D. B. Baker, P. T. Gallagher, T. J. Donohoe, *Tetrahedron* **2013**, *69*, 3690–3697.

[371] Q. Cai, J. Yan, K. Ding, *Org. Lett.* **2012**, *14*, 3332–3335.

[372] W. Li, D. P. Nelson, M. S. Jensen, S. R. Hoerrner, D. Cai, R. D. Larsen, *Org. Synth.* **2005**, *81*, 89–97.

[373] A. C. Kinsman, M. A. Kerr, *J. Am. Chem. Soc.* **2003**, *125*, 14120–14125.

[374] T. B. Poulsen, L. Bernardi, J. Alemán, J. Overgaard, K. A. Jørgensen, *J. Am. Chem. Soc.* **2007**, *129*, 441–449.

[375] J. K. Vandavasi, X. Y. Hua, H. Ben Halima, S. G. Newman, *Angew. Chemie - Int. Ed.* **2017**, *56*, 15441–15445.

[376] C. X. Yang, H. H. Patel, Y. Y. Ku, R. Shah, D. Sawick, *Synth. Commun.* **1997**, *27*, 2125–2132.

[377] C. Wang, S. Wang, H. Li, J. Yan, H. Chi, X. Chen, Z. Zhang, *Org. Biomol. Chem.* **2014**, *12*, 1721–1724.

[378] A. Banerji, D. Bandyopadhyay, B. Basak, *Heterocycles* **2004**, *63*, 2371–2377.

[379] J. Zhou, J. Li, Y. Li, C. Wu, G. He, Q. Yang, Y. Zhou, H. Liu, *Org. Lett.* **2018**, *20*, 7645–7649.

[380] S. Dvorácskó, A. Keresztes, A. Mollica, A. Stefanucci, G. Macedonio, S. Pieretti, F. Zádor, F. R. Walter, M. A. Deli, G. Kékesi, et al., *Eur. J. Med. Chem.* **2019**, *178*, 571–588.

[381] Z. D. Cooper, J. L. Poklis, F. Liu, *Neuropharmacology* **2018**, *134*, 92–100.

[382] E. Kumaran, W. Y. Fan, W. K. Leong, *Org. Lett.* **2014**, *16*, 1342–1345.

[383] W. Lee, N. Cho, J. Kwon, J. Ko, J. I. Hong, *Chem. - An Asian J.* **2012**, *7*, 343–350.

[384] Z. Wu, Z. An, X. Chen, P. Chen, *Org. Lett.* **2013**, *15*, 1456–1459.

[385] T. Niu, Y. Zhang, *Tetrahedron Lett.* **2010**, *51*, 6847–6851.

[386] J. H. Kim, H. U. Kim, D. Mi, S. H. Jin, W. S. Shin, S. C. Yoon, I. N. Kang, D. H. Hwang, *Macromolecules* **2012**, *45*, 2367–2376.

[387] K. Komeyama, R. Asakura, K. Takaki, *Org. Biomol. Chem.* **2015**, *13*, 8713–8716.

[388] S. Shome, S. P. Singh, *Chem. Commun.* **2018**, *54*, 7322–7325.

[389] G. Schimperna, G. Bianchi, *Process for the Preparation of Benzohetero [1,3] - Diazole Compounds Disubstituted with Heteroaryl Groups*, **2014**, US2014221663 (A1).

[390] R. Agosta, R. Grisorio, L. De Marco, G. Romanazzi, G. P. Suranna, G. Gigli, M. Manca, *Chem. Commun.* **2014**, *50*, 9451–9453.

[391] S. Chen, D. Zhang, M. Wang, L. Kong, J. Zhao, *New J. Chem.* **2016**, *40*, 2178–2188.

[392] S. Maiti, R. G. Jadhav, S. M. Mobin, T. K. Mukherjee, A. K. Das, *ChemPhysChem* **2019**, *20*, 2221–2229.

[393] L. Wang, W. Huang, R. Li, D. Gehrig, P. W. M. Blom, K. Landfester, K. A. I. Zhang, *Angew. Chemie - Int. Ed.* **2016**, *55*, 9783–9787.

[394] T. Li, Y. Yang, B. Li, P. Yang, *Chem. Commun.* **2019**, *55*, 353–356.

[395] T. Qi, W. Qiu, Y. Liu, H. Zhang, X. Gao, Y. Liu, K. Lu, C. Du, G. Yu, D. Zhu, *J. Org. Chem.* **2008**, *73*, 4638–4643.

[396] P. Cai, X. Xu, J. Sun, J. Chen, Y. Cao, *RSC Adv.* **2017**, *7*, 20440–20450.

[397] C. T. Chen, J. S. Lin, M. V. R. K. Moturu, Y. W. Lin, W. Yi, Y. T. Tao, C. H. Chien, *Chem. Commun.* **2005**, 3980–3982.

[398] B. Shaik, J. H. Park, T. K. An, Y. R. Noh, S. B. Yoon, C. E. Park, Y. J. Yoon, Y. H. Kim, S. G. Lee, *Tetrahedron* **2013**, *69*, 8191–8198.

[399] F. A. Arroyave, C. A. Richard, J. R. Reynolds, *Org. Lett.* **2012**, *14*, 6138–6141.